

This PDF was created from the British Library's microfilm copy of the original thesis. As such the images are greyscale and no colour was captured.

Due to the scanning process, an area greater than the page area is recorded and extraneous details can be captured.

This is the best available copy

DX

184780

THE BRITISH LIBRARY

BRITISH THESIS SERVICE

TITLE SYNTHESSES, STRUCTURE AND STABILITY OF
SOME ALKYLPHOSPHONIC ACIDS AND THEIR
METAL COMPLEXES.

AUTHOR Maria
CONSTANTINOU

DEGREE Ph.D

**AWARDING
BODY** University of North London

DATE 1994

**THESIS
NUMBER** DX184780

THIS THESIS HAS BEEN MICROFILMED EXACTLY AS RECEIVED

The quality of this reproduction is dependent upon the quality of the original thesis submitted for microfilming. Every effort has been made to ensure the highest quality of reproduction. Some pages may have indistinct print, especially if the original papers were poorly produced or if awarding body sent an inferior copy. If pages are missing, please contact the awarding body which granted the degree.

Previously copyrighted materials (journals articles, published texts etc.) are not filmed.

This copy of the thesis has been supplied on condition that anyone who consults it is understood to recognise that its copyright rests with its author and that no information derived from it may be published without the author's prior written consent.

Reproduction of this thesis, other than as permitted under the United Kingdom Copyright Designs and Patents Act 1988, or under specific agreement with the copyright holder, is prohibited.

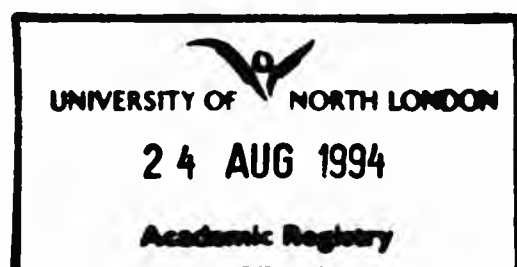
C12.

**Syntheses, Structure and Stability of Some
Alkylphosphonic Acids and Their Metal
Complexes**

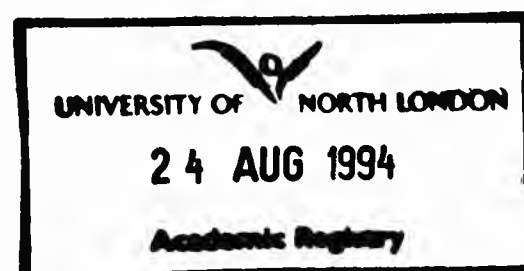
MARIA CONSTANTINO

**A thesis submitted in partial fulfilment of the
requirements of the University of North London for
the degree of Doctor of Philosophy**

**This research programme was carried out in the School of Applied
Chemistry at the University of North London, and (in part) in
collaboration with Interlox Research and Development**



August 1994



To my parents and Chris

Syntheses, Structure and Stability of Some Alkylphosphonic Acids and Their Metal Complexes

ABSTRACT

The protonation and complexation behaviour of the α -aminomethylenephosphonic acids diethylaminomethylenephosphonic acid (DEAMPH₂), *N*-ethyliminobis(methylenephosphonic acid) (NEIBMPH₄), (\pm)-*trans*-1,2-diaminocyclohexanetetraakis(methylenephosphonic acid) (CDTMPH₃), and 5,8-dioxadodecane-1,12-diaminetetraakis(methylenephosphonic acid) (DDDTMPH₃) were studied by potentiometry and nmr spectroscopy. Adaptations of the Mannich reaction were used to prepare these acids. Protonation constants in aqueous solution were determined potentiometrically ($I = 0.1 \text{ mol dm}^{-3}$, KNO_3 , $25.0 \pm 0.1 \text{ }^\circ\text{C}$), and ^{31}P nmr spectra were used to elucidate the microscopic protonation schemes. In the case of CDTMPH₃, the particular complex pH-dependence of the two ^{31}P nmr resonances was successfully rationalised by assuming that certain features of the hydrogen-bonded scheme in the solid state structure are carried over into solution. The X-ray crystal structures of both CDTMPH₃ and DEAMPH₂ were determined in this work.

The complexation behaviour of DEAMPH₂, NEIBMPH₄, CDTMPH₃ and DDDTMPH₃ with some metal ions [variously Mn(II), Co(II), Ni(II), Pb(II), Cd(II), Zn(II), Cu(II), Fe(III) and Gd(III)] was investigated by determining stability constants ($\log \beta$) for species which in equilibrium, represented a 'best-fit' model for replication of the experimentally determined potentiometric titration curves. The metal-ligand species determined were mainly complexes with a metal:ligand ratio of 1:1; only in three cases were $[\text{ML}_2]$ complexes indicated. The order of stability for complexes of $[\text{ML}]^{2-}$ with NEIBMPH₄ follows the Irving-Williams series. The order of stability for the complexes $[\text{MLH}]^{5-}$ with DDDTMPH₃ also follows the Irving-Williams series. The order of stability of the species $[\text{MLH}]^{5-}$ for CDTMPH₃ follows the Irving-Williams series except for Co(II) and Ni(II), where the stability is reversed. For DEAMPH₂, NEIBMPH₄, and DDDTMPH₃ the stability of Pb(II) complexes were almost as strong as the Cu(II) complexes. As expected, Fe(III) forms the most stable complexes with NEIBMPH₄ and CDTMPH₃.

The effect of hydrogen peroxide on DEAMPH₂ and NEIBMPH₄ was investigated, and the solid N-oxide derivative of NEIBMPH₄ obtained. The $\delta(^{31}\text{P})$ vs pH profile suggests that hydrogen peroxide reacts with the amino group at above pH ca. 7, probably yielding the N-oxide. The protonation and complexation behaviour of this derivative with Cu(II) is reported.

Novel clusters formed from the condensation reactions of organostannonic acids with carboxylic and/or phosphonic acids have been previously synthesised. Attempts were made to investigate the mechanism by which combination of sodium stannate and aminophosphonic acids leads to enhanced stability of aqueous hydrogen peroxide by studying the possible reactions of organostannonic acids with phosphorus and carboxylic-based acids and, specifically with aminophosphonic acids.

Acknowledgements

I would like to thank my supervisor Dr. Matthews for all his help, time, useful comments and suggestions. I would like to thank both my industrial supervisors from Interlox Research and Development; Dr. Candy for his help and in supplying information about aminomethylenephosphonic acids and Dr. Lynch for his attentiveness and helpfulness when I visited Interlox Research and Development for a week's safety training in handling hydrogen peroxide.

I would like to thank Prof. McPartlin and Mr N. Y. Choi for their help in the determination of crystal structures.

I would like to thank all the technicians in the School of Applied Chemistry for the routine examination of my samples: *i.e.* Mr J. Crowder for running nmr spectra, Mr S. Boyer and Ms P. Haria for micro analysis, Mr W. Dissanayake for mass spectra; and Dr. P. Baillie for assistance in locating various chemicals.

I would also like to thank the following for making my time in and out of the University of North London both enjoyable and memorable: Mr N. Choi, Ms S. Choudhury, Ms S. Darvies, Ms N. Ereira, Mr E. G. Evagorou, Mr I. Khan, Ms C. McGrath, Mr I. Mitchell, Mrs E. Mitchell, Dr. I. J. Scowen and Dr. S. Waikar. Last but not least, I would especially like to thank Mr. C. J. L. Silwood for his continual support, sense of humour and for putting up with me; and my parents for their support and encouragement.

I gratefully acknowledge a studentship (No. 90314686) from the SERC for financial support and from Interlox Research and Development for the duration of my post-graduate study at the University of North London.

I also gratefully acknowledge funding from the SERC and the School of Applied Chemistry for a conference to America; and from the School of Applied Chemistry for a conference to Poland.

CONTENTS

	Page
Title page	ii
Abstract	iii
Acknowledgements	iv
Contents	v
Chapter 1 Introduction	
1.1 Alkylaminoalkylphosphonic acids	1
1.1.1 Preparation	1
1.1.2 Applications	2
1.2 Stabilisation of hydrogen peroxide	2
1.2.1 Applications	3
1.2.2 Stability of hydrogen peroxide	4
1.3 Equilibrium analysis	6
1.3.1 Nomenclature of metal complexes	6
1.3.2 Equilibrium constants and mass-balance equations	6
1.3.3 Determination of stability constants by potentiometry	10
1.3.4 Stability constants	12
1.3.5 Computational methods for the determination of stability constants	13
1.3.6 SUPERQUAD; a general program for stability constant calculation	13
1.3.7 Thermodynamic stability of metal complexes	14
1.4 Organotin cluster chemistry	16
1.4.1 Synthesis	16
1.4.2 Drum and ladder organotin clusters based on carboxylic acids	17
1.4.3 Organotin clusters based on phosphorus-based acids	19
1.5 Aims	20
1.5.1 Context	20
1.5.2 Aims of present work	20
1.6 References	22
Chapter 2 Experimental Methods	
2.1 Synthesis of alkyl/aryl stannonic acid and their cluster derivatives	25
2.1.1 Starting materials and solvents	25

	Page
2.1.2 Preparation of methylstannonic acid, $[\text{CH}_3\text{SnO}_2\text{H}]$	25
2.1.3 Preparation of <i>n</i> -butylstannonic acid, $[\text{CH}_3(\text{CH}_2)_3\text{SnO}_2\text{H}]$	26
2.1.4 Preparation of the hydrochloride salt of phenylstannonic acid, $[\text{C}_6\text{H}_5\text{SnO}_2\text{H}]\cdot\text{HCl}$.	27
2.1.5 Preparation of hexameric methyloxotin acetate, $[\text{CH}_3\text{Sn}(\text{O})\text{O}_2\text{CCH}_3]_6$	27
2.1.6 Preparation of methyltin tris(diphenylphosphate), $[\text{CH}_3\text{Sn}(\text{O}_2\text{P}(\text{OC}_6\text{H}_5)_2)_3]$	27
2.1.7 Preparation of the cage cluster, $[(\text{CH}_3)_2\text{Sn}_2(\text{OH})(\text{O}_2\text{P}(\text{OC}_6\text{H}_5)_2)_3(\text{O}_3\text{POC}_6\text{H}_5)]_2$	28
2.1.8 Preparation of methyltin tris(styrenephosphonate), $[\text{CH}_3\text{Sn}(\text{O}_2\text{P}(\text{OH})\text{CH}=\text{CHC}_6\text{H}_5)_3]$	28
2.1.9 Preparation of hexameric methyloxotin benzoate, $[\text{CH}_3\text{Sn}(\text{O})\text{O}_2\text{CC}_6\text{H}_5]_6$	29
2.1.10 Preparation of $[(\text{CH}_3(\text{CH}_2)_3\text{Sn}(\text{O})\text{O}_2\text{CCH}_3)_2(\text{CH}_3(\text{CH}_2)_3\text{Sn}(\text{O}_2\text{CCH}_3)_3)]_2$ in a 'ladder' form	30
2.1.11 Preparation of hexameric <i>n</i> -butyloxotin benzoate, $[\text{CH}_3(\text{CH}_2)_3\text{Sn}(\text{O})\text{O}_2\text{CC}_6\text{H}_5]_6$	30
2.1.12 Preparation of <i>n</i> -butyloxotin diethylaminomethylene-phosphonate, $[\text{CH}_3(\text{CH}_2)_3\text{SnO}(\text{O}_2\text{P}(\text{OH})\text{CH}_2\text{N}(\text{CH}_2\text{CH}_3)_2)]_6$	31
2.1.13 Preparation of hexameric <i>n</i> -butyloxotin hippurate, $[\text{CH}_3(\text{CH}_2)_3\text{Sn}(\text{O})\text{O}_2\text{CCH}_2\text{NH}(\text{CO})\text{C}_6\text{H}_5]_6$	31
2.1.14 Preparation of hexameric phenyloxotin acetate, $[\text{C}_6\text{H}_5\text{Sn}(\text{O})\text{O}_2\text{CCH}_3]_6\cdot\text{C}_7\text{H}_8$	32
2.1.15 Preparation of hexameric phenyloxotin benzoate, $[\text{C}_6\text{H}_5\text{Sn}(\text{O})\text{O}_2\text{CC}_6\text{H}_5]_6$	32
2.1.16 Preparation of the 'cage' $[(\text{CH}_3\text{CH}_2\text{CH}_2\text{CH}_2)_2\text{Sn}_2\text{O}(\text{O}_2\text{P}(\text{OH})\text{CH}_2\text{C}_6\text{H}_5)_4]_2$	33
2.1.17 Preparation of the 'cage' $[(\text{CH}_3)_2\text{Sn}_2\text{O}(\text{O}_2\text{P}(\text{OH})\text{C}(\text{CH}_3)_3)_4]_2$	33
2.1.18 Preparation of the 'cage' cluster $[(\text{CH}_3\text{CH}_2\text{CH}_2\text{CH}_2)_2\text{Sn}_2\text{O}(\text{O}_2\text{P}(\text{OH})\text{C}(\text{CH}_3)_3)_4]_2$	34
2.1.19 Preparation of the copper complex of, $[\text{CH}_3\text{CH}_2\text{CH}_2\text{CH}_2\text{Sn}(\text{O})\text{O}_2\text{CC}_6\text{H}_5]_6$	35
2.2 Preparation of some alkylaminomethylenephosphonic acids, their N-oxides, and complexes with selected metal ions	35
2.2.1 Starting materials and solvents	35

	Page
2.2.2 Preparation of <i>N</i> -ethyliminobis(methylenephosphonic acid), NEIBMPH ₄	36
2.2.3 A novel method for recrystallising diethylaminomethylene-phosphonic acid DEAMPH ₂	37
2.2.4 Preparation of (±)- <i>trans</i> -cyclohexane-1,2-diaminotetrakis(methylenephosphonic acid), CDTMPH ₃	38
2.2.5 Preparation of the <i>N</i> -oxide derivative of NEIBMPH ₄	39
2.2.6 Characterisation of 5,8-dioxadodecane-1,12-diaminotetrakis(methylenephosphonic acid), DDDTMPH ₃	40
2.2.7 Preparation of [Cd(NEIBMPH ₃) ₂]	40
2.2.8 Preparation of [Cu(NEIBMPH ₃) ₂]	41
2.2.9 Preparation of [Mn(NEIBMPH ₃) ₂]	41
2.2.10 Preparation of [Co(NEIBMPH ₃) ₂]	42
2.2.11 Preparation of [Zn(NEIBMPH ₃) ₂].H ₂ O	42
2.3 Determination of protonation and stability constants for some alkylaminomethylenephosphonic acids and their metal complexes by potentiometric titration	42
2.3.1 Reagents and solvents used during potentiometric titrations	42
2.3.2 Preparation of solutions	43
2.3.3 Data acquisition	47
2.3.4 Cell calibration	50
2.3.5 Conditions for ligand and ligand/metal potentiometric titrations	50
2.3.6 Data processing	56
2.3.7 Computational methods	57
2.3.8 Species' abundance vs pH diagrams	59
2.4 Determination of pH-dependence ³¹ P nmr chemical shift for some alkylaminomethylenephosphonic acids and their derivatives	59
2.4.1 Reagents used	60
2.4.2 ³¹ P nmr spectra	60
2.4.3 pH Measurements	61
2.4.4 Preparation of <i>aqueous</i> solutions for ³¹ P nmr/pH titrations	61
2.4.5 ³¹ P nmr/pH titrations of DEAMPH ₂	62
2.4.6 pH dependence of ³¹ P nmr spectrum of DEAMPH ₂ treated with <i>aqueous</i> hydrogen peroxide	63
2.4.7 ³¹ P nmr/pH titration of DEAMPH ₂ in the presence of sodium stannate	63

	Page
2.4.8 ^{31}P nmr/pH titration of NEIBMPH ₄ and its N-oxide derivative	63
2.4.9 ^{31}P nmr/pH titration of DDDTMPH ₃	64
2.4.10 ^{31}P nmr/pH titration of DDDTMPH ₃ in the absence of excess acid	64
2.4.11 ^{31}P nmr/pH titration of DDDTMPH ₃ against tetraethylammonium hydroxide	65
2.5 Instrumental methods	65
2.5.1 Infrared spectra	65
2.5.2 ^1H nmr spectra	65
2.5.3 ^{13}C nmr spectra	65
2.5.4 ^{31}P nmr spectra	66
2.5.5 ^{119}Sn nmr spectra	66
2.5.6 Elemental analysis	66
2.5.7 Mass spectra	66
2.5.8 UV-visible spectra	67
2.5.9 Magnetic susceptibilities	67
2.6 Single crystal X-Ray diffraction methods	69
2.6.1 Data collection	69
2.6.2 Structure solution and refinement of diethylaminomethylene phosphonic acid	69
2.6.3 Structure solution and refinement of (\pm)- <i>trans</i> -cyclohexane-1,2-diaminetetrakis(methylenephosphonic acid)	70
2.7 References	71
 Chapter 3 Organotin cages, clusters and drums	
3.1 Introduction	73
3.1.1 Preparation of the 'cage' cluster I, $[\text{Me}_2\text{Sn}_2(\text{OH})(\text{O}_2\text{P}(\text{OPh})_2)_3(\text{O}_3\text{POPh})]_2$	73
3.2 The Preparation of some novel organotin clusters with phosphonic and/or carboxylic acids	78
3.2.1 Preparation of <i>n</i> -butylstannonic acid	78
3.2.2 Preparation of the hydrochloride salt of phenylstannonic acid	78
3.2.3 Preparation of the novel compound <i>n</i> -butyltinbis-(diethylaminomethylenephosphonic acid)	79
3.2.4 Preparation of the novel hexameric alkyloxotin carboxylates	80
3.2.5 Preparation of the novel 'ladder' form of $[\text{CH}_3\text{CH}_2\text{CH}_2\text{CH}_2\text{Sn}(\text{O})\text{O}_2\text{CCH}_3]_2(\text{CH}_3\text{CH}_2\text{CH}_2\text{CH}_2\text{Sn}(\text{O}_2\text{CCH}_3)_3)_2$	82

	Page
3.2.6 Preparation of the novel compound methyltin tris(styrene-phosphonic acid)	83
3.2.7 Preparation of some 'cages' with phosphorus-based acids	83
(a) Preparation of the 'cage', $[(CH_3)_2Sn_2O(O_2P(OH)C(CH_3)_3)_4]_2$,	83
(b) Preparation of the novel 'cage'	86
$[(CH_3CH_2CH_2CH_2)_2Sn_2O(O_2P(OH)C(C_6H_5)_4)]_2$	
(c) Preparation of the novel 'cage'	86
$[(CH_3CH_2CH_2CH_2)_2Sn_2O(O_2P(OH)C(CH_3)_3)_4]_2$	
3.2.8 The possible clathration of metals by organotin compounds	86
3.3 References	89

Chapter 4 Protonation constants of some alkylaminomethylenephosphonic acids

4.1 Introduction	90
4.2 Syntheses of some alkylaminomethylenephosphonic acids	93
4.2.1 Synthesis and characterisation of DEAMPH ₂ and NEIBMPH ₄	93
4.2.2 Synthesis and characterisation of CDTMPH ₃	96
4.2.3 Characterisation of DDDTMPH ₃	100
4.2.4 Infrared spectra	101
4.3 Protonation equilibria for diethylaminomethylenephosphonic acid, DEAMPH ₂	102
4.4 Protonation constants for <i>N</i> -ethyliminobis(methylenephosphonic acid), NEIBMPH ₄	112
4.5 Protonation equilibria for (±)- <i>trans</i> -1,2-diaminecyclohexane-tetrakis(methylenephosphonic acid), CDTMPH ₃	117
4.6 Protonation equilibria determined for DDDTMPH ₃	131
4.7 References	142

Chapter 5 Metal complexes of some alkylaminomethylenephosphonic acids

5.1 The stability of some metal complexes of two 'simple' α-aminomethylenephosphonic acids, DEAMPH ₂ and NEIBMPH ₄	147
5.1.1 Stability constants for metal ion complexes with DEAMPH ₂	147
(a) Zinc(II) and cadmium(II)	148
(b) Cobalt(II)	150
(c) Lead(II)	151
5.1.2 Stability constants for metal ion complexes with NEIBMPH ₄	153
(a) Manganese(II)	153

	Page
(b) Iron(III)	156
(c) Cobalt(II)	158
(d) Nickel(II)	159
(e) Copper(II)	163
(f) Zinc(II)	166
(g) Lead(II)	167
(h) Cadmium(II)	169
5.1.3 Species abundance plots of some metal ions with DEAMPH ₂ and NEIBMPH ₄	171
5.1.4 Possible structures of metal complex species in solution	176
5.2 The stability of some metal complexes of two 'complex' α-amino- methylene phosphonic acids, CDTMPH ₃ and DDDTMPH ₃	186
5.2.1 Stability constants for metal ion complexes with CDTMPH ₃	186
(a) Manganese(II)	187
(b) Iron(III)	188
(c) Cobalt(II)	190
(d) Nickel(II)	192
(e) Zinc(II)	193
(f) Lead(II)	194
(g) Copper(II)	196
(h) Gadolinium(III)	197
5.2.2 Stability constants for some metal ions complexes with DDDTMPH ₃	201
(a) Copper(II)	201
(b) Zinc(II)	203
(c) Cadmium(II)	205
(d) Lead(II)	207
5.2.3 Species distribution plots of some metals with CDTMPH ₃ and DDDTMPH ₃	209
5.2.4 Comparison with previous work for CDTMPH ₃	216
5.2.5 The configuration and orientation of the ligating groups and its effect on the resulting complex stability	216
5.2.6 Possible structures of metal complex species in solution	219
5.3 Preparation of some solid metal complexes of N-ethyliminobis- (methylene phosphonic acid), NEIBMPH ₄	222
5.3.1 Characterisation of some metal complexes of NEIBMPH ₄	224
5.4 References	227

Chapter 6 Alkylaminomethylenephosphonic acids: Some studies relevant to their stabilising action on hydrogen peroxide	
6.1	The effect of hydrogen peroxide on some α -aminomethylene-phosphonic acids 231
6.1.1	The pH-dependence of the ^{31}P nmr chemical shift for DEAMP $_2$ after treatment with aqueous hydrogen peroxide 232
6.1.2	Synthesis and characterisation for the N-oxide derivative of NEIEMPH $_4$ 234
6.1.3	Protonation equilibria for the N-oxide derivative of NEIEMPH $_4$ 237
	(a) Preliminary examination of the stability of Cu(II) complexes of the N-oxide derivative 242
6.1.4	Preliminary investigations of the possible interaction between DEAMP $_2$ and sodium stannate 245
	(a) The pH-dependence of the ^{31}P nmr chemical shift of DEAMP $_2$ in the presence of sodium stannate 245
6.2	References 248
 Chapter 7 Determination of the solid state structures of <i>N,N</i>-diethylaminomethylenephosphonic acid and (\pm)-trans-cyclohexane-1,2-diaminetetrakis(methylenephosphonic acid) by single crystal X-ray diffraction	
7.1	Introduction 250
7.2	Description of the solid structure of <i>N,N</i> -diethylaminomethylene-phosphonic acid, DEAMP $_2$ 252
7.2.1	Classification of phosphorus to oxygen bond lengths 255
7.2.2	Hydrogen bonding interactions 256
7.3	Description of the solid structure of (\pm)-trans-cyclohexane-1,2-diaminetetrakis(methylenephosphonic acid), CDTMPH $_8 \cdot \text{H}_2\text{O}$ 258
7.3.1	Classification of phosphorus to oxygen bond lengths 262
7.3.2	Intramolecular hydrogen bonding interactions 264
7.3.3	Intermolecular hydrogen bonding interactions 266
7.3.4	Conformation of the cyclohexyl ring of CDTMPH $_8 \cdot \text{H}_2\text{O}$ 268
7.3.5	The configuration of the substituent groups 272
7.4	References 274

- Appendix 1 X-Ray crystallographic data for DEAMPH₂
Appendix 2 X-Ray crystallographic data for CDTMPH₂·H₂O
Appendix 3 Publications

Chapter 1 Introduction

1.1 Alkylaminoalkylphosphonic acids

The first natural compound with a carbon-phosphorus bond, 2-aminoethylphosphonic acid (β -ciliatine), was discovered by Horiguchi and Kandastu from sea anemone.¹ Subsequently, other workers, e.g. Kitteredge and Hughes, discovered other aminoalkylphosphonic acids and their derivatives, e.g. 2-amino-3-phosphonopropionic acid and *N*-methylaminoethylphosphonic acid to name but two.² These compounds belong to the large class of aminoalkylphosphonic acids, whose chemistry has been widely summarised in a number of reviews³⁻⁵ and whose wide variety of applications continues to stimulate vigorous investigation of its chemistry.

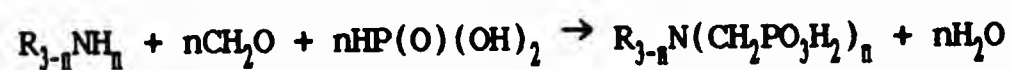
1.1.1 Preparation

There are a variety of methods that can be used to prepare aminoalkylphosphonic acids.⁶ For example, the Kabachnik-Fields reaction involves reaction of ammonia (or an amine) with a carbonyl compound and a dialkyl phosphite to yield the aminophosphonic acid ester. This ester can then be hydrolysed to form the free acid.⁶

Another reaction involves the amidoalkylation of phosphorus trichloride with a carbonyl compound and an amide; these are reacted with acetic acid and then subsequent hydrolysis leads to the formation of the aminophosphonic acid.

The Arbuzov and Michaelis-Becker reactions are also important in the chemistry of organophosphorus compounds and were among the first methods used to prepare the phosphorus analogue of glycine, aminomethylenephosphonic acid.

However, a method that has become widely used to prepared many alkylamino-methylenephosphonic acids is the Moedritzer-Irani reaction:^{7,8}



where $n = 1, 2$ and 3 . A major advantage of this reaction is the availability and cheapness of the starting materials and use of a 'one-pot' reacting vessel. However, the products prepared by this method are often impure and need to be isolated from syrupy oils which is often very difficult.

1.1.2 Applications

Aminophosphonic acids are analogues of aminocarboxylic acids and are known to have widespread use in industrial and medicinal applications, e.g. hydrogen peroxide stabilisation,⁹ disinfecting solutions for contact lens.¹⁰ Aminoalkylphosphonic acids are also used as anticorrosive agents upon adsorption by steel pipes.¹¹ Some cycloalkylaminomethylenebis(phosphonic acids) are being used as bone resorption inhibitors and anti-inflammatory.¹² In some colour photographic processing, cyclohexanediamine-tetra acetic and phosphonic acid derivatives are used as bleaching agents to improve silver removal of colour-developed photographic material for rapid processing.¹³ Diethylenetriamine-pentakis(methylenephosphonic acid) is a well known aminomethylenephosphonic acid, effective for both bleaching paper and for stabilising hydrogen peroxide.^{13,14} Their potential as spectroscopic diagnostic agents, e.g. as a contrasting agent in the nmr imaging of calcified tissues, is emerging.¹⁵⁻¹⁷ Platinum complexes of some aminophosphonic acids are now being investigated as possible antitumour agents in cancer chemotherapy.¹⁸

Another use of aminoalkylphosphonic acids which has become more important over the last 25 years, is the sequestration of metals in some industrial applications. Some polyaminoalkylphosphonic acids have replaced certain aminocarboxylic acids in stabilising hydrogen peroxide¹⁴ and in textile processing. Polyaminoalkylphosphonic acids can also act as detergents, dispersing soil in solution and they are also known to form stable metal complexes over a wide pH range.¹⁴

1.2 Stabilisation of hydrogen peroxide

Hydrogen peroxide is a clear, colourless, slightly viscous liquid, which is miscible with water. Hydrogen peroxide is produced commercially by the 'Autoxidation Process' (AO). This AO process (Figure 1.2.1) involves the reduction of an anthraquinone to anthraquinol followed by oxidation to the same anthraquinone with hydrogen peroxide as a by-product.¹⁹

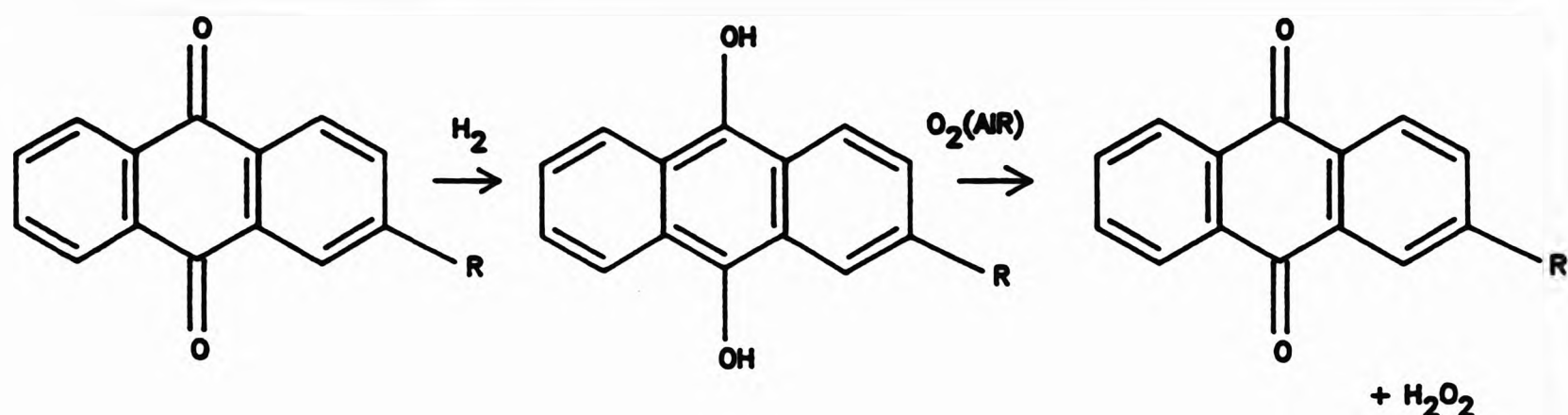
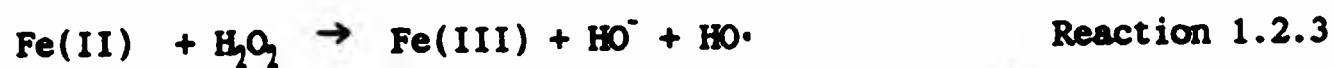
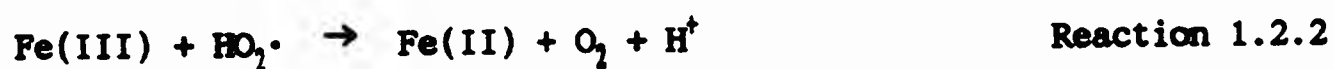
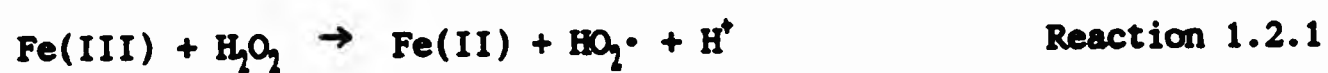


Figure 1.2.1 The autoxidation (AO) process for the preparation of hydrogen peroxide.

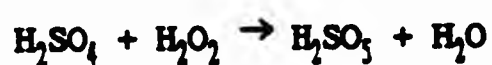
1.2.1 Applications

Hydrogen peroxide can react as an oxidizing or reducing agent in both basic and acidic solution. Hydrogen peroxide can also form other inorganic and organic peroxy salts e.g. peroxonium (H_2OOH^+), hydroperoxide (OOH^-) and peroxides (O_2^{2-}). Hydrogen peroxide can, however, undergo decomposition to water and oxygen via various reactions,¹⁹ the exact mechanism of decomposition depending on the nature of the materials present, e.g. with iron by the Fenton reaction (Reaction 1.2.3) by some of the following reactions.²⁰



An example of the use of hydrogen peroxide in chemical synthesis is the oxidation of tertiary amines to produce amine oxides. Secondary amines give substituted hydroxylamines and primary aromatic amines give nitro compounds.²¹ Hydrogen peroxide is known to readily oxidise aminoalkylphosphonic acids to their N-oxide derivatives (Chapter 6).²²

Hydrogen peroxide is a very useful reagent in metallurgy because its decomposition products (water and oxygen) are harmless. However, one of its limitations is the tendency to decompose in the presence of transition metal ions at elevated temperatures. This can be overcome by converting hydrogen peroxide to Caro's acid, H_2SO_5 , (which is a much stronger oxidant than hydrogen peroxide) by the following reaction.¹⁹



An example from metallurgy where hydrogen peroxide is converted to Caro's acid is that of the extraction of uranium. Uranium is leached from its ores using a mixture of sulphuric acid and oxidant to convert insoluble uranium(IV) to soluble uranium(VI). Caro's acid is the most suitable oxidant to use as it combines 'environmentally friendly' by-products with being easy to use and control. Caro's acid acts by oxidising iron(II) to iron(III) which in turn oxidises uranium.¹⁹



Hydrogen peroxide is also one of the most versatile bleaching agents for paper available. Some of its many advantages are: ease of application, potential for reducing process times, minimisation of effluent problems, produces paper of a high and stable degree of whiteness, preservation of fibre quality, and harmless decomposition products *i.e.* water and oxygen.^{13,14}

There are several areas in which hydrogen peroxide can assist environmental protection in water and effluent treatment. Since its own decomposition products are water and oxygen, it is not itself a source of pollution. Injection of hydrogen peroxide in the sewers can both eliminate any hydrogen sulphide present and maintain aerobic conditions which will prevent any further hydrogen sulphide being produced. Hydrogen peroxide also provides an effective way of treating certain toxic industrial pollutants such as cyanides, phenols, nitrites and sulphides.²¹

1.2.2 Stability of hydrogen peroxide

Hydrogen peroxide when first produced is very pure and the decomposition rate is very slow.²¹ However, if the hydrogen peroxide is contaminated with low levels of metal ions (e.g. a few parts per million) such as iron, copper, chromium, nickel, or other metals from the platinum group, then fast decomposition to water and oxygen occurs.²¹ This is known as homogeneous decomposition and the most active catalysts are those giving rise to multi-valent ions. In addition, the solution pH also affects the rate of decomposition. Fast decomposition may also occur if hydrogen peroxide is brought into contact with insoluble solids; this is known as heterogeneous decomposition. Hydrogen peroxide will decompose to some extent on any surface

even at normal temperatures, although the rate will vary according to the nature and state of the surface. For example, the rate of decomposition on silver is 10 times faster than that on polyethylene, which is one of the common storage materials. Some of the solids which catalyse the decomposition of hydrogen peroxide are the hydroxides and oxides of the heavy metals, the most active being iron, gold, lead, cobalt, silver and mercury. These are most active when their surface area is large, as with colloids and powdered metals.²¹

Most manufacturers of hydrogen peroxide add stabilisers to keep decomposition to a minimum. Two types of stabilisers are in current use: a) complexing agents, e.g. aminocarboxylic acids and alkylaminomethylenephosphonic acids and b) colloidal. It is believed that these stabilisers can either 'neutralise' small amounts of catalysts or adsorb/absorb impurities.²¹

Pure hydrogen peroxide of any concentration, in the absence of contaminating catalysts in a thoroughly clean container of non-catalytic material, is a very stable substance. For example, data obtained with high quality unstabilised hydrogen peroxide in a container indicates the decomposition rate of 90 % hydrogen peroxide at 50 °C as not in excess of 0.0010 % per hour. In the presence of a small quantity of stabiliser, such as sodium stannate, this figure may fall to approximately to 0.0003 % per hour at 50 °C.²¹

If hydrogen peroxide could be prepared and kept in the total absence of catalytically active materials, no stabilisers would be needed to enhance storage for long periods at normal temperatures without noticeable loss by decomposition. Therefore, pure hydrogen peroxide is commercially available in a form nearly free of stabilisers, and it may also be transported and stored safely in aluminum tanks.²¹

In general terms, the stabilisation process, apart from control of the pH and temperature of the hydrogen peroxide solution, consists of deactivating catalytically active substances which may be present, either dissolved or suspended in the solution, or in the walls of the container. Sodium stannate, $\text{Na}_2\text{SnO}_3 \cdot 3\text{H}_2\text{O}$, forms colloidal hydrous stannic oxide on hydrolysis, which may adsorb ferric ions and hence improve the stability of the hydrogen peroxide solutions.^{21,23}

There is also an optimum pH at which sodium stannate is most effective *i.e.* between pH 3.5 and 6. However, if sodium stannate is added in excess, the hydrolysis of sodium stannate increases the pH of the hydrogen peroxide to a point which may result in a reduction of its stability. In hydrogen peroxide, hydrous stannic oxide is present as a negatively charged colloid which may coagulate and 'neutralise' positive metal ions.²¹

1.3 Equilibrium analysis

1.3.1 Nomenclature of metal complexes

A 'complex' may be defined as a species formed by the association of two or more simpler species, each capable of independent existence.²⁴ The central atom, or nucleus is usually a Lewis acid (electron acceptor, *e.g.* a metal) and this is surrounded by a number of ligands (electron donors, Lewis bases).²⁵

A ligand is said to be multidentate if it contains more than one electron donating atom used to coordinate to metal ions. Many multidentate ligands can also form chelate complexes which have a higher degree of stability than the corresponding straight chain analogs.²⁶ The term 'chelation' was first used by Morgan and Drew and the word is derived from the Greek meaning "claw".²⁶ Ligands may be bound to metal ions by one, two, or three or more donor atoms. Such ligands can be classified as *mono-*, *bis-*, *trisidentate* and so on (*dentis* meaning tooth).

1.3.2 Equilibrium constants and mass-balance equations

Bronsted (1923) defined an acid as any substance that can ionize in solution to give a solvated hydrogen ion (*i.e.* a proton stabilised by interaction with the solvent or a substance in solution).²⁷ Conversely, a base is a substance which accepts a proton. Thus, the proton donor (acid) and proton acceptor (base) are known as conjugate acid-base pairs. Here the proton is shared



between the two bases and the equilibrium is determined by the relative strengths of the acids.

The law of mass action was developed by Guldberg and Waage and is sometimes

known as the *law of chemical equilibrium*.²⁸ It states that the velocity of a chemical reaction is proportional to the product of active masses of the reacting substances. Applying the law of mass action to homogenous systems (*i.e.* in which all the molecules are present in one phase) a mathematical expression can be determined for the reversible reaction of Equation 1.3.1:²⁸

$$K_c = \frac{[A_2][B_1]}{[A_1][B_2]} \quad \text{Equation 1.3.2}$$

where the square brackets [] represent the concentrations of the species and K_c is the stoichiometric equilibrium constant. Therefore, an equilibrium constant is a quotient involving the concentration or activities of reacting species in solution at equilibrium.²⁵ At constant temperature and pressure the



free energy change (ΔG) for the Equation 1.3.3 must be zero, and the expression for the thermodynamic equilibrium constant (K_t) is:

$$K_t = \frac{\{C\}^c \{D\}^d}{\{A\}^a \{B\}^b} \quad \text{Equation 1.3.4}$$

where {A} represents the activity of the species A and the thermodynamic equilibrium constant (K_t) is independent of concentrations.²⁵ The activity (a_i) of the *i*th component is related to the concentration (c_i) of the component:

$$a_i = c_i \gamma_i$$

where γ_i is the activity coefficient of the component (*i*). Therefore, the thermodynamic equilibrium constant K_t can also be written in terms of activity coefficient and concentration:

$$K_t = \frac{[C]^c [D]^d}{[A]^a [B]^b} \times \frac{y_C^c y_D^d}{y_A^a y_B^b} \quad \text{Equation 1.3.5}$$

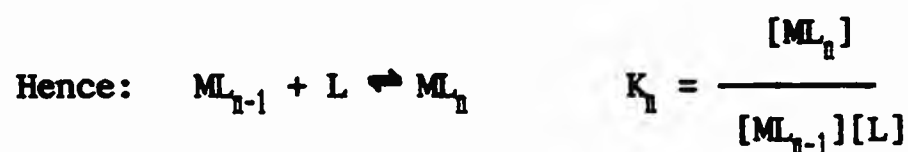
where [A] indicates the concentration, and y_A is the activity coefficient, of

the species A. The activity coefficient (γ) varies with the concentration and as infinite dilution approaches, the activity (a) becomes equal to the concentration ($\gamma = 1$) for weak electrolytes and hence the stoichiometric equilibrium concentration constant (K_c) becomes numerically equal to the thermodynamic constant (K_t). Therefore, for determining the stoichiometric equilibrium constant (K_c), the activity coefficient (γ) must also be constant. One way to, achieve this is to use an ionic medium of high concentration, consisting of ions that are expected not to interfere with the reactions occurring in solution. The ionic strength (I) of the ionic medium is the measure of the electrical field in solution:

$$I = \frac{1}{2} \sum c_i z_i^2$$

where c_i is the concentration of the ion, i , and z_i its charge.

In an *aqueous* solution containing aquated metal ions (M) and unidentate ligands (L) and where only soluble mononuclear complexes are formed, the system at equilibrium may be described by the following equations.²⁸



Hence, β_n (the overall stability constant) is expressed by the following equations.²⁸





Hence:
$$\beta_n = \prod_{i=1}^{i=n} K_i = K_1 K_2 K_3 \dots K_n \quad \text{Equation 1.3.6}$$

In the above equilibria it is assumed that no polynuclear species or insoluble products are formed. The overall stability constant (β) for the complex $[M_p L_q H_r]$ formed according to Equation 1.3.7 is:^{25,28}

$$\beta = \frac{[M_p L_q H_r]}{[M]^p [L]^q [H]^r}$$



This equilibrium condition, together with the mass balance conditions for the three components (metal, M, ligand, L, and proton, H), gives rise to the following mass-balance equations:²⁵

$$[M]_{\text{tot}} = [M] \sum_{p=1}^P \sum_{q=1}^Q \sum_{r=1}^R p [M_p L_q H_r] = m + \sum_{p=1}^P \sum_{q=1}^Q \sum_{r=1}^R p \beta_{pqr} m^p l^q h^r$$

$$[L]_{\text{tot}} = [L] \sum_{p=1}^P \sum_{q=1}^Q \sum_{r=1}^R q [M_p L_q H_r] = l + \sum_{p=1}^P \sum_{q=1}^Q \sum_{r=1}^R q \beta_{pqr} m^p l^q h^r$$

$$[H]_{\text{tot}} = [H] \sum_{p=1}^P \sum_{q=1}^Q \sum_{r=1}^R r [M_p L_q H_r] = h + \sum_{p=1}^P \sum_{q=1}^Q \sum_{r=1}^R r \beta_{pqr} m^p l^q h^r$$

where m , l and h are the 'free' concentrations of the components M, L and H. P, Q and R are the maximum values for p , q and r under the experimental conditions used. It was assumed that in the law of mass action, that the

effective concentrations of the components can be expressed by the stoichiometric concentrations.²⁸ However, this is not true: the equilibrium constant (K_i) which represents the components in terms of activities is the true thermodynamic equilibrium constant.²⁷

1.3.3 Determination of stability constants by potentiometry

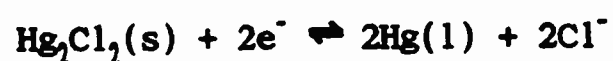
Potentiometry is one of the most convenient and successful techniques used for measuring the extent of metal complexation (equilibrium/stability constants).²⁹ Some workers use specific ion selective electrodes for measuring metal ion concentrations, but it is usually sufficient to use an accurate glass electrode for measuring the hydrogen ion $[H^+]$ concentration.²⁹

To determine the concentration of an analyte, an indicating electrode is used in conjunction with a reference electrode (by convention the reference electrode is always treated as the anode).³⁰ The potential of the reference electrode is independent of the concentration of the analyte or any other ions in the solution under study.³⁰

In present work, the reference electrode was a saturated calomel electrode (Section 2.3) and the indicating electrode is a silver/silver chloride internal reference electrode built into a glass electrode (which has been assigned to measure hydrogen ion concentration). The calomel electrode can be represented by the following half-cell formula. The electrode potential



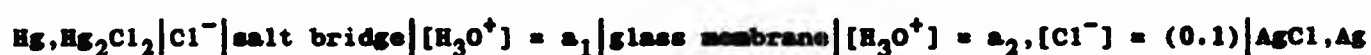
for the calomel electrode is based upon the half-cell reaction.



The electrode system has a salt bridge with a glass sinter that provides an electrical contact between the calomel electrode and the solution under examination. The indicator (glass) electrode consists of a thin, pH-sensitive glass membrane sealed onto a heavy glass tube. A small volume of dilute hydrochloric acid saturated with silver chloride is contained in the tube. A silver wire in this solution forms an internal silver/silver chloride reference electrode. The half-cell reaction for the indicator (glass) electrode is.



Therefore, in the present work, the entire electrode system can be summarised as follows.



The electromotive force of the whole electrode system (E) is given by the following equation:

$$E = E_{\text{right}} - E_{\text{left}}$$

where E_{right} is the half-cell reaction for the glass electrode and E_{left} is the half-cell for the calomel electrode. Experimentally, E can be further resolved into its components.

$$E = E(\text{Ag}|\text{AgCl}) + E(\text{Hg}|\text{Hg}_2\text{Cl}_2) + E_j + E_{\text{asym}} + E_b$$

where E_j is the junction potential of the salt bridge, E_{asym} is the asymmetry potential of the glass electrode and E_b the boundary potential of the glass electrode. The junction potential is caused by the unequal distribution of cations and anions across the membrane of the salt bridge and is due to differences in the rates at which the various ions diffuse across the membrane resulting in a separation of charges. The boundary potential (E_b) of the glass membrane is related to the hydrogen ion activities of the solutions in contact with each of the glass membrane and is made up from the potentials (V_2 and V_1). The boundary potential is responsible for the sensitivity of the glass electrode to hydrogen ions [H^+].

The asymmetry potential is caused by differences in the manufacture of the glass membrane in the glass electrode and to mechanical abrasion. In order to reduce this error, all membrane electrodes should be calibrated at least once a day or when in heavy use³⁰, e.g. calibration (under the standard conditions) using either standard pH buffers (NBS Standard) or standardised alkali and acid.³¹

The relation by which E (emf) is related to the hydrogen ion concentration was developed by Nernst:

$$E = E_0 - \frac{RT \log [H^+]}{nF}$$

where E_0 is the standard potential, E is the measured potential, R is the gas constant, T the absolute temperature, F is Faraday's constant and n is the number of electrons involved in the equilibrium.

In the present work, the electrode system is calibrated at least once a day and this involves titration of standardised base against nitric acid (Section 2.3). The calibration titration involves the programs S.SCMTITR³² and S.SCMCAL³². The program S.SCMTITR initiates and controls the calibration titration from start to finish and also asks for input certain parameters (Section 2.3). The calibration titration uses fixed increments of base which are used in the calculation of the end-point. At the end of the titration the program S.SCMCAL, is automatically run to calculate both E_0 and pK_a from the titration data obtained. The program S.SCMCAL reads in data from the calibration titration, including the number of points used in the titration, the concentration of base, the volume of acid and the ionic strength. With this data, S.SCMCAL, determines the end-point from the second derivative of the mV vs volume of base curve, i.e. $d^2(\text{mV})/d(\text{vol})^2$ vs volume.

The program S.SCMCAL then calculates E_0 at each successive data point and this is averaged with the previous running average until E_0 for a data point differs by more than 1 mV (normally E_0 is calculated from the first 30-40 data points). The constant pK_a is also calculated using the S.SCMCAL program from the data in basic solution. Both the values of E_0 and pK_a are saved to data disc which are read into each sample titration data set. The titration data obtained for a ligand on its own, or with a metal, is transferred to the VAX mainframe computer (along with the values for E_0 , pK_a , temperature, initial concentrations of base, ligand, acid, ionic strength) and the SUPERQUAD³³ program is used to calculate the stability constants of the system under examination (Section 1.3.5).

1.3.4 Stability constants

Stability (equilibrium) constants have been widely used as an effective measure of the affinity of a ligand for a metal cation in solution. Early workers such as Bodlander and von Euler developed the quantitative determination of overall formation constants.²⁹ Bjerrum was the first to

measure the stepwise stability constants for monodentate ligands on the formation of transition metal-ammonia complexes in aqueous solution. This early work began the interest in determining stability constants.³⁴

In recent years, the measurement of stability constants has been made more important by the increased interest in several areas; e.g. the development of macrocyclic complexes, and development of synthetic designs for new and better complexing ligand systems for medicinal and industrial use.

1.3.5 Computational methods for the determination of stability constants

Before computers and computer programs were used to determine stability constants, graphical analysis was used. Rossotti and Rossotti²⁴ have published one of the complete guides on graphical analysis used to determine stability constants.

For example, Sillen *et al.* wrote Pit-Mapping,³⁵ one of the first computer programs reported for the determination of stability constants (1961). Many computer programs for the determination of stability constants³⁶ have now been developed by independent research groups, including; LETAGROP,³⁷ MINIQUAD,³⁸ MAGEC,³⁹ BEST,⁴⁰ ACBA⁴¹ and more recently (in 1985) the SUPERQUAD³³ program used in this work.

1.3.6 SUPERQUAD; a general program for stability constant calculation

Developed by Gans *et al.*, SUPERQUAD³³ is a FORTRAN 77 program widely used for the determination of stability constants. The program uses a minimisation of an error-squared sum based on the measured electrode potentials (this is the refinement algorithm):

$$\sigma^2 = \sigma_E^2 + (\partial E / \partial V) \sigma_V^2$$

where σ^2 is the calculated variance of the measurement, σ_E^2 and σ_V^2 are the estimated variances of the electrode and volume readings taken individually and $\partial E / \partial V$ is the slope of the titration curve. The unknown quantities [M], [L], and [H] are found by solving the three non-linear mass balance equations in these three unknowns (different at each titration point) by iteration. The data consists of values of volume and electrode potential, v_i , E_i at each data point. Each pair of data also carries a 'flag' to include it (1), or exclude it (-1), or to hold it constant (0) during the refinement. Estimates of some

parameters are also needed and in some cases these need to be fairly good estimates for the minimisation to be successful.⁴²

Refinement of the data involves selecting a model for the equilibria that may be occurring in solution (based on other results). Along with the model (*i.e.* for a metal:ligand ratio of 1:1, the following species may be refined: 110, 111, 112 and so on), estimates for values of $\log \beta$ for each process for the formation of the species is also placed into the SUPERQUAD³³ files. Once a model has been selected, the data points are 'cut-back' to the region in the titration curve where these species may be formed. The calculation in the SUPERQUAD³³ program involves an iterative process to fit the calculated curve (for the model selected) as closely as possible to the experimental curve. The best fit model is taken as the one with a low sample standard deviation (s or σ), χ^2 less than 12.60 (based on weighted residuals) and no ill-defined formation constants. The procedure is repeated until a best-fit model is found for describing the system being examined.

1.3.7 Thermodynamic stability of metal complexes

The main factors affecting the thermodynamic stability of transition metal complexes are shown below.²⁶ These metal cations have also been categorised as belonging to one of three main groups (Table 1.1.1).

Class A metal ions are 'hard' acids; having a high charge and being small ions they also have a low polarisability. Class B metal ions are 'soft' acids; with low oxidation states and large atoms, they are easy to polarise. Hard class 'A' metal ions form their most stable complexes with ligands containing hard donors (bases) such as those with oxygen and N donor atoms. Soft class 'B' metal ions form their most stable complexes with soft donors, *e.g.* ligands containing sulphur or phosphorus donor atoms. This is known as Pearson's Hard and Soft Acid Base (HSAB) theory.²⁶

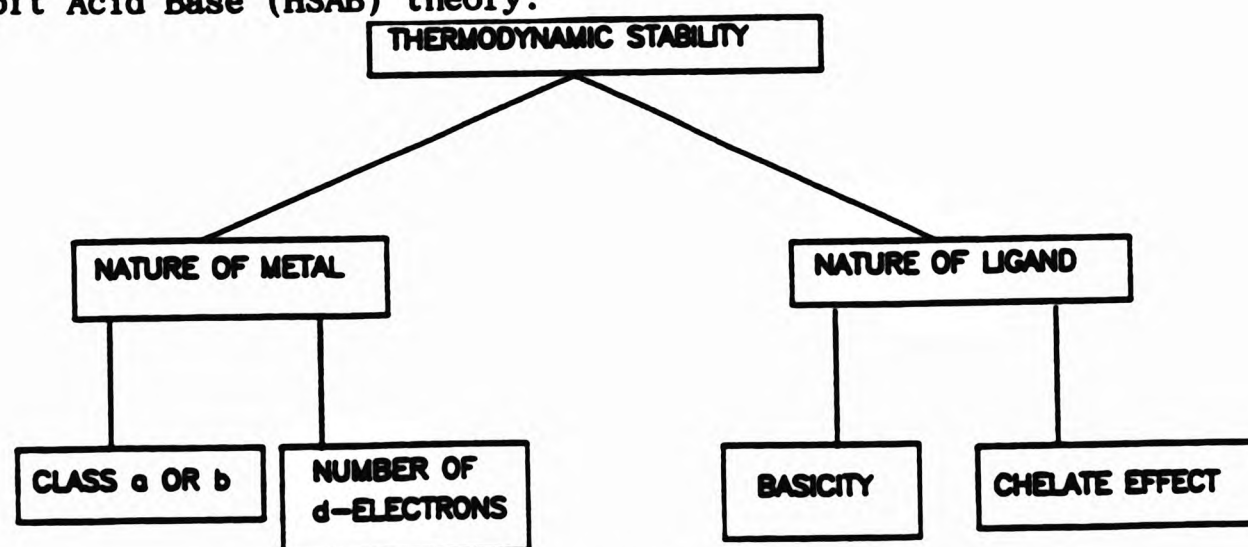


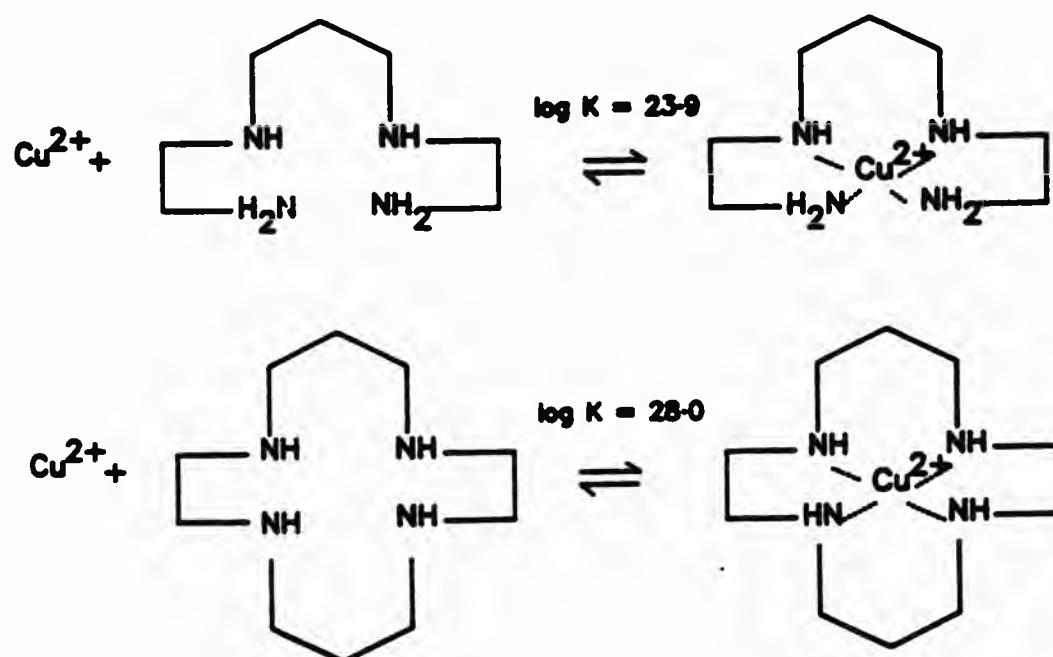
Table 1.3.1 The three classes of metal ions.²⁶

CLASS A	BORDERLINE	CLASS B
H ⁺ Li ⁺ Na ⁺ K ⁺ Be ²⁺ Mg ²⁺ Ca ²⁺ Sr ²⁺	Fe ²⁺ Co ²⁺	Cu ⁺ Ag ⁺ Au ⁺ Tl ⁺
Mn ²⁺ Al ³⁺ Sc ³⁺ Ga ³⁺ In ³⁺ La ³⁺ Fe ³⁺	Ni ²⁺ Cu ²⁺	Hg ²⁺ Pd ²⁺ Pt ²⁺
Cr ³⁺ Co ³⁺ Ti ⁴⁺ Sn ⁴⁺	Zn ²⁺ Pb ²⁺	Pt ⁴⁺ Tl ³⁺

However, some metal ions frequently form complexes whose stabilities cannot be predicted on the basis of the HSAB theory and these are therefore placed into the borderline class. The stabilities of complexes of the first row transition metal ions (+2) in the borderline class with a given ligand are almost invariably in the order: Mn(II) < Fe(II) < Co(II) < Ni(II) < Cu(II) > Zn(II). This is known as the Irving-Williams series.^{26,43}

The 'chelate effect' was first used as early as 1952 by Schwarzenbach.⁴⁴ The 'chelate effect' refers to the enhanced stability of a system containing chelate rings as compared to an almost similar system in which there are fewer, or no chelate rings.²⁶

Therefore, complexes of chelating ligands are in general more stable thermodynamically than those with an equivalent number of monodentate ligands.²⁶ The size of the chelate ring also influences the stability of the complex formed. As a rule five-membered rings are more stable than six-membered rings which in turn are more stable than seven-membered rings.²⁶ Also the greater the



number of chelate rings in the resulting complex, the greater the stability

of the complex formed.²⁶ Previous workers have experimented with various chelate compounds and come to the conclusion that the 'chelate effect' is due to both entropy and enthalpy factors.⁴⁴

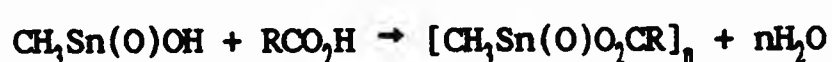
The complexing ability of aminoalkylphosphonic acids, and especially polyaminomethylenephosphonic acids, have been widely studied by potentiometry e.g. ref. 45. Potentiometric titrations are the most widely used method for investigating the solution chemistry of these ligands, and result in determination of the stoichiometries of the species in solution and calculation of their stability constants.⁴⁶

1.4 Organotin cluster chemistry

1.4.1 Synthesis

In the last ten years, new classes of organotin cluster compounds have been prepared and investigated.⁴⁷⁻⁵⁴ These new classes are based on the bonds formed in reactions between carboxylic and/or phosphorus based acids with organostannonic acids, i.e. forming bridged carboxylate and phosphate ligands to central tin atoms.⁵⁵

One of the first workers to investigate the structure of methylstannonic acid and its derivatives was Lambourne in the early 1920's. Lambourne established the composition of organotin carboxylate compounds and proposed possible structures for these compounds resulting from the condensation reaction of methylstannonic acids with carboxylic acids.⁵⁶



where $n = 3$ or 6 and $\text{R} = \text{H}, \text{CH}_3, \text{C}_6\text{H}_5$ and CH_2Cl .⁵⁶

There was a long period when only occasional reports based on Lambourne's work were published; and there were little if no advances in structural elucidation. This inert period may be partly due to the difficulty with working with these classes of compounds;⁵⁵ e.g., using reactions such as condensation, intermediates were formed resulting in mixtures usually in the form of oils. Other side reactions may also occur which inhibit the formation of the desired pure product. Some of the products are also highly insoluble

in many organic solvents, and longer aliphatic chain lengths may be required to aid solubility and characterisation.⁵⁵ With the aid of modern nmr techniques, especially the use of the magnetically active ¹¹⁹Sn isotope, characterisation of these compounds is being made easier. X-ray structural analysis of their structures in the solid state, has also clarified their compositions.⁵⁵

1.4.2 Drum and ladder organotin clusters based on carboxylic acids

During the purification of triphenyltin cyclohexanecarboxylate in 1985, Chandrasekhar noticed a small amount of crystalline material forming.⁴⁷ Following X-ray structural analysis, this crystalline material was shown to have the composition of $[\text{PhSn}(\text{O})\text{O}_2\text{CC}_6\text{H}_{11}]_6$ and occupy a 'drum' arrangement.⁴⁷

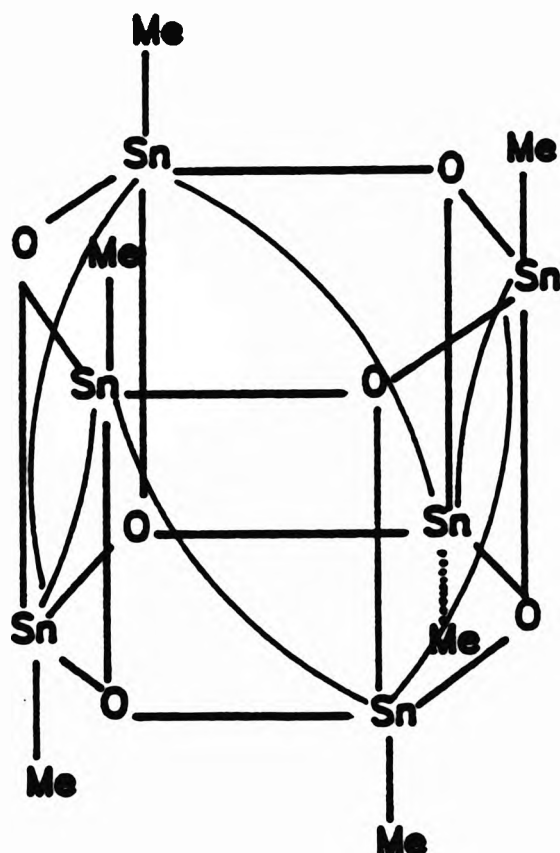
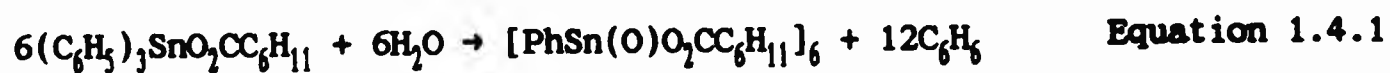


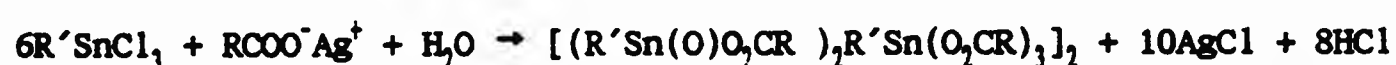
Figure 1.4.1 Schematic diagram of a 'drum' structure.

The six tin atoms are chemically equivalent and are in an octahedral arrangement. This established a new structural class for tin. The hydrolysis reaction (Equation 1.4.1) for synthesising $[\text{PhSn}(\text{O})\text{O}_2\text{CC}_6\text{H}_{11}]_6$ involved phenyl-tin bond cleavage.⁴⁷



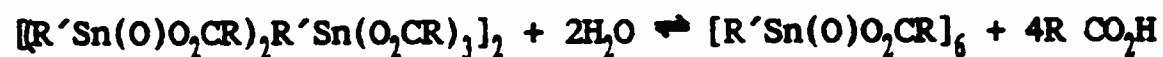
Other drum derivatives could also be formed more directly by the condensation

of an organostannonic acid with a carboxylic acid.^{48,49} An analogous condensation reaction was also carried out by Lambourne to produce a different composition e.g. $[(R'Sn(O)OCR)_2R'Sn(O_2CR)_3]_2$ where $R' = Me$ and $R = C_6H_{11}$.⁵⁶ This type of organotinocarboxylate can also be obtained by the reaction of the alkyltin trichloride with the silver salt of the carboxylic acid ($R' = n-Bu$ and $R = C_6H_{11}, C_6H_5$ and CH_3 ^{48,49}).



Subsequent X-ray structural analysis showed these products to have a 'open-drum' or 'ladder' composition (Figure 1.4.2).^{48,49} Retention of the 'drum' and 'ladder' structures of these compounds in solution was supported from ¹¹⁹Sn nmr spectroscopy;⁴⁸⁻⁵⁰ for the 'drum' structure a single resonance was observed and for the 'ladder' form three resonances were observed.

Using ¹¹⁹Sn nmr spectroscopy, Chandrasekhar established that the 'drum' and 'ladder' compositions were reversibly interconverted by hydrolysis.⁴⁹



He also found that the 'drum' composition was more hydrolytically stable. However, the mechanism by which this interconversion was not fully understood.⁴⁹

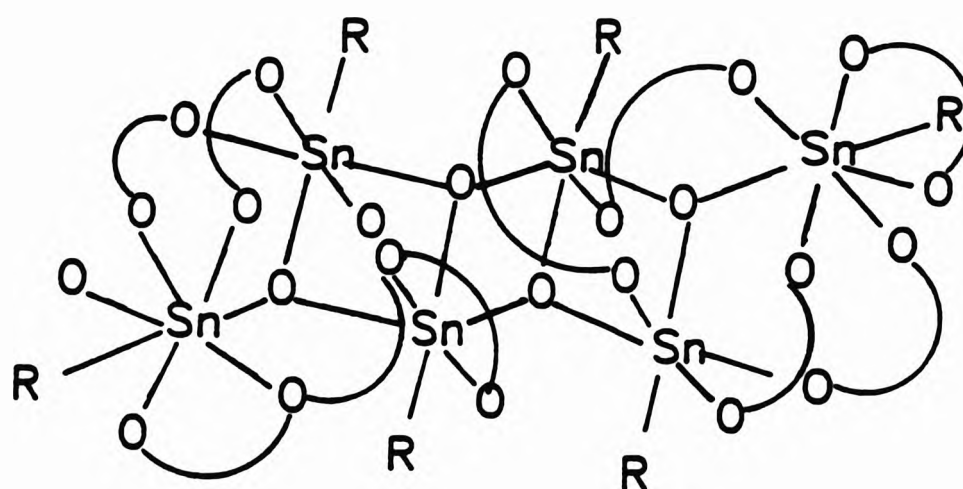
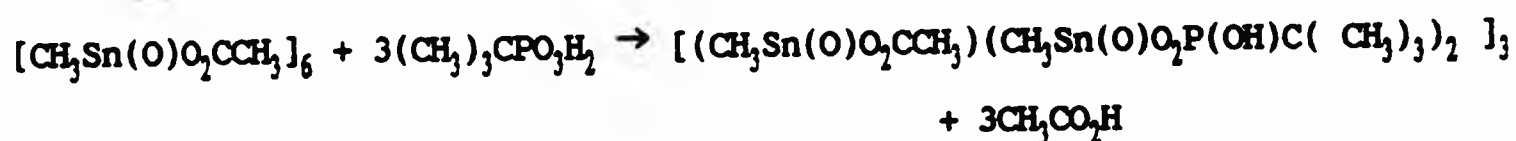


Figure 1.4.2 Schematic diagram of a 'ladder' structure.

1.4.3 Organotin clusters with phosphorus-based acids

Reaction of phosphorus-based acids with organostannonic acids instead of carboxylic acids provided a much wider variety of organotin clusters, e.g. drum⁵⁰, cube^{51,52}, butterfly⁵² and oxygen-capped cluster^{50,52,53}. The preparation of these different structural types of organotin cluster usually involves varying the stoichiometries of the reactants used in the reactions. Sometimes, a reaction may also occur by using an earlier prepared cluster (e.g. a 'drum') with a phosphorus based acid:



In 1990, yet another new structural class of organotin cluster was reported by Kumara Swamy *et al.*; the 'cage' composition.⁵⁴ Kumara Swamy *et al.* used both preparative methods described before to synthesise tetranuclear 'cages' i.e. $[(n\text{-Bu})_2\text{Sn}_2\text{O}(\text{O}_2\text{P}(\text{OH})t\text{-Bu})_4]_2$ and $[\text{Me}_2\text{Sn}_2(\text{OH})(\text{O}_2\text{P}(\text{OPh})_2)_3(\text{O}_3\text{POPh})]_2$.⁵⁴

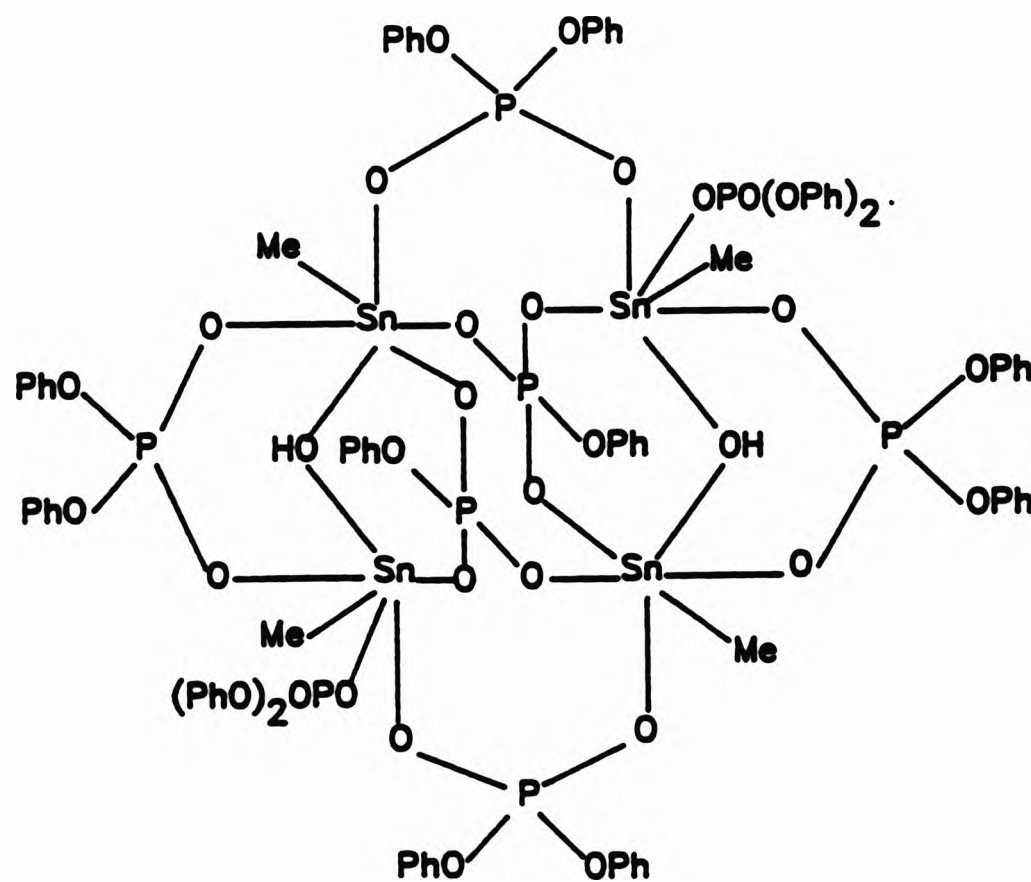


Figure 1.4.3 Schematic diagram of a cage, $[\text{Me}_2\text{Sn}_2(\text{OH})(\text{O}_2\text{P}(\text{OPh})_2)_3(\text{O}_3\text{POPh})]_2$.⁵⁴

1.5 Aims

1.5.1 Context

This project continues and extends investigations of the chemistry of alkylaminomethylenephosphonic acids and their metal complexes. These investigations have been the subject of collaboration between the University of North London and Interlox Research & Development over the last six years and aim to elucidate the role of aminomethylenephosphonic acids in the stabilisation of hydrogen peroxide. During the earlier work, the potentiometric titration apparatus necessary to measure protonation and stability constants of ligand and metal-ligand systems, respectively, was developed, tested and applied to several model α -aminomethylenephosphonic acids.⁵⁷ Protonation constants and stability constants for complexes of these ligands with a variety of metal cations were determined. Extension of potentiometric techniques to dilute hydrogen peroxide solutions of these ligands were complicated by solution instability and evidence of ligand decomposition.⁵⁸ Preliminary investigations of the effect of hydrogen peroxide on the related aminomethylenephosphonic acids using ^{13}C , ^{31}P nmr has implicated ligand oxidation in basic 35 % hydrogen peroxide solutions.⁵⁸

1.5.2 Aims of present work

On the assumption that the stabilising properties of alkylaminomethylenephosphonic acids towards hydrogen peroxide involve complex formation with metal ions, the protonation (Section 4) and complexation behaviour (Section 5) of some α -aminomethylenephosphonic acids were examined using potentiometry and nmr spectroscopy. Attempts were made to isolate the free acids (Section 4) and metal complexes (Section 5) of some α -aminomethylenephosphonic acids in crystalline form suitable for X-ray structural analysis (Section 7) in order to aid characterisation and to provide indications of the types of structure which might be adopted in solution.

In particular, (\pm)-*trans*-1,2-diaminecyclohexane *tetrakis*(methylenephosphonic) acid, CDTMPH₈, along with another polyamino *tetrakis*(methylenephosphonic) acid, has potential for stabilising solutions of hydrogen peroxide under certain conditions. Hence, detailed examination of the protonation (Section 4) and complexation behaviour (Section 5) of these two acids was carried out.

The effect of hydrogen peroxide on some aminomethylenephosphonic acids was

examined and the derivative of the reaction of hydrogen peroxide with an aminomethylenephosphonic acid isolated and characterised by nmr spectroscopy (Section 6).^{22,57} Examination of the protonation scheme of this derivative and its complexing ability with Cu(II) was carried out by potentiometry (Section 6).

The improved stability of *aqueous* solutions of hydrogen peroxide when both sodium stannate and an aminomethylenephosphonic acid are added as stabilisers was examined by the reaction of organotin compounds with an aminomethylenephosphonic acid (Section 3). The syntheses of novel clusters formed from the condensation reactions between organostannonic and phosphonic acids and more importantly, the probable reaction with aminomethylenephosphonic acids was examined. Synthesis of such compounds have been recently reported and some of these compounds have cage like geometries which also contain cavities displaying considerable flexibility, giving rise to the possibility of these compounds being involved in metal ion clathration. Therefore, synthetic and characterisation techniques for organotin and phosphonic acid clusters were developed by repeating selected syntheses from the literature and applying these to the synthesis of new compounds containing aminophosphonic acids.

1.6 References

1. M. Horiguchi and M. Kandatsu, *Nature*, 1959, 184, 901.
2. M. Horiguchi in *Analytical Chemistry of Phosphorus Compounds*, 1972, Ed. M. Halmann, Wiley-Interscience, New York.
3. M. I. Kabachnik, T. Ya. Medved', N. M. Dyatlova and M. V. Rudomino, *Russ. Chem. Revs.*, 1974, 43, 733.
4. M. I. Kabachnik, T. Ya. Medved', N. M. Dyatlova, O. G. Arkhipova and M. V. Rudomino, *Russ. Chem. Revs.*, 1968, 37, 503.
5. N. M. Dyatlova and R. P. Lastovskii, *Russ. Chem. Revs.*, 1965, 34, 1153.
6. V. P. Kukhar' and V. A. Solodenko, *Russ. Chem. Revs.*, 1987, 56, 859.
7. K. Moedritzer and R. R. Irani, *J. Org. Chem.*, 1966, 31, 1603.
8. P. B. Iveson, M. P. Lowe and J. C. Lockhart, *Polyhedron*, 1993, 12, 2313.
9. E.g. M. Hollmann, O. Rudolf and K. Haage, *Ger. (East) 144073, CA 94*, 210645f, 1985; Y. Machida, T. Yoshida, N. Kimura and M. Watanabe, *Jpn. Kokai Tokkyo Koho JP 62185797, CA 108*, 39593u, 1988; G. W. Morris, N. D. Feasy, P. A. Ferguson, D. Van Hemelnijk and M. Charlot, *PCT Int. Appl. WO 9001034, CA 113*, 6601v, 1990.
10. F. P. Tsao, *EP 265381, CA 109*, 11797k, 1988.
11. J. Kubicki and B. Purranov, *Pr. Nauk. Inst. Technol. Nieorg. Nawozow. Miner. Politech. Wroclaw*, 1987, 33, 54; *CA 108*, 154221h, 1988.
12. Y. Isomura, M. Takeuchi and S. Sakamoto, *EP 325482, CA 112*, 21140s, 1990.
13. K. Kuczynski, H. Nijs and B. H. May, *Tappi J.*, 1988, 71, 142, 171, *CA 109*, 112280s, 131082v, 1988.
14. R. D. Gillard, P. D. Newman and J. D. Collins, *Polyhedron*, 1989, 8, 2077.
15. P. J. Sadler, C. T. Harding, J. D. Kelly and A. B. McEwen, *EP 210043, CA 110*, 36204y, 1989.
16. I. K. Adzami, H. Gries, D. Johnson and M. Blau, *J. Med. Chem.*, 1989, 32, 139, *CA 110*, 36204y, 1989.
17. K. F. Kraft, S. C. Quay, S. M. Rocklage and D. Tursh, *EP 258616, CA 109*, 226271v, 1988.
18. M. J. Bloemink, J. P. Dorenbos, R. J. Heetebrij, B. K. Keppler, J. Reedijk and H. Zahn, *Inorg. Chem.*, 1994, 33, 1127.
19. N. N. Greenwood and A. Earnshaw, *Chemistry of the Elements*, 1986, Pergamon Press, Oxford.
20. S. Croft, B. C. Gilbert, J. R. L. Smith, J. K. Stell and W. R. Sanderson, *J. Chem. Soc., Perkin Trans. 2*, 1992, 153.
21. W. C. Schumb, C. N. Satterfield and R. L. Wentworth, *Hydrogen Peroxide*,

- 1955, Reinhold Publishing, New York.
22. R. P. Carter, M. M. Crutchfield and R. R. Irani, *Inorg. Chem.*, 1967, 6, 943.
 23. T. J. Lewis and T. M. Walters, *J. Appl. Chem.*, 1960, 10, 396, 403.
 24. F. J. C. Rossotti and H. Rossotti, *The Determination of Stability Constants and other Equilibrium Constants in Solution*, 1961, McGraw-Hill, New York.
 25. M. Heloun, J. Havel and E. Hogfeldt, *Computation of Solution Equilibria*, 1988, Ellis Horwood Ltd., Chichester.
 26. K. F. Purcell and J. C. Kotz, *Inorganic Chemistry*, 1985, Holt Saunders, Japan.
 27. A. Albert and E. P. Serjeant, *The Determination of Ionization Constants*, 1971, Chapman and Hall, London.
 28. J. Bassett, R. C. Denney, G. H. Jeffery and J. Mendham, *Vogels: Text book of Quantitative Inorganic Analysis, Fourth Edition*, 1987, Longman, New York.
 29. A. E. Martell and R. J. Motekaitis, *The Determination and Use of Stability Constants*, 1988, VCH Publishers, New York.
 30. D. A. Skoog, D. M. West, F. J. Holler, *Fundamentals of Analytical Chemistry*, 1988, Saunders College Publishers, New York.
 31. P. W. Linder, R. G. Torrington and D. R. Williams, *Analysis using Glass Electrodes*, 1984, Open University Press, Milton Keynes.
 32. P. L. Biggins, S. E. Edwards, T. A. Lucas, R. W. Matthews, I. J. Scowen and C. J. L. Silwood, unpublished BBC BASIC program S.SCMITR. P. L. Biggins, S. E. Edwards, T. A. Lucas and R. W. Matthews, unpublished BBC BASIC program S.SCMCAL.
 33. P. Gans, A. Sabatini and A. Vacca, *J. Chem. Soc., Dalton Trans.*, 1985, 1195.
 34. E.g. A. E. Martell and R. Smith, *Critical Stability Constants*, 1976 check.
 35. D. Dyrssen, N. Ingri and L. G. Sillen, *Acta. Chem. Scand.*, 1961, 15, 694.
 36. E.g. *Computational Methods for the Determination of Stability Constants*, Ed. D. J. Leggett, 1985, Plenum Press, New York.
 37. L. G. Sillen, *Acta. Chem. Scand.*, 1962, 16, 159.
 38. A. Sabatini, A. Vacca and P. Gans, *Talanta*, 1974, 21, 53.
 39. P. M. May, D. R. Williams, P. W. Linder and R. G. Torrington, *Talanta*, 1982, 29, 249.
 40. R. J. Motekaitis and A. E. Martell, *Can. J. Chem.*, 1982, 60, 2403.

41. G. Arena, E. Rizzarelli, S. Sammartano and C. Rigano, *Talanta*, 1979, 26, 1.
42. P. Gans, *Data Fitting in the Chemical Sciences*, 1992, John Wiley & Sons, Chichester.
43. H. Irving and R. J. P. Williams, *J. Chem. Soc.*, 1953, 3192.
44. A. E. Martell in *Werner Centennial: Advances in Chemistry Series*, 1962, 62, Ed. R. F. Gould, AMC Publishers, Washington DC.
45. E.g. E. N. Rizkalla, *Revs. Inorg. Chem.*, 1983, 5, 203.
46. R. J. Motekaitis and A. E. Martell, *J. Coord. Chem.*, 1985, 14, 139; M. S. Mohan and E. H. Abbott, *J. Coord. Chem.*, 1978, 8, 175; K. Sawada, T. Araki and T. Suzuki, *Inorg. Chem.*, 1987, 26, 1199; I. Ya. Polyakova, A. Ya. Fridman, N. M. Dyatlova, *Koord. Khim.*, 1987, 13, 147; T. Kiss, J. Balla, G. Nagy, H. Kozlowski and J. Kowalik, *Inorg. Chim. Acta.*, 1987, 138, 25; M. I. Kabachnik, V. G. Dasheveskii, T. Ya. Medved and A. P. Baranov, *Teor. Eksp. Khim.*, 1985, 21, 660, CA 104, 76131e, 1986.
47. V. Chandrasekhar, R. O. Day and R. R. Holmes, *Inorg. Chem.*, 1985, 24, 1970.
48. R. R. Holmes, C. G. Schmid, V. Chandrasekhar, R. O. Day and J. M. Holmes, *J. Am. Chem. Soc.*, 1987, 109, 1408.
49. V. Chandrasekhar, C. G. Schmid, S. D. Burton, J. M. Holmes, R. O. Day and R. R. Holmes, *Inorg. Chem.*, 1987, 26, 1050.
50. R. O. Day, V. Chandrasekhar, K. C. Kumara Swamy, J. M. Holmes, S. D. Burton and R. R. Holmes, *Inorg. Chem.*, 1988, 27, 2887.
51. K. C. Kumara Swamy, R. O. Day and R. R. Holmes, *J. Am. Chem. Soc.*, 1987, 109, 5546.
52. R. R. Holmes, K. C. Kumara Swamy, C. G. Schmid and R. O. Day, *J. Am. Chem. Soc.*, 1988, 110, 7060.
53. R. O. Day, J. M. Holmes, V. Chandrasekhar and R. R. Holmes, *J. Am. Chem. Soc.*, 1987, 109, 940.
54. K. C. Kumara Swamy, C. G. Schmid, R. O. Day and R. R. Holmes, *J. Am. Chem. Soc.*, 1990, 112, 223.
55. R. R. Holmes, *Acc. Chem. Res.*, 1989, 22, 190.
56. H. Lambourne, *J. Chem. Soc.*, 1922, 2533; 1924, 2013.
57. P. Biggins, S. E. Edwards, T. Lucas, R. W. Matthews, G. Morris, I. J. Scowen and C. J. L. Silwood, unpublished results.
58. I. J. Scowen, Ph.D Thesis, University of North London, 1993.

Chapter 2 Experimental Methods

2.1 Synthesis of alkyl/aryl stannonic acids and their cluster derivatives

2.1.1 Starting materials and solvents

Origins and purities of reagents used in syntheses of organotin compounds are given in Table 2.1.1. General purpose grade solvents were used without further purification except for GPR grade toluene which was dried over sodium wire before use.

Table 2.1.1 Origin and purity of reagents used in syntheses of organotin compounds.

Compound	Source	Purity ^a
Tin(II) chloride	Hopkin & Williams	99 %
Potassium hydroxide (pellets)	Aldrich	> 85 %
Diphenylphosphate	Lancaster	99 %
Benzoic acid	Aldrich	99 %
Styrene phosphonic acid ^b	Albright & Wilson	
<i>n</i> -Butyltin trichloride	Aldrich	95 %
Phenyltin trichloride	Aldrich	98 %
Phenylphosphonic acid	Aldrich	98 %
<i>t</i> -Butylphosphonic acid	Aldrich	98 %
Hippuric acid	BDH	99 %
Methyliodide	Aldrich	99.5 %

^a Manufacturer's estimate. ^b Micro analysis: calc. for C₉H₉O₃P: C, 45.7; H, 4.9 %. Found: C, 46.7; H, 5.0 %. ¹H NMR (CD₃OD): δ/ppm 6.47 [approx. t, 1H, ²J(HP) = 17.7 Hz]; 7.30-7.53 (m's, 6H). ¹³C NMR (CD₃OD): δ/ppm 118.28 [d, CH-P, ¹J(CP) = 187.8 Hz]; 128.49, 129.87, 130.90 (all aromatic carbons); 136.55 [d, CH=CH-P, ²J(CP) = 22.9 Hz]; 146.68 [d, aryl C-CH, ³J(CP) = 5.9 Hz].

2.1.2 Preparation of methylstannonic acid, [CH₃SnO₂H]

The method described by Lambourne was used.¹ Potassium hydroxide (KOH) pellets (25.0 g, 0.45 mol) were dissolved in water (100 cm³) and the solution was slowly added, with stirring, to a freshly prepared solution of tin(II) chloride (10.5 g, 0.06 mol) in water (25 cm³) at 0 °C. On addition of potassium hydroxide the solution turned cloudy. When nearly all the potassium hydroxide had been added, the grey precipitate which had initially formed turned black; this was taken as a sign of completion of the reaction. The

mixture was filtered and methyl iodide (5.0 g, 0.4 mol) was then added to the filtrate, resulting in two layers. Sufficient methanol (350 cm³) was then added to make the mixture homogeneous. Carbon dioxide, generated by slow addition of spirit (IMS 99) to solid carbon dioxide, was bubbled through the solution for three days. A heavy, white, crystalline precipitate of potassium methylstannoyl carbonate formed. This precipitate was filtered off and then decomposed by boiling with water to produce methylstannonic acid. The white, amorphous solid (methylstannonic acid) was filtered off and dried in a vacuum desiccator over conc. sulphuric acid.

Yield: 1.3 g (23 %). M.p., 313.4–323.8 °C.

Micro analysis: calculated for CH₃O₂Sn: C, 7.2; H, 2.4 %. Found: C, 7.3; H, 2.5 %.

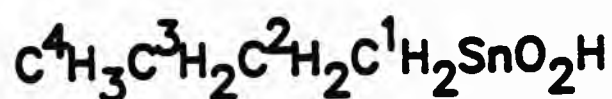
IR (16 mm KBr disc): $\bar{\nu}_{\text{max}}/\text{cm}^{-1}$ ca. 3500br (OH); 3000–2920w (CH₃); 1390w (CH₃); 1200m (OH); 720 (CH₃ rock); 640br (Sn–O).

¹H NMR (CF₃CO₂D): δ/ppm 1.47 [s, CH₃, ²J(H–¹¹⁹Sn) = 143.9 Hz, ²J(H–¹¹⁷Sn) = 138.5 Hz].

¹³C NMR (CF₃CO₂D): δ/ppm 9.4 (CH₃).

2.1.3 Preparation of *n*-butylstannonic acid, [CH₃(CH₂)₃SnO₂H]

The method described by Davies *et al.* was used.² Aqueous ammonia (3 mol dm⁻³) was added dropwise to a solution of *n*-butyltin trichloride (7.0 g, 0.025 mol) in water (40 cm³). On addition of the aqu. ammonia (while stirring), a white precipitate formed and the temperature of the solution rose from 25 to 35 °C. The solution was allowed to cool and further aqu. ammonia was added until precipitation had ceased. The precipitate was collected by filtration and washed with boiling water until free from chloride. The product was dried in a vacuum desiccator over conc. sulphuric acid.



Yield: 4.4 g (85 %). M.p., 270–303 °C decomposed.

Micro analysis: calculated for C₄H₁₀O₂Sn: C, 23.0; H, 4.8 %. Found: C, 23.2; H, 5.0 %.

IR (16 mm KBr disc): $\bar{\nu}_{\text{max}}/\text{cm}^{-1}$ ca. 3500br (OH); 2956, 2925, 2858m (CH₃); 1462m (CH₂); 688; 620br (Sn–O); 540br.

¹H NMR (CF₃CO₂D): δ/ppm 1.01 [H⁴, t, ³J(HH) = 7.3 Hz]; 1.51 [H³, approx. sextet,

$^3\text{J}(\text{HH}) \approx 7.4 \text{ Hz}$]; 1.91 [H^2 , approx. quintet, $^3\text{J}(\text{HH}) \approx 7.3 \text{ Hz}$]; 2.29 [H^1 , t, $^3\text{J}(\text{HH}) = 8.0 \text{ Hz}$, $^2\text{J}(\text{H}-^{117/119}\text{Sn}) \approx 135 \text{ Hz}$].

$^{13}\text{C NMR}$ ($\text{CF}_3\text{CO}_2\text{D}$): δ/ppm 13.8 (C^A); 26.8, 28.3, 33.3 (C^1 , C^2 , C^3).

2.1.4 Preparation of the hydrochloride salt of phenylstannonic acid, [$\text{C}_6\text{H}_5\text{SnO}_2\text{H}$].HCl

The method used was based on that described by Davies *et al.*² To a solution of phenyltin trichloride (10.0 g, 0.033 mol) in water (160 cm^3), *aqu. ammonia* (3 mol dm^{-3}) was added. The solution turned cloudy and a white precipitate formed. The precipitate was collected, washed with water and dried over conc. sulphuric acid in a vacuum desiccator.

Yield: 6.1 g (69 %). M.p., > 250 °C decomposed.

Micro analysis: calculated for $\text{C}_6\text{H}_5\text{O}_2\text{Sn.HCl}$: C, 27.2; H, 2.7 % Found: C, 27.1; H, 2.8 %.

2.1.5 Preparation of hexameric methyloxotin acetate, [$\text{CH}_3\text{Sn}(\text{O})\text{O}_2\text{CCH}_3$]₆

The method described by Day *et al.* was used.³ Methylstannonic acid (3.90 g, 0.0234 mol) was dissolved in glacial acetic acid (20 cm^3 , 0.349 mol) in a 100 cm^3 round-bottomed flask, and methanol (15 cm^3) was added. The solution was heated under reflux for 6 h. Within 2 h, a white precipitate was observed. After reflux, the mixture was allowed to cool to room temperature before the white amorphous solid was collected, washed thoroughly with methanol followed by three portions of diethylether (10 cm^3) and dried in air.

Yield: 4.1 g (83 %). M.p., 300–350 °C decomposed.

Micro analysis: calculated for $\text{C}_{18}\text{H}_{36}\text{O}_{18}\text{Sn}_6$: C, 17.3; H, 2.9 %. Found: C, 17.3; H, 2.9 %.

IR (16 mm KBr disc): $\bar{\nu}_{\text{MI}}/\text{cm}^{-1}$ ca. 3400br (OH); 3000–2820w (CH_2); 1600s (COO^-); 1530s (COO^-); 1450s; 1410sh; 1350ms (CH_2); 1190m; 1050m; 1030m; 770ms (CH_2 rock); 620s (Sn–O).

The product was insufficiently soluble for the determination of nmr spectra.

2.1.6 Preparation of methyltin tris(diphenylphosphate), [$\text{CH}_3\text{Sn}(\text{O}_2\text{P}(\text{OC}_6\text{H}_5)_2)_3$]

The method described by Kumara Swamy *et al.* was used.⁴ A mixture of hexameric methyloxotin acetate (1.6 g, 0.0013 mol) and diphenylphosphate (5.7 g, 0.023 mol) was heated under reflux in toluene (100 cm^3) using a Dean-Stark trap for 7 h. The solvent was removed by rotary evaporator to yield the title

compound as a brown viscous oil.

Yield: 5.3 g (81 %).

Micro analysis: calculated for $C_{37}H_{33}O_{12}P_3Sn$: C, 50.4; H, 3.9 %. Found: C, 50.7; H, 3.8 %.

1H NMR ($CDCl_3$): δ /ppm 1.26 (s, CH_3); 6.74–7.36 (br, aromatic CH). The spectrum also showed impurities due to toluene (2.3, 7.2), acetic acid (2.0, 10.4) and further proton-containing impurities (0.2–0.9). The product was insufficiently soluble for the determination of ^{13}C nmr spectra.

2.1.7 Preparation of the cage cluster, $[(CH_3)_2Sn_2(OH)(O_2P(OC_6H_5)_2)_3(O_3POC_6H_5)]_2$
The method described by Kumara Swamy *et al.* was used.⁴ Methyltin tris(di-phenylphosphate) (3.6 g, 0.0041 mol) was dissolved in a mixture of diethyl-ether (50 cm^3) and acetonitrile (80 cm^3). Water (0.5 g, 0.028 mol) was added to the solution. Reduction of the volume of the solution by about 50 % by slow evaporation over a period of a hours yielded a white precipitate. The solution was covered with Parafilm and left at room temperature for 24 h. The product was filtered off and washed with three portions of cold acetonitrile (10 cm^3). The product was dried over silica gel.

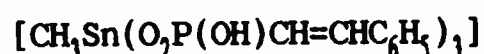
Yield: 2.4 g (96 %). M.p., 206.2–208.5 °C.

Micro analysis: calculated for $C_{38}H_{34}O_{34}P_3Sn_4$: C, 43.9; H, 3.5 %. Found: C, 44.3; H, 3.5 %.

IR (16 mm KBr disc): $\bar{\nu}_{IR}/cm^{-1}$ ca. 3430br (OH); 3069w (CH aryl); 2910w; 2851w (CH_3); 2500br (PO–H); 1593s, 1490s (C=C); 1229–1193br,s (PO); 1084–1057br,s (PO); 963s; 944s; 905sh; 779s (CH o.o.p., aryl); 754sh; 689s; 526br (Sn–O).

1H NMR ($CDCl_3$): δ /ppm 0.22 (CH_3); 0.57 (CH_3); 6.91–7.35 (m's, overlapped aromatic CH). The spectrum also showed impurities due to acetic acid (1.3), acetonitrile (1.6), toluene (7.3) and further proton-containing impurities (0.9, 9.0) arising from the starting materials. The product was insufficiently soluble for the determination of ^{13}C nmr spectra.

2.1.8 Preparation of methyltin tris(styrenephosphonate),



Hexameric methyloxotin acetate (1.00 g, 0.0008 mol), toluene (100 cm^3) and styrene phosphonic acid (2.66 g, 0.02 mol) were placed into a round-bottomed flask. The solution was heated under reflux using a Dean-Stark trap for 6 h. After 3 h, a white precipitate had formed. After reflux, the mixture was

allowed to cool to room temperature before the product was collected and washed with three portions (10 cm³ each) of toluene and diethylether. The product was dried in a vacuum desiccator over conc. sulphuric acid.

Yield: 3.0 g (92 %). M.p., 319-346 °C decomposed.

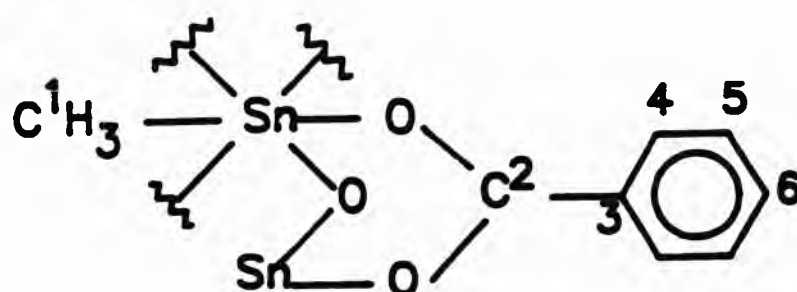
Micro analysis: calculated for C₂₅H₂₇O₉P₃Sn: C, 44.0; H, 4.0 %. Found: C, 44.7; H, 3.9 %.

IR (16 mm KBr disc): $\bar{\nu}_{\text{max}}/\text{cm}^{-1}$ ca. 3100-2800vbr,s; ca. 2320br (PO-H); 1617m (C=C); 1583m; 1497m (C=C aryl); 1438m; 1240-935vbr,s; 1150-1100br (PO); 803s; 733s (CH o.o.p., aryl); 689s; 526s (Sn-O); 514sh; 503sh.

The product was insufficiently soluble for the determination of ¹³C or ¹H nmr spectra.

2.1.9 Preparation of hexameric methyloxotin benzoate, [CH₃Sn(O)₂CC₆H₅]₆

Benzoic acid (0.73 g, 0.006 mol), toluene (100 cm³), methylstannonic acid (1.00 g, 0.006 mol) and methanol (15 cm³) were placed into a round-bottomed flask. The solution was heated under reflux using a Dean-Stark trap for ca. 6 h. A white precipitate formed during the reaction. After reflux, the precipitate was collected and washed with three portions of diethylether (10 cm³) and dried in a desiccator over silica gel.



Yield: 1.1 g (65 %). M.p., >340 °C.

Micro analysis: calculated for C₄₈H₄₈O₁₈Sn₆: C, 35.5; H, 3.0 %. Found: C, 35.3; H, 2.9 %.

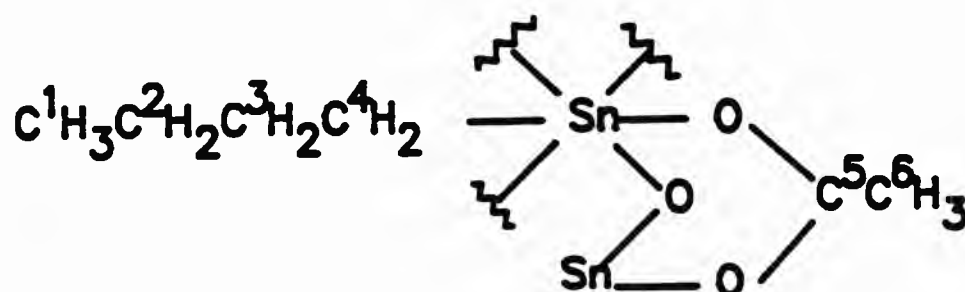
IR (16 mm KBr disc): $\bar{\nu}_{\text{max}}/\text{cm}^{-1}$ ca. 3386br (OH); 3058w; 3048w; 3023w (C-H aryl); 2933w (CH₃); 1711br; 1600s (COO⁻); 1550s (COO⁻); 1444s; 1389-950vbr,s; 833s; 806s; 706s (CH o.o.p., aryl); 678s; 633s; 567br (Sn-O); 510br; 420br.

¹H NMR (CF₃COOD): δ/ppm 1.47 [H¹, overlapped with a pair of doublets (satellites) ²J(H-¹¹⁹Sn) = 145.5 Hz, ²J(H-¹¹⁷Sn) = 140.4 Hz]; 7.52 [H⁵, approx. t, ³J(HH) \approx 7.7 Hz]; 7.71 [H⁶, t, ³J(HH) = 7.4 Hz]; 8.14 [H⁴, d, ³J(HH) = 7.4 Hz].

¹³C NMR (CF₃COOD): δ/ppm 9.7 (C¹); 129.59, 130.6, 132.3 (C³, C⁴, C⁵); 137.0 (C⁶) 176.2 (C²).

2.1.10 Preparation of $[(\text{CH}_3(\text{CH}_2)_3\text{Sn}(\text{O})\text{O}_2\text{CCH}_3)_2(\text{CH}_3(\text{CH}_2)_3\text{Sn}(\text{O}_2\text{CCH}_3)_3)]_2$ in a 'ladder' form

Methanol (15 cm³) was added to a solution of *n*-butylstannonic acid (1.0 g, 0.0048 mol) in glacial acetic acid (4.1 cm³, 0.072 mol) and the solution heated under reflux for 5 h. The mixture was left at room temperature for 3 days, after which the solvent was removed by using a rotary evaporator to yield a white crystalline solid. The product was collected by filtration, washed with three portions of water (10 cm³), acetone (10 cm³) and dried in a vacuum desiccator over conc. sulphuric acid.



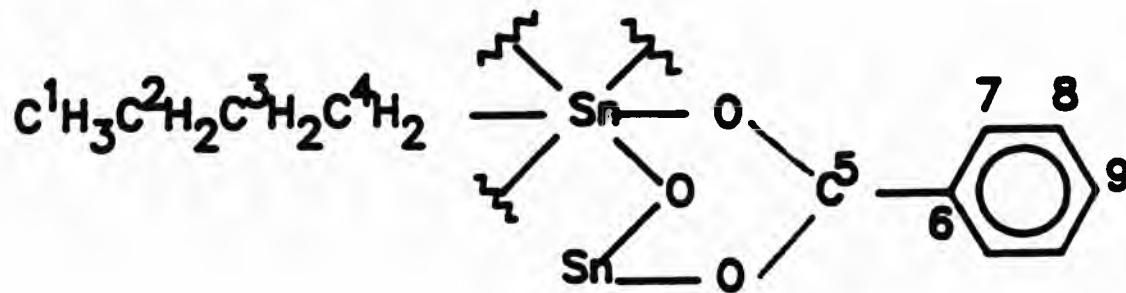
Yield: 1.5 g (65 %). M.p., 287–294 °C decomposed.

Micro analysis: calculated for $\text{C}_{44}\text{H}_{84}\text{O}_{24}\text{Sn}_6$: C, 30.9; H, 4.9 %. Found: C, 30.2; H, 4.9 %.

IR (16 mm KBr disc): $\bar{\nu}_{\text{MI}}/\text{cm}^{-1}$ ca. 3409br (OH); 2963w, 2929w, 2871w (CH_3, CH_2); 1598–1563br,s (COO^-); 1433br (COO^-); 1377sh; 1344m; 1293m; 1080w; 1022m; 664s (Sn–O); 613s; 583s; 551br,s.

¹H NMR (CDCl_3): δ/ppm 0.92 [H^1 , approx. t, $^3\text{J}(\text{HH}) \approx 7.5$ Hz]; 1.23–1.73 [$\text{H}^2, \text{H}^3, \text{H}^4$, br]; 2.09 (H^6 , s). The product was insufficiently soluble for the determination of ¹³C nmr spectra.

2.1.11 Preparation of hexameric *n*-butyloxotin benzoate, $[\text{CH}_3(\text{CH}_2)_3\text{Sn}(\text{O})\text{O}_2\text{CC}_6\text{H}_5]_6$
Benzoic acid (0.73 g, 0.006 mol), toluene (100 cm³), methanol (15 cm³) and *n*-butylstannonic acid (1.25 g, 0.006 mol) were placed into a round-bottomed flask. The solution was heated under reflux using a Dean-Stark trap for 5 h. After 3 h a white precipitate had appeared. After cooling, the precipitate was collected, washed with three portions of diethylether (5 cm³) and dried in a desiccator over silica gel.



Yield: 0.8 g (40 %). M.p., 298-315 °C decomposed.

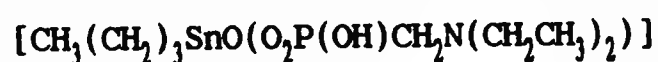
Micro analysis: calculated for $C_{66}H_{84}O_{18}Sn_6$: C, 42.2; H, 4.5 %. Found: C, 43.1; H, 4.6 %.

IR (16 mm KBr disc): $\bar{\nu}_{\text{max}}/\text{cm}^{-1}$ ca. 3409br (OH); 3073w (CH aryl); 2962w, 2860w, (CH₃, CH₂); 1597s (COO⁻); 1550-1529br,s (COO⁻); 1405s (C=C aryl); 1176m; 1068w; 1022w; 710s (CH o.o.p., aryl); 680m; 612sh; 585s (Sn-O); 533s; 502s; 466s.

¹H NMR (CF₃COOD): δ/ppm 1.01 [H¹, t, ³J(HH) = 7.3 Hz]; 1.53 [H², approx. sextet, ³J(HH) \approx 7.4 Hz]; 1.95 [H³, approx. pentet, ³J(HH) \approx 7.7 Hz]; 2.30 [H⁴, approx. t, ³J(HH) \approx 8.0 Hz]; 7.52 [H⁸, t, ³J(HH) = 7.6 Hz]; 7.70 [H⁹, t, ³J(HH) = 7.0 Hz]; 8.15 [H⁷, d, ³J(HH) = 7.5 Hz].

¹³C NMR (CF₃COOD): δ/ppm 13.83 (C¹); 26.82, 28.34, 33.45 (C², C³, C⁴); 129.60, 130.62, 132.30 (C⁶, C⁷, C⁸); 136.95 (C⁹); ca. 175.5 (C⁵).

2.1.12 Preparation of *n*-butyloxotin diethylaminomethylenephosphonate,



n-Butylstannonic acid (0.39 g, 0.0019 mol), toluene (100 cm³), diethylaminomethylenephosphonic acid (0.62 g, 0.0037 mol) and potassium hydroxide (0.1 g) were placed in a round bottomed flask and heated under reflux using a Dean-Stark trap for 5.25 h. After reflux, a small amount of crystalline material was filtered from the solution (this was thought to be un-reacted starting materials). The resulting mixture was left for 2 days at room temperature. After this time, the solvent was removed by rotary evaporator to yield a white solid. The product was washed with three portions of diethylether (10 cm³) and dried in a desiccator over silica gel.

Yield: 0.5 g (75 %). M.p., 213-238 °C decomposed.

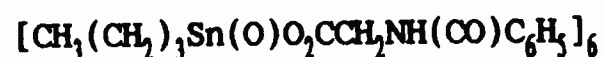
Micro analysis: calculated for $C_9H_{12}NO_4\text{PSn}$: C, 30.2; H, 6.2; N, 3.9 %. Found: C, 30.9; H, 6.8; N, 4.2 %.

IR (16 mm KBr disc): $\bar{\nu}_{\text{max}}/\text{cm}^{-1}$ 3411br (OH); 2957w, 2927w, 2864w, 2855w (CH₃ aliphatic); 1636w; 1465m (CH₂); 1091-1144br (PO); 992s (PO); 776w; 678w; 579m (Sn-O); 512m.

The ¹H nmr spectrum was very complex and could not be assigned.

¹H NMR (CD₃OD): δ/ppm 0.86-3.39 (all bands are multiplets with complex spitting patterns).

2.1.13 Preparation of hexameric *n*-butyloxotin hippurate,



n-Butylstannonic acid (1.00 g, 0.0048 mol), toluene (100 cm³), methanol

(15 cm³) and hippuric acid (Ph(CO)NHCH₂CO₂H) (0.86 g, 0.0048 mol) were placed in a round-bottomed flask. The mixture was heated under reflux for ca. 8 h using a Dean-Stark trap. After reflux, the solvent was removed to leave a clear oil, which was redissolved in diethylether. Small amounts of hexane were added, whereupon the solution turned cloudy. The solution was covered with Parafilm and left to stand at room temperature. After one hour, a white precipitate was collected by filtration (the mother liquor had turned pink) and dried in a desiccator over silica gel for 24 h.

Yield: 0.7 g (40 %). M.p., 301-307 °C decomposed.

Micro analysis: calculated for C₇₈H₁₀₂N₆O₂₄Sn₆: C, 42.2; H, 4.6; N, 3.8 %. Found: C, 42.6; H, 4.6; N; 3.5 %.

IR (16 mm KBr disc): $\bar{\nu}_{\text{max}}/\text{cm}^{-1}$ 3330s (NH); 3045w (CH aryl); 2960w, 2909w; 2873w (CH₃, CH₂); 1650s (C=O); 1601s (COO⁻); 1577s; 1547s (COO⁻); 1489m; 1432s (CH₃); 1233w; 1310s; 1078w; 1000m; 778m (CH o.o.p., aryl); 591s (Sn-O); 539s.

The product was insufficiently soluble for the determination of ¹³C or ¹H nmr spectra.

2.1.14 Preparation of hexameric phenyloxotin acetate, [C₆H₅Sn(O)O₂CCH₃]₆·C₇H₈
Glacial acetic acid (3.75 cm³, 0.0655 mol) was added to a solution of phenylstannonic acid (1.00 g, 0.0044 mol), methanol (15 cm³) and toluene (20 cm³) in a round-bottomed flask. The mixture was heated under reflux for ca. 8 h using a Dean-Stark trap. After 1.75 h, a white precipitate was observed. After reflux, the solution was left to stand for 3 days at room temperature. The product was collected by filtration and washed with three portions of diethylether (5 cm³) and dried in a desiccator over silica gel.

Yield: 0.4 g (34 %). M.p., 334.5-349.9 °C decomposed.

Micro analysis: calculated for C₃₅H₃₆O₁₈Sn₆: C, 38.5; H, 3.3 %. Found: C, 38.4; H, 3.2 %.

IR (16 mm KBr disc): $\bar{\nu}_{\text{max}}/\text{cm}^{-1}$ ca. 3409br (OH); 3080; 3050w (CH aryl); 1591s (COO⁻); 1542s (COO⁻); 1452s (CH); 736m (CH o.o.p., aryl); 698m; 620s (Sn-O); 553m; 498m; 452m.

The product was insufficiently soluble for the determination of ¹³C or ¹H nmr spectra.

2.1.15 Preparation of hexameric phenyloxotin benzoate, [C₆H₅Sn(O)O₂CC₆H₅]₆
Phenylstannonic acid (1.50 g, 0.0066 mol) in methanol (15 cm³), toluene

(100 cm³), and benzoic acid (0.80 g, 0.0067 mol) were added to a round bottomed flask (250 cm³). The mixture was heated under reflux for 6.5 h using a Dean-Stark trap. After 45 minutes, a white precipitate was formed. After cooling the mixture to room temperature, the product was collected by filtration, washed with three portions of diethylether (5 cm³) and dried in a desiccator over silica gel.

Yield: 1.0 g (46 %). M.p., >355.9 °C.

Micro analysis: calculated for C₇₈H₆₀O₁₈Sn₆: C, 46.9; H, 3.0 %. Found: C, 46.9; H, 3.0 %.

IR (16 mm KBr disc): $\bar{\nu}_{\text{MI}}/\text{cm}^{-1}$ ca. 3409br(OH); 3074w, 3047w (CH aryl); 1604s (C=C aryl); 1553s (COO⁻); 1529s; 1409br,s (COO⁻); 1178m; 1022m; 715s (CH o.o.p., aryl); 691s; 595s (Sn-O); 504m; 475m; 444m.

¹H NMR (CF₃COOD): δ/ppm 7.31-8.14 (br, aromatic CH).

¹³C NMR (CF₃COOD): δ/ppm 129.5, 130.1, 130.5, 131.3, 131.9, 132.2, 133.3, 133.6, 134.6, 136.0, 136.8 (aromatic CH); 176.0 (CO₂).

2.1.16 Preparation of the cage, [(CH₃(CH₂)₃)₂Sn₂O(O₂P(OH)CH₂C₆H₅)₄]₂

The method from Kumara Swamy *et al.* was used.⁴ To a solution of phenylphosphonic acid (0.70 g, 0.0044 mol) in acetone (35 cm³), *n*-butylstannonic acid (0.46 g, 0.0022 mol) was added. The solution was filtered and then stirred until all the reactants had dissolved. After 10 mins the mixture became cloudy, the solvent was then allowed to evaporate to dryness to yield a colourless solid.

Yield: 0.78 g (18 %). M.p., 301-319 °C decomposed.

Micro analysis: calculated for C₆₄H₈₄O₂₆P₈Sn₄: C, 38.6; H, 4.3 %. Found: C, 38.9; H, 4.2 %.

IR (16 mm KBr disc): $\bar{\nu}_{\text{MI}}/\text{cm}^{-1}$ ca. 3234-2609br (OH); 3058w (CH aryl); 2961w, 2929w, 2859w (CH₃, CH₂); 1436m (CH); 1203-933br,s (PO); 750s (CH o.o.p., aryl); 720m; 695s; 553br,s (Sn-O).

The product was insufficiently soluble for the determination of ¹³C and ¹H nmr spectra.

2.1.17 Preparation of the cage [(CH₃)₂Sn₂O(O₂P(OH)C(CH₃)₃)₄]₂

Methylstannonic acid (1.00 g, 0.006 mol), toluene (100 cm³), and *t*-butylphosphonic acid (0.83 g, 0.006 mol) were added to a round-bottomed flask and heated under reflux for 9 h. The solvent was evaporated to leave a white

solid.

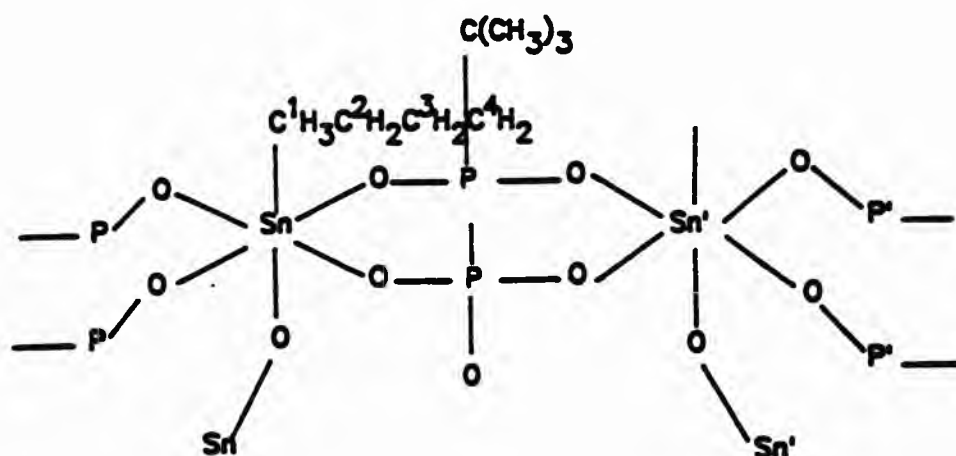
Yield: 1.0 g (10 %). M.p., > 352 °C.

Micro analysis: calculated for $C_{36}H_{92}O_{26}P_8Sn_4$: C, 26.0; H, 5.6 %. Found: C, 26.0; H, 5.5 %.

IR (KBr disc): $\bar{\nu}_{\text{MI}}/\text{cm}^{-1}$ ca. 3516-3234br (OH); 2980m, 2912m, 2870m (CH_2); 2789w; 2703br,w (PO-H); 1651w; 1483m (CH_2); 1198-1048br,s (PO); 1031s; 951m; 829m; 762m; 658s; 503s (Sn-O).

$^1\text{H NMR}$ (DMSO- D_6): δ/ppm 0.33 (s, CH_3); 1.01 (approx. d, $^3J(\text{HP}) \approx 14.53$ Hz, *t*-butyl protons).

2.1.18 Preparation of the cage cluster,⁴ $[(\text{CH}_2(\text{CH}_2)_3)_2\text{Sn}_2\text{O}(\text{O}_2\text{P}(\text{OH})\text{C}(\text{CH}_3)_3)_4]_2$
The method described by Kumara Swamy *et al.* was used.⁴ *n*-Butylstannonic acid (0.38 g, 0.0018 mol) was added to a solution of *t*-butylphosphonic acid (0.5 g, 0.0036 mol) in acetone (40 cm^3), with stirring. The solution was covered with Parafilm and left for 10 mins at room temperature, after which a white crystalline precipitate was observed. The product was collected by filtration and washed with two portions of acetone (5 cm^3). The product was dried in a dessicator over silica gel.



Yield: 0.6 g (18 %). M.p., 280-370 °C decomposed.

Micro analysis: calculated for $C_{48}H_{116}O_{25}P_8Sn_4$: C, 31.5; H, 6.4 %. Found: C, 31.5; H, 6.3 %.

IR (16 mm KBr disc): $\bar{\nu}_{\text{MI}}/\text{cm}^{-1}$ ca. 3375br (OH); 3051w, 3009w, 2939w (CH_3 , CH_2); 2719br (PO-H); 1652-1637br,w; 1440m (CH_3 , CH_2); 1139s (PO); 1044-922br,s (PO); 751m; 720m (CH_3 rock); 695m; 644m; 568s (Sn-O); 511s; 418s.

$^1\text{H NMR}$ (CDCl_3): δ/ppm 0.90 [t, CH_3 , $^3\text{J}(\text{HH}) = 7.3$ Hz]; 1.10 [d, $(\text{CH}_3)_3$, $^3\text{J}(\text{HP}) = 4.9$ Hz]; 1.16 [d, $(\text{CH}_3)_3$, $^3\text{J}(\text{HP}) = 4.7$ Hz]; 1.28 [approx. t, $\text{CH}_2\text{-Sn}$, $^3\text{J}(\text{HH}) \approx 8.0$ Hz]; 1.38 [approx. sextet, $-\text{CH}_2-$, $^3\text{J}(\text{HH}) \approx 7.3$ Hz]; 1.64 [approx. pentet, $-\text{CH}_2-$, $^3\text{J}(\text{HH}) \approx 7.5$ Hz]; 4.50 [s, OH, overlapped with a pair of doublets (satellites), $^2\text{J}(\text{H-}^{117/119}\text{Sn}) = 26.6$ Hz].

$^{31}\text{P NMR}$ (CDCl_3): δ/ppm 22.62 [s, $^2\text{J}(\text{P-}^{117}\text{Sn}) = 273.9$ Hz, $^2\text{J}(\text{P-}^{119}\text{Sn}) = 286.6$ Hz]; 31.33 [s, $^2\text{J}(\text{P}'\text{-}^{117}\text{Sn}) = 228.1$ Hz, $^2\text{J}(\text{P}'\text{-}^{119}\text{Sn}) = 238.7$ Hz].

$^{119}\text{Sn NMR}$ (CDCl_3): δ/ppm -630.4 [tt, $^2\text{J}(\text{}^{117/119}\text{Sn-O-P})$ and $^2\text{J}(\text{}^{117/119}\text{Sn-O-P}')$ = 239.3 Hz, 286.4 Hz].

2.1.19 Preparation of a copper complex of $[\text{CH}_3\text{CH}_2\text{CH}_2\text{CH}_2\text{Sn}(\text{O})\text{O}_2\text{CC}_6\text{H}_5]_6$

To a solution of copper (II) perchlorate (0.10 g, 0.000266 mol) in methanol (35 cm^3), $[\text{CH}_3\text{CH}_2\text{CH}_2\text{CH}_2\text{Sn}(\text{O})\text{O}_2\text{CC}_6\text{H}_5]_6$ (0.50 g, 0.000266 mol) was added. The mixture was heated under reflux for ca. 1.5 h. After ca. 30 mins of reflux, the solution had turned to a clear pale blue colour. The mixture was allowed to cool to room temperature overnight, before being reduced in volume using a rotary evaporator to yield a pale blue solid. The solid was dried in a desiccator over silica gel.

Yield: 0.4 g (70 %). M.p., 177-181.7 °C decomposed.

Micro analysis: calculated for $\text{C}_{66}\text{H}_{96}\text{O}_{32}\text{Sn}_6\text{Cl}_2\text{Cu}$: C, 35.3; H, 4.3 %. Found: C, 34.1; H, 3.9 %.

IR (16 mm KBr disc): $\bar{\nu}_{\text{IR}}/\text{cm}^{-1}$ ca. 3422br (OH); 3070w (aryl CH), 2959w, 2959w, 2929w (aliphatic CH_3 , CH_2); 1597s (COO^-); 1547, 1531br,s (COO^-); 1407s (aryl C=C); 1146m; 1115m; 1088m; 1027m; 718s (o.o.p., CH aryl); 674m; 625m; 586s (Sn-O); 472m.

2.2 Preparation of some alkylaminomethylenephosphonic acids, their N-oxides, and complexes with selected metal ions

2.2.1 Starting materials and solvents

Origins and purities of reagents used as precursors for the synthesis of alkylaminomethylenephosphonic acids, some metal complexes, and the N-oxide derivative of NEIBMPH₄ are shown in Table 2.2.1. All solvents used were general purpose grade except for ethanol which was absolute.

Table 2.2.1 Origin and purity of synthetic precursors.

Compound	Source	Purity ^a
DEAMP ₂	b	b
Ethylamine	Aldrich	30 % <i>aqu.</i>
Phosphorous acid	Aldrich	99 %
Formaldehyde	Hopkin & Williams	37 % <i>aqu.</i>
(±)- <i>Trans</i> -1,2-diaminocyclohexane	Aldrich	99 %
Hydrogen peroxide ^c	Interox R & D	
Cadmium(II)chloride	Hopkin & Williams	99 %
Manganese(II)perchlorate	Research organic/inorganic chemical corp	99.5 %
Cobalt(II)chloride	BDH	98 %
Copper(II)bromide	Hopkin & Williams	99 %
Zinc(II)acetate	Hopkin & Williams	98 %

^a Manufacturers' estimate. ^b *N*, *N*-Diethylaminomethylenephosphonic acid. Prepared by I. J. Scowen, Ph.D. Thesis, University of North London, 1993; purity confirmed by (a) micro analysis: calc. for C₅H₁₄NO₃P: C, 35.9; H, 8.4; N, 8.4 %. Found: C, 36.6; H, 8.7; N, 8.5 %; (b) nmr spectroscopy; ¹H NMR (D₂O): δ/ppm 1.31 [t, CH₃, ³J(HH) = 7.3 Hz]; 3.27 [d, CH₂-P, ²J(HP) = 13.0 Hz]; 3.36 (m, CH₂CH₂). ¹³C NMR (D₂O): δ/ppm 11.04 (CH₃); 51.38 [d, CH₂-P, ¹J(CP) = 136.3 Hz]; 52.16 [d, CH₂CH₂, ³J(CP) = 4.4 Hz]. ³¹P NMR (D₂O): δ/ppm 8.28. ^c unstabilised.

2.2.2 Preparation of *N*-ethyliminobis(methylenephosphonic acid), NEIBMPH₄
N-ethyliminobis(methylenephosphonic acid) was prepared using a method adapted from a procedure given by Moedritzer *et al.*⁵

Ethylamine (5.0 g, 0.11 mol), hydrochloric acid (8 cm³, 35 % w/w) and phosphorous acid (18.2 g, 0.22 mol) were slowly added to water (50 cm³). The mixture, which started to fume, was allowed to cool and then heated under reflux for 1 h. Over the course of the next hour, formaldehyde solution (36.0 g, 0.44 mol) was added dropwise with stirring, and then heating under reflux was continued for a further 4 h. After standing overnight, the mixture was reduced in volume using a rotary evaporator to leave a yellow oil. Ethanol (100 cm³) was added to the oil and within 30 mins. a white precipitate was observed. The product was collected by Büchner filtration, washed with three

portions of ethanol (10 cm³) and diethylether (5 cm³). The product was dried in a desiccator over silica gel.

Yield: 15.6 g (60 %). M.p., 214.9–217.1 °C.

Micro analysis: calculated for C₄H₁₂NO₆P₂: C, 20.6; H, 5.6; N, 6.0 %. Found: C, 20.8; H, 5.7; N, 6.0 %.

IR (16 mm KBr disc): $\bar{\nu}_{\text{max}}/\text{cm}^{-1}$ ca. 3409 (OH); 3009w, 2972w (aliphatic CH str.); 2912–2546br (PO–H str.); 1479br; 1446br (aliphatic CH def.); 1281s,br; 1214–1124s,br (PO); 975–939br (P=O); 851s; 794s; 757s; 710s; 597s.

¹H NMR (D₂O): δ/ppm 1.37 [t, CH₃, ³J(HH) = 7.2 Hz]; ca. 3.58 [m, CH₃CH₂, overlapped by doublet at 3.61]; 3.61 [d, CH₂-P, ²J(PH) = 12.9 Hz].

¹³C NMR (D₂O): δ/ppm 10.84 (CH₃); 52.72 [dd, CH₂-P, ¹J(CP) = 139.3 Hz, ³J(CP) = 4.4 Hz]; 55.04 [t, CH₃CH₂, ³J(CP) = 4.0 Hz].

³¹P NMR (D₂O): δ/ppm 9.11

2.2.3 A novel method for recrystallising diethylaminomethylenephosphonic acid, DEAMP₂

DEAMP₂ (0.30 g, 0.002 mol) was added to a solution of *n*-butylstannonic acid (0.40 g, 0.002 mol) in toluene (100 cm³). The mixture was heated under reflux for 6 h using a Dean–Stark trap. The mixture was left to stand overnight at room temperature before being filtered. The solution was stoppered and left for four months, after which clear, square crystals were discovered. These crystals were suitable for X-ray diffraction and the structure was determined (Chapter 7).

Recovery: 0.27 g (87 %). M.p., 210–212.1 °C.

Micro analysis: calculated for C₃H₁₄NO₃P: C, 35.9; H, 8.4; N, 8.4 %. Found: C, 35.8; H, 8.5; N, 8.3%.

IR (16 mm KBr disc): $\bar{\nu}_{\text{max}}/\text{cm}^{-1}$ ca. 3420br (OH); 2964m, 2935m, 2873m (aliphatic CH str.); 2758w; 2660w (PO–H str.); 1636m; 1468m (aliphatic CH def.); 1124s,br (PO); 1005s (PO); 878w; 772w; 686w; 576m; 513s.

¹H NMR (D₂O): δ/ppm 1.31 [t, CH₃, ³J(HH) = 7.3 Hz]; 3.28 [d, CH₂-P, ²J(PH) = 13.4 Hz]; 3.37 (m, CH₃CH₂).

¹³C NMR (D₂O): δ/ppm 11.15 (CH₃); 51.44 [d, CH₂-P, ¹J(CP) = 136.8 Hz]; 52.39 [d, CH₃CH₂, ³J(CP) = 4.4 Hz].

³¹P NMR (D₂O): δ/ppm 8.45.

2.2.4 Preparation of (*±*)-trans-cyclohexane-1,2-diaminetetrakis(methylene-phosphonic acid), CDTMPH₈

(*±*)-Trans-cyclohexane-1,2-diamine was initially distilled to yield a colourless liquid which was then used without further purification in the next stage. The freshly distilled amine (10.0 g, 0.09 mol) was added to a solution of phosphorous acid (28.7 g, 0.35 mol) in water (100 cm³) and hydrochloric acid (13 cm³ of 35 % w/w, 0.15 mol). The resulting mixture was heated under reflux for 1h. Over the course of the next hour, formaldehyde (56.7 g, 0.72 mol) was slowly added and the solution turned yellow. Heating under reflux was continued for an additional 3.75 h. The mixture was left to stand overnight at room temperature. Reducing the volume using a rotary evaporator yielded a dark yellow oil. Water (50 cm³) was added to the oil and the resulting solution was extracted with three portions of diethylether (25 cm³). The resulting aqueous layer was left at room temperature for nine months, after which colourless rectangular crystals were isolated. The crystals were collected by Büchner filtration and washed with three portions of cold water (10 cm³) and allowed to dry in the air.

Yield: 1.0 g (3 %).

Micro analysis: calculated for C₁₀H₂₆N₂O₁₂P₄: C, 24.5; H, 5.4; N, 5.7 %. Found: C, 24.4; H, 5.3; N, 5.6 %.

¹H NMR (D₂O): δ/ppm ca. 1.2-1.5 [m's, 4H, ring CH₂'s]; ca. 1.89 [m, 2H, ring CH₂'s]; ca. 2.22 [m, 2H, ring CH₂'s]; ca. 3.02-3.72 [m's, 10H, CH₂-P and CH].

¹³C NMR (D₂O): δ/ppm 25.3, 26.5 (ring CH₂'s); 49.1 [dd, CH₂-P, ¹J(CP) = 147.8 Hz, ³J(CP) = 13.9 Hz]; 51.9 [d, CH₂-P, ¹J(CP) = 146.6 Hz]; 66.1, 66.28 (CH).

³¹P NMR (D₂O): δ/ppm 15.27, 16.55.

A pure sample of CDTMPH₈ (ca. 2 g) was also obtained from Interlox Research and Development and used to measure protonation and metal complex stability constants (Section 2.3). The purity of CDTMPH₈ from this source was confirmed by elemental analysis and nmr spectra.

Micro analysis: calculated for C₁₀H₂₆N₂O₁₂P₄: C, 24.5; H, 5.4; N, 5.7 %. Found: C, 24.4; H, 5.4; N, 5.7 %.

IR (16 mm KBr disc): $\bar{\nu}_{\text{max}}$ /cm⁻¹ 3465sh (OH); 3043m, 2943m, 2872m (aliphatic CH str.); 2546-2796br (PO-H str.); 1657br,m; 1444br,m (aliphatic CH def.); ca. 1200v,br; 1007s,br (PO); 949s (P=O); 604m; 553m.

¹H NMR (D₂O): δ/ppm ca. 1.2-1.5 [m's, 4H, ring CH₂'s]; ca. 1.89 (2H, ring

CH_2 's); ca. 2.22 (2H, ring CH_2 's); ca. 3.03-3.72 [m's, 10H, CH_2 -P and CH].
 ^{13}C NMR (D_2O): δ /ppm 25.6, 26.8 (ring CH_2 's); 49.4 [dd, CH_2 -P, $^1\text{J}(\text{CP}) = 146.5$ Hz, $^3\text{J}(\text{CP}) \approx 11.7$ Hz]; 52.3 [d, CH_2 -P, $^1\text{J}(\text{CP}) = 146.5$ Hz]; 66.46, 66.63 (CH).
 ^{31}P NMR (D_2O): δ /ppm 15.44, 16.71.

A small amount of crystalline material of CDTMPH_3 was prepared by I. Hales[†] and this was used to determine the single crystal X-ray structure (Chapter 7). The purity of the sample was confirmed as noted below.

Micro analysis: calculated for $\text{C}_{10}\text{H}_{26}\text{N}_2\text{O}_{12}\text{P}_4$: C, 24.5; H, 5.4; N, 5.7 %. Found: C, 24.6; H, 5.0; N, 5.6 %.

^1H NMR (D_2O): δ /ppm 1.2-1.5 [m's, 4H, ring CH_2 's]; ca. 1.88 (2H, ring CH_2 's); ca. 2.22 (2H, ring CH_2 's); 3.01-3.72 [m's, 10H, CH_2 -P and CH].
 ^{13}C NMR (D_2O): δ /ppm 25.6, 26.8 (ring CH_2 's); 49.6 [dd, CH_2 -P, $^1\text{J}(\text{CP}) = 143.4$ Hz, $^3\text{J}(\text{CP}) = 11.6$ Hz]; 52.3 [d, CH_2 -P, $^1\text{J}(\text{CP}) = 146.3$ Hz]; 66.4, 66.6 (CH).
 ^{31}P NMR (D_2O): δ /ppm 15.15, 16.47. Small amounts of phosphorus-containing impurities were also observed.

2.2.5 Preparation of the N-oxide derivative of NEIBMPH_4

All glassware used in contact with hydrogen peroxide was soaked in concentrated nitric acid for 24 h, then thoroughly rinsed with deionised water.

To a solution of NEIBMPH_4 (0.5 g, 0.0022 mol) in water (20 cm^3), hydrogen peroxide (35 % v/v, 10 cm^3) was slowly added. This mixture was carefully heated under reflux (at 60 °C) for 24 h. The solution was decomposed by passing dry air through the solution until a residue was left. On addition of ethanol (100 cm^3) the mixture was left to stand at room temperature. After a period of one week, a white precipitate was collected by Büchner filtration, and then recrystallised from water. The resulting white precipitate was washed with two portions of ethanol (5 cm^3) and dried in a desiccator over silica gel.

Yield: 0.4 g (76 %). M.p., 126.3-127.6 °C.

Micro analysis: calculated for $\text{C}_4\text{H}_{13}\text{NO}_7\text{P}_2$: C, 19.3; H, 5.3; N, 5.6 %. Found: C, 19.6; H, 5.2; N, 5.5 %.

[†] I. D. C. Hales, BSc project, University of North London, 1992.

$^1\text{H NMR}$ (D_2O): δ/ppm 1.17 [t, CH_3 , $^3\text{J}(\text{HH}) = 7.1$ Hz]; 4.04 [q, CH_2CH_2 , $^3\text{J}(\text{HH}) = 7.2$ Hz]; 4.05–4.25 [AB subspectra of an ABX spin system].

$^{13}\text{C NMR}$ (D_2O): δ/ppm 11.11 (CH_3); 64.38 [dd, $\text{CH}_2\text{-P}$, $^1\text{J}(\text{CP}) = 133.4$ Hz, $^3\text{J}(\text{CP}) = 3.3$ Hz]; 67.97 [t, CH_2CH_2 , $^3\text{J}(\text{CP}) = 3.2$ Hz].

$^{31}\text{P NMR}$ (D_2O): δ/ppm 5.19.

2.2.6 Characterisation of 5,8-dioxadodecane-1,12-diaminetetrakis(methylene-phosphonic acid), DDDTMPH_3

A sample of DDDTMPH_3 was prepared by P. B. Iveson[†] and kindly supplied by J. Lockhart. The synthesis of DDDTMPH_3 was achieved by a modification of the Moedritzer-Irani reaction. Characterisation of DDDTMPH_3 was carried out to confirm purity.

Micro analysis: calculated for $\text{C}_{12}\text{H}_{22}\text{N}_2\text{O}_{14}\text{P}_4$: C, 26.1; H, 5.8; N, 5.1 %. Found: C, 26.3; H, 5.9; N, 5.0 %.

$^1\text{H NMR}$ (D_2O): δ/ppm 2.11 [approx. pentet, $\text{CH}_2\text{CH}_2\text{CH}_2$, $^3\text{J}(\text{HH}) \approx 6.3$ Hz]; 3.60–3.73 [complex multiplets, $\text{CH}_2\text{-P}$, $\text{CH}_2\text{CH}_2\text{-N}$, $\text{CH}_2\text{-OCH}_2$, $\text{CH}_2\text{-OCH}_2$].

$^{13}\text{C NMR}$ (D_2O): δ/ppm 26.4 ($\text{CH}_2\text{CH}_2\text{CH}_2$); 54.2 [dd, $\text{CH}_2\text{-P}$, $^1\text{J}(\text{CP}) = 137.8$ Hz; $^3\text{J}(\text{CP}) = 4.3$ Hz]; 59.1 [t, $\text{CH}_2\text{CH}_2\text{-N}$, $^3\text{J}(\text{CP}) = 4.0$ Hz]; 71.5, 72.5 ($\text{CH}_2\text{-OCH}_2$, $\text{CH}_2\text{-OCH}_2$).

$^{31}\text{P NMR}$ (D_2O): δ/ppm 8.83.

2.2.7 Preparation of $[\text{Cd}(\text{NEIBMPH}_3)_2]$

To an aqueous solution (50 cm^3) of NEIBMPH_3 (0.8 g, 0.0034 mol) cadmium(II) chloride (0.31 g, 0.002 mol) was added and the mixture was stirred for 20 mins. After slow evaporation at room temperature, a white powder was collected by Büchner filtration and washed with portions of cold water. The product was allowed to dry in a desiccator over silica gel.

Yield: 0.95 g (48 %). M.p., > 305 °C dec.

Micro analysis: calculated for $\text{C}_8\text{H}_{14}\text{N}_2\text{O}_{12}\text{P}_4\text{Cd}$: C, 16.7; H, 4.2; N, 4.9 %. Found: C, 16.7; H, 4.2; N, 4.8 %.

IR (16 mm KBr disc): $\bar{\nu}_{\text{max}}/\text{cm}^{-1}$ ca. 3449br (OH); 3083w, 2839w, 2760w (CH_3 , CH_2); 3000–2760br (PO–H); 1422m; 1356m; 1278m; 1218sh; 1200s; 1163–1132br (PO_2^-); 1079s (PO_2^-); 931s (PO–H); 769s; 694s; 600s; 561s; 489s.

$^1\text{H NMR}$ (NaOH): δ/ppm 1.09 [t, CH_3 , $^3\text{J}(\text{HH}) = 6.8$ Hz]; 2.80 [d, $\text{CH}_2\text{-P}$, $^2\text{J}(\text{HP}) = 12.0$ Hz]; 3.25 [approx. q, CH_2CH_2 , $^3\text{J}(\text{HH}) \approx 6.6$ Hz].

[†] P. B. Iveson, Ph.D. Thesis, University of Newcastle Upon Tyne, 1991.

^{13}C NMR (NaOH): δ/ppm 9.4 (CH_3); 53.2 [t, CH_2CH_2 , $^3\text{J}(\text{CP}) = 6.1$ Hz]; 55.1 [dd, $\text{CH}_2\text{-P}$, $^1\text{J}(\text{CP}) = 138.6$ Hz, $^3\text{J}(\text{CP}) = 7.6$ Hz].

^{31}P NMR (NaOH): δ/ppm 17.47.

M. s.: 577, (33.1 %) [$\text{M}+\text{H}^+$].

2.2.8 Preparation of $[\text{Cu}(\text{NEIBMPH}_3)_2]$

To an aqueous solution (50 cm^3) of NEIBMPH_4 (0.5 g, 0.0022 mol) copper(II) bromide (0.5 g, 0.0022 mol) was added and the resulting solution turned blue. Small portions of acetone was added, just until the solution turned cloudy. The mixture was then left to stand in a fridge overnight. A pale blue product was collected by Büchner filtration and washed with portions of IMS 99. The product was allowed to dry in a desiccator over phosphorus pentoxide.

Yield: 0.40 g (35 %). M.p., > 250 °C dec.

Micro analysis: calculated for $\text{C}_8\text{H}_{24}\text{N}_2\text{O}_{12}\text{P}_4\text{Cu}$: C, 18.2; H, 4.6; N, 5.3 %. Found: C, 18.2; H, 4.7; N, 5.3 %.

IR (16 mm KBr disc): $\bar{\nu}_{\text{III}}/\text{cm}^{-1}$ 3618s; ca. 3557-3114br (OH); 3114-2500br (PO-H); 3048s; 2961w, 2843w, 2790w (CH_3 , CH_2); 1463m; 1222br; 1158s (PO_2^-); 1067s (PO_2^-); 967m; 933s (PO-H); 768m; 718m; 572m.

2.2.9 Preparation of $[\text{Mn}(\text{NEIBMPH}_3)_2]$

The pH of an aqueous solution (25 cm^3) of NEIBMPH_4 (0.8 g, 0.0034 mol) was adjusted to pH 11 using sodium hydroxide (2 mol dm^{-3}). An aqueous solution (25 cm^3) of manganese(II) perchlorate (0.4 g, 0.0017 mol) was added to the ligand solution. The resulting mixture was left to stand overnight at room temperature. A white product was collected by Büchner filtration and washed with three portions of water (5 cm^3) and allowed to dry in a vacuum desiccator over phosphorus pentoxide.

Yield: 1.25 g (42 %).

Micro analysis: calculated for $\text{C}_8\text{H}_{24}\text{N}_2\text{O}_{12}\text{P}_4\text{Mn}$: C, 18.5; H, 4.7; N, 5.4 %. Found: C, 18.6; H, 4.6; N, 5.2 %.

IR (16 mm KBr disc): $\bar{\nu}_{\text{III}}/\text{cm}^{-1}$ ca. 3414br (OH); 3071-2500br,s (PO-H); 2848w, 2767w (CH_3 , CH_2); 2406-2047 br; 1422m; 1359m; 1289m; 1219br,s; 1159-1143br,s (PO_2^-); 1073br,s (PO_2^-); 1000s; 932s (PO-H); 766s; 713s; 594s; 566s.

M. s.: 520, (5.3 %) [$\text{M}+\text{H}^+$].

2.2.10 Preparation of $[\text{Co}(\text{NEIBMPH}_3)_2]$

To an aqueous solution (50 cm^3) of NEIBMPH_4 (0.5 g, 0.0022 mol), cobalt (II) chloride (0.3 g, 0.001 mol) was added. The resulting pale purple mixture was left to stand at room temperature for 48 h. A pink product was collected by Büchner filtration and washed with portions of water and allowed to dry in a vacuum desiccator over silica gel.

Yield: 0.6 g (100 %).

Micro analysis: calculated for $\text{C}_8\text{H}_{24}\text{N}_2\text{O}_{12}\text{P}_4\text{Co}$: C, 18.3; H, 5.0; N, 5.3 %. Found: C, 18.7; H, 4.9; N, 5.2 %.

IR (16 mm KBr disc): $\bar{\nu}_{\text{max}}/\text{cm}^{-1}$ ca. 3386br (OH); 3042s; 2909–2546br; 2857w (CH_3 , CH_2); 2409–2068br; 1422m; 1389m; 1361m; 1278m; 1219s; 1200s; 1132br (PO_2^-); 1074s (PO_2^-); 933s (PO–H); 811m; 767s; 709m; 600s; 567s; 489m; 478m.

M. s.: 524, (9.6 %) $[\text{M}+\text{H}^+]$.

2.2.11 Preparation of $[\text{Zn}(\text{NEIBMPH}_3)_2]\cdot\text{H}_2\text{O}$

To an aqueous solution (25 cm^3) of NEIBMPH_4 (0.5 g, 0.0022 mol), zinc (II) acetate (0.5 g, 0.0022 mol) was added. After 10 mins a white product was collected by Büchner filtration and washed with three portions of water (5 cm^3) and allowed to dry in a vacuum desiccator over silica gel.

Yield: 0.30 g (25 %). M.p., $> 300^\circ\text{C}$.

Micro analysis: calculated for $\text{C}_8\text{H}_{26}\text{N}_2\text{O}_{13}\text{P}_4\text{Zn}$: C, 17.1; H, 4.7; N, 4.9 %. Found: C, 17.1; H, 4.5; N, 5.2 %.

M. s.: 548, (3.8 %) $[\text{M}+\text{H}^+]$.

2.3 Determination of protonation and stability constants for some alkylamino-methylenephosphonic acids and their metal complexes by potentiometric titration

Protonation constants for the ligands, and equilibrium constants for metal-ligand complexes were determined potentiometrically using a computer controlled titration system developed to acquire data under conditions of high thermal and potentiometric stability (Section 2.3.4).

2.3.1 Reagents and solvents used during potentiometric titrations

Origins and purities of the reagents used in potentiometric titrations are

outlined in Table 2.3.1. The purity of ligand samples used for potentiometric titrations were confirmed using C, H, and N elemental analysis, ^1H , ^{13}C , and when appropriate ^{31}P nmr spectroscopy.

Table 2.3.1 Origin and purity of reagents used in potentiometric titrations.

Reagent	Source	Grade
Nitric acid	BDH	concentrated solution ^a
Potassium hydroxide	BDH	concentrated solution ^a
Hydrochloric acid	BDH	concentrated solution ^a
Potassium nitrate	BDH	ARISTAR, > 99.5 % ^b
Disodium tetraborate decahydrate	BDH	AnalaR, > 99.5 % ^c
Nitrogen	BOC	'Oxygen free' ^d
Soda lime	BDH ^e	
Mercury	Thorn EMI	Triple distilled
Mercury(I)chloride	Aldrich	AnalaR
Potassium Chloride	BDH	ARISTAR, > 99.5 %

^a 'ConVol' solutions prepared from AnalaR grade reagents. ^b Conforms to A.C.S. specification. ^c Recrystallised according to a standard procedure¹⁶ before use. ^d Passed over soda lime and saturated with solvent before use. ^e Mesh size 3-9 or 10-16; self-indicating type used.

Water used for the preparation of solutions was obtained by the following method. Deionised water, produced to BS3978 specification using a RO50-100-200 Reverse Osmosis unit (Purite Ltd.), was used without further purification, except for the preparation of base solutions where the water was degassed by sonication under vacuum at the water pump for at least 2 h before being stored under nitrogen.

2.3.2 Preparation of solutions

2.3.2(a) Aqueous nitric acid

Nitric acid was made up to 500 cm³ with water to give a stock solution of concentration ca. 0.1 mol dm⁻³.

2.3.2(b) Aqueous hydrochloric acid

Hydrochloric acid, made up to 500 cm³ with water to give a concentration of ca.

0.1 mol dm⁻³, was standardised against disodium tetraborate decahydrate (borax) using methyl red indicator, according to a standard procedure.^{7a}

2.3.2(c) Aqueous potassium nitrate/nitric acid for potentiometric titrations
An aliquot (20 cm³) of the nitric acid stock solution was pipetted into a volumetric flask (500 cm³). Potassium nitrate (4.85 g) was added to give [KNO₃] = 0.096 mol dm⁻³. The solution was made up to the mark with water to give an acid concentration of 0.004 mol dm⁻³ and hence an ionic strength of 0.1 mol dm⁻³.

2.3.2(d) Aqueous potassium hydroxide

Aqueous potassium hydroxide was made up to 500 cm³ with water (which had been degassed by sonication under vacuum at the water pump until bubble evolution had stopped) to give a concentration of ca. 0.1 mol dm⁻³. The resultant solution was further degassed by sonication under vacuum as before. The solution was stored in the reservoir of the motorised burette used in all titrations. All solution transfers were carried out while purging the receiving vessel with nitrogen to minimise exposure to air and, therefore, to carbon dioxide. The base (ca. 0.1 mol dm⁻³, KOH) was then standardised against previously standardised aqu. hydrochloric acid (ca. 0.1 mol dm⁻³) using methyl red indicator according to the standard procedure.^{7b}

2.3.2(e) Aqueous metal ion solutions

Solutions of metal ions susceptible to hydrolysis during storage, e.g. Fe(III), were prepared by dissolving the hydrated metal nitrate in nitric acid stock solution (20.0 cm³) and making up to the mark in a 500 cm³ volumetric flask to give a metal ion concentration of ca. 0.05 mol dm⁻³ and an acid concentration of ca. 0.004 mol dm⁻³. Solutions of metal ions not susceptible to hydrolysis during storage, e.g. Cu(II), Ni(II), Co(II), Pb(II), Cd(II) and Zn(II), were made up by dissolving the hydrated metal nitrate in water to give a metal ion concentration of ca. 0.1–0.05 mol dm⁻³. The concentration of the metal ion in solution was determined by either atomic absorption spectroscopy [Ni(II), Cu(II), and Co(II)] or by complexometric titration of the metal ion solution with EDTA [Zn(II), Pb(II), and Cd(II)].^{7c}

2.3.2(f) Solution for the salt bridge

Potassium nitrate (2.5275 g) was added to a volumetric flask (250 cm³) and made

up to the mark with water to give a concentration of $[\text{KNO}_3] = I = 0.1 \text{ mol dm}^{-3}$, i.e. the same ionic strength as that used in the cell during potentiometric titrations.

2.3.2(g) Preparation of calomel reference electrode

The calomel reference electrode was prepared using experimental methods adapted from those described by Vogel.^{7d}

All experimental procedures for preparing the calomel electrode took place in a fume cupboard. The calomel electrode cell was thoroughly cleaned with water and finally with methanol, and allowed to dry completely before use. The electrolyte solution was prepared by dissolving potassium nitrate (2.40 g, $0.095 \text{ mol dm}^{-3}$) and potassium chloride (0.093 g, 0.05 mol dm^{-3}) in water and making up to the mark in a volumetric flask (250 cm^3).

A layer of mercury (ca. 1 cm depth) was gently poured into the calomel cell using a long-stemmed funnel. Calomel paste was prepared by rubbing together mercury(I) chloride (ca. 5 g) and mercury (ca. 5 cm^3). In a glass pestle and mortar for a few minutes a small portion of the electrolyte solution was added (enough to keep a small layer of liquid above the paste). After standing for 5 mins. the excess electrolyte was poured off and then fresh electrolyte was added and grinding was continued. This process was repeated 4 to 5 times until a smooth paste was obtained.

A layer of calomel paste was applied to the mercury such that the mercury was completely covered (ca. 1 cm thick). Electrolyte was then carefully added to the electrode cell so that the calomel layer was not disturbed and so that the level of the top of the electrolyte was approximately the same as the level in the measurement cell with all its fittings present. The electrode was allowed to equilibrate by standing for one week prior to use.

The composition of the electrode is shown in Table 2.3.2 and a schematic diagram is shown in Figure 2.3.1.

Table 2.3.2 Composition of calomel reference electrode used for potentiometric titrations in aqueous solution.

Electrolyte ^a	Calomel half cell ^b
KNO_3	$\text{KNO}_3 (0.095), \text{KCl} (0.005), \text{Hg}_2\text{Cl}_2(\text{s}) \text{Hg}(\text{s})$

^a Ionic strength = 0.1 mol dm^{-3} . ^b Concentrations ($/\text{mol dm}^{-3}$) are given in parentheses.

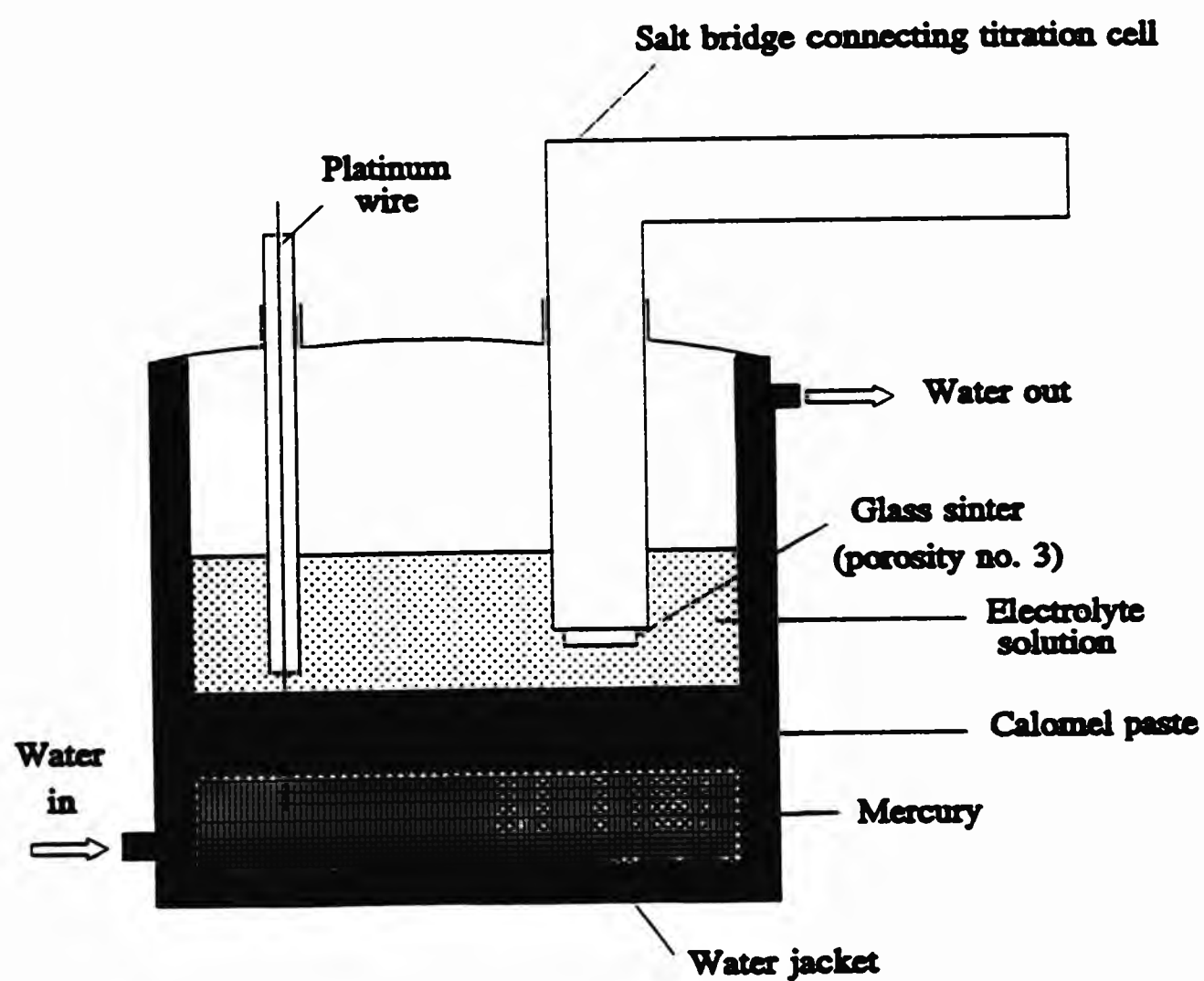


Figure 2.3.1 Schematic diagram of the calomel reference electrode.

2.3.3 Data acquisition

Potentiometric acid/base titrations were carried out using a previously 'in-house' built, automated titration apparatus based on a motorised piston burette (Metrohm Dosimat 655 fitted with an anti-diffusion tip) and driven by a BBC Microcomputer and 6502 second processor (Figure 2.3.2). All titrations were performed under an atmosphere of water-saturated, carbon dioxide-free nitrogen in a water-jacketed sample cell (Figure 2.3.3). The solution potential was measured using a glass electrode (Corning 003 11 101J) referenced to a thermostated calomel electrode *via* a salt bridge composed of electrolyte solution (KNO_3 , $I = 0.1 \text{ mol dm}^{-3}$). The liquid-liquid junctions between the salt bridge, the calomel electrode and the titration solutions were maintained by glass sinters (No. 4 porosity).

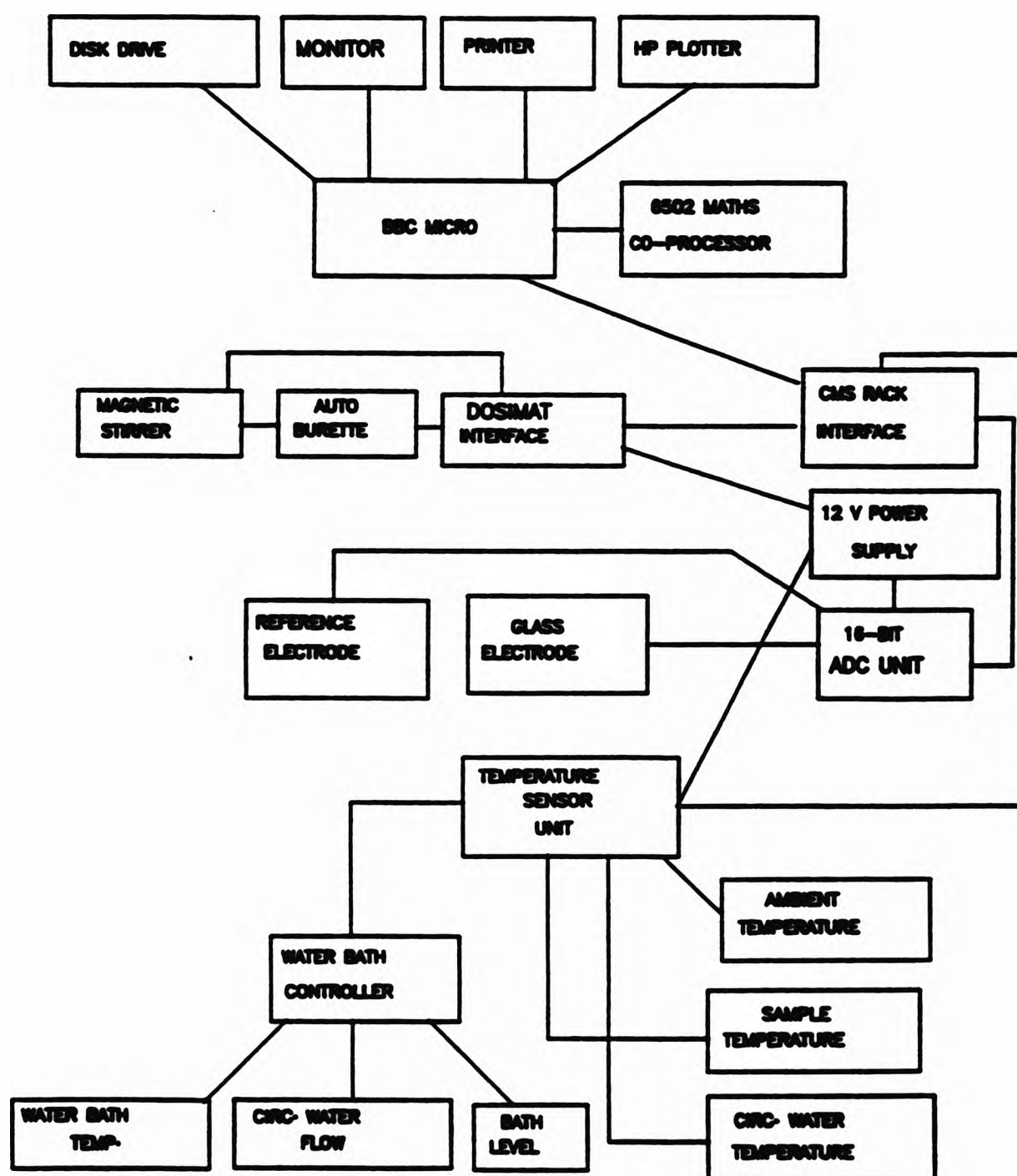


Figure 2.3.2 Schematic diagram of the titration apparatus.

The titration environment was maintained at 25.0 ± 0.1 °C by a circulating water system based on a Grant SE15 water bath. Sample, circulating and ambient temperatures, obtained from platinum resistance thermometer probes (SDL Pt-100 glass encased, SDL Pt-100 steel encased and RS Pt-100 respectively) were calculated and displayed during execution of the titration program, S.SCMTITR.⁸

If the temperature exceeded a preset tolerance of ± 0.1 °C (in early experiments, a tolerance of ± 0.2 °C was used) during a titration, the run was suspended until the temperature was within the correct range. The water flow was monitored during the titrations and any failure resulted in the titration being suspended until the water flow was restored. The titration data, *i.e.* the potential (mV) of the solution in the cell, volume of base added and sample temperature, were printed out and saved on to disc after every five data points.

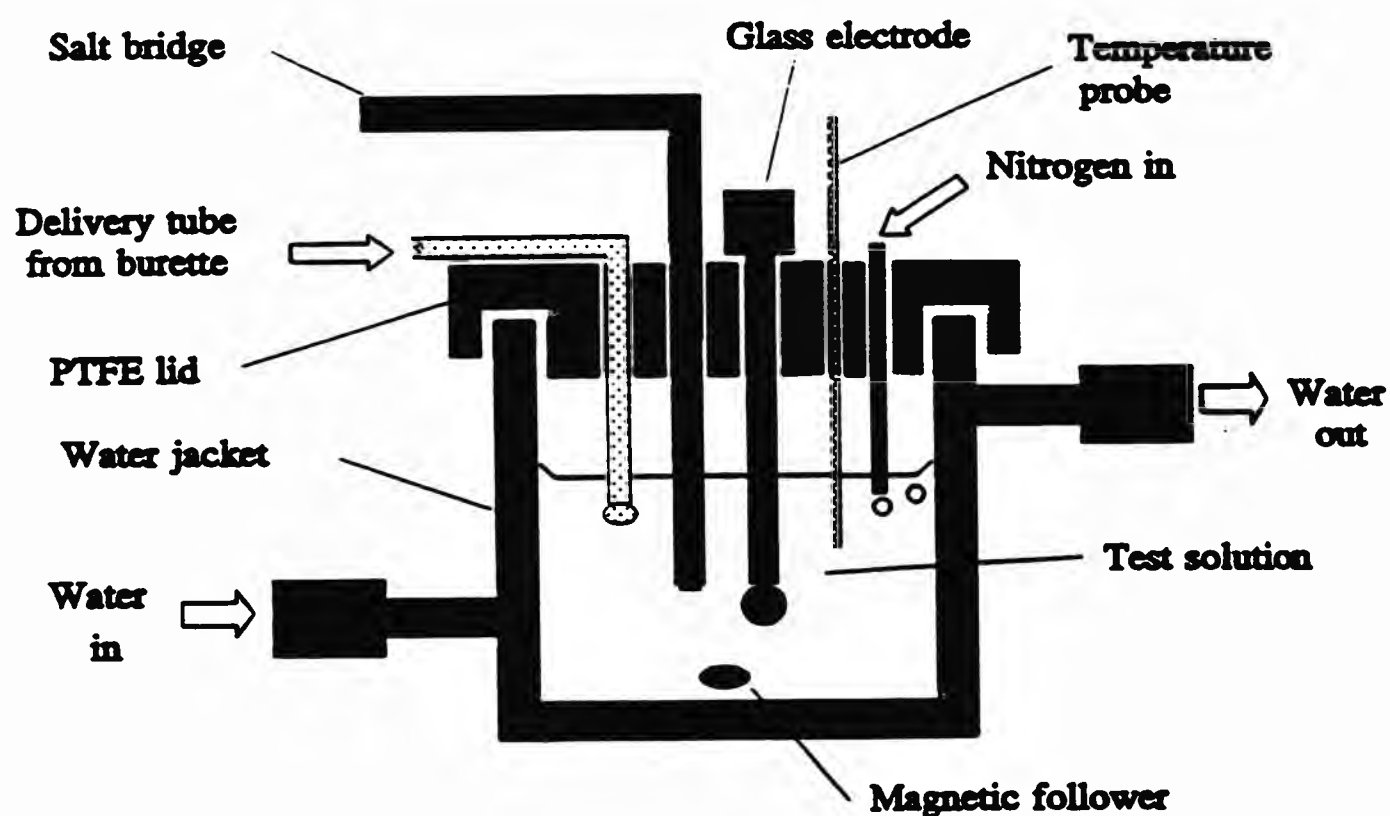


Figure 2.3.3 Schematic diagram of the titration cell used for potentiometric measurements.

The titration program, S.SCMTITR,⁸ allows certain input parameters (Table 2.3.3) to be varied according to the conditions required; e.g. a metal ion which is inert may require a different set of input parameters compared to a labile metal ion, in order to allow the system to reach equilibrium before emf readings are taken. This is achieved by ensuring that the mV reading at each titration point is within a chosen tolerance (typically ± 0.05 mV).

The titration system is designed so that the sample solution reaches equilibrium before an aliquot of base is added to the sample solution in the titration cell. The sequence of addition of base, delay and collection of mV readings can be summarised as follows. The motorised piston burette delivers a fixed increment of base. Then there is a delay of 45 s (delay between points, a 'mixing delay') before 60 (readings per point: 30-99) mV readings are taken and averaged. Then another 60 mV readings are taken without delay, and these readings are averaged. The second average is taken as the final mV value for the titration point and if the two averaged mV values are within ± 0.05 mV, the motorised piston burette delivers another fixed increment of base and the titration continues. If the readings are not within the tolerance specified, then the processes of obtaining the averaged readings are repeated until the tolerance condition is satisfied or the 'read limit' (chosen between 50-300 readings) has been reached. If the read limit is reached, then the final averaged mV reading is recorded. The next aliquot of base is then added.

Table 2.3.3 Input parameters which can be varied for a titration under the control of the program S.SCMTITR.

Parameter	Typical value
Number of readings per point	60
Minimum increment /cm ³	0.0100
Millivolt tolerance /mV	0.0500
Fixed increment /cm ³	0.0100
Unknown concentration at each titration point	1
Volume of base to add /cm ³	2.0000
Delay between points /s	45
Read limit	150
Temperature tolerance /°C	0.1000
Water bath temperature /°C	25.55

2.3.4 Cell calibration

The electrode system was calibrated using a strong acid and assuming it to be fully ionised. The cell parameters (E_0 and pK_a) were obtained by direct titration of the strong acid solution ($[H^+] \approx 0.004 \text{ mol dm}^{-3}$) against standard base solution ($[KOH] \approx 0.1 \text{ mol dm}^{-3}$), using the same ionic background ($[KNO_3] = 0.096 \text{ mol dm}^{-3}$) which was to be used for the equilibria under study. Titrations were performed over the same pH range as that used for the sample titrations. E_0 and pK_a were calculated by the computer program S.SCMCAL.⁹

Standard calibration titration conditions: number of readings per point: 30; volume of base delivered: 2 cm^3 ; delay between points: 30 secs; read limit: 50 points; tolerance for recording points: $\pm 0.05 \text{ mV}$; temperature tolerance: $\pm 0.1^\circ\text{C}$.

2.3.5 Conditions for ligand and ligand/metal potentiometric titrations

For 'ligand only' titrations, solution preparation was carried out using a standard procedure. A sample of the ligand (to give a concentration of ca. $0.001\text{--}0.0005 \text{ mol dm}^{-3}$) was weighed out by difference using a five-figure balance (Mettler AE163), and placed in the titration cell. An aliquot of *aqu.* KNO_3/HNO_3 ($I = 0.1 \text{ mol dm}^{-3}$) was then added (25.0 cm^3) using a pipette. For ligand/metal titrations, the above procedure was repeated and then a small aliquot of the metal stock solution, (between 0.25 cm^3 and 0.05 cm^3), sufficient to give the desired ratio metal to ligand ratio (*e.g.* M:L; 1:1, 1:2, 1:3) was delivered to the titration cell using a micropipette (Gilson Microman M250). In both types of titration, the cell was then placed in position on the titration apparatus and connected up to the circulating constant temperature water system. The nitrogen delivery tube, temperature probe, base solution delivery tube, glass electrode and the salt bridge liquid/liquid junction were washed and wiped dry before being placed into the titration solution (Figure 2.3.2). Initially, and under computer control, the solution temperature was allowed to stabilise to within the preset tolerance about 25.0°C ($\pm 0.1^\circ\text{C}$) and then the potential of the solution was recorded at five minute intervals. When two successive readings were within $\pm 0.2 \text{ mV}$ of each other, the automatic titration began. It was possible to adjust the temperature of the circulating water during the titration in order to minimise the time taken to reach thermal equilibrium in the cell.

Standard titration conditions: number of readings per point: 60; volume of

base delivered: 2 cm³; delay between points: normally 45 s, but increased to 150 s where equilibrium might be slow to be established [e.g. Ni(II), Fe(II)]; read limit: 150 points; tolerance for recording points: ± 0.05 mV; temperature tolerance: ± 0.1 °C.

Table 2.3.4 Experimental conditions used for titrations of DEAMPH₂.

Data file	Ligand ^a		Metal salt solution [M]:[L]			
	/mg	/μmol	/mol dm ⁻³ ^b	aliquot/cm ³	/mol dm ⁻³ ^b	
M040	4.80	28.72	0.001149 ^c			
M041	1.57	9.39	0.000376 ^c			
				Pb(NO ₃) ₂ ^d		
M032	4.56	27.28	0.001081	0.2483	0.000990	1:1.09
M033	3.84	22.97	0.000914	0.1241	0.000498	1:1.84
M082	4.48	26.80	0.001069	0.0827	0.000332	1:3.32
				Co(NO ₃) ₂ ^e		
M011	4.69	28.06	0.001090	0.7323	0.000972	1:1.12
M012	4.23	25.31	0.001003	0.2441	0.000330	1:3.04
M010				0.7323	0.000971	
				Zn(NO ₃) ₂ ^f		
M083	4.25	25.43	0.001007	0.2500	0.000989	1:1.02
M084	4.36	26.09	0.001040	0.0834	0.000332	1:3.13
				Cd(NO ₃) ₂ ^g		
M085	4.61	27.58	0.001099	0.0895	0.000329	1:3.34
M086	3.79	22.68	0.000904	0.0895	0.000329	1:2.75

^a RMM = 167.14; Section 2.2.1. ^b Calculated for a starting volume of 25.0 cm³ plus volume of metal aliquot unless otherwise stated. ^c Calculated for starting volume of 25.0 cm³. ^d [Pb(II)] = 0.1007 mol dm⁻³; BDH AR Pb(NO₃)₂·6H₂O (> 99 %). ^e [Co(II)] = 0.03414 mol dm⁻³; BDH AR Co(NO₃)₂·6H₂O (> 99 %). ^f [Zn(II)] = 0.0999 mol dm⁻³; BDH AR Zn(NO₃)₂·6H₂O (> 99 %). ^g [Cd(II)] = 0.09215 mol dm⁻³; BDH AR Cd(NO₃)₂·6H₂O (> 99 %).

Ligand concentrations, together with metal ion concentrations for ligand/metal titrations, are collected for each of the alkylaminomethylenephosphonic acids, examined in this work; DEAMPH₂, NEIBMPH₄, the N-oxide derivative of NEIBMPH₄, CDTMPH₃ and DDDTMPH₃ in Tables 2.3.4, 2.3.5, 2.3.6, 2.3.7 and 2.3.8, respectively.

Table 2.3.5 Experimental conditions used for titrations of NEIBMPH₄.

Data file	Ligand ^a		Metal salt solution		[M]:[L]
	/mg	/μmol	/mol dm ⁻³ b	aliquot/cm ³ /mol dm ⁻³ b	
M096	3.08	13.21	0.000529 ^c		
M097	2.66	11.41	0.000456 ^c		
M100	2.58	11.07	0.000443 ^c		
M078	6.06	25.99	0.001040 ^c		
				Mn(NO ₃) ₂ ^d	
NMn1	5.89	25.27	0.000999	0.2949	0.000326 1:3.06
NMn3	5.98	25.65	0.001014	0.2949	0.000326 1:3.11
				Fe(NO ₃) ₃ ^{e,f}	
M074	5.98	25.66	0.001019	0.1856	0.000331 1:3.08
M075	6.16	26.43	0.001049	0.1856	0.000331 1:3.17
M077	6.19	26.56	0.001054	0.1856	0.000331 1:3.18
				Co(NO ₃) ₂ ^g	
M005	5.90	25.31	0.000998	0.3661	0.000493 1:2.02
M006	6.12	26.26	0.001040	0.2441	0.000330 1:3.15
				Ni(NO ₃) ₂ ^h	
M063	6.16	26.43	0.001032	0.6188	0.000998 1:1.03
M047	5.56	23.85	0.000942	0.3094	0.000499 1:1.89
M059	6.51	27.93	0.001108	0.2063	0.000333 1:3.33
				Cu(NO ₃) ₂ ⁱ	
M049	5.68	24.37	0.000951	0.6231	0.000976 1:0.97
M050	6.35	27.24	0.001076	0.3116	0.000494 1:2.18
M051	5.89	25.27	0.001002	0.2077	0.000319 1:3.14
				Zn(NO ₃) ₂ ^j	
M052	6.06	25.99	0.001030	0.2500	0.000989 1:1.04
M053	5.84	25.05	0.000997	0.1250	0.000497 1:2.01
M054	5.82	25.01	0.000997	0.0830	0.000331 1:3.01

[Table 2.3.5 continued]

				$\text{Cd}(\text{NO}_3)_2^{\text{k}}$		
M056	5.29	22.69	0.000898	0.271	0.000988	1:0.91
M057	5.25	22.52	0.000896	0.136	0.000499	1:1.80
M058	6.37	27.33	0.001089	0.0903	0.000332	1:3.28
				$\text{Pb}(\text{NO}_3)_2^{\text{l}}$		
M028	5.84	25.05	0.000992	0.2483	0.000990	1:1.00
M031	6.32	27.11	0.001079	0.1241	0.000497	1:2.17
M030	6.32	27.11	0.001081	0.0826	0.000332	1:3.26

^a RMM = 233.095; Section 2.2.2. ^b Calculated for a starting volume of 25.0 cm³ plus volume of metal aliquot unless otherwise stated. ^c Calculated for starting volume of 25.0 cm³. ^d [Mn(II)] = 0.02797 mol dm⁻³; BDH AR Mn(NO₃)₂·6H₂O (> 99 %). ^e [Fe(III)] = 0.04485 mol dm⁻³; H & W Fe(NO₃)₃·6H₂O (> 98 %). ^f Metal ion solution contained *aqu.* nitric acid, [H⁺] ca. 0.004 mol dm⁻³. ^g [Co(II)] = 0.03414 mol dm⁻³; BDH AR Co(NO₃)₂·6H₂O (> 99 %). ^h [Ni(II)] = 0.0404 mol dm⁻³; H & W Ni(NO₃)₂·6H₂O (> 98 %). ⁱ [Cu(II)] = 0.04012 mol dm⁻³; H & W Cu(NO₃)₂·3H₂O (> 98 %). ^j [Zn(II)] = 0.09990 mol dm⁻³; BDH AR Zn(NO₃)₂·6H₂O (> 99 %). ^k [Cd(II)] = 0.09215 mol dm⁻³; BDH AR Cd(NO₃)₂·4H₂O (> 99 %). ^l [Pb(II)] = 0.1007 mol dm⁻³; BDH AR Pb(NO₃)₂·6H₂O (> 99 %).

Table 2.3.6 Experimental conditions used for titrations of the N-oxide derivative of NEIBMPH₄.

Data file	Ligand ^a		Metal salt solution aliquot/cm ³	[M]:[L]
	/mg	/μmol		
M087	7.11	24.09	0.000964 ^c	
M088	3.45	11.69	0.000468 ^c	
M090	5.85	19.82	0.000793 ^c	
			$\text{Cu}(\text{NO}_3)_2^{\text{d}}$	
M091	7.16	24.26	0.000947	1:0.97
M092	6.99	23.68	0.000936	1:1.89

^a RMM = 295.165; Section 2.2.5. ^b Calculated for a starting volume of 25.0 cm³ plus volume of metal aliquot unless otherwise stated. ^c Calculated for starting volume of 25.0 cm³. ^d [Cu(II)] = 0.04012 mol dm⁻³; H & W Cu(NO₃)₂·3H₂O (> 98 %).

Table 2.3.7 Experimental conditions used for titrations of CDTMPH₃.

Data file	Ligand ^d		Metal salt solution		[M]:[L]
	/mg	/μmol	/mol dm ⁻³ b	aliquot/cm ³	
TC2	6.06	12.36	0.000494 ^c		
TC3	6.35	12.95	0.000518 ^c		
TC4	6.60	13.46	0.000539 ^c		
				Mn(NO ₃) ₂ ^d	
TMn1	6.29	12.83	0.000504	0.4469	0.000491 1:1.03
TMn2	6.38	13.02	0.000511	0.4469	0.000491 1:1.04
TMn3	7.06	14.40	0.000566	0.4469	0.000491 1:1.15
				Fe(NO ₃) ₃ ^{e,f}	
TFe1	6.88	14.03	0.000559	0.0929	0.000166 1:3.37
TFe2	5.64	11.51	0.000459	0.0929	0.000166 1:2.76
TFe3	6.10	12.44	0.000496	0.0929	0.000166 1:2.99
				Co(NO ₃) ₂ ^g	
TCo1	6.04	12.32	0.000486	0.3661	0.000493 1:0.99
TCo2	5.77	11.77	0.000464	0.3661	0.000493 1:0.94
TCo3	5.91	12.06	0.000475	0.3661	0.000493 1:0.96
				Ni(NO ₃) ₂ ^h	
TNi2	6.01	12.26	0.000484	0.3094	0.000494 1:0.98
TNi3	6.42	13.10	0.000517	0.3094	0.000494 1:1.05
TNi4	6.28	12.81	0.000506	0.3094	0.000494 1:1.03
				Cu(NO ₃) ₂ ⁱ	
TCu1	6.60	13.46	0.000532	0.3116	0.000494 1:1.08
TCu4	5.93	12.10	0.000478	0.3116	0.000494 1:0.97
TCu5	6.38	13.01	0.000514	0.3116	0.000494 1:1.04
				Zn(NO ₃) ₂ ^j	
TZn1	6.03	12.30	0.000490	0.1250	0.000497 1:0.99
TZn2	6.68	13.63	0.000542	0.1250	0.000497 1:1.09
TZn3	6.07	12.38	0.000493	0.1250	0.000497 1:0.99
				Pb(NO ₃) ₂ ^k	
TPb1	6.67	13.61	0.000452	0.1241	0.000497 1:1.09
TPb2	6.03	12.30	0.000490	0.1241	0.000497 1:0.99
TPb3	5.82	11.87	0.000473	0.1241	0.000497 1:0.95

[Table 2.3.7 continued]

Data file	Ligand ^a		Metal salt solution			[M]:[L]
	/mg	/μmol	/mol dm ⁻³ ^b	aliquot/cm ³	/mol dm ⁻³ ^b	
TGd1	5.54	11.30	0.000447	0.2790	0.000494	1:0.91
TGd2	6.33	12.91	0.000514	0.1395	0.000248	1:2.07
TGd5	6.22	12.69	0.000502	0.2790	0.000494	1:1.02
TGd6	5.83	11.89	0.000473	0.1395	0.000248	1:1.91
TGd8	5.80	11.83	0.000472	0.0930	0.000166	1:2.84

^a RMM = 490.21; Section 2.2.4. ^b Calculated for starting volume of 25.0 cm³ plus volume of metal aliquot unless otherwise stated. ^c Calculated for a starting volume of 25.0 cm³. ^d [Mn(II)] = 0.02797 mol dm⁻³; BDH AR Mn(NO₃)₂·6H₂O (> 99 %). ^e [Fe(III)] = 0.04485 mol dm⁻³; H & W Fe(NO₃)₃·6H₂O (> 98 %). ^f Metal ion solution contained aqueous nitric acid, [H⁺] ca. 0.004 mol dm⁻³. ^g [Co(II)] = 0.03414 mol dm⁻³; BDH AR Co(NO₃)₂·6H₂O (> 99 %). ^h [Ni(II)] = 0.0404 mol dm⁻³; H & W Ni(NO₃)₂·6H₂O (> 98 %). ⁱ [Cu(II)] = 0.04012 mol dm⁻³; H & W Cu(NO₃)₂·3H₂O (> 98 %). ^j [Zn(II)] = 0.0999 mol dm⁻³; BDH AR Zn(NO₃)₂·6H₂O (> 99 %). ^k [Pb(II)] = 0.1007 mol dm⁻³; BDH AR Pb(NO₃)₂·6H₂O (> 99 %). ^l [Gd(III)] = 0.04479 mol dm⁻³; BDH AR Gd(NO₃)₃·6H₂O (> 99 %).

Table 2.3.8 Experimental conditions used for titrations of DDDTMPH₃.

Data file	Ligand ^a		Metal salt solution		[M]:[L]	
	/ng	/μmol	/mol dm ⁻³ ^b	aliquot/cm ³ /mol dm ⁻³ ^b		
PBI3	6.78	12.28	0.000491 ^c			
PBI9	3.83	6.93	0.000277 ^c			
PB10	3.88	7.03	0.000281 ^c			
PB11	3.78	6.84	0.000274 ^c			
				Cu(NO ₃) ₂ ^d		
PCu1	6.30	11.40	0.000450	0.3115	0.000494	1:0.91
PCu2	6.94	12.57	0.000496	0.3115	0.000494	1:1.00
PCu3	6.68	12.09	0.000478	0.3115	0.000494	1:0.97
				Zn(NO ₃) ₂ ^e		
PZn1	7.12	12.87	0.000513	0.1250	0.000497	1:1.03
PZn2	6.88	12.46	0.000497	0.0625	0.000249	1:2.00
PZn3	6.09	11.03	0.000440	0.0625	0.000249	1:1.77
PZn4	6.41	11.61	0.000462	0.1250	0.000497	1:0.93
PZn5	6.65	12.04	0.000479	0.1250	0.000497	1:0.96
				Cd(NO ₃) ₂ ^f		
PCd1	6.33	11.46	0.000456	0.1356	0.000497	1:0.92
PCd2	6.86	12.42	0.000494	0.1356	0.000497	1:0.99
PCd3	6.25	11.32	0.000450	0.1356	0.000497	1:0.91
				Pb(NO ₃) ₂ ^g		
PPb1	6.70	12.13	0.000483	0.1240	0.000497	1:0.97
PPb2	6.44	11.66	0.000464	0.1240	0.000497	1:0.93
PPb3	6.54	11.84	0.000471	0.1240	0.000497	1:0.95

^a RMM = 552.282; Section 2.2.6. ^b Calculated for starting volume of 25.0 cm³ plus metal aliquot unless otherwise stated. ^c Calculated for starting volume of 25.0 cm³. ^d [Cu(II)] = 0.04012 mol dm⁻³; H & W Cu(NO₃)₂·3H₂O (> 98 %). ^e [Zn(II)] = 0.0999 mol dm⁻³; BDH AR Zn(NO₃)₂·6H₂O (> 99 %). ^f [Cd(II)] = 0.09215 mol dm⁻³; BDH AR Cd(NO₃)₂·4H₂O (> 99 %). ^g [Pb(II)] = 0.1007 mol dm⁻³; BDH AR Pb(NO₃)₂·6H₂O (> 99 %).

2.3.6 Data processing

Data files from 'ligand only' and ligand/metal titrations were created and

stored on disc during execution of the BBC program S.SCMTITR.⁸ They contained values for E_0 , pK_a , initial reactant concentrations, mean sample temperature and data for potential vs volume of base added. These data files were converted into ASCII format using the BBC program DECDATA,¹⁰ and then transferred to a DEC VAX 11-780 mainframe computer (VMS version 5.4-3) using the Termulator¹¹ file transfer utility.

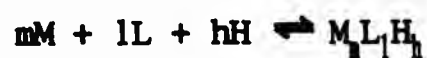
Stability constants from ligand and ligand/metal titration data were obtained using the FORTRAN 77 program SUPERQUAD¹² operating on the DEC VAX 11-780 mainframe computer. Refinement of the results for a specific equilibrium model (e.g. MLH, MLH₂ etc.) was achieved by minimisation of the 'fit' parameters [*i.e.* chi-squared (χ^2 , a statistic based on the weighted residuals) and sigma (σ , the sample standard deviation)]; these are generated as part of the program's output. Variation of the pH range of the data (by elimination of consecutive data points from either 'end' of the full data set) was used to obtain an acceptable fit between calculated and experimental data. Ligand, metal and base concentrations were held constant during refinement, whereas, the total acid concentration, $[H^+]$, was not fixed, but was recalculated during the execution of the program. Protonation constants, obtained from analysis of titration data for the ligand, were held constant during analysis of data in ligand/metal files.

2.3.7 Computational methods

The computer program SUPERQUAD¹² (coded in FORTRAN 77) has been developed from the programs MINIQAD¹³⁻¹⁵ and MIQUV,¹⁶ and is widely used to calculate formation constants of species used in solution equilibria from data obtained from potentiometric titrations. It is an extremely powerful general purpose computer program for stability constant determination. It can handle data from all known systems of potentiometric titration, including batch titrations, electrode readings in pH or millivolts, and systems where the number of electrodes is equal to the number of reactants. It also caters for ion-selective electrodes whose response is other than Nernstian. Refinement of ligand, metal, and proton concentrations and standard potentials (obtained from cell calibration) are individually possible, and concentrations can be refined individually or they can be constrained to refine together.

SUPERQUAD (as well as MINIQAD AND MIQUV) uses the Newton least-squares method to refine the overall formation constants (β) of species in an assumed model

of the equilibrium system. The formation of each species is represented:



where M, L, H ... are the uncomplexed reactant species (up to four are allowed), $M_l L_l H_h$... is the product species and m, l, h, are the stoichiometric reaction coefficients.

The overall formation constants (β) are defined as follows:

$$\beta_{alh} = \frac{[M_l L_l H_h]}{[M]^m [L]^l [H]^h}$$

where $[M_l L_l H_h]$ is the concentration of the complex species, and [M], [L], and [H] are the concentrations of the uncomplexed reactant species, at equilibrium. The program calculates the free concentration of metal ion [M], ligand [L] and proton $[H^+]$ from the emf data for each titration data point using mass-balance equations applicable to each reactant in the system *i.e.* M, L, H (Section 1.3.2).

SUPERQUAD calculates β values which minimise the sum of the squared residuals between the observed, E^{exp} , and calculated, E^{calc} , emf values. The sum of squared residuals function, U, is given by the following equation.

$$U = \sum_i^i w_i (E_i^{exp} - E_i^{calc})^2$$

where w_i is the weighting factor assigned to the *i*th observation. The calculated stability constants, the 'fit parameters' (*i.e.* χ^2 , σ and the relative standard deviation for each $\log \beta$), together with a graphical display of the weighted residuals for each titration data point (a plot of the error in the difference between the measured electrode potentials and the calculated electrode potentials for each titration point) are generated after a successful convergence of U.¹² A fit at a confidence level of 95 % or greater is associated with an experimentally determined χ^2 of less than 12.60.

The refinement of ligand protonation and metal/ligand stability constants to fit the experimental data involved input of estimated values of $\log \beta$ for each species in the equilibrium models being refined. The pH range under study was

then varied by elimination of data points from the full data set in order to achieve an acceptable fit as measured by χ^2 and σ values after each separate refinement of the selected models. Refined $\log \beta$'s with their relative standard deviations were produced. This procedure was repeated until χ^2 was less than 12.60, σ and relative standard deviations for each $\log \beta$ were as low as possible, and the graphical display of weighted residuals was acceptable. The strategy employed here in calculations of metal/ligand stability constants was to fix values of previously determined protonation constants and then refine for several different model systems for the equilibrium. The concentration of acidic protons from both the acid stock solution (HNO_3 , $0.004 \text{ mol dm}^{-3}$) and the ligand was treated as a refinable parameter in processing all data files.

2.3.8 Species' abundance vs pH diagrams

Protonation and metal/ligand stability constants refined by SUPERQUAD¹² were input into the program SPE¹⁷ (as $\log \beta$'s) along with reactant concentrations and equilibrium models. SPE creates a numerical file, as output, containing information about species' distributions. These files, and hence species' distributions, were initially viewed graphically with the program SPECIES¹⁸ and finally obtained as a hard copy using the GW-BASIC program HPLOT¹⁹ adapted for the Hewlett-Packard plotter.

2.4 Determination of pH-dependence of ^{31}P nmr chemical shift for some alkyl-aminomethylenephosphonic acids and their derivatives

Using *aqueous* solutions of the alkylaminomethylenephosphonic acids DEAMP₂, NEIBMP₄, CDTMP₃ and DDDTMP₃ (see Section 2.3) in nmr tubes, small volume acid/base titrations were performed. The ^{31}P nmr spectrum was recorded for each titration point in order to establish the dependence of ^{31}P chemical shift (δ) on pH for these and related compounds.

The interaction of DEAMP₂ with *aqueous* solutions of hydrogen peroxide under similar conditions as a function of pH, was also studied using ^{31}P nmr/pH titrations.

The possible interaction of DEAMP₂ with sodium stannate as a function of pH in *aqu.* solution was also studied using the same procedure.

2.4.1 Reagents used

The origins and purities of reagents used in studying the alkylaminomethylene-phosphonic acids by ^{31}P nmr/pH titrations, are shown in Table 2.4.1.

Table 2.4.1 Origin and purity of reagents used in ^{31}P nmr/pH titrations.

Reagent	Source	Purity ^a
Phosphoric acid	BDH	AnalaR, <i>aqu.</i> > 85 %
Deuterium oxide	Goss	99.9 %
Potassium nitrate ^b	BDH	ARISTAR, > 99.5 %
Nitric acid	BDH	AnalaR ^c
Potassium hydroxide	BDH	AnalaR ^c
Hydrogen peroxide ^d	Laporte	<i>aqu.</i> 35 %
Nitric acid	May & Baker	68 % ^e
Ammonia ^f	BDH	35 %
Sodium stannate	Laporte	not known
Tetraethylammonium hydroxide	Aldrich	<i>aqu.</i> 20 % w/w
Water	§	§

^a Manufacturer's estimate. ^b Dried in an oven for one day at 120 °C and stored in a desiccator over silica gel before use. ^c 'ConVol' solutions prepared from AR grade reagents. ^d Unstabilised hydrogen peroxide. ^e 68 % minimum; used for adjusting pH of hydrogen peroxide solutions. ^f Specific gravity 0.888. [§] Purified by reverse osmosis to BS3978 specification on a R050-100-200 Reverse Osmosis unit.

2.4.2 ^{31}P nmr spectra

During nmr/pH titrations, spectra were obtained in the broad band proton decoupled mode at 32.392 MHz on a Bruker WP80 or WP80SY FT nmr spectrometers, using *aqu.* 85 % phosphoric acid (H_3PO_4) as an external reference. For experiments on DEAMPH₂, two nmr tubes were used to provide the reference by sample substitution. A 5 mm outside diameter (o.d.) co-axial tube containing the reference was inserted into a 10 mm o.d. nmr tube containing the ligand solution. The sample solution upon which the titration was performed was contained in a separate 10 mm o.d. nmr tube. This method (the 'two tube method') was used to overcome the unfavourable dynamic ranges encountered when the reference solution was contained in a co-axial tube of 5 mm o.d. within

the titration sample.

In later experiments, a 'one tube method' was used. This involved a co-axial tube (8 mm o.d.) containing the ligand solution for titration, inserted into a 10 mm o.d. nmr tube containing the reference. This arrangement resulted in a thin capillary film of reference solution between the two tubes. Deuterium oxide (D_2O) in the sample solution was used as a lock signal throughout.

Typical spectrometer operating parameters: pulse length, 1 μ s; offset (01), 2700 Hz; delay, 3.0 s; spectral width, 1602.6 Hz; acquisition time, 5.1 s; number of scans, 110; data points, 16 K; line broadening, 1 Hz; temperature, ambient (298 K).

2.4.3 pH Measurements

All pH measurements were carried out using a Corning Series 180 pH/Ion Meter. The pH was recorded with a thin stem combination electrode (CMAWL/3.7/200, Russell pH Ltd.) placed in the nmr tube. The electrode was calibrated, before a two-day run, by using NBS standard 0.05M potassium hydrogen phthalate and 0.025M phosphate buffers, prepared using standard procedures.^{7e} The pH values of the buffer were corrected for temperature.^{7e}

2.4.4 Preparation of aqueous solutions for ^{31}P nmr/pH titrations

2.4.4(a) Acid stock solution

Aqu. nitric acid (40 cm^3 , 0.1 $mol\ dm^{-3}$), potassium nitrate (9.706 g), and deuterium oxide (10 cm^3) were placed into a volumetric flask (100 cm^3) and made up to the mark with water.

2.4.4(b) Base solution

Degassed aqu. potassium hydroxide (1.0 $mol\ dm^{-3}$) was prepared by sonication and placed into a motorised piston burette (Metrohm 655 Dosimat) under nitrogen as described in Section 2.3.3.

2.4.4(c) Ligand stock solution

The concentration of ligand used in the stock solution depended on the protonation sites, *i.e.* it was necessary to use sufficient acid in order to ensure that all the protonation sites of the ligand were protonated. A concentration of ca. 0.02 $mol\ dm^{-3}$ in the phosphonic acid group was found to be satisfactory in these experiments. The ligand was weighed out by

difference into a sample tube (15 cm³) and an aliquot of the acid stock solution (10.0 cm³) was added to give a solution of specification (for example for DEAMPH₂): [DEAMPH₂] = 0.02 mol dm⁻³, [HNO₃] = 0.04 mol dm⁻³, [KNO₃] = 0.96 mol dm⁻³, 10 % D₂O, and ionic strength I = 1.0 mol dm⁻³.

2.4.5 ³¹P nmr/pH titrations of DEAMPH₂

Into each of two 10 mm diameter nmr tubes, an aliquot of the ligand stock solution (3.0 cm³) was added. One tube, the 'sample', was used without further addition, and to the other, the 'reference', a co-axial tube (5 mm o.d.) containing *aqu.* 85 % phosphoric acid was added.

Initially, the pH was determined for the ligand solution both the sample and reference tubes. The ³¹P nmr spectrum was then obtained for the reference, and the H₃PO₄ signal was assigned to 0.00 ppm. The ³¹P nmr spectrum of the sample was determined and δ³¹P obtained.

A fixed aliquot (0.012 cm³) of base solution was added to the sample from the motorised piston burette. The tip of the burette was washed with water and wiped dry before being inserted into the sample solution. After addition of the base, the tip was slowly withdrawn to minimise the amount of solution extracted with the tip. The nmr tube was then gently shaken and the pH continuously monitored until the reading was stable (*i.e.* within ±0.01 pH units). Care was also taken to withdraw the electrode in such a way as to minimise loss of sample solution. The ³¹P nmr spectrum of the sample was determined. The cycle of addition of base, determination of pH and ³¹P nmr spectrum was then repeated to cover the pH range 1.5-13.0. As the pH change *per* aliquot of base varied (*e.g.* became larger near the endpoint regions) the aliquot was decreased or increased as appropriate.

The H₃PO₄ reference signal was (*via* sample substitution) recorded after every 5 titration points and reassigned to 0.00 ppm. In no case did the reference signal deviate from its original position by more than 0.05 ppm and the deviation was generally much less than this. The pH of the 'reference' ligand solution was also recorded and shown to be constant. Usually 25-30 points were recorded for each nmr/pH titration.

At the end of the titration, a volume of base solution, equal to the total volume delivered into the sample solution, was added to the sample solution

surrounding the *aqu.* phosphoric acid reference. Determination of the ^{31}P nmr spectrum indicated that the position of the H_3PO_4 reference signal was independent of the pH of the sample solution surrounding the co-axial tube and providing the deuterium lock.

2.4.6 pH Dependence of ^{31}P nmr spectrum of DEAMPH_2 treated with aqueous hydrogen peroxide

All glassware in contact with hydrogen peroxide was pre-treated with conc. nitric acid and washed thoroughly with water.

The ligand solution ($[\text{DEAMPH}_2] = 0.02 \text{ mol dm}^{-3}$) was prepared by dissolving DEAMPH_2 in 35 % hydrogen peroxide (20 cm^3) and deuterium oxide (10 % v/v). The solution was divided into four parts (1-4) each of 5 cm^3 volume. The pH of each solution was adjusted to the required value using conc. nitric acid and/or *aqueous ammonia* (Section 2.4.3). The solutions were left to stand for one week, and the hydrogen peroxide was then decomposed by adding a platinum wire catalyst and heating the solution to *ca.* 50°C until bubble evolution had stopped (*ca.* 3 hours).

The pH and the ^{31}P nmr spectrum of each solution (1-4) after decomposition were determined. $\delta^{31}\text{P}$ was referenced to *aqueous* 85 % phosphoric acid by sample substitution.

2.4.7 ^{31}P nmr/pH titration of DEAMPH_2 in the presence of sodium stannate

A solution (10 cm^3) of DEAMPH_2 and sodium stannate was prepared from acid stock solution to give a solution of specification: $[\text{DEAMPH}_2] = 0.01 \text{ mol dm}^{-3}$, $[\text{sodium stannate}] = 0.02 \text{ mol dm}^{-3}$, $[\text{HNO}_3] = 0.04 \text{ mol dm}^{-3}$, $[\text{KNO}_3] = 1.0 \text{ mol dm}^{-3}$, $\text{D}_2\text{O} = 10 \text{ % v/v}$. The resulting solution, which was slightly cloudy, was filtered through a fine glass filter paper (under a positive pressure of nitrogen gas) into a sample tube. Two aliquots (3 cm^3) of this solution were placed in 10 mm o.d. nmr tubes, one to be treated as the 'sample', and the other as the 'reference', for nmr/pH titrations by the 'two tube' method.

The titration procedure was followed as in Section 2.4.5 to obtain both the pH and the ^{31}P nmr spectrum for each titration point.

2.4.8 ^{31}P nmr/pH titration of NEIBMPH_4 and its *N*-oxide derivative

The ligand, NEIBMPH_4 (0.02348 g, 0.01 mol dm^{-3}) was weighed into a sample

bottle (15 cm³), into which the acid stock solution (10.0 cm³) was added. From this solution, 3.0 cm³ was pipetted into an nmr tube (8 mm o.d.). Initially, the pH was determined for the ligand solution in the internal nmr tube (8 mm o.d.). The ³¹P nmr spectrum was then obtained for the sample and the reference using the 'one-tube' method. The H₃PO₄ reference signal was assigned to 0.00 ppm. A fixed aliquot of base solution was then added to the sample from the motorised piston burette. The nmr tube was gently shaken and the pH monitored until stable (± 0.01 pH units). The ³¹P nmr spectrum of the sample and the reference was determined. The cycle of addition of base, determination of pH and ³¹P nmr spectrum was repeated to cover the pH range (2-13).

The reference signal was reassigned to 0.00 ppm after every 5 titration points. In no case did the reference signal deviate from its original position by more than 0.07 ppm and the deviation was generally much less than this. Usually 20-26 points were recorded for each nmr/pH titration.

The N-oxide (0.02453 g, 0.01 mol dm⁻³) was weighed into a sample tube (15 cm³). Acid stock solution (10.0 cm³) was pipetted into the sample tube. Subsequently, 3.0 cm³ of this solution was pipetted into an nmr tube (8 mm o.d.) and the titration was carried out as for NEIBMPH₄.

2.4.9 ³¹P nmr/pH titration of DDDTMPH₉

The ligand, DDDTMPH₉ (0.02724 g), was weighed into a sample bottle (15 cm³). To this, acid stock solution (10.0 cm³) was added (pipette) and then 3.0 cm³ of this solution was added to the nmr tube (8 mm o.d.) to give a ligand concentration of 0.0049 mol dm⁻³. The titration procedure was followed as described in Section 2.4.8.

2.4.10 ³¹P nmr/pH titration of DDDTMPH₉ in the absence of excess acid

A stock solution was prepared by placing potassium nitrate (10.1261 g, 1.0 mol dm⁻³) and D₂O (10 cm³) in a volumetric flask (100 cm³) and making up to the mark with water.

The ligand, DDDTMPH₉ (0.02689 g), was weighed into a sample tube into which the stock solution (10.0 cm³) was pipetted to give a solution with [DDDTMPH₉] = 0.00487 mol dm⁻³. 3.0 cm³ of this solution was pipetted into the nmr tube (8 mm o.d.) and the titration procedure described in Section 2.4.8 was followed.

2.4.11 ^{31}P nmr/pH titration of DDDTMPH₃ against tetraethylammonium hydroxide
An aqueous solution of tetraethylammonium hydroxide, (20 % w/w, 250 cm³) was made up to the mark in a 500 cm³ volumetric flask with water. The solution was standardised against hydrochloric acid using methyl red indicator; [tetraethylammonium hydroxide] = 0.69 mol dm⁻³.^{7d}

No attempt was made to maintain constant ionic strength during titrations using tetraethylammonium hydroxide. The ligand, DDDTMPH₃ (0.02792 g), was weighed into a sample tube and 10.0 cm³ of D₂O/H₂O solution (10 % v/v) was added. 3.0 cm³ of this solution was pipetted into the nmr tube (8 mm o.d.) to yield a solution with [DDDTMPH₃] = 0.00506 mol dm⁻³, and titrated against aqueous tetraethylammonium hydroxide following the method described in Section 2.4.8.

2.5 Instrumental methods

2.5.1 Infrared spectra

Samples were prepared as KBr discs (16 mm diameter). All infrared spectra were obtained using either of the instruments noted below (typical conditions are given in parentheses): Perkin-Elmer 781 (range 4000–600 cm⁻¹, scan time 3 mins, noise filter 1); BIO-RAD FTS40 Fourier transform infrared spectrometer [background spectra were obtained from KBr discs (16 mm diameter), range 4000–400 cm⁻¹, number of scans 16, resolution 8 cm⁻¹].

2.5.2 ^1H nmr spectra

^1H nmr spectra were obtained using a Bruker AM250 spectrometer operating at 250.13 MHz in pulse Fourier transform (pFt) mode. Samples for ^1H nmr were dissolved in deuterated solvents containing tetramethylsilane (SiMe₄) as an internal standard. Spectra of water soluble samples were obtained in deuterated water (D₂O) containing sodium trimethylsilylpropionate (TSP-d₄) as the internal standard; all nmr spectra were recorded at the natural pH of the ligand solution. Typical operating conditions: ambient temperature (300 K), pulse width 2.0 μs, delay 5 s, acquisition time 3 s, number of points 16 K.

2.5.3 ^{13}C nmr spectra

^{13}C nmr spectra were obtained using a Bruker AM250 pFt spectrometer operating

at 62.90 MHz. Samples were dissolved in deuterated solvents and tetramethylsilane (SiMe_4) was used as the internal standard. Spectra of water soluble samples were obtained in deuterated water (D_2O) containing sodium trimethylsilylpropionate (TSP-d_4) as the internal standard; all nmr spectra were recorded at the natural pH of the ligand solution. Typical operating conditions: ambient temperature (300 K), pulse width 2.0 μs , acquisition time 1 s, delay 3 s, number of points 32 K.

2.5.4 ^{31}P nmr spectra

^{31}P nmr spectra, other than for ^{31}P nmr/pH titrations, were obtained using a Bruker AM250 pFt spectrometer operating at 101.26 MHz. Samples were dissolved in deuterated solvents and aqueous phosphoric acid (H_3PO_4 , 85 %) was used as the external standard.

All nmr spectra were recorded at the natural pH of the ligand solution. Typical operating conditions: ambient temperature (300 K), pulse width 3.0 μs , acquisition time 2 s, delay 5 s, number of points 32 K.

2.5.5 ^{119}Sn nmr spectra

^{119}Sn nmr spectra were obtained using a Bruker AM250 pFt spectrometer operating at 93.28 MHz. Samples were dissolved in deuterated solvents and tetramethyltin (SnMe_4) was used as the external standard. Typical operating conditions: ambient temperature (300 K), pulse width 6.0 μs , acquisition time 0.5 s, number of points 64 K.

2.5.6 Elemental analysis

Analyses for the carbon, hydrogen and nitrogen content of samples were obtained using a Carlo Erba 1106 Elemental Analyser.

2.5.7 Mass spectra

Electron impact (e.i.) spectra were obtained using an AEI MS-9, or a Kratos Profile, Mass Spectrometer operating in positive ion mode.

2.5.8 UV-visible spectra

The absorption spectra of aqueous solutions of metal complexes of alkylamino-methylenephosphonic acids were obtained on a Shimadzu UV-2100 UV-visible spectrophotometer in the range 190-700 nm at concentrations ranging from

0.001–0.006 mol dm⁻³ depending upon the sample solubility. Quartz cells of 1 cm path length were used.

2.5.9 Magnetic susceptibilities

Magnetic susceptibilities were measured at 24.4 °C (297.4 K) by the Gouy method using a JMC magnetic susceptibility balance with a permanent magnet. The balance was calibrated against the solid complex Hg[Co(NCS)₄].²⁰

2.5.9(a) Procedure used to measure magnetic susceptibilities

The Gouy tube was cleaned with dilute sulphuric acid, rinsed thoroughly with distilled water, and dried using a stream of nitrogen gas. When the Gouy tube was completely dry, the weight of the Gouy tube was noted down (4 decimal-place balance).

The JMC balance was zeroed, and the Gouy tube was then placed into the sample holder. The reading was allowed to settle (a few minutes) and then noted. The Gouy tube was taken out of the sample holder and the calibration sample [HgCo(SCN)₄], which had been ground before hand using a pestle and mortar, was slowly added with a plastic spatula. The Gouy tube was gently tapped on the bench a few times after addition of each small portion of calibrant, to ensure that the packing of calibration sample was homogenous. Enough calibration sample was added to ensure that the length of the calibration sample in the Gouy tube was between 2.5–3.5 cm. The tube and contents were weighed as before. The Gouy tube was then placed in the sample holder of the JMC balance, and the reading allowed to settle for a few minutes. The reading and the temperature were noted.

2.5.9(b) Sample preparation

The sample was ground using a pestle and mortar to produce a uniform powder. The Gouy tube was cleaned as before and allowed to dry. The empty Gouy tube was weighed, and then placed into the sample holder. The reading was noted after the reading had stabilised. The temperature was also noted.

Enough sample was added to the Gouy tube, using a plastic spatula, to ensure the length of the sample was between 2.5–3.5 cm. Again, the Gouy tube was gently tapped on the bench during addition to ensure homogenous packing. The sample was then placed in the sample holder, the temperature noted, and the reading allowed to stabilise before being noted.

2.5.9(c) Calculation

The calibration constant, c , was determined from the following equation:

$$X_g = \frac{c \times l \times (R - R_0)}{m \times 10^9}$$

where X_g is the mass susceptibility (c.g.s), l is the sample length (cm), m is the mass in (g), R is the balance reading for the Gouy tube plus the sample and R_0 is the balance reading for the empty Gouy tube. The calibration procedure was repeated; the results are shown in Table 2.5.1.

Armed with the value of c , the mass susceptibility (X_g) of the sample was determined. The molar susceptibility (X_M) of the sample was obtained from:

$$X_M = \text{RMM} \times X_g$$

A diamagnetic correction was calculated for all the atoms in the sample²² and then added to the molar susceptibility (X_M) to produce the actual molar susceptibility (X'_M). This value is then used to calculate the effective magnetic moment (μ_{eff}) of the sample under investigation:

$$X'_M = X_M + \text{diamagnetic correction}$$

$$\mu_{\text{eff}} = 2.84 \sqrt{(T \times X'_M)}$$

where T is the absolute temperature in Kelvin.

Table 2.5.1 Measurements made for the calibration sample $\text{HgCo}(\text{SCN})_4$.

	(C1)	(C2)	Mean
Mass of $\text{HgCo}(\text{SCN})_4$ used /g	0.3326	0.3118	
Length of $\text{HgCo}(\text{SCN})_4$ used /cm	3.2	3.2	
Reading of empty Gouy tube (R_0)	-006	-006	
Reading of Gouy tube plus $\text{HgCo}(\text{SCN})_4$ (R)	605	571	
Mass susceptibility X_g / 10^{-6} c.g.s	16.198	16.204	
Calibration constant	2.6190	2.7944	2.707
Temperature / °C	24.5	24.4	24.4

Table 2.5.2 Measurements made for the sample.

	[Cu(NEIBMPH ₃) ₂]
Mass of sample used /g	0.2031
Length of sample used /cm	3.1
Reading of empty Gouy tube (R ₀)	-004
Reading of Gouy tube plus sample (R)	67
Mass susceptibility X _g /10 ⁻⁶ c.g.s	2.9333
Molar susceptibility X _m /10 ⁻³ c.g.s	1.5479
Diamagnetic correction X' _d /10 ⁻⁶ c.g.s	339.48
X' _m /10 ⁻⁶ c.g.s	188.75
Average temperature / °C	24.4
Effective magnetic moment (μ) /BM	2.1

2.6 Single crystal X-ray diffraction methods

2.6.1 Data collection²¹

X-Ray data for single crystals of DEAMPH₂ and CDTMPH₃ (Chapter 7), were collected on a Philips PW1100 four-circle diffractometer with graphite crystal monochromated Mo-Kα radiation (λ = 0.7107 Å) in the θ-range of 3-25° and a scan width of 0.8°.

The computer systematically adjusts the four-circles, which brings all the sets of planes into the diffracting position. The three-circles (ω, χ, φ,) are needed to get the crystal into the correct orientation, the fourth-circle (2θ) brings the counter into position. Initially, the computer moves the four circles in small increments until 25 diffracted beams(reflections) have been detected and recorded (Peak hunting). From the 25 sets of data (for the four-circles) the computer calculates a,b,c and α,β,γ for the unit cell. Lastly, the computer is then set to drive the four circles to all the settings of ω, χ, φ and 2θ to record all the reflections produced by the crystal.

2.6.2 Structure solution and refinement of diethylaminomethylenephosphonic acid, DEAMPH₂

The coordinates of the carbon, nitrogen and phosphorus atoms were located by direct methods.²² Absorption corrections were applied to the data after initial refinement with isotropic thermal parameters for all atoms; before

application of absorption corrections, $R = 0.101$. After absorption corrections has been applied, $R = 0.0778$. Difference Fourier synthesis, calculated using data with $\sin \theta < 0.35$, revealed the positions of the hydrogen atoms H(01) and H(n1). The remaining hydrogen atoms, H(1a), H(1b), H(21a), H(21b), H(22a), H(22b), H(22c), H(31a), H(31b), H(32a), H(32b) and H(32c) were given idealised positions; C-H 1.08 Å, $U = 0.08 \text{ \AA}^2$. After several cycles of refinement with anisotropic thermal parameters assigned to all the non-hydrogen atoms, the refinement converged with $R = 0.0498$ and $R_w = 0.489$.²³

2.6.3 Structure solution and refinement of (\pm)-trans-cyclohexane-1,2-diamine-tetrakis(methylenephosphonic acid), $CDTMPH_8 \cdot H_2O$.

The coordinates of the phosphorus atoms, P(1a), P(1b), P(1c), and P(1d), some of the oxygen atoms, O(1a), O(1b), O(2c), O(3c), O(1d), O(2d) and O(3d), the two nitrogens, N(1) and N(2), and some of the carbon atoms C(1a), C(1b), C(1), C(2) and C(4) were located from direct methods.²² These coordinates were included in the first Fourier synthesis to calculate the scale factor, with one cycle of least-square refinement of the coordinates and thermal parameters converging at $R = 0.1796$ and $R_w = 0.1822$. The Fourier map revealed the positions of all remaining non-hydrogen atoms, including the water molecule. Absorption corrections were applied to the data after initial refinement with isotropic parameters for all the non-hydrogen atoms. Refinement of the data gave R values before and after absorption correction as 0.0778 and 0.0752, respectively. Difference Fourier syntheses, calculated using data with $\sin \theta < 0.35$, revealed the positions of the following hydrogen atoms; H(2n), H(1wa), H(1wb), H(2oa), H(3oa), H(2ob), H(2oc), H(3oc), H(2od), H(3od), H(3a), H(4b), H(5a), H(5b), H(6a), H(1a1), H(1b2), H(1c1) and H(1d2). However, all the carbon-bonded hydrogen atoms were placed in idealised positions (C-H 1.08 Å) and their thermal parameters fixed at 0.08 \AA^2 . In the final cycles of full-matrix least-squares refinement, all of the non-hydrogen atoms were assigned anisotropic thermal parameters, and this refinement converged with $R = 0.0420$ and $R_w = 0.0420$.²³

2.7 References

1. H. Lambourne, *J. Chem. Soc.*, 1922, 121, 2533.
2. A. G. Davies, L. Smith and P. J. Smith, *J. Organomet. Chem.*, 1972, 39, 279.
3. R. O. Day, V. Chandrasekhar, K. C. Kumara Swamy, J. M. Holmes S. D. Burton and R. R. Holmes, *Inorg. Chem.*, 1988, 27, 2887.
4. K. C. Kumara Swamy, C. G. Schmid, R. O. Day and R. R. Holmes, *J. Am. Chem. Soc.*, 1990, 112, 223.
5. K. Moedritzer and R. R. Irani, *J. Org. Chem.*, 1966, 31, 1603.
6. P. L. Biggins, S. E. Edwards, T. A. Lucas, R. W. Matthews, I. J. Scowen and C. J. L. Silwood, unpublished results.
7. A. Vogel, *Textbook of Quantitative Inorganic Analysis*, 4th Edition, 1978, Longman, Great Britain, 7(a) p 301; 7(b) p 304; 7(c) pp 316-336; 7(d) pp 569-570; 7(e) 587.
8. P. L. Biggins, S. E. Edwards, T. A. Lucas, R. W. Matthews, I. J. Scowen and C. L. J. Silwood, 'S.SCMITR,' unpublished BBC BASIC program.
9. P. L. Biggins, S. E. Edwards, T. A. Lucas and R. W. Matthews, 'S.SCMCAL,' unpublished BBC BASIC program.
10. P. L. Biggins, S. E. Edwards, R. W. Matthews, I. J. Scowen and C. J. L. Silwood, 'DECDATA,' unpublished BBC BASIC program.
11. 'TERMULATOR,' terminal emulation for the BBC MICRO, University of Surrey, 1984.
12. P. Gans, A. Sabatini and A. Vacca, *J. Chem. Soc., Dalton Trans.*, 1985, 1195.
13. A. Sabatini, A. Vacca and P. Gans, *Talanta*, 1974, 21, 53.
14. P. Gans, A. Sabatini and A. Vacca, *Inorg. Chim. Acta.*, 1976, 18, 237.
15. M. Micheloni, A. Sabatini and A. Vacca, *Inorg. Chim. Acta.*, 1977, 25, 41; A. Sabatini and A. Vacca, in *Computational Methods for the Determination of Stability Constants*, Ed. D. J. Leggett, 1985, Plenum Press, New York.
16. A. Vacca and A. Sabatini, in *Computational Methods for the Determination of Stability Constants*, Ed. D. J. Leggett, 1985, Plenum Press, New York.
17. R. J. Motekaitis, FORTRAN 77 program SPE, 1987; A. E. Martell and R. J. Motekaitis, *The Determination and Use of Stability Constants*, 1988, VCH Publishers, New York.
18. C. Crees, TURBO C program SPECIES, 1990.
19. C. J. L. Silwood, GW-BASIC program HPLOT, 1990.
20. B. N. Figgis and J. Lewis in, *Modern Coordination Chemistry: Principles*

and Methods, Eds. J. Lewis and R. G. Wilkins, 1960, Interscience, New York.

21. M. K. Cooper, P. J. Guerney and M. McPartlin, *J. Chem. Soc., Dalton Trans.*, 1987, 757.
22. N. Walker and D. Stuart, *Acta Cryst.*, 1983, A39, 158.
23. N. Y. Choi, unpublished results, 1994.

Chapter 3 Organotin cages, clusters and drums

3.1 Introduction

Over the last ten years', a new cluster chemistry of organotin compounds has been developed.¹⁻⁹ This class of compounds is based on the bonds formed between carboxylic and/or phosphorus based acids with organotin acids, *i.e.* bridged carboxylate and phosphate ligands to central tin atoms. It has been discovered that some of the organotin compounds prepared have demonstrated catalytic activity in polymerization and/or transesterification processes.¹⁰

It is well known that hydrogen peroxide is decomposed by small amounts of transition metal ions *e.g.* Fe(III), Cu(II) and Ni(II).¹¹ However, the presence of small quantities of alkylaminoalkylphosphonic and/or aminocarboxylic acids are known to stabilize hydrogen peroxide.¹²⁻¹⁴ In general stabilizers may act by either complexing metal impurities or forming colloids which adsorb impurities onto its surface.¹⁵ Hydrogen peroxide is also known to be stabilized by combination of both sodium stannate and aminomethylenephosphonic acids; this combination provides enhanced stability.¹⁶ In an attempt to understand the mechanism by which α -aminomethylenephosphonic acids and sodium stannate improve stability of hydrogen peroxide, it was assumed that some reaction between the two different types of stabilizers yielded species which complex or adsorb the offending metal ion impurities present in *aqueous* solutions of hydrogen peroxide.

It has been reported that reactions between organotin acids and phosphorus-based and/or carboxylic acids can produce many of the organotin clusters mentioned in Section 1.4;¹⁻¹⁰ the organotin compounds formed contain cavities which may play a role in sequestering metal ions (Section 3.2.8). To explore these possibilities, some previously prepared and some new organotin clusters were synthesised. Attempts were also made to synthesis clusters based on aminomethylenephosphonic acids.

All the organotin compounds prepared in this work were characterised by C, H, N elemental analysis, ir and nmr spectroscopy, where possible.

3.1.1 Preparation of the 'cage' cluster I,



In order to gain some experience in this relatively new field of organotin

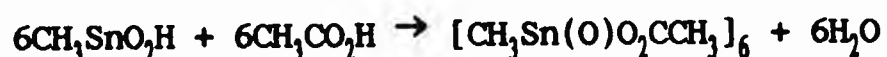
chemistry, a previously reported route was followed to prepare the 'cage' cluster I, $[(\text{CH}_3)_2\text{Sn}_2(\text{OH})(\text{O}_2\text{P}(\text{OC}_6\text{H}_5)_2)_3(\text{O}_3\text{POC}_6\text{H}_5)]_2$.⁹

The preparation of I involved the synthesis of the precursor methylstannonic acid, $\text{CH}_3\text{SnO}_2\text{H}$.¹ Organotin hydroxides and oxides are commonly obtained by the hydrolysis of the corresponding organotin chlorides under basic conditions. Methylstannonic, is a white, amorphous solid, which is insoluble in common organic solvents but soluble in some organic acids, e.g. acetic acid and trifluoroacetic acid. C, H, and N Elemental analysis was satisfactory with the formulation of $[\text{CH}_3\text{SnO}_2\text{H}]$ (Section 2.1.2). The melting point of $\text{CH}_3\text{SnO}_2\text{H}$ (313.4–328.8 °C) is characteristic of many organostannonic acids;^{1,17-19} the organostannonic acids are all solids which usually do not melt but decompose at temperatures above 300 °C.¹⁷ The low-molecular weight acids are insoluble in the common organic solvents and water; the higher-molecular weight acids are soluble in most organic solvents except petroleum ether and water.^{1,17} The stannonic acids are amphoteric, dissolving in sodium or potassium hydroxide and also in the halogen acids. Lambourne suggested that the stannonic acids, when freshly prepared, exist as cyclic trimers.¹ However, further condensation may occur on standing.¹

¹³C and ¹H nmr spectra for methylstannonic acid were obtained in deuterated trifluoroacetic acid ($\text{CF}_3\text{CO}_2\text{D}-d_1$) (Section 2.5). The ¹H nmr spectrum gave a singlet at 1.47 ppm overlapped with a pair of doublets (^{119/117}Sn satellites) due to the methyl protons coupling to the tin nuclei (I = -1/2) isotopes ¹¹⁹Sn (abundance: 8.6 %) and ¹¹⁷Sn (abundance: 7.6 %).

The ¹³C nmr spectrum for methylstannonic acid is unremarkable and showed a single resonance at 9.4 ppm due to the methyl carbon; there was no observable coupling between carbon and the tin nuclei (^{117/119}Sn).

The next stage in the preparation of the 'cage' cluster, I, was the synthesis of hexameric methyloxotin acetate, $[\text{CH}_3\text{Sn}(\text{O})\text{O}_2\text{CCH}_3]_6$.⁵ The method involved a condensation reaction between methylstannonic acid and glacial acetic acid,



described by Day *et al.*, who succeeded in obtaining colourless, cubic crystals of hexameric methyloxotin acetate. These crystals were subsequently examined

by X-ray crystallography and the hexamer was found to have a 'drum' structure.⁵

The 'drum' structure of hexameric methyloxotin acetate consists of cyclic hexamers with carboxylate groups bridging two tin atoms (Figure 3.1.1).⁵

The ¹¹⁹Sn nmr spectrum obtained by Chandrasekhar⁴ for a related 'drum' hexameric *n*-butyloxotin cyclohexanoate, $[\text{CH}_3\text{CH}_2\text{CH}_2\text{CH}_2\text{Sn}(\text{O})\text{O}_2\text{C}_6\text{H}_{11}]_6$, shows only one signal, indicating the equivalence of the six tin atoms in the cyclic hexamer.⁴

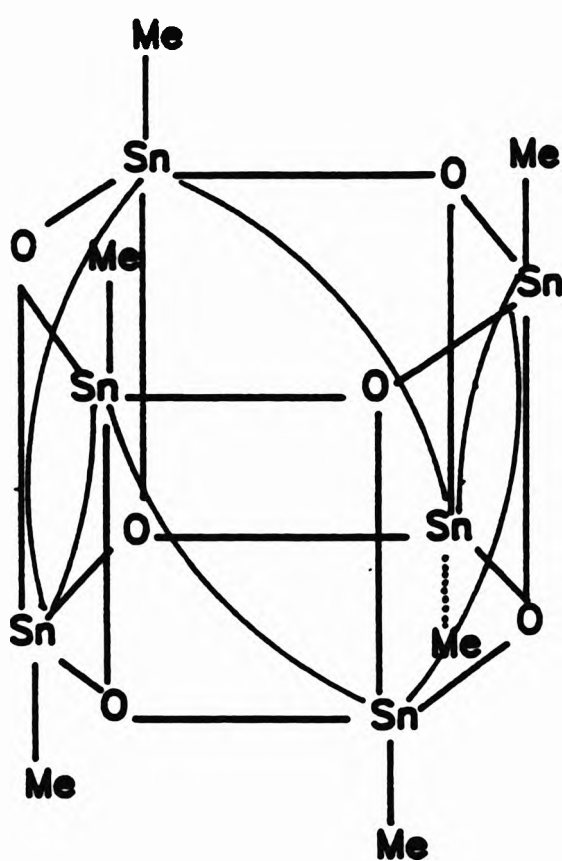


Figure 3.1.1 Schematic diagram of the 'drum' structure of hexameric methyloxotin acetate, $[\text{CH}_3\text{Sn}(\text{O})\text{O}_2\text{CCH}_3]_6$.⁵

A possible mechanism for the condensation reaction of methylstannonic acid with glacial acetic acid has not been discussed in the literature to date.

As the product was insoluble in common organic solvents as well as some organic acids (*i.e.* acetic and trifluoroacetic acid) characterisation by nmr spectroscopy was precluded. Nevertheless, Day *et al.* managed to determine the ¹¹⁹Sn nmr spectrum of $[\text{CH}_3\text{Sn}(\text{O})\text{O}_2\text{CCH}_3]_6$ in phenol, but decomposition was

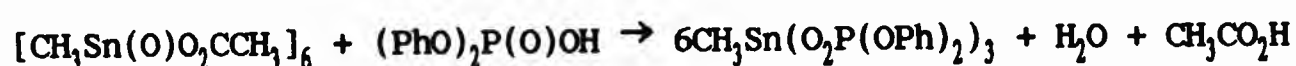
indicated.⁵ The ir spectrum of hexameric methyloxotin acetate was obtained and the bands assigned (Table 3.1.1).

Table 3.1.1 Assignment of the bands in the ir spectrum ($\bar{\nu}/\text{cm}^{-1}$) of methyloxotin acetate, $[\text{CH}_3\text{Sn}(\text{O})\text{O}_2\text{CCH}_3]_6$.^a

$\text{sym}(\text{Sn}-\text{O})^b$	$(\text{CH}_3 \text{ rock})$	$(\text{C}-\text{O})^b$	$\text{sym}(\text{CH}_3)^c$	$\text{asym}(\text{COO}^-)^b$	$\text{sym}(\text{COO}^-)^b$	$(\text{C}-\text{H})^b$
620s	770ms	1030m	1350ms	1530s	1600s	3000-2020w ^d
623 ^e				1525 ^e	1595 ^e	

^a M.p. = 300-350 °C dec. ^b Stretch. ^c Deformation. ^d Two bands also observed at 2820 cm^{-1} . ^e Data taken from ref. 5.

Hexameric methyloxotin acetate, $[\text{CH}_3\text{Sn}(\text{O})\text{O}_2\text{CCH}_3]_6$, was used as a precursor to prepare the methyltin tris(diphenylphosphate).⁹ The method (previously described by Kumara Swamy *et al.*) involved heating the starting materials, $[\text{CH}_3\text{Sn}(\text{O})\text{O}_2\text{CCH}_3]_6$ and diphenylphosphate, under reflux for seven hours in an apparatus fitted with a Dean-Stark trap.



The product was obtained as a viscous red/brown oil; C, H, and N elemental analysis showed that the product contained some impurities, probably acetic acid and toluene. These impurities were observed in the ¹H and ¹³C nmr spectra. The ¹H nmr spectrum obtained in deuterated chloroform (CDCl_3) (Table 3.1.2) is consistent with that obtained by Kumara Swamy *et al.*⁹

Table 3.1.2 Assignment of the bands in the ¹H nmr spectrum (δ/ppm) of methyltin tris(diphenyl phosphate).

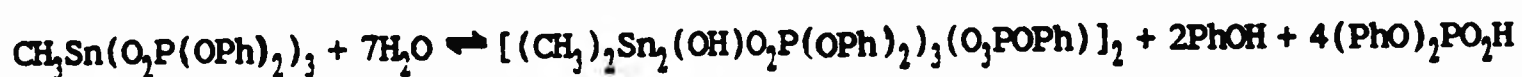
acetic acid impurities	CH_3^a	toluene impurity	aromatic protons
0.20-0.87	1.26	2.3, 7.2	6.74-7.36 ^b
0.20-0.90 ^c			6.60-7.40 ^c

^a Singlet. ^b Very complex splitting pattern. ^c Ref. 9, bands are quoted as being broad.

The ¹³C nmr spectrum of methyltin tris(diphenyl phosphate), showed a resonance

at 21.5 ppm due to the methyl carbon. A ^{13}C DEPT 90 spectrum obtained for methyltintris(diphenylphosphate) indicated that all the signals were positive and due to CH_3 or CH groups.

The last stage in the preparation of the 'cage' cluster, I, involved hydrolysis of methyltin tris(diphenyl phosphate) in a diethylether/acetonitrile mixture at room temperature to yield a white powder, the 'cage' cluster, I.⁹



Kumara Swamy *et al.* obtained crystals of the 'cage' cluster I which when examined by X-ray crystallography and found to have a tetranuclear 'cage' composition (Figure 3.1.2).⁹

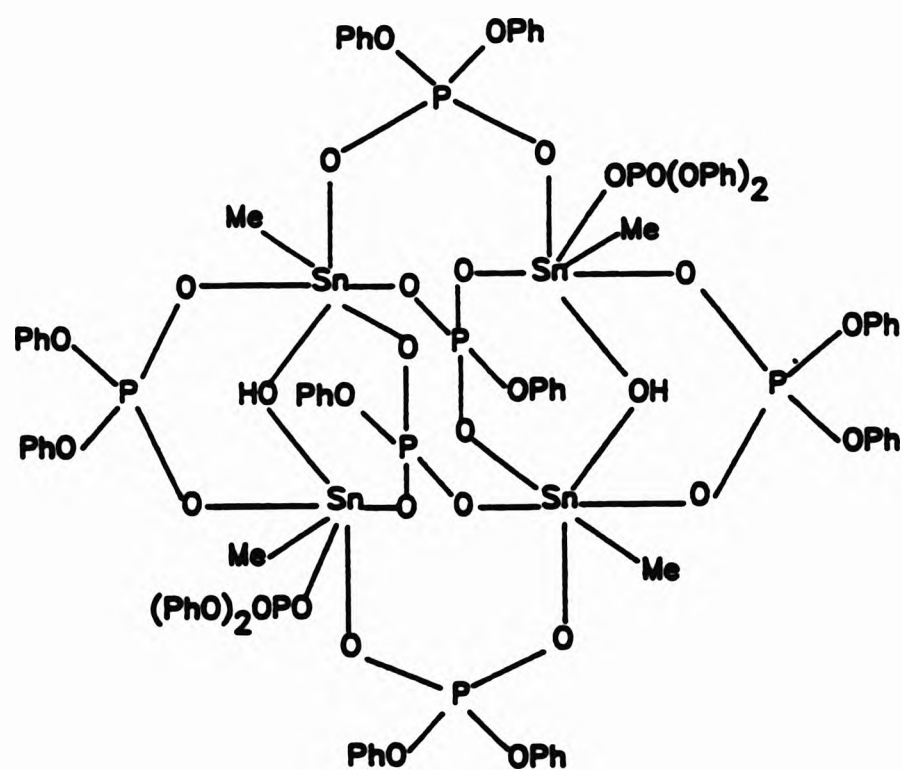


Figure 3.1.2 Schematic diagram of the 'cage' cluster, I,
 $[(\text{CH}_3)_2\text{Sn}_2(\text{OH})(\text{O}_2\text{P}(\text{OC}_6\text{H}_5)_2)_3(\text{O}_3\text{POC}_6\text{H}_5)]_2$.

The ^1H nmr spectrum of the 'cage' cluster I was obtained in deuterated chloroform (CDCl_3) and the results are consistent with those determined by Kumara Swamy⁹ (Table 3.1.3).

Table 3.1.3 Assignment of the signals in the ^1H nmr spectrum (δ/ppm) for the 'cage' cluster, $[(\text{CH}_3)_2\text{Sn}_2(\text{OH})(\text{O}_2\text{P}(\text{OC}_6\text{H}_5)_2)_3(\text{O}_3\text{POC}_6\text{H}_5)]_2$.

CH_3^{a}	CH_3^{a}	aromatic protons	OH^{b}	$^2\text{J}(\text{CH}-^{119}\text{Sn}) / \text{Hz}$	$^2\text{J}(\text{CH}-^{117}\text{Sn}) / \text{Hz}$
0.22	0.57	6.91-7.35	9.18	147.0	144.0
0.22 ^c	0.58 ^c	6.80-7.40 ^c	^d	146, 145 ^e	

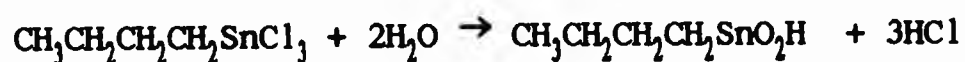
^a Two types of methyl groups. ^b Broad singlet. ^c Ref. 9, all bands are quoted as being broad. ^d The position of the OH could not be determined exactly. ^e Approximate values.

3.2 The preparation of some novel organotin clusters with phosphonic and/or carboxylic acids

The main purpose for the previous reactions (Section 3.1.1) was to gain some experience and understanding of this organotin cluster area.

3.2.1 Preparation of *n*-butylstannonic acid

To overcome solubility problems and to aid characterisation by nmr spectroscopy, *n*-butylstannonic acid was prepared from the hydrolysis of *n*-butyltintrichloride.²⁰



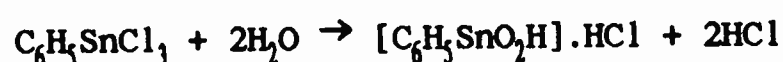
The product *n*-butylstannonic acid was a white amorphous solid which was insoluble in common organic solvents except for some organic acids. The melting point of $\text{CH}_3\text{CH}_2\text{CH}_2\text{CH}_2\text{SnO}_2\text{H}$ was determined and found to be in agreement with other organostannonic acids.¹⁷ The ir spectrum obtained for *n*-butylstannonic acid contained the characteristic band $\bar{\nu}_{\text{as}}(\text{Sn}-\text{O})$ at 620 cm^{-1} .

The ^1H and ^{13}C nmr spectra for *n*-butylstannonic acid (Section 2.5) were obtained in deuterated trifluoroacetic acid. The ^1H nmr spectrum showed evidence of tin satellites.

3.2.2 Preparation of the hydrochloride salt of phenylstannonic acid

The hydrochloride salt of phenylstannonic acid was prepared by a method described by Davies *et al.*²⁰ Phenyltin trichloride was hydrolysed in basic

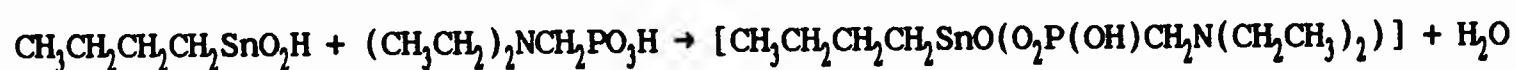
conditions.



On addition of *aqueous ammonia* solution, a white precipitate was collected and dried in a desiccator over conc. sulphuric acid. From C, H and N elemental analysis the product was found to be the hydrochloride salt of phenylstannonic acid.

3.2.3 Preparation of the novel compound *n*-butyloxotin diethylaminomethylene-phosphonate

The preparation of a cluster of an organostannonic acid with an aminomethylenephosphonic acid, DEAMP₂, was attempted. The reactants were heated under reflux for 5.5 hours in an apparatus fitted with a Dean-Stark trap. The resulting mixture was filtered and reduced in volume to leave a yellow solid.



The ir spectrum obtained showed characteristic stretching bands for the phosphonic acid group and for tin-oxygen stretching. Comparison of the ir bands obtained for *n*-butylstannonic acid (Table 3.2.1) with that for *n*-butyloxotin diethylaminomethylenephosphonate, showed a lowering of the values for the frequencies of the bands assigned to the Sn-O stretch.

Table 3.2.1 Comparison of the bands in the ir spectrum ($\bar{\nu}/\text{cm}^{-1}$) for *n*-butyloxotin diethylaminomethylenephosphonate and *n*-butylstannonic acid.

	sym(Sn-O) ^a	(PO)	sym, asym(PO ₂ ⁻) ^a	sym(CH ₃) ^b	(C-H) ^{a,c}
	579m	992s	1091-1144br	1464m	2855-2957
<i>n</i> -butylstannonic acid	620br			1462m	2858-2956m

^a Stretch. ^b Deformation. ^c A number of bands due to aliphatic CH groups.

The ¹H nmr spectrum determined for *n*-butyloxotin diethylaminomethylene-phosphonate in deuterated acetic acid, was complex and could not be assigned.

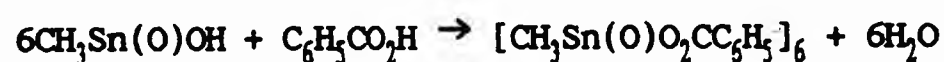
The above results are inconclusive as to whether a new compound was prepared

or a mixture of products. Much time was spent on this area without success. The preparation of other new organotin clusters were examined in order to determine their compositions by X-ray crystallography. However, many were only obtained in powder form with little or no proof of their structures in solution (due to insolubility) and solid state (lack of crystals). What follows is a discussion of the preparation of new compounds prepared and the probable structures in the solid state based on previous work.

3.2.4 Preparation of the novel hexameric alkyloxotin carboxylates

(a) Hexameric methyloxotin benzoate

Hexameric methyloxotin benzoate was prepared by reacting methylstannonic acid with benzoic acid under reflux for five hours. A white powder was obtained in 65 % yield.



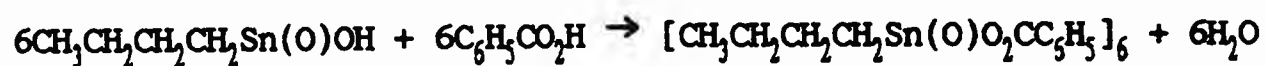
C, H and N elemental analysis was found to be satisfactory and suggested the formulation of the compound was that of a 'drum' (i.e. a similar structure to $[\text{CH}_3\text{Sn}(\text{O})\text{O}_2\text{CCH}_3]_6$ already determined by Kumara Swamy). The ^1H nmr spectrum of hexameric methyloxotin benzoate was determined in deuterated trifluoroacetic acid ($\text{CF}_3\text{COOD}-d_1$) (Section).

The methyl protons (CH_3) are coupled through two bonds to the tin atom to give a doublet overlapping the singlet ($^2J = 145.5$ Hz) and is consistent with the value determined for methylstannonic acid (143.9 Hz).

Examination of the ^1H nmr data available for other hexameric alkyloxotin carboxylates, e.g. hexameric *n*-butyloxotin cyclobutanoate and cyclopropanoate⁵ and hexameric *n*-butyloxotin cyclohexanoate⁴ also show multiplets arising from only one monomeric unit, i.e. $[\text{RSn}(\text{O})\text{O}_2\text{CR}']$. This suggests, that all the monomeric units are equivalent. This assignment of the ^1H nmr spectra of these types of 'drum' structures by Day *et al.* and Chandrasekhar *et al.*, also provide some evidence of the 'drum' structure of hexameric methyloxotin benzoate.

(b) Hexameric *n*-butyloxotin benzoate

The condensation reaction of benzoic acid with *n*-butylstannonic acid heated under reflux with a Dean-Stark trap produced a white powder.



The product was very soluble in acetic acid but not in chloroform. The product was expected to have the same structure as hexameric methyloxotin acetate *i.e.* a 'drum' structure. The ^1H and ^{13}C nmr spectra were obtained in deuterated trifluoroacetic acid and indicated the equivalence on the monomeric units $[\text{RSn}(\text{O})\text{O}_2\text{CR}']$ (Table 3.2.2).

Table 3.2.2 Assignment of the bands in the ^1H nmr spectrum (δ/ppm) of hexameric *n*-butyloxotin benzoate, $[\text{CH}_3\text{CH}_2\text{CH}_2\text{CH}_2\text{Sn}(\text{O})\text{O}_2\text{CC}_6\text{H}_5]_6$.

H^i	H^2	H^3	H^4	H^7	H^8	H^9
1.01 ^a	1.53 ^b	1.95 ^c	2.30 ^d	8.15 ^e	7.52 ^f	7.70 ^g

^a Triplet, $^3\text{J}(\text{HH}) = 7.3$ Hz. ^b An approx. sextet, $^3\text{J}(\text{HH}) \approx 7.4$ Hz. ^c An approx. pentet, $^3\text{J}(\text{HH}) \approx 7.7$ Hz. ^d An approx. triplet, $^3\text{J}(\text{HH}) \approx 8.0$ Hz. ^e Doublet, $^3\text{J}(\text{HH}) = 7.5$ Hz. ^f Triplet, $^3\text{J}(\text{HH}) = 7.6$ Hz. ^g Triplet, $^3\text{J}(\text{HH}) = 7.0$ Hz.

Table 3.2.3 Assignment of the bands in the ^{13}C nmr spectrum (δ/ppm) of hexameric *n*-butyloxotin benzoate, $[\text{CH}_3\text{CH}_2\text{CH}_2\text{CH}_2\text{Sn}(\text{O})\text{O}_2\text{CC}_6\text{H}_5]_6$.

C^1	$\text{C}^2, \text{C}^3, \text{C}^4$	CO_2^5	$\text{C}^6, \text{C}^7, \text{C}^8$	C^9
13.83	26.82, 28.34, 33.45	ca.175.5	129.60, 130.62, 132.30	136.95

Comparison of the nmr data available for other hexameric butyloxotin carboxylates^{4,5}, suggests that from the evidence of the nmr spectra obtained for hexameric *n*-butyloxotin benzoate that it does have the 'drum' formulation and is retained in solution.

(c) *Hexameric n-butyloxotin hippurate*

The reaction of hippuric acid $[\text{C}_6\text{H}_5\text{C}(\text{O})\text{NHCH}_2\text{CO}_2\text{H}]$ with *n*-butylstannonic acid heated under reflux for eight hours, after cooling small amounts of diethylether and hexane were added and a white precipitate isolated. The product was soluble in pyridine and acetic acid. C, H and N elemental analysis was found to be consistent with the 'drum' structure, $[\text{CH}_3\text{CH}_2\text{CH}_2\text{CH}_2\text{Sn}(\text{O})\text{O}_2\text{CCH}_2\text{NHCOC}_6\text{H}_5]_6$. However, nmr spectra were not obtained because of the solubility problem.

(d) *Hexameric phenyloxotin acetate*

The reaction of phenylstannonic acid (in toluene) with glacial acetic acid was carried out and a white precipitate collected. C, H and N elemental analysis indicated the product to have a 'drum' formulation, *i.e.* $[\text{PhSn}(\text{O})\text{O}_2\text{CPh}]_6 \cdot \text{PhCH}_3$. The ir spectrum was obtained and showed the presence of the characteristic stretches for the carboxylate group (COO^-) (Section 2.1.14).

(e) *Hexameric phenyloxotin benzoate*

The reaction of phenylstannonic acid with benzoic acid heated under reflux for six hours, produced a white precipitate. The product also had a 'drum' formulation which was confirmed by C, H and N elemental analysis, $[\text{C}_6\text{H}_5\text{Sn}(\text{O})\text{O}_2\text{CC}_6\text{H}_5]_6$.

The preparation of phenylstannonic and *n*-butylstannonic acids was to aid the solubilities of any organooxotin compounds formed and hence aid characterisation by nmr spectroscopy and X-ray crystallography. Again the use of phosphonic acids with differing R groups, in the preparation of new organooxotin compounds, was to aid characterisation. However, many of the new organooxotin compounds formed were insoluble in the common organic solvents. Therefore, recrystallisation and determination of their solid state structures were unsuccessful and hence their solid structures have been based on the results of other workers in this area.

3.2.5 *Preparation of the novel 'ladder' form of $[(\text{CH}_3\text{CH}_2\text{CH}_2\text{CH}_2\text{Sn}(\text{O})\text{O}_2\text{CCH}_3)_2 - (\text{CH}_3\text{CH}_2\text{CH}_2\text{CH}_2\text{Sn}(\text{O}_2\text{CCH}_3)_3)]_2$*

The reaction of *n*-butylstannonic acid with glacial acetic acid heated under reflux for five hours produced a white crystalline solid.



The condensation reaction between *n*-butylstannonic acid and glacial acetic acid was expected to produce the 'drum' structure *i.e.* $[\text{CH}_3\text{CH}_2\text{CH}_2\text{CH}_2\text{Sn}(\text{O})\text{O}_2\text{CCH}_3]_6$. However, C, H and N elemental analysis indicated the formulation of the product to be that of the 'ladder' $[(\text{CH}_3\text{CH}_2\text{CH}_2\text{CH}_2\text{Sn}(\text{O})\text{O}_2\text{CCH}_3)_2(\text{CH}_3\text{CH}_2\text{CH}_2\text{CH}_2\text{Sn}(\text{O}_2\text{CCH}_3)_3)]_2$.⁴ The product was sparingly soluble in CCl_4 , CHCl_3 and acetic acid, but insoluble in DMSO, methanol, acetone and acetonitrile. The possible structure of this compound could be similar to that determined by Chandrasekhar *et al.* for the organotin cluster

$[(\text{CH}_3\text{CH}_2\text{CH}_2\text{CH}_2\text{Sn}(\text{O})\text{O}_2\text{CC}_6\text{H}_{11})_2 \text{CH}_3\text{CH}_2\text{CH}_2\text{CH}_2\text{Sn}(\text{O}_2\text{CC}_6\text{H}_{11})_3]_2$ which was also found to have the 'ladder' composition (Figure 3.2.1).

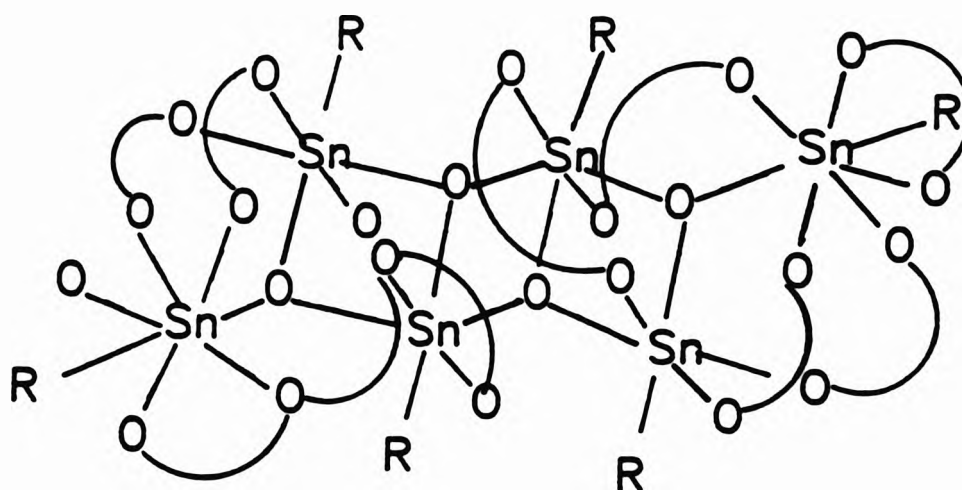


Figure 3.2.1 Schematic diagram of the 'ladder' form of $(\text{CH}_3\text{CH}_2\text{CH}_2\text{CH}_2\text{Sn}(\text{O})\text{O}_2\text{CC}_6\text{H}_{11})_2 \text{CH}_3\text{CH}_2\text{CH}_2\text{CH}_2\text{Sn}(\text{O}_2\text{CC}_6\text{H}_{11})_3]_2$.

3.2.6 Preparation of the novel compound, methyltin tris(styrenephosphonate),

The reaction of styrene phosphonic acid with hexameric methyloxotin acetate heated under reflux in toluene (6 hours) produced a white precipitate after three hours. C, H and elemental analysis indicated the product not to have a 'cage' or 'drum' formulation, but to have the following structure $[\text{CH}_3\text{Sn}(\text{O}_2\text{P}(\text{OH})\text{CH}=\text{CHC}_6\text{H}_5)_3]$. The product was insoluble in CCl_4 , ether, acetone, methanol in chloroform.

3.2.7 Preparation of some 'cages' with phosphorus-based acids

(a) Preparation of the 'cage' $[(\text{CH}_3\text{CH}_2\text{CH}_2\text{CH}_2)_2\text{Sn}_2\text{O}(\text{O}_2\text{P}(\text{OH})\text{C}(\text{CH}_3)_3)_4]_2$

A previously reported route was followed for the reaction of *t*-butylphosphonic acid with *n*-butylstannonic acid.⁹ To a solution of *t*-butylphosphonic acid, *n*-butylstannonic acid was added to give a light-brown coloured solution. A light-brown crystalline material was collected.

C, H and N elemental analysis indicated the product to have the same formulation $[(\text{CH}_3(\text{CH}_2)_3)_2\text{Sn}_2\text{O}(\text{O}_2\text{P}(\text{OH})\text{C}(\text{CH}_3)_3)_4]_2$ as determined by Kumara Swamy *et al.*⁹ All nmr spectra were determined in deuterated chloroform (CDCl_3) and are in agreement with the results (Table 3.2.4) determined by Kumara Swamy *et al.*⁹ Kumara Swamy *et al.*, noted that the reaction of *n*-butylstannonic acid with *t*-butylphosphonic acid, proceeds via a condensation:



where R = *t*-butyl group.

Table 3.2.4 Assignment of the bands in the ^1H nmr spectrum (δ/ppm) of $[(\text{CH}_3\text{CH}_2\text{CH}_2\text{CH}_2)_2\text{Sn}_2\text{O}(\text{O}_2\text{P}(\text{OH})\text{C}(\text{CH}_3)_3)_4]_2$.

	CH_3CH_2-	$(\text{CH}_3)_3\text{-C-}$	$\text{CH}_2\text{-Sn}$	$-\text{CH}_2\text{CH}_2-$	C-P-OH
	0.90 ^a	1.10 ^b , 1.16 ^b	1.28 ^c	1.38 ^d , 1.64 ^e	4.50 ^f
Ref.9	0.88	1.10, 1.15		1.37, 1.65	4.49

^a Triplet, protons of *n*-butyl group, $^3\text{J}(\text{HH}) = 7.3$ Hz. ^b Two doublets from two different *t*-butyl groups, $^3\text{J}(\text{HP}) = 4.9$ Hz, 4.7 Hz. ^c An approx. triplet, $^3\text{J}(\text{HH}) \approx 8.0$ Hz. ^d An approx. sextet, methylene protons of *n*-butyl group, $^3\text{J}(\text{HH}) \approx 7.3$ Hz. ^e An approx. pentet of the *n*-butyl group, $^3\text{J}(\text{HH}) \approx 7.5$ Hz. ^f Singlet, two types of bridging OH groups. Overlapped with a pair of doublets, $^2\text{J}(\text{H}-^{117/119}\text{Sn}) = 26.6$ Hz.

The ^{31}P nmr spectrum for the cage showed two signals (P and P') both overlapped with a pair of doublets, due to coupling to the tin nuclei [$^2\text{J}(\text{P}'-^{119}\text{Sn}) = 238.7$ Hz, $^2\text{J}(\text{P}'-^{117}\text{Sn}) = 228.1$ Hz and $^2\text{J}(\text{P}-^{119}\text{Sn}) = 286.6$ Hz, $^2\text{J}(\text{P}-^{117}\text{Sn}) = 273.9$ Hz.

The ^{119}Sn nmr spectrum obtained for the cage shows nine symmetrical lines with the central line being the chemical shift of the tin atoms in the cage cluster (Figure 3.2.3). The signal (centred at -630.4 ppm) is coupled through two bonds to two phosphorus atoms (P) to give a triplet, $^2\text{J}(^{117/119}\text{Sn-O-P}) = 286.4$ Hz and is further coupled to two different phosphorus atoms (P') $^2\text{J}(^{117/119}\text{Sn-O-P}') = 239.3$ Hz, to give a triplet of triplets (Figure 3.2.2). These results are consistent with those determined by Kumara Swamy.⁹

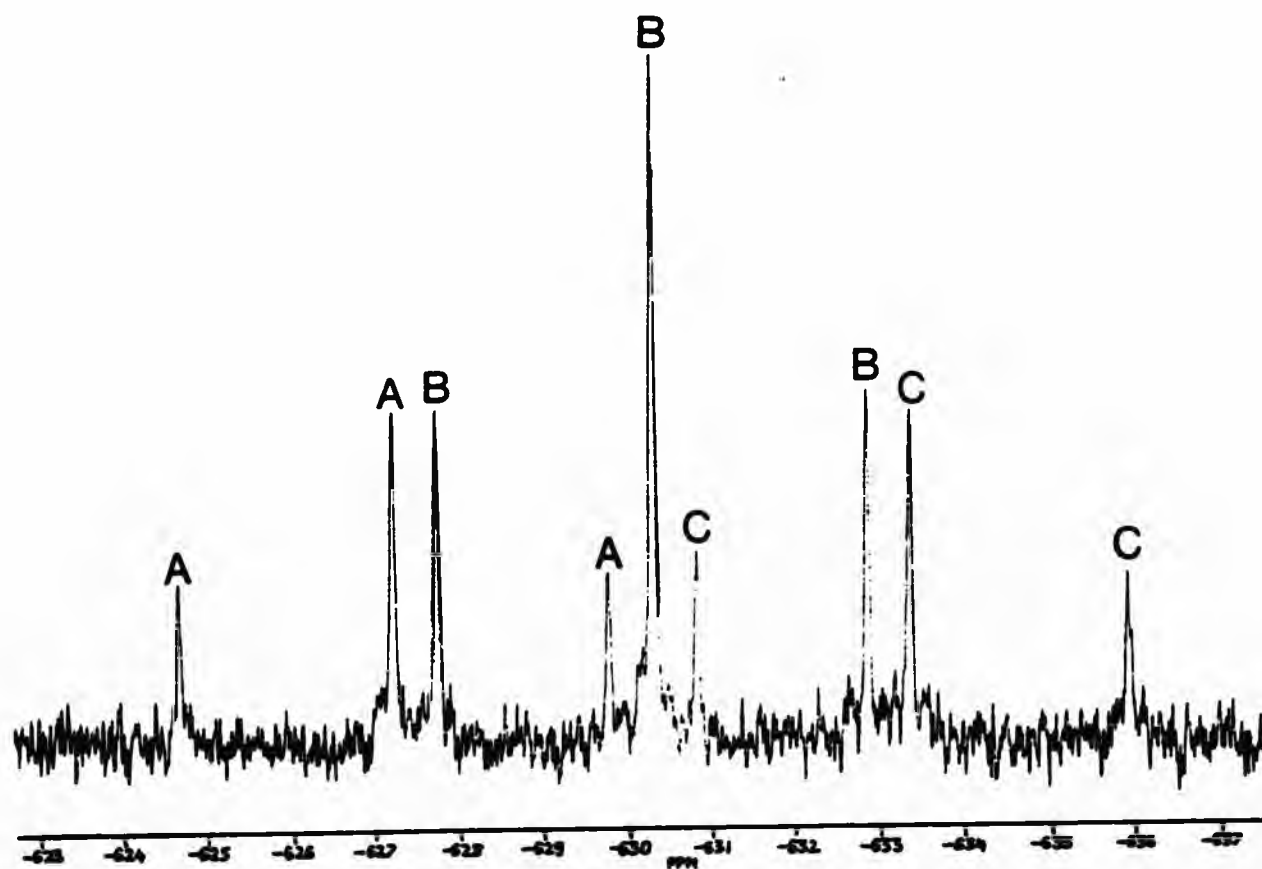


Figure 3.2.2 ^{119}Sn nmr spectrum of $[(\text{CH}_3\text{CH}_2\text{CH}_2\text{CH}_2)_2\text{Sn}_2\text{O}(\text{O}_2\text{P}(\text{OH})\text{C}(\text{CH}_3)_3)_4]_2$ in deuterated chloroform.

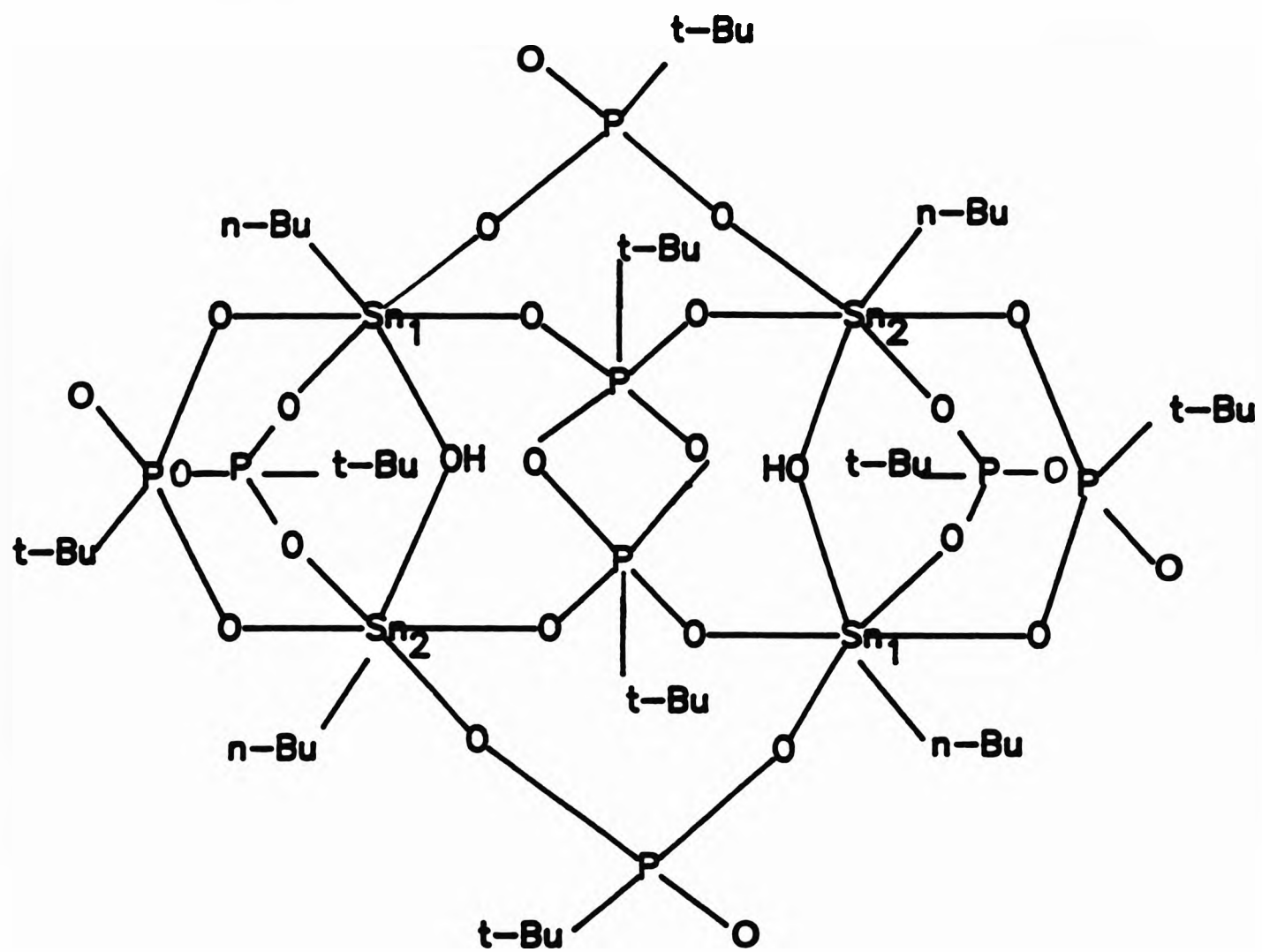


Figure 3.2.3 Schematic diagram of the 'cage', $[(\text{CH}_3(\text{CH}_2)_3)_2\text{Sn}_2\text{O}(\text{O}_2\text{P}(\text{OH})\text{C}(\text{CH}_3)_3)_4]_2$.

The reaction of the *t*-butylphosphonic acid and *n*-butylstannonic acid yielded a compound which is much more soluble in the common organic solvents (in this case, chloroform). This aided characterisation of the compound by nmr spectroscopy and X-ray crystallography as determined by Kumara Swamy *et al.*⁹ (Figure 3.2.3).

(b) Preparation of the novel 'cage' $[(\text{CH}_2\text{CH}_2\text{CH}_2\text{CH}_2)_2\text{Sn}_2\text{O}(\text{O}_2\text{P}(\text{OH})\text{CH}_2\text{C}_6\text{H}_5)_4]_2$

Therefore, in order to produce compounds which were more soluble in the common organic solvents, different alkylphosphonic acids were used in the reactions to prepared cage compounds.

The reaction of phenylphosphonic acid in acetone with *n*-butylstannonic acid was carried out. This reaction produced a colourless solid which was soluble in dimethylformamide (DMF) but was insoluble in acetone, methanol, dimethylsulphoxide (DMSO), chloroform and acetonitrile. C, H and N elemental analysis indicated that the formulation of the product was that of a 'cage', $[(\text{CH}_2\text{CH}_2\text{CH}_2\text{CH}_2)_2\text{Sn}_2\text{O}(\text{O}_2\text{P}(\text{OH})\text{CH}_2\text{C}_6\text{H}_5)_4]_2$. However, as the sample was insoluble in many of the common organic solvents, characterisation by nmr spectroscopy was precluded.

(c) Preparation of the novel 'cage' $[(\text{CH}_3)_2\text{Sn}_2\text{O}(\text{O}_2\text{P}(\text{OH})\text{C}(\text{CH}_3)_3)_4]_2$

Another simple condensation reaction was used which involved the reaction of methylstannonic acid with *t*-butylphosphonic acid. The mixture of methylstannonic acid and *t*-butylphosphonic acid in toluene was heated under reflux for nine hours in an apparatus fitted with a Dean-Stark trap to yield a white powder, $[(\text{CH}_3)_2\text{Sn}_2\text{O}(\text{O}_2\text{P}(\text{OH})\text{C}(\text{CH}_3)_3)_4]_2$. C, H and N elemental analysis indicated the product to have the 'cage' formulation, *i.e.* similar to that determined for the 'cage' cluster of $[(n\text{-Bu})_2\text{Sn}_2\text{O}(\text{O}_2\text{P}(\text{OH})t\text{-Bu})_4]_2$ by Kumara Swamy *et al.* (Figure 3.2.3). The product was soluble in DMF, DMSO and sparingly soluble in acetic acid, methanol and chloroform.

Again, as the sample was only sparingly soluble in some of the common organic solvents and hence nmr spectra were not determined.

3.2.8 The possible clathration of metal ions by organotin drums

The stabilisation of aqueous solutions of hydrogen peroxide by amino-phosphonic acids is well known. It is possible that in aqueous solutions of hydrogen peroxide that reaction between sodium stannate $[\text{Na}_2\text{Sn}(\text{OH})_6]$ and an α -

aminoalkylphosphonic acids (Chapter 6) may take place. The resulting compound may involve large 'cage's or cluster formations which sequester metal ions (Figure 3.2.4). However, this proposal has not been successful in this work. Kumara Swamy *et al.* suggested that the organotin compounds prepared from the reactions of phosphonic and stannonic acids, contained flexible cavities that may have the potential to be used as clathration agents, but this has not been carried out to date.

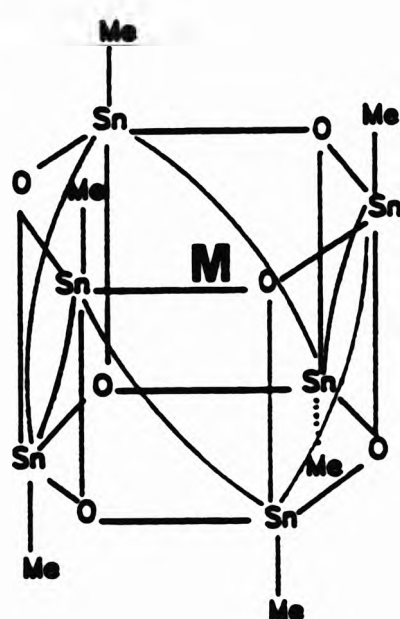


Figure 3.2.4 Possible clathration of metals by the 'drum' formulation of hexameric *n*-butyloxotin benzoate, $[\text{CH}_3\text{CH}_2\text{CH}_2\text{CH}_2\text{Sn}(\text{O})\text{O}_2\text{CC}_6\text{H}_5]_6$.

In this work, it was possible to react copper perchlorate with hexameric *n*-butyloxotin benzoate, $[\text{CH}_3\text{CH}_2\text{CH}_2\text{CH}_2\text{Sn}(\text{O})\text{O}_2\text{CC}_6\text{H}_5]_6$, previously prepared (Section 2.1.11) in which a pale blue precipitate was collected. The resulting compound was soluble in acetone and hot methanol, but crystallisation was unsuccessful. C, H and N elemental analysis and ir spectrum, suggested that the basic 'drum' formulation of $[\text{CH}_3\text{CH}_2\text{CH}_2\text{CH}_2\text{Sn}(\text{O})\text{O}_2\text{CC}_6\text{H}_5]_6$ was still present, but the exact nature of the solid state structure remains unknown. The ir spectrum was obtained and comparison with the ir bands obtained for $[\text{CH}_3\text{CH}_2\text{CH}_2\text{CH}_2\text{Sn}(\text{O})\text{O}_2\text{CC}_6\text{H}_5]_6$ (Table 3.2.5) showed some differences.

It may be possible to sequester metal ions by using organotin 'cage' compounds with carboxylic and/or alkylaminoalkylphosphonic acid derivatives but this needs to be examined more thoroughly with the aid of nmr spectroscopy and X-ray crystallography.

Table 3.2.5 Comparison of the bands in the ir spectrum ($\bar{\nu}/\text{cm}^{-1}$) of $[\text{CH}_3\text{CH}_2\text{CH}_2\text{CH}_2\text{Sn}(\text{O})\text{O}_2\text{CC}_6\text{H}_5]_6 \cdot \text{Cu}(\text{ClO}_4)_2 \cdot 6\text{H}_2\text{O}$ and in hexameric *n*-butyloxotin benzoate (Drum).

	sym(Sn-O) ^a	(C-H) ^b	(C-H)	(COO ⁻) ^a
Cu(II)-Drum	586m	718 ^c	1407s	1531, 1547, 1597
Drum	585s	710s	1405s	1529-1550br, 1597s

^a Stretch. ^b Out of plane vibration of aryl C-H group. ^c Perchlorate counter ion at 674 cm^{-1} and 1088 cm^{-1} .

3.3 References

1. H. Lambourne, *J. Chem. Soc.*, 1922, 2533; 1924, 2013.
2. V. Chandrasekhar, R. O. Day and R. R. Holmes, *Inorg. Chem.*, 1985, 24, 1970.
3. R. R. Holmes, C. G. Schmid, V. Chandrasekhar, R. O. Day and J. M. Holmes, *J. Am. Chem. Soc.*, 1987, 109, 1408.
4. V. Chandrasekhar, C. G. Schmid, S. D. Burton, J. M. Holmes, R. O. Day and R. R. Holmes, *Inorg. Chem.*, 1987, 26, 1050.
5. R. O. Day, V. Chandrasekhar, K. C. Kumara Swamy, J. M. Holmes, S. D. Burton and R. R. Holmes, *Inorg. Chem.*, 1988, 27, 2887.
6. K. C. Kumara Swamy, R. O. Day and R. R. Holmes, *J. Am. Chem. Soc.*, 1987, 109, 5546.
7. R. R. Holmes, K. C. Kumara Swamy, C. G. Schmid and R. O. Day, *J. Am. Chem. Soc.*, 1988, 110, 7060.
8. R. O. Day, J. M. Holmes, V. Chandrasekhar and R. R. Holmes, *J. Am. Chem. Soc.*, 1987, 109, 940.
9. K. C. Kumara Swamy, C. G. Schmid, R. O. Day and R. R. Holmes, *J. Am. Chem. Soc.*, 1990, 112, 223.
10. R. R. Holmes, *Acc. Chem. Res.*, 1989, 22, 190.
11. W. C. Schumb, C. N. Satterfield and R. L. Wentworth, *Hydrogen Peroxide*, Reinhold Publishing, New York, 1955.
12. S. Croft, B. C. Gilbert, J. R. L. Smith, J. K. Stell and W. R. Sanderson, *J. Chem. Soc., Perkin Trans. 2*, 1992, 153.
13. R. D. Gillard, P. D. Newman and J. D. Collins, *Polyhedron*, 1989, 8, 2077.
14. M. Hollmann, R. Opitz, K. Haage, *Ger. (East)* 144073, 1980; *CA* 94, 21045f. Y. Machida, T. Yoshida, N. Kimura, and M. Watanabe, *Jpn. Kokai Tokkyo Koho JP* 62185797, 1986; *CA* 108, 39593u. G. W. Morris, N. D. Feasey, P. A. Ferguson, D. Van Hemelrijk and M. Charlot, *PCT Int. Appl. WO* 9001034, 1990; *CA* 113, 6601v.
15. T. J. Lewis and T. M. Walters, *J. Appl. Chem.*, 1960, 10, 396, 403.
16. S. Lynch, R. W. Matthews and G. W. Morris, personal communication.
17. R. K. Ingham, S. D. Rosenberg and H. Gilman, *Chem. Revs.*, 1960, 60, 459.
18. J. G. F. Druce, *J. Chem. Soc.*, 1922, 1859.
19. J. G. F. Druce, *J. Chem. Soc.*, 1921, 758.
20. A. G. Davies, L. Smith and P. J. Smith, *J. Organometal. Chem.*, 1972, 39, 279.

*Chapter 4 Protonation constants of some
alkylaminomethylenephosphonic acids*

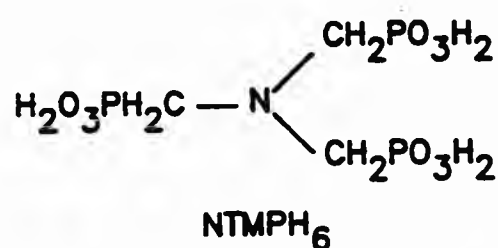
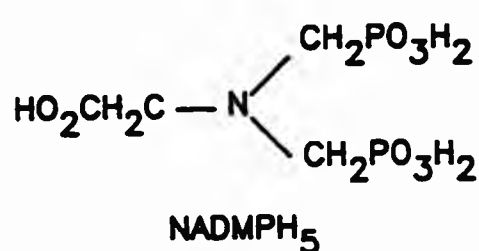
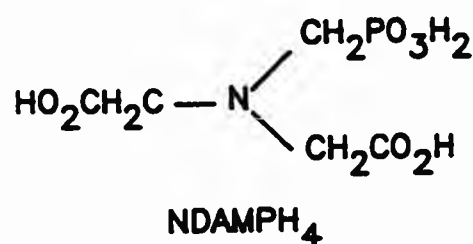
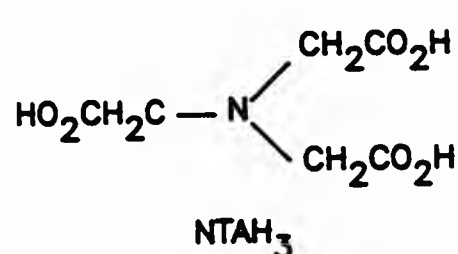
4.1 Introduction

The development of alkylaminomethylenephosphonic acids as complexing ligands with a high affinity for a variety of metal cations has led to widespread use of such ligand systems in many different areas of industry and medicine.¹ Their study has proved to be interesting from both a fundamental and a practical point of view, and their main advantage over phosphates is the high stability of the former ligands to hydrolysis which is attributed to the presence of the strongly covalent carbon to phosphorus bond.² α -Alkylaminomethylenephosphonic acids, $RR'NCH_2PO_3H_2$ are analogs of α -alkylaminomethylene-carboxylic acids, $RR'NCH_2COOH$.[†] An obvious difference is that the phosphonic acid group is diprotic. Alkylaminomethylenephosphonic acids share with alkylaminomethylenecarboxylic acids many properties which are useful in a variety of applications, e.g. their colour reactions with ninhydrin and its derivatives are useful in analysis.³⁻⁵ However, replacement of a carboxylic acid group by a phosphonic acid group results in considerable changes in the specificity of the chelating agent which can be related to differences in stereochemistry, polarisability, inductive effects and π -bonding, between the two groups.⁶ The properties of alkylaminomethylenephosphonic acids were first reported as early as 1949 by Schwarzenbach⁷ simultaneously with those of alkylaminomethylenecarboxylic acids and, since then, this new class of chelating ligands has expanded rapidly in importance.⁸⁻¹⁸

Many reports in the literature in recent years have been concerned with the stabilities of metal complexes with alkylaminomethylenephosphonic acids (e.g. refs. 6, 19-25) and some have described investigations of their structures in aqueous solution.²⁶ Martell *et al.*¹⁹⁻²² have determined the protonation and metal complex stability constants of a series of related aminocarboxylic and aminophosphonic acid ligands in order to explain differences in their coordinating abilities. It was suggested by Martell^{20,21} that if two or more phosphonate groups were present in a ligand, then the bi-negative charges of the phosphonate groups would prevent all the groups from coordinating around a single divalent metal cation. In this context, Carter *et al.*²³ determined the stability constants for complexes between Ca(II) and Mg(II) and a series of acids in which the acetic acid groups of nitrilotriacetic acid (NTAH₃) were substituted, stepwise, by methylenephosphonic acid groups to give the

[†] Although alkylaminomethylenephosphonic acids usually exist as zwitterions, $RR'NH^+CH_2PO_3H^-$, they will be written in the unionised form, $RR'NCH_2PO_3H_2$ unless the zwitterion form is being emphasised.

compounds nitrilodiaceticmethylenephosphonic acid (NDAMPH₄), nitriloaceticdi-(methylenephosphonic acid) (NADMPH₅) and nitrilotris(methylenephosphonic acid) (NTMPH₆):



The values of $\log K_{ML}$ on advancing from NTAH₃ to NTMPH₆ for Ca²⁺ and Mg²⁺ complexes are shown in Table 4.1.1.

Table 4.1.1 Stability constants for Ca²⁺ and Mg²⁺ complexes for a series of related acids.

	NTAH ₃ ^a	NDAMPH ₄ ^a	NADMPH ₅ ^b	NTMPH ₆ ^c
$\log K_{CaL}$	6.41	7.18	6.17	6.68
$\log K_{MgL}$	5.41	6.28	-	6.49

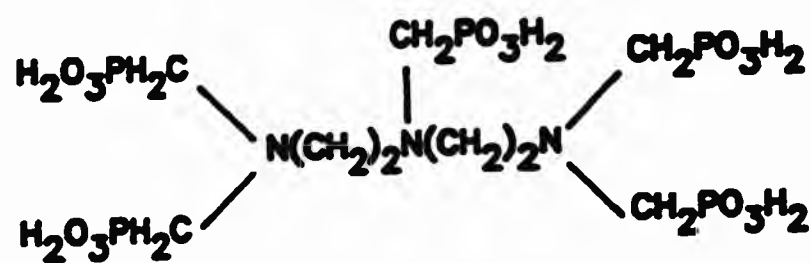
^a Ref. 23, I = 0.1 mol dm⁻³ KCl at 25 °C. ^b Ref. 23, I = 0.1 mol dm⁻³ KNO₃ at 25 °C. ^c Ref. 20, I = 1.0 mol dm⁻³ KNO₃ at 25 °C.

For Ca²⁺, the value of $\log K_{CaL}$ increases from NTAH₃ to NDAMPH₄ on replacement of an acetic acid group by a phosphonic acid group, but this increase does not continue in going from NDAMPH₄ to NTMPH₆. Martell¹⁹⁻²² suggested that this unexpected behaviour was due to the electrostatic repulsion of the negatively charged phosphonate groups which were, as a result, not able to completely coordinate around the metal cation;^{23,24} replacement of two of the acetate groups in NTAH₃ by methylenephosphonate groups to give NADMPH₅ does not result in an increase in the value of $\log K_{CaL}$. The stability of the complex ML is influenced by the repulsion of the donor groups (*i.e.* PO₃²⁻), the metal coordination geometry and the possible coordination of the nitrogen to the central metal cation. However, such ligands may be especially effective for

ions having a greater charge than +2; such ions can neutralise charge to charge repulsions and produce a higher stability for the resulting complex.¹⁹ Oakes *et al.*²⁵ studied complexes of various metal ions with ethylenediamine-tetrakis(methylenephosphonic acid) (EDTMPH₄) to determine the hydration numbers of these complexes in *aqueous* solution and found that the hydration numbers were greater than in the carboxylate analogs (*i.e.* EDTAH₄). These authors argued that the repulsion between the donating groups (*i.e.* phosphonate groups) around the metal atom leaves the metal coordination sphere incomplete, which is then satisfied by other donor molecules in the system. In *aqueous* solution, this increases the number of water molecules coordinated to the central metal atom. There are some examples of complexes of α -alkylamino-methylenephosphonic acids in which the coordination sphere of the metal is completed by water molecules.^{27,28}

The use of alkylaminomethylenephosphonic acids as stabilisers for hydrogen peroxide is well known.²⁹ However, the solution chemistry of this stabilisation process is not fully understood. The decomposition of hydrogen peroxide is catalysed by transition metal ions; α -alkylaminomethylenephosphonic acids may stabilise hydrogen peroxide by acting as sequestering agents (Chapter 6) for these metal ion impurities and contaminants.²⁹ Knowledge of the species present in solutions containing alkylaminomethylenephosphonic acid stabilisers and metal ions would be an important element in understanding the process. Hence, analysis of the solution chemistry of some α -alkylaminomethylenephosphonic acids and their complexes with metal ions was undertaken using the potentiometric titration technique. However, while this method can give an indication of the stoichiometries of species in solution and provide a measure of their stabilities, it cannot discriminate at the microscopic level. Nmr spectroscopy, on the other hand, when used in conjunction with potentiometric studies, can often provide the required insights at the molecular level.

Alkylaminomethylenephosphonic acids used industrially for hydrogen peroxide stabilisation generally contain several phosphonic acid groups (*e.g.* diethylenetriaminepentakis(methylenephosphonic acid), DTPMPH₁₀, has three basic nitrogen sites and five methylenephosphonic acid groups). DTPMPH₁₀ has various trade names including 'BRIQUEST 543-45AS' and 'DEQUEST 2060'.²⁶ The equilibria in *agu.* solution, and even more so in hydrogen peroxide, are likely to be very complex. In order to facilitate study of the solution chemistry of alkylaminomethylenephosphonic acids, model compounds with either one, two or

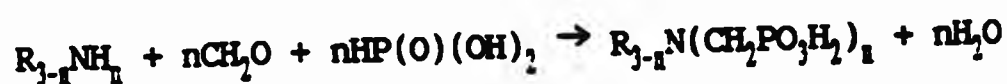


DTPMPH₁₀

four methylenephosphonic acid groups were selected. Hence, protonation of *N*-ethyliminobis(methylenephosphonic acid), NEIBMPH₄, diethylaminomethylenephosphonic acid, DEAMPH₂, *trans*-cyclohexane-1,2-diamine tetrakis(methylenephosphonic acid), CDTMPH₄ and 5,8-dioxadodecane-1,12-diamine tetrakis(methylenephosphonic acid) DDDTMPH₄, have been investigated by means of potentiometry and nmr spectroscopy. Their complexation behaviour with various metal cations (Chapter 5), has also been investigated by means of potentiometry.

4.2 Syntheses and characterisation of some alkylaminomethylenephosphonic acids

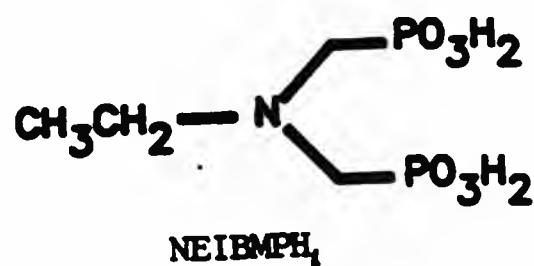
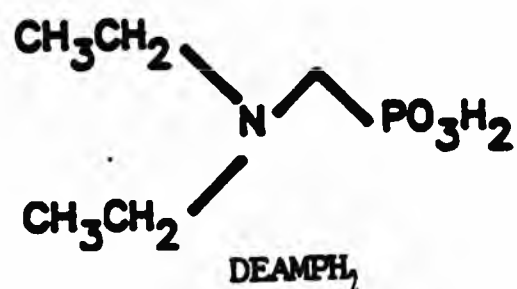
One of the major routes for the preparation of α -aminomethylenephosphonic acids is by the procedure given by Moedritzer and Irani.³⁰ However, it has been noted both by industry³¹ and other workers^{32,33} that the products prepared by this method (Moedritzer-Irani) are often impure. On the other hand, the preparation of α -aminomethylenephosphonic acids (by this route) which are insoluble in water, is often achieved in high yields. The reaction involves heating the appropriate amine, formaldehyde and phosphorous acid under reflux with concentrated hydrochloric acid:



where $n = 1, 2, 3$. To date, examination of the mechanism of this reaction has not appeared in the literature.

4.2.1 Synthesis and characterisation of DEAMPH₂ and NEIBMPH₄

Two simple aminomethylenephosphonic acids, DEAMPH₂ (Section 2.2.1) and NEIBMPH₄,



(Section 2.2.2), were prepared according to the Moedritzer-Irani reaction³⁰ and characterised by C, H, and N elemental analysis and nmr spectroscopy. The nmr spectra (¹H, ¹³C and ³¹P) for DEAMP₂ and NEIBMP₄, were determined in D₂O with deuterated sodium trimethylsilylpropionate (TSP-d₄) used as the internal reference for both ¹H and ¹³C nmr spectra. For ³¹P nmr spectra, aqueous phosphoric acid (85 %) was used as an external reference. Assignments for ¹H and ¹³C nmr spectra of both DEAMP₂ and NEIBMP₄ are given in sections 2.2.1 and 2.2.2, respectively.

The ¹H nmr spectrum of NEIBMP₄ is unremarkable, with only one feature worth noting, *i.e.* the coupling of the methylenephosphonate protons (CH₂-P) through two bonds to the adjacent phosphorus atom; ²J(HP) = 12.9 Hz.

In the ¹H nmr spectrum of DEAMP₂, the signals due to the methylene protons of CH₂-P and CH₂CH₂-N are more clearly resolved than in the ¹H nmr spectrum obtained for NEIBMP₄. A triplet is observed (at 1.31 ppm) arising from the methyl protons (CH₃) and a doublet at 3.28 ppm can be ascribed to the methylene-phosphonate protons CH₂-P, which are coupled through two bonds to the adjacent phosphorus atom. The value of the coupling constant [²J(HP) = 13.4 Hz] obtained for DEAMP₂, is consistent with that found for NEIBMP₄. The remaining two protons of the ethyl group give rise to an approximate quintet at 3.37 ppm. This quintet could arise from a number of possibilities. The CH₂CH₂-N protons are coupled through three bonds to the CH₃ protons to give a quartet whose components may be further coupled (through four bonds) to the phosphorus atom. The value of the coupling constant ⁴J(HP) (< 1) found for a similar α -aminomethylenephosphonic acid, 1-aminopropylphosphonic acid,³⁴ suggests that this possibility is unlikely. A second possibility is that the components of the quartet (arising from the coupling of CH₂CH₂-N to CH₃) are further coupled through four bonds to the methylenephosphonate protons, CH₂-P. But this also is unlikely as the methylenephosphonate protons CH₂-P show only coupling to the phosphorus [²J(HP)]. The value of the coupling constant ⁴J(HP) (< 1; found for 1-aminopropylphosphonic acid³⁴) also suggests that this possibility is unlikely. A third possibility is that the CH₂CH₂-N protons are anisochronous and therefore each proton (H^a and H^b) gives a quartet on coupling through three bonds to the adjacent methyl protons. These two quartets could then be overlapped to give the appearance of a quintet, but this explanation requires that ²J(H^aH^b) \approx 0 Hz. This explanation might apply if the nitrogen is *prochiral*, which may arise if the nitrogen is protonated and proton (H^f) exchange is sufficiently slow, or if the rate of *nitrogen inversion* is slow

enough at the non-protonated nitrogen.³⁵ To conclude, there is no obvious first order assignment of this quintet, and the $^1\text{H}\{-^{31}\text{P}\}$ nmr experiment which would have been helpful was not available in this work.

The ^{13}C nmr spectrum of NEIBMPH₂ is shown in Figure 4.2.1. The resonance of the methylene carbon of the methylenephosphonate group is split into a doublet by coupling with an adjacent phosphorus [$^1\text{J}(\text{CP})$] and is split further into a doublet by a three-bond coupling with phosphorus. The methylene carbon of the ethyl group splits into a triplet through three bond coupling with both phosphorus atoms.

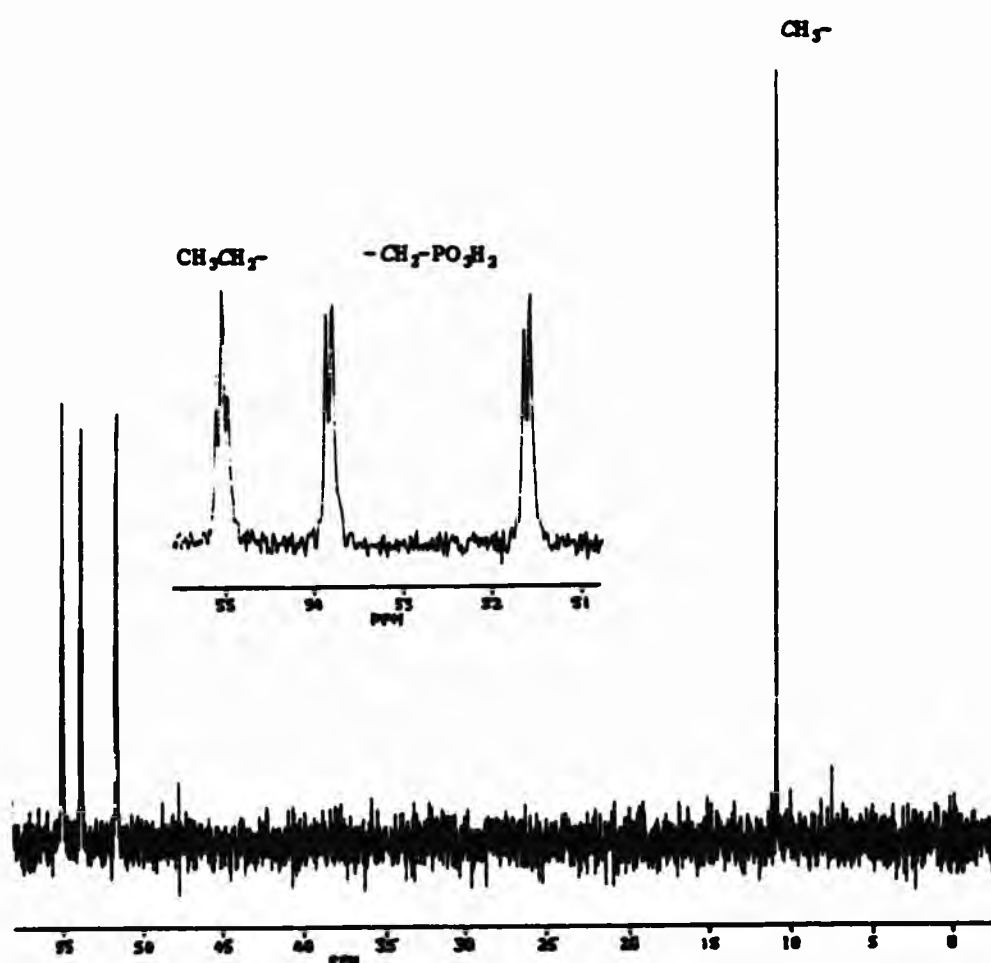


Figure 4.2.1 The ^{13}C nmr spectrum of NEIBMPH₂ in D₂O at 62.9 MHz.

The ^{13}C nmr spectrum obtained for DEAMPH₂ is substantially simpler than that for NEIBMPH₂. The resonance of the methylene carbon of the methylenephosphonate group is split only into a doublet by coupling with the adjacent phosphorus atom [$^1\text{J}(\text{CP})$]. The resonance of the methylene carbons of the ethyl groups is split into a doublet by a three bond coupling to phosphorus.

The values of the coupling constants [$^1\text{J}(\text{CP})$ and $^3\text{J}(\text{CP})$] obtained for DEAMPH₂ and NEIBMPH₂ are consistent with those reported by Sawada *et al.*³⁶ for

ethylenediamine *tetrakis*(methylenephosphonic acid), EDTMPH₈.

The ³¹P nmr spectra obtained for NEIBMPH₄ and DEAMPH₂ confirm the presence of only one phosphorus environment, with single resonances at 9.11 ppm and 8.28 ppm, respectively. Hence, the rapid exchange of protons between all the species present in solution produces an average chemical shift for the phosphorus atoms.

4.2.2 Synthesis and characterisation of CDTMPH₈

The preparation of another alkylaminomethylenephosphonic acid, CDTMPH₈, was attempted by various adaptations of the Moedritzer-Irani method³⁰ (Section 2.2.4). The (±)-*trans*-1,2-diaminocyclohexane isomer was used in the synthesis. The *trans* isomer of the diamine has two possible conformations of the substituent groups attached to the cyclohexyl ring in the chair form, *i.e.* *aa* or *ee*,[†] which are inter-convertible. The di-equatorial (*ee*) conformation is normally the more stable conformation.³⁷ With the two chiral carbons in the *ee* conformation, there are two possible stereoisomers, *i.e.* *RR* and *SS*.

Due to the high solubility of this compound in water, it was found to be extremely difficult to isolate the product in significant yields in the solid form. With some good fortune, a small amount of solid CDTMPH₈ was obtained after many attempts. The successful method involved extraction of the reaction mixture with diethylether (Section 2.2.4). It was thought that the diethylether was removing some of the excess hydrochloric acid present in the oil. However, C, H, N elemental analysis of this material showed that it could be approximately formulated as CDTMPH₈.3HCl. The ir spectrum of this sample, obtained as a KBr micro disc, indicated the presence of the characteristic stretching bands of the phosphonate group (PO₃²⁻). However, characterisation by ³¹P nmr spectroscopy indicated the presence of a number of phosphorus-containing impurities.

In order to determine the stability constants of CDTMPH₈, a pure sample of CDTMPH₈ was kindly supplied by Interlox Research & Development and its purity was confirmed by characterisation. Elemental analysis (C, H and N) was consistent with formulation as C₁₀H₂₆N₂O₁₂P₄, indicating that the sample did not contain hydrochloric acid.

[†] *a* = axial and *e* = equatorial.

The ^1H nmr spectrum obtained for this pure sample of CDTMPH_3 in D_2O (pH ca. 2) was complicated by various couplings to phosphorus and to other protons in the molecule. The multiplets were also broad, suggesting that the cyclohexyl ring is 'flipping' at a rate which is intermediate on the nmr time scale. It is

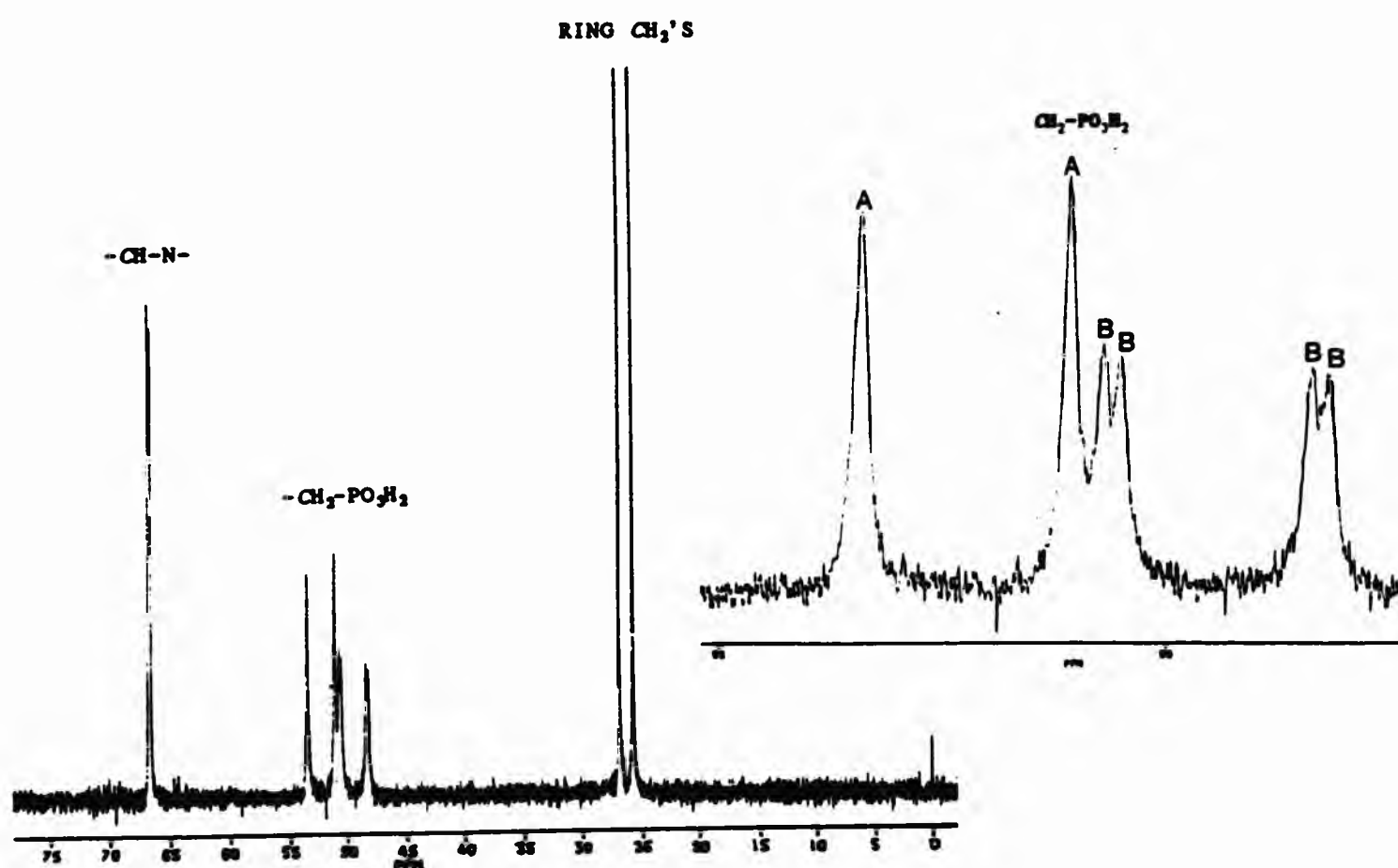
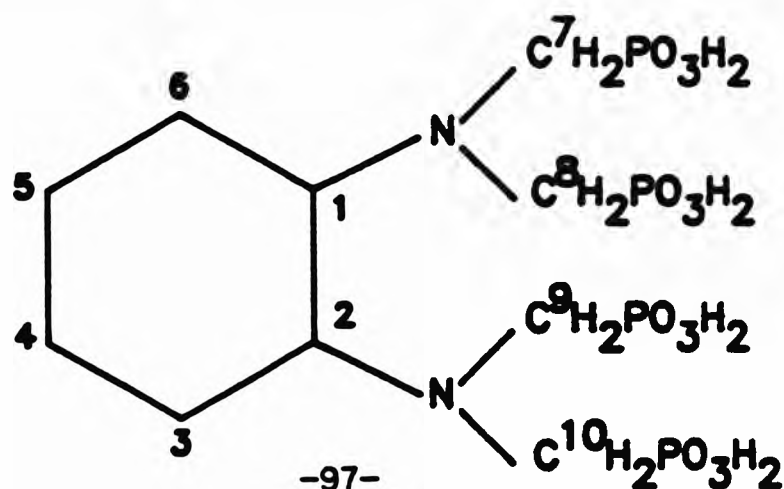


Figure 4.2.2 The ^{13}C nmr spectrum of CDTMPH_3 with an expanded region (at ca. 50 ppm) shown in the inset.

noted that the line broadening does not arise from the rather concentrated and hence relatively viscous solution used;^{38,39} the TSP resonance remains sharp. The line widths of the resonances in the ^{13}C nmr spectrum are also slightly broad (ca. 11 Hz), which again indicates the possibility of that the cyclohexyl ring is slowly 'flipping' at room temperature.

The observed pattern of the resonances in the ^{13}C nmr spectrum of CDTMPH_3 in D_2O (pH ca. 2) was more complicated than those for DEAMPH_2 and NEIBMPH_4 (Figure 4.2.2).



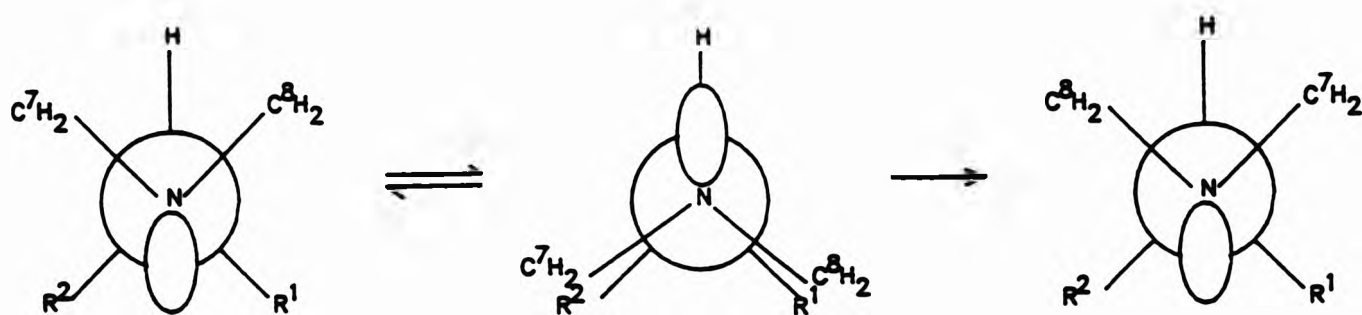
The two single resonances at 25.6 and 26.8 ppm, can be assigned to the methylene carbons of the cyclohexyl ring (3,6 and 4,5). The remaining signals can be divided into two groups; two at ca. 66.6 ppm and six between ca. 45 and 55 ppm. These groups can be assigned on the basis of chemical shift. The former are assigned to the CH carbons of the cyclohexyl ring, and the latter group is ascribed to the carbons of the four methylene phosphonate groups, CH₂-P. There are two possible assignments, and hence explanations, of the splitting patterns due to C-P spin-spin coupling for these CH and CH₂-P signals.

The two equatorial amine groups are expected to be equivalent because they are related by a two-fold axis. Then, if the N(CH₂PO₃)₂ groups are identical, only one ¹³C nmr multiplet for CH₂-P would be expected (as observed for NEIBMPH₄). However, in contrast to the ³¹P nmr spectra obtained for DEAMPH₂ and NEIBMPH₄, two resonances were observed in the ³¹P nmr spectrum of CDTMPH₃ (at 15.4 and 16.7 ppm). This behaviour suggests either that the two nitrogen atoms are not in the same environment, or that the ³¹P nuclei in the two CH₂PO₃H₂ groups (e.g. in C⁷H₂PO₃H₂ and C⁸H₂PO₃H₂) on a particular nitrogen atom are anisochronous.

The latter case could arise from the proximity of the chiral CH carbons on the ring, giving rise to isochronous pairs (say) C⁷, C⁹ and C⁸, C¹⁰ and, by the same token, two ³¹P resonances at differing chemical shifts. The pattern of the CH₂-P signals in the ¹³C nmr spectrum can then be assigned as follows: the resonance of one of the methylene carbons of the methylenephosphonate groups on each nitrogen atom (say) C⁷ and C⁹, splits into a doublet by coupling with the phosphorus in the α-position. For the other methylene carbons (i.e. C⁸, C¹⁰) the resonance is split to give a doublet by coupling through one bond to phosphorus and then again into a doublet of doublets by coupling to the phosphorus three bonds away. On this basis, the ¹³C nmr spectrum can be interpreted as (say) C⁷, C⁹ δ = 52.3 ppm, ¹J(CP) = 146.5 Hz; C⁸, C¹⁰ δ = 49.4 ppm, ¹J(CP) = 146.4 Hz and ³J(CP) = 11.6 Hz.

It is relevant to this interpretation that *nitrogen inversion*³⁵ will render the two methylenephosphonate groups (previously diastereotopic, i.e. differing in chemical shift) on a particular nitrogen atom, equivalent.

However, for quaternary ammonium compounds, nitrogen inversion is not possible and chiral ions may be separated into its enantiomers that are relatively stable.³⁵



Thus, if the nitrogen atoms were not protonated, the anisochronous behaviour of the two CH_2 groups within each amino group would be lost. Clearly, this interpretation requires that nitrogen inversion is inhibited by some means on *both* amino groups, and a full interpretation can only be advanced in the knowledge of the protonation scheme.

The alternative assignment of the ^{13}C and ^{31}P nmr spectra is based on the supposition that the amino groups are not equivalent due to some special feature(s) of the molecule and of the $-\text{N}(\text{CH}_2\text{PO}_3\text{H}_2)_2$ groups in particular (see later). Under these circumstances, (say) C^7 and C^8 would be isochronous and exhibit both one bond and three bond coupling to phosphorus (*i.e.* an $\text{AA}'\text{XX}'$ spin system), and C^9 and C^{10} would be an isochronous pair exhibiting only one bond coupling to phosphorus ($[\text{MP}]_2$ spin system).

It should be noted that the ^{13}C nmr CH resonances at 66.7 and 66.5 ppm do not give unambiguous distinction between the two alternative assignments. In the assignments in which C^7 and C^8 are anisochronous, the two signals may be components of a doublet due to three bond coupling to just *one* of the phosphorus atoms in the $\text{N}(\text{CH}_2\text{PO}_3\text{H}_2)_2$ groups.

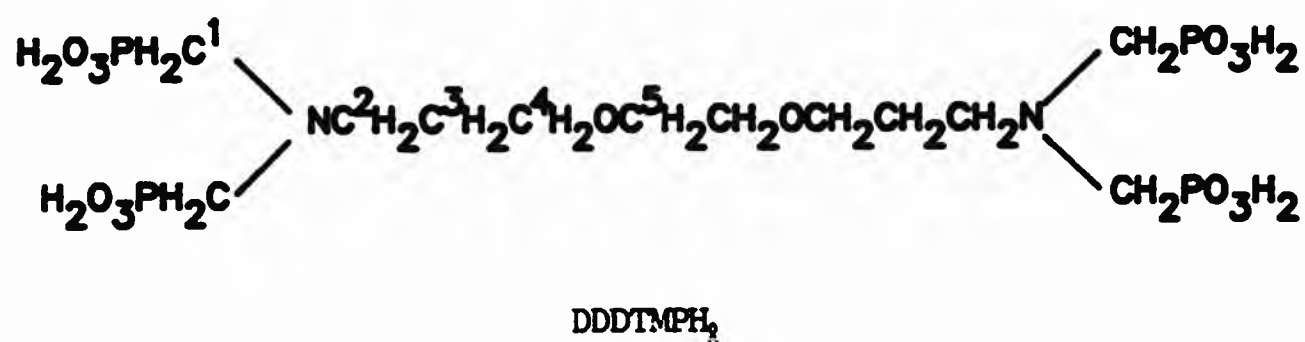
On the other hand, the assignment which assumes the amino groups to be non-equivalent should, at least, generate two separate resonances for the two anisochronous CH carbon atoms. In this case, $^3\text{J}(\text{CP})$ would be close to zero. The crucial $^{13}\text{C}\{-^{31}\text{P}\}$ experiment, which would have determined the separation of the CH signal as a coupling or as a chemical shift phenomenon, was not available in this work.

As mentioned previously, the protonation scheme for CDTMPH_2 has an important

bearing on these two alternative assignments and so the assignments will be considered further (Section 4.5) when the protonation scheme has been established.

4.2.3 Characterisation of DDDTMPH₃

A sample of DDDTMPH₃ was kindly supplied by J. Lockhart and P. Iveson[†] from the University of Newcastle Upon Tyne and the purity of the sample was confirmed by C, H, N elemental analysis. Nmr spectra were obtained in D₂O with deuterated TSP-d₄ as the internal standard reference for both ¹H and ¹³C nmr spectra, and aqueous phosphoric acid (85 %) as the external reference for ³¹P nmr spectra.



Allowing for the symmetry in the molecule, the expected five signals were observed for the 12 carbon atoms in the ¹³C nmr spectrum (Figure 4.2.3). The resonance of the methylene carbons of the methylenephosphonate group (C¹) at

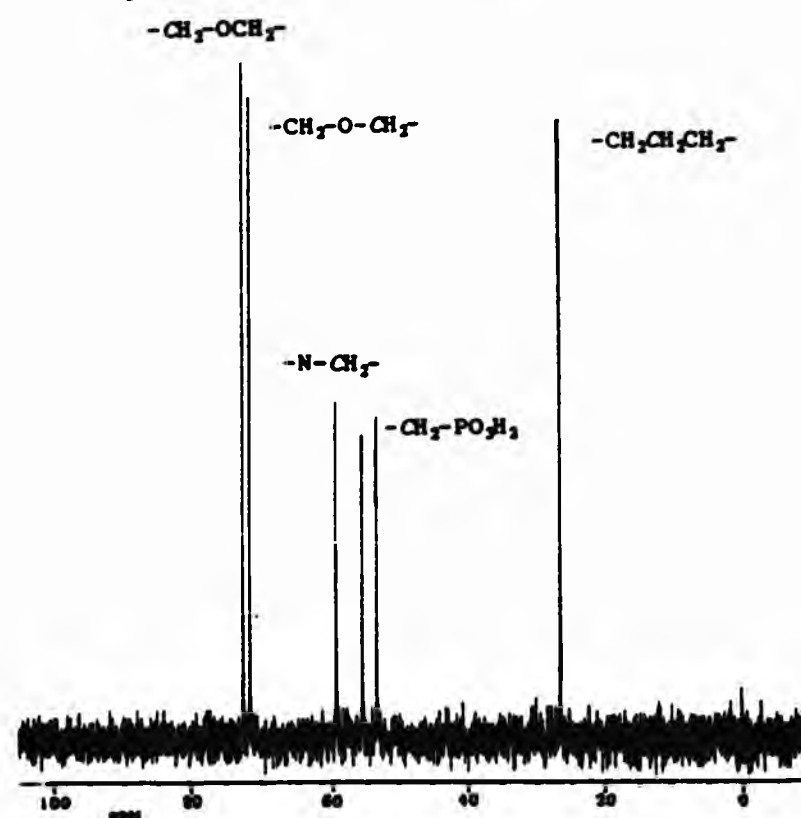


Figure 4.2.3 ¹³C nmr spectrum of DDDTMPH₃ in D₂O.

[†] P. Iveson, Ph.d Thesis, University of Newcastle Upon Tyne, 1991.

ca. 54 ppm, splits into a doublet by coupling with an adjacent phosphorus [$^1J(\text{CP})$] and the components are further split into doublets by a three-bond coupling with phosphorus. The resonance of the methylene carbon (C^2) of the aliphatic backbone, splits into a triplet by coupling through three bonds with two phosphorus atoms. The other carbons (C^3 , C^4 and C^5) in the molecule are assigned to the remaining three singlet resonances on the basis of chemical shift.

The ^{31}P nmr spectrum of DDDTMPH_3 , showed only one signal at 8.83 ppm, indicating that the four phosphorus atoms are in one environment. Presumably, rapid exchange of protons between all the species present in aqueous solution produces an averaged chemical shift.

4.2.4 Infrared spectra

The ir spectra of the alkylaminomethylenephosphonic acids, DEAMPH_2 , NEIBMPH_4 and CDTMPH_3 , were all obtained as 16 mm KBr discs (Section 2.5).

The ir spectra of aminomethylenephosphonic acids are usually quite difficult to assign. The more interesting features lie in the fingerprint region ($900\text{--}1500\text{ cm}^{-1}$). Bands due to deformation of the aliphatic CH_2 group ($1400\text{--}1470\text{ cm}^{-1}$) and the phosphonate stretching bands (νPO) at ($850\text{--}1300\text{ cm}^{-1}$) are usually observed.^{39,40}

The ir spectra of alkylaminomethylenephosphonic acids show a wide range of characteristic stretching bands for the phosphonate group giving rise to complex patterns of absorptions which are further complicated by the formation of hydrogen bonding (lowers the frequency of the band). Possible vibrations are; (P-OH); (P=O); asym (PO_2^-); sym (PO_2^-); asym (PO_3^-) and sym (PO_3^-).⁴⁰ The combined effect usually results in a broad cluster of bands in the fingerprint region. The associated OH stretch of the phosphonate group occurs as a group of broad, medium bands in the region $2560\text{--}2700\text{ cm}^{-1}$.

Assignments of these bands in the ir spectra of DEAMPH_2 , NEIBMPH_4 and CDTMPH_3 , are summarised in Table 4.2.1.

Table 4.2.1 Assignments for selected bands in the ir spectra of some alkyl-aminomethylenephosphonic acids ($\bar{\nu}/\text{cm}^{-1}$).

Ligand	(PO-H) ^a	(CH ₂) ^a	(CH ₂) ^b	asym,sym(PO ₂ ⁻)	(P-O)
DEAMPH ₂	2484-2758br	2964,2935,2873	1468	1124br	1005
NEIBMPH ₄	2546-2704br	2972,2912,2808	1446br	1214-1124br	975-939
CDTMPH ₈	2546-27950	2962,2943,2872	1444m ^c	1084-1007br	949

^a Stretch. ^b Deformation. ^c Not fully resolved.

4.3 Protonation equilibria for diethylaminomethylenephosphonic acid, DEAMPH₂

Diethylaminomethylenephosphonic acid, DEAMPH₂, contains one basic nitrogen site and one methylenephosphonic acid group. Potentiometric titrations of the acid were carried out in the absence of metal ions over the pH range 2-12 (Figure 4.3.1), generating two data files. Analysis of the data files, using SUPERQUAD,⁴¹ yielded two protonation constants (Table 4.3.1). The protonation constants ($\log \beta_{011}$ and $\log \beta_{012}$) obtained from data file M040 are characterised by satisfactory statistics and agree closely with the values determined by Wozniak *et al.*⁴² The protonation constants for DEAMPH₂ determined by Carter *et*

*al.*²³ are substantially different to those determined in this work and this could be ascribed to the different ionic strength used. The value of $\log K_{011}$ (11.55) determined by a previous worker at the University of North London⁴³ under the same conditions as those used in the present work is also significantly different. This may be due to the lower reliability associated with data at high pH and/or it may reflect the improvements in the stability constant determination procedures which have taken place since the earlier work. Data file M041 yielded protonation constants of lower reliability than those from file M040, as indicated by high χ^2 and σ values. The results from the file M041, shown here for comparison, were not used in further work on this ligand.

Table 4.3.1 Protonation constants for DEAMPH₂ (L = [Et₂NCH₂PO₃]²⁻).

Datafile	log β ₀₁₁	log β ₀₁₂	log K ₀₁₂
MO40 ^{a,b}	11.92(0.016)	17.22(0.024)	5.30
MO41 ^{a,c}	11.78(0.072)	16.81(0.170)	5.03
Literature ^d	11.81(0.03)	17.09(0.03)	5.28
Literature ^e	12.32 ± 0.19	18.11 ± 0.11	5.79
Literature ^f	11.55 ± 0.12	16.92 ± 0.15	5.37

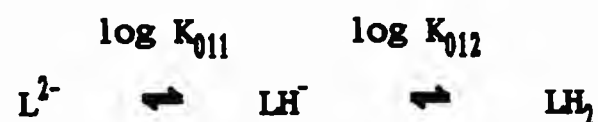
^a Data obtained at I = 0.1 mol dm⁻³ KNO₃, 25.0 ± 0.1 °C. Figures in parentheses are standard deviations obtained from SUPERQUAD. Convention: β_{MLH} for M_nL_mH_n.

^b Fit parameters obtained from SUPERQUAD, χ² = 3.26, σ = 0.345; pH 2.75–11.22, 152 data points. ^c Fit parameters obtained from SUPERQUAD, χ² = 16.12, σ = 0.655; pH 2.89–11.25, 125 data points. ^d Ref. 42, at I = 0.1 mol dm⁻³ KNO₃, 25.0 °C. Figures in parentheses are 3σ. ^e Ref. 23, at I = 1.0 mol dm⁻³ KNO₃, 25.0 °C. ^f Ref. 43 at I = 0.1 mol dm⁻³ KNO₃, 25.0 °C.

The two buffer regions (Figure 4.3.1) correspond approximately to the two stepwise protonation constants, *i.e.* pH 4.5–5.5 and pH 11–12. DEAMPH₂ has three protonation sites, the basic nitrogen and the two phosphonic acid oxygens, and hence three protonation constants might be expected for determinations in an initially acidic solution:



The two log K values determined from the analysis using SUPERQUAD⁴¹, were assigned to the protonation scheme for DEAMPH₂ as:



rather than the alternative two sequential protonations resulting in LH₃⁺. This assignment is based on comparison with the results of potentiometric studies of some other alkylaminomethylenephosphonic acids^{23,42,44} *i.e.* three simple aminomethylenephosphonic acids, containing three, two and one

methylenephosphonate groups respectively (Table 4.3.2).

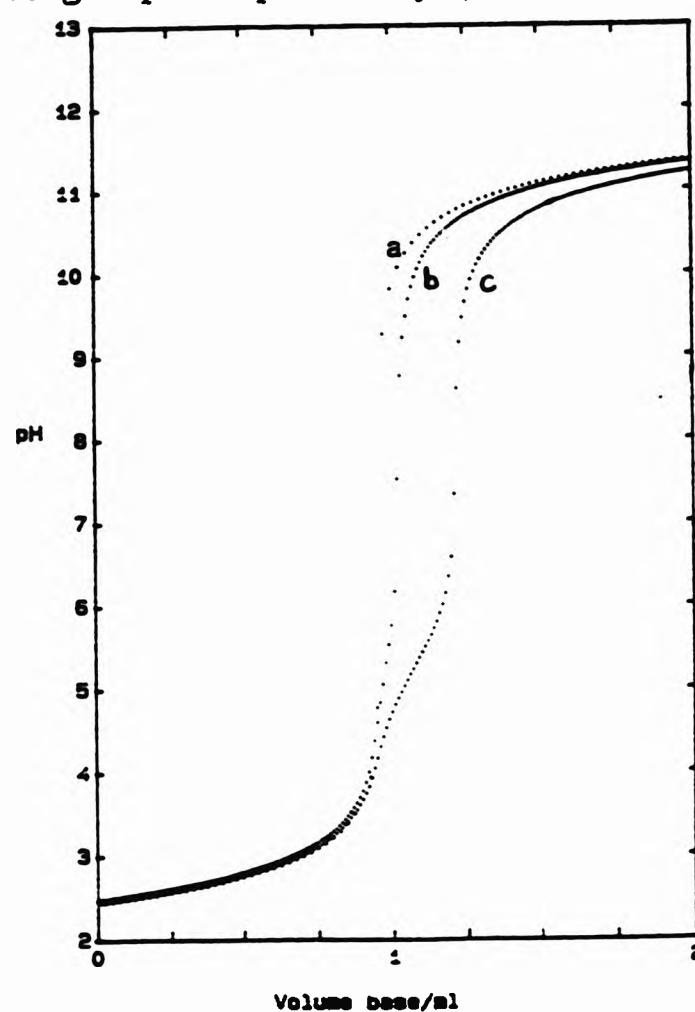


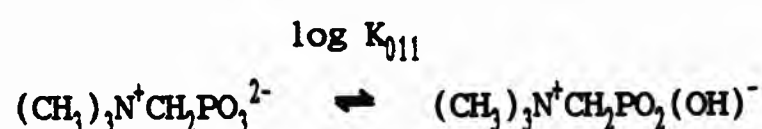
Figure 4.3.1 Titration curves (pH vs volume of base added) for DEAMPH₂; (a) calibration curve, (b) [DEAMPH₂] = 0.0004 mol dm⁻³, and (c) [DEAMPH₂] = 0.001 mol dm⁻³.

Table 4.3.2 Protonation constants for some α -aminomethylenephosphonic acids.

M L H	log K _{MLH}			
	NTMPH ₂ ^a	IDMPH ₂ ^b	DMAMPH ₂ ^c	TMAMPH ₂ ^d
0 1 1	12.34	10.62	11.06	5.10
0 1 2	6.66	5.82	5.19	
0 1 3	5.46	4.83	0.45 ^e	
0 1 4	4.30	<2		
0 1 5	<2			
0 1 6	<2			

^a Ref. 23, I = 1.0 mol dm⁻³ KNO₃, 25.0 °C. ^b Ref. 43, I = 1.0 mol dm⁻³ KNO₃, 25.0 °C. ^c Ref. 42, I = 0.1 mol dm⁻³ KNO₃, 25.0 °C. ^d Ref. 42, I = 0.1 mol dm⁻³ KNO₃, 25.0 °C. ^e For fully protonated species LH₃⁺.

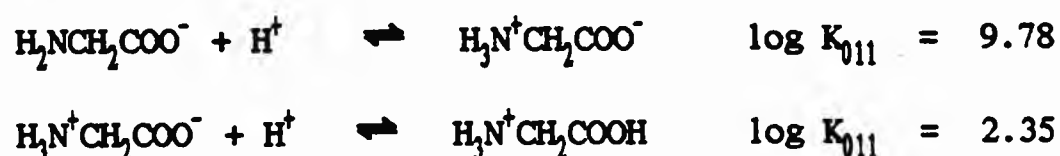
Also of relevance is another simple alkylaminomethylenephosphonic acid, trimethylammoniummethylenephosphonic acid (TMAMPH₂), (CH₃)₃N⁺CH₂PO₃H₂, in which the nitrogen is in a quaternary environment and hence cannot be protonated. Only one protonation constant (Table 4.3.2) was determined by Wozniak⁴² and must represent protonation of the phosphonate function:



The value of log K₀₁₁ for each of the three alkylaminomethylenephosphonic acids NTMPH₆, IDMPH₄ and DMAMPH₂ is greater than ten. However, in the case of TMAMPH₂, where the quaternary nitrogen cannot be protonated, log K₀₁₁ (5.10) is very much less than ten and is also very similar to the log K₀₁₂ for DMAMPH₂ (5.19). This strongly suggests that the log K value of 5.30 for DEAMPH₂ corresponds to the first protonation of the phosphonate oxygen and that log K₀₁₁ for DEAMPH₂ is due to the protonation of the basic nitrogen site to give the species LH⁻. Log K values for IDMPH₄ and NTMPH₆, each with one nitrogen, also fit this pattern.

Furthermore, during analysis of the data files for DEAMPH₂ using SUPERQUAD,⁴¹ inclusion of the fully protonated species LH₃⁺ in the model for the equilibria in solution over the pH range 2-12 did not lead to successful refinement. It is likely, therefore, that the fully protonated species LH₃⁺ exists only in very acidic conditions (*i.e.* less than pH 2). Previously determined protonation constants for DEAMPH₂ were also similarly assigned (Table 4.3.1).^{23,42}

Alkylaminomethylenephosphonic acids are difunctional compounds containing both a basic and an acidic group. α-Aminomethylenephosphonic acids are analogous to α-aminomethylenecarboxylic acids, *e.g.* glycine (GlyH) and L-proline; these are amphoteric and exist as zwitterions in solution and the solid state.³⁵ Glycine exists as the fully protonated species, GlyH₂⁺, in very acidic media (*i.e.* less than pH *ca.* 2.5). Two protonation constants have been determined for glycine:³⁵



schemes.

The ^{31}P nmr spectra for DEAMP H_2 were determined as a function of pH in order to confirm the protonation scheme proposed above. The conditions employed for the nmr/pH titrations were qualitatively similar to those used in the potentiometric titrations. It was necessary, however, to use a ligand concentration *ca.* ten-fold greater so that the ^{31}P nmr signal could be detected within a reasonable time scale. Concentrations of other components of the solution were likewise increased (*i.e.* $I = 1.0 \text{ mol dm}^{-3} \text{ KNO}_3$, initial $[\text{HNO}_3] = 0.04 \text{ mol dm}^{-3}$). A base (*aqu.* KOH) concentration of 1.0 mol dm^{-3} was used in order to minimise volume changes which would effect ionic strength during the titration. As only 10 % D_2O was employed, it was assumed that the deuterium isotope effect⁶³ would not significantly affect solution pH, and therefore pH values were not corrected.

In the pH range studied (1.37-12.79), the ^{31}P nmr spectra obtained showed only one signal indicating that there is rapid exchange of protons between all the species present in solution at each point. The plot of $\delta(^{31}\text{P})$ against pH showed a distinctive curve similar to that obtained for other simple α -aminomethylenephosphonic acids (Figure 4.3.2a).^{23,24,30,43,57,58,60,64-66} The pH dependence of $\delta(^{31}\text{P})$ for DEAMP H_2 broadly correlates with that determined by Carter *et al.*²³

Comparison of the species distribution curves with the plot of $\delta(^{31}\text{P})$ vs pH for DEAMP H_2 (Figure 4.3.2) shows a correspondence between the 'half-neutralisation points' at *ca.* pH 5 and *ca.* pH 12 on the species curves and the approximate positions of inflections on the $\delta(^{31}\text{P})$ vs pH curve. The 'half neutralisation points' also correspond approximately to the two pK_a values determined by using SUPERQUAD.⁴¹ Hence, it is reasonable to assume that the upfield shift of the phosphorus signal between *ca.* pH 4 and 6 (*ca.* 2 ppm) is associated with the deprotonation of the species LH_2 to form the species LH^- . Then the large downfield shift of $\delta(^{31}\text{P})$ at *ca.* pH 11-13 (*ca.* 5.5 ppm) is assigned to deprotonation of LH^- to form the fully deprotonated species L^{2-} . On this basis, the slight upfield shift of the phosphorus signal at *ca.* pH 1-4 (Figure 4.3.2b) would be due to the deprotonation of the species LH_2^+ to give the neutral species LH_2 .

There is substantial evidence from previous work on α -aminomethylenephosphonic acids which indicates that an upfield shift (usually at low pH) of the phosphorus signal with increasing pH is due to deprotonation of the

phosphonate oxygen and that the sharp downfield shift (usually at high pH) is due to the nitrogen-bound proton being neutralised.^{23,30,58,60,61,66,68}

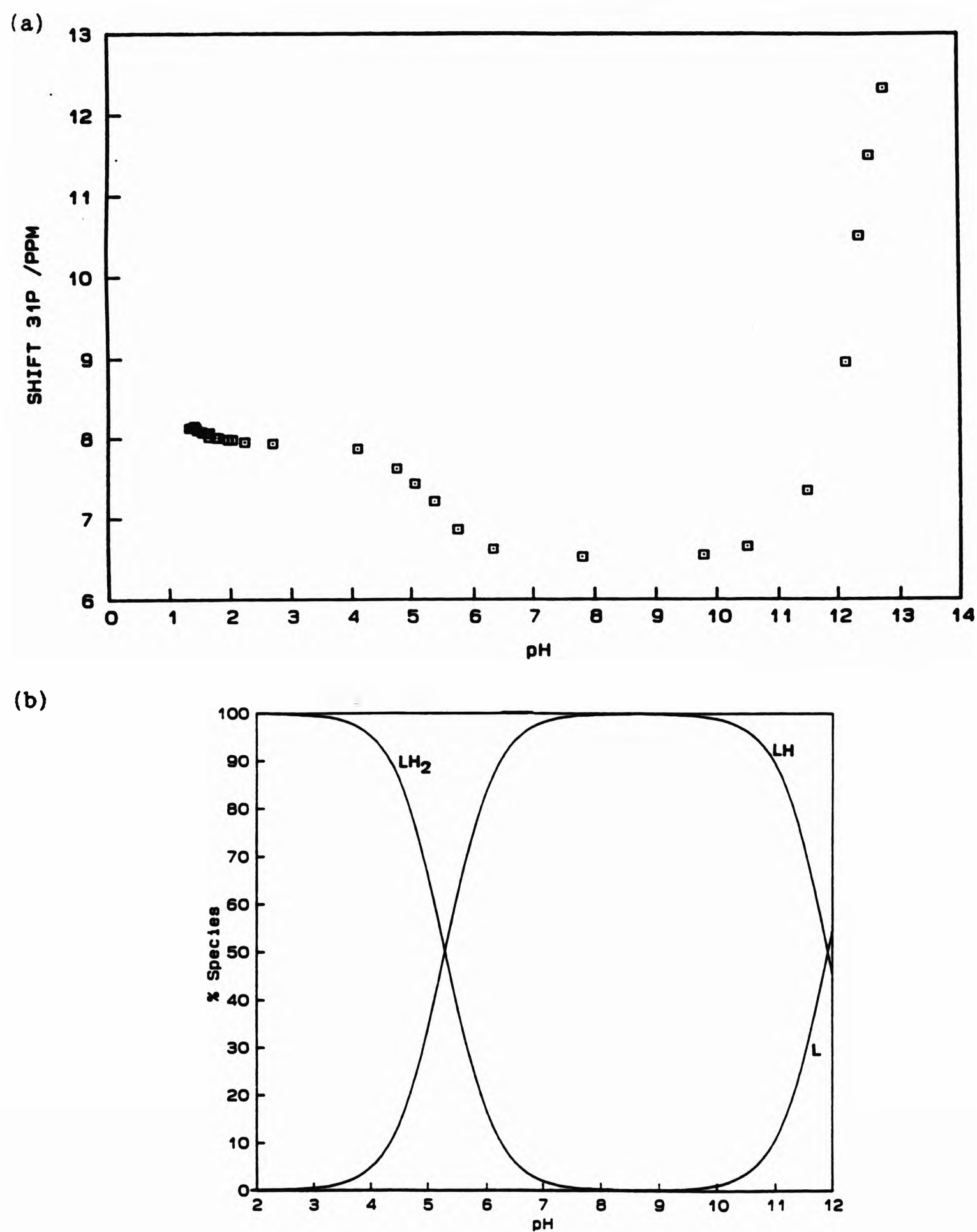
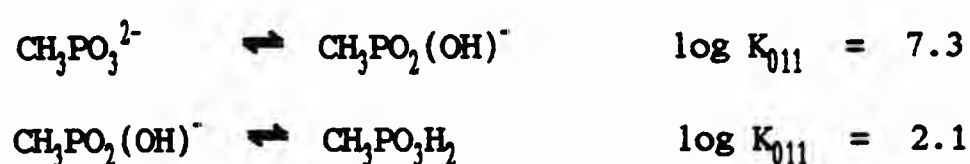


Figure 4.3.2 (a) The pH dependence of $\delta(^{31}\text{P})$ for DEAMPH_2 in *aqu.* solution; (b) species distribution plots⁶⁷ as a function of pH for DEAMPH_2 .

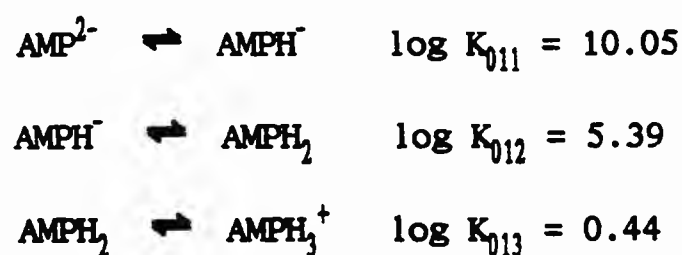
Appleton determined the variation of the ^{31}P chemical shift as a function of pH (pD) for a simple alkylphosphonic acid, methylphosphonic acid, $\text{CH}_3\text{PO}_3\text{H}_2$ (MPH_2).⁶⁰ The resulting plot of $\delta^{31}\text{P}$ vs pD showed two inflections in the curve, at pD 2.3 and 7.8, which corresponded to the two successive protonations of MP^{2-} and their log K values.⁶⁰



As the pH is increased, there is a large upfield shift in the phosphorus signal in the region pD 0-2.5 [$\Delta(\delta^{31}\text{P})$ ca. 7 ppm] with an inflection corresponding to the deprotonation of MPH_2 to form MPH^- . Between pD ca. 2.5-6, there is a levelling off of the curve. As the pD is further increased, there is another upfield shift in the phosphorus signal between pH 6.5-10 [$\Delta(\delta^{31}\text{P})$ ca. 4 ppm]. Again, this upfield shift coincides with the second inflection at pD 7.8, indicating that the species MPH^- is being deprotonated to form the fully deprotonated species MP^{2-} . Above pD 10, there is a final levelling off of the curve.

Comparing the results determined by Appleton for MPH_2 ⁶⁰ with that obtained for DEAMPH_2 , a major difference is observed. For MPH_2 , there is no downfield shift in the phosphorus signal above pD 8; instead as already mentioned there is a levelling off of the curve. This strongly indicates that the upfield shift of the phosphorus signal for DEAMPH_2 as pH increases is due to the deprotonation of the phosphonate oxygens.

Appleton also studied the variation of the $\delta^{31}\text{P}$ as a function of pD for aminomethylenephosphonic acid, $\text{NH}_2\text{CH}_2\text{PO}_3\text{H}_2$ (AMPH_2) and the resulting plot of $\delta^{31}\text{P}$ vs pD was significantly different to that obtained for MPH_2 .⁶⁰ In the case of AMPH_2 , the three inflections in the curve at ca. pD 10, 6 and 1 correspond to the successive protonations of AMP^{2-} and the log K values determined.⁶⁰



At low pD (0-1.5), there is a small upfield shift in the phosphorus signal [$\Delta(\delta^{31}\text{P})$ ca. 4 ppm] which corresponds to the deprotonation of the fully protonated species AMPH_3^+ to give AMPH_2 . Between pD 2-4, there is a slight levelling off of the curve, with another slight upfield shift in the phosphorus signal between pD 4-6, which corresponds to the deprotonation of AMPH_2 to give AMPH^- . Above pD 10, there is a rather large downfield shift of the phosphorus signal [$\Delta(\delta^{31}\text{P})$ ca. 11 ppm] and, by comparison with the pD dependence of $\delta^{31}\text{P}$ for MPH_2 , this downfield shift corresponds to the process in which the nitrogen bound proton is being neutralised to form the fully deprotonated species AMP^{2-} .⁶⁰

Comparison of the results for MPH_2 and AMPH_2 , and for several other aminomethylenephosphonic acids,^{23,26,30,59,60,64-66} with those for DEAMPH_2 , leads to the conclusion that the downfield shift of the phosphorus nucleus in DEAMPH_2 can be assigned to the deprotonation of the basic nitrogen.

The origins of the downfield shift of the phosphorus signal on nitrogen deprotonation are the subject of some debate, and several factors have been identified as being important. The possibility of formation of intramolecular hydrogen bonds between the phosphonate oxygens and the neighbouring protonated nitrogen, and hence the state of protonation of the basic nitrogen and phosphonate oxygen atoms, is expected to greatly influence $\delta(^{31}\text{P})$ for the various species in solution.^{59,60} Recently, Dhansay *et al.*⁵⁹ also suggested that disruption of intramolecular hydrogen bonds on deprotonation of the nitrogen was responsible for the dramatic downfield shift in the phosphorus signal.

Appleton *et al.*⁶⁰ studied the pH dependence of $\delta(^{31}\text{P})$ for a sequence of aminoalkylphosphonic acids, $\text{NH}_3(\text{CH}_2)_n\text{PO}_3\text{H}_2$ (where $n = 1, 2$ and 3). At a pH of greater than 11, the change in $\delta(^{31}\text{P})$ for the three aminoalkylphosphonic acids decreased as n increased from 1 to 3. Appleton⁶⁰ suggested the presence of *cyclic* structures in which strong hydrogen bonds are formed between the protonated nitrogen and the phosphonate oxygens. These structures involved five, six and seven membered rings ($n = 1, 2$ and 3 respectively). Appleton proposed that as the carbon chain increased and hence the size of the ring formed in solution also increased, the hydrogen bonds became weaker resulting in less interaction between the amine and phosphonate groups. This in turn was assumed to lead to a decrease in the change in $\delta(^{31}\text{P})$.⁶⁰

A typical feature of the solid state structures of the many α -aminomethylene

phosphonic acids whose structures have been determined by X-ray crystallography^{45,46,48,50,52-57} is the extensive nature of their hydrogen bonding interactions. For example, in the solid state structure of DEAMPH₂ (Section 7.2), there are two very strong intermolecular hydrogen bonds, one between a protonated phosphonate oxygen and an unprotonated phosphonate oxygen, O(3)...HO(2), and the other between the protonated nitrogen and an unprotonated phosphonate oxygen, H(n1)...O(1), but no intramolecular hydrogen bonding was found. In fact, only in one instance has an intramolecular hydrogen bond found between a protonated nitrogen and a phosphonate oxygen forming a five membered ring, *i.e.* for ethylenediaminebis(methylenephosphonic acid).⁵⁴ This intramolecular hydrogen bond has to be classified as being weak, (N)H...O(1) = 2.68(4) Å and the angle at hydrogen, N-H...O(1), is 96(5) °.⁵⁴ However, in a mixed aminophosphonic and carboxylic acid, a six membered intramolecular hydrogen bond between a nitrogen-bound proton and phosphonate oxygen was found, *i.e.* for 2-amino-3-phosphonopropionic acid, NH₂CH(COOH)CH₂PO₃H₂.⁶⁹ This hydrogen bond can be classified as being stronger than the intramolecular hydrogen bond formed in ethylenediaminebis(methylenephosphonic acid), (N)H...O(1) = 2.04(4) Å and N-H...O(1) is 145(4) °.

Therefore, examination of the solid state structures of α -aminomethylene-phosphonic acids suggests that five membered rings involving intramolecular hydrogen bonds between the protonated nitrogen and the phosphonate oxygen are rare. Ring formation may be more favourable where the possibility of a six-membered ring exists.

Sawada *et al.*²⁴ later proposed that Appleton's observations were due instead to a through-bond electronic effect [P-(CH₂)_n-N], *i.e.* as the carbon chain increased, the electron-withdrawing effect of the phosphonate group on the nitrogen decreased.

Another explanation offered for the downfield shift of the phosphorus signal as the pH is increased, and the nitrogen-bound proton is neutralised, is centred around the hybridisation changes at nitrogen.^{30,66} The dramatic deshielding of the phosphorus atom is attributed to conversion of the nitrogen atom from tetrahedral (sp³) to an uncharged pyramidal environment (sp³). Letcher and van Wazer⁶⁶ further developed this idea using quantum mechanical methods and separated the effects into opposing contributions to the ³¹P chemical shift from the inductive effects of proton dissociation and the accompanying effects due to changes in the pi-bonding between the phosphorus

and oxygen atoms.⁵⁶

Thus, the actual mechanisms which produce this downfield chemical shift of the phosphorus signal when nitrogen is deprotonated still remain unresolved.

Species distribution curves (species abundances vs pH, obtained using the program SPE⁶⁷, Section 2.3.9) for DEAMPH₂ (Figure 4.3.2a), show that the neutral (zwitterion) LH₂ and the monoprotonated species LH⁻ are dominant over the pH range 2-12.

4.4 Protonation constants for N-ethyliminobis(methylenephosphonic acid), NEIBMPH₄

N-ethyliminobis(methylenephosphonic acid), NEIBMPH₄, contains three functional groups, *i.e.* one basic nitrogen site and two methylenephosphonic acid groups. The potentiometric titrations of the free ligand were carried out, as for DEAMPH₂, in the absence of metal ions over the same pH range (Figure 4.4.1). NEIBMPH₄ contains 5 possible protonation sites but analysis, using SUPERQUAD,⁴¹

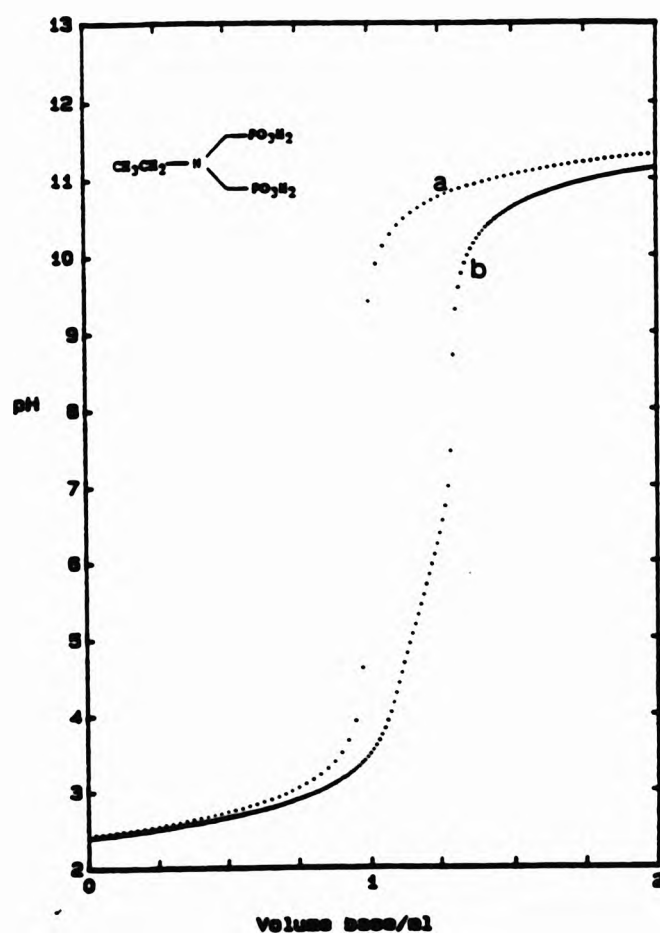


Figure 4.4.1 Titration curve (pH vs volume of base added) for NEIBMPH₄; (a) calibration curve; (b) [NEIBMPH₄] = 0.0005 mol dm⁻³.

of the three data files obtained, gave only the four protonation constants shown in Table 4.4.1. The results obtained for all the data files are considered reliable as judged by low χ^2 and σ values, and satisfactory weighted residuals output.⁴¹ The buffer regions (Figure 4.4.1) correspond approximately to the four stepwise protonation constants determined.

Thermodynamic equilibrium constants are strictly defined in terms of activities of the species in solution at equilibrium. The activity (a_i) of a species is its effective concentration in solution and is defined as:

$$a_i = \gamma_i c_i$$

where γ_i is the activity coefficient and c_i is the actual concentration of the i th species in the solution. Ionic activity coefficients vary with concentration and in very dilute solutions approach unity. The ionic activity coefficient also varies with the total ionic strength of the solution. Therefore, working in a medium of constant ionic strength minimises changes in ionic activity coefficients and hence the activities of the species. Under these circumstances, 'concentration equilibrium constants', calculated from the concentrations of ions rather than their activities, become useful. It follows that when comparing two equilibrium constants at different ionic strengths, the activity coefficients of ions in the two solutions will be slightly different and hence the measured equilibrium constants will also be different. As the activity coefficient, pH and ionic strength are inter-related, it is important to state the sample temperature, ionic strength and solvent composition for protonation or stability constant determination in order to allow comparison of data or duplication of results.⁷⁰

The protonation constants for NEIBMPH₄ determined by Carter *et al.*²³ and Bel'skii *et al.*⁴⁴ at $I = 1.0 \text{ mol dm}^{-3} \text{ KNO}_3$ (Table 4.4.1) vary significantly from the results determined here, presumably because of the difference in ionic strengths used for the two determinations. The agreement between the value of $\log \beta_{011}$ obtained in this work and that by a previous worker at the University of North London⁴³ is somewhat unsatisfactory, but values of $\log K_{011}$ are particularly sensitive to a number of factors including the low abundance of the fully deprotonated ligand in the pH range studied in the refinement, the possible interaction of the ligand with the background electrolyte, as found by Anderegg,⁷¹ and the unreliability of the data obtained at high pH, as measured with a glass electrode.⁷²

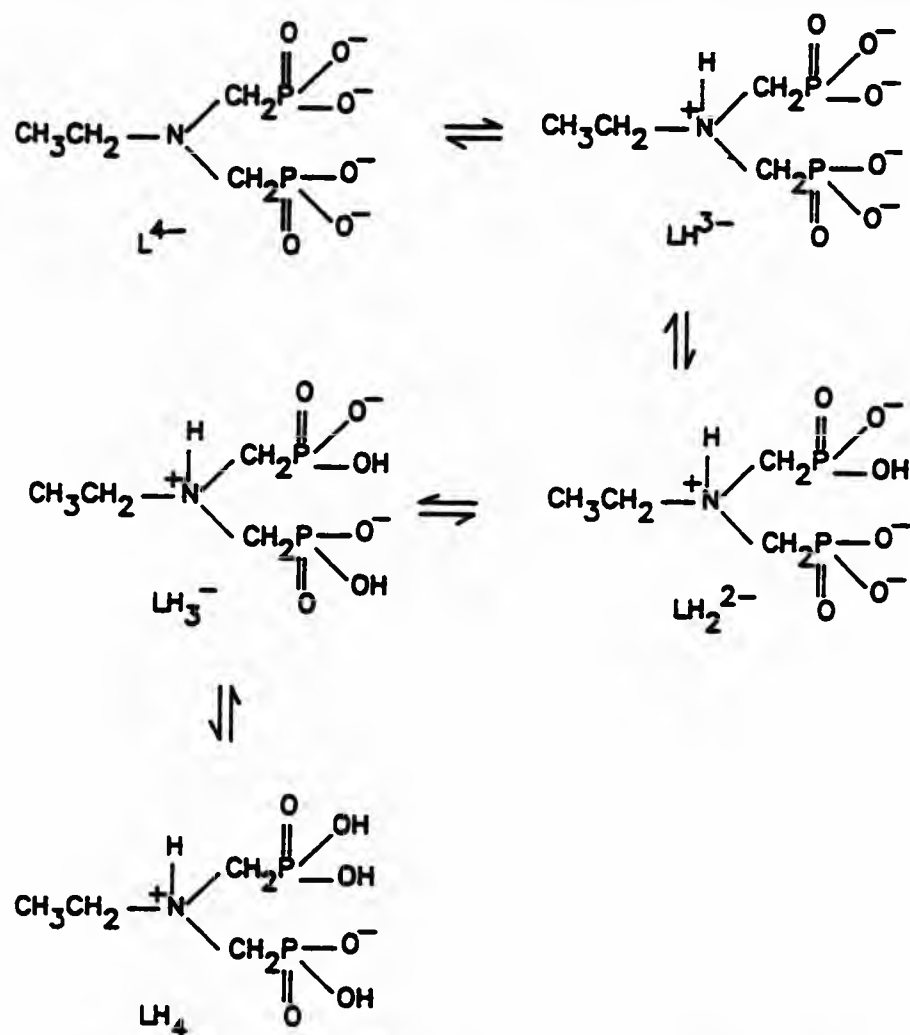
Table 4.4.1 Protonation constants for NEIBMPH₄ (L = [EtN(CH₂PO₃)₂]⁴⁻).^a

Data file:	M096 ^b	M097 ^c	M0100 ^d	Mean ^e
log β ₀₁₁	12.11(0.01)	12.16(0.02)	11.74(0.03)	12.00 ±0.26
log β ₀₁₂	18.35(0.02)	18.45(0.03)	18.02(0.03)	18.27 ±0.25
log K ₀₁₂	6.25	6.29	6.29	6.28 ±0.03
log β ₀₁₃	23.23(0.03)	23.34(0.03)	22.92(0.04)	23.16 ±0.24
log K ₀₁₃	4.88	4.89	4.89	4.89 ±0.01
log β ₀₁₄	25.02(0.04)	25.43(0.04)	24.87(0.06)	25.11 ±0.32
log K ₀₁₄	1.78	2.09	1.96	1.94 ±0.16

	log β ₀₁₁	log K ₀₁₂	log K ₀₁₃	log K ₀₁₄
Literature ^f	12.42 ±0.10	5.92 ±0.04	4.70 ±0.04	<2
Literature ^g	11.98 ±0.05	5.92 ±0.03	4.68 ±0.03	<2
Literature ^h	11.73 ±0.08	6.34 ±0.07	5.00 ±0.14	2.1 ±0.4

^a This work: I = 0.1 mol dm⁻³ KNO₃, 25.0 ±0.1 °C. Figures in parentheses are standard deviations obtained from SUPERQUAD. Convention: β_{MLH} for M_nL_mH_n. ^b Fit parameters obtained from SUPERQUAD, χ² = 5.14, σ = 0.0771; pH 2.81-11.12; 130 data points. ^c Fit parameters obtained from SUPERQUAD, χ² = 7.13, σ = 0.0607; pH 2.97-11.09; 111 data points. ^d Fit parameters obtained from SUPERQUAD, χ² = 5.40, σ = 0.0940; pH 2.77-10.98; 105 data points. ^e Unweighted mean of values from each refinement; error limits are derived from the ranges obtained for each log β_{MLH} (and log K_{MLH}). ^f Ref. 23, at I = 1.0 mol dm⁻³ KNO₃, 25.0 °C. ^g Ref. 44, at I = 1.0 mol dm⁻³ KNO₃, 25.0 °C. ^h Ref. 43, at I = 0.1 mol dm⁻³ KNO₃, 25.0 °C.

Using arguments previously applied to the determination of the protonation scheme for DEAMPH₂ (Section 4.3), the protonation scheme shown below is proposed for NEIBMPH₄. The scheme is consistent with the pH-dependence of δ³¹P for this molecule reported by Scowen⁴³ and in this work (Chapter 6). The neutral ligand exists as a zwitterion in solution, with the fully protonated species NEIBMPH₄, occurring only in very acidic conditions *i.e.* less than pH 2. Furthermore, during analysis of the data files for NEIBMPH₄ using SUPERQUAD,⁴¹ inclusion of the fully protonated species LH₅⁺ in the model for the reactions occurring in solution over the pH range 2-12 did not lead to successful refinement. Therefore, the protonation constants have been assigned to the following protonation scheme:



Species distribution curves⁶⁷ for NEIBMPH₄ (Figure 4.4.2) show that the dominant species over the pH range 2-12 are LH₃⁻, LH₂²⁻, and LH₃⁻.

Protonation constants (Table 4.4.2) are useful in deciphering the electronic effects of the phosphorus-containing substituents (*i.e.* phosphonate groups) on the relative basicity of the nitrogen in ethylamine, DEAMPH₂, NEIBMPH₄ and NIMPH₆.

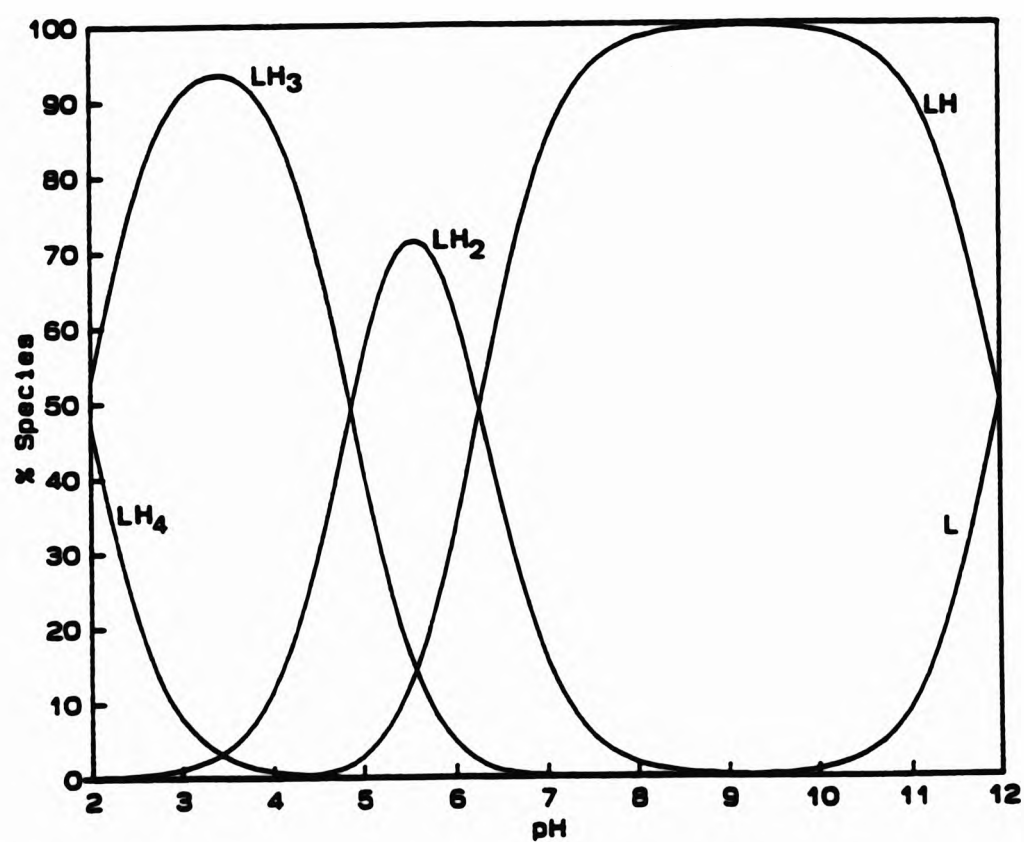


Figure 4.4.2 Species distribution curves⁶⁷ for NEIBMPH₄.

The first protonation of the ligand ($\log K_{011}$) increases with increasing number of methylenephosphonic acid groups, whereas that of aminopolymethylene-carboxylate ligands is scarcely changed by the number of carboxylate groups [$\log K_{011} = 9.78, 9.65$ and 9.71 for *N,N*-dimethylglycine, *N*-methyliminobis-(acetic acid) and nitrilotriacetic acid respectively]. The high negative charge of the phosphonate groups (PO_3^{2-}) compared with the carboxylate group (CO_2^-) may induce the higher and, indeed, increasing basicity of the nitrogen atom of the alkylaminomethylenephosphonic acids.²⁴ For example, on replacement of one of the hydrogens of ethylamine by a methylenephosphonate group to give DEAMPH_2 , there is a large increase in the value of $\log K_{011}$ for DEAMPH_2 (ca. 1 log unit). This increase in $\log K_{011}$ also continues from DEAMPH_2 to NTMPH_6 .

Table 4.4.2 Protonation constants of some related ligands.

Ligand	$\log K_{011}$	$\log K_{012}$	$\log K_{013}$	$\log K_{014}$	$\log K_{015}$	$\log K_{016}$
EtNH_2^a	10.72					
DEAMPH_2^b	11.92	5.30				
NEIBMPH_4^b	12.00	6.28	4.89	1.94		
NTMPH_6^c	12.34	6.66	5.46	4.30	< 2	< 2
DEGH_2^d	10.47	2.04				

^a Ref. 6; ethylamine. ^b This work; carried out at $I = 0.1 \text{ mol dm}^{-3}$, $25.0 \pm 0.1 \text{ }^\circ\text{C}$. ^c Ref. 23; nitrilotris(methylenephosphonic acid); $I = 1.0 \text{ mol dm}^{-3} \text{ KNO}_3$, $25.0 \pm 0.1 \text{ }^\circ\text{C}$. ^d Ref. 42; *N,N*-diethylglycine; $I = 0.1 \text{ mol dm}^{-3} \text{ KNO}_3$, $25.0 \pm 0.1 \text{ }^\circ\text{C}$.

This increase in basicity has been ascribed by some workers²⁴ to the increase in electron density on the nitrogen arising from the negatively charged phosphonate groups (-1 in the carboxylate to -6 in *tris*phosphonate). A similar result is also seen when comparing $\log K_{011}$ of DEGH_2 with DEAMPH_2 . On replacing the carboxylate group of DEGH_2 with a phosphonic acid group, there is an increase in the value of $\log K_{011}$ for DEAMPH_2 ca. 1.5 log units.

The increase in the value of $\log K_{011}$ for NEIBMPH_4^{4-} (12.00) over that of DEAMPH_2^{2-} (11.92) corresponds to the substitution of an ethyl group of DEAMPH_2 with a methylenephosphonate group. This increase in the basicity of the nitrogen atom has been ascribed (see above) to the extremely electron-rich phosphonate group, which counteracts the loss of the +inductive effect of one of the ethyl

groups. Further substitution at the nitrogen site of NEIBMP⁴⁻, by replacing the ethyl group with another methylenephosphonate group, gives rise to an even more basic nitrogen atom as found by Sawada for NTMP⁸⁻; $\log K_{011} = 12.80$ (at $I = 0.1 \text{ mol dm}^{-3} \text{ KNO}_3$).

Sawada suggested, from the closeness of the values of $\log K_{012}$ and $\log K_{013}$ determined for NTMPH₆, that these values could hence be assigned to the protonation of each of the unprotonated phosphonate groups (PO_3^{2-}) in NTMPH⁷⁻.²⁴ This suggests that, in an aminopolymethylenephosphonic acid, if the values of $\log K$ corresponding to the protonation of the phosphonate oxygens were close to each other then protonation would occur on each of the unionized phosphonate groups. The reason for this has been suggested to be due to charge repulsions between the negatively charged phosphonate groups (PO_3^{2-}). This will be at its maximum if free rotation about the C-N bond is possible.^{24,43} In the case of NEIBMPH₄, the values of $\log K_{012}$ (6.78) and $\log K_{013}$ (4.89) are close, suggesting that charge repulsion will be at its maximum. This is consistent with their assignment to successive protonation of each of the unprotonated phosphonate groups (PO_3^{2-}). The $\text{p}K_a$ value of 1.94 is much less than for $\log K_{012}$ and $\log K_{013}$ and can be ascribed to protonation of one of the protonated phosphonate groups (PO_3H^-).

4.5 Protonation equilibria for (±)-*trans*-1,2-diaminocyclohexane tetrakis-(methylenephosphonic acid), CDTMPH₆

CDTMPH₆ is known to be very effective in the prevention of hydrogen peroxide decomposition in the presence of metal ions.³¹ It is likely, therefore, that understanding the efficiency of CDTMPH₆ in this application requires knowledge of the possible equilibria in *aqueous* solution.

The two ligands, CDTMPH₆ and DDDTMPH₆ (Section 4.6) have in common two nitrogen atoms and four methylenephosphonate groups. However, the major difference between these two ligands is in their backbone structure. CDTMPH₆ has a 'rigid' cyclohexane backbone³⁷ and DDDTMPH₆ has a flexible aliphatic/ether type chain. This variation may have a considerable effect on the stability of any metal complexes formed in *aqueous* solution (see Chapter 5).

Potentiometric titrations of the 'free-ligand', CDTMPH₆ (Section 2.3), were carried out in the absence of metal ions over the pH range 2-12.

Potentiometric titration curves obtained for CDTMPH₃ (Figure 4.5.1) have an inflection corresponding to ca. five equivalents of base being consumed by the ligand system by ca. pH 9. An approximate indication of the values of the protonation constants can be obtained by inspection of the buffer regions observed in the titration curve (Figure 4.5.1), *i.e.* pK_a's values are expected at ca. 2, 5, 6.5 and greater than 9.

Analysis, using SUPERQUAD⁴¹, of the three data files obtained for CDTMPH₃ (Section 2.3.6), yielded the protonation constants given in Table 4.5.1. Theoretically there are ten possible protonation constants (log K_{MLH}), allowing that the fully neutralised anion, LH₃⁻, can accept two protons to become the acid salt:

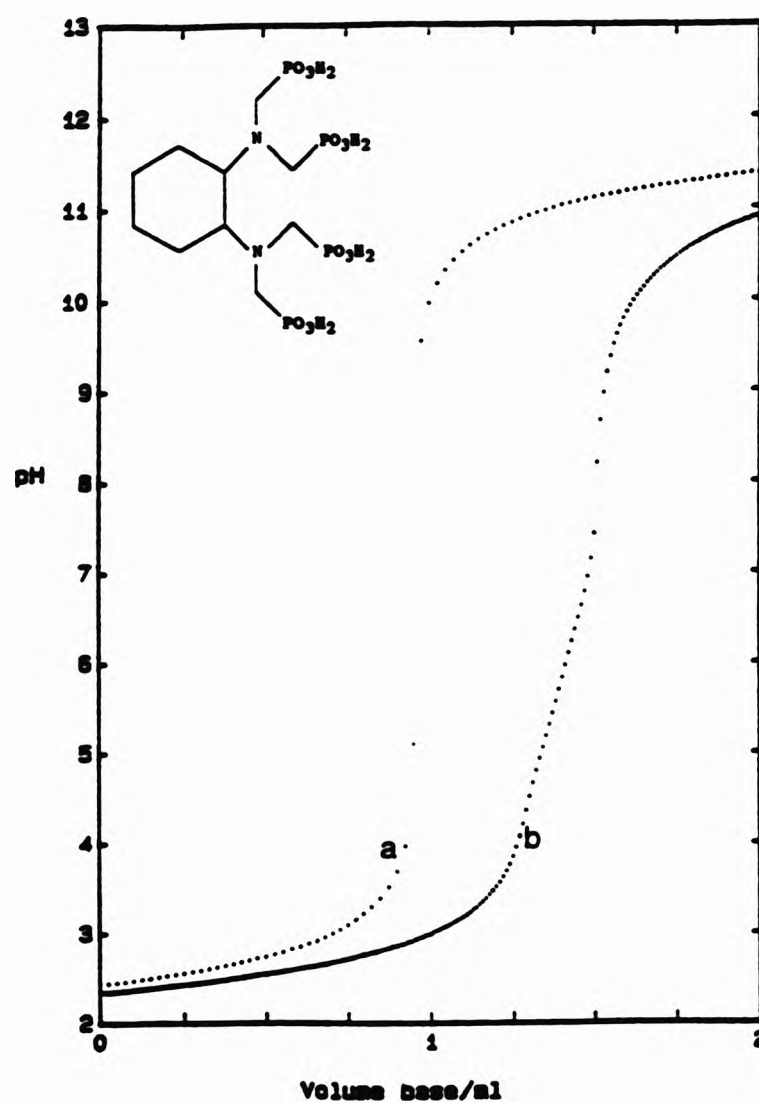
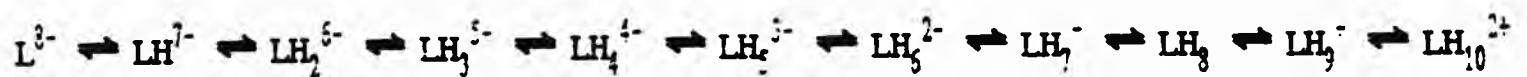
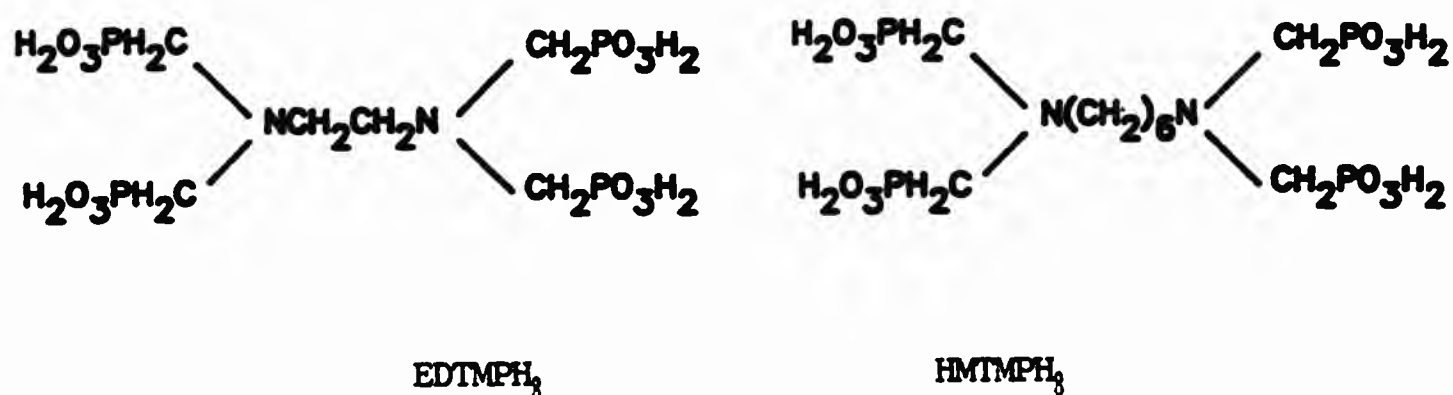


Figure 4.5.1 A typical titration curve (pH vs volume of base added) for CDTMPH₃; (a) calibration curve; (b) [CDTMPH₃] = 0.0005 mol dm⁻³.

However, only five out of the ten possible protonation constants could be determined in this work.

Initial refinement of data file TC2 for a model consisting of species where MLH = 011 to 016 was unsuccessful; the log K value for the species 015 became negative on refinement and hence was removed from the final output. Another model, which was tried for all three data files, included the species where MLH = 011 to 017. Again, this refinement was unsuccessful, as indicated by high χ^2 and σ values. A model which only included the species where MLH = 011 to 015 was found to be successful for all three data files, as indicated in Table 4.5.1. The results were characterised by acceptable χ^2 and σ values. It is assumed that the five protonation constants determined apply to successive protonation steps (*i.e.* none remained undetected between log K values of 2.05 and 11.26). However, assignment of each log K value to a particular protonation step is not trivial. Thus the log K values given in Table 4.5.1 could be assigned to any of the following protonation sequences; sequential protonation of the species L^{8-} resulting in the species LH_1^{7-} , or sequential protonation of the species LH_1^{4-} resulting in LH_2^{3-} , and so on. The 'classical' method of assignment has been to compare with protonation constants for other related ligands. For example, in this case, comparison with ethylenediamine tetrakis(methylenephosphonic acid), EDTMPH₃ and 1,6-hexa-methylenetetraakis(methylenephosphonic acid), HMTMPH₃ (Table 4.5.2) is appropriate.



The protonation constants of CDTMPH₃ were previously determined by Banks *et al.* on the octa-sodium salt by potentiometry in 1959.¹⁷ Compared to the work reported here, there are two differences in the method by which Banks determined the protonation constants of CDTMPH₃. One was that the titrations were carried out using a different ionic medium, *i.e.* sodium perchlorate ($I = 0.1 \text{ mol dm}^{-3}$), and the other difference was the method used to calculate the

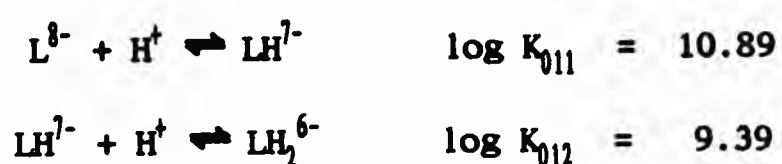
log K values. This method involved graphical analysis, by hand, of the buffer regions in the titration curves, and the fact that each titration point can be expressed as a function of the total concentration of CDTMPH₃, the hydrogen ion concentration, the moles of base added per mole of CDTMPH₃, the eight protonation constants and the various species of CDTMPH₃ present in solution. Banks calculated the log K values from expressions derived from simultaneous equations.⁷⁷

Table 4.5.1 Protonation constants for CDTMPH₃ (L = [C₈H₁₀N₂(CH₂PO₃)₃(CH₂PO₃H)]⁷⁻).^a

Datafile	TC2 ^b	TC3 ^c	TC4 ^d	Mean ^e
log β ₀₁₁	11.33(0.016)	11.21(0.015)	11.23(0.019)	11.26 ±0.07
log β ₀₁₂	21.38(0.020)	21.25(0.016)	21.25(0.018)	21.29 ±0.09
log K ₀₁₂	10.05	10.04	10.02	10.04 ±0.02
log β ₀₁₃	27.99(0.033)	27.83(0.025)	27.82(0.027)	27.88 ±0.11
log K ₀₁₃	6.61	6.58	6.57	6.58 ±0.02
log β ₀₁₄	33.01(0.046)	32.86(0.034)	32.83(0.036)	32.90 ±0.11
log K ₀₁₄	5.02	5.03	5.01	5.02 ±0.01
log β ₀₁₅	35.37(0.067)	34.95(0.070)	34.52(0.113)	34.95 ±0.42
log K ₀₁₅	2.36	2.10	1.69	2.05 ±0.36

^a The monoprotonated ligand is denoted as L; see text. Data obtained at I = 0.1 mol dm⁻³ KNO₃, 25.0 ±0.1 °C. Figures in parentheses are standard deviations obtained from SUPERQUAD. Convention: β_{M_nL_nH_n} for M_nL_nH_n. ^b Fit parameters obtained from SUPERQUAD, χ² = 8.40, σ = 0.1415; pH 2.75–11.21, 152 data points. ^c Fit parameters obtained from SUPERQUAD, χ² = 5.60, σ = 0.1012; pH 3.03–10.70, 87 data points. ^d Fit parameters obtained from SUPERQUAD, χ² = 5.74, σ = 0.1165; pH 2.95–10.66, 92 data points. ^e Unweighted mean of values from each refinement; error limits are derived from the ranges obtained from each log β_{M_nL_nH_n} (and log K_{M_nL_nH_n}).

Banks determined eight out of the ten possible protonation constants (Table 4.5.2). Protonation constants with values 10.89 and 9.39 were assigned to the processes of successive protonation of the two nitrogen atoms:⁷⁷



The remaining six protonation constants ($\log K_{013}$ to $\log K_{018}$) were assigned to the successive protonations of the phosphonate oxygen atoms.

Table 4.5.2 Protonation constants for some related ligands.

MLH	$\log K_{MLH}$							
	011	012	013	014	015	016	017	018
EDTMPH ₃ ^a	10.60	9.22	7.43	6.63	6.18	5.05	2.72	1.46
EDTMPH ₃ ^b	(13.14)	10.01	8.13	6.57	5.26	3.15	(1.37)	
EDTMPH ₃ ^c	12.99	9.78	7.94	6.42	5.17	3.02	1.33	
EDTMPH ₃ ^d	12.10	10.18	8.08	6.54	5.23	3.00		
HMTMPH ₃ ^e	11.82	7.71	6.23	5.68	5.12	3.25		
CDTMPH ₃ ^f	11.26	10.04	6.58	5.02	2.05			
CDTMPH ₃ ^g	10.89	9.39	7.69	6.97	6.46	5.32	3.70	2.40

^a Ref. 20, $I = 0.1 \text{ mol dm}^{-3} \text{ KNO}_3$. Values in parentheses estimated by extrapolation. ^b Ref. 73, $I = 0.1 \text{ mol dm}^{-3} \text{ KNO}_3$. ^c Ref. 74, $I = 0.1 \text{ mol dm}^{-3} \text{ KNO}_3$. ^d Ref. 75, $I = 0.1 \text{ mol dm}^{-3} \text{ KCl}$. ^e Ref. 76, $I = 0.1 \text{ mol dm}^{-3} \text{ KNO}_3$. ^f This work $I = 0.1 \text{ mol dm}^{-3} \text{ KNO}_3$, $25.0 \pm 0.1^\circ\text{C}$. ^g Ref. 77, $I = 0.1 \text{ mol dm}^{-3} \text{ NaClO}_4$, 25.0°C .

There are a number of factors that can significantly affect the values of the protonation constants determined by potentiometry. These include the concentration and nature of the ionic medium used, differences in sample preparation and hence purity,⁷⁴ and the reliability associated with the data at high pH.⁷² Anderegg also noted that some association of the species in aqueous solution with the electrolyte ions cannot be completely ruled out.⁷¹

The protonation constants of CDTMPH₃ determined in this work are significantly different to those determined by Banks.⁷⁷ The components that are likely to be causing the disparities in the $\log K$ values are differences in sample preparation and the methods used to calculate the protonation constants.

The protonation constants of ethylenediaminetetrakis(methylenephosphonic acid), EDTMPH₃, have been determined by a number of workers over the last 20 years, e.g. Motekaitis,^{73,74} Westerback,²⁰ Kabachnik⁷⁵ and Rizkalla.⁷⁸ EDTMPH₃ also has ten possible protonation constants, allowing that the fully neutralised anion can accept two protons to become of acid salt (LH_{10}^{2+}), but

only five out of the ten possible protonation constants were determined *directly* by the potentiometric method, *i.e.* $\log K_{012}$ to $\log K_{016}$. Motekaitis *et al.*⁷³ determined the values of $\log K_{011}$ and $\log K_{017}$ by a linear extrapolation of the differences in the values between the other protonation constants determined at two different ionic strengths ($I = 0.1 \text{ mol dm}^{-3}$ and $I = 3.0 \text{ mol dm}^{-3}$).⁷³ Motekaitis suggested that sequence of protonation of the anion, EDTMP^{8-} , based on the values of the protonation constants determined, corresponds to the initial successive protonation of the two basic nitrogen atoms ($\log K_{011}$ and $\log K_{012}$). This assignment was also based on comparison between the relatively high basicity of the nitrogen atoms expected through migration of the negative charge (from the phosphonate groups, -8) towards the nitrogen atoms, and the basicity of the nitrogen atoms in the parent amine (ethylenediamine $\log K_{011} = 10.04$ and $\log K_{012} = 9.89$).⁷⁴

There is significant variation in the values of $\log K_{011}$ for EDTMPH_2 determined by the different groups of workers (Table 4.5.2), *i.e.* $\log K_{011} = 10.60^{20}$, 13.14 (estimated by extrapolation of the results determined by potentiometry at two different ionic strengths, $I = 3.0$ and $0.1 \text{ mol dm}^{-3} \text{ KNO}_3$)⁷³, 12.99⁷⁴ and 12.10⁷⁵. The large variation in the value of $\log K_{011}$ of *ca.* 2.56 log units could be ascribed to differences in sample preparation and hence purity, or the lower reliability associated with data obtained at high pH.^{6,74} The value of $\log K_{011} = 12.10$ ($I = 0.1 \text{ mol dm}^{-3} \text{ KCl}$) determined by Kabachnik⁷⁵ is similar to the values obtained at $I = 0.1 \text{ mol dm}^{-3} \text{ KNO}_3$, but could be ascribed to the differing ionic medium used.

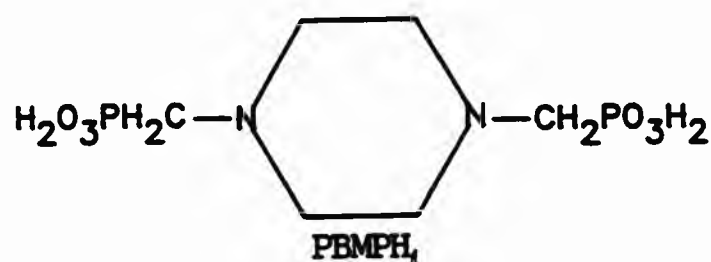
The protonation constants, $\log K_{011}$ and $\log K_{012}$, determined for 1,6-hexamethylenetetraakis(methylenephosphonic acid), HMTMPH_8 , have also been assigned to the protonation of the basic nitrogens.⁷⁶ Zaki proposed that the formation of five-membered rings between the nitrogen-bound proton and phosphonate oxygens produced enhanced stability of these protonated species.⁷⁶

Comparisons between these results leads to the conclusion that the pK_a values for the process of neutralisation of the nitrogen-bound protons can vary quite significantly (Table 4.5.2). The process of protonating the first nitrogen atom can have an associated $\log K$ value anywhere between 10.6 to 13.1 log units. Again, the process of protonating the second nitrogen atom can also have a $\log K$ value between 7.7 and 10.2 log units. These rather large variations in the values of $\log K$ for the process of protonating nitrogen atoms for related alkylaminomethylenephosphonic acids makes it unreliable to

assign the macroscopic protonation constants of CDTMPH_3 to a protonation scheme on this basis.

Nevertheless, it was initially thought that the values of $\log K_{011}$ (11.26) and $\log K_{012}$ (10.04) could be assigned to the successive protonation of the two basic nitrogens of CDTMP^{3-} , which was the conclusion reached by Banks.⁷⁷

The protonation constants determined for piperazine-1,4-bis(methylene-phosphonic acid), PBMPH_4^\dagger (Table 4.5.3), also imply, on this basis, that the



values of $\log K_{011}$ (10.00) and $\log K_{012}$ (7.15) are for the processes of successively protonating the two nitrogen atoms. However, examination of the dependence of $\delta^{31}\text{P}$ on pH indicates a totally unexpected protonation sequence for PBMP^{4-} .[†] Assuming the relationships between shielding of the ^{31}P nucleus and protonation of the phosphonate group (PO_3^{2-}) and the nitrogen atom (described in Section 4.3), the results suggest that the value of $\log K_{011}$ corresponds to protonation of one of the piperazine nitrogens, but the values of $\log K_{012}$ (7.15) and $\log K_{013}$ (5.10) are for protonation of two phosphonate oxygens. Quite unexpectedly, the remaining piperazine nitrogen is protonated only at a relatively high pH ($\log K_{014} = 3.20$).

Table 4.5.3 Protonation constants for PBMPH_4 .[‡]

$\log K_{011}$	$\log K_{012}$	$\log K_{013}$	$\log K_{014}$
10.00	7.15	5.20	3.20

[‡] Ref. 79, $I = 0.1 \text{ mol dm}^{-3} \text{ KNO}_3$, $25.0 \pm 0.1 \text{ }^\circ\text{C}$.

Therefore, as already mentioned in Section 4.3, the macroscopic protonation constants for a ligand, determined by potentiometry, do not reveal the sequence of protonation of the available sites on the ligand. In order to

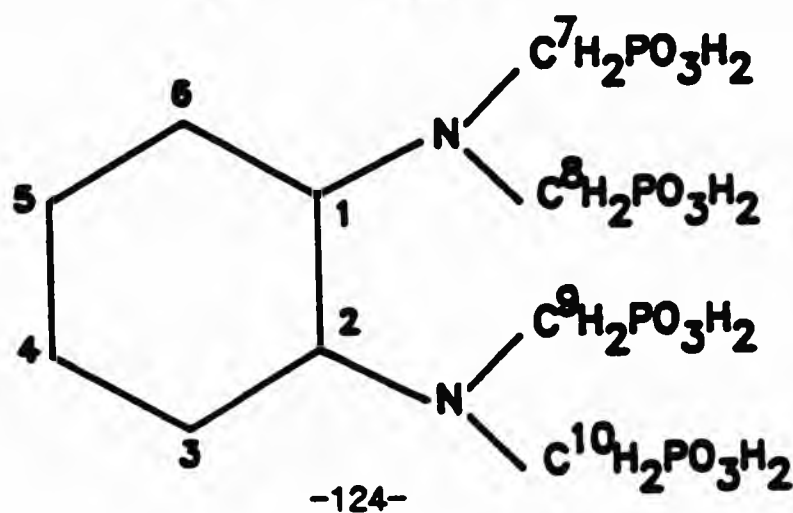
[†] I. Khan, M. Phil. Thesis, University of North London, 1994.

elucidate the protonation scheme for CDTMP^{3-} , ^{31}P nmr spectra as a function of the degree of titration, τ [$\tau = (\text{moles of titrator})/(\text{moles of titrant})$] were determined (Figure 4.5.2a and 4.5.2b) by Hägele *et al.* at Heinrich Heine University using the Stopped Flow NMR (SFNMR) technique.⁸⁰

In this method, ^{31}P nmr spectra are determined on a non-spinning sample contained in an nmr tube connected to a PC-controlled titration system. After each addition of the titrant to the sample in the titration cell, the solution is pumped through the entire system (*i.e.* cell, nmr tube and connecting tubes) until a constant pH is attained. The solution flow is then stopped and the nmr spectrum is acquired on the titration sample. The entire titration is computer controlled and spectra are conveniently displayed on a two-dimensional plot (contour plot) vs degree of titration, τ .

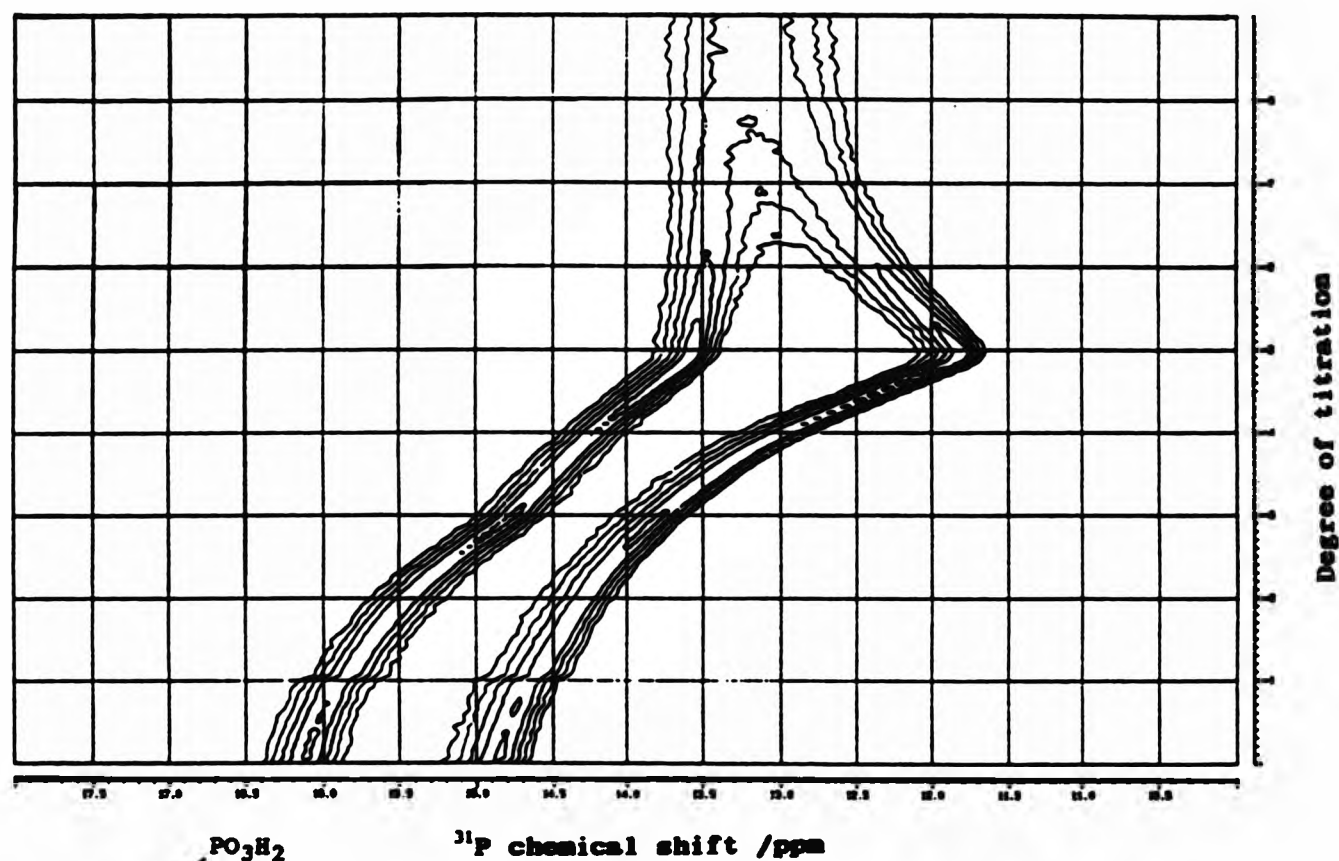
The ^{31}P SFNMR plot for CDTMPH_2 (Figure 4.5.2a and 4.5.2b) shows two single resonances at the start of the titration (ca. 15.0 ppm and 16.0 ppm) confirming the presence of two averaged environments for the phosphorus atoms, as previously noted for CDTMPH_2 in aqueous solution (Section 4.2.1). As the titration proceeds to five equivalents of base, there is an upfield shift in both the signals (15 ppm and 16 ppm) of ca. 2.5 ppm and 3 ppm, respectively. This is indicative (Section 4.3) of the neutralisation of five phosphonate oxygen-bound protons of CDTMPH_2 . On addition of the sixth equivalent of base, the signal originally at 15 ppm shifts downfield by ca. 0.5 ppm, but the signal originally at ca. 16 ppm shifts only slightly; instead it levels off at ca. 13.5 ppm. Again, on addition of the seventh and eight equivalent of titrant, the signal originally at 15.0 ppm continues to shift downfield by ca. 0.5 ppm to merge with the other signal, into a broad signal centred at ca. 13.0 ppm.

As previously discussed in section 4.2.2, there are two possible assignments of the ^{13}C nmr spectra, with respect to the methylenephosphonate carbons. In one assignment the close proximity of the chiral carbons (1 and 2) gives rise to isochronous pairs (say) C^7, C^9 and $\text{C}^8, \text{C}^{10}$. The alternative assignment is



based on the supposition that the amino groups are not equivalent and hence C^7 and C^8 would be isochronous and C^9 and C^{10} would be an isochronous pair.

(a)



(b)

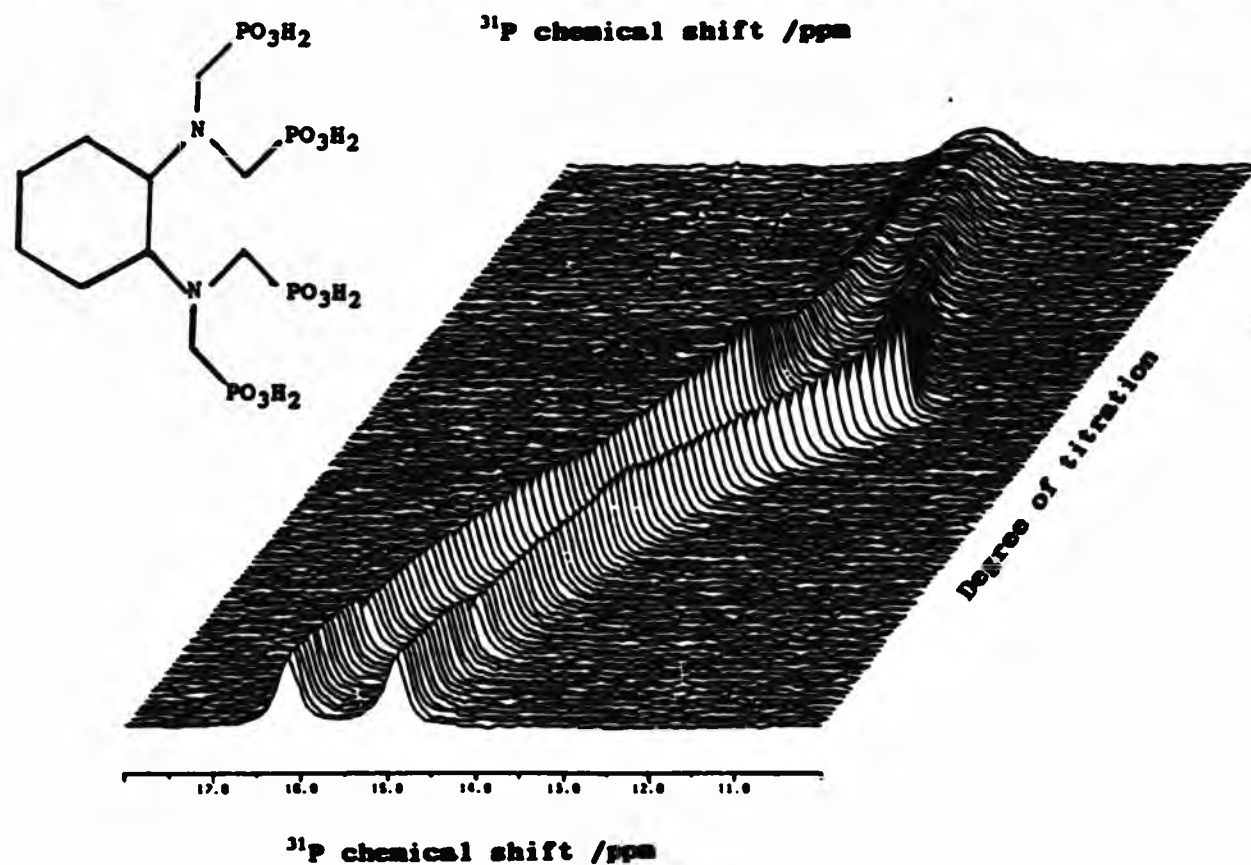


Figure 4.5.2 (a) Dependence of $\delta^{31}\text{P}$ on degree of titration (τ) for titration of an aqueous solution of CDTMPH₃ against the titrant (NaOH) by the SFNMR technique; (b) stacked plot of ^{31}P nmr spectra vs degree of titration, τ .⁸⁰

Given this ambiguity, and the lack of success in elucidating the protonation scheme from comparison of the log K values determined for CDTMPH_8 with those of related acids, it was hoped that determination of the SFNMR plot of $\delta^{31}\text{P}$ vs τ would be helpful in resolving both problems.

Other workers, *i.e.* Clegg *et al.*,⁵⁷ have suggested that assignments of the protonation schemes of polyaminomethylenephosphonic acids from plots of $\delta^{31}\text{P}$ vs pH can be unclear, even though they are usually based on the rule that phosphonate and nitrogen protonations would deshield and shield the phosphorus nuclei, respectively. However, several possible electronic effects (potentially of opposite signs) may also contribute to the shift in the phosphorus signal. Clegg⁵⁷ noted that although the protonation of a phosphonate group is likely to deshield the phosphorus atom in the same phosphonate group (of a polyaminomethylenephosphonic acid), it may have the opposite effect on the phosphorus atom in another phosphonate group. Since exchange processes for protonation equilibria are normally fast, the observed chemical shift is a weighted average for the two or more phosphorus atoms in the ligand. This may result in the phosphorus signal being shielded or deshielded in the corresponding ^{31}P spectrum.

These considerations notwithstanding, it is tempting to consider the protonation behaviour of CDTMPH_8 in the light of its solid state structure (Chapter 7). However, one has to first question whether the protonation constant $\log K_{011}$ (11.26) does indeed represent the value for the first protonation of CDTMP^{8-} or is there a higher value(s) missed by the potentiometric method. The two reasonably high values of $\log K_{011}$ (11.26) and $\log K_{012}$ (10.04) are consistent with two high pK_2 's found for EDTMPH_8 (Table 4.5.2). It is therefore reasonable to assume from that both $\log K_{011}$ and $\log K_{012}$ can be ascribed to successive protonations of the two nitrogen atoms. However, the value of 11.26 does fall in the lower end of the range for the process of protonating the first nitrogen atom of EDTMP^{8-} , *i.e.* 11.82-13.14 [the pK_2 value of 10.60 determined for EDTMPH_8 ²⁰ is not included in this range because it is significantly lower than the other values of $\log K_{011}$ (Table 4.5.2)]. This may suggest that there is another pK_2 value for CDTMPH_8 greater than 11.26.

An indication of the total number of ionizable protons available on CDTMPH_8 , comes from the refinable parameter TOTMM (total number of millimoles of available proton initially present in the titration vessel) in the SUPERQUAD⁴¹

input files. When a value that corresponds to eight available protons on CDTMPH_3 was used as input into the SUPERQUAD⁴¹ files, subsequent refinement of the data files for the model which included the formation of the species LH^{7-} to LH_3^{3-} was unsuccessful. Whereas, when a value that corresponded to seven available protons on CDTMPH_3 was used, subsequent refinement of the data files for the same model was successful (Table 4.5.1).

Further evidence is available from the potentiometric titration curves (Figure 4.5.1). The curves exhibit an inflection which corresponds to ca. 5 equivalents of base being consumed by the ligand system by ca. pH 9. This suggests that there are three $\text{p}K_a$ values greater than 9, but only two were determined by potentiometry, *i.e.* 10.04 and 11.26, and therefore, one $\text{p}K_a$ value remains undetected. Taken together, the arguments constitute substantial evidence to support the suggestion that the log K value of 11.26 in fact corresponds to $\log K_{12}$.

In the solid state structure of CDTMPH_3 all eight protons were located by X-ray crystallography (Section 7.3). Seven phosphonate oxygens are protonated and only one nitrogen atom was found to be protonated (Figure 4.6.3). Two very

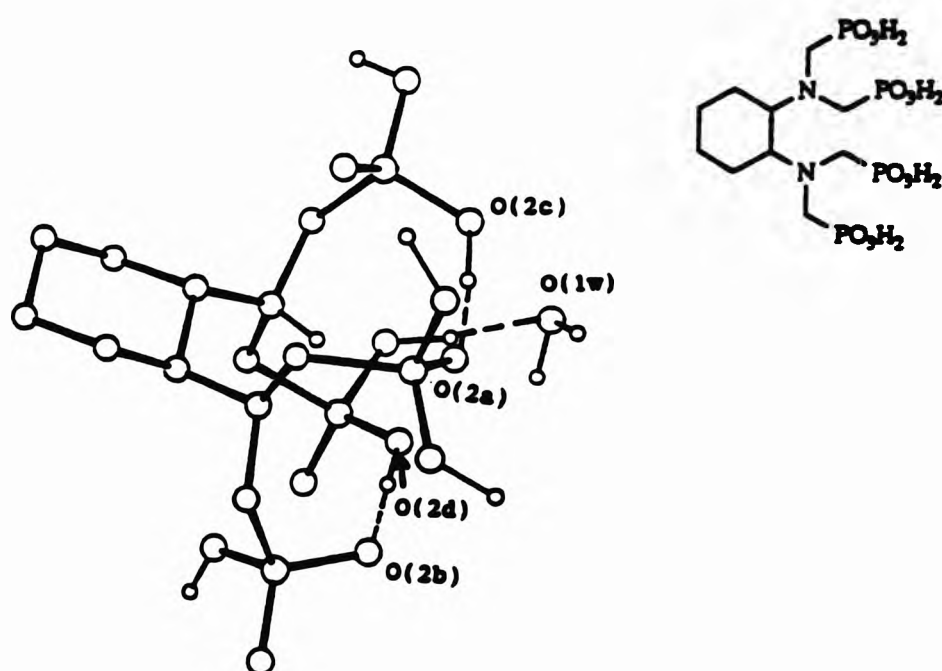


Figure 4.5.3 Solid state structure of CDTMPH_3 showing the two intramolecular hydrogen bonds.

strong intramolecular hydrogen bonds were found, *i.e.* $\text{O}(2c)\dots\text{O}(2a) = 2.57 \text{ \AA}$ and $\text{O}(2d)\dots\text{O}(2b) = 2.48 \text{ \AA}$. The protonated nitrogen, however, is not involved in any intramolecular hydrogen bonding with either phosphonate oxygen atoms

or the other nitrogen atom, even though it is quite close to the latter (2.78 Å). Each of the two very strong hydrogen bonds involves a phosphonate oxygen atom from two *different* aminobis(methylenephosphonate) substituents, thus effectively holding each methylenephosphonate group in a fixed position relative to the other three groups. This produces a *rigid* structure and (in the solid state) gives rise to non-equivalence of the methylenephosphonate groups. In addition, the fact that only one nitrogen atom is protonated (NH^+) in the solid state is also a source of non-equivalence between the amino-methylenephosphonate groups.

These observations may be useful in assigning the ^{13}C nmr spectrum of CDTMPH_8 . As previously discussed in Section 4.2.2, there are two possible assignments of the ^{13}C nmr spectrum with respect to the methylenephosphonate carbons. In one assignment the two $\text{N}(\text{CH}_2\text{PO}_3)_2$ groups are equivalent and the close proximity of the chiral carbons gives rise to two pairs of isochronous methylenephosphonate carbons (*i.e.* C^7, C^9 and $\text{C}^8, \text{C}^{10}$). The alternative assignment is based on the supposition that the amino groups are not equivalent and hence the four methylenephosphonate carbons can be classified into two pairs of isochronous nuclei, one pair within each methylenephosphonate group. If the solid state structure of CDTMPH_8 were retained in solution, the latter assignment would apply, *i.e.* there would be two pairs of isochronous methylenephosphonate carbons, C^7C^8 and C^9C^{10} .

There must be a reasonable possibility that the essentially *rigid* structure of CDTMPH_8 is retained in solution because of the forced crowding of the methylenephosphonate groups (due to their 1,2 *ee* disposition) and the likelihood that the strong hydrogen bonding found in the solid state structure persists in solution. Ring flipping of the cyclohexyl ring which might separate the aminobis(methylenephosphonate) groups through *ee/aa* equilibrium can be ruled out (at ambient temperature) from inspection of the ^1H nmr spectrum. The complexity of the methylene/methine region of the spectrum (^1H) supports the absence of fast *ee/aa* exchange, and, indeed, the slight broadening of the signals observed in the spectra (Section 4.2.2) suggests that any lack of rigidity in the molecule arises from relatively slow exchange.

If the essentially *rigid* structure of CDTMPH_8 is retained in solution, it is also tempting to explain the SFNMR plot of CDTMPH_8 as follows. On the basis that deprotonation of a nitrogen-bound proton causes a downfield shift in $\delta^{31}\text{P}$,

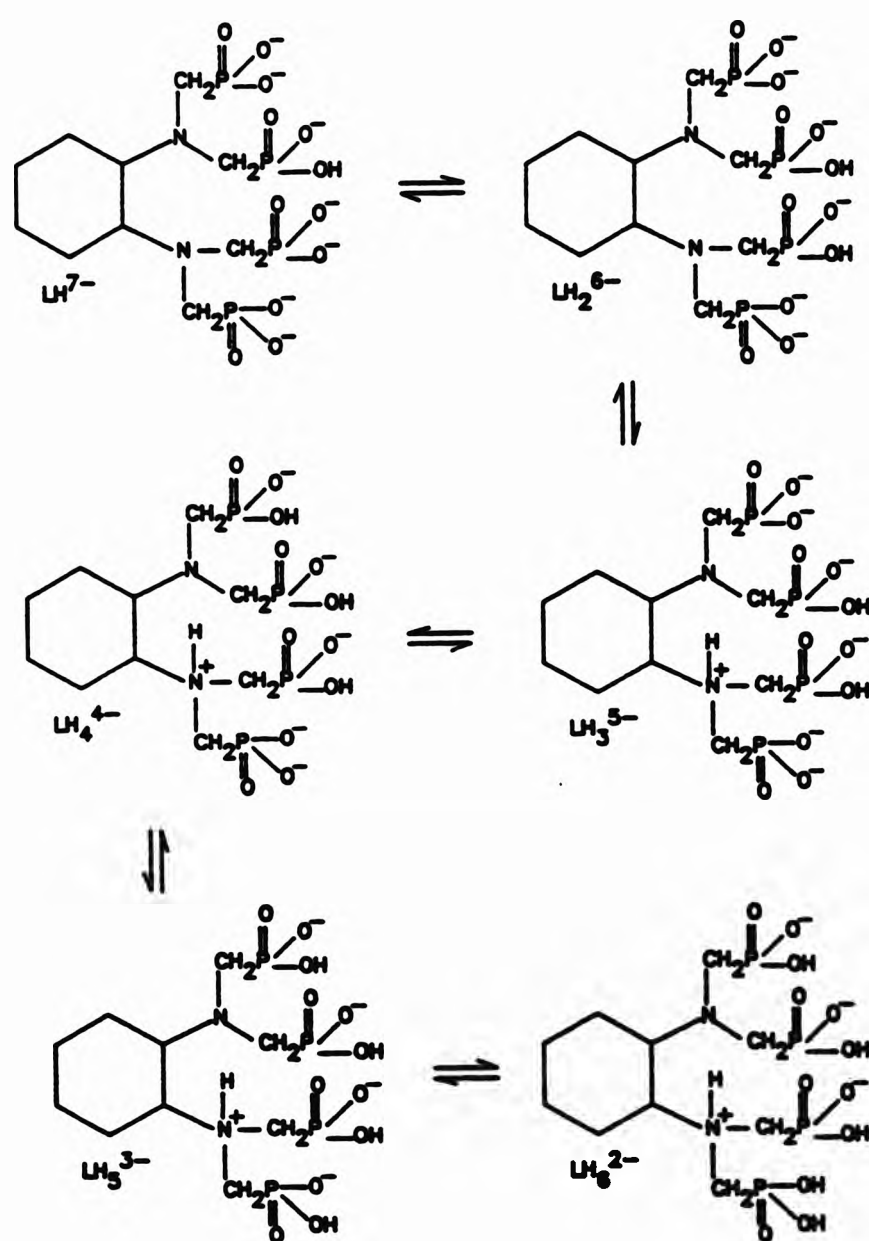
then one can assign the phosphorus signal at 15 ppm in the SFNMR plot of CDTMPH_6 as being due to the phosphorus atoms of the two methylenephosphonate groups attached to the protonated nitrogen. The other phosphorus signal at 16 ppm in the SFNMR plot can then be ascribed to the phosphorus atoms of the two methylenephosphonate groups attached to the unprotonated nitrogen atom. As the titration proceeds, five phosphonate oxygen-bound protons are neutralised and this process produces the expected upfield shift in both phosphorus nuclei (*i.e.* these will be the five protons not strongly held by hydrogen bonding). As the sixth equivalent of titrant is added, the SFNMR plot of $\delta^{31}\text{P}$ shows only nitrogen deprotonation for the signal originally upfield (15 ppm), but not for the signal that was originally downfield (16 ppm). The signal originally at 16 ppm continues to move slightly upfield.

On addition of the seventh equivalent of base, the signal originally at 16 ppm shifts by very little and levels off about *ca.* 13.3 ppm, whereas the signal originally at 15 ppm continues to move downfield (by *ca.* 0.5 ppm), though less steeply, and the two signals broaden and begin to coalesce. On addition of the eighth equivalent of base the two signals continue to coalesce at *ca.* 13 ppm. The behaviour of the signals during addition of the seventh and eighth equivalents of base is consistent with neutralisation of the two strongly hydrogen bonded phosphonate protons at very high pH. As deprotonation of CDTMPH_6 nears completion, the structure becomes less rigid and the amino groups become equivalent. Hence the two signals broaden and coalesce.

The clear implication of this interpretation is that the first five deprotonations are of the phosphonate protons that are not held by intramolecular hydrogen bonding. On addition of the sixth equivalent of titrant the nitrogen-bound proton is neutralised and this process corresponds to a log K value of 10.04. On addition of the seventh and eighth equivalents of base the two strongly hydrogen-bonded phosphonate protons are neutralised and these processes of successively neutralising the two phosphonate protons (at high pH) correspond to log K = 11.26, with the other log K value being greater than 11.5.

The assumption that the rigid solid state structure of CDTMPH_6 is retained in solution allows satisfactory rationalisation of both the ^{13}C nmr and ^{31}P SFNMR nmr spectra. Combining this model of the protonation processes with the evidence for assignment of the potentiometrically-determined log K values

discussed earlier leads to the conclusion that the 'species' L in the SUPERQUAD⁴¹ input files should be assigned to the monoprotinated species, CDTMPH⁷⁻ in the chemical system, with $\log K_{012}$ corresponding to protonation of one of the nitrogen atoms. The protonation scheme based on these arguments is shown below.



The species distribution curves⁶⁷ for CDTMPH₃ (Figure 4.5.4) show that the dominant ligand species are LH₅, LH₄, and LH₃ with the monoprotinated ligand

being produced above pH 10 (LH^{7-}).

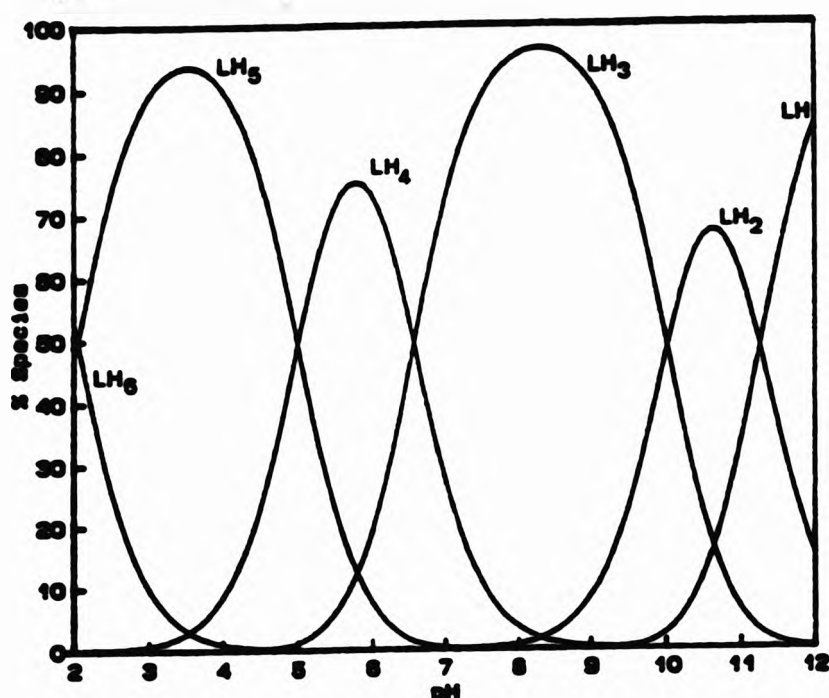
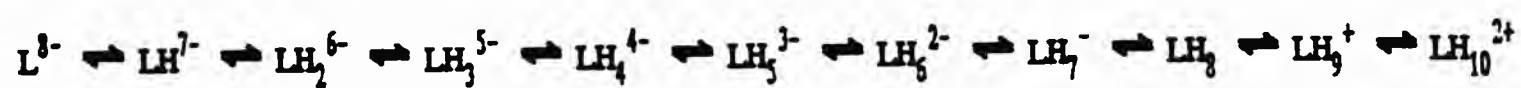


Figure 4.5.4 Species distribution curves for CDTMPH₃.

4.6 Protonation equilibria determined for DDDTMPH₃

Potentiometric titrations of the 'free-ligand', DDDTMPH₃, were carried out as before over the pH range ca. 2-12. The titration curves (Figure 4.6.1) have an inflection corresponding to ca. six equivalents of base per mole of ligand at ca. pH 9. The appearance of the curves in the region ca. pH 4-7 indicates the presence of overlapping equilibria. Analysis, using SUPERQUAD⁴¹, of the four data files obtained at two different concentrations (Table 2.3.8) yielded the protonation constants given in Table 4.6.1. Only five out of the ten possible protonation constants could be determined.

Two regions of the titration curves (Figure 4.6.1) contain buffer regions which correspond approximately to the five protonation constants, *i.e.* between pH 4-7 and pH 10-12. DDDTMPH₃ has ten possible protonation sites available from the two nitrogen atoms and four phosphonate groups.



To assign the pK_a 's determined for DDDTMPH₃ to a protonation scheme, comparison with results for some other related alkylaminomethylenephosphonic acids was again examined; *i.e.* ethylenediaminetetrakis(methylenephosphonic acid) (EDTMPH₃), 1,6-hexamethylene tetrakis(methylenephosphonic acid) (HMTMPH₃), pentamethylenediaminebis(isopropylidene phosphonic acid) (PMBISPH₄) and oxadiazinebis(ethyleneisopropylidene phosphonic acid) (OBEISPH₄).

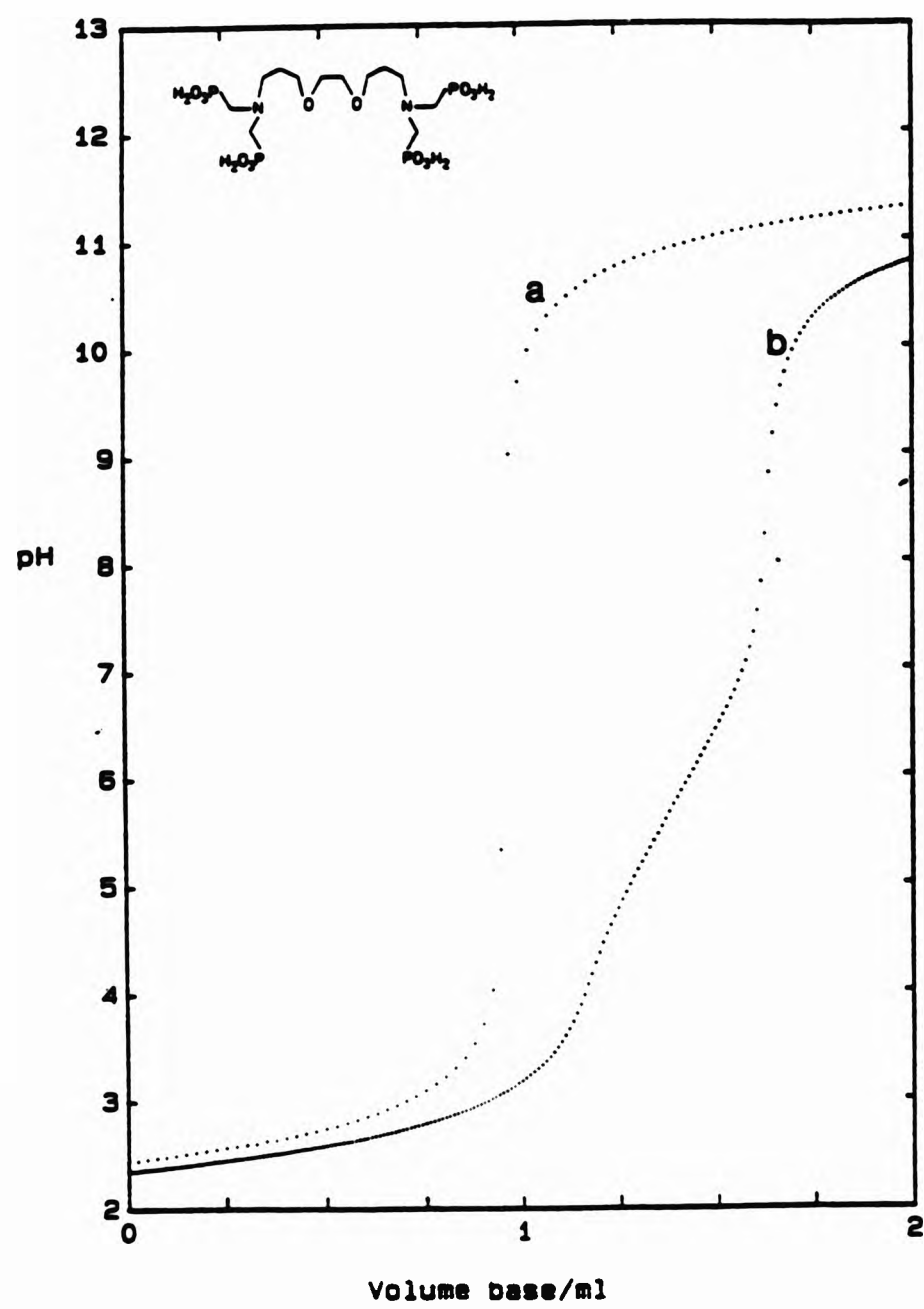
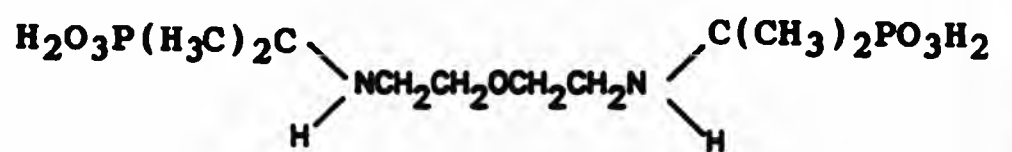
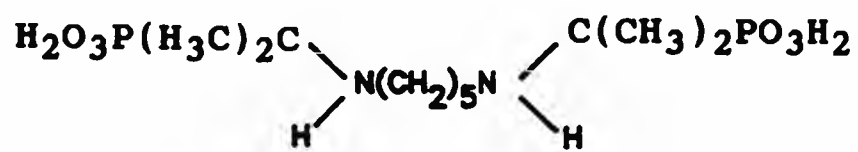
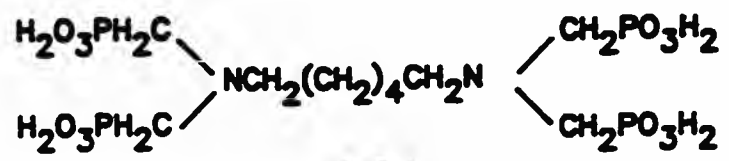
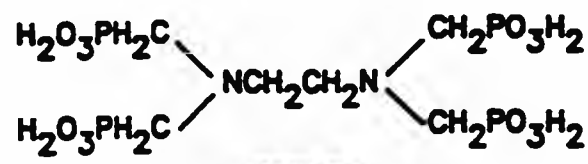


Figure 4.6.1 Titration curves (pH vs volume of base added) for DDDTMPH₃; (a) calibration curve, (b) [DDDTMPH₃] ca. 0.0005 mol dm⁻³.

As already mentioned in Section 4.4, the protonation constants of EDTMPH₃ reported by a number of workers (Table 4.6.2) (at the same ionic strength and in the same medium) are significantly different and hence one must ascribe these differences to either sample preparation and purity and/or the lower reliability associated with the data obtained at high pH. Nevertheless, comparison of the data for EDTMPH₃ with that for HMTMPH₃ where the same functional groups are separated by a much longer aliphatic chain, is useful in relation to the protonation of DDDTMPH₃. The values of log K₀₁₁ and log K₀₁₂ for both EDTMPH₃ and HMTMPH₃⁴⁶ (Table 4.6.2) have been assigned to the processes of successively protonating the two nitrogen atoms.

Table 4.6.1 Protonation constants for DDDTMPH₃ (L = [C₈H₁₆O₂N₂H⁺(CH₂PO₃²⁻)₄]).^a

Datfile	PBI3 ^b	PBI9 ^c	PB10 ^d	PB11 ^e	Mean ^f
log β ₀₁₁	11.24(0.020)	11.15(0.010)	10.96(0.014)	10.93(0.035)	11.07 ±0.17
log β ₀₁₂	18.22(0.031)	18.01(0.019)	17.84(0.030)	17.87(0.061)	17.99 ±0.23
log K ₀₁₂	6.98	6.86	6.88	6.94	6.92 ±0.06
log β ₀₁₃	24.37(0.033)	24.17(0.020)	24.02(0.027)	23.97(0.064)	24.13 ±0.24
log K ₀₁₃	6.15	6.15	6.18	6.10	6.15 ±0.05
log β ₀₁₄	29.82(0.036)	29.55(0.021)	29.41(0.030)	29.40(0.069)	29.55 ±0.27
log K ₀₁₄	5.44	5.39	5.39	5.43	5.41 ±0.03
log β ₀₁₅	34.37(0.046)	34.20(0.028)	34.15(0.036)	33.95(0.092)	34.17 ±0.22
log K ₀₁₅	4.56	4.64	4.74	4.56	4.63 ±0.12

^a The monoprotonated ligand is denoted as L; see text. Data obtained at I = 0.1 mol dm⁻³ KNO₃, 25.0 ±0.1 °C. Figures in parentheses are standard deviations obtained from SUPERQUAD. Convention: β_{M_nL_nH_n} for M_nL_nH_n. ^b Fit parameters obtained from SUPERQUAD, χ² = 6.73, σ = 0.1398; pH 3.60-10.79, 89 data points. ^c Fit parameters obtained from SUPERQUAD, χ² = 9.55, σ = 0.0495; pH 3.22-10.93, 77 data points. ^d Fit parameters obtained from SUPERQUAD, χ² = 7.45, σ = 0.0898; pH 3.26-10.70, 94 data points. ^e Fit parameters obtained from SUPERQUAD, χ² = 10.79, σ = 0.1230; pH 3.31-10.60, 57 data points. ^f Unweighted mean of values for each refinement; error limits are derived from the ranges obtained for each log β_{M_nL_nH_n} (and log K_{M_nL_nH_n}).

The difference between the value of log K₀₁₁ and the value of log K₀₁₂ (Table 4.6.2) increases with increasing chain length between the two nitrogen atoms,

i.e. the differences for EDTMPH₈ are 3.13,⁷³ 3.21,⁷⁴ 1.38²⁰ and 0.12⁷⁶ whereas for HMTMPH₈ the difference is 4.11.⁷⁶ This suggests that the processes for successively protonating the nitrogen atoms on HMTMP⁸⁻ are in themselves, significantly different, whereas, the processes for successively protonating EDTMP⁸⁻ at the nitrogen atoms are similar^{20,76}. Zaki⁷⁶ noted that this increase in the difference between the value of log K₀₁₁ and the value log K₀₁₂ for EDTMPH₈ compared with HMTMPH₈ has been attributed to the increase in basicities of the nitrogen atoms due in turn to the decrease in repulsive forces between the positively charged nitrogen atoms on increasing the backbone chain.

However, since the only difference between EDTMPH₈ and HMTMPH₈ is the length of the backbone chain, and the resulting pK_a's are very different (Table 4.6.2), it may be that the value of log K₀₁₁ for HMTMPH₈ has not been

Table 4.6.2 Protonation constants for some related ligands.

MLH	log K _{MLH}							
	011	012	013	014	015	016	017	018
EDTMPH ₈ ^a	(13.14)	10.01	8.13	6.57	5.26	3.15	(1.37)	
EDTMPH ₈ ^b	12.99	9.78	7.94	6.42	5.17	3.02	1.33	
EDTMPH ₈ ^c	10.60	9.22	7.43	6.63	6.18	5.05	2.72	1.46
EDTMPH ₈ ^d	10.60	10.48	9.27	7.39	5.63	3.80		
HMTMPH ₈ ^e	11.82	7.71	6.23	5.68	5.12	3.25		
PMBISPH ₄ ^f	11	11	6.13	5.77				
OBEISPH ₄ ^g	11.48	10.56	6.40	5.15				

^a Ref. 73. I = 0.1 mol dm⁻³ KNO₃, 25.0 °C. ^b Ref. 74. I = 0.1 mol dm⁻³ KNO₃, 25.0 °C. ^c Ref. 20. I = 0.1 mol dm⁻³ KNO₃, 25.0 °C. ^d Ref. 76. I = 0.1 mol dm⁻³ KNO₃, 25.0 °C. ^e Ref. 76. I = 0.1 mol dm⁻³ KNO₃, 25.0 °C. ^f Ref. 82. I = 0.1 mol dm⁻³ KNO₃, 25.0 °C. ^g Ref. 82. I = 0.1 mol dm⁻³ KNO₃, 25.0 °C.

determined, *i.e.* log K₀₁₁ is greater than 12 and the value of 11.82 (HMTMPH₈) is for the process of protonating the second nitrogen atom. Increasing the backbone chain length between the aminobis(methylenephosphonic acid) groups, one might expect the two groups to behave as independent 'fragments' and hence protonation of the nitrogen atoms would result in similar log K values.

The protonation constants of two related acids, PMBISPH₄ and OBEISPH₄ (Table 4.6.2) are similar and Kabachnik has noted that introduction of an heteroatom (such as oxygen, sulphur or nitrogen) into the backbone chain has no significant effect on the pK_a's of the corresponding acids.⁸² It is worth noting that the differences between the log K values of log K₀₁₁ and log K₀₁₂ for HMTMPH₃ and PMBISPH₄/OBEISPH₄ may be due to the number of methylenephosphonate substituent groups present, *i.e.* 4 rather than 2, respectively. The two high log K values for PMBISPH₄ and OBEISPH₄ have been ascribed to the successive protonations of the two nitrogen atoms.⁸²

The structure of DDDTMPH₃ is similar to that of HMTMPH₃ and, since the introduction of an heteroatom is not expected to significantly affect the pK_a values,⁸² the two log K values corresponding to the successive protonation of the nitrogen atoms should be of the same order. The pattern of determined log K's for DDDTMPH₃ is indeed similar to that for HMTMPH₃ and the amino-tetrakisphosphonate groups are also well separated in DDDTMPH₃. So, on this basis, there is a possibility that log K₀₁₁ for DDDTMPH₃ has not been determined by the potentiometric method in this work. Motekaitis had similar problems in determining the values of log K₀₁₁ and log K₀₁₇ for EDTMPH₃.⁷³

Such comparisons with pK_a's values for similar compounds suggest that assignment of the log K value of 11.07 for DDDTMPH₃ to log β₀₁₁ may be incorrect.

Extensive efforts were made to try and refine data files PBI3 and PBI9 for a model including two log K values at or about 11, but this proved to be unsuccessful as indicated by the resulting high χ^2 and/or σ values obtained and 'excessive'⁴¹ deviations for individual log β values.

Some evidence that one of the protons of the acid remained unionised in the pH range of the titration was provided by the results of refinements of the datafiles under different conditions. Although [H⁺] was treated as a variable parameter in refinements using SUPERQUAD⁴¹, the total number of millimoles of proton in the SUPERQUAD⁴¹ input files was varied over several different refinements. On refinement of datafile PBI3 with values of the total number of millimoles of proton corresponding to 6, 7 and 8 ionisable protons, the following results were obtained. For data file PBI3, on changing the input value of the total number of millimoles of proton, the value either increased or decreased during refinement to a value which corresponded to *ca.* seven

ionisable protons on the ligand. Only the first pK_a ($\log K_{011} = 11.00$) varied significantly between the refinements, but the values of the subsequent pK_a 's only varied by ca. ± 0.15 log units. This is evidence that the removal of the last nitrogen-bound proton may be occurring at a high pH, *i.e.* > 12 .

This possibility is supported by the qualitative appearance of the titration curves. The four titration curves all show an end-point corresponding to ca. 6 equivalents of base per mole of DDDTMPH₈ at ca. pH 9, suggesting that there are two protons remaining to be neutralised at a higher pH (> 9.5).

As previously mentioned in sections 4.3 and 4.5, the macroscopic protonation constants determined for a ligand by potentiometry do not reveal the sequence of protonation of basic sites on a ligand. By following the chemical shift of a ligand's phosphorus atoms as a function of pH, the microscopic protonation schemes can often be clarified.

Therefore, the ^{31}P nmr spectra for DDDTMPH₈ were determined as a function of pH as described in section 2.4. Three different ^{31}P nmr titrations were carried out, with the conditions employed for one of the ^{31}P nmr titrations (against *aqueous* potassium hydroxide) being qualitatively similar to those used in the potentiometric titrations (Section 2.4.9). A second ^{31}P nmr titration experiment (also against *aqueous* potassium hydroxide) involved using a stock solution which did not contain an excess of nitric acid (Section 2.4.10) and the normal titration procedure was followed (Section 2.4.8). The final ^{31}P nmr titration experiment involved using a stock solution without both supporting electrolyte and excess nitric acid (Section 2.4.11) and titration against *aqueous* tetraethylammonium hydroxide instead of potassium hydroxide (Section 2.4.8).

In all three ^{31}P titration experiments, the ^{31}P nmr spectra obtained showed only one phosphorus signal over the pH ranges studied. This is indicative of rapid exchange of protons between the species present in *aqueous* solution at each titration point for all three titrations.

The profile of $\delta^{31}\text{P}$ vs pH resulting from the titration where the stock solution used contained nitric acid [Figure 4.6.2(a); curve denoted as "□"] is similar to that obtained for other alkylaminomethylenephosphonic acids (Section 4.3).^{23,24,30,42,56,57,59,63-65} This curve, and that for $\delta^{31}\text{P}$ vs pH obtained for DDDTMPH₈ from titrations where the stock solution did not contain nitric acid [Figure

4.6.2(a); curve denoted as "▲"] are similar within experimental error in the pH range common to both, *i.e.* pH 2-12.5. One difference between the two profiles [Figure 4.6.2(a)] is that there is an extra inflection at *ca.* pH 2 for the titration carried out in the presence of extra acid.

Comparison of the species distribution curves⁶⁶ (calculated from the pK_a values) [Figure 4.6.2(b)] with the profiles of $\delta^{31}\text{P}$ vs pH for DDDTMPH_3 [Figure 4.6.2(a)] shows a correlation between the 'half-neutralisation' points on the species distribution curves⁶⁶ [Figure 4.6.2(b)] and the approximate positions of the inflections on the profiles of the $\delta^{31}\text{P}$ vs pH [Figure 4.6.2(a)]. In particular, increasing shielding of the ^{31}P nucleus between *ca.* pH 4-7 [Figure 4.6.2(a)] clearly correlates with a series of overlapping equilibria [Figure 4.6.2(b)] and the pK_a value of 11.07 (Table 4.6.1) correlates with the presence of species causing a large downfield shift in the phosphorus signal, *i.e.* *ca.* 4 ppm [Figure 4.6.2(a)].

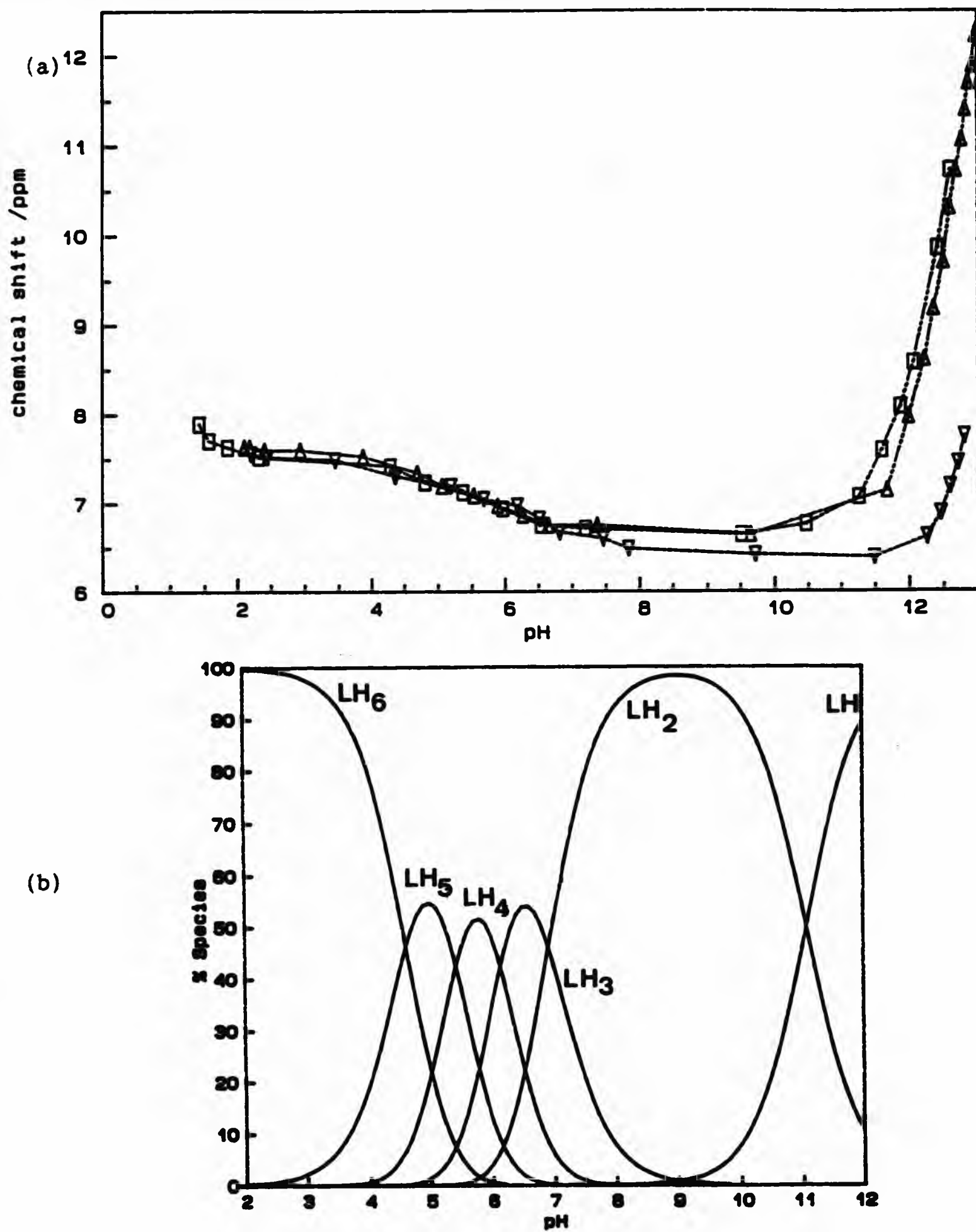


Figure 4.6.2 (a) The pH dependence of $\delta^{31}\text{P}$ for DDDTMPH_3 in aqueous solution; \square = titration vs aqueous KOH, stock solution containing nitric acid; Δ = titration vs aqueous KOH, stock solution without nitric acid; ∇ = titration vs aqueous Et_4NOH , stock solution without supporting electrolyte. (b) Species distribution curves⁶⁶ for DDDTMPH_3 .

An alternative way of presenting the results of a ^{31}P nmr titration to determine the sequence of neutralisation of the protons on a ligand, is to plot $\delta^{31}\text{P}$ vs τ , (τ = degree of titration, defined in Section 4.5). It is convenient to carry out a ^{31}P nmr titration to be presented in this way in the absence of an initial excess of acid (*i.e.* without aqueous nitric acid in this case). The resulting plot of $\delta^{31}\text{P}$ vs τ (Figure 4.6.3, curve denoted as " Δ ") shows that increasing degree of titration results in shielding of the phosphorus nucleus until $\tau = 6-7$. This shielding can be ascribed to the deprotonation of six phosphonate oxygens, as discussed in Section 4.3.^{23,30,57,59,60,65,67}

Thereafter, the phosphorus nucleus is deshielded as τ increases beyond *ca.* 7 and this can be ascribed to deprotonation of the nitrogen-bound protons.^{23,26,29,30,58,59,63-65} The conclusion reached is that six phosphonate oxygens are deprotonated between *ca.* pH 2-9, resulting in the shielding of the phosphorus nucleus and two nitrogen bound protons are neutralised above pH 9.5 ($\tau > 6.5$) resulting in the large downfield shift [Figure 4.6.2(a)].

This implies that there are two pK_a 's greater than 9.5 log units for the processes of successively deprotonating the two nitrogen atoms. However, only one log K value above this has been determined (11.07). This conclusion seems

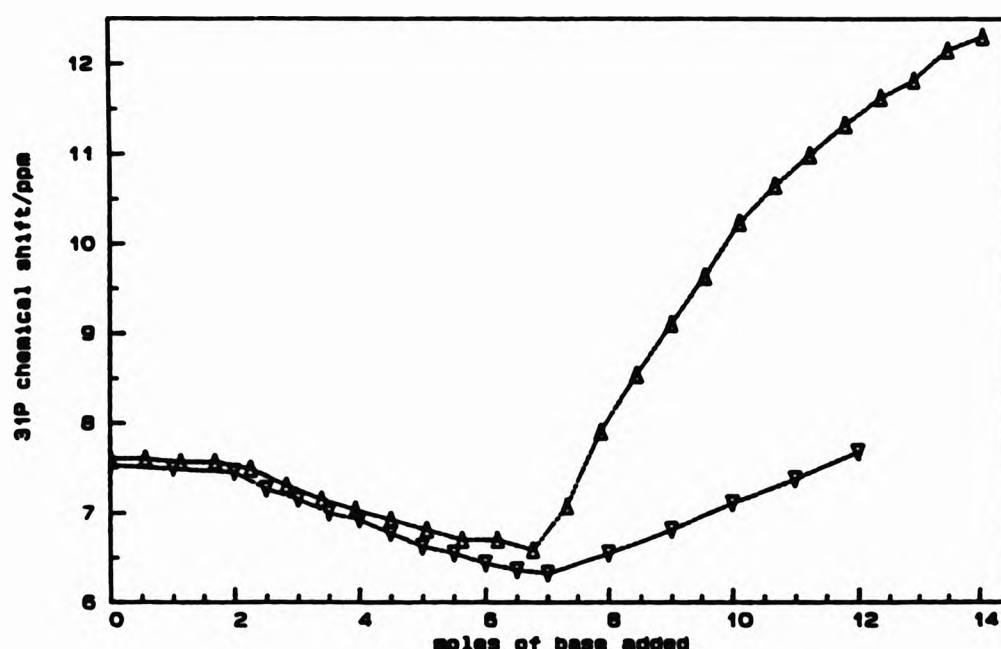
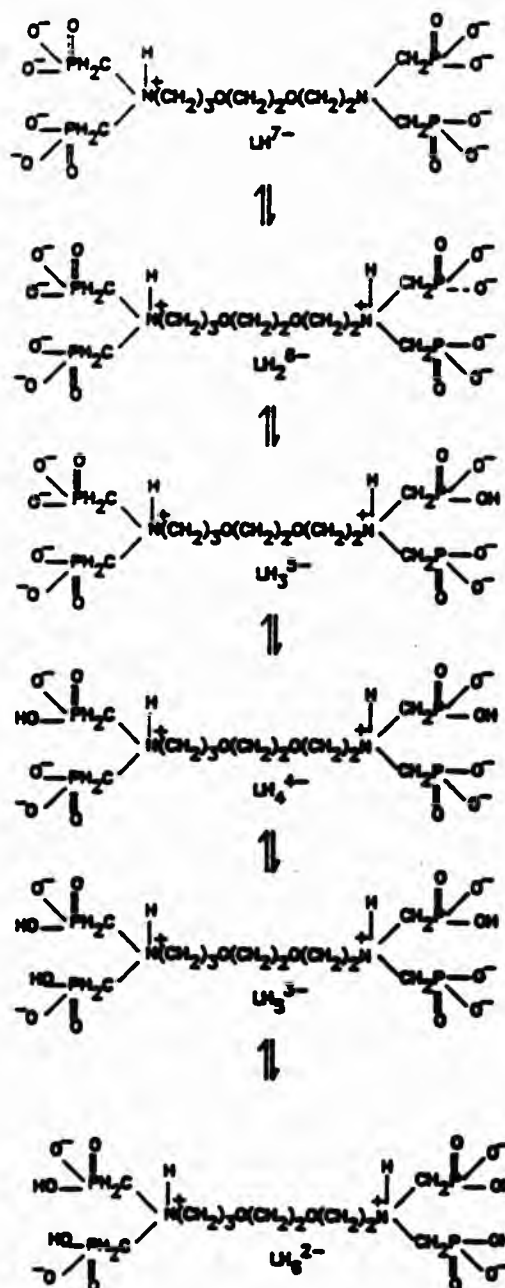


Figure 4.6.3 Profiles of $\delta^{31}\text{P}$ vs τ (degree of titration) for DDDTMPH₆ in aqueous solution, Δ = titration against potassium hydroxide, stock solution without nitric acid; ∇ = titration against aqueous tetraethylammonium hydroxide, stock solution without supporting electrolyte.

to be consistent with the comparison of $\delta^{31}\text{P}$ vs pH profiles [Figure 4.6.2(a)] with the species distribution curves [Figure 4.6.2(b)]. The broad 'well' between pH values of ca. 6 and 9.5 [Figure 4.6.2(a)] coincides with the dominance of a single species in the range pH 8-11 [Figure 4.6.2(b)]. Also the rather low value of $\delta^{31}\text{P}$ for this species [Figure 4.6.2(a)] would support its formulation of a species with both nitrogens fully protonated. This is also consistent agrees with the titration curves (Figure 4.6.1) in which the inflection at pH ca. 9 corresponds to ca. six equivalents of base being consumed by the ligand system with two protons remaining to be neutralised at a higher pH (> 9.5), only one of which was determined using the potentiometric method.

Based on these arguments, the protonation constants for DDDTMPH_3^\dagger have been assigned to the following scheme:



[†] The 'species' L in the SUPERQUAD⁴¹ input files must therefore be assigned to the monoprotonated species DDDTMPH^\dagger in the chemical system and the value corresponding to the first protonation of the one of the nitrogens of the species DDDTMP^\dagger remains undetermined.

Since DDDTMPH₃ contains the ether linkage $-O-CH_2CH_2-O-$, it might be expected that potassium ions in the stock solution (and/or base) used in the potentiometric and the two ^{31}P nmr titration experiments (Section 2.3, 2.4.9 and 2.4.10) [Figure 4.6.2(a)] would coordinate to the ether oxygens of the ligand. Pedersen found that some macrocyclic crown ethers he prepared were able to form stable complexes with alkali metal ions, especially potassium.⁸³ Such coordination might affect the pH determination using the glass electrode and/or the shielding of the phosphorus nucleus.

In order to investigate this possibility, the $\delta^{31}P$ vs pH titration of DDDTMPH₃ against aqueous tetraethylammonium hydroxide (Section 2.4.11) was carried out. The resulting plot of $\delta^{31}P$ vs τ (degree of titration) (Figure 4.6.3, curve denoted as "v") is similar to the profile of $\delta^{31}P$ vs τ for the titration against aqueous potassium hydroxide (Figure 4.6.3, curve denoted as "Δ"), except at high pH (> ca. 10), where the downfield shift in the phosphorus nucleus is less than 1 ppm. The difference between the two curves (Figure 4.6.3) provides evidence for complexation of potassium ions with the ligand at high pH (> 10).

The difference between the plots of $\delta^{31}P$ vs pH at pH ca. 8 for the titrations of the stock solutions with (□) and without (Δ) nitric acid, and the plot of the titration without supporting electrolyte (v) [Figure 4.6.2 (a)] indicates that there is either a complexation effect and/or an alkali metal ion effect in which the glass electrode responds to alkali metal ions at high pH resulting in a lower pH value than the true pH.⁸⁴ However, the $\delta^{31}P$ vs τ (degree of titration) (Figure 4.6.3) shows that at least part of this difference is due to complexation of potassium ions.

4.7 References

1. E.g. L. J. Matienzo, D. K. Shaffer, W. C. Moshier and G. D. Davis, *ACS. Symp. Ser.*, 1986, 322, 234; CA 106, 51736j. D. A. Johnson, U.S. Patent 4,642,194, 1987; CA 106, 162364f. J. Wasel-Nielen and L. Fischer, Ger. Offen. De 3526640 1987; CA 106, 162363e. A. Stehlin and C. Guth, Eur. Pat. Appl. EP 210952, 1987; CA 106, 178074x. A. Harris, J. Burrows and J. R. Hargreaves, Ger. Offen., 2231206, 1972; CA 78, 91868p. A. Harris, J. Burrows and J. R. Hargreaves, Ger. Offen., 2230832, 1972; CA 78, 150164f. M. Hollmann, R. Opitz and K. Haage, Ger. (East) 144073, 1980; CA 94, 210645f. B. Szpoganicz and A. E. Martell, *Biochimie*, 1987, 71, 591. M. Horiguchi and M. Kandatsu, *Nature (London)*, 1959, 184, 901. P. J. Sadler, C. T. Harding, J. D. Kelly and A. B. McEwen, Eur. Pat. Appl. EP 210043, 1987; CA 108, 128096b. A. J. Hutchinson, K. R. Shaw and J. A. Schneider, Eur. Pat. Appl. EP 203891, 1986; CA 108, 112743x.
2. E. J. Griffith, *Ind. Eng. Chem.*, 1959, 51, 240.
3. J. S. Kittredge, E. Roberts and D. G. Simonsen, *Biochem.*, 1962, 1, 624.
4. B. L. Roop and W. E. Roop, *Anal. Biochem.*, 1968, 25, 260.
5. J. Fourche, H. Jensen and E. Neuzil, *Anal. Chem.*, 1976, 48, 155.
6. E. N. Rizkalla, *Rev. Inorg. Chem.*, 1983, 5, 223, and references therein.
7. G. Schwarzenbach, H. Ackermann and P. Ruchstuhl, *Helv. Chim. Acta.*, 1949, 32, 1175.
8. R. Tyka, G. Hagele and J. Peters, *Synth. Comm.*, 1988, 18, 425.
9. R. Tyka, G. Hagele and R. Boetzel, *Phosphorus, Sulphur and Silicon*, 1991, 62, 75.
10. G. Bartels, Ger. Offen. De 3445300, 1984; CA 106, 504502z.
11. L. Maier, Ger. 1292654, 1965; CA 71, 39166z. L. Maier, *Helv. Chim. Acta.*, 1967, 50, 1723.
12. K. B. Yatsimirskii, M. D. Konstantinovskaya and E. I. Sinyavskaya, *Zh. Neorg. Khim.*, 1989, 34, 2217; CA 112, 12629f.
13. Yu. M. Polikarpov, F. I. Bel'skii, A. S. Pisareva and M. I. Kabachnik, *Izu. Akad. Nauk. SSSR, Ser. Khim.*, 1989, 9, 2112; CA 112, 198536b.
14. Z. H. Kudzin and M. W. Majchrzak, *J. Organomet. Chem.*, 1989, 376, 245.
15. L. Maier and P. J. Diel, *Phosphorus Sulphur Silicon Relat. Elem.*, 1991, 62, 15; CA 115, 280130k.
16. I. Ya. Polyakova, A. Ya. Fridman and N. M. Dyatlova, *Koord. Khim.*, 1987, 13, 147.
17. D. Cameron, H. R. Hudson, I. Lagerlund and M. Pianka, Eur. Pat. 153 284; CA. 104, 207445k.

18. J. E. Franz, Ger. Pat. 2152826, 1972; CA.
19. R. J. Motekaitis, I. Murase and A. E. Martell, *J. Inorg. Nucl. Chem.*, 1971, 33, 3353.
20. S. Westerback, K. S. Rajan and A. E. Martell, *J. Am. Chem. Soc.*, 1965, 87, 2567.
21. K. S. Rajan, I. Murase and A. E. Martell, *J. Am. Chem. Soc.*, 1969, 91, 4408.
22. N. Ockerbloom and A. E. Martell, *J. Am. Chem. Soc.*, 1958, 80, 2351.
23. R. P. Carter, R. L. Carroll and R. R. Irani, *Inorg. Chem.*, 1967, 6, 939.
24. K. Sawada, T. Araki and T. Suzuki, *Inorg. Chem.*, 1987, 26, 1199.
25. J. Oakes and E. G. Smith, *J. Chem. Soc., Dalton Trans.*, 1983, 601.
26. R. D. Gillard, P. D. Newman and J. D. Collins, *Polyhedron*, 1989, 8, 2077.
27. N. Choi, I. Khan, R. W. Matthews, M. McPartlin and B. P. Murphy, *Polyhedron*, 1994, 13, 847.
28. E.g. T. Glowiak, W. Sawka-Dobrowolska and B. Jezowska-Trzebiatowska, *Inorg. Chim. Acta.*, 1980, 45, L105. A. Schier, S. Gamper, G. Muller, *Inorg. Chim. Acta.*, 1990, 177, 179.
29. E.g. W. C. Schumb, C. N. Satterfield and R. L. Wentworth, *Hydrogen Peroxide*, Reinhold, New York, 1955. G. W. Morris, N. D. Feasey, P. A. Ferguson, D. Van Hemelrijk and M. Charlot, PCT Int. Appl. WO 9001034, 1990; CA 113, 6601v. K. J. Radimer, Eur. Pat. Appl. EP 97305, 1984; CA 100, 123537w. M. Hollmann, R. Opitz and K. Haage, Ger. (East) 144073, 1980; CA 94, 21045f. Y. Machida, T. Yoshida, N. Kimura and M. Watanabe, Jpn. Kokal Tokkyo Koho JP 62185797, 1986; CA 108, 39593u. S. Croft, B. C. Gilbert, J. R. L. Smith, J. K. Stell and W. R. Sanderson, *J. Chem. Soc. Perkin Trans. 2*, 1992, 153.
30. K. Moedritzer and R. R. Irani, *J. Org. Chem.*, 1966, 31, 1603.
31. T. Candy, Interlox Research & Deveolpement, personal communication.
32. P. B. Iveson, M. P. Lowe and J. C. Lockhart, *Polyhedron*, 1993, 12, 2313.
33. R. W. Matthews and I. Khan, unpublished work.
34. D. Green, G. Hägele, H. R. Hudson, R. Lee, R. W. Matthews, M. McPartlin, I. J. Scowen and C. J. L. Silwood, unpublished results.
35. A. Steitweiser and C. H. Heathcock, *Introduction to Organic Chemistry*, MacMillian, New York, 1985.
36. K. Sawada, T. Miyagawa, T. Sakaguchi and K. Doi, *J. Chem. Soc., Dalton Trans.*, 1993, 3777.
37. E. L. Eliel, N. L. Allinger, S. J. Angyual and G. A. Morrison, *Conformational Analysis*, Interscience Publishers, 1967.
38. A. E. Derome, *Modern Nmr Techniques for Chemistry Research*, Pergamon

- Press, Oxford, 1987.
39. D. H. Williams and I. Fleming, *Spectroscopic Methods in Organic Chemistry*, McGraw-Hill, London, 1980.
 40. R. T. Conley, *Infrared Spectroscopy*, Allyn Bacon, Boston, 1972.
 41. P. Gans, A. Sabatini and A. Vacca, *J. Chem. Soc., Dalton Trans.*, 1985, 1195.
 42. M. Wozniak and G. Nowogrocki, *Talanta*, 1979, 26, 1135.
 43. I. J. Scowen, Ph.D Thesis, University of North London, 1993.
 44. F. I. Bel'skii, I. B. Goryunova, P. V. Petrovskii, T. Ya. Medved' and M. I. Kabachnik, *Bull. Acad. Sci. USSR*, 1982, 31, 93.
 45. J. J. Daly and P. J. Wheatley, *J. Chem. Soc.*, 1967, 212.
 46. W. Sawka-Dobrowolska, *Acta. Cryst.*, 1985, C41, 84.
 47. J. Kowalik, W. Sawka-Dobrowolska and T. Glowiak, *J. Chem. Soc. Chem Comm.*, 1984, 446.
 48. W. Sawka-Dobrowolska and J. Kowalik, *Acta. Cryst.*, 1988, C44, 1624.
 49. W. Sawka-Dobrowolska, T. Glowiak and J. Kowalik, *Acta. Cryst.*, 1992, C48, 286.
 50. Z. Galdecki and W. M. Wolf, *Acta. Cryst.*, 1990, C46, 271.
 51. I. Lazar, D. C. Hrnar, W.-D. Kim, G. E. Kiefer and A. D. Sherry, *Inorg. Chem.*, 1992, 31, 4422.
 52. B. I. Makaranets, N. T. Polynova, V. K. Bel'skii, S. A. Ii'ichev and M. A. Porai-Koshits, *Zh. Strukt. Khim.*, 1985, 26, 131.
 53. L. M. Shkol'nikova, G. V. Polyanchuk, N. M. Dyatlova, T. Ya. Medved, I. B. Goryunova and M. I. Kabachnik, *Izv. Akad. Nauk SSSR, Ser. Khim.*, 1985, 5, 1035.
 54. L. M. Shkol'nikova, G. V. Polyanchuk, V. E. Zavodnik, M. V. Rudomino, S. A. Pisareva, N. M. Dyatlova, B. V. Zhadanov and I. A. Polyakova, *Zh. Strukt. Khim.*, 1987, 28, 124.
 55. M. Darriet, J. Darriet, A. Cassaigne and E. Neuzil, *Acta. Cryst.*, 1975, B31, 469.
 56. G. V. Polyanchuk, L. M. Shkol'nikova, M. V. Rudomino, N. M. Dyatlova and S. S. Makarevich, *Zh. Strukt. Khim.*, 1985, 26, 109.
 57. W. Clegg, P. B. Iveson and J. C. Lockhart, *J. Chem. Soc., Dalton Trans.*, 1992, 3291.
 58. C. F. G. C. Geraldès, A. D. Sherry and W. P. Cacheris, *Inorg. Chem.*, 1989, 28, 3336.
 59. M. A. Dhansay, P. W. Linder, R. G. Torrington and T. A. Modro, *J. Phys. Org. Chem.*, 1990, 3, 248 and references therein.
 60. T. G. Appleton, J. R. Hall, A. D. Harris, H. A. Kimlin and I. J. McMahon,

- Aust. J. Chem.*, 1984, 37, 1833.
61. Z. Glowacki, M. Hoffmann, M. Topolski and J. Rachon, *Phosphorus, Sulphur Silicon Relat. Elem.*, 1991, 60, 67.
 62. J. L. Sudmeier and C. N. Reilley, *Anal. Chem.*, 36, 1964, 1699.
 63. K. Mikkelsen and S. O. Nielsen, *J. Phys. Chem.*, 1960, 64, 632.
 64. P.-M. L. Robitaille, P. A. Robitaille, G. G. Brown Jr. and G. G. Brown, *J. Magn. Reson.*, 1991, 92, 73.
 65. T. G. Appleton, J. R. Hall and I. J. McMahon, *Inorg. Chem.*, 1986, 25, 726.
 66. K. Moedritzer, *Inorg. Chem.*, 1967, 6, 936, 943 and references therein.
 67. R. J. Motekaitis, FORTRAN 77 program SPE, 1987. C. Crees, TURBO C, program SPECIES, unpublished, 1990. C. J. L. Silwood, GW-BASIC program, HPLOT, unpublished, 1990.
 68. R. J. Grabenstetter, O. T. Quimby and T. J. Flautt, *J. Phys. Chem.*, 1967, 71, 4194.
 69. W. Sawka-Dobrowolska, T. Glowiak, Z. Siatecki and M. Soroka, *Acta Cryst.*, 1985, C41, 453.
 70. A. Albert, E. P. Serjeant, *The Determination of Ionization Constants*, Chapman and Hall, London, 1971.
 71. G. Anderegg, *Talanta*, 1993, 40, 243.
 72. D. A. Skoog and D. M. West, *Fundamentals of Analytical Chemistry*, 1982, 4th Edition, CBS College Publishing, New York.
 73. R. J. Motekaitis, I. Murase and A. E. Martell, *Inorg. Nucl. Chem. Lett.*, 1971, 7, 1103.
 74. R. J. Motekaitis, I. Murase and A. E. Martell, *Inorg. Chem.*, 1976, 15, 2303.
 75. M. I. Kabachnik, N. M. Dyatlova, T. Ya. Medved', Yu. F. Belugin and V. V. Sidorenko, *Dokl. Akad. Nauk SSSR*, 1967, 175, 351.
 76. M. T. M. Zaki and E. N. Rizkalla, *Talanta*, 1980, 27, 709.
 77. C. V. Banks and R. E. Yerrick, *Anal. Chim. Acta.*, 1959, 20, 301.
 78. E. N. Rizkalla and M. T. M. Zaki, *Talanta*, 1979, 26, 507.
 79. I. Khan. M. Phil. Thesis, University of North London, 1994.
 80. G. Hägele, S. Varbanov, J. Ollig and H.-W. Kropp, *Z. Anorg. Allg. Chem.*, 1994, 620, 914; G. Hägele, *Phosphorus-31 NMR Spectral Properties in Compound Characterisation and Structural Analysis*, Eds. L. D. Quin and J. G. Verkade, VCH Publishers.
 81. A. E. Martell and R. M. Smith, *Critical Stability Constants, Volume 2: Amino acids*, Plenum Press, New York, 1974.
 82. M. I. Kabachnik, T. Ya. Medved', O. G. Arkhipova and M. V. Rudomino,

- Russ. Chem. Revs.*, 1968, 37, 503.
83. N. N. Greenwood and A. Earnshaw, *Chemistry of the Elements*, Pergamon Press, Oxford, 1986. C. J. Pedersen, *J. Am. Chem. Soc.*, 1967, 89, 7017.
84. D. A. Skoog, D. M. West and F. J. Holler, *Fundamentals of Analytical Chemistry*, Saunders College Publishing, New York, 1988.

*Chapter 5 Metal complexes of some
alkylaminomethylenephosphonic acids*

5.1 The stability of some metal complexes of two 'simple' α -aminomethylene-phosphonic acids, DEAMPH₂ and NEIBMPH₄

The complexing ability of α -aminomethylenephosphonic acids with various metal cations has been widely investigated, usually by means of potentiometry (e.g. ref. 1) and occasionally using nmr spectroscopy (e.g. ref's. 2-9).

After analysis of the protonation behaviour of both DEAMPH₂ (Section 4.3) and NEIBMPH₄ (Section 4.4), there was a need to examine the complexation behaviour of these two acids. Of particular concern is the need to establish the identity of the species in solution in order to probe the means by which these types of α -aminomethylenephosphonic acids may stabilise *aqueous* solutions of hydrogen peroxide.

The potentiometric method was exclusively used in this work, the titrations being performed exactly as for the protonation studies, but with the addition of appropriate quantities of metal ions. The previously determined protonation constants for DEAMPH₂ and NEIBMPH₄ were held constant during analysis of the titration data using the SUPERQUAD program.¹⁰ In the refinement of all the datafiles for both DEAMPH₂ and NEIBMPH₄, the fully deprotonated ligand, *i.e.* DEAMP²⁻ and NEIBMP⁴⁻ respectively, was defined as L.

5.1.1 Stability constants for metal ion complexes with DEAMPH₂

The coordination behaviour of DEAMPH₂ has received some attention previously; Wozniak¹¹ and Carter¹² reported stability constants for DEAMPH₂ with Ca(II), Mg(II) and Cu(II). Several protonated species of Cu(II) with DEAMPH₂ were reported by Wozniak, *i.e.* [CuL], [CuLH]⁺ and [CuL(OH)]⁻.¹¹ However, only one species, [ML], was reported by Carter for DEAMPH₂ with Mg(II) and Ca(II).¹²

The coordination behaviour of DEAMPH₂ with Cu(II) and Ni(II) was also investigated using potentiometric titrations by a previous worker at the University of North London.¹³ However, precipitation of Cu(II) and Ni(II) complexes, or hydrolysis products, in basic solution this precluded refinement of the data to determine stability constants.¹³

Potentiometric titrations of DEAMPH₂ in the presence of metal ions were carried out over the pH range 2-12 (Section 2.3.6). The following metal ions were examined: Zn(II), Cd(II), Pb(II) and Co(II). For each metal ion, at least two

potentiometric titrations were carried out, and where possible, differing ratios of ligand to metal were used (*i.e.* M:L ratios of 1:1, 1:2 and 1:3).

5.1.1(a) Zinc(II) and Cadmium(II)

Potentiometric titration curves for DEAMP₂ with the metal ions Zn(II) and Cd(II) (Figure 5.1.1) show characteristic signs of hydrolysis. The discontinuities in the curves at, respectively, pH > 8 and > 7, and the associated scatter of points, are reasonably ascribed to hydrolysis and subsequent precipitation of the hydrolysis products. The slight deviation of the titration curves in the presence of the metal ions from the 'ligand-only' curve indicates only weak complexation in the pH range below the onset of hydrolysis. The concentrations of DEAMP₂ used in the titration of DEAMP₂ alone [Figure 5.1.1 (a)] and with Zn(II) [Figure 5.1.1(b)] are different. This results in the 'ligand-only' curve being slightly to the right of the 'metal-ligand' curve in Figure 5.1.1 (b).

Values of stability constants (only log β_{110}) for DEAMP₂ with Cd(II) and Zn(II) were only determined from one datafile in each case (Table 5.1.1). Refinements of the datafiles for DEAMP₂ with Zn(II) and Cd(II) involved 'cutting-back' the data region to exclude the area of the curve which was ascribed to hydrolysis. Although values for log β_{110} were obtained, they dictate that the complexes have only small abundance (< 10 %) in the pH range studied. The values must therefore be regarded as very approximate. Refinements of the datafiles for DEAMP₂ with Cd(II) and Zn(II) using a model which included metal-ligand hydrolysis products were also unsuccessful.

Metal stability constants for a similar ligand, *N,N*-dimethylaminomethylene-phosphonic acid (DMAMP₂) with Mn(II), Zn(II), Fe(II), Co(II) and Cd(II) also gave unreliable titration curves at high pH.¹⁴ This was ascribed to precipitation of the metal complex or of metal hydroxide. The stability constants determined for DEAMP₂ with Cd(II) and Zn(II) show reasonable agreement with the results reported for *N,N*-dimethylaminomethylene-phosphonic acid.¹⁴

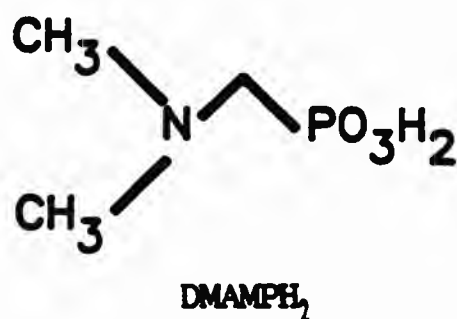


Table 5.1.1 Stability constants for complexes of DEAMPH₂ and DMAMPH₂.

	Log β_{CdL}	Log β_{ZnL}	Log β_{CuL}	Log β_{MgL}	Log β_{CaL}
DEAMPH ₂	5.62(0.016) ^{a,b}	6.52(0.017) ^{a,c}	7.46 ^d	ca. 2 ^{e,f}	1.28 ± 0.18 ^e
DMAMPH ₂	5.17 ± 0.1 ^g	5.45 ± 0.1 ^g			

^a This work, $I = 0.1 \text{ mol dm}^{-3} \text{ KNO}_3$, $25.0 \pm 0.1 \text{ }^\circ\text{C}$. Figures in parentheses are relative standard deviations obtained using SUPERQUAD. These values should be taken as very approximate estimates (see text). ^b Datafile M085. Fit parameters determined using SUPERQUAD, $\chi^2 = 4.30$, $\sigma = 0.0688$, pH range 3.60–8.98, number of points = 37. ^c Datafile M084. Fit parameters determined using SUPERQUAD, $\chi^2 = 6.32$, $\sigma = 0.1750$, pH range 3.00–7.84, number of points = 53. ^d Ref. 11, $I = 0.1 \text{ mol dm}^{-3} \text{ KNO}_3$, $25.0 \text{ }^\circ\text{C}$. ^e Ref. 12, $I = 1.0 \text{ mol dm}^{-3} \text{ KNO}_3$, $25.0 \text{ }^\circ\text{C}$. ^f Estimate; precipitation prevented precise measurement. ^g *N,N*-dimethylaminomethylenephosphonic acid, Ref. 14, $I = 0.1 \text{ mol dm}^{-3} \text{ KNO}_3$, $25.0 \pm 0.1 \text{ }^\circ\text{C}$.

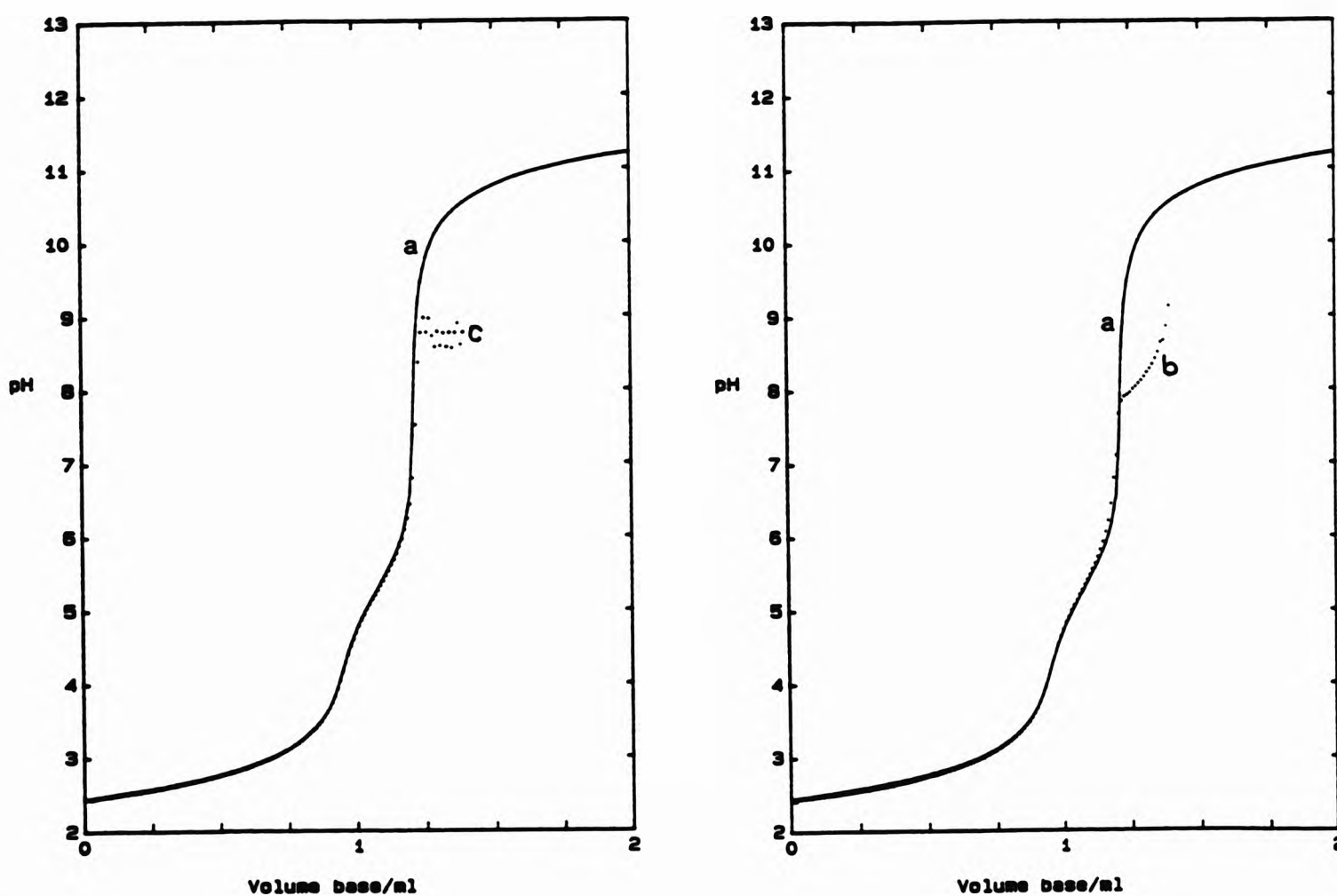


Figure 5.1.1 Titration curves (pH vs volume of base added) for acidified solutions of (a) DEAMPH₂, [DEAMPH₂] ca. $0.001 \text{ mol dm}^{-3}$, (b) $\text{Zn}(\text{NO}_3)_2$ with DEAMPH₂, [M]:[L] ca. 1:1 and (c) $\text{Cd}(\text{NO}_3)_2$ with DEAMPH₂, [M]:[L] ca. 1:1.

5.1.1(b) Cobalt(II)

The potentiometric titration curve obtained for Co(II) with DEAMPH₂ (Figure 5.1.2) showed some slight deviation of the 'metal-ligand' curve from the 'ligand-only' curve, but the deviation (between pH 3 and 8) is partly attributed to the small difference in concentrations of base used in the two potentiometric titrations. The potentiometric titration curve obtained for Co(NO₃)₂ in the absence of DEAMPH₂ is shown in Figure 5.1.2(c) and shows irregularities in the curve at pH ca. 8.5 which must be ascribed to precipitation of metal hydrolysis products. On this basis, the discontinuities observed in the metal-ligand curve at pH ca. 8-9 [Figure 5.1.2(b)] must be also be ascribed to precipitation of metal hydrolysis products.

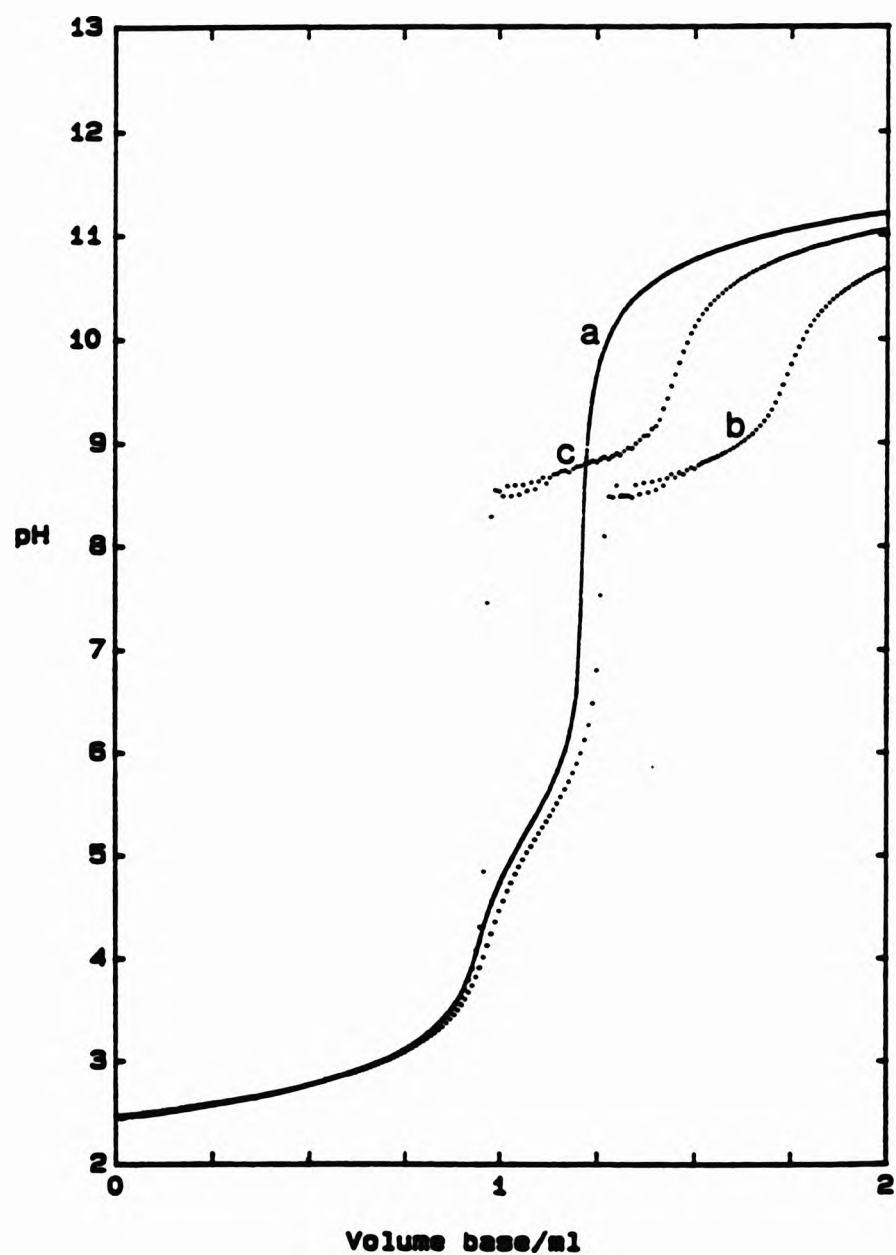


Figure 5.1.2 Titration curves (pH vs volume of base added) for acidified solutions of (a) DEAMPH₂, [DEAMPH₂] ca. 0.001 mol dm⁻³, (b) Co(NO₃)₂ with DEAMPH₂, [M]:[L] ca. 1:1 and (c) Co(NO₃)₂.

Attempts to fit the data for Co(II)-ligand titrations to different models of the equilibria which might occur in solution failed. The models tried involved species with stoichiometries ($M_nL_mH_p$) of 110, 111 and 112.

Stability constant determinations by Sawada¹⁴ for the analogue of DEAMPH₂, DMAMPH₂, gave a value of $\log \beta_{110} = 4.80$, which suggests that, in spite of the results obtained here, DEAMPH₂ may have some affinity for the metal Co(II).¹⁴

5.1.1(c) Lead(II)

In contrast to titrations in the presence of Zn(II), Cd(II) and Co(II), the titration curves of DEAMPH₂ with the metal ion Pb²⁺ (Figure 5.1.3) show no evidence of precipitation. Determination of stability constants for metal complexes of a variety of aminomethylenephosphonic acids have shown^{11,13}

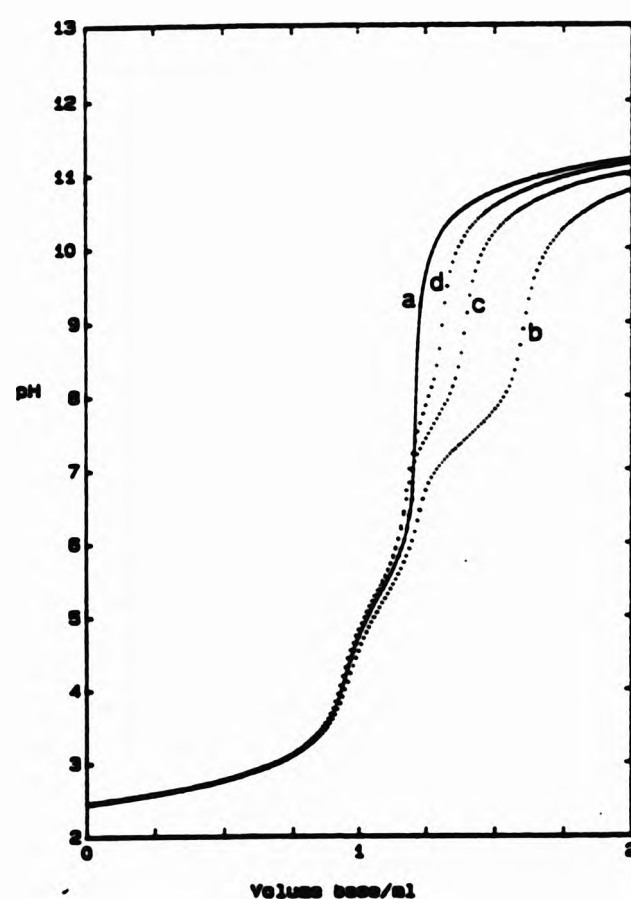


Figure 5.1.3 Titration curves (pH vs volume of base added) for acidified solutions of (a) DEAMPH₂, [DEAMPH₂] ca. 0.001 mol dm⁻³, (b) Pb(NO₃)₂ with DEAMPH₂, [M]:[L] ca. 1:1, (c) Pb(NO₃)₂ with DEAMPH₂, [M]:[L] ca. 1:2 and (d) Pb(NO₃)₂ with DEAMPH₂, [M]:[L] ca. 1:3.

(examples also given in E. N. Rizkalla, *Rev. Inorg. Chem.*, 1983, 5, 223) that complexes with M:L ratios of 1:1 and 1:2 can be formed in solution. Therefore, in order to increase the likelihood of forming complexes with M:L ratios of 1:2 and possibly 1:3, and hence measure their stability constants, the concentration of the metal ion was decreased through the three titrations involving Pb(II) (datafiles M032, M033 and M082).

Analysis, using the program SUPERQUAD,¹⁰ of the three datafiles gave the stability constants summarized in Table 5.1.2. These analyses were characterized by satisfactory χ^2 and σ values, and by weighted residuals plots which displayed a reasonably random distribution of points. During the refinement of the titration data from file M082 ([M]:[L] = 1:3.32), inclusion of the species [ML₂] in the model for equilibria occurring in solution was partially successful. The value of χ^2 was somewhat high and the weighted

Table 5.1.2 Stability constants for DEAMP₂ with Pb(II).^a

Datafile	M032 ^b	M033 ^c	M082 ^d	Mean ^e
[M]:[L]	1:1.09	1:1.84	1:3.32	
log β_{110}	7.32(0.047)	7.64(0.047)	7.73(0.036)	7.56 ±0.24
log β_{111}	14.50(0.043)	14.81(0.053)	15.15(0.039)	14.82 ±0.33
log K_{111}	7.18	7.17	7.42	7.26 ±0.16
log β_{11-1} ^f	0.084(0.014)	-0.16(0.027)	-0.63(0.035)	-0.24 ±0.39
log K_{11-1} ^g	-7.24	-7.80	-8.36	-7.80 ±0.56

^a I = 0.1 mol dm⁻³ KNO₃, 25.0 ±0.1 °C. Figures in parentheses are relative standard deviations obtained using SUPERQUAD. Convention: β_{MLH} for $M_nL_mH_p$.

^b Fit parameters determined using SUPERQUAD, $\chi^2 = 2.53$, $\sigma = 0.063$, pH range 5.19-7.36, number of points = 30. ^c Fit parameters determined using SUPERQUAD, $\chi^2 = 4.93$, $\sigma = 0.078$, pH range 4.91-7.75, number of points = 29. ^d Fit parameters determined using SUPERQUAD, $\chi^2 = 4.00$, $\sigma = 0.051$, pH range 5.21-8.23, number of points = 24. ^e Unweighted mean of values from each refinement; error limits are derived from the ranges obtained for each log β_{MLH} (and

log K_{MLH}).

^f $\{\text{Pb}(\text{H}_2\text{O})\}^{2+} + \text{DEAMP}^{2-} \rightleftharpoons \{\text{Pb}(\text{DEAMP})(\text{OH})\}^- + \text{H}^+$;

$\beta_{11-1} = [\{\text{Pb}(\text{DEAMP})(\text{OH})\}^-][\text{H}^+]/[\{\text{Pb}(\text{H}_2\text{O})\}^{2+}][\text{DEAMP}^{2-}]$.

^g $\{\text{Pb}(\text{DEAMP})(\text{H}_2\text{O})\} \rightleftharpoons \{\text{Pb}(\text{DEAMP})(\text{OH})\}^- + \text{H}^+$;

$K_{11-1} = [\{\text{Pb}(\text{DEAMP})(\text{OH})\}^-][\text{H}^+]/[\{\text{Pb}(\text{DEAMP})(\text{H}_2\text{O})\}]$; log $K_{11-1} = \log \beta_{11-1} - \log \beta_{110}$.

residuals output showed evidence of systematic errors¹⁰ and hence the value of $\log \beta_{120}$ was not considered satisfactory.

The possibility that some Pb(II) hydrolysis reactions could also be occurring in solution was investigated. However, attempted refinement of datafile M032 for a model including $\log \beta_{10-1}$ $\{[\text{Pb}(\text{OH})]^{\dagger}\}$ along with values for the other species ($\log \beta_{110}$, $\log \beta_{111}$ and $\log \beta_{11-1}$) failed, $\log \beta_{10-1}$ being rejected in all cases. In datafile M033, refinement for a model which only involved the species *i.e.* MLH = 110, 111 and 112 was unsuccessful.

The potentiometric titration curves for DEAMP₂ with Pb(II) (Figure 5.1.3) show four buffer regions at *ca.* pH 2-3, 5, 7.5 and 11. Up to pH *ca.* 9, approximately two equivalents of base is consumed by the 'metal-ligand' system suggesting the formation of the species [PbL]. There is fairly close correspondence between the 'ligand-only' curve and the 'metal-ligand' curves up to pH *ca.* 5.5.

5.1.2 Stability constants for metal ion complexes with NEIBMPH₄

The iminobis(methylenephosphonic acid) moiety is present in a number of more 'complex' α -aminomethylenephosphonic acids, *e.g.* CDTMPH₃ and DDDTMPH₃. Therefore NEIBMPH₄ provides a model system for the investigation of the possible species in solution and the ways in which two or more ligating methylenephosphonate substituent groups can affect the stability of any resulting metal complexes.

The complexation behaviour of NEIBMPH₄ has been previously studied with a number of transition metals, Cu(II), Co(II), Ni(II) and Mn(II)¹⁵, and the alkaline earth metals Ca(II) and Mg(II).¹² The majority of the species determined in these studies were species with a 1:1 metal:ligand ratio. A previous worker at the University of North London examined the coordination behaviour of NEIBMPH₄ with Cu(II) and Ni(II) and investigated the possible formation of species with metal:ligand ratios of 1:1 and 1:2 and some metal complex hydrolysis products.¹³

5.1.2(a) Manganese(II)

Knowing the readiness with which manganese can form hydrolysis species or oxidise to form oxidation products (*i.e.* MnO₂) at high pH, titration datafiles for NEIBMPH₄ with Mn(II) were obtained at metal:ligand ratios of 1:3 only.

Smooth titration curves were observed and these show only some deviation of the 'metal-ligand' curve from the 'ligand-only curve', indicating the formation of weak metal complexes (Figure 5.1.4).

Refinement of each datafile for the model describing the formation of species with metal:ligand ratios of 1:1 was successful for only two datafiles (NMn1 and NMn3, Table 5.1.3). It was not possible to obtain a successful refinement for a model involving the species $[ML_2]$.

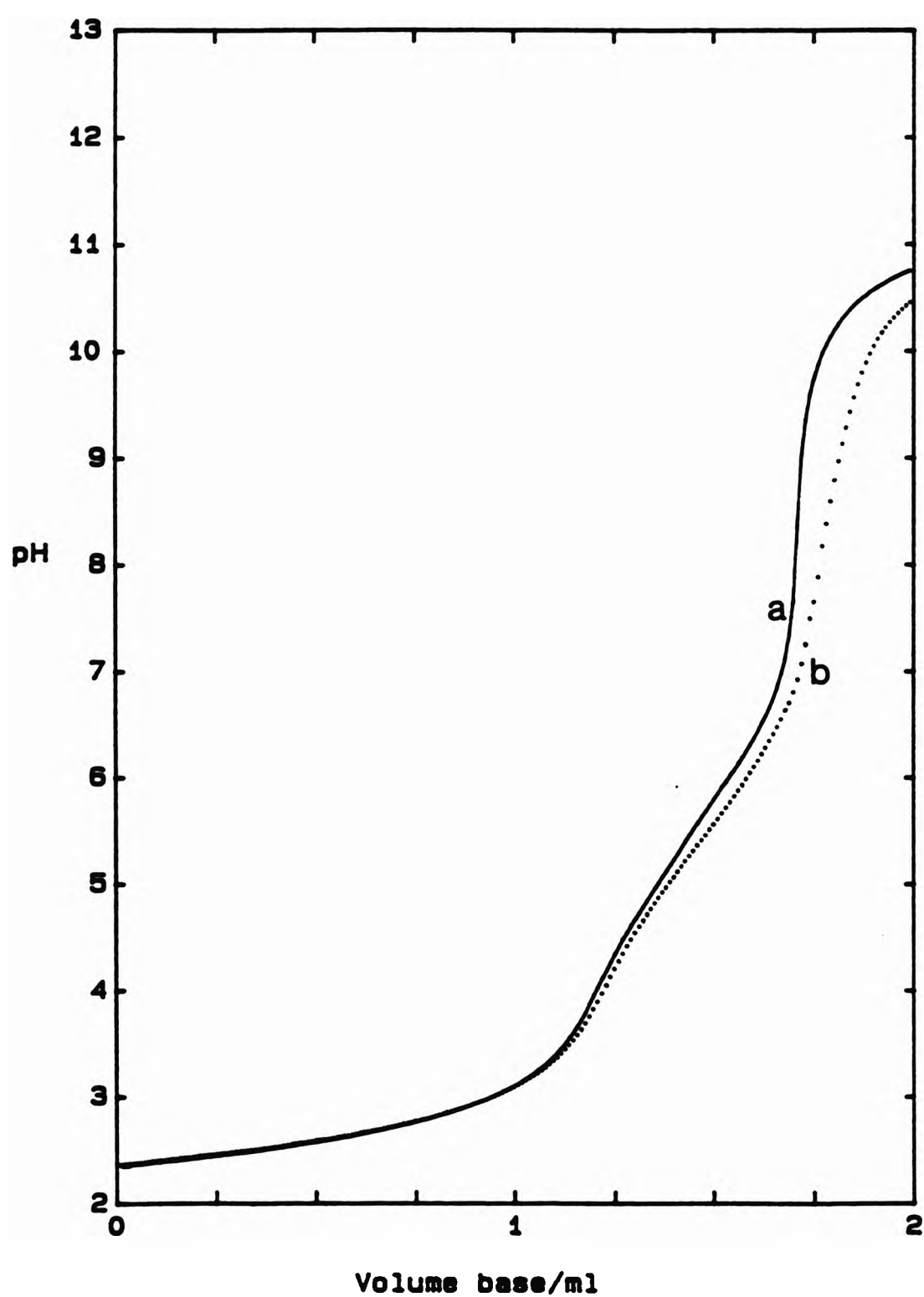


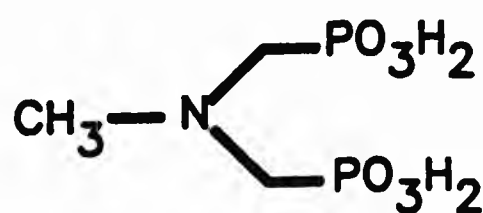
Figure 5.1.4 Titration curves (pH vs volume of base added) for acidified solutions of $NEIBMPH_4$ (a) $[NEIBMPH_4]$ ca. $0.001 \text{ mol dm}^{-3}$; (b) $Mn(NO_3)_2$ with $NEIBMPH_4$, $[M]:[L]$ ca. 1:3.

Table 5.1.3 Stability constants for NEIBMPH₄ with Mn(II).^a

Datafile: [M]:[L]	NMn1 ^b 1:3.06	NMn3 ^c 1:3.11	Mean ^d
log β ₁₁₀	6.95(0.012)	6.83(0.0425)	6.89 ±0.06
log β ₁₁₁	15.74(0.007)	15.09(0.0379)	15.42 ±0.33
log K ₁₁₁	8.79	8.26	8.53 ±0.27
log β ₁₁₂	20.73(0.021)		20.73
log K ₁₁₂	4.99		4.99

^a I = 0.1 mol dm⁻³ KNO₃, 25 ±0.1 °C. Figures in parentheses are standard deviations obtained using SUPERQUAD. Convention: β_{M_nL_nH_n} for M_nL_nH_n. ^b Fit parameters determined using SUPERQUAD, χ² = 4.33, σ = 0.0297, pH range 4.64-10.23, number of points = 57. ^c Fit parameters determined using SUPERQUAD, χ² = 10.03, σ = 0.0686, pH range 5.56-8.79, number of points = 31. ^d Unweighted mean of values from each refinement; error limits are derived from the ranges obtained for each log β_{M_nL_nH_n} (and log K_{M_nL_nH_n}).

The coordination behaviour of NEIBMPH₄ with some metal ions has also been investigated by Bel'skii in aqueous potassium nitrate (1.0 mol dm⁻³), i.e. Ca(II), Cu(II), Co(II), Ni(II) and Mn(II). The value of log β₁₁₀ (6.89) determined in this work is similar to the value obtained by Bel'skii for the species [MnL] (log β₁₁₀ = 6.94). However, there was significant variation between the value of log K₁₁₁ found in this work (8.53) and that found by Bel'skii (log K₁₁₁ = 3.29).¹⁵ The values of log K₁₁₀ and log K₁₁₁ for MIBMPH₄, the



MIBMPH₄

methyl analogue of NEIBMPH₄, with Mn(II) are closely agree with the values found in this work, i.e. log K₁₁₀ = 8.24 and log K₁₁₁ = 7.93.¹⁴

5.1.2(b) Iron(III)

It is known that iron(III) can readily form hydroxy species at pH 7 and above; therefore three potentiometric titration datafiles were obtained at a metal:ligand ratio of 1:3 in order to limit the possibility of metal hydrolysis. A variable increment in the volume of base added was used in one titration (datafile M074); this allowed more data points to be recorded in the end-point regions where a small volume of base can result in a large increase in the mV reading [Figure 5.1.5(c)]. The titration curves obtained show discontinuities in the data above pH 7 and the associated scatter of points can be ascribed to precipitation of hydrolysis products of the metal or metal

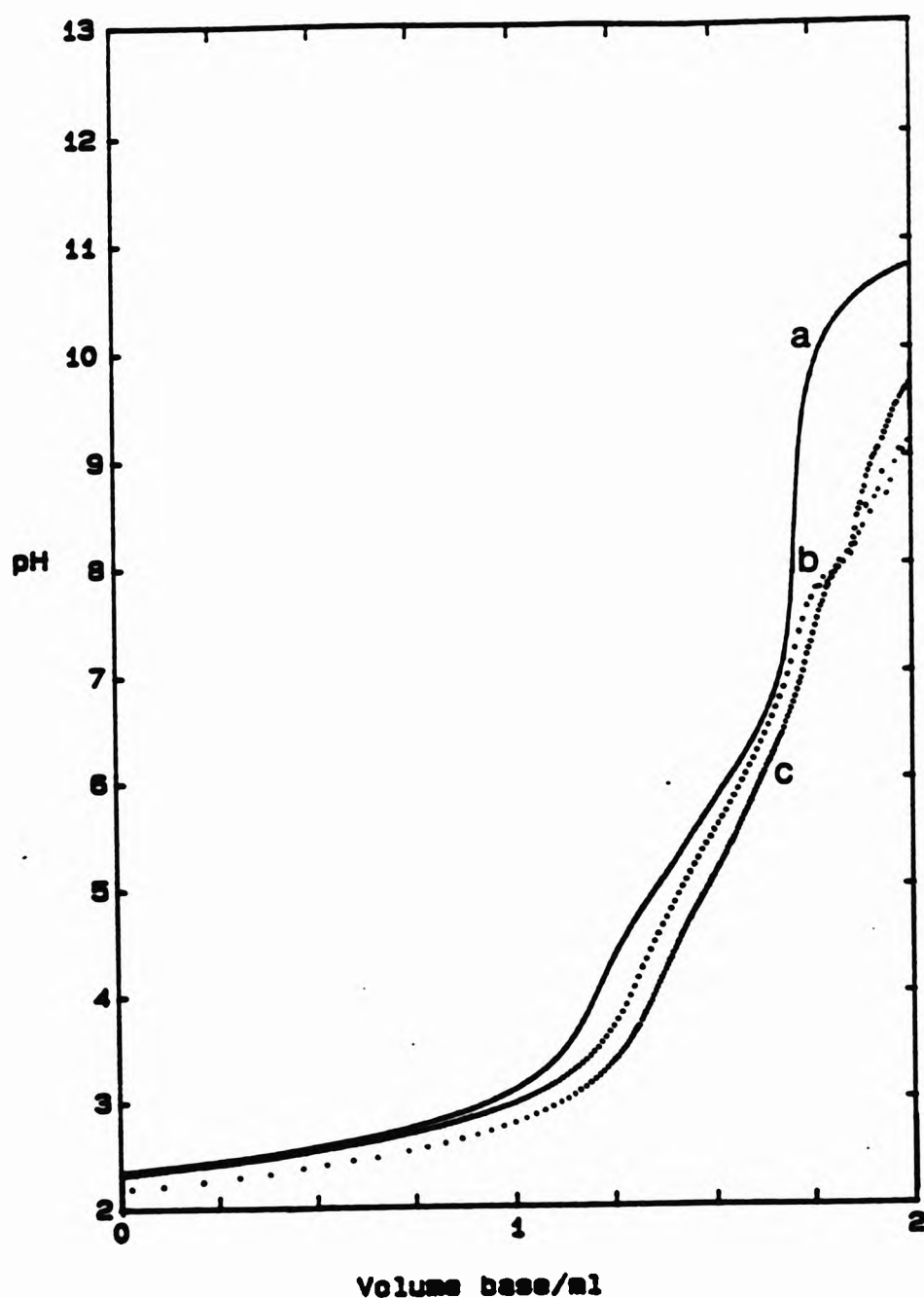


Figure 5.1.5 Titration curves (pH vs volume of base added) for acidified solutions of NEIBMPH₄ (a) [NEIBMPH₄] ca. 0.001 mol dm⁻³; (b) Fe(NO₃)₃ with NEIBMPH₄, [M]:[L] ca. 1:3 and (c) Fe(NO₃)₃ with NEIBMPH₄, [M]:[L] ca. 1.3; curve is offset to show effects of variable increment used in addition of base.

complexes. The titration curves were not as smooth as those normally obtained [Figure 5.1.5(b) and (c)] and may suggest that precipitation of hydrolysis products and/or colloid formation.^{16(a)}

Refinement of all three datafiles for a model which only involved species with a metal:ligand ratio of 1:1 was unsuccessful. A successful refinement for a model involving the species 110, 111 and 112 was obtained only if the following metal hydrolysis constants were used in the SUPERQUAD input files as constant: $\log \beta_{10-3} = -11.10$ {for $[\text{Fe}(\text{OH})_3]$ }, and $\log \beta_{10-4} = -20.50$ {for $[\text{Fe}(\text{OH})_4]^-$ }.^{16(a),17} Refinement for this model was achieved by limiting the data to the region of pH below that at which the signs of hydrolysis appeared in the titration curves (at pH ca. 7.5). The values for $\log \beta_{110}$ obtained from each datafile (Table 5.1.4) show a degree of variation not seen for complexes of other metals with NEIBMPH₄ examined in this work; e.g. the difference between the values of $\log \beta_{110}$ in datafiles M074 and M075 is ca. 0.6 log units. This difference may be ascribed to the small amount of $[\text{FeL}]^-$ present (< 20 %)

Table 5.1.4 Stability constants for NEIBMPH₄ with Fe(III).^a

Datafile:	M074 ^b	M075 ^c	M077 ^d	Mean ^e
[M]:[L]	1:3.08	1:3.17	1:3.18	
$\log \beta_{110}$	20.68(0.045)	20.06(0.066)	20.44(0.042)	20.39 ±0.29
$\log \beta_{111}$	28.40(0.034)	27.88(0.029)	28.18(0.028)	28.15 ±0.27
$\log K_{111}$	7.72	7.82	7.74	7.76 ±0.06
$\log \beta_{112}$	33.41(0.036)	33.17(0.052)	33.34(0.030)	33.31 ±0.14
$\log K_{112}$	5.01	5.29	5.16	5.15 ±0.14

^a I = 0.1 mol dm⁻³ KNO₃, 25 ±0.1 °C. Figures in parentheses are standard deviations obtained using SUPERQUAD. Convention: β_{MLH} for $M_nL_nH_n$. Log β values for metal hydroxy species were included in all refinements as constants:

$\log \beta_{10-3} = -11.10$ and $\log \beta_{10-4} = -20.50$.^{16(a),17} ^b Fit parameters determined using SUPERQUAD, $\chi^2 = 5.82$, $\sigma = 0.0365$, pH range 5.69–7.76, number of points = 44.

^c Fit parameters determined using SUPERQUAD, $\chi^2 = 9.24$, $\sigma = 0.0740$, pH range 5.69–7.75, number of points = 25. ^d Fit parameters determined using SUPERQUAD,

$\chi^2 = 5.48$, $\sigma = 0.0394$, pH range 5.39–7.77, number of points = 29. ^e Unweighted mean of values from each refinement; error limits are derived from the ranges obtained for each $\log \beta_{MLH}$ (and $\log K_{MLH}$).

in the pH region examined in each of the successfully refined datafiles, or it may be attributed to the presence of hydrolysed metal complex species (not modelled for) which are important above pH 8 and which may have some importance in the pH regions examined in the datafiles. Although, the results were judged to be acceptable according to the fit parameters χ^2 and σ (Table 5.1.4), the log β values must be subject to some uncertainty in view of the evidence for hydrolysis in the pH range used for data refinement.

5.1.2(c) Cobalt(II)

Two datafiles were obtained for NEIBMPH₄ with Co(II) at metal:ligand ratios of ca. 1:2 and 1:3, respectively. The potentiometric titration curves (Figure 5.1.6) show that the 'metal-ligand' curve closely follows the shape of the 'ligand-only' curve up to pH ca. 5 and that thereafter, there is slight but increasing deviation indicating the formation of weak metal complexes.

Successful refinements for a model involved only species with a metal:ligand ratio of 1:1 (*i.e.* MLH = 110, 111 and 112) were obtained for both datafiles (Table 5.1.5). Refinements of datafile M006 for models which only involved

Table 5.1.5 Stability constants for NEIBMPH₄ with Co(II).^a

Datafile: [M]:[L]	M005 ^b 1:2.02	M006 ^c 1:3.15	Mean ^d
log β_{110}	8.10(0.025)	8.15(0.049)	8.13 \pm 0.03
log β_{111}	15.64(0.018)	15.75(0.031)	15.70 \pm 0.06
log K_{111}	7.54	7.60	7.57 \pm 0.03
log β_{112}	20.88(0.026)	20.94(0.042)	20.91 \pm 0.03
log K_{112}	5.24	5.19	5.22 \pm 0.03

^a I = 0.1 mol dm⁻³ KNO₃, 25.0 \pm 0.1 °C. Figures in parentheses are standard deviations obtained using SUPERQUAD. Convention: β_{MLH} for $M_L L_H H_H$. ^b Fit parameters determined using SUPERQUAD, $\chi^2 = 4.06$, $\sigma = 0.0342$, pH range 4.46–7.49, number of points = 49. ^c Fit parameters determined using SUPERQUAD, $\chi^2 = 9.33$, $\sigma = 0.0559$, pH range 4.66–7.95, number of points = 48. ^d Unweighted mean of values from each refinement; error limits are derived from the ranges obtained for each log β_{MLH} (and log K_{MLH}).

species with a metal:ligand ratio of 1:2 (*i.e.* MLH = 120, 121 and 122) were not successful.

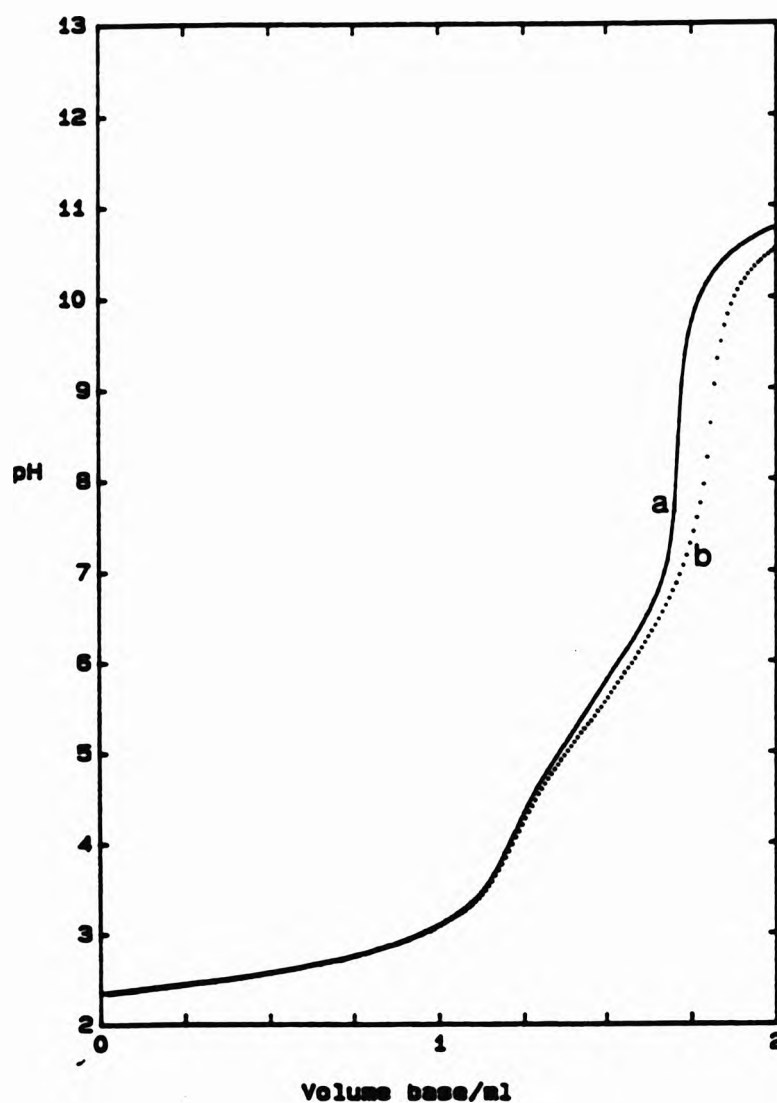


Figure 5.1.6 Titration curves (pH vs volume of base added) for acidified solutions of NEIBMPH₄ (a) [NEIBMPH₄] *ca.* 0.001 mol dm⁻³; (b) Co(NO₃)₂ with NEIBMPH₄, [M]:[L] *ca.* 1:3.

The value of $\log \beta_{110}$ (8.13) determined in this work is similar to the value obtained by Bel'skii, $\log \beta_{110} = 7.86$.¹⁵ The values of $\log K_{110}$ (9.27) and $\log K_{111}$ (6.59) found by Sawada for MIBMPH₄ with Co(II)¹⁴ bear a relationship to each other which is similar to the values found in this work, $\log K_{110} = 8.13$ and $\log K_{111} = 7.57$, but, the latter is quite different to the value determined by Bel'skii for the formation of the species [CoLH]⁻ ($\log K_{111} = 2.86$).¹⁵

5.1.2(d) Nickel(II)

Potentiometric titration datafiles were obtained for NEIBMPH₄ with Ni(II) at

metal:ligand ratios of ca. 1:1, 1:2 and 1:3. The titration curves were smooth and show no evidence of precipitation of metal complexes or metal hydrolysis products. The 'metal-ligand' curve closely follows the 'ligand-only' curve up to pH ca. 6 but diverges at higher pH, indicating the formation of some metal complex species. The small deviation between the curves at lower pH can be attributed to the slightly larger concentration of the ligand used in Figure 5.1.7(a) and the slightly larger concentration of base used in the titration of NEIBMPH₄ with Ni(II) in Figure 5.1.7(b).

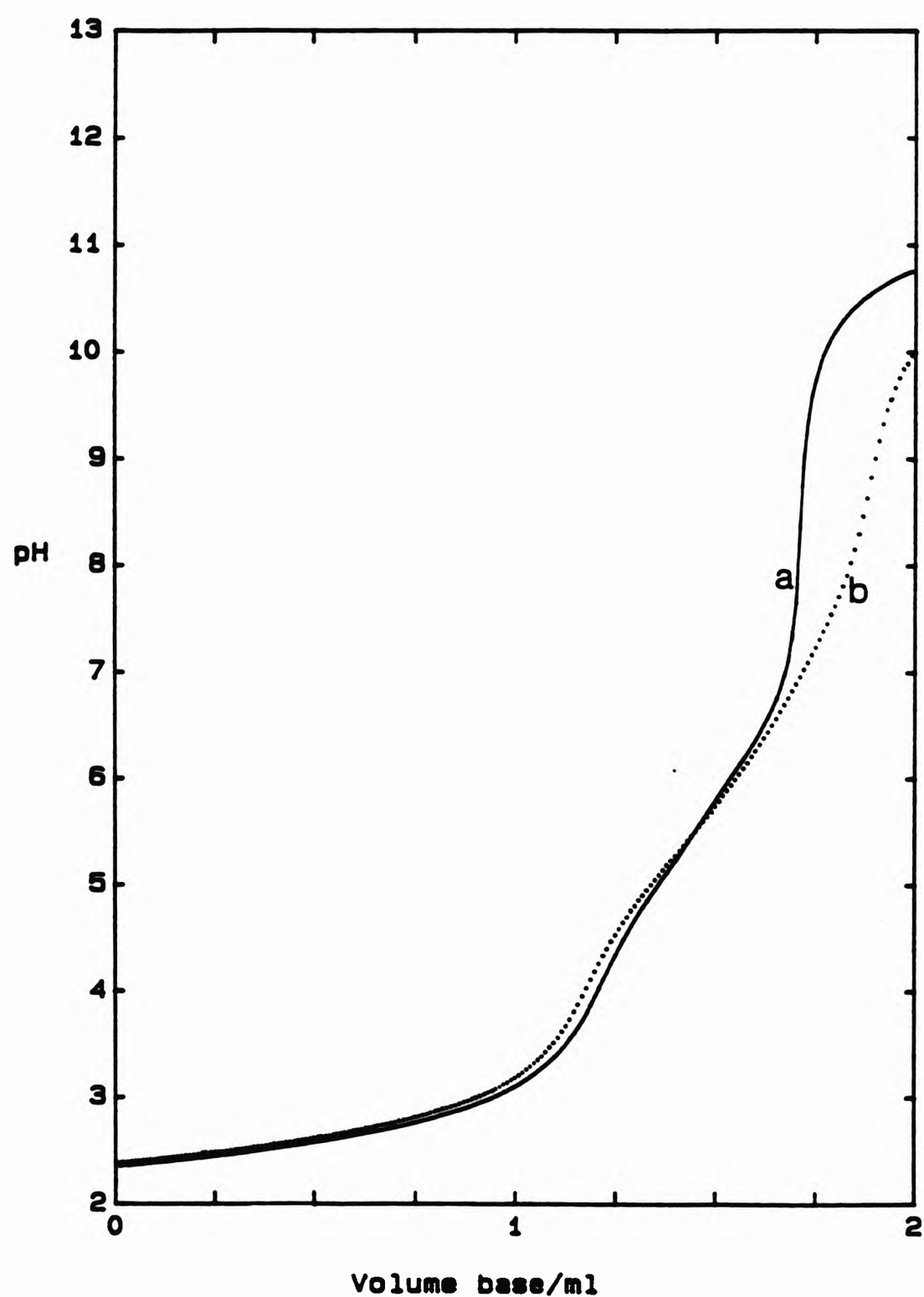


Figure 5.1.7 Titration curves (pH vs volume of base added) for acidified solutions of NEIBMPH₄ (a) [NEIBMPH₄] ca. 0.001 mol dm⁻³; (b) Ni(NO₃)₂ with NEIBMPH₄, [M]:[L] ca. 1:1.

Refinement for a model involving three species where the metal:ligand ratio of 1:1 (*i.e.* MLH = 110, 111 and 112) was only successful for datafile M063. Whereas, for datafiles M047 and M059, a model which involved only the species $[ML]^{2-}$ and $[MLH]^-$ facilitated successful refinement. The stability constants determined are summarised in Table 5.1.6.

Table 5.1.6 Stability constants for NEIBMPH₄ with Ni(II).^a

Datafile:	M063 ^b	M047 ^c	M059 ^d	Mean ^e
[M]:[L]	1:1.03	1:1.89	1:3.33	
log β_{110}	8.03(0.012)	8.21(0.007)	8.28(0.030)	8.17 ±0.14
log β_{111}	15.19(0.013)	15.29(0.007)	15.50(0.019)	15.33 ±0.17
log K_{111}	7.16	7.08	7.22	7.15 ±0.07
log β_{112}	19.82(0.120)			19.82
log K_{112}	4.96			4.96

^a I = 0.1 mol dm⁻³ KNO₃, 25 ±0.1 °C. Figures in parentheses are standard deviations obtained using SUPERQUAD. Convention: β_{MLH} for $M_nL_mH_p$. ^b Fit parameters determined using SUPERQUAD, $\chi^2 = 10.23$, $\sigma = 0.0339$, pH range 4.19–7.32, number of points = 57. ^c Fit parameters determined using SUPERQUAD, $\chi^2 = 16.13$, $\sigma = 0.0367$, pH range 4.40–9.00, number of points = 55. ^d Fit parameters determined using SUPERQUAD, $\chi^2 = 5.16$, $\sigma = 0.0579$, pH range 5.43–8.96, number of points = 37. ^e Unweighted mean of values from each refinement; error limits are derived from the ranges obtained for each log β_{MLH} (and log K_{MLH}).

Determination of the stability constants for NEIBMPH₄ with Ni(II) was also carried out by a previous worker at the University of North London.¹³ Refinement of the datafile IS2N2 (see Table 5.1.7, [M]:[L] ca. 1:.00) obtained by Scowen for a model which included the species with a metal:ligand ratio of 1:1 (*i.e.* MLH = 110, 111, 112, 121 and 11-1) also included the single hydrolysis constant for Ni(II), log $\beta_{10-1} = -9.86$ $[Ni(OH)]^-$ as a constant in the SUPERQUAD input files. The results determined by Scowen for this file are similar to the results obtained in this work (Table 5.1.7) except for the value of log β_{112} . Scowen noted that, for datafile IS2N2, the titration curve shows two discontinuities at pH ca. 9 and pH ca. 10. Therefore, he excluded

the data points above this first discontinuity (increasing pH) in refinement of this datafile. The difference in the value of $\log \beta_{112}$ obtained in this work (19.82) and that obtained from datafile IS2N2 (21.35)¹³ could be ascribed to the inclusion of the hydrolysis constants for Ni(II) in successful refinement of the latter file, or it may be attributed to the difference in refinement strategy used for IS2N2 and the inclusion of the species 121 in successful refinement.

Table 5.1.7 Stability constants for NEIBMPH₄ with Ni(II).

MLH	$\log \beta_{MLH}$						
	110	111	112	120	121	122	11-1
IS2N1 ^{a,b}	8.62	16.26	21.86	13.96	23.80	30.18	
IS2N2 ^{a,c}	8.54	15.84	21.35	-	23.44	-	-1.62 ^d
This work ^e	8.17	15.33	19.82	-			
Bel'skii ^f	7.97	10.69					

^a Ref. 13, I = 0.1 mol dm⁻³ KNO₃, 25.0 ± 0.1 °C. The Ni(II) hydrolysis constant was also included in the refinement, $\log \beta_{10-1} = -9.86$. ^b [M]:[L] = 1:2.06. ^c [M]:[L] = 1:1.00. ^d Represents the overall formation of the species [NiL(OH)]⁻. ^e I = 0.1 mol dm⁻³ KNO₃, 25.0 ± 0.1 °C. Log β values are obtained from Table 5.1.6. ^f Ref. 15, I = 1.0 mol dm⁻³ KNO₃, 25.0 °C.

Successful refinement of datafile IS2N1 ([M]:[L] = 1:2.06) by Scowen¹³ was for a model which included more species with a metal:ligand ratio of 1:2.

However, it was noted by Scowen¹³ that data collection gave more reproducible results for the study of NEIBMPH₄ with Cu(II) after improvements to the potentiometric titration apparatus stability and installation of air conditioning had been undertaken.¹³ The study of NEIBMPH₄ with Ni(II) had been carried out before these improvements had been effected. In summary, the variation in the values of $\log \beta$ for Ni(II) determined in this work for NEIBMPH₄ and those found by Scowen¹³ can be attributed to the difference in refinement strategies used, the inclusion of the Ni(II) hydrolysis constant in the SUPERQUAD input files (IS2N1 and IS2N2) and the improvements made to the apparatus for determining stability constants.¹³

The value of 8.17 ($\log K_{110}$) found in this work is similar to that found by Bel'skii ($\log K_{110} = 7.97$).¹⁵ However, there is a discrepancy in the values of $\log \beta_{111}$ found by Bel'skii¹⁵ and in this work of ca. 4.5 log units. The value of $\log \beta_{111}$ (15.85) determined¹⁴ for the analogue MIBMPH₄ with Ni(II) is of the same order as that found in this work.

5.1.2(e) Copper(II)

Titration datafiles for NEIBMPH₄ with Cu(II) were obtained at metal:ligand ratios of ca. 1:1, 1:2 and 1:3. In each case, a smooth titration curve was observed and there was no evidence of precipitation of metal complexes or hydrolysed species. The small deviation between the curves at lower pH can be attributed to the slightly greater concentration of base used in curves

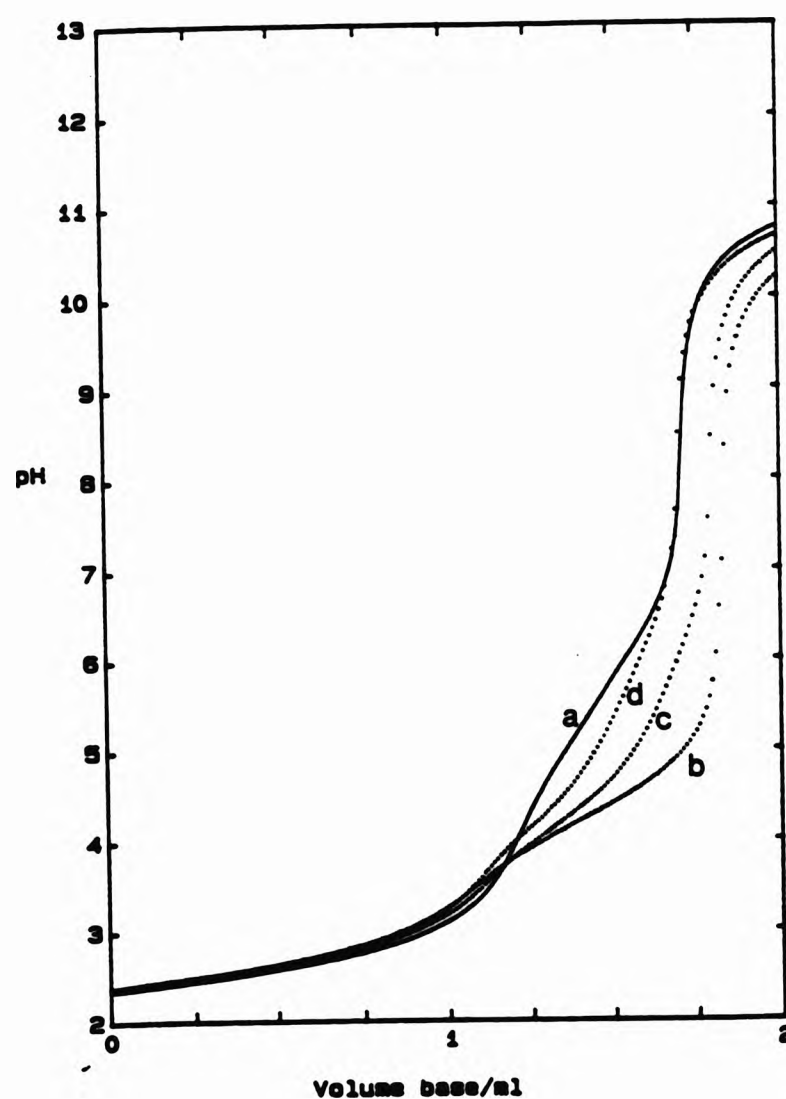


Figure 5.1.8 Titration curves (pH vs volume of base added) for acidified solutions of NEIBMPH₄ (a) [NEIBMPH₄] ca. 0.001 mol dm⁻³; (b) Cu(NO₃)₂ with NEIBMPH₄, [M]:[L] ca. 1:1; (c) Cu(NO₃)₂ with NEIBMPH₄, [M]:[L] ca. 1:2; (d) Cu(NO₃)₂ with NEIBMPH₄, [M]:[L] ca. 1:3.

(b), (c) and (d) in Figure 5.1.8. The 'metal-ligand' curve (at a metal:ligand ratio of ca. 1:1) shows a deviation from the 'ligand-only' curve which is larger than for any other metal ions with NEIBMPH₄. This suggests that Cu(II) complexes with NEIBMPH₄ are more stable than those for the other divalent metal ions examined in this work.

The potentiometric titration curves for NEIBMPH₄ with Cu(II) are shown in Figure 5.1.8. The end-point on the titration curve at pH ca. 7.5 corresponds to ca. 4 equivalents of base, one greater than in the ligand system. This suggests that the species LH³⁻ present in the 'ligand-only' system in this region loses a proton on complexation with Cu(II) resulting in the formation of [CuL]²⁻.

Table 5.1.8 Stability constants for NEIBMPH₄ with Cu(II).^a

Datafile:	M049 ^b	M050 ^c	M051 ^d	Mean ^e
[M]:[L]	1:0.97	1:2.18	1:3.14	
log β_{110}	13.38(0.006)	13.24(0.007)	13.21(0.004)	13.28 ±0.10
log β_{111}	18.03(0.003)	17.99(0.002)	17.99(0.004)	18.00 ±0.03
log K_{111}	4.65	4.75	4.87	4.73 ±0.08
log β_{112}	21.47(0.026)	21.04(0.051)	-	21.26 ±0.22
log K_{112}	3.44	3.05	-	3.25 ±0.20
log β_{120}			18.44(0.035) ^f	18.44
log K_{120}			5.23	5.23

^a I = 0.1 mol dm⁻³ KNO₃, 25.0 ±0.1 °C. Figures in parentheses are standard deviations obtained using SUPERQUAD. Convention: β_{MLH} for $M_nL_mH_p$. ^b Fit parameters determined using SUPERQUAD, $\chi^2 = 4.49$, $\sigma = 0.0467$, pH range 3.06–4.72, number of points = 74. ^c Fit parameters determined using SUPERQUAD, $\chi^2 = 3.67$, $\sigma = 0.0150$, pH range 3.29–4.74, number of points = 48. ^d Fit parameters determined using SUPERQUAD, $\chi^2 = 5.33$, $\sigma = 0.0265$, pH range 3.30–4.59, number of points = 36. ^e Unweighted mean of values from each refinement; error limits are derived from the ranges obtained for each log β_{MLH} (and log K_{MLH}). ^f Log β_{120} obtained in a refinement in which log β_{110} , log β_{111} and log β_{112} were held constant. Fit parameters determined using SUPERQUAD, $\chi^2 = 1.56$, $\sigma = 0.1360$, pH range 6.98–10.30, number of points = 18.

Refinements of datafiles M049 and M050 for a model which involved species with a metal:ligand ratio of 1:1 (*i.e.* MLH = 110, 111 and 112) were successful. However, satisfactory refinement of datafile M051 could only be obtained for a model which involved the species $[\text{CuL}]^{2-}$ and $[\text{CuLH}]^-$. A separate refinement of datafile M051 for a model which only involved species with a metal:ligand ratio of 1:2 (*i.e.* MLH = 120, 121 and 122) was unsuccessful, but refinement for the species $[\text{CuL}_2]^{6-}$ on its own was successful. The results are summarised in Table 5.1.8.

A more comprehensive study of the coordination of NEIBMPH₄ with Cu(II) at the same ionic strength used in this study was carried out by Scowen.¹³ This study involved examination of the titration data for formation of species with metal:ligand ratios of 1:1 and 1:2 (Table 5.1.9). Refinement of datafile M060 for a model which involved the species 110, 111 and 112 was successful when two hydrolysis constants for Cu(II) were placed into the SUPERQUAD input files as constants.¹³ The results determined from this datafile (*i.e.* $\log \beta_{110}$, $\log \beta_{111}$ and $\log \beta_{112}$) are comparable with those determined in this work (Table 5.1.9). Refinement of datafiles M061 and M062 by Scowen, which also included the two Cu(II) hydrolysis constants, yielded more species with a metal:ligand

Table 5.1.9 Stability constants for NEIBMPH₄ with Cu(II).

MLH	$\log \beta_{\text{MLH}}$					
	110	111	112	120	121	122
M060 ^{a,b}	13.54	18.10	21.97			
M061 ^{a,c}	13.72	18.14	22.13	18.94	28.41	34.28 ^d
M062 ^{a,e}	13.74	18.05	22.14	18.91	28.51	34.19
This work ^f	13.28	18.00	21.26	18.44		
Bel'skii ^g	13.09	18.49	22.09			

^a Ref. 13, I = 0.1 mol dm⁻³ KNO₃, 25.0 ± 0.1 °C. Also included in the refinement were the two hydrolysis constant for Cu(II), $[\text{Cu}(\text{OH})]^+$ and $[\text{Cu}_2(\text{OH})_2]^{2+}$. ^b [M]:[L] = 1:1.02. ^c [M]:[L] = 1:2.12. ^d A large relative error is associated with this $\log \beta$ value. ^e [M]:[L] = 1:3.04. ^f I = 0.1 mol dm⁻³ KNO₃, 25.0 ± 0.1 °C. Log β values are obtained from Table 5.1.8. ^g Ref. 15, I = 1.0 mol dm⁻³ KNO₃, 25.0 °C.

ratio of 1:2 than in this work. The value of $\log \beta_{120}$ found in this work is similar to the value found by Scowen in both datafiles M061 and M062.

The average values of $\log \beta_{110}$, $\log \beta_{111}$ and $\log \beta_{112}$ determined in this work (Table 5.1.9) are also similar to the values determined by Bel'skii at $I = 1.0 \text{ mol dm}^{-3} \text{ KNO}_3$.¹⁵

5.1.2(f) Zinc(II)

Potentiometric titration curves for NEIBMPH_4 with Zn(II) at metal:ligand ratios of ca. 1:1, 1:2 and 1:3 are shown in Figure 5.1.9. There is a close correspondence between the 'ligand-only' curve and the 'metal-ligand' curve up to ca. pH 4.5. Approximately 4 equivalents of base are consumed in the metal-ligand system by an end-point at ca. pH 8 [as observed for Cu(II)] and this suggests the formation of $[\text{ML}]^{2-}$.

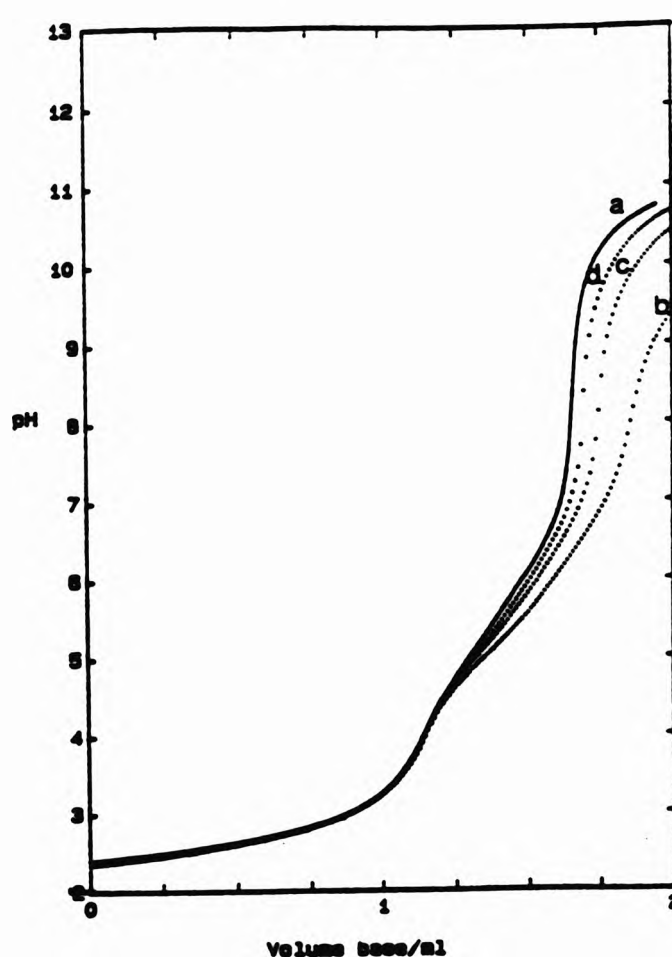


Figure 5.1.9 Titration curves (pH vs volume of base added) for acidified solutions of NEIBMPH_4 (a) $[\text{NEIBMPH}_4]$ ca. $0.001 \text{ mol dm}^{-3}$; (b) $\text{Zn(NO}_3)_2$ with NEIBMPH_4 , $[\text{M}]:[\text{L}]$ ca. 1:1; (c) $\text{Zn(NO}_3)_2$ with NEIBMPH_4 , $[\text{M}]:[\text{L}]$ ca. 1:2; (d) $\text{Zn(NO}_3)_2$ with NEIBMPH_4 , $[\text{M}]:[\text{L}]$ ca. 1:3.

Successful refinements of two datafiles (M052 and M053) was obtained for a model involving only three species *i.e.* MLH = 110, 111 and 112, whereas, in datafile M054, a successful refinement could only be obtained for a model which involved the species $[ML]^{2-}$ and $[MLH]^-$. A particular refinement of M054 for a model comprising of species with a metal:ligand ratio of 1:2 (*i.e.* MLH = 120, 121 and 122) was unsuccessful, but, a satisfactory refinement for the species $[ML_2]$ alone was obtained for datafile M054 in a high pH region. The results are summarised in Table 5.1.10.

Table 5.1.10 Stability constants for NEIBMPH₄ with Zn(II).^a

Datafile:	M052 ^b	M053 ^c	M054 ^d	Mean ^e
[M]:[L]	1:1.04	1:2.01	1:3.01	
log β_{110}	9.31(0.017)	9.42(0.012)	9.13(0.006)	9.29 ±0.16
log β_{111}	15.93(0.013)	15.93(0.008)	15.80(0.005)	15.89 ±0.09
log K_{111}	6.62	6.51	6.67	6.60 ±0.09
log β_{112}	20.18(0.111)	20.00(0.133)		20.09 ±0.09
log K_{112}	4.25	4.07		4.16 ±0.09
log β_{120}			14.35(0.051) ^f	14.35
log K_{120}			5.22	5.22

^a I = 0.1 mol dm⁻³ KNO₃, 25.0 ±0.1 °C. Figures in parentheses are standard deviations obtained using SUPERQUAD. Convention: β_{MLH} for $M_nL_mH_p$. ^b Fit parameters determined using SUPERQUAD, $\chi^2 = 10.00$, $\sigma = 0.0705$, pH range 4.02–6.91, number of points = 62. ^c Fit parameters determined using SUPERQUAD, $\chi^2 = 5.83$, $\sigma = 0.0220$, pH range 4.18–6.47, number of points = 46. ^d Fit parameters determined using SUPERQUAD, $\chi^2 = 2.80$, $\sigma = 0.0281$, pH range 3.69–6.62, number of points = 51. ^e Unweighted mean of values from each refinement; error limits are derived from the ranges obtained for each log β_{MLH} (and log β_{MLH}). ^f Log β_{120} obtained in a refinement in which log β_{110} , log β_{111} and log β_{112} were held constant. Fit parameters determined using SUPERQUAD, $\chi^2 = 7.15$, $\sigma = 0.3049$, pH range 6.01–10.40, number of points = 39.

5.1.2(g) Lead(II)

Three potentiometric titration curves were obtained for NEIBMPH₄ with Pb(II) at metal:ligand ratios of *ca.* 1:1, 1:2 and 1:3 (Figure 5.1.10). The 'metal-

ligand' curves closely follow the 'ligand-only' curve up to pH ca. 3, with significant deviation occurring above pH 4.5. Again, the end-points on the titration curves (Figure 5.1.10) at pH ca. 8.5 is equivalent to 4 moles of proton being neutralised in the metal-ligand system [see Cu(II)] and provides evidence for the formation of the species $[ML]^{2-}$.

Refinements of all three datafiles for a model involving only $[PbL]^{2-}$, $[PbLH]^{-}$ and $[PbLH_2]$ was successful (Table 5.1.11). Refinement of datafile M030 using $[PbL_2]^{6-}$, $[PbL_2H]^{5-}$ and $[PbL_2H_2]^{4-}$ as a model was unsuccessful, as was an attempted refinement for $[PbL_2]^{6-}$ on its own.

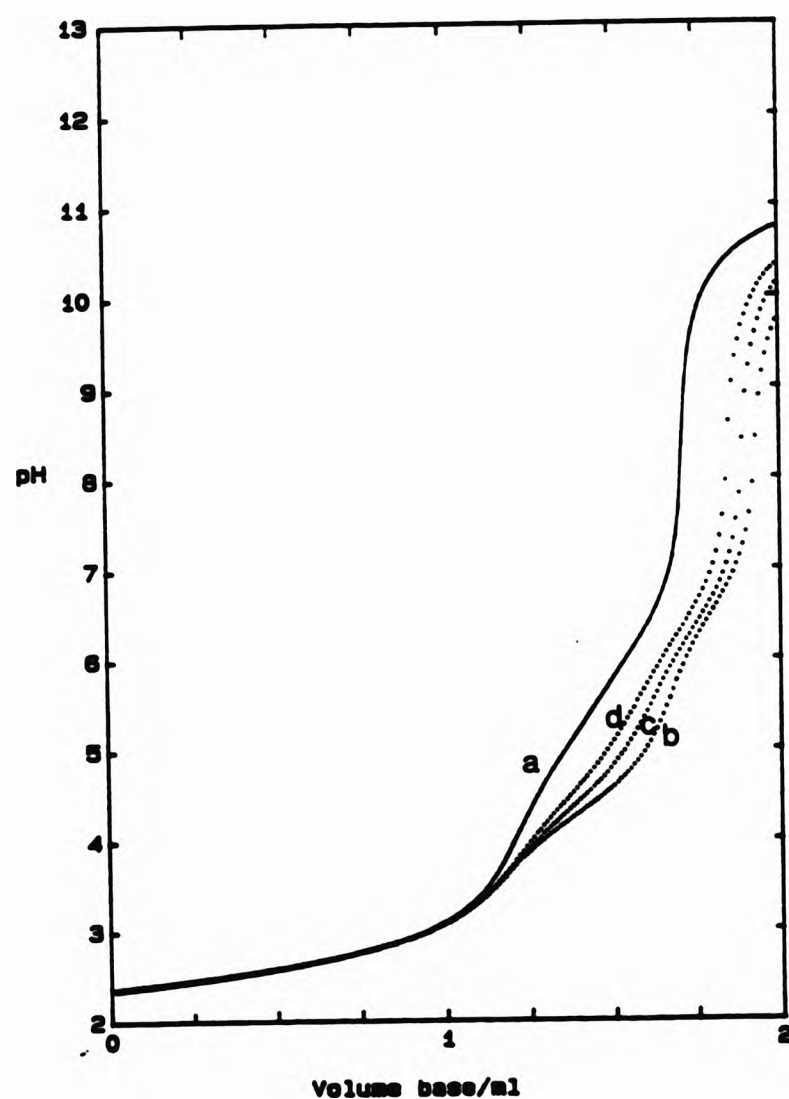


Figure 5.1.10 Titration curves (pH vs volume of base added) for acidified solutions of NEIBMPH₄ (a) $[NEIBMPH_4]$ ca. $0.001 \text{ mol dm}^{-3}$; (b) $Pb(NO_3)_2$ with NEIBMPH₄, $[M]:[L]$ ca. 1:1; (c) $Pb(NO_3)_2$ with NEIBMPH₄, $[M]:[L]$ ca. 1:2; (d) $Pb(NO_3)_2$ with NEIBMPH₄, $[M]:[L]$ ca. 1:3.

Table 5.1.11 Stability constants for NEIBMPH₄ with Pb(II).^a

Datafile:	M028 ^b	M031 ^c	M030 ^d	Mean ^e
[M]:[L]	1:1.00	1:2.17	1:3.26	
log β ₁₁₀	11.30(0.004)	11.16(0.008)	11.07(0.018)	11.18 ±0.12
log β ₁₁₁	17.85(0.002)	17.70(0.003)	17.64(0.007)	17.73 ±0.12
log K ₁₁₁	6.55	6.54	6.57	6.55 ±0.02
log β ₁₁₂	21.77(0.005)	21.58(0.010)	21.67(0.018)	21.67 ±0.09
log K ₁₁₂	3.92	3.88	4.03	3.94 ±0.09

^a I = 0.1 mol dm⁻³ KNO₃, 25.0 ±0.1 °C. Figures in parentheses are standard deviations obtained using SUPERQUAD. Convention: β_{MLH} for M_nL_mH_p. ^b Fit parameters determined using SUPERQUAD, χ² = 6.87, σ = 0.0178, pH range 4.15-6.48, number of points = 46. ^c Fit parameters determined using SUPERQUAD, χ² = 5.63, σ = 0.0276, pH range 4.07-6.63, number of points = 51. ^d Fit parameters determined using SUPERQUAD, χ² = 8.92, σ = 0.0420, pH range 4.07-6.84, number of points = 52. ^e Unweighted mean of values from each refinement; error limits are derived from the ranges obtained for each log β_{MLH} (and log K_{MLH}).

5.1.2(h) Cadmium(II)

Potentiometric titration curves for NEIBMPH₄ with Cd(II) at metal:ligand ratios of ca. 1:1, 1:2 and 1:3 were obtained; the curve for the 1:2 (metal:ligand ratio) titration is shown in Figure 5.1.11. Up to ca. pH 4 there is close agreement between the 'ligand-only' curve and the 'metal-ligand' curve. Thereafter, as the titration proceeds, approximately four equivalents of base are consumed by the 'metal-ligand' system by pH ca. 8.5, indicating the formation of [CdL]²⁻ in this region [see Cu(II)], with significant deviation of the 'metal-ligand' curve occurring above ca. pH 5.

Refinements of all three datafiles (M056, M057 and M058) for a model which only involved species MLH = 110, 111 and 112 was successful (Table 5.1.12). Refinement of datafile M058 for a model which only involved the species [ML₂]⁶⁻, [ML₂H]⁵⁻ and [ML₂H₂]⁴⁻ was unsuccessful, as was refinement for a model with only one species, [ML₂]⁶⁻.

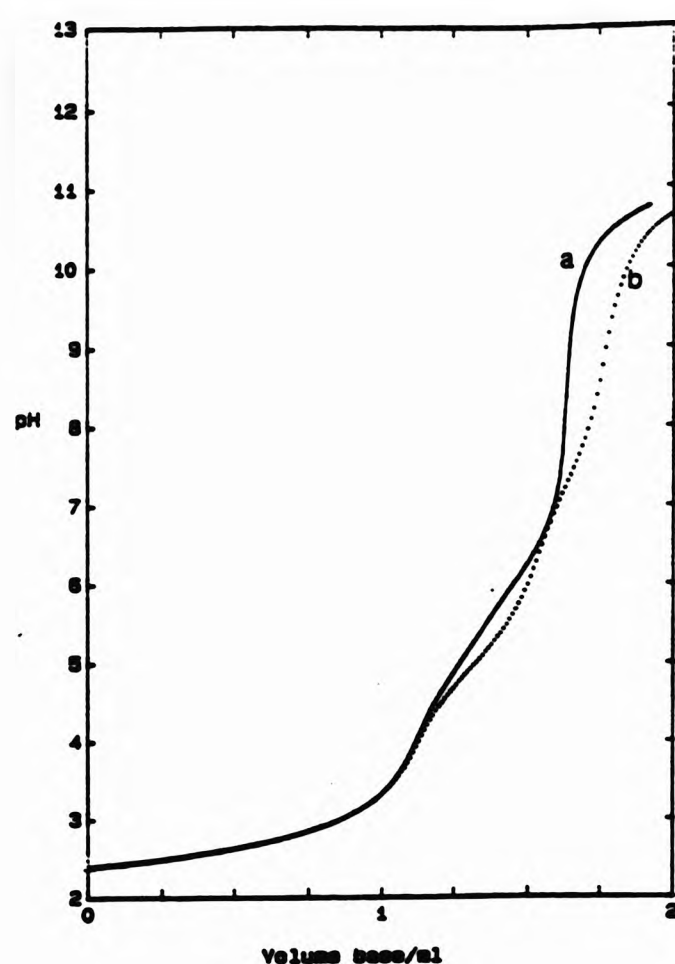


Figure 5.1.11 Titration curves (pH vs volume of base added) for acidified solutions of NEIBMPH₄ (a) [NEIBMPH₄] ca. 0.001 mol dm⁻³; (b) Cd(NO₃)₂ with NEIBMPH₄, [M]:[L] ca. 1:2.

Table 5.1.12 Stability constants for NEIBMPH₄ with Cd(II).^a

Datafile:	MO56 ^b	MO57 ^c	MO58 ^d	Mean ^e
[M]:[L]	1:0.91	1:1.80	1:3.28	
log β ₁₁₀	9.10(0.013)	8.91(0.015)	8.74(0.001)	8.92 ±0.18
log β ₁₁₁	16.39(0.007)	16.29(0.009)	16.28(0.005)	16.32 ±0.06
log K ₁₁₁	7.29	7.38	7.54	7.40 ±0.14
log β ₁₁₂	21.17(0.014)	21.08(0.017)	21.08(0.010)	21.11 ±0.06
log K ₁₁₂	4.78	4.79	4.80	4.79 ±0.01

^a I = 0.1 mol dm⁻³ KNO₃, 25.0 ±0.1 °C. Figures in parentheses are standard deviations obtained using SUPERQUAD. Convention: β_{ML_nH_n} for M_nL_nH_n. ^b Fit parameters determined using SUPERQUAD, χ² = 7.41, σ = 0.0313, pH range 4.85-7.15, number of points = 34. ^c Fit parameters determined using SUPERQUAD, χ² = 7.14, σ = 0.0415, pH range 3.87-8.24, number of points = 56. ^d Fit parameters determined using SUPERQUAD, χ² = 2.35, σ = 0.0184, pH range 4.67-7.15, number of points = 46. ^e Unweighted mean of values from each refinement; error limits are derived from the ranges obtained for each log β_{ML_nH_n} (and log K_{ML_nH_n}).

5.1.3 Species abundance plots of some metal ions with DEAMPH₂ and NEIBMPH₄. Species distribution curves¹⁸ show the abundances of the various species present in solution over the pH 2-12 relative to the total ligand concentration (taken as 100 %). The curves depend on the species modelled for in solution and on the values of log β obtained, in this case from SUPERQUAD¹⁰. The relative abundances of the species are affected by the metal:ligand ratios used in the input files, e.g. in a system with a metal:ligand ratio of 1:3 then the metal-containing species have a total abundance of 33.3 %.

The species distribution curves¹⁸ can only be regarded as valid in the pH range used for a successful refinement of 'ligand-only' and 'metal-ligand' datafiles. Species not modelled for may be important in the regions outside this pH range, and hence some uncertainty will arise in the relative abundances of the species outside the pH range examined.

Using log β values obtained in this work together with the protonation constants for the ligand and appropriate relative concentration of metal and ligand the species distribution curves¹⁸ for DEAMPH₂ with Pb(II) (Figure 5.1.12) and for NEIBMPH₄ with Mn(II), Co(II), Ni(II), Cu(II), Zn(II), Pb(II), Cd(II) and Fe(III) [Figure 5.1.13 (a) to (h)] were computed.

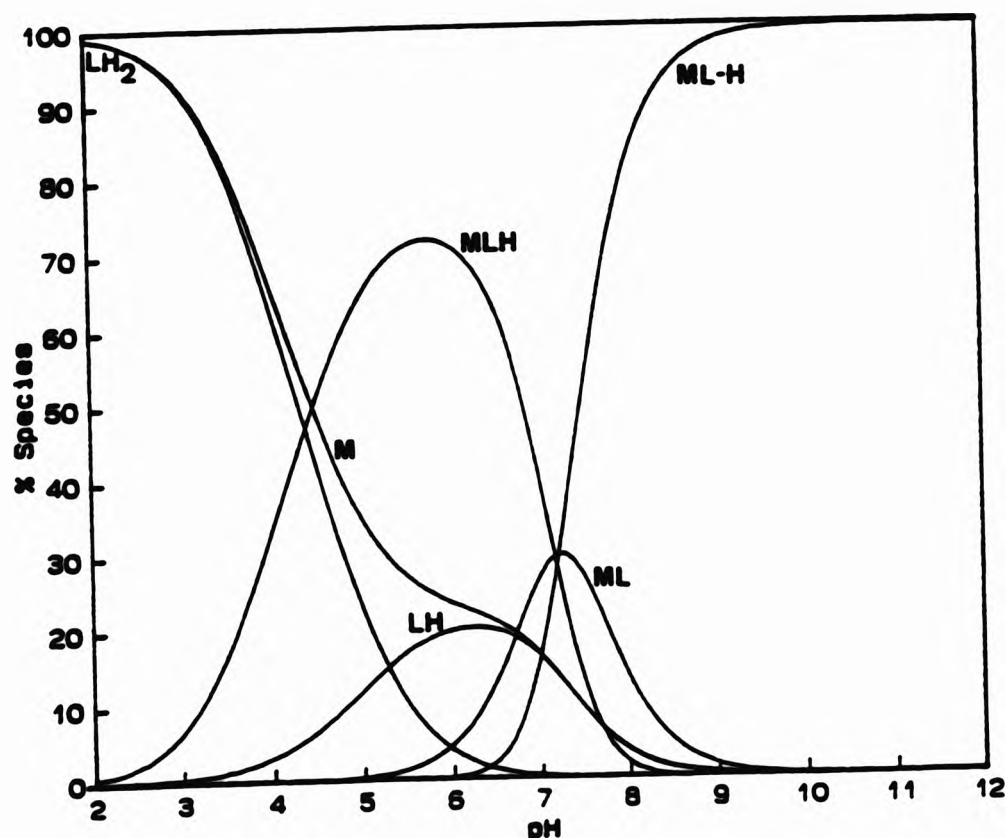


Figure 5.1.12 Species distribution curves¹⁸ for DEAMPH₂ with Pb(II), [M]:[L] ca. 1:1.

The species distribution curves¹⁸ for DEAMPH₂ with Pb(II) at a metal:ligand ratio of ca. 1:1 are shown in Figure 5.1.12. The curves are valid in the pH range ca. 3-9, based on the pH ranges of data used in refinements for protonation and stability constants. In the pH range 5-9, the metal complex species are dominant, *i.e.* [PbLH]⁺, [PbL] and [PbL(OH)]⁻. Ligand species LH₂ and LH⁻ are also present in this region.

The species distribution curves¹⁸ for NEIBMPH₄ with the metal ions Mn(II), Co(II), Ni(II), Cu(II), Zn(II), Pb(II) and Cd(II) [Figure 5.1.13(a) to (h), respectively] were computed for a metal:ligand ratio of ca. 1:1. The three metal-ligand species [MLH₂], [MLH]⁻ and [ML]²⁻ were determined for all the metals in this work, and this results in species distribution curves¹⁸ which are similar in character. The curves are only valid in the pH range 3-10, based on the pH regions used of data refinements. The increasing value of log β₁₁₀ on going from Mn(II) to Cu(II) in the first transition metal series, *i.e.* 6.89 to 13.28 log units, results in increasing importance of the metal-ligand species at a lower pH. For example, the species distribution curves¹⁸ for NEIBMPH₄ with Cu(II) show that [CuL]²⁻ begins to form at pH ca. 3.5 [Figure 5.1.13.(d)], whereas, for Mn(II) the species [MnL]²⁻ begins to form at a much higher pH (ca. 7) [Figure 5.1.13(a)].

Only two examples were studied in which a refinement for the species [ML₂]⁶⁻ was successful, *i.e.* for NEIBMPH₄ with Cu(II) and Zn(II). The species distribution curves¹⁸ for NEIBMPH₄ with Cu(II) [Figure 5.1.13(d)] and Zn(II) [Figure 5.1.13(f)] however, shows that the species [ML₂]⁶⁻ is not present to any significant extent at a metal:ligand ratio of 1:1, presumably because the ratio of metal:ligand does not favour the formation the [ML₂]⁶⁻.

The extremely high log β₁₁₀ (20.39) value determined for NEIBMPH₄ with Fe(III) has a considerable effect on the resulting species distribution curves¹⁸ [Figure 5.1.13(i)]. The valid pH range for the curves is ca. 3-8. The formation of metal-ligand species are significant at a much lower pH (ca. 2) than that observed for NEIBMPH₄ with the other metals examined in this work. Another significant feature is that the species [FeLH₂]⁺, [FeLH] and [FeL]⁻ account for nearly 100 % of the available metal over the valid pH range. Above pH ca. 8, the curves show that the hydrolysis of Fe(III) is important; however, above this region, other species not modelled for may be important. There is therefore a strong possibility that the curves above pH 8 do not

truly represent the equilibria occurring in solution.

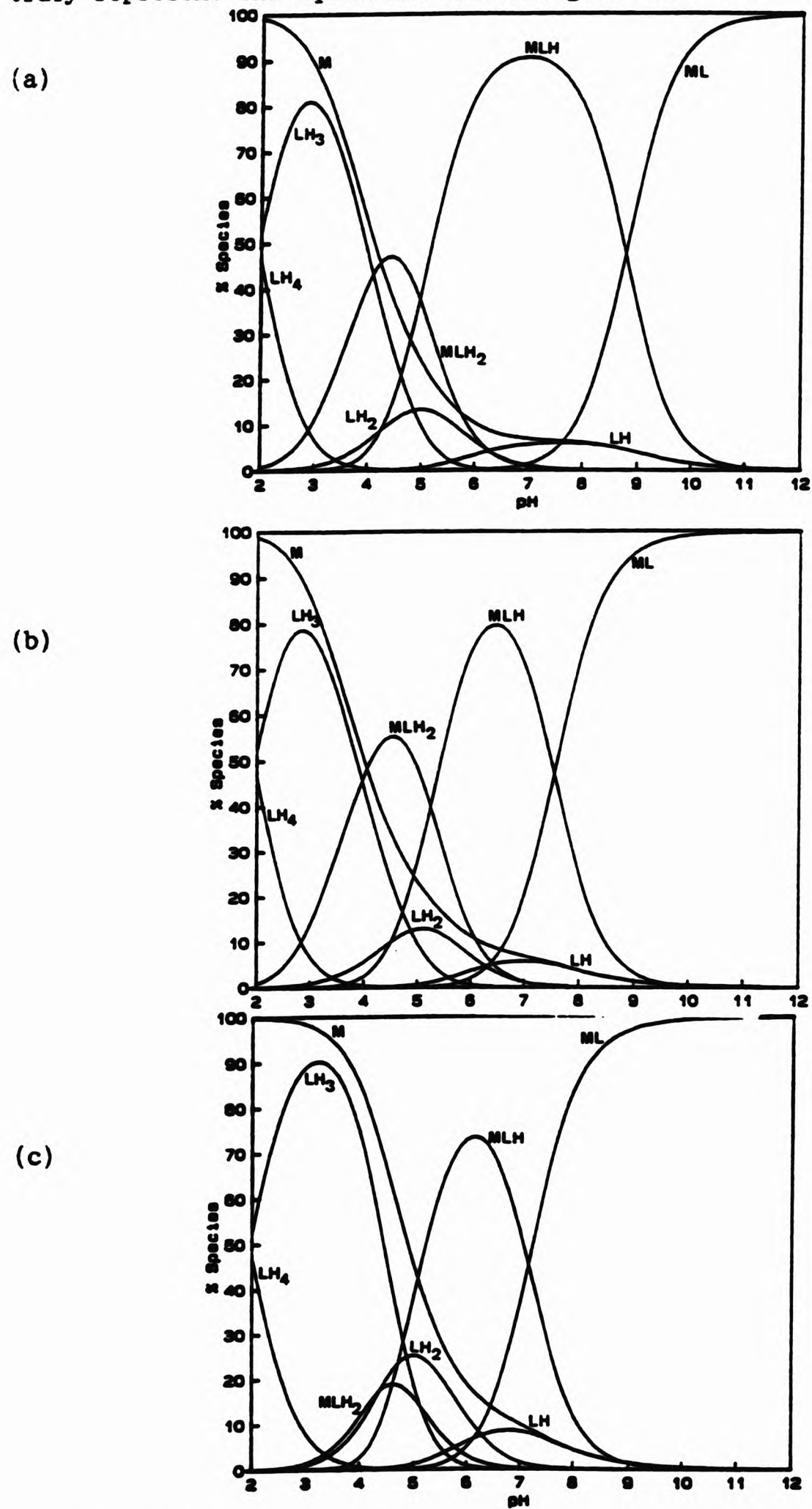


Figure 5.1.13 Species distribution curves¹⁸ for NEIBMPH₄ with metal ions at [M]:[L] ca. 1:1 (a) Mn(II) (b) Co(II) and (c) Ni(II).

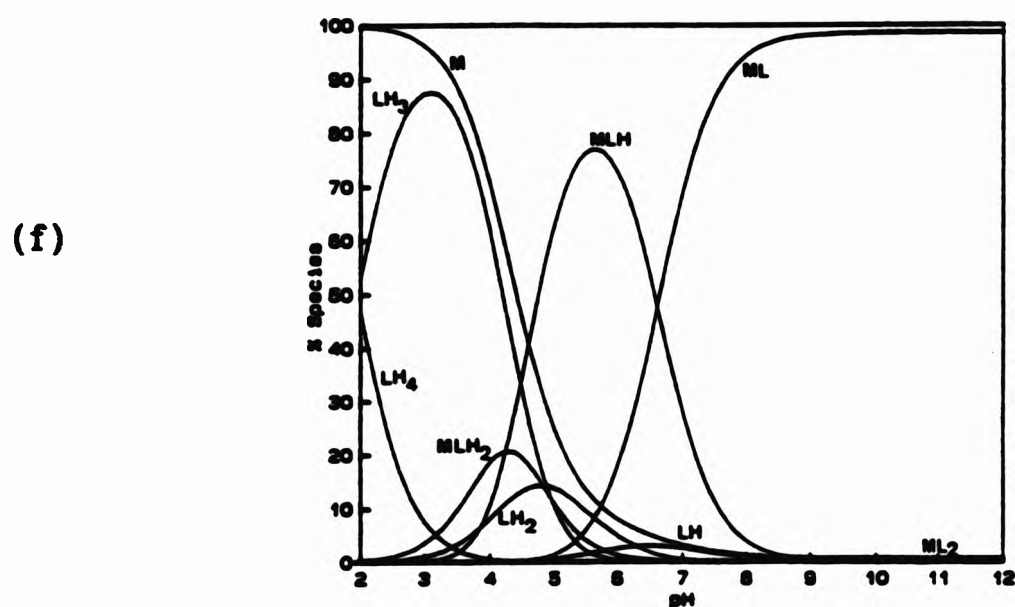
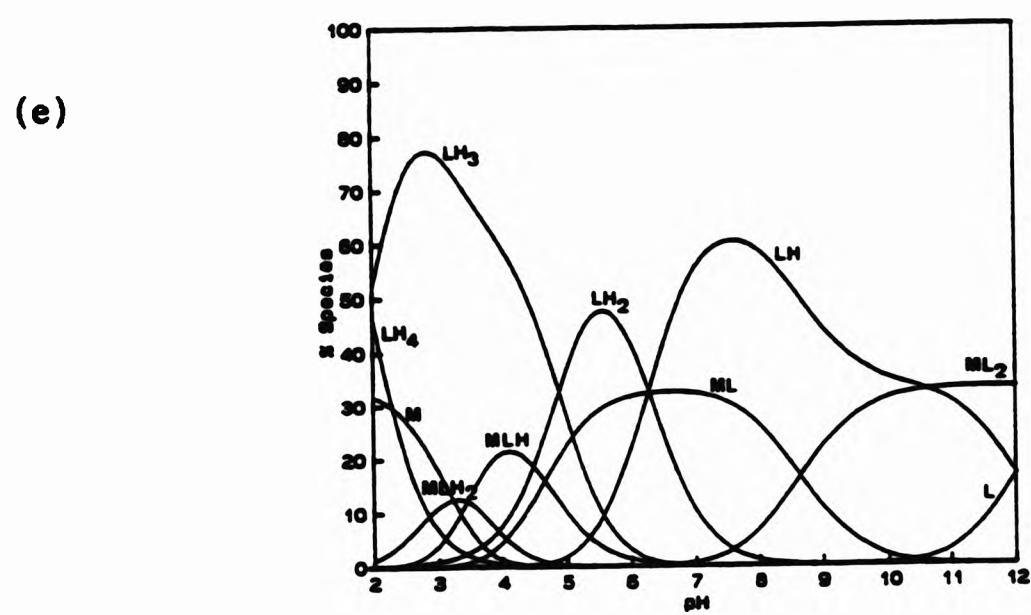
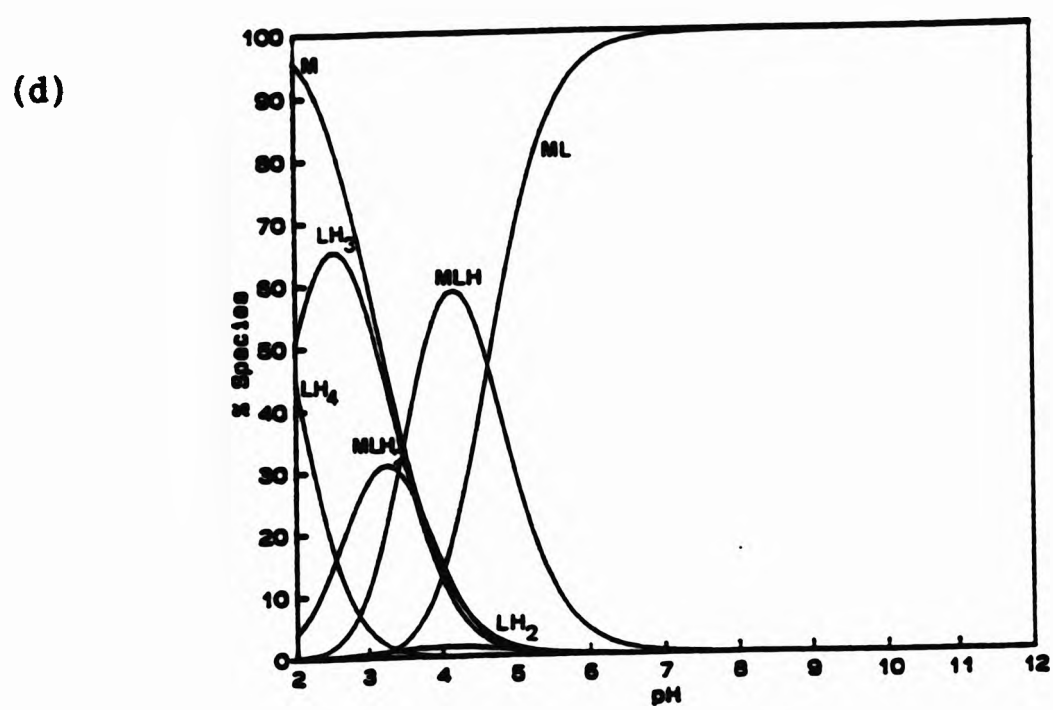
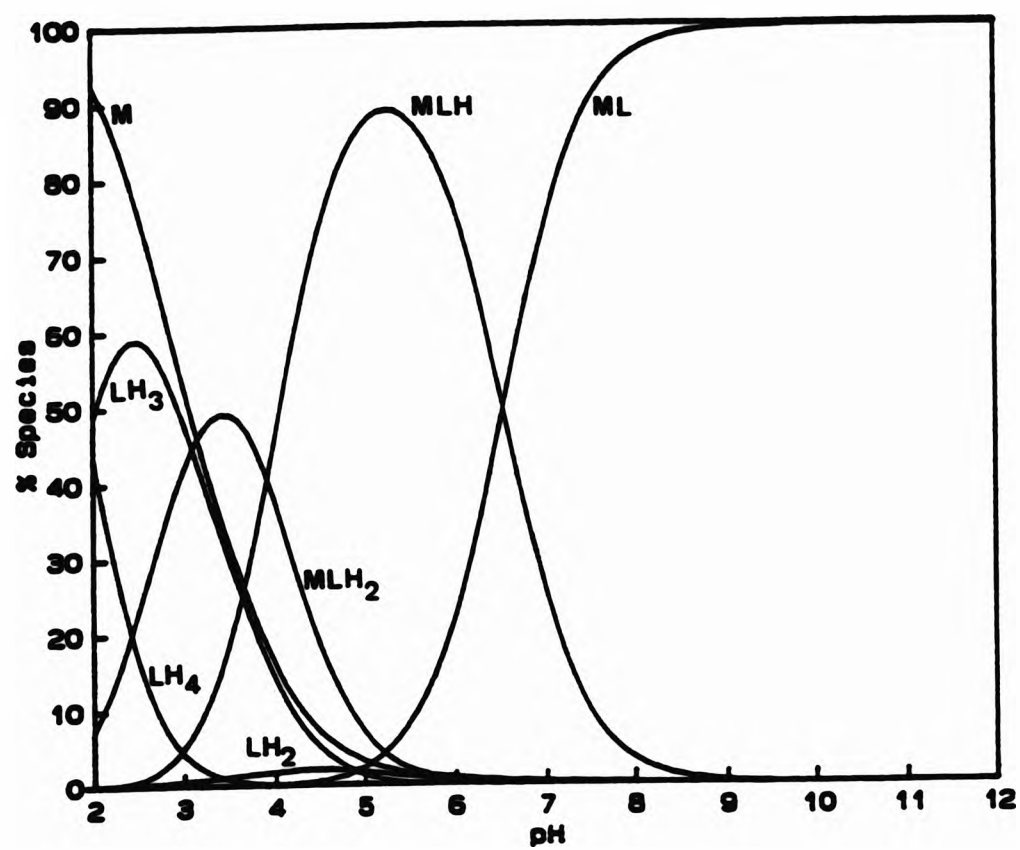


Figure 5.1.13, continued. Species distribution curves¹⁸ for NEIBMPH₄ with metal ions at $[M]:[L]$ ca. 1:1 (d) Cu(II) (e) Cu(II) at $[M]:[L]$ ca. 1:3 and (f) Zn(II).

(g)



(h)

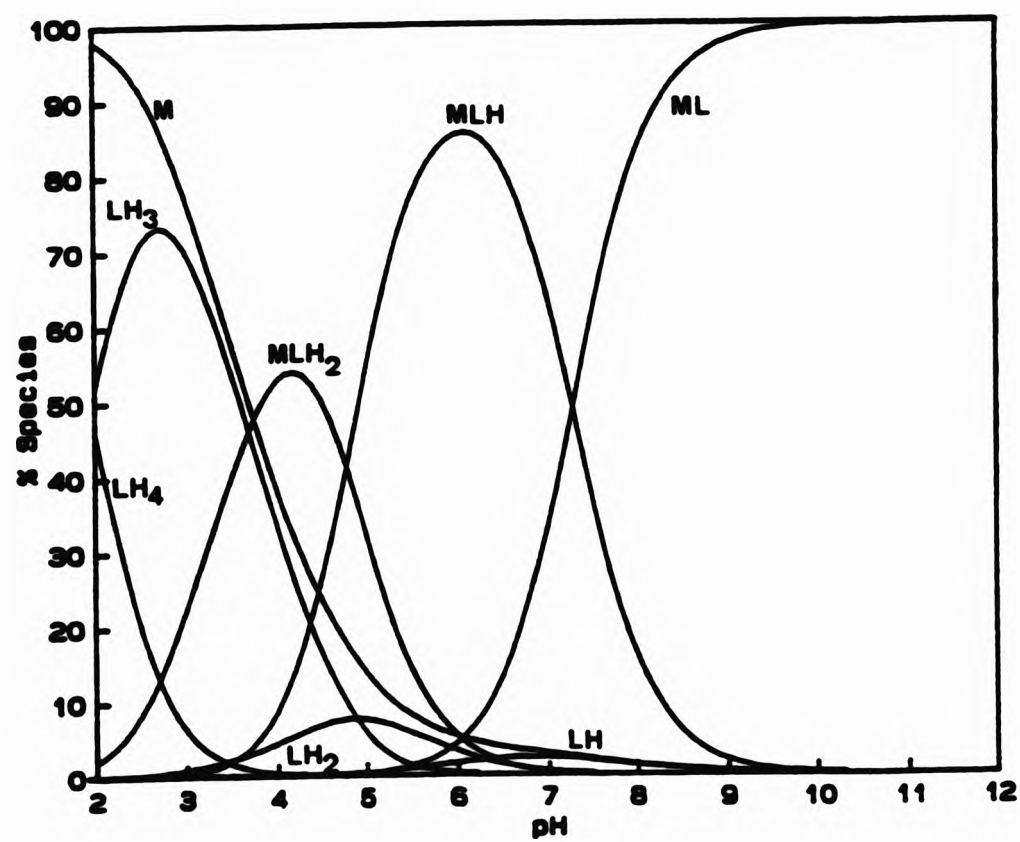


Figure 5.1.13, continued. Species distribution curves¹⁸ for NEIBMP₄ with metal ions (g) Pb(II), [M]:[L] ca. 1:1 and (h) Cd(II).

(i)

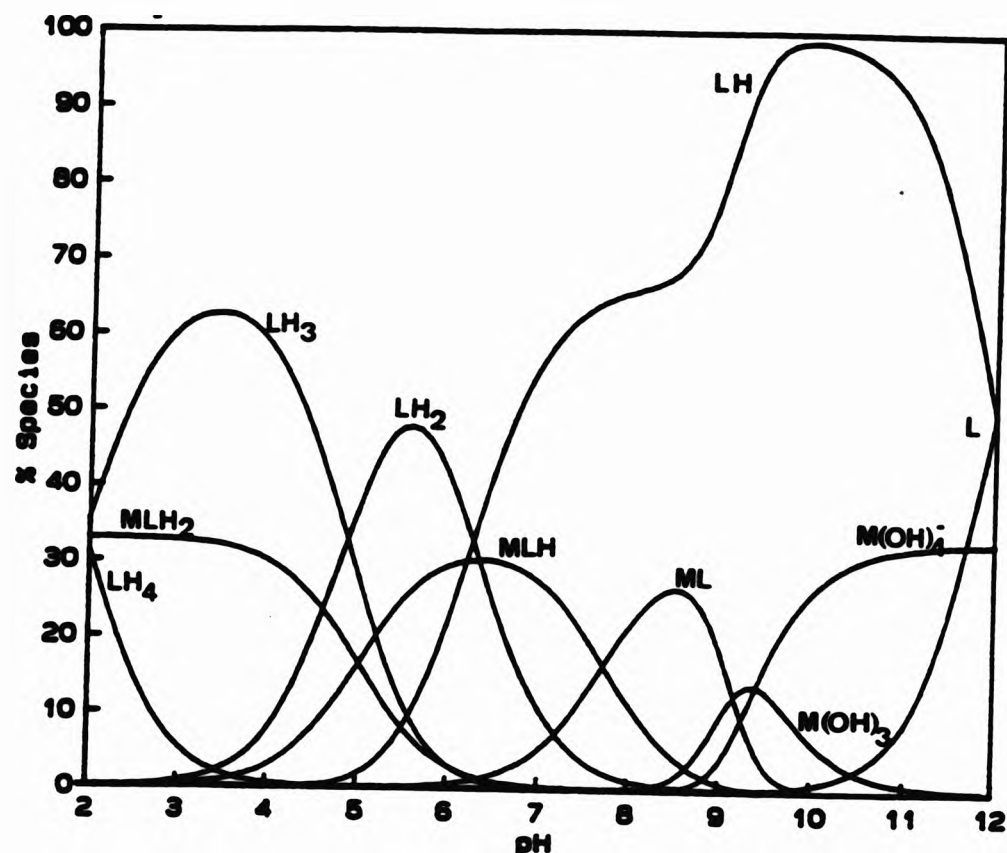


Figure 5.1.13, continued. Species distribution curves¹⁸ for NEIBMPH₄ with metal ion (i) Fe(III), [M]:[L] ca. 1:3.

5.1.4 Possible structures of metal complex species in solution

Examination of the results determined in this work and elsewhere for complexes of metal ions with DEAMP₂ show that the species [ML] was determined to be present in all cases (Table 5.1.13). There are only two examples in which more than one species were determined, *i.e.* for Pb(II) and Cu(II).¹¹ The values for the process of forming the species [ML] ($\log \beta_{110}$) for the transition metal ions with DEAMP₂ follow the Irving-Williams series: Co(II) << Cu(II) > Zn(II) > Cd(II).^{5,19}

The transition metal complexes formed by DEAMP₂ are more stable than those formed with the alkaline earth metals (Table 5.1.13). This was also observed for the methyl analogue of DEAMP₂, *i.e.* dimethylaminomethylenephosphonic acid, DMAMP₂.¹⁴

The value of $\log \beta_{110}$ (7.56) determined for Pb(II) with DEAMP₂ in this work is identical (within experimental error) to the value determined for $\log \beta_{110}$ (7.46) for Cu(II) with DEAMP₂.¹¹ This suggests that the process for forming

the species [ML] for DEAMPH₂ with Pb(II) may be similar to that for Cu(II). This strong complexing ability of DEAMPH₂ for Pb(II) may be of some use in the sequestration of the toxic, heavy metal.

Table 5.1.13 Stability Constants for some metal ions with DEAMPH₂.

MLH	log β_{MLH}			
	110	111	11-1	122
Metal				
Mg(II) ^a	ca. 2 ^b			
Ca(II) ^a	1.28			
Co(II) ^c	—very weak—			
Cu(II) ^d	7.46	14.12	-0.02	27.56
Zn(II) ^c	6.5 ^e			
Cd(II) ^c	5.6 ^e			
Pb(II) ^c	7.56	14.82	0.07	

^a Ref. 12. I = 1.0 mol dm⁻³ KNO₃, 25.0 °C. ^b Estimate. ^c This work. I = 0.1 mol dm⁻³ KNO₃, 25.0 ± 0.1 °C. ^d Ref. 11. I = 0.1 mol dm⁻³ KNO₃, 25.0 °C. ^e Approximate values.

As discussed in section 5.1.2, the coordination chemistry of NEIBMPH₄ with various metals examined by Bel'skii *et al.*¹⁵ and Scowen¹³ shows some agreement with that determined in this work. The present work indicates formation of the species [ML]²⁻, [MLH]⁻ and [MLH₂] in all cases. There were only two examples in which the formation of the species [ML₂]⁶⁻ were determined with some certainty, *i.e.* for Cu(II) and Zn(II). The stability constants for NEIBMPH₄ are collected in Table 5.1.14.

The values of the stability constants for the formation of the species [ML]²⁻ for transition metal complexes with NEIBMPH₄ follow the Irving-Williams series^{5,19} except that log β_{110} for Ni(II) and Co(II) are of similar magnitude: *i.e.* Mn < Co ≈ Ni < Cu > Zn > Cd. The Irving-Williams series is based upon the stabilities of complexes of divalent metal ions of the first transition series. The Irving-Williams series for transition metal ions is: Mn(II) < Fe(II) < Co(II) < Ni(II) < Cu(II) > Zn(II) > Cd(II)^{5,19} which is the reverse of

the order of the size of the cationic radii for this series.²⁰ The Irving-Williams series is rationalised on the basis of the metal ion and its charge, and it arises from a number of factors including d-orbital contribution to the metal-ligand bond,²¹ and the second ionisation potential of the metal.¹⁹ The stability of any metal and ligand is greater if the oxidation state of the metal is +3 rather than +2.²⁰ For example, the value of $\log \beta_{110}$ determined for Fe(III) with NEIBMPH₄ is 20.39, which is considerably larger than the estimated value of $\log \beta_{110}$ for Fe(II) from the Irving-Williams series in this work, of *ca.* 7.5.

Table 5.1.14 Stability Constants for some metal ions with NEIBMPH₄.

MLH	$\log \beta_{MLH}$			
	110	111	112	120
Metal				
Mg(II) ^a	4.42			
Ca(II) ^a	3.36			
Mn(II) ^b	6.89	15.42	20.73	
Co(II) ^b	8.13	15.70	20.91	
Ni(II) ^b	8.17	15.33	19.82	
Cu(II) ^b	13.28	18.00	21.26	18.44
Zn(II) ^b	9.29	15.59	20.09	14.35
Cd(II) ^b	8.92	16.32	21.11	
Pb(II) ^b	11.18	17.73	21.67	
Fe(III) ^b	20.39	28.15	33.31	

^a Ref. 12. $I = 1.0 \text{ mol dm}^{-3} \text{ KNO}_3$, 25.0 °C. ^b This work. $I = 0.1 \text{ mol dm}^{-3} \text{ KNO}_3$, 25.0 ± 0.1 °C.

The values of $\log \beta_{110}$ determined in this work for the metal ions [*e.g.* Mn(II), Co(II), Ni(II), Cu(II), Zn(II) and Cd(II)] with NEIBMPH₄, are each *ca.* 1 log unit less than the $\log \beta_{110}$ values determined for *N*-methyliminobis(methylene-phosphonic acid), MIBMPH₄ (Table 5.1.15). The effect of substitution of the methyl group at nitrogen in MIBMPH₄ with an ethyl group to give NEIBMPH₄ seems to result in lower stability of complexes with NEIBMPH₄, possibly due to the substituent effect of the ethyl group resulting in the reduced basicity of

both the nitrogen and phosphonate oxygen atoms.

Table 5.1.15 Stability constants for complexes of NEIBMPH₄^a and MIBMPH₄.

	log K _{MnL}	log K _{CoL}	log K _{NiL}	log K _{CuL}	log K _{ZnL}	log K _{CdL}
NEIBMPH ₄ ^a	6.89	8.13	8.17	13.28	9.29	8.92
MIBMPH ₄ ^b	8.24	9.27	9.59	14.32	10.44	10.18

^a This work. I = 0.1 mol dm⁻³ KNO₃, 25.0 ± 0.1 °C. ^b Ref. 14. I = 0.1 mol dm⁻³ KNO₃, 25.0 °C.

The relatively high stability constant (log K_{MnL}) determined for NEIBMPH₄ with Cu(II) compared to the values determined with Ni(II) and Co(II) can be explained by the Irving-Williams series, *i.e.* the smaller the cationic radius of the metal then the greater the stability of the metal complex formed.²⁰ The values of log β₁₁₀ determined for the analogue MIBMPH₄ with Ni(II) (9.59)¹⁴ and Co(II) (9.27)¹⁴ are close and this close agreement was also observed for the values of log β_{CoL} and log β_{NiL} for NEIBMPH₄, in this work.

On the other hand, the low values of log β₁₁₀ determined for NEIBMPH₄ with Co(II) and Ni(II) may also be explained in terms of the metal's requirements for its coordination sphere. For example, the higher stability constant observed for the complex [CuL]²⁻ may be ascribed to the Cu(II) ion preferring a tetrahedral arrangement,²² whereas Ni(II) and Co(II) may prefer octahedral coordination and this may lead to an overcrowding of the donor groups (PO₃²⁻) on the surface of the metal ion. This in turn increases the electrostatic repulsions and the steric forces between the donor groups and hence lowers the stability of the complex formed.²³ If all the donor groups cannot completely satisfy the coordination sphere of the metal ion then extra donor atoms (*e.g.* water) are needed to satisfy the coordination sphere.⁴

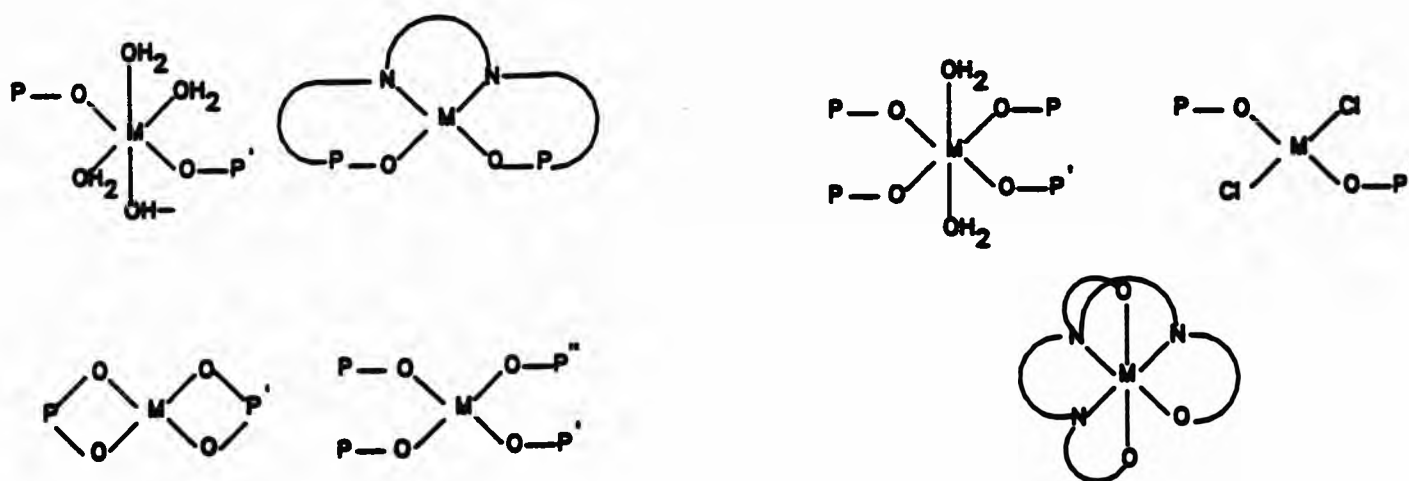
The stability constants for metal ions with DEAMPH₂ are much lower than those with NEIBMPH₄, *e.g.* log β₁₁₀ for Cu(II) with DEAMPH₂ is 7.46,¹¹ whereas with NEIBMPH₄ the value of log β₁₁₀ is substantially greater (13.28). This is consistent with the results determined by Sawada for MIBMPH₄ and DMAMPH₂¹⁴ (the difference between the values of log β₁₁₀ for MIBMPH₄ for Cu(II) and with that for DMAMPH₂ is *ca.* 6.3 log units). This suggests that in both NEIBMPH₄ and MIBMPH₄ complex stability is enhanced through increased basicity of the ligands

Table 5.1.16 Stability constants for complexes of some metal(II) ions with some related ligands.

	log β_M				
	Co	Ni	Cu	Zn	Pb
DEAMPH ₂	-	-	7.46 ^a	6.52 ^b	7.56 ^b
NEIBMPH ₄ ^b	8.13	8.14	13.28	9.29	11.18
IBMPH ₄ ^c	7.75	8.32	12.84	9.03	10.17
EBISPH ₄ ^d	11.19	11.23	20.35	13.38	16.00
OBEISPH ₄ ^e	9.02	8.84	16.18	11.17	11.68

^a Ref. 11. I = 0.1 mol dm⁻³ KNO₃, 25.0 °C. ^b This work. I = 0.1 mol dm⁻³ KNO₃, 25.0 ± 0.1 °C. ^c Ref. 24. I = 0.1 mol dm⁻³ KNO₃, 25.0 °C. ^d Ref. 26. I = 0.1 mol dm⁻³ KNO₃, 25.0 °C. ^e Ref. 25. I = 0.1 mol dm⁻³ KNO₃, 25.0 °C.

Insight into possible structures of the species in solution is available from the (relatively few) reported X-ray crystallographic structure determinations of metal complexes with aminomethylenephosphonic acids.²⁷⁻³⁴ A typical feature of such complexes is their polymeric nature, although it is unlikely (on solubility grounds) that such structures would be present to any significant extent in solution. The known structures all contain a single metal ion coordinated to the phosphonate oxygen atoms and/or the nitrogen atoms. The following diagram represents the coordination modes of the metal ions in the structures available at this time.



There are only three examples in which the nitrogen atoms are coordinated to the metal ion forming relatively stable five-membered chelate rings.^{28,33,34} For example, Shkol'nikova *et al.*²⁸ isolated crystals of a copper(II) complex with ethylenebis(amineisopropylphosphonic acid) (EDISPH₄) which was subsequently examined by X-ray crystallography.²⁸ The solid state structure of [Cu(EDDIPH₂)] shows the copper ion to have a square-pyramidal geometry with both nitrogen atoms and two phosphonate oxygen atoms coordinated to the metal.

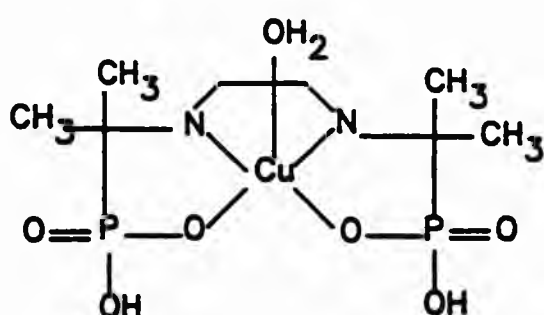


Figure 5.1.14 Schematic diagram of the solid state structure of [Cu(EDISPH₄)].²⁸

Coordination of the Cu(II) ion to the nitrogen atoms and the phosphonate oxygen atoms produces three relatively stable, five-membered chelate rings. In similar case, Kabachnik *et al.* prepared and isolated the copper(II) complex of *N,N,N*-1,4,7-triazacyclononane4, in which the copper ion is coordinated to the three ring nitrogen atoms and to two phosphonate oxygen atoms.³³ The copper(II) ion also has a square-pyramidal geometry with five five-membered chelate rings formed (Figure 5.1.15).

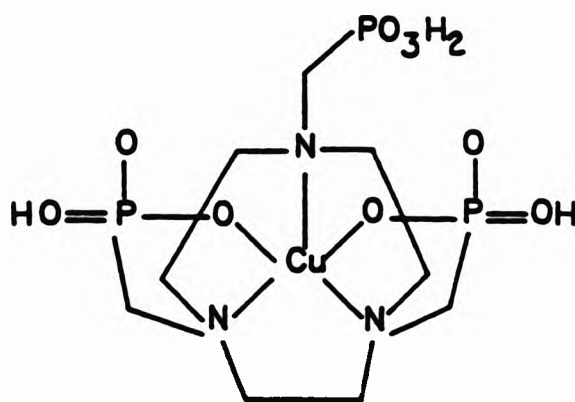


Figure 5.1.15 Schematic diagram of the solid state structure of [Cu(TACNTMPH₄)].³³

Another example of nitrogen coordination to the metal ion was found for the Fe(III) complex with *N,N,N*-1,4,7-triazacyclononanetrakis(methylenephosphonic acid), TACNTMPH₉.³⁴ The Fe(III) ion is in a distorted octahedral environment coordinated to all three nitrogen atoms and three phosphonate oxygen atoms (Figure 5.1.16) producing six five-membered chelate rings.

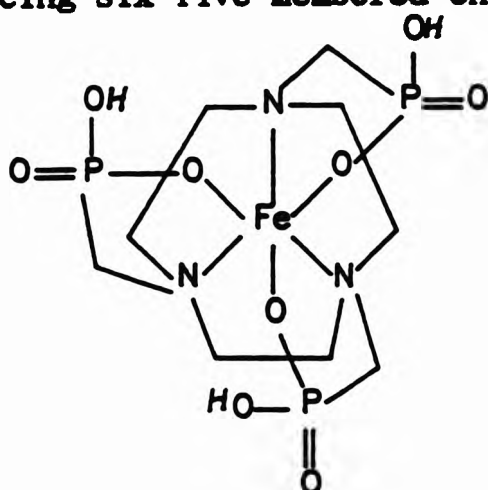


Figure 5.1.16 Schematic diagram of the solid state structure of [Fe(TACNTMPH₉)].³⁴

There are a few examples of metal complexes with aminomethylenephosphonic acids in which the metal to ligand ratio is greater than 1:1 and where the structure is known. For example, the complex of Zn(II) with aminomethylphosphonic acid (AMPH₂) has the structure shown in Figure 5.1.17.²⁹ The Zn(II)

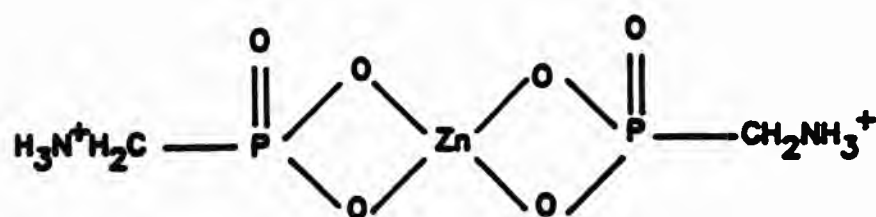
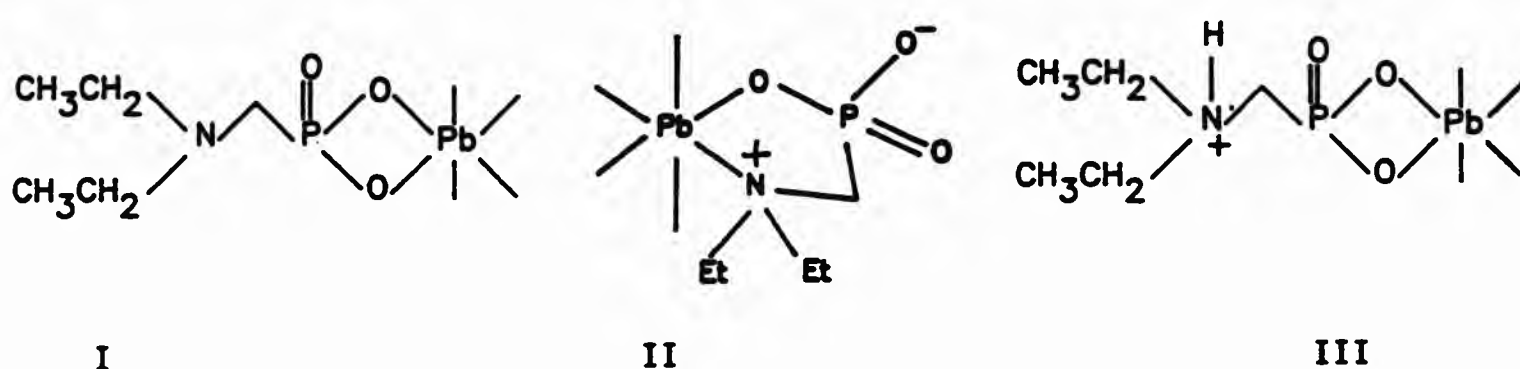


Figure 5.1.17 Schematic diagram of the solid state structure of [Zn(AMPH₂)₂].4H₂O.²⁹

ion is in a tetrahedral environment, coordinated to four phosphonate oxygen atoms from two different molecules of AMPH₂. This results in two four-membered chelate rings.

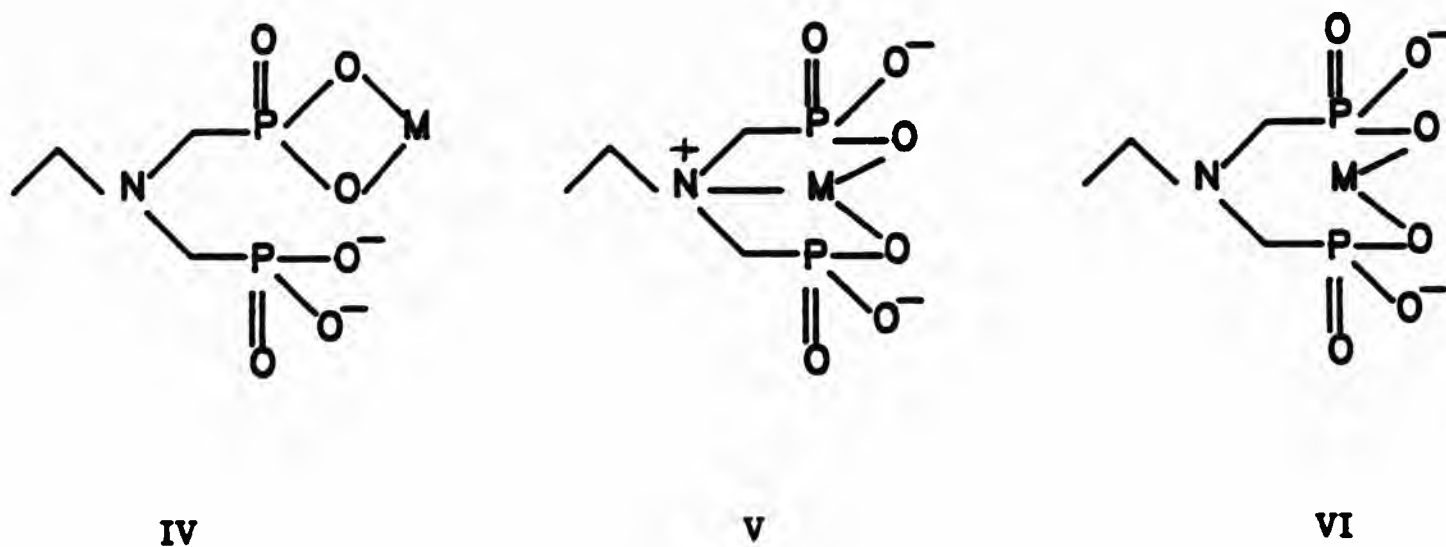
Some indication of the microscopic nature of the metal complexes in solution can also be inferred from their stability constants as proposed by Sawada.^{2,14} The basicity of uncoordinated oxygens (*i.e.* O⁻) on the ligands is expected to decrease on coordination of the ligand to the metal cation. Consequently, if the first protonation of the complex [ML] occurs on the phosphonate oxygen (O⁻)

uncoordinated to the metal cation, then the first protonation constant for the complex [ML] ($[ML] + H^+ = [MLH^+]$), $\log K_{MLH}$ should be less than that of the phosphonate oxygen of the 'free-ligand' (i.e. $\log K_{012}$ for DEAMP₂ and NEIBMPH₄). For the complex of DEAMP₂ with Pb(II) there are two possible structures for the refined species [PbL].

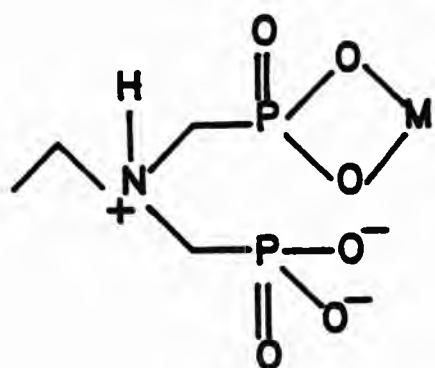


Since the value $\log K_{111}$ (7.26) is greater than the value for the process of protonating a phosphonate oxygen in the free ligand, i.e. $\log K_{012} = 5.30$, then it is likely that protonation occurs at the nitrogen atom in I to form III. Although it may be tempting to assume that the species [PbL] does not contain a M-N bond, there is no evidence to distinguish between I and II. The rest of the coordination sphere of Pb(II) is satisfied by other donor molecules i.e. in this case water^{4,27} and hydrolysis of one of the water molecules results in the hydroxy metal complex [PbL(OH)]⁻.

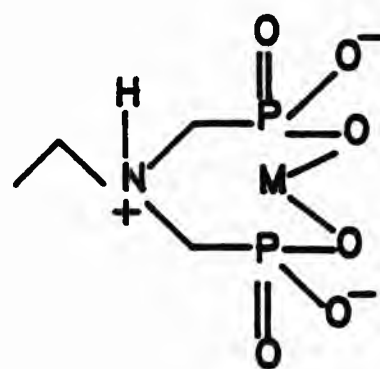
The method described by Sawada¹⁴ for inferring the possible structures of metal complexes in solution was used for complexes of NEIBMPH₄. The possible structures of the species [ML]²⁺ are based on the crystal structures available.



However, since structures containing eight-membered chelate rings have not been found structure VI is unlikely. The stability constants determined for protonating the species $[ML]^{2-}$ for the metal ions Mn(II), Co(II), Ni(II), Zn(II), Cd(II), Pb(II) and Fe(III) ($\log K_{MLH} = 6.55-8.53$) are all greater than the value for the process of protonating a phosphonate oxygen of the free ligand ($\log K_{012} = 6.28$). In analogous work on MIBMPH₄, Sawada¹⁴ suggested that this could be ascribed to the protonation of the species $[ML]^{2-}$ at the nitrogen atom to form the monoprotonated species $[MLH]^-$ (structures VII or VIII).¹⁴

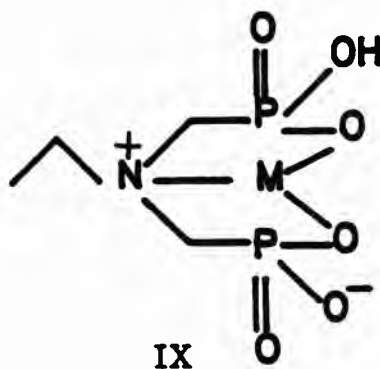


VII



VIII

The process for protonating the species $[CuL]^{2-}$ to form $[CuLH]^-$ has a value of $\log K_{CuLH} = 4.73$. This suggests that in the protonation of $[CuL]^{2-}$, the proton does not attack the nitrogen but, instead, an uncoordinated phosphonate oxygen atom (PO_3^{2-}) (structure IX). This is evidence for the persistence of a Cu-N bond.



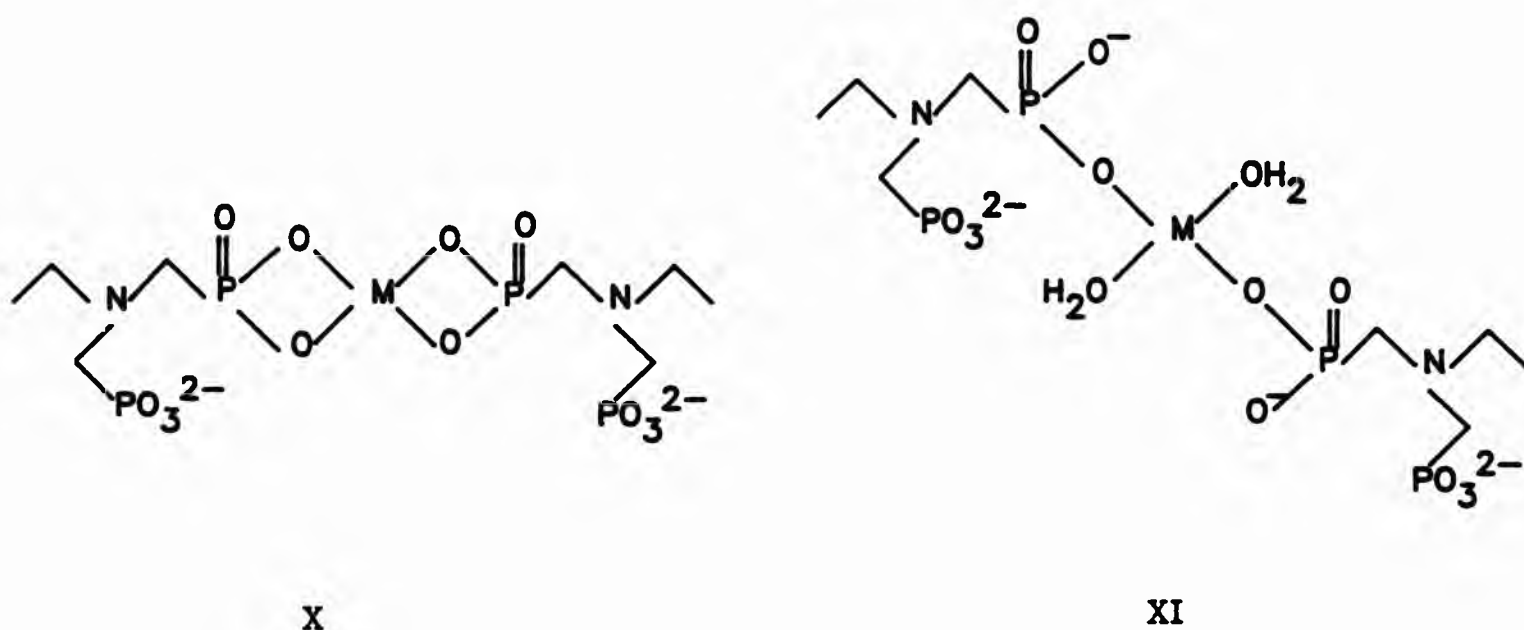
IX

For copper(II) in particular, coordination of both the nitrogen atom and phosphonate oxygen atoms to form two relatively stable five membered chelate rings has been found in the solid state.^{28,33}

A similar interpretation has been placed on stability constants for a Cu(II) complex of the related ligand, iminobis(methylenephosphonic acid), IBPH₄ with Cu(II).²⁴ The protonation of the complex $[ML]$ (where $L = IDP^{4-}$) has a value of $\log K_{012}$ (4.60), *i.e.* smaller than the value for the second protonation constant of the free ligand ($\log K_{012} = 6.08$), representing the first proton

attacking an uncoordinated phosphonate oxygen atom.

There are a number of crystal structures which involve the metal coordinated to two or more aminomethylenephosphonate ligands^{27,29-32} and on this basis structures X or XI are proposed for $[\text{ZnL}_2]^{6-}$ and $[\text{CuL}_2]^{6-}$.



5.2 The stability of some metal complexes of two 'complex' α -aminomethylene-phosphonic acids, CDTMPH_3 and DDDTMPH_3

The coordination behaviour of two 'complex' α -aminomethylenephosphonic acids, *i.e.* *trans*-cyclohexane-1,2-diamine *tetrakis*(methylenephosphonic acid), CDTMPH_3 and 5,8-dioxadodecane-1,12-diamine *tetrakis*(methylenephosphonic acid), DDDTMPH_3 , was studied under similar conditions ($I = 0.1 \text{ mol dm}^{-3}$, KNO_3). The protonation equilibria of both CDTMPH_3 and DDDTMPH_3 have been determined to establish the various species in *aqueous* solution (Chapter 4).

The structures of CDTMPH_3 and DDDTMPH_3 are significantly different, *i.e.* there is a 'rigid' cyclohexyl ring in CDTMPH_3 and DDDTMPH_3 has a flexible, aliphatic ether type backbone. However, both CDTMPH_3 and DDDTMPH_3 contain the basic *iminobis*(methylenephosphonate group). The differences in their structures may significantly affect the stability of metal complexes formed in solution.

5.2.1 Stability constants for metal ion complexes with CDTMPH_3

The coordination behaviour of CDTMPH_3 with the following metals was examined by potentiometric titration over the pH range 2-12; Mn(II), Fe(III), Co(II), Ni(II), Cu(II), Zn(II), Cd(II), Pb(II) and Gd(III). For the metal ions, Co(II), Ni(II), Cu(II), Zn(II) and Pb(III), three potentiometric titrations

were obtained at metal to ligand ratio of *ca.* 1:1. For the metal ion Mn(II) only two potentiometric titrations were obtained at a metal:ligand ratio of *ca.* 1:1. In the case of CDTMPH₃ with Fe(III) three datafiles were obtained at a metal:ligand ratio of *ca.* 1:3 in order to prevent any precipitation of unwanted metal complex or metal hydroxy species. For CDTMPH₃ with Gd(III), five datafiles were obtained covering metal:ligand ratios of *ca.* 1:1, 1:2, and 1:3. The previously determined protonation constants (Section 4.4) for CDTMPH₃ were used as constants in the SUPERQUAD¹⁰ input files, and subsequent refinement of the datafiles yielded the metal-complex stability constants. Recalling that the first protonation constant of CDTMPH₃ was not determined by potentiometry (Section 4.5), refinement of all datafiles obtained for CDTMPH₃ with metals was carried out on the assumption that L was defined as the monoprotinated ligand, *i.e.* CDTMPH⁷⁻.

5.2.1(a) Manganese

Two titration curves were obtained for CDTMPH₃ with Mn(II), and one is shown in Figure 5.2.1. There is a close correspondence between the 'ligand-only'

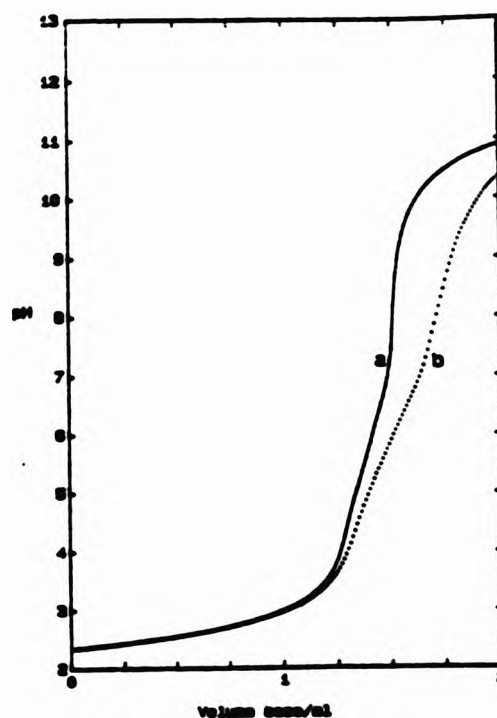


Figure 5.2.1 Titration curves (pH vs volume of base added) for acidified solutions of CDTMPH₃; (a) [CDTMPH₃] *ca.* 0.0005 mol dm⁻³; (b) Mn(NO₃)₂ with CDTMPH₃, [M]:[L] *ca.* 1:1.

curve and the 'metal-ligand' curve up to pH ca. 3 with significant deviation occurring at higher pH. An end-point region of the titration curve at pH ca. 9 corresponds to ca. seven equivalents of base being consumed by the 'metal-ligand' system, *i.e.* one greater than in the ligand-only system (Section 4.5). This suggests that the species LH_2^{6-} complexes with the metal ion to form the species $[\text{MLH}]^{5-}$ in this region.[†]

Refinements of both datafiles for a model involving the species $[\text{MnLH}_3]^{3-}$, $[\text{MnLH}_2]^{4-}$ and $[\text{MnLH}]^{5-}$ was successful.

Table 5.2.1 Stability constants for CDTMPH_3 with Mn(II) .^a

Datafile [M]:[L]	Tm1 ^b 1:1.03	Tm2 ^c 1:1.04	Mean ^d
log β_{110}	10.11(0.025)	10.49(0.033)	10.00 ±0.35
log β_{111}	18.56(0.008)	18.62(0.014)	18.56 ±0.01
log K_{111}	8.45	8.18	8.57 ±0.33
log β_{112}	25.14(0.009)	25.13(0.019)	25.18 ±0.20
log K_{112}	6.58	6.51	6.62 ±0.21

^a The monoprotonated ligand (CDTMPH^{7-}) is denoted as L; see text. Data obtained at $I = 0.1 \text{ mol dm}^{-3} \text{ KNO}_3$, $25.0 \pm 0.1 \text{ }^\circ\text{C}$. Figures in parentheses are standard deviations obtained from SUPERQUAD. Convention: β_{MLH} for $\text{M}_n\text{L}_m\text{H}_n$. ^b Fit parameters obtained from SUPERQUAD, $\chi^2 = 6.00$, $\sigma = 0.0326$; pH 4.76–7.56, 32 data points. ^c Fit parameters obtained from SUPERQUAD, $\chi^2 = 8.82$, $\sigma = 0.0660$; pH 4.79–7.59, 34 data points. ^d Unweighted mean of values from each refinement; error limits are derived from the ranges obtained from each log β_{MLH} (and log K_{MLH}).

5.2.1(b) Iron (III)

The potentiometric titration curves obtained for CDTMPH_3 with Fe(III) were smooth and showed no evidence of precipitation. One example of the titration curves obtained is shown in Figure 5.2.2. Seven equivalents of base were

[†] Note: In the SUPERQUAD¹⁰ input files, L has been denoted as CDTMPH^{7-} and so the stability constant for (for example) $[\text{MLH}]^{3-}$ is log β_{110} ; that for $[\text{MLH}_2]^{4-}$ is log β_{111} , etc.

consumed by the 'metal-ligand' system at the end-point on the titration curve at pH ca. 9, indicating the formation of $[\text{MLH}]^{4-}$ in this region.

Refinements of datafiles TFe1, TFe2 and TFe3 for a model which only involved the species $[\text{MLH}]^{4-}$, $[\text{MLH}_2]^{3-}$ and $[\text{MLH}_2]^{2-}$ were successful (Table 5.2.2). Separate refinements for two datafiles (Tfe1 and Tfe2) for a model with only one species $[\text{ML}_2\text{H}_2]^{11-}$ were successful (Table 5.2.2).

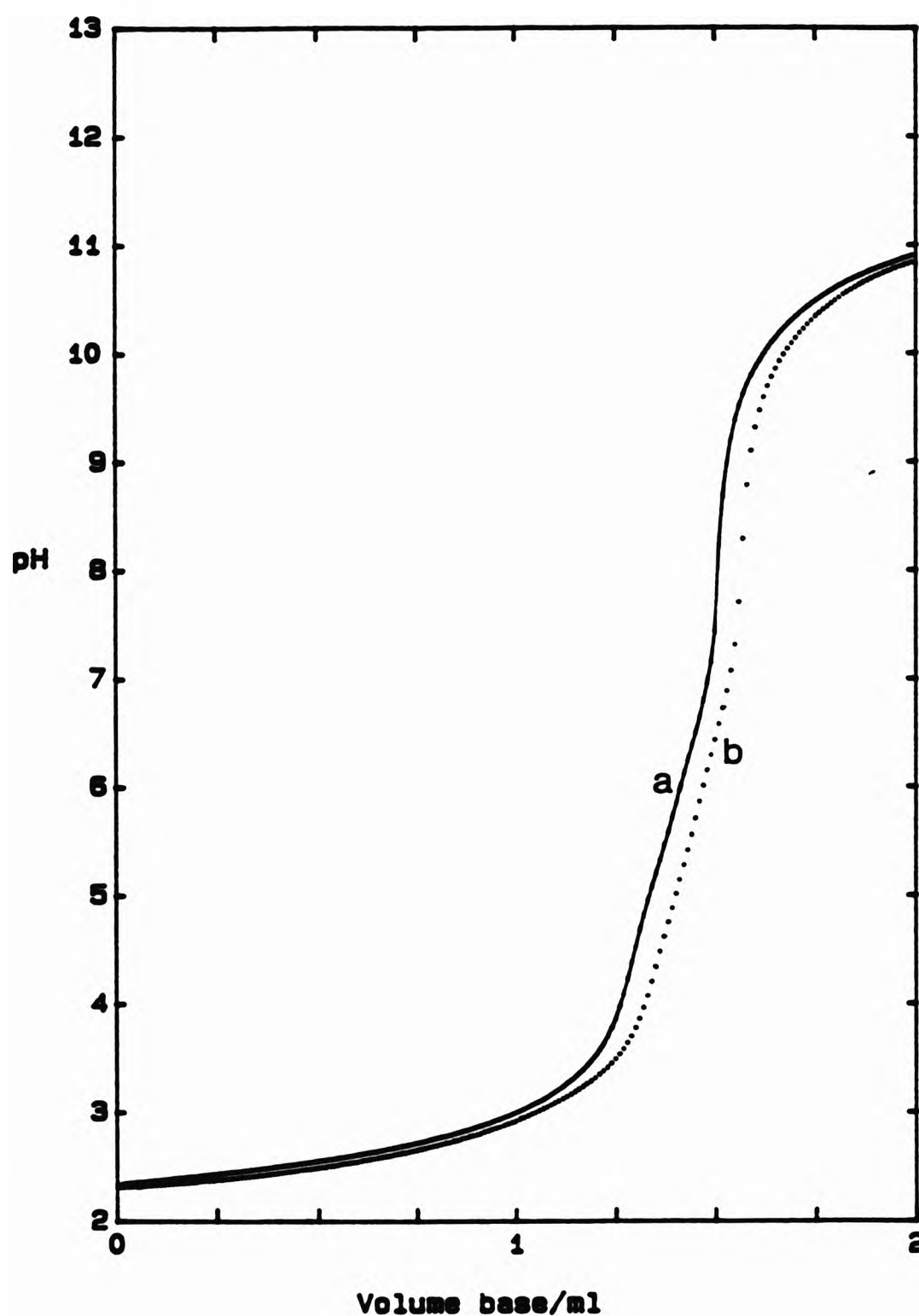


Figure 5.2.2 Titration curves (pH vs volume of base added) for acidified solutions of CDTMPH_3 ; (a) $[\text{CDTMPH}_3]$ ca. $0.0005 \text{ mol dm}^{-3}$; (b) $\text{Fe}(\text{NO}_3)_3$ with CDTMPH_3 , $[\text{M}]:[\text{L}]$ ca. 1:3.

Table 5.2.2 Stability constants for CDTMPH₃ with Fe(III).^a

Datafile [M]:[L]	Tfe1 ^b 1:3.37	Tfe2 ^c 1:2.76	Tfe3 ^d 1:2.99	Mean ^e
log β ₁₁₀	18.60(0.045)	18.75(0.063)	18.94(0.076)	18.76 ±0.16
log β ₁₁₁	25.09(0.027)	25.28(0.040)	25.38(0.047)	25.25 ±0.16
log K ₁₁₁	6.49	6.53	6.44	6.49 ±0.05
log β ₁₁₂	29.89(0.010)	30.16(0.018)	30.15(0.020)	30.07 ±0.18
log K ₁₁₂	4.80	4.88	4.77	4.82 ±0.06
log β ₁₂₀	22.99(0.043) ^f	22.79(0.138) ^g		22.89 ±0.10

^a The monoprotonated ligand (CDTMPH⁷⁻) is denoted as L; see text. Data obtained at I = 0.1 mol dm⁻³ KNO₃, 25.0 ±0.1 °C. Figures in parentheses are standard deviations obtained from SUPERQUAD. Convention: β_{MLH} for M_nL_mH_p. ^b Fit parameters obtained from SUPERQUAD, χ² = 7.20, σ = 0.0284; pH 3.30–7.65, 41 data points. ^c Fit parameters obtained from SUPERQUAD, χ² = 7.89, σ = 0.0557; pH 3.28–8.75, 38 data points. ^d Fit parameters obtained from SUPERQUAD, χ² = 8.38, σ = 0.0582; pH 3.29–8.29, 39 data points. ^e Unweighted mean of values from each refinement; error limits are derived from the ranges obtained from each log β_{MLH} (and log K_{MLH}). ^f Fit parameters obtained from SUPERQUAD, χ² = 6.00 σ = 0.0896; pH 8.69–10.29, 16 data points. ^g Fit parameters obtained from SUPERQUAD, χ² = 8.00 σ = 0.0939; pH 8.75–10.18, 12 data points.

5.2.1(c) Cobalt

One example of the potentiometric titration curves obtained for CDTMPH₃ with Co(II) is shown in Figure 5.2.3. Again the formation of [MLH]⁵⁻ is inferred from the equivalents of base consumed by the metal-ligand system on the titration curve at pH ca. 8 [see Mn(II)].

Successful refinements were obtained for all datafiles for a model which involved the species with a metal:ligand ratio of 1:1 (i.e. [MLH]⁵⁻, [MLH₂]⁴⁻ and [MLH₃]³⁻) and they were characterised by satisfactory fit parameters (Table 5.2.3).

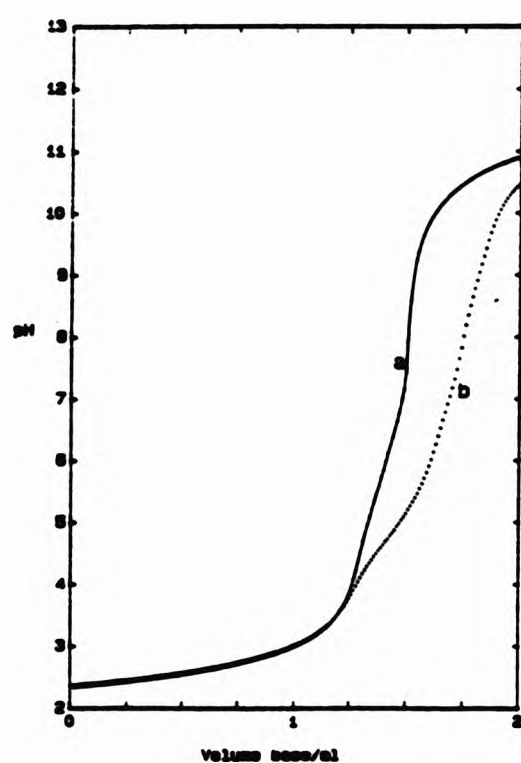


Figure 5.2.3 Titration curves (pH vs volume of base added) for acidified solutions of CDTMPH₃; (a) [CDTMPH₃] ca. 0.0005 mol dm⁻³; (b) Co(NO₃)₂ with CDTMPH₃, [M]:[L] ca. 1:1.

Table 5.2.3 Stability constants for CDTMPH₃ with Co(II).^a

Datafile	TCo1 ^b	TCo2 ^c	TCo3 ^d	Mean ^e
[M]:[L]	1:0.99	1:0.94	1:0.96	
log β ₁₁₀	10.39(0.029)	10.13(0.036)	10.38(0.034)	10.30 ±0.17
log β ₁₁₁	19.32(0.020)	19.12(0.023)	19.30(0.022)	19.25 ±0.13
log K ₁₁₁	8.93	8.99	8.91	8.94 ±0.05
log β ₁₁₂	26.19(0.020)	26.04(0.019)	26.14(0.018)	26.12 ±0.08
log K ₁₁₂	6.86	6.92	6.84	6.87 ±0.05

^a The monoprotonated ligand (CDTMPH⁷⁻) is denoted as L; see text. Data obtained at I = 0.1 mol dm⁻³ KNO₃, 25.0 ±0.1 °C. Figures in parentheses are standard deviations obtained from SUPERQUAD. Convention: β_{MLH} for M_nL_mH_n. ^b Fit parameters obtained from SUPERQUAD, χ² = 2.18, σ = 0.0846; pH 5.73–10.49, 44 data points. ^c Fit parameters obtained from SUPERQUAD, χ² = 5.82, σ = 0.1008; pH 5.55–10.46, 44 data points. ^d Fit parameters obtained from SUPERQUAD, χ² = 6.41, σ = 0.0885; pH 5.62–10.38, 41 data points. ^e Unweighted mean of values from each refinement; error limits are derived from the ranges obtained from each log β_{MLH} (and log K_{MLH}).

5.2.1(d) Nickel(II)

Smooth potentiometric titration curves obtained for CDTMPH₃ with Ni(II) and show no evidence of precipitation; one example is shown in Figure 5.2.4.

In order to obtain successful refinements for all three datafiles for a model involving the species [MLH₂]²⁻, [MLH₃]³⁻, [MLH₂]⁴⁻ and [MLH]⁵⁻, it was necessary to add two Ni(II) hydrolysis constants (log β₁₀₋₁ and log β₁₀₋₂) into the SUPERQUAD input files as constants.^{16(b),17} The results are given in Table 5.2.4. In spite of this, the reproducibility for all the log β values for Ni(II) complexes was significantly poorer than those normally obtained in this work [*cf.*, *e.g.* Co(II), 5.2.1(c)]. It is therefore likely that the best-fit model for the equilibria has not been obtained.

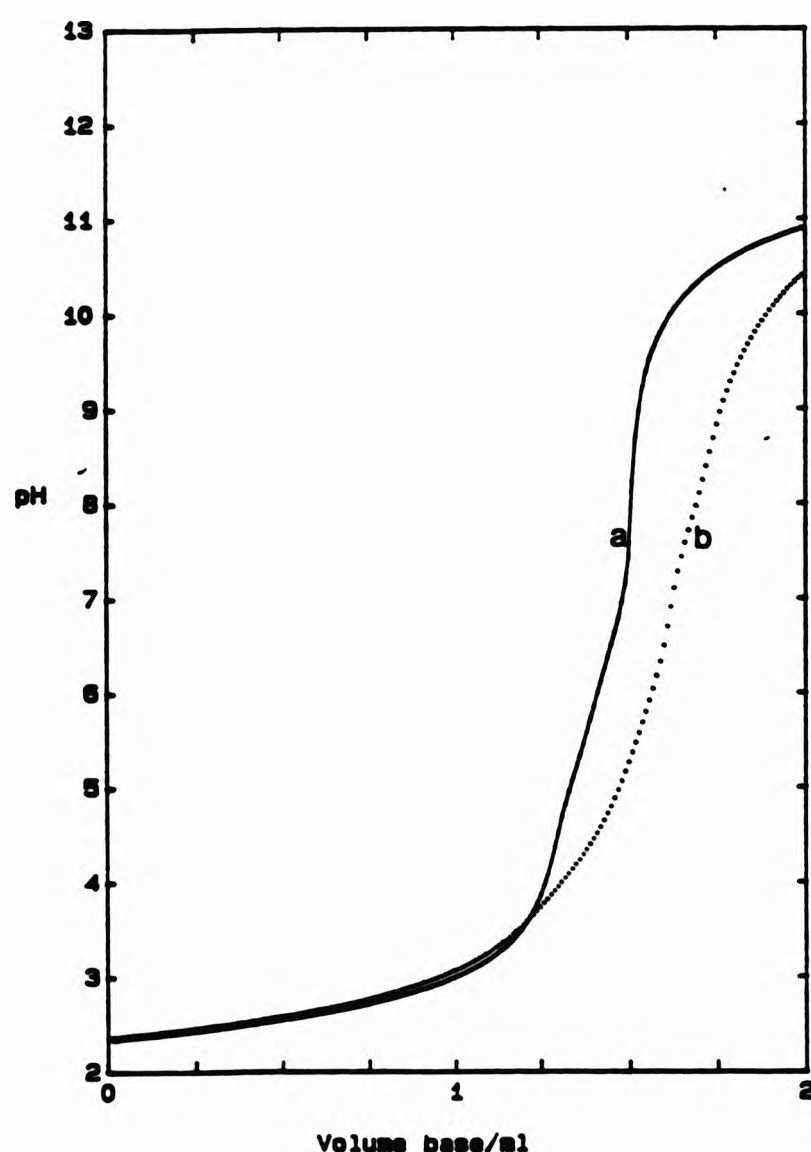


Figure 5.2.4 Titration curves (pH vs volume of base added) for acidified solutions of CDTMPH₃; (a) [CDTMPH₃] ca. 0.0005 mol dm⁻³; (b) Ni(NO₃)₂ with CDTMPH₃, [M]:[L] ca. 1:1.

Another source of irreproducibility in $\log \beta$ values might be the provision of insufficient time for equilibrium at each data point; Ni(II) is known to be an 'inert' species.³⁵ However, in generating one datafile (TNi4), a longer time delay of 300 s per point was used (total titration time ca. 20 h) and the values of $\log \beta$ determined were not significantly different to those in datafile TNi3 which was run at the normal delay of 150 s.

Table 5.2.4 Stability constants for CDTMPH₃ with Ni(II).^a

Datafile	TNi2 ^b	TNi3 ^c	TNi4 ^d	Mean ^e
[M]:[L]	1:0.98	1:1.05	1:1.03	
$\log \beta_{110}$	9.38(0.027)	8.64(0.057)	8.73(0.036)	8.92 ±0.43
$\log \beta_{111}$	18.90(0.023)	18.25(0.034)	18.30(0.022)	18.48 ±0.42
$\log K_{111}$	9.52	9.61	9.58	9.57 ±0.05
$\log \beta_{112}$	26.61(0.024)	26.16(0.025)	26.15(0.017)	26.31 ±0.30
$\log K_{112}$	7.71	7.91	7.84	7.82 ±0.09
$\log \beta_{113}$	32.03(0.048)	31.53(0.032)	31.49(0.029)	31.68 ±0.35
$\log K_{113}$	5.42	5.38	5.34	5.38 ±0.04

^a The monoprotonated ligand (CDTMPH⁷⁻) is denoted as L; see text. Data obtained at I ca. 0.1 mol dm⁻³ KNO₃, 25.0 ±0.1 °C. Figures in parentheses are standard deviations obtained from SUPERQUAD. Convention: β_{MLH} for $M_nL_mH_n$. The following Ni(II) hydrolysis values were input and held constant in all three datafiles; $\log \beta_{10-1} = -8.00$ and $\log \beta_{10-2} = -17.50$.^{16(b),17} ^b Fit parameters obtained from SUPERQUAD, $\chi^2 = 5.26$, $\sigma = 0.0839$; pH 4.92–10.52, 54 data points. ^c Fit parameters obtained from SUPERQUAD, $\chi^2 = 5.43$, $\sigma = 0.1556$; pH 4.49–10.29, 56 data points. ^d Fit parameters obtained from SUPERQUAD, $\chi^2 = 6.55$, $\sigma = 0.1290$; pH 4.58–10.41, 58 data points. ^e Unweighted mean of values from each refinement; error limits are derived from the ranges obtained from each $\log \beta_{MLH}$ (and $\log K_{MLH}$).

5.2.1(e) Zinc(II)

One example of the potentiometric titration curves obtained for CDTMPH₃ with Zn(II) is shown in Figure 5.2.5. The metal-ligand system consumes ca. seven equivalents of base by the end-point on the titration curve at pH ca. 9, indicating the formation of [MLH]⁵⁻.

Successful refinements of all three datafiles were obtained for a model which only involved species with a metal:ligand ratio of 1:1 (i.e. $[\text{MLH}]^{5-}$, $[\text{MLH}_2]^{4-}$ and $[\text{MLH}_3]^{3-}$).

Table 5.2.5 Stability constants for CDTMPH_3 with Zn(II) .^a

Datafile [M]:[L]	TZn1 ^b 1:0.99	TZn2 ^c 1:1.09	TZn3 ^d 1:0.99	Mean ^e
log β_{110}	11.77(0.030)	11.86(0.036)	11.78(0.032)	11.80 \pm 0.06
log β_{111}	20.57(0.019)	20.61(0.023)	20.57(0.020)	20.58 \pm 0.03
log K_{111}	8.80	8.75	8.78	8.78 \pm 0.03
log β_{112}	26.72(0.011)	26.77(0.013)	26.73(0.011)	26.74 \pm 0.03
log K_{112}	6.15	6.15	6.16	6.16 \pm 0.01
log β_{113}	30.96(0.049)	31.17(0.045)	30.96(0.052)	31.03 \pm 0.14
log K_{113}	4.24	4.40	4.23	4.29 \pm 0.11

^a The monoprotonated ligand (CDTMPH^{7-}) is denoted as L; see text. Data obtained at I ca. $0.1 \text{ mol dm}^{-3} \text{ KNO}_3$, $25.0 \pm 0.1 \text{ }^\circ\text{C}$. Figures in parentheses are standard deviations obtained from SUPERQUAD. Convention: β_{MLH} for $M_L H_L$. ^b Fit parameters obtained from SUPERQUAD, $\chi^2 = 4.80$, $\sigma = 0.0442$; pH 4.57–9.26, 40 data points. ^c Fit parameters obtained from SUPERQUAD, $\chi^2 = 5.24$, $\sigma = 0.0567$; pH 4.58–9.10, 41 data points. ^d Fit parameters obtained from SUPERQUAD, $\chi^2 = 7.20$, $\sigma = 0.0474$; pH 4.56–9.19, 40 data points. ^e Unweighted mean of values from each refinement; error limits are derived from the ranges obtained from each log β_{MLH} (and log K_{MLH}).

5.2.1(f) Lead(II)

The potentiometric titrations curves obtained for CDTMPH_3 with Pb(II) were smooth and show no evidence of precipitation. One titration curve is shown in Figure 5.2.6. Again, the metal-ligand system consumes ca. seven equivalents of base by the end-point on the titration curve at pH ca. 9, hence $[\text{MLH}]^{5-}$ is being formed.

Refinements of datafiles TPb1, TPb2 and TPb3 for a model involving the species $[\text{PbLH}_4]^{2-}$, $[\text{PbLH}_3]^{3-}$, $[\text{PbLH}_2]^{4-}$ and $[\text{PbLH}]^{5-}$ were successful (Table 5.2.6).

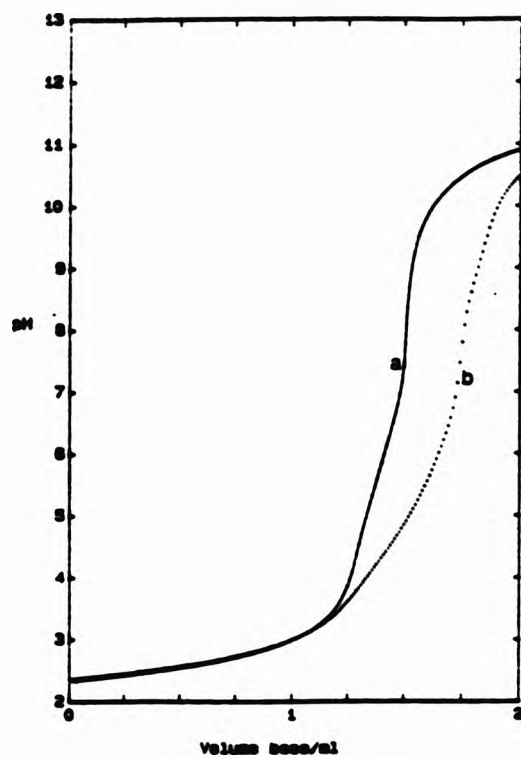


Figure 5.2.5 Titration curves (pH vs volume of base added) for acidified solutions of CDTMPH_3 ; (a) $[\text{CDTMPH}_3]$ ca. $0.0005 \text{ mol dm}^{-3}$; (b) $\text{Zn}(\text{NO}_3)_2$ with CDTMPH_3 , $[\text{M}]:[\text{L}]$ ca. 1:1.

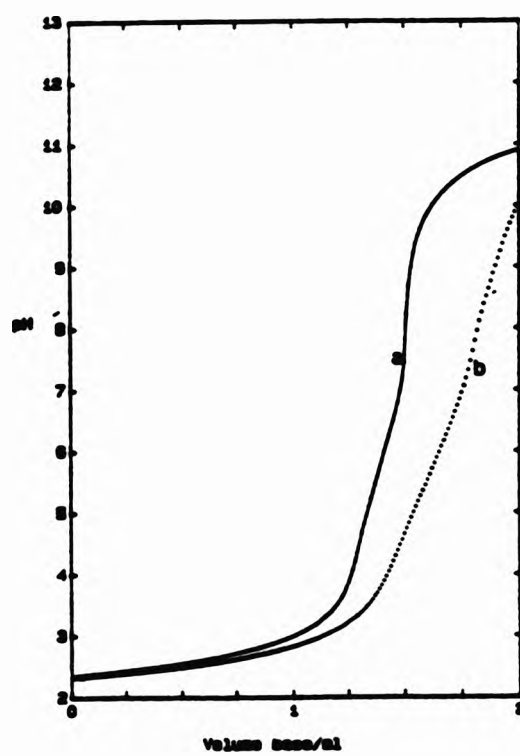


Figure 5.2.6 Titration curves (pH vs volume of base added) for acidified solutions of CDTMPH_3 ; (a) $[\text{CDTMPH}_3]$ ca. $0.0005 \text{ mol dm}^{-3}$; (b) $\text{Pb}(\text{NO}_3)_2$ with CDTMPH_3 , $[\text{M}]:[\text{L}]$ ca. 1:1.

Table 5.2.6 Stability constants for CDTMPH₃ with Pb(II).^a

Datafile [M]:[L]	TPb1 ^b 1:1.09	TPb2 ^c 1:0.99	TPb3 ^d 1:0.95	Mean ^e
log β ₁₁₀	10.51(0.093)	10.61(0.036)	10.66(0.038)	10.60 ±0.09
log β ₁₁₁	19.28(0.061)	19.43(0.025)	19.45(0.026)	19.39 ±0.11
log K ₁₁₁	8.77	8.82	8.79	8.79 ±0.03
log β ₁₁₂	26.13(0.045)	26.27(0.018)	26.28(0.019)	26.23 ±0.10
log K ₁₁₁	6.85	6.84	6.83	6.84 ±0.01
log β ₁₁₃	31.49(0.047)	31.64(0.020)	31.64(0.020)	31.61 ±0.12
log K ₁₁₃	5.36	5.37	5.36	5.36 ±0.01

^a The monoprotonated ligand (CDTMPH⁷⁻) is denoted as L; see text. Data obtained at I = 0.1 mol dm⁻³ KNO₃, 25.0 ±0.1 °C. Figures in parentheses are standard deviations obtained from SUPERQUAD. Convention: β_{MLH} for M_nL_mH_n. ^b Fit parameters obtained from SUPERQUAD, χ² = 10.64, σ = 0.0974; pH 4.65–9.49, 45 data points. ^c Fit parameters obtained from SUPERQUAD, χ² = 9.65, σ = 0.0394; pH 4.66–9.71, 43 data points. ^d Fit parameters obtained from SUPERQUAD, χ² = 6.74, σ = 0.0280; pH 4.75–9.46, 39 data points. ^e Unweighted mean of values from each refinement; error limits are derived from the ranges obtained from each log β_{MLH} (and log K_{MLH}).

5.2.1(g) Copper(II)

The three potentiometric titration curves obtained for CDTMPH₃ with Cu(II) were smooth and showed no signs of precipitation; one of the titration curves obtained is shown in Figure 5.2.7. Deviation of the 'metal-ligand' curve from the 'ligand-only' started at a much lower pH (2.5) than for CDTMPH₃ with the other divalent metals investigated in this work, suggesting greater stability of the Cu(II) complexes. The formation of the species [CuLH]⁵⁻ is inferred from the equivalents of base consumed by the metal-ligand system at pH ca. 9 [see Mn(II)].

Initial refinements of all three datafiles for a model which involved five species (i.e. MLH = 110, 111, 112, 113 and 114) was unsuccessful. Further refinement of the datafiles for a new model which excluded the species [MLH₅]⁻ was successful. These results are summarised in Table 5.2.7.

Table 5.2.7 Stability constants for CDTMPH₄ with Cu(II).^a

Datafile [M]:[L]	TCu1 ^b 1:1.08	TCu4 ^c 1:0.97	TCu5 ^d 1:1.04	Mean ^e
log β ₁₁₀	13.20(0.043)	13.36(0.035)	13.23(0.046)	13.26 ±0.10
log β ₁₁₁	21.70(0.032)	21.89(0.025)	21.72(0.033)	21.77 ±0.12
log K ₁₁₁	8.51	8.52	8.49	8.51 ±0.02
log β ₁₁₂	28.52(0.021)	28.66(0.018)	28.52(0.021)	28.57 ±0.09
log K ₁₁₁	6.81	6.77	6.80	6.79 ±0.02
log β ₁₁₃	33.11(0.023)	33.14(0.022)	33.03(0.019)	33.09 ±0.06
log K ₁₁₃	4.59	4.48	4.51	4.53 ±0.06

^a The monoprotonated ligand (CDTMPH⁷⁻) is denoted as L; see text. I = 0.1 mol dm⁻³ KNO₃, 25.0 ±0.1 °C. Figures in parentheses are standard deviations obtained from SUPERQUAD. Convention: β_{M_nL_nH_n} for M_nL_nH_n. ^b Fit parameters obtained from SUPERQUAD, χ² = 3.70, σ = 0.0602; pH 4.02–9.39, 43 data points. ^c Fit parameters obtained from SUPERQUAD, χ² = 6.28, σ = 0.0663; pH 3.86–10.02, 47 data points. ^d Fit parameters obtained from SUPERQUAD, χ² = 1.67, σ = 0.0762; pH 3.75–9.58, 48 data points. ^e Unweighted mean of values from each refinement; error limits are derived from the ranges obtained from each log β_{M_nL_nH_n} (and log K_{M_nL_nH_n}).

5.2.1(h) Gadolinium(III)

An imaging technique that is becoming widely used in medical diagnostic technology is magnetic resonance imaging (MRI).³⁶ In this technique, metal complexes (usually of lanthanide metals) are used as image enhancement agents, with complexes of gadolinium (III) being the most common used.

To be useful in MRI applications, a critically important feature of a metal complex is that it should have a high stability constant for binding between the metal ion and the ligand.³⁷ This can be achieved by using a multidentate ligand which is capable of coordinating to a metal ion *via* several ligating groups. The large number of ligands synthesised for use as MRI agents have usually contained nitrogen and oxygen donor atoms (e.g. α-aminomethylene-carboxylates). For example, the lanthanide complexes of the macrocyclic ligand 1,4,7,10-tetraazacyclododecane-1,4,7,10-tetraacetic acid (DOTA₄) are being thoroughly investigated as an MRI agent.³⁸

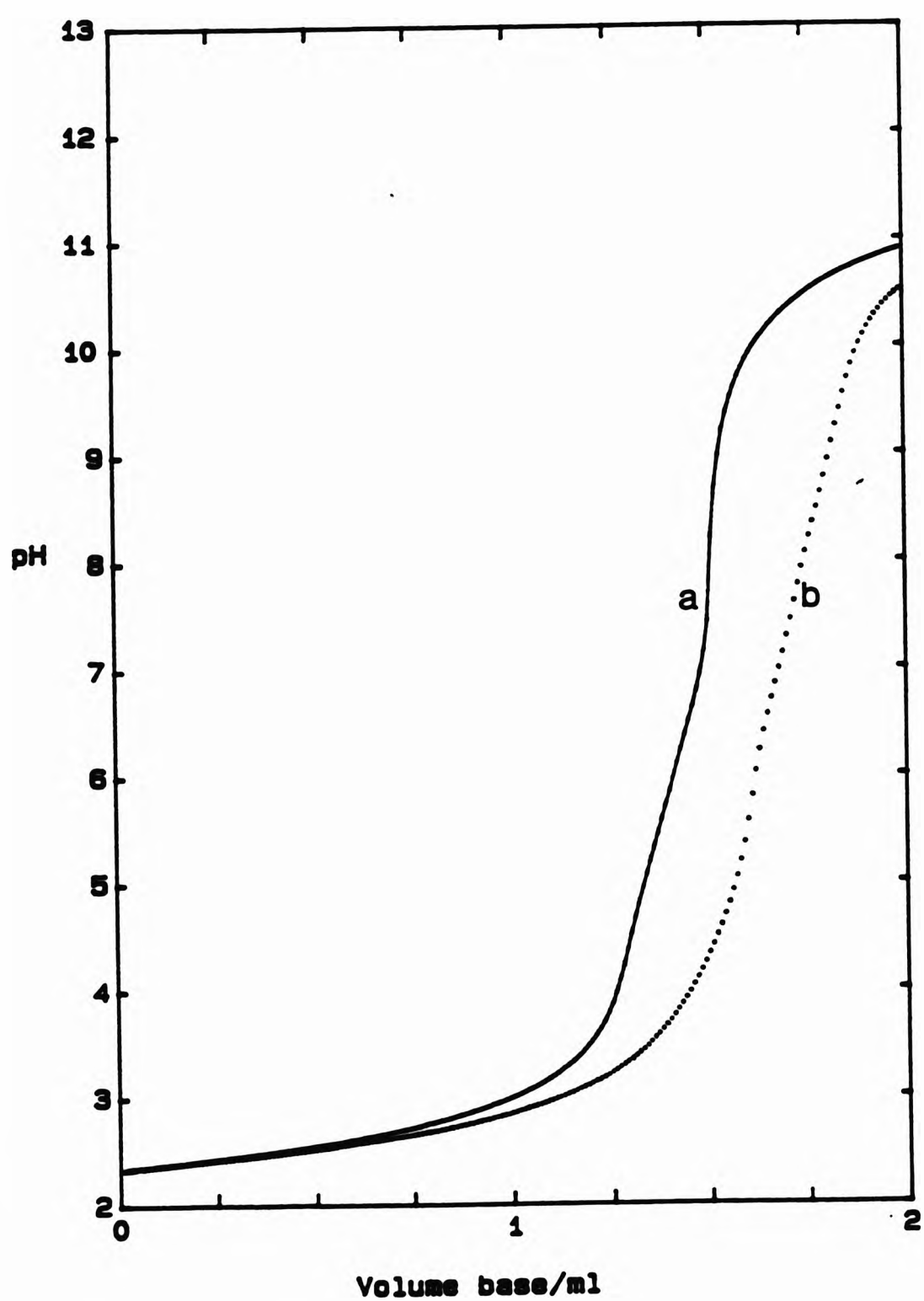
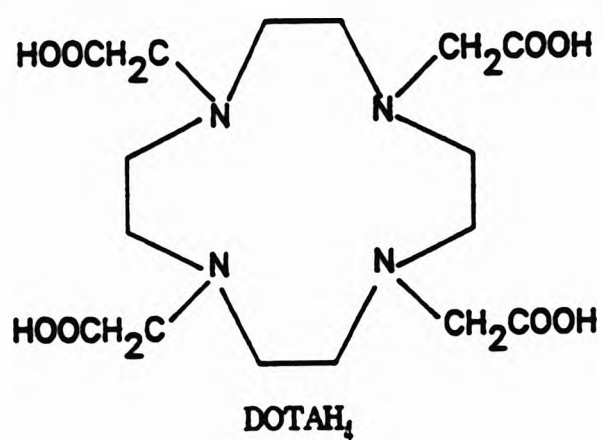


Figure 5.2.7 Titration curves (pH vs volume of base added) for acidified solutions of CDTMPH₃; (a) [CDTMPH₃] ca. 0.0005 mol dm⁻³; (b) Cu(NO₃)₂ with CDTMPH₃, [M]:[L] ca. 1:1.

Attention is now turning towards the complexation of the phosphorus analogs of carboxylic acids (*i.e.* aminophosphonic acids) with lanthanide metals such as Gd(III) for possible use as new MRI agents.³⁹⁻⁴⁰ Since CDTMPH₃ has the potential to coordinate to a metal ion *via* several functional groups and thereby form relatively stable complexes an investigation of the coordination behaviour of CDTMPH₃ with Gd(III) was undertaken.

Potentiometric titrations for CDTMPH₃ with Gd(III) at metal:ligand ratios of *ca.* 1:1, 1:2 and 1:3 were obtained. Three curves at metal:ligand ratios

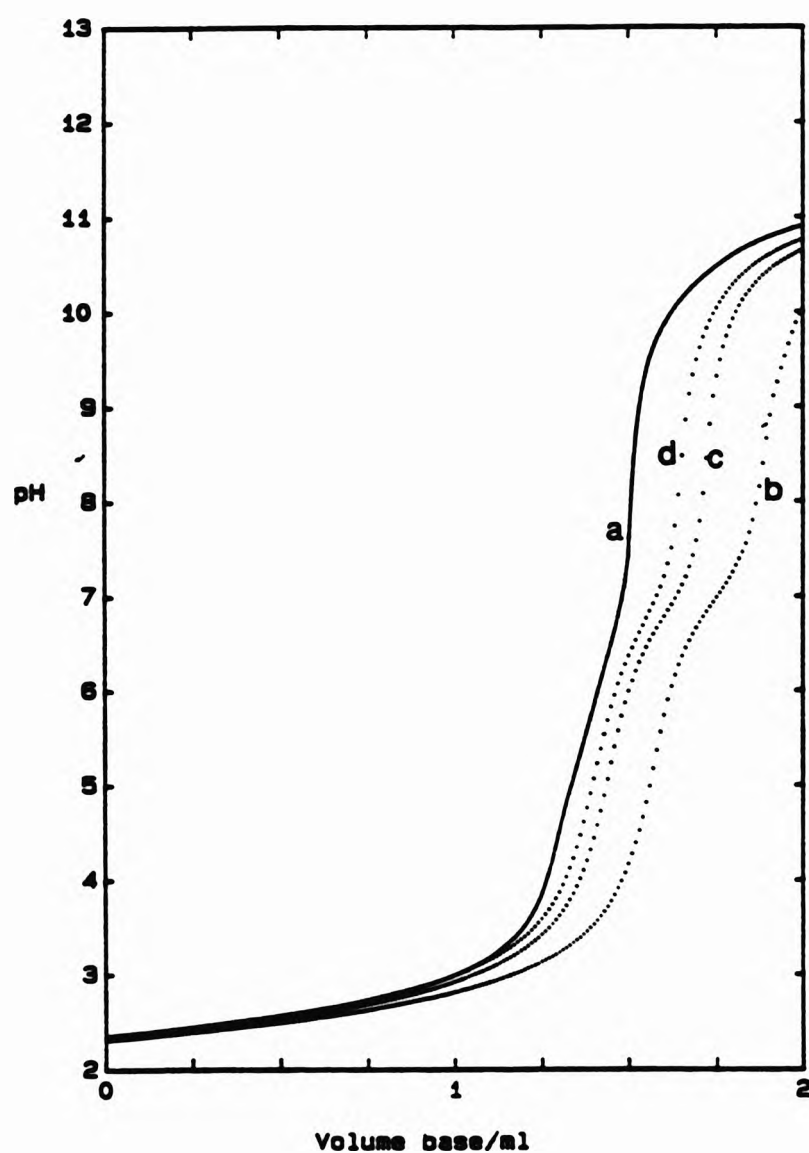


Figure 5.2.8 Titration curves (pH vs volume of base added) for acidified solutions of CDTMPH₃; (a) [CDTMPH₃] *ca.* 0.0005 mol dm⁻³; (b) Gd(NO₃)₃ with CDTMPH₃, [M]:[L] *ca.* 1:1; (c) Gd(NO₃)₃ with CDTMPH₃, [M]:[L] *ca.* 1:2; (d) Gd(NO₃)₃ with CDTMPH₃, [M]:[L] *ca.* 1:3.

of ca. 1:1, 1:2 and 1:3 are shown in Figure 5.2.8. The titration curves clearly show deviation of the 'metal-ligand' curve from the 'ligand-only' curve at low pH (> ca. 2.5) be ascribed to the excess nitric acid (Section 2.3.2) contained in the gadolinium stock solution. This excess acid in the

Table 5.2.8 Stability constants for CDTPH₃ with Gd(III).^a

Datafile	log β_{110}	log β_{11-1}	log β_{11-2}	χ^2	σ	[M]:[L]
TGd1	12.62(0.074)	5.13(0.102)		3.20 ^b	0.3488 ^b	1:0.91
TGd2	12.05(0.026)	4.56(0.062)		9.00 ^c	0.1226 ^c	1:2.07
	12.18(0.047)		-2.82(0.134)	5.57 ^d	0.0312 ^d	
	12.27(0.038)	constant	-2.67(0.102)	10.14 ^e	0.0283 ^e	
TGd5	12.02(0.032)	4.57(0.096)		5.00 ^f	0.1837 ^f	1:1.02
	12.80(0.106)		-2.04(0.172)	2.80 ^g	0.0685 ^g	
	12.60(0.084)	constant	-2.39(0.158)		0.0659 ^h	
TGd6	12.01(0.040)	4.43(0.143)		6.00 ⁱ	0.1957 ⁱ	1:1.91
	12.13(0.048)		-2.90(0.131)	7.33 ^j	0.0213 ^j	
	12.21(0.039)	constant	-2.76(0.120)	7.33 ^k	0.0194 ^k	
TGd8	11.97(0.020)	4.51(0.049)		6.11 ^l	0.0377 ^l	1:2.84
	12.19(0.057)		-2.80(0.170)	12.60 ^m	0.0203 ^m	
	12.25(0.048)	constant	-2.70(0.170)	12.60 ⁿ	0.0183 ⁿ	
Average ^o	log β_{110}	log β_{11-1}	log K_{11-1}	log β_{11-2}	log K_{11-2}	
	12.25 ± 0.55	4.64 ± 0.49	-7.63	-2.64 ± 0.60	-14.91	

^a The monoprotonated ligand (CDTPH⁷⁻) is denoted as L; see text. Data obtained at I = 0.1 mol dm⁻³ KNO₃, 25.0 ± 0.1 °C. The following Gd(III) hydrolysis constants^{16(c),17} were added to the SUPERQUAD input files; log β_{10-1} = -8.00, log β_{10-2} = -15.60, log β_{10-3} = -25.20, log β_{10-4} = -37.00. Convention: β_{MLH} for $M_nL_nH_n$. ^b pH 6.44-8.76, 20 data points. ^c pH 6.63-8.82, 15 data points. ^d pH 6.69-7.11, 7 data points. ^e pH 6.69-7.11, 7 data points. ^f pH 6.74-8.16, 7 data points. ^g pH 6.74-7.20, 10 data points. ^h pH 6.68-7.15, 10 data points. ⁱ pH 6.57-9.01, 17 data points. ^j pH 6.75-7.11, 6 data points. ^k pH 6.75-7.11, 6 data points. ^l pH 6.79-8.36, 9 data points. ^m pH 6.72-7.08, 5 data points. ⁿ pH 6.72-7.08, 5 data points. ^o Unweighted mean of values from each refinement; error limits are derived from the ranges obtained from each log β_{MLH} (and log K_{MLH}).

metal stock solution is to prevent the metal hydrolysing on storage. In

addition, there is further deviation between the 'metal-ligand' curve and 'ligand-only' curves above pH ca. 3.5, suggesting the formation of protonated metal complex species. However, refinement of datafile TGd1 for a model which involved the species 110, 111 and 112 was unsuccessful.

If four metal hydrolysis constants were placed into the SUPERQUAD input files as constants: $\log \beta_{10-1} = -8.00$ {for $\text{Gd}(\text{OH})^{2+}$ }, $\log \beta_{10-2} = -15.60$ {for $\text{Gd}(\text{OH})_2^+$ }, $\log \beta_{10-3} = -25.20$ {for $\text{Gd}(\text{OH})_3$ }, $\log \beta_{10-4} = -37.00$ {for $\text{Gd}(\text{OH})_4^-$ }^{16(c),17} successful refinements for datafiles were obtained for models variously involving the species [GdLH], [GdL] and [GdL(OH)]. The results are reported in Table 5.2.8 in the manner of Brown *et al.*;⁴¹ where a value appears under a particular $\log \beta$, that species was included in the model for refinement.

5.2.2 Stability constants for metal ion complexes with DDDTMPH₃

The complexing properties of DDDTMPH₃ (Section 2.2.4) with four metals were examined: Pb(II), Cd(II), Zn(II) and Cu(II). For Cu(II), Cd(II) and Pb(II), three potentiometric titrations were obtained at a metal:ligand ratio of ca. 1:1. For Zn(II), five titrations were obtained variously at metal:ligand ratios of ca. 1:1 or ca. 1:2.

The previously determined protonation constants (Section 4.5) for DDDTMPH₃ were held as constant in the SUPERQUAD¹⁰ input files, and with subsequent refinement of the datafiles, the metal-complex stability constants were obtained. Since the first protonation constant of DDDTMPH₃⁸⁻ was not determined potentiometrically (Section 4.6), L was defined, for use in the SUPERQUAD program, as the monoprotonated species DDDTMPH₃⁷⁻.

5.2.2(a) Copper(II)

One of the three potentiometric titration curves obtained for DDDTMPH₃ with Cu(II) is shown in Figure 5.2.9. There is considerable deviation of the metal-ligand curve from the ligand-only curve from ca. pH 3.5 upwards suggesting that the complexes formed are more stable than those for DDDTMPH₃ with the other metals examined in this work. The end-point on the titration curve at pH ca. 8 represents the metal-ligand system consuming ca. seven equivalents of base, *i.e.* one greater than in the ligand-only system at the end-point at this pH. This is taken as evidence for the formation of the species [MLH]⁵⁻, in this region.

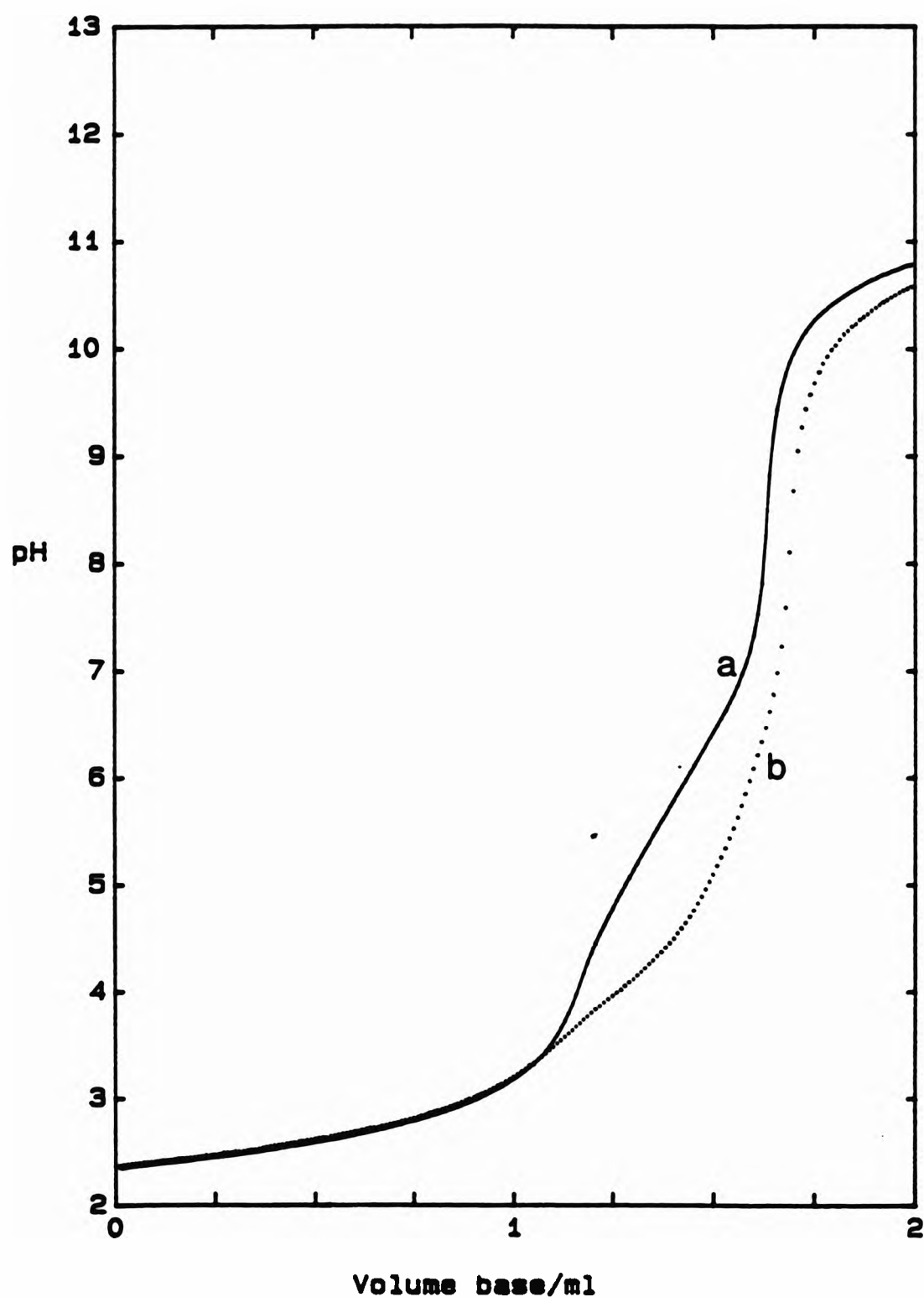


Figure 5.2.9 Titration curves (pH vs volume of base added) for acidified solutions of DDDTMPH₃ (a) [DDDTMPH₃] ca. 0.0005 mol dm⁻³; (b) Cu(NO₃)₂ with DDDTMPH₃, [M]:[L] ca. 1:1.

Refinements of datafiles (PCu1 and PCu2) for a model which only involved the species [MLH]⁵⁻, [MLH₂]⁴⁻, [MLH₃]³⁻, [MLH₄]²⁻ and [MLH₅]⁻ were successful. One titration curve showed clear signs of precipitation of either the metal complexes or metal hydrolysis products at ca. pH 9.5 and higher and a successful refinement of this datafile for a model involving the species

$[\text{MLH}_2^-]$, $[\text{MLH}_4^{2-}]$, $[\text{MLH}_3^{3-}]$, $[\text{MLH}_2^{4-}]$ and $[\text{MLH}]^{5-}$ was achieved by limiting the data to the region of pH below that at which hydrolysis had become evident in the titration curve. The stability constants are summarised in Table 5.2.9.

Table 5.2.9 Stability constants for DDDTMPH₅ with Cu(II).^a

Datafile	PCu1 ^b	PCu2 ^c	PCu3 ^d	Mean ^e
[M]:[L]	1:0.91	1:1.00	1:0.97	
log β_{110}	13.36(0.021)	13.19(0.037)	13.31(0.038)	13.29 ±0.10
log β_{111}	20.03(0.013)	19.95(0.024)	20.01(0.023)	19.99 ±0.05
log K_{111}	6.67	6.77	6.70	6.71 ±0.06
log β_{112}	25.40(0.010)	25.44(0.017)	25.44(0.017)	25.43 ±0.03
log K_{112}	5.37	5.49	5.43	5.43 ±0.06
log β_{113}	29.75(0.005)	29.81(0.010)	29.79(0.009)	29.78 ±0.03
log K_{113}	4.35	4.37	4.35	4.36 ±0.01
log β_{114}	32.94(0.051)	33.16(0.052)	33.11(0.057)	33.07 ±0.13
log K_{114}	3.18	3.36	3.32	3.29 ±0.11

^a The monoprotonated ligand (DDDTMPH⁷⁻) is denoted as L; see text. Data obtained at I = 0.1 mol dm⁻³ KNO₃, 25.0 ±0.1 °C. Figures in parentheses are standard deviations obtained from SUPERQUAD. Convention: β_{MLH} for $M_nL_mH_p$. ^b Fit parameters obtained from SUPERQUAD, $\chi^2 = 5.05$, $\sigma = 0.0354$; pH 2.96–6.34, 76 data points. ^c Fit parameters obtained from SUPERQUAD, $\chi^2 = 7.78$, $\sigma = 0.0388$; pH 3.10–6.40, 72 data points. ^d Fit parameters obtained from SUPERQUAD, $\chi^2 = 7.17$, $\sigma = 0.0383$; pH 3.10–6.20, 69 data points. ^e Unweighted mean of values from each refinement; error limits are derived from the ranges obtained from each log β_{MLH} (and log K_{MLH}).

5.2.2(b) Zinc(II)

One out of the five potentiometric titration curves obtained for DDDTMPH₅ with Zn(II) (PZn2) showed evidence of precipitation at and above pH ca. 9. One example of the titration curves with no precipitation is shown in Figure 5.2.10. The deviation of the metal–ligand curve from the ligand-only curve occurs at pH ca. 3 with ca. 6.5–7 equivalents of base have been consumed by the end-point on the titration curve at pH ca. 9 (for curves where [Zn]:[L] is ca. 1:1). This suggests that the formation of $[\text{ZnLH}]^{5-}$ in this region [Section 5.2.2(a)].

Successful refinements of datafiles, PZn1, PZn3, PZn4 and PZn5 for a model which only involved the species $[\text{MLH}]^{5-}$, $[\text{MLH}_2]^{4-}$, $[\text{MLH}_3]^{3-}$ and $[\text{MLH}_4]^{2-}$ were obtained (Table 5.2.10). A separate refinement of datafile PZn2 for a model involving species with a metal:ligand ratio of 1:2 was unsuccessful, as were refinements for datafile PZn1 for a model with species having a metal:ligand ratio of 2:1 (*i.e.* $[\text{ML}_2\text{H}_2]^{-12}$, $[\text{ML}_2\text{H}_3]^{-11}$, $[\text{ML}_2\text{H}_4]^{-10}$).

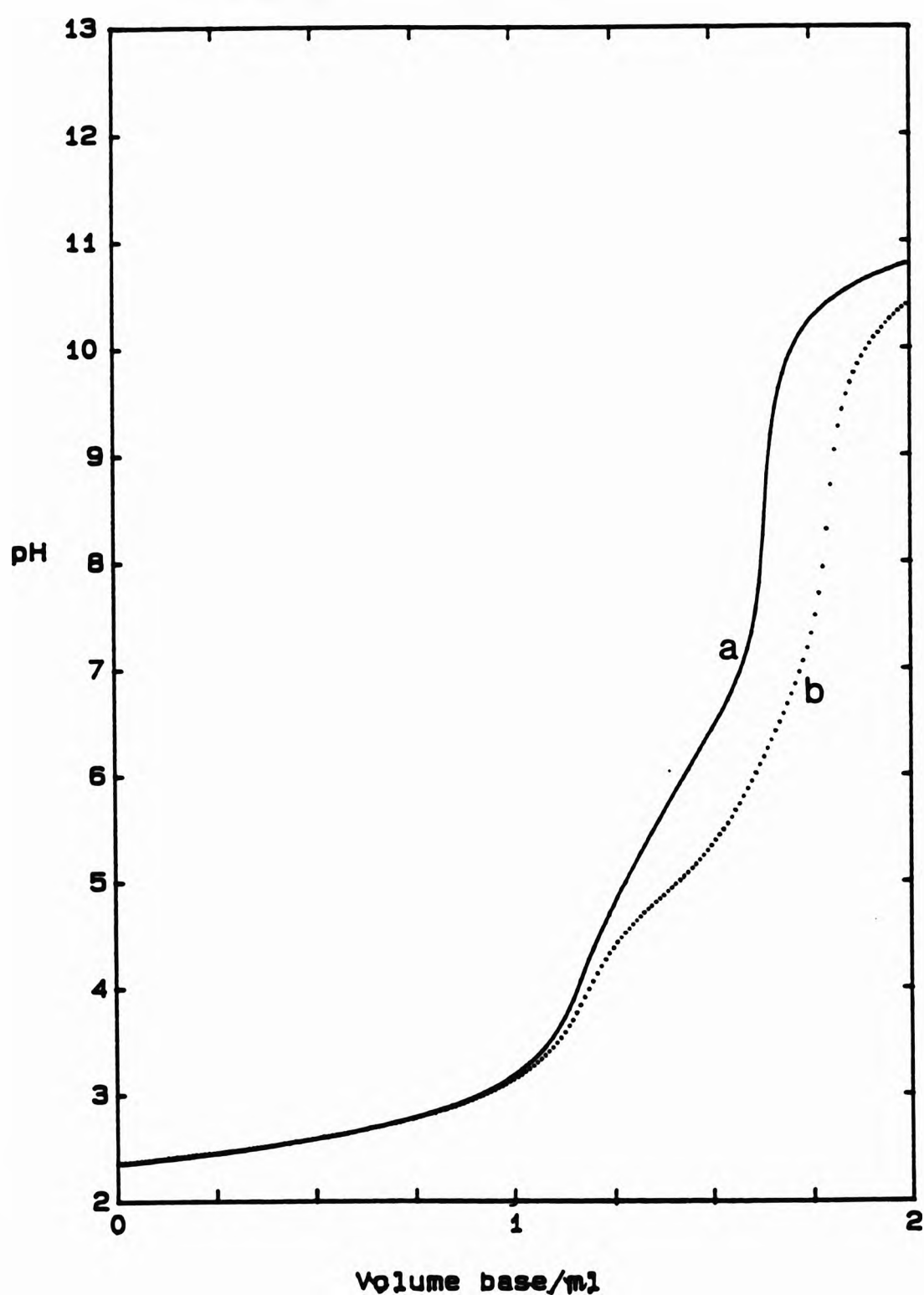


Figure 5.2.10 Titration curves (pH vs volume of base added) for acidified solutions of DDDTMPH₃ (a) [DDDTMPH₃] ca. 0.0005 mol dm⁻³; (b) Zn(NO₃)₂ with DDDTMPH₃, [M]:[L] ca. 1:1.

Table 5.2.10 Stability constants for DDDTMPH₃ with Zn(II).^a

Datafile	PZn1 ^b	PZn2 ^c	PZn3 ^d	PZn4 ^e	PZn5 ^f	Mean ^g
[M]:[L]	1:1.03	1:2.00	1:1.77	1:0.93	1:0.96	
log β ₁₁₀	9.89 (0.007)	9.71 (0.012)	9.68 (0.017)	9.93 (0.010)	9.98 (0.006)	9.84 ±0.16
log β ₁₁₁	17.13 (0.005)	16.83 (0.009)	16.94 (0.012)	17.16 (0.007)	17.25 (0.004)	17.06 ±0.23
log K ₁₁₁	7.24	7.12	7.26	7.23	7.27	7.22 ±0.10
log β ₁₁₂	23.17 (0.003)	23.03 (0.005)	23.08 (0.006)	23.16 (0.004)	23.21 (0.002)	23.13 ±0.10
log K ₁₁₂	6.03	6.19	6.15	6.00	5.96	6.06 ±0.13
log β ₁₁₃	27.73 (0.010)	27.78 (0.014)	27.81 (0.020)	27.72 (0.015)	27.67 (0.009)	27.74 ±0.07
log K ₁₁₃	4.56	4.76	4.73	4.56	4.46	4.61 ±0.15

^a The monoprotonated ligand (DDDTMPH⁷⁻) is denoted as L; see text. Data obtained at I = 0.1 mol dm⁻³ KNO₃, 25.0 ±0.1 °C. Figures in parentheses are standard deviations obtained from SUPERQUAD. Convention: β_{MLH} for M_nL_mH_n. ^b Fit parameters obtained from SUPERQUAD, χ² = 10.59, σ = 0.0375; pH 3.33–7.19, 68 data points. ^c Fit parameters obtained from SUPERQUAD, χ² = 5.33, σ = 0.0350; pH 3.34–7.00, 60 data points. ^d Fit parameters obtained from SUPERQUAD, χ² = 10.59, σ = 0.0439; pH 3.44–7.25, 54 data points. ^e Fit parameters obtained from SUPERQUAD, χ² = 2.57, σ = 0.0521; pH 3.24–7.07, 65 data points. ^f Fit parameters obtained from SUPERQUAD, χ² = 2.40, σ = 0.0279; pH 3.45–7.00, 60 data points. ^g Unweighted mean of values from each refinement; error limits are derived from the ranges obtained from each log β_{MLH} (and log K_{MLH}).

5.2.2(c) Cadmium(II)

Two of the three datafiles obtained for DDDTMPH₃ with Cd(II) (*i.e.* datafiles PCd2 and PCd3) showed signs of precipitation above *ca.* pH 9. The titration curve for datafile PCd1 is shown in Figure 5.2.11. Deviation of the 'metal-ligand' curve from that of the 'ligand-only' curve occurs above a pH of *ca.* 4, and with *ca.* seven equivalents of base are consumed by the 'metal-ligand' system by the end-point at pH *ca.* 9. This infers the formation of the monoprotonated species [CdLH]⁵⁻ in this pH region.

Successful refinements was obtained for the titration datafiles for a model which only involved species with a metal:ligand ratio of 1:1 (Table 5.2.11).

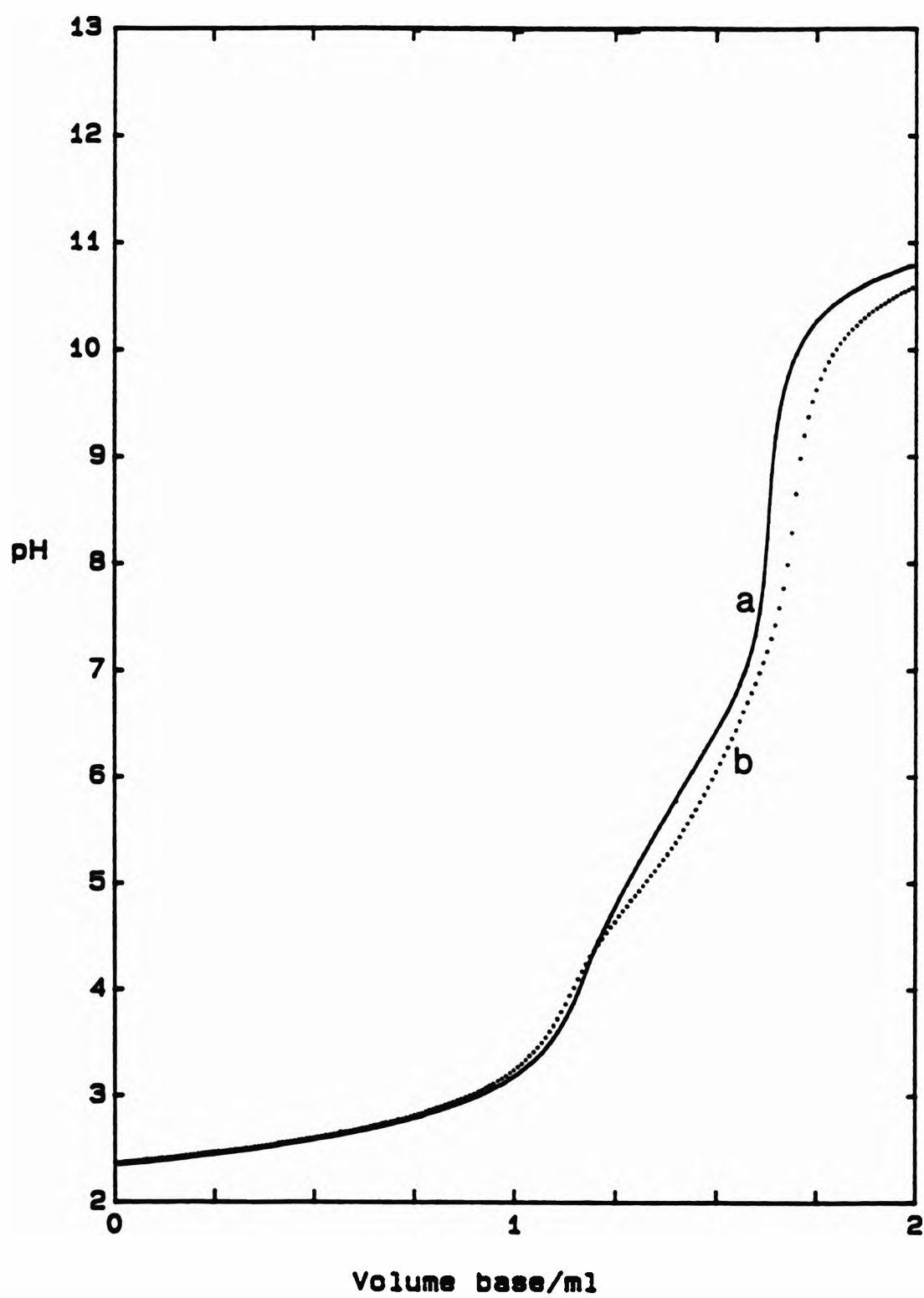


Figure 5.2.11 Titration curves (pH vs volume of base added) for acidified solutions of DDDTMPH_3 (a) $[\text{DDDTMPH}_3]$ ca. $0.0005 \text{ mol dm}^{-3}$; (b) $\text{Cd}(\text{NO}_3)_2$ with DDDTMPH_3 , $[\text{M}]:[\text{L}]$ ca. 1:1.

Table 5.2.11 Stability constants for DDDTMPH₃ with Cd(II).^a

Datafile	PCd1 ^b	PCd2 ^c	PCd3 ^d	Mean ^e
[M]:[L]	1:0.92	1:0.99	1:0.91	
log β ₁₁₀	9.25(0.006)	9.22(0.021)	9.33(0.011)	9.27 ±0.06
log β ₁₁₁	16.56(0.005)	16.58(0.016)	16.60(0.008)	16.58 ±0.02
log K ₁₁₁	7.31	7.36	7.27	7.31 ±0.05
log β ₁₁₂	22.83(0.003)	22.82(0.012)	22.83(0.006)	22.83 ±0.01
log K ₁₁₂	6.27	6.25	6.23	6.25 ±0.02
log β ₁₁₃	28.00(0.005)	28.05(0.018)	28.00(0.010)	28.02 ±0.03
log K ₁₁₃	5.17	5.23	5.17	5.19 ±0.04

^a The monoprotonated ligand (DDDTMPH⁷⁻) is denoted as L; see text. Data obtained at I = 0.1 mol dm⁻³ KNO₃, 25.0 ±0.1 °C. Figures in parentheses are standard deviations obtained from SUPERQUAD. Convention: β_{MLH} for M_nL_mH_p. ^b Fit parameters obtained from SUPERQUAD, χ² = 4.94, σ = 0.0305; pH 3.27-7.18, 63 data points. ^c Fit parameters obtained from SUPERQUAD, χ² = 2.40, σ = 0.1369; pH 3.11-8.33, 80 data points. ^d Fit parameters obtained from SUPERQUAD, χ² = 5.11, σ = 0.0623; pH 3.20-8.41, 72 data points. ^e Unweighted mean of values from each refinement; error limits are derived from the ranges obtained from each log β_{MLH} (and log K_{MLH}).

5.2.2(d) Lead(II)

The potentiometric titrations for DDDTMPH₃ with Pb(II) showed no evidence of precipitation. One of the three titration curves is shown in Figure 5.2.12. The titration curves for DDDTMPH₃ with Pb(II) show deviation of the 'metal-ligand' curve from the 'ligand-only' curve above ca. pH 3.5. Approximately seven equivalents of base are consumed by the metal-ligand system by an endpoint at ca. pH 9, suggesting the formation of [PbLH]⁵⁻.

Refinements of each datafile for a model which involved only species with a metal:ligand ratio of 1:1 (i.e. [MLH]⁵⁻, [MLH₂]⁴⁻, [MLH₃]³⁻ and [MLH₄]²⁻) were successful (Table 5.2.12).

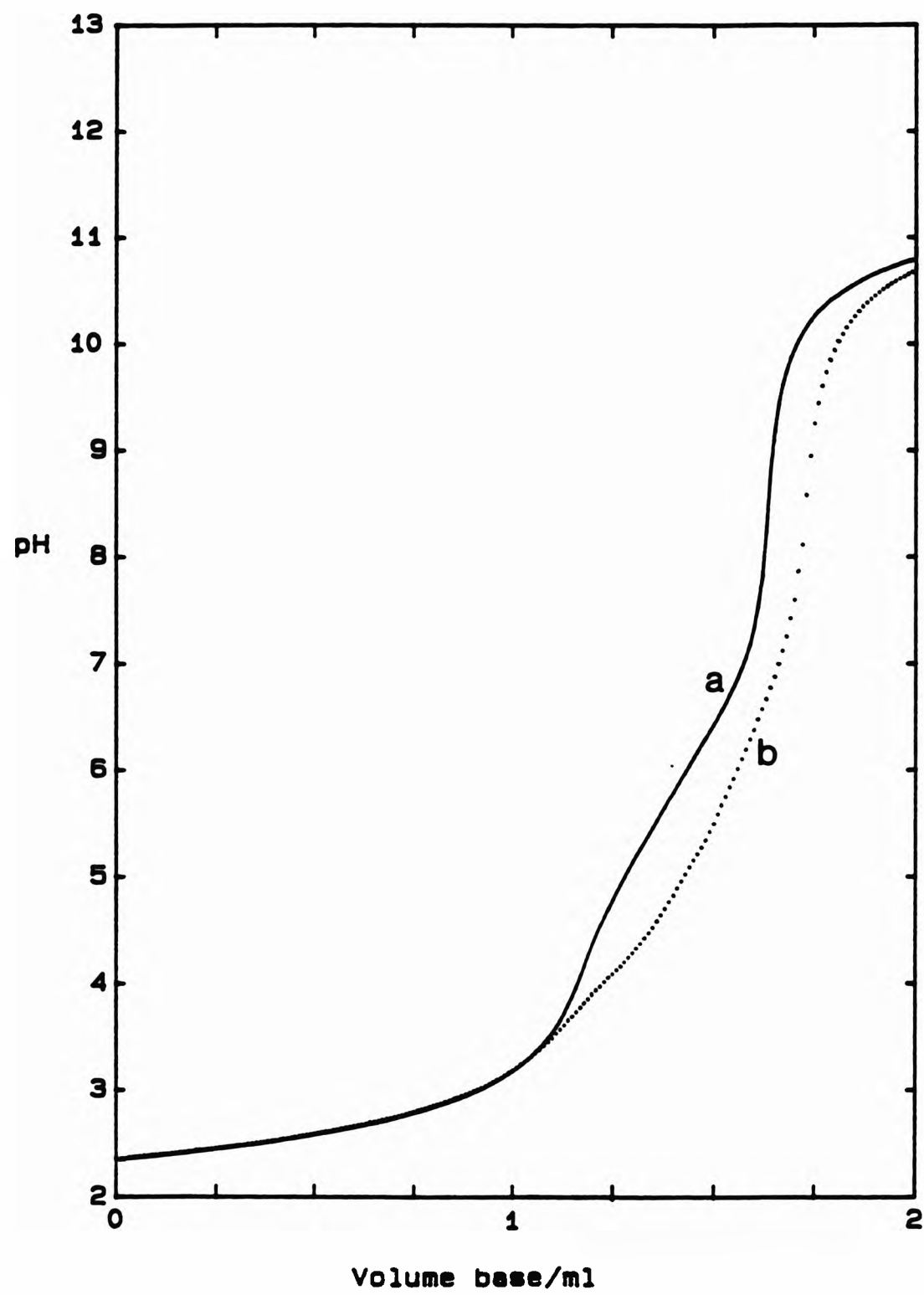


Figure 5.2.12 Titration curves (pH vs volume of base added) for acidified solutions of DDDTMPH₃ (a) [DDDTMPH₃] ca. 0.0005 mol dm⁻³; (b) Pb(NO₃)₂ with DDDTMPH₃, [M]:[L] ca. 1:1.

Table 5.2.12 Stability constants for DDDTMPH₃ with Pb(II).^a

Datafile	PPb1 ^b	PPb2 ^c	PPb3 ^d	Mean ^e
[M]:[L]	1:0.97	1:0.93	1:0.95	
log β ₁₁₀	10.72(0.022)	10.83(0.021)	10.75(0.025)	10.77 ±0.05
log β ₁₁₁	18.12(0.014)	18.20(0.014)	18.12(0.017)	18.15 ±0.05
log K ₁₁₁	7.40	7.37	7.37	7.38 ±0.02
log β ₁₁₂	24.24(0.010)	24.28(0.010)	24.23(0.012)	24.25 ±0.03
log K ₁₁₂	6.12	6.08	6.11	6.10 ±0.02
log β ₁₁₃	29.35(0.007)	29.36(0.007)	29.33(0.009)	29.35 ±0.02
log K ₁₁₃	5.11	5.09	5.10	5.10 ±0.01

^a The monoprotonated ligand (DDDTMPH⁷⁻) is denoted as L; see text. Data obtained at I = 0.1 mol dm⁻³ KNO₃, 25.0 ±0.1 °C. Figures in parentheses are standard deviations obtained from SUPERQUAD. Convention: β_{MLH} for M_nL_mH_n. ^b Fit parameters obtained from SUPERQUAD, χ² = 8.00, σ = 0.0775; pH 3.19–7.13, 68 data points. ^c Fit parameters obtained from SUPERQUAD, χ² = 9.11, σ = 0.0851; pH 3.11–7.25, 71 data points. ^d Fit parameters obtained from SUPERQUAD, χ² = 2.90, σ = 0.0759; pH 3.32–7.22, 63 data points. ^e Unweighted mean of values from each refinement; error limits are derived from the ranges obtained from each log β_{MLH} (and log K_{MLH}).

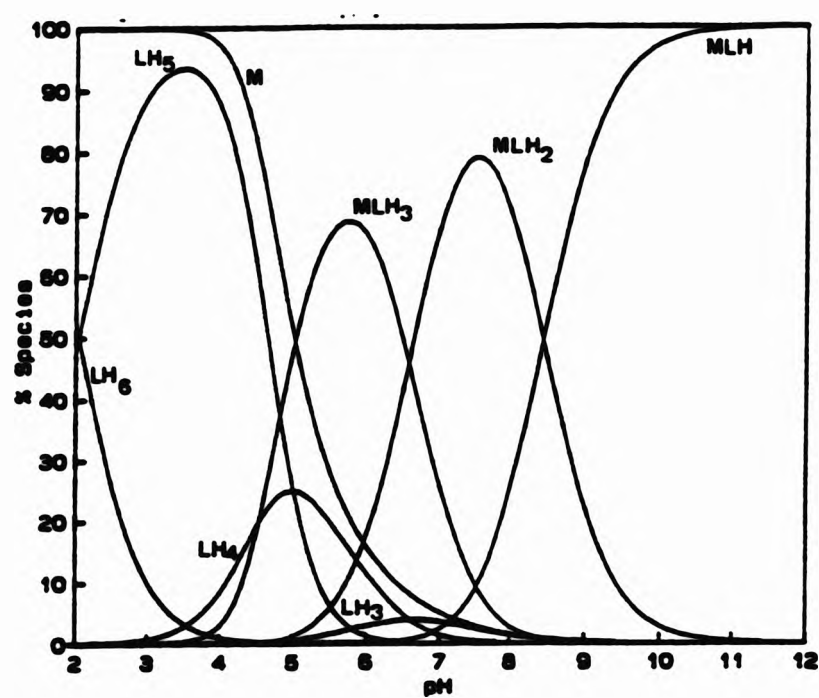
5.2.3 Species distribution plots of some metals with CDTMPH₃ and DDDTMPH₃

The species distribution curves¹⁸ obtained for CDTMPH₃ with the metal ions examined in this work are valid in the pH range based on the data used in refinements for protonation and stability constants, as mentioned in section 5.2.1. For the metal ions Co(II), Ni(II), Pb(II) and Cu(II) the valid pH region is between 3 and 10; and for the ions Mn(II) and Zn(II) it is between pH 3 and 9.

The species distribution curves obtained for CDTMPH₃ with the metal ions Mn(II) and Co(II) are similar with only three metal-ligand species, *i.e.* [MLH]⁵⁻, [MLH₂]⁴⁻ and [MLH₃]³⁻ determined from the refinements of the datafiles. Whereas the species distribution curves for the metal ions Ni(II), Cu(II), Zn(II) and Pb(II) are in themselves similar but are different to the curves for Mn(II) and Co(II), because four metal-ligand species were determined from the

refinements. However, most of the divalent metal ions are sequestered above pH 5-6, with the metal-ligand species dominating the region above this pH.

(a)



(b)

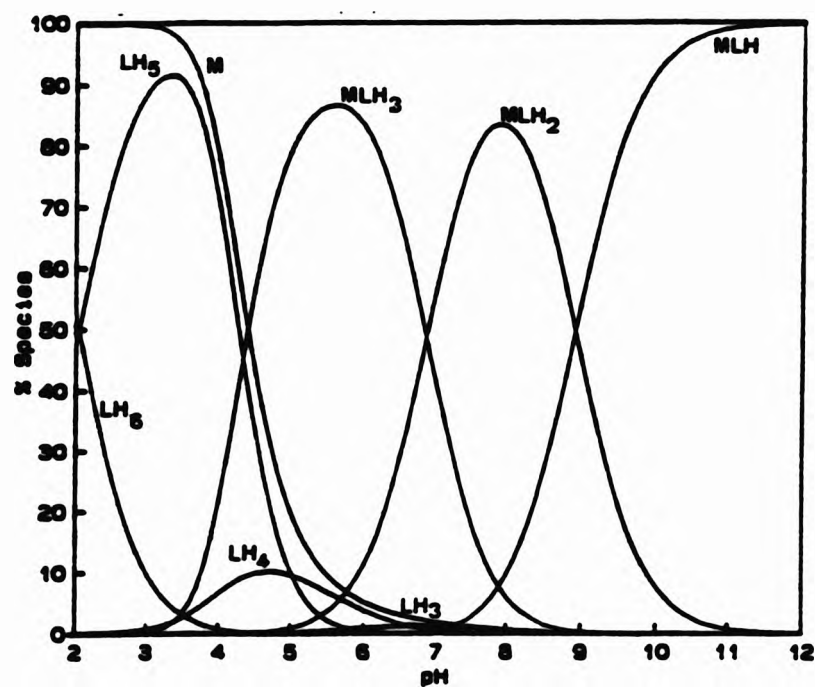
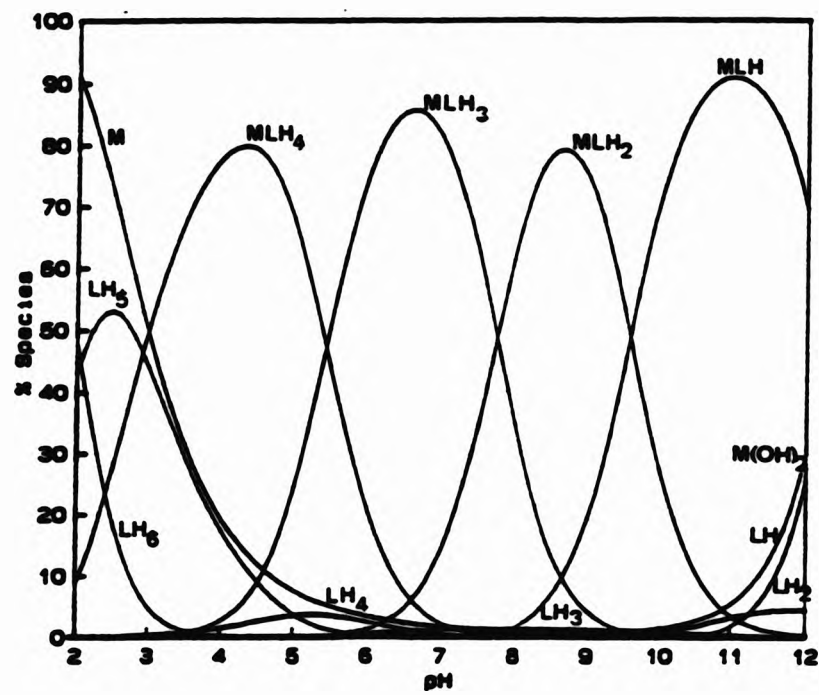


Figure 5.2.13 Species distribution curves¹⁸ for CDTMPH₃ with metal ions at [M]:[L] ca. 1:1 (a) with Mn(II) and (b) with Co(II).

(c)



(d)

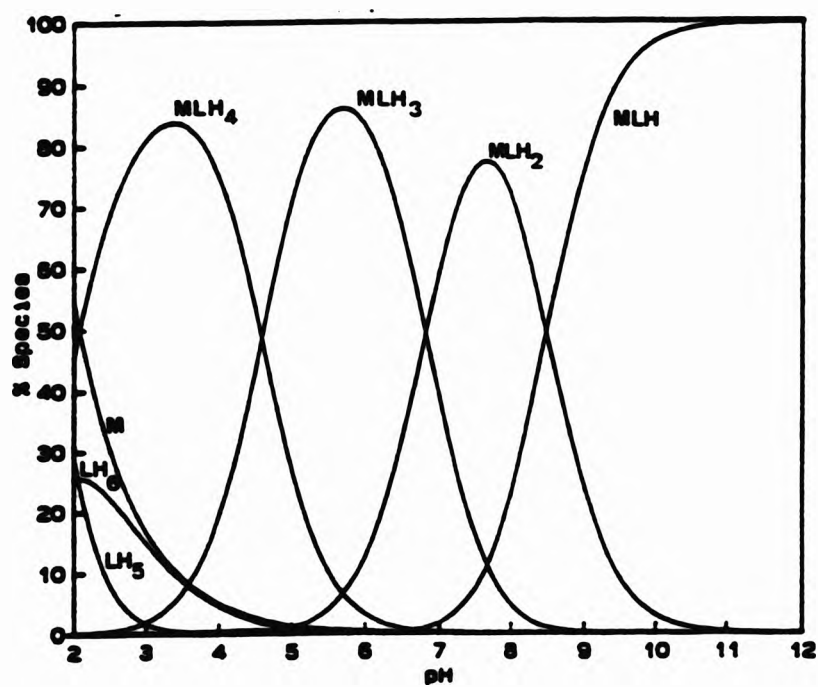
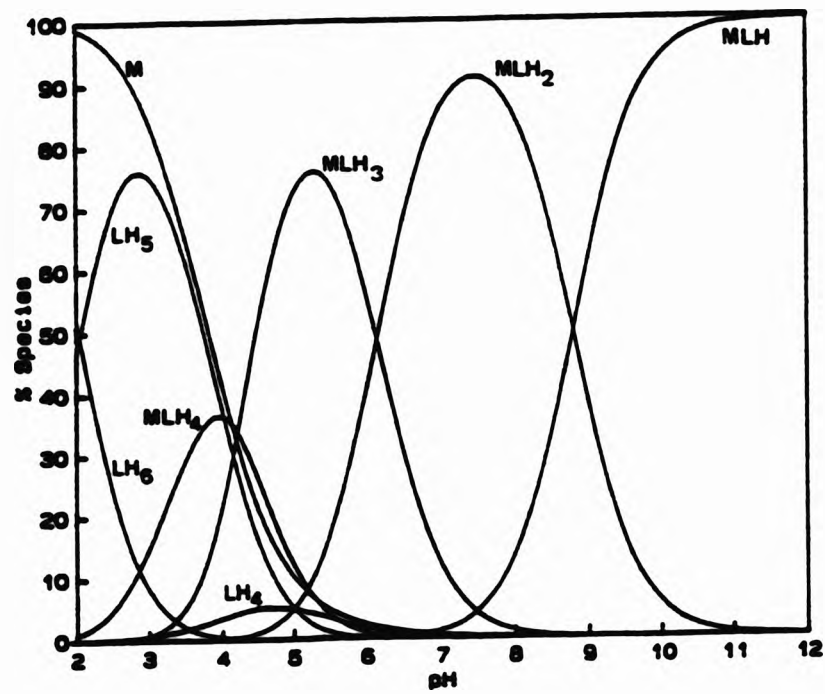


Figure 5.2.13, continued. Species distribution curves¹⁸ for CDTMPH₅ with metal ions at [M]:[L] ca. 1:1 (c) with Ni(II) and (d) with Cu(II).

(e)



(f)

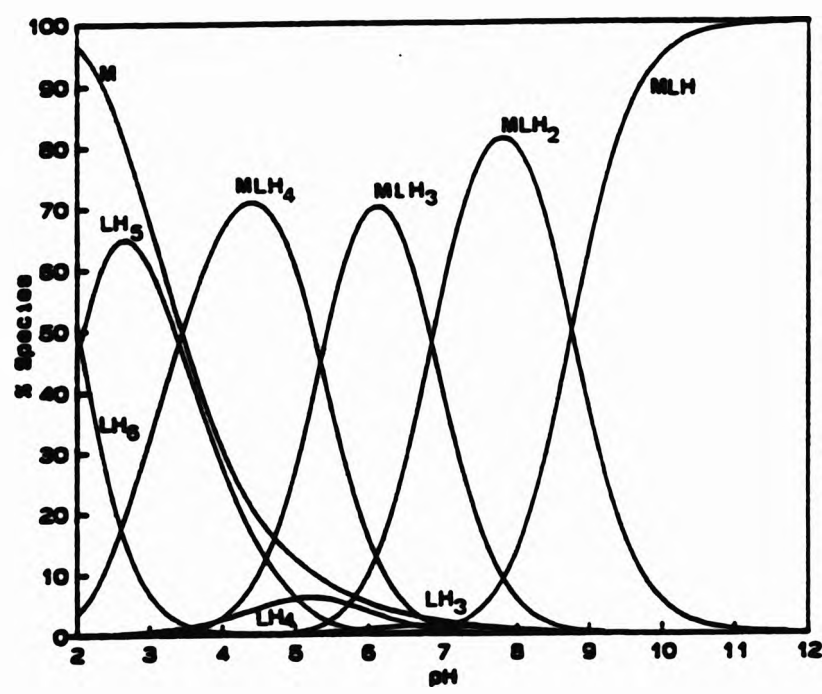
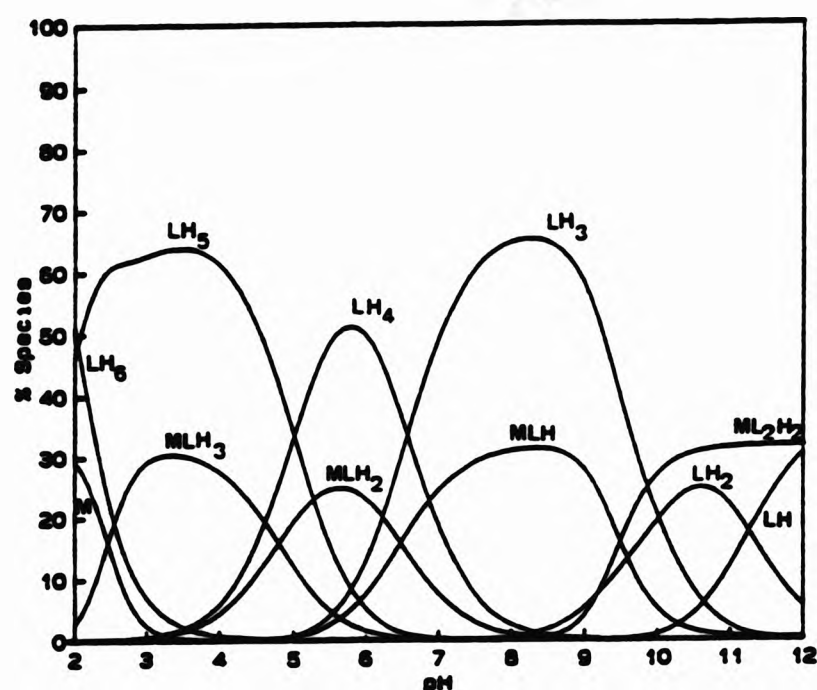


Figure 5.2.13, continued. Species distribution curves¹⁸ for CDTMPH₃ with metal ions at [M]:[L] ca. 1:1 (f) with Zn(II) and (g) with Pb(II).

Fe(III) is known to catalyse the decomposition of *aqueous* solutions of hydrogen peroxide and therefore the sequestration of this metal is important. The species distribution curves for CDTMPH₃ with Fe(III) are, as expected, different to the curves for CDTMPH₃ with the divalent metal ions determined in this work. The valid pH range for the curves computed for CDTMPH₃ with Fe(III) is between 3 and 9. Most of the metal ion [Fe(III)] is complexed by ca. pH 3 and above pH ca. 10, the species [FeL₂H₂]⁻¹² is becoming important.

(g)



(h)

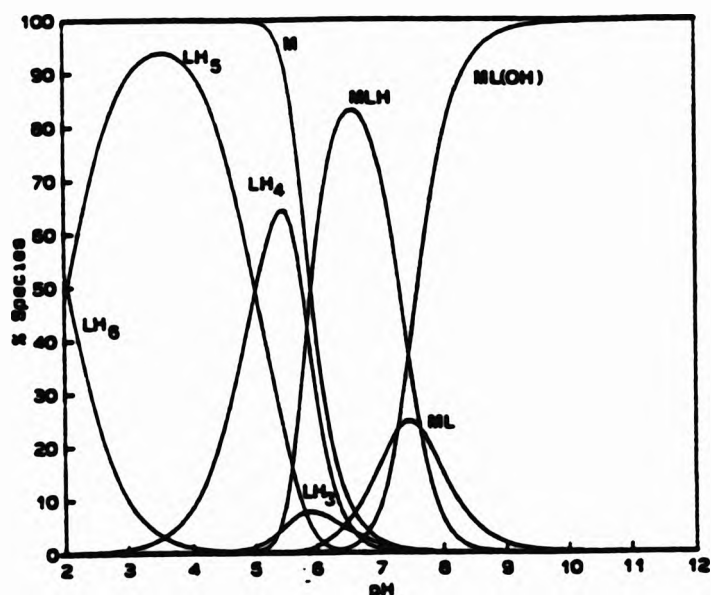


Figure 5.2.13, continued. Species distribution curves¹⁸ for CDTMPH₃ (g) Fe(III) at [M]:[L] of ca. 1:3 and (h) Gd(III) at [M]:[L] of ca. 1:1.

The valid pH range for the species distribution curves obtained for CDTMPH₃ with for Gd(III) [Figure 5.2.13(h) are between pH 3 and 8. The Gd(III) ion does not complex until pH ca. 6.5-7 which coincides with the formation of the monoprotonated species [GdLH]⁴⁻. Thereafter, deprotonated species appear to be important, *i.e.* [GdL]⁵⁻ and [GdL(OH)]⁶⁻.

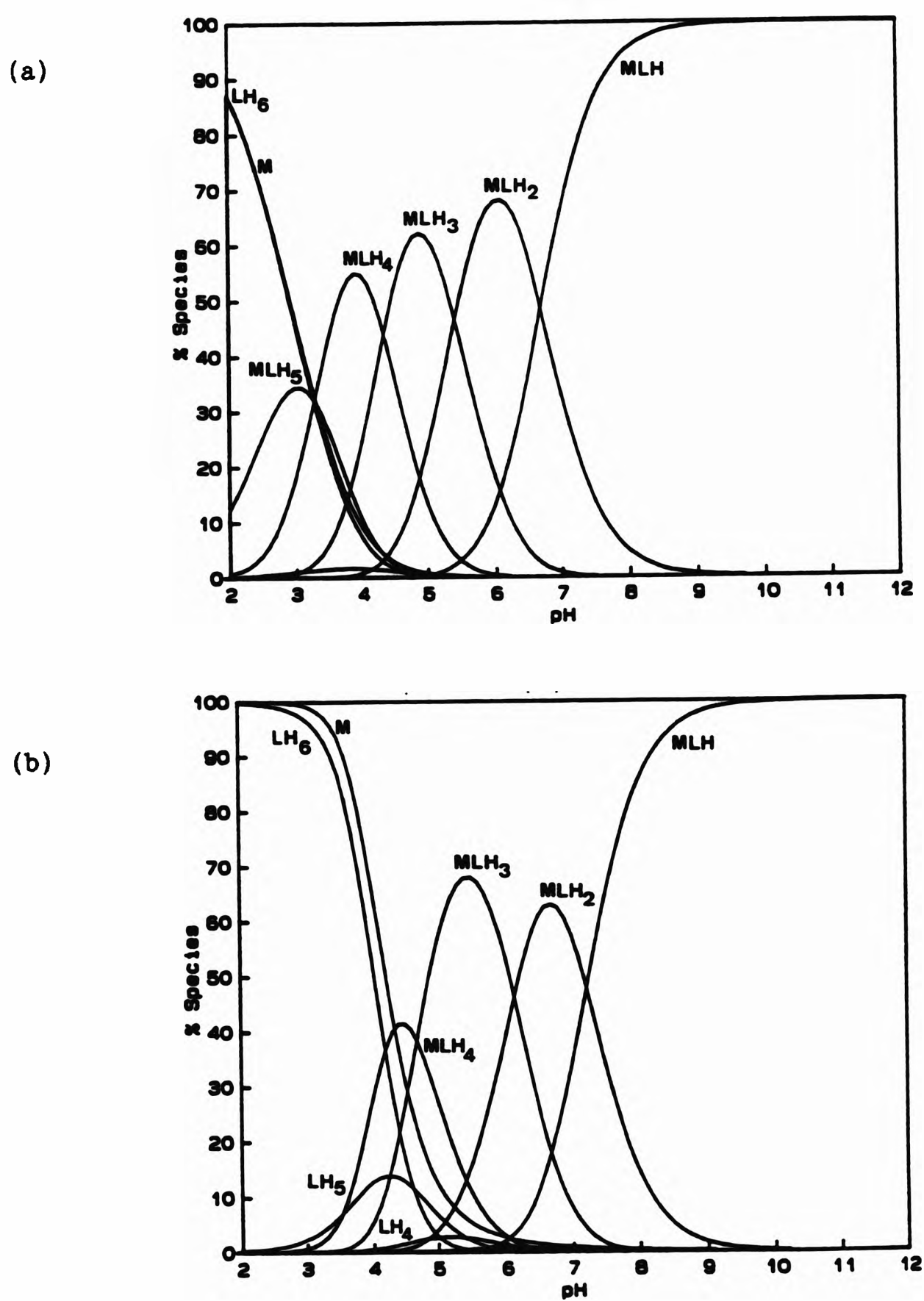


Figure 5.2.14 Species distribution curves¹⁸ for DDDTMPH₃ with metal ions at [M]:[L] ca. 1:1 (a) with Cu(II) and (b) with Zn(II).

The species distribution curves computed for DDDTMPH_6 with the metal ions Pb(II) , Cd(II) , Zn(II) and Cu(II) are valid in the pH range 3 to ca. 8, based on data refinements used. The curves for DDDTMPH_6 with the metal ions Zn(II) , Cd(II) and Pb(II) are similar, *i.e.* they all contain four metal-ligand species, $[\text{MLH}]^{5-}$, $[\text{MLH}_2]^{4-}$, $[\text{MLH}_3]^{3-}$ and $[\text{MLH}_4]^{2-}$. With most of the metal ions being complexed by pH ca. 5-6.

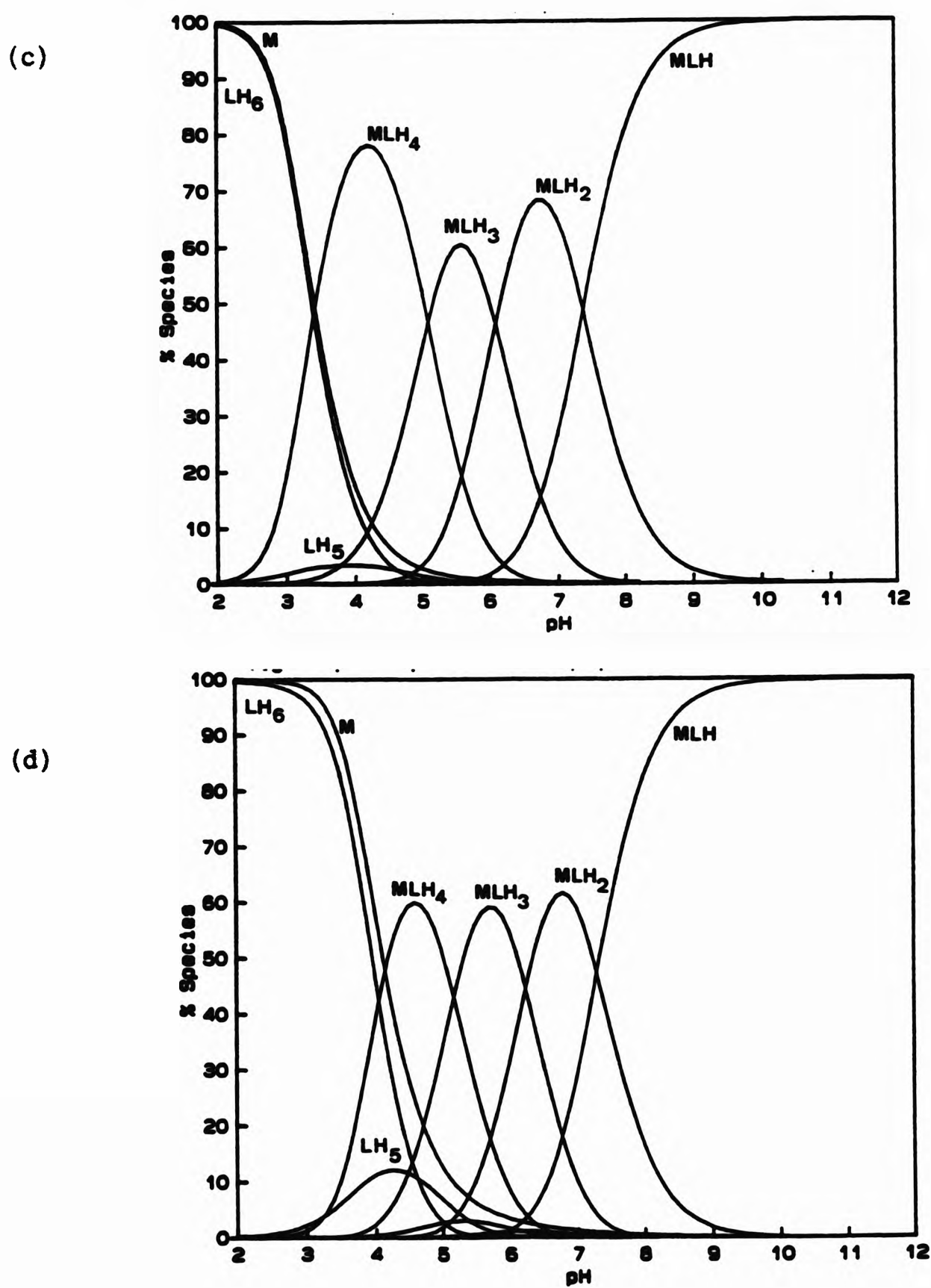


Figure 5.2.14, continued. Species distribution curves¹⁸ for DDDTMPH_6 with metal ions at $[\text{M}]:[\text{L}]$ ca. 1:1 (c) with Pb(II) and (d) with Cd(II) .

The curves obtained for DDDTMPH₃ with Cu(II) are different in that they contain five metal-ligand species, *i.e.* [CuLH]⁵⁻, [CuLH₂]⁴⁻, [CuLH₃]³⁻, [CuLH₄]²⁻ and [MLH₅]⁻. With most of the Cu(II) ion being sequestered by pH ca. 4, with the species [CuLH₅]⁻ being important below pH 3.

5.2.4 Comparison with previous work for CDTMPH₃

The metal stability constants determined by Banks⁴² for CDTMPH₃ with a variety of metal ions seem quite low compared to those determined for EDTAH₄ and those in this work.⁴³ Kabachnik⁴³ noted that the low values of stability constants determined by Banks⁴² may be ascribed to assumption of an incorrect model for the species in solution; in particular, protonated complexes were not considered. Alternatively, the differences between stability constants determined for CDTMPH₃ in this work and by Banks⁴² may be due to differences in ligand purity and ionic media, and other conditions.⁴⁴ The potentiometric titrations for CDTMPH₃ with various metal ions carried out by Banks⁴² were using a different ionic medium, *i.e.* sodium perchlorate and in this work potassium nitrate was used. The titration curves obtained by Banks⁴² only have 20 points in total, whereas in this study, 200 points were normally used, although, x-y were utilised in refinement. Bank's⁴² titrations for CDTMPH₃ with various metals were carried out with a metal:ligand ratio of 20:1. The present work carried out with the advantages of computer controlled acquisition of the data and analysis using a sophisticated computer program, represents an appropriate advance on the work carried out by Banks in 1959. In particular, the importance of protonated species has been confirmed as suggested by Kabachnik⁴³.

5.2.5 The configuration and orientation of the ligating groups and its effect on complex stability

It has been noted by Hancock and Martell⁴⁵ that the values of metal complex constants of CDTAH₄, *trans*-cyclohexane-1,2-diaminetetraacetic acid, are greater than those for the straight chain analogue, EDTAH₄, ethylenediaminetetraacetic acid (Table 5.2.13).^{45,46}

Hancock *et al.*⁴⁵ suggested that for the acid, EDTAH₄ in *aqueous* solution, there is free rotation about the central carbon-carbon bond and hence the free ligand may adopt a *trans* configuration which maximises the charge separation between the substituent groups. Indeed, this configuration is found in the solid state.⁴⁷ In contrast, the cyclohexyl ring of CDTAH₄ inhibits rotation

about the corresponding C-C bond, and the two *trans*-iminodiacetate substituent groups are most likely to be in an *ee* configuration.⁴⁸ This arrangement of the ligating groups in CDTAH₄, is pre-organised for complexation which leads to the increase in complex stability.^{45,46} Thus, energy is not expended in orienting the ligating groups for complexation, e.g. the stability of transition metal complexes of CDTAH₄, are ca. 2 log units greater than those of EDTAH₄ (Table 5.2.13).⁴⁶

Table 5.2.13 Comparison of some stability constants (log K_{ML}) of some related acids.

Metal ion	CDTAH ₄ ^a	EDTAH ₄ ^b
Mn(II)	17.43	13.81
Fe(II)	18.90	14.27
Co(II)	19.58	16.26
Ni(II)	20.2	18.52
Cu(II)	21.92	18.70
Zn(II)	19.35	16.44
Fe(III)	30.0	25.0
Gd(III)	19.47	17.35

^a Ref. 46. I = 0.1 mol dm⁻³ KNO₃, 25.0 °C. ^b Ref. 46. I = 0.1 mol dm⁻³ KNO₃, 25.0 °C.

Hancock⁴⁵ suggested that in EDTAH₄ type ligands, orientation of the ligating groups from the *trans* to the *pre-organised* configuration must involve overcoming the electrostatic repulsions of the negatively charged groups on bringing the ligating groups together for complexation.

The values of log K_{MLH}^{LH} for CDTAH₄ for the transition metal ions are still slightly greater than those for EDTAH₄ (ca.1 log unit). This suggests that the higher stability observed for protonated complexes [MLH] for CDTAH₄ may be ascribed to the *pre-organisation* of the ligating groups in CDTAH₄ compared to the re-organisation of the substituent groups in EDTAH₄.⁴⁵

Since the value for the first protonation constant for CDTMP^{δ-} could not be determined (Section 4.5) it was necessary to compare the values for log K_{MLH}^{LH} determined for CDTMPH₃ with some metal ions with the corresponding values for

other related ligands (Table 5.2.14). The values of $\log K_{MLH}^{LH}$ determined for CDTMPH₃ in this work for the transition metal ions, except for Mn(II), are ca. 2-4 log units less than those for EDTMPH₃, suggesting that another factor other than *pre-organisation* is affecting the stability of the protonated metal complexes [MLH]. The higher stability of the protonated complex [FeLH]⁴⁻ of CDTMPH₃ ($\log K_{MLH}^{LH} = 18.76$) compared with EDTMPH₃ ($\log K_{MLH}^{LH} = 13.75$) may indicate that *pre-organisation* of the substituent groups in CDTMPH₃ (*c.f.* to EDTMPH₃) enhances the stability of the larger metal ions such as iron(III). Whereas, the value of $\log K_{MLH}^{LH}$ for CDTMPH₃ with Gd(III) is ca. 4 log units less than the value calculated for EDTMPH₃.

Table 5.2.14 Comparison of some stability constants $\log K_{MLH}^{LH}$ of some related acids.^a

Metal ion	CDTAH ₄ ^b	EDTAH ₄ ^b	CDTMPH ₃ ^c	EDTMPH ₃ ^b
Mn(II)	7.98	6.74	10.30	8.77
Co(II)	10.22	9.09	10.30	12.43
Ni(II)	d	d	8.84	12.33
Cu(II)	12.80	11.53	13.26	17.78
Zn(II)	9.97	9.27	11.80	14.08
Fe(III)	d	d	18.75	13.75
Gd(III)	9.40	d	12.25	16.20

^a The values of the stability constants ($\log K_{MLH}^{LH}$) are for the process for forming the monoprotonated complex [MLH] by the reaction, $M^{n+} + LH^{n-} \rightleftharpoons MLH^{n-1}$ and is calculated as $\log K_{MLH}^{LH} = \log K_{MLH}^{ML} + \log K_{ML}^L - \log K_{LH}^L$. ^b The values of the stability constants used to calculate $\log K_{MLH}^{LH}$ for each metal ions were obtained from ref. 46. ^c In this work, the monoprotonated ligand CDTMPH⁷⁻ is denoted as L. I = 0.1 mol dm⁻³ KNO₃, 25.0 ± 0.1°C. ^d Values for $\log K_{MLH}^{LH}$ could not be calculated.

This indicates that the stability of the protonated complexes of CDTMPH₃ is being affected by other factors, such as, strong intramolecular hydrogen-bonding (Section 7) which may be need to be broken for coordination of the metal ion to the ligand to be favoured, the crowding of the phosphonate groups around the nitrogen atoms thus inhibiting coordination of the metal ion to nitrogen.

It is worth noticing that the values of $\log K_{MLH}^{ii}$ for $CDTMPH_3$ are all greater than those calculated for the $EDTAH_4$ and $CDTAH_4$, suggesting that the protonated species $[MLH]^{5-}$ formed with $CDTMPH_3$ are more stable than those for $EDTAH_4$, possibly due to *pre-organisation* of the methylenephosphonate groups in $CDTMPH_3$ compared to $EDTAH_4$. Whereas, the lower stability constants ($\log K_{MLH}^{ii}$) for $CDTAH_4$ compared to $CDTMPH_3$, suggests that *pre-organisation* is not the main factor affecting the stability of the complexes, but may be influenced by the repulsion of the PO_3^{2-} groups, the metal coordination geometry and possible coordination of the nitrogen atom to the metal.

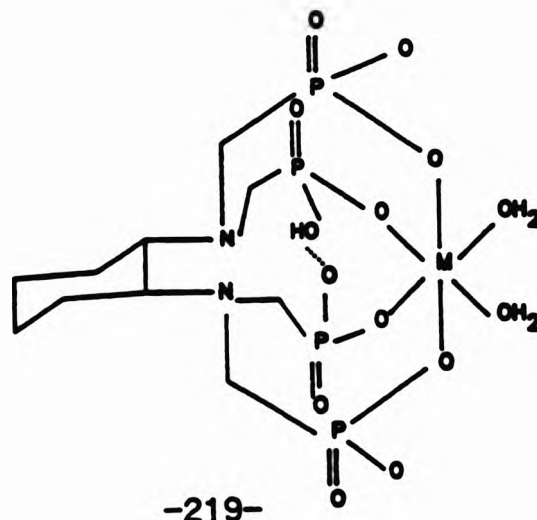
As expected from the Irving-Williams series and noted by Gillard *et al.*⁵, Cu(II) is by far the strongest complexing divalent transition metal ion with respect to $CDTMPH_3$. The stabilities of the $[MLH]^{5-}$ complexes of $CDTMPH_3$ with the divalent metal ions examined in this work are of the order Mn(II) < Co(II) > Ni(II) < Cu(II) > Zn(II) > Cd(II). Except for the reserved order for Co(II) and Ni(II) this follows the Irving-Williams series.

The order of stability of the metal complexes $[MLH]^{5-}$ of $DDDTMPH_3$ with the divalent metals examined in this work is Cu(II) > Zn(II) > Cd(II) < Pb(II).

5.2.6 Possible structures of metal complex species in solution

The possible structures of metal complexes with $CDTMPH_3$ and $DDDTMPH_3$ in solution were not examined by the method of Sawada¹⁴ because it was not possible to determine the values for the first protonation constant of the free ligands, *i.e.* $\log K_{011}$ for $CDTMP^{3-}$ and $DDDTMP^{3-}$.

Determination of the solid state structure of $CDTMPH_3$ (Section 7) shows the methylenephosphonate substituent groups are *pre-organised* for complexation as observed in the solid state structure of $CDTAH_4$; strong intramolecular hydrogen bonding between methylenephosphonate groups hold the substituent groups close together and results in the 'crowding' of the phosphonate groups.

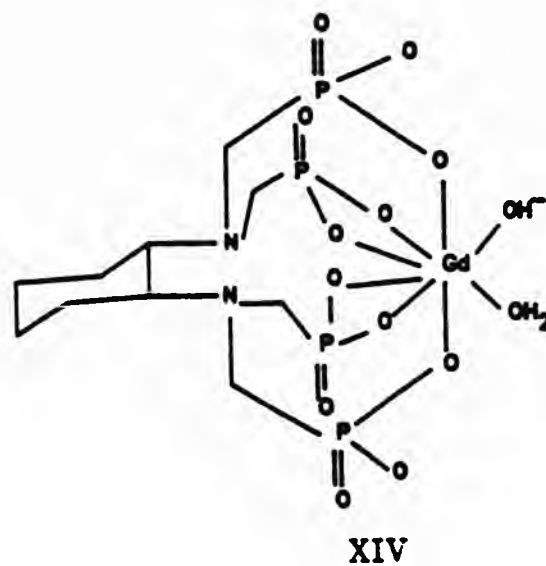
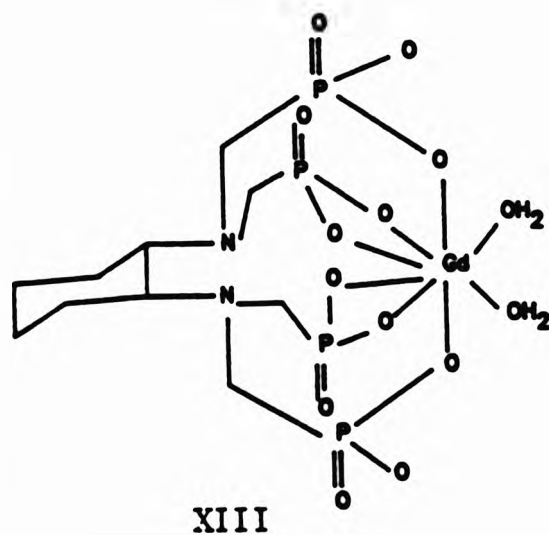


The assumption that a proton is retained by the ligand (CDTMPH^{7-}) in solution is a reasonable one, because the two strongly hydrogen bonded protons on the methylenephosphonate oxygen atoms hold the ligating groups ready for complexation and still leaves six potentially coordinating oxygen atoms.

The complexation behaviour of lanthanide metals with aminocarboxylic acids had been investigated by potentiometry as early as 1974, before any evidence appeared that these lanthanide complexes would be of interest in medicine and the MRI technique.⁴⁹

Prados *et al.*⁵⁰ noted that during potentiometric titrations of some aminocarboxylic acids with lanthanide metals [e.g. La(III)], the deprotonation of the ammonium group usually took place after lanthanide hydrolysis. Also, in acidic solutions of the simple amino acids, the lanthanide ions tend to coordinate to the carboxylate residue with the ammonium group remaining protonated and unbound.⁵⁰ Therefore, complexes of La(III) ions with aminocarboxylic acids do not involve coordination of the nitrogen atom to the metal ion and hence the nitrogen atoms remains protonated until relatively high pH.⁵⁰

The increased multidentate character of alkylaminomethylenephosphonic acids (PO_3^{2-}) compared to alkylaminomethylenecarboxylic acids (CO_2^-) favours formation of complexes with rare-earth metals, which are known to be characterised by a high coordination capacity and a strong affinity for oxygen. For the lanthanide metal ions [e.g. Gd(III)] a possible structure for $[\text{GdL}]^{5-}$ ($\log \beta_{110} = 4.64$) (XIII) involves the coordination sphere being satisfied by donor molecules (*i.e.* in this case water) since the normal coordination number of Gd(III) can be six, eight or nine.³⁵



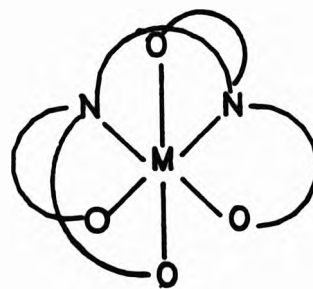
The species $[\text{GdL}]^{5-}$ can then undergo subsequent hydrolysis and lose a proton to form the deprotonated species $[\text{GdL}(\text{OH})]^{6-}$ (XIV). Since coordination of the amino groups in aminocarboxylic acids to lanthanide metal ions is unlikely,⁵⁰ and the because of the *pre-organisation* of the methylenephosphonate groups in CDTMPH_3 resulting in a 'crowding' effect of these groups, then coordination of the nitrogen atoms to $\text{Gd}(\text{III})$ is also unlikely.

Table 5.2.15 Metal stability constants ($\log K_{\text{MLH}}^{\text{LH}}$) for some related ligands.^a

Ligand	Cu(II)	Zn(II)	Cd(II)	Pb(II)
HMTMPH_3 ^{b,c}	10.08	^d	6.88	^d
EDTMPH_4 ^e	17.78	14.08	^d	^d
DDDTMPH_3 ^f	13.29	9.84	9.27	10.77

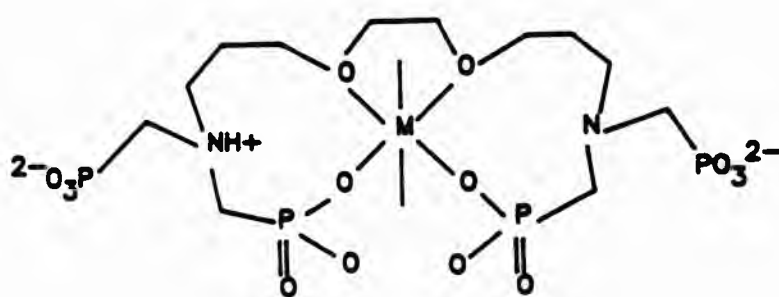
^a The values of the stability constants ($\log K_{\text{MLH}}^{\text{LH}}$) are for the process for forming the monoprotonated complex $[\text{MLH}]$ by the reaction, $\text{M}^{n+} + \text{LH}^{n-} \rightleftharpoons \text{MLH}^{n-1}$ and is calculated as $\log K_{\text{MLH}}^{\text{LH}} = \log K_{\text{MLH}}^{\text{ML}} + \log K_{\text{ML}}^{\text{L}} - \log K_{\text{LH}}^{\text{L}}$. ^b It is assumed that these values are for the process for forming the monoprotonated species $[\text{MLH}]^{5-}$ because the value of $\log K_{011}$ (11.82) is for protonating only one nitrogen atom and the value of $\log K_{012}$ (7.71) is for the process of protonating a phosphonate oxygen (see section 4.6). ^c Values for calculating $\log K_{\text{MLH}}^{\text{LH}}$ are taken from ref. 26. ^d Values for $\log K_{\text{MLH}}^{\text{LH}}$ could not be calculated. ^e Values for calculating $\log K_{\text{MLH}}^{\text{LH}}$ are taken from ref. 46. ^f This work. $I = 0.1 \text{ mol dm}^{-3}$ KNO_3 , 25.0 ± 0.1 °C.

The values of $\log K_{\text{MLH}}^{\text{LH}}$ for EDTMPH_4 with the metal ions Cu(II) (17.78) and Zn(II) (14.08) are all greater than those determined for DDDTMPH_3 in this work (Table 5.2.15). This suggests that increasing the aliphatic chain between the two nitrogen atoms in HMTMPH_3 ⁵¹ compared to EDTMPH_4 decreases the stability of the resulting complex. Motekaitis⁵² suggested that the two nitrogen atoms and the four phosphonate oxygen atoms were all able to coordinate to the metal (XVII).



XVII

However, increasing the aliphatic chain from HMTMPH₃ to DDDTMPH₃ results in an increasing stability of the [MLH] complexes. This may be ascribed to the inability of the two nitrogens and all the phosphonate groups of HMTMPH₃ to fully coordinate around the divalent metal (*c.f.* to EDTMPH₃). Kabachnik suggested that the insertion of heteroatoms (O, S or N) into the aliphatic chain between the two nitrogen atoms may take part in coordination to the metal ion.²⁵ This may be the case in DDDTMPH₃ (XVIII), and may explain the higher stability of the resulting complexes compared to HMTMPH₃.⁵¹



XVIII

Therefore, increasing the chain length between the two nitrogens as in DDDTMPH₃ may provide some steric hinderance for complexation (*c.f.* EDTMPH₃) but may also promote coordination of the ether oxygen atoms to the metal ions.

5.3 The preparation of some metal complexes of an α -aminomethylenephosphonic acid, *N*-ethyliminobis(methylenephosphonic acid)

It has already been noted that the complexation behaviour of aminomethylenephosphonic acids has been widely studied by potentiometry (Section 5.1) with the major interest being centred on the various species in *aqueous* solution. However, information about the nature of the metal-ligand species in *aqueous* solution is hindered by the lack of knowledge about the ways in which these ligands coordinate to metal ions. Relatively few *X*-ray crystal structures of metal complexes of alkylaminomethylenephosphonic acids have been reported.²⁷⁻³⁴

Metal complexes of alkylaminomethylenephosphonic acids in the solid state have not been widely studied. However, the early 1980's, produced a growing interest in the preparation and characterisation (*i.e.* by ir spectroscopy, uv-visible spectroscopy, nmr spectroscopy and thermal analysis) of these types of complexes.⁵³⁻⁶¹

The majority of metal complexes prepared with alkylaminomethylenephosphonic acids have been found to have one of the following formulations: e.g. $M_2L(OH)_n \cdot xH_2O$ ($x = 1, 2$ or 4 ; $n = 1, 2$),⁵³ or $M_4L \cdot xH_2O$, or $M_2L \cdot xH_2O$, or M_2Na_4L .⁵⁴⁻⁵⁶ This suggests that alkylaminomethylenephosphonic acids can coordinate to bivalent metals in a variety of ways, and hence produce solid complexes with varying metal to ligand ratios.

In the present work, the preparation of some solid complexes of NEIBMPH₄ with bivalent metal ions were investigated. All the solids were isolated from *aqueous* solution as amorphous powders and were characterised by C, H and N elemental analysis, ir, nmr spectroscopy (where possible), and mass spectroscopy. These complexes were found to have either one of the following stoichiometries $[M(LH_3)_2]$ or $[M(LH_3)_2] \cdot H_2O$ (Table 5.3.1).

Attempted preparations of bivalent metal complexes with CDTMPH₃ were unsuccessful. Many of these products could not be fully analysed, as the complexes obtained from *aqueous* solutions were either oily/sticky residues or glassy type solids. This again emphasises the difficulty in obtaining crystals of these metal complexes, suitable for analysis by X-ray crystallography.

Table 5.3.1 Analytical data obtained for some metal complexes of NEIBMPH₄.^a

Complex	colour	$[M + H^+]$	% yield	M.p. °C
$[Cu(NEIBMPH_3)_2]$	pale blue	^b	47	250 dec.
$[Zn(NEIBMPH_3)_2] \cdot H_2O$	white	563	25	> 300
$[Cd(NEIBMPH_3)_2]$	white	577	48	> 250
$[Co(NEIBMPH_3)_2]$	pink	578	40	> 300
$[Mn(NEIBMPH_3)_2]$	white	520	42	^c

^a This work. ^b Not enough sample to obtain a mass spectrum. Magnetic susceptibility calculated (μ_{eff}) at 24.4 °C = 2.13 BM. ^c Metal perchlorate used.

Mitrofanova *et al.*^{55,56} has also investigated the preparation of some, solid metal complexes of NEIBMPH₄, *i.e.* Cu(II), Ni(II) and Co(II). The composition calculated for the copper complex with NEIBMPH₄ in this work, is in agreement

with one of the compositions calculated by Mitrofanova *et al.* Mitrofanova also isolated complexes of Co(II) with varying metal to ligand ratios, *e.g.* 1:1 and 1:2.⁵⁵ In this work, the Co(II) complex was found to have the formulation [Co(LH₃)₂].

5.3.1 Characterisation of some metal complexes of NEIBMPH₄

The ir bands considered to be important in the metal complexes are the stretches of the phosphonic acid group because these are likely to be involved in coordination (Table 5.3.2).

The 'free ligand' as well as the complexes exhibited bands due to $\nu_{\text{asy}} \text{PO}_2^{2-}$ and $\nu_{\text{sym}} \text{PO}_2^{2-}$ vibrations and it is these bands that give clues regarding the complexation behaviour of the ligand. Owing to the electron withdrawing nature of the metal ions, electron density is withdrawn from the phosphorus atoms which may result in an increase in the bond order of P=O. Therefore, an increase in the frequency of the bands of $\nu_{\text{sym}} \text{PO}_2^{2-}$ and $\nu_{\text{asy}} \text{PO}_2^{2-}$ and a decrease in the frequency of $\nu_{\text{sym}} \text{P-OH}$ are expected when the metal is coordinated to the ligand through the phosphonate oxygen atoms.⁶¹ It was noted that the splitting of the band at 1044-1088 $\nu_{\text{sym}} \text{PO}_2^{2-}$ can also be assigned to the bending motion of the (O-P-C) linkage in the complex [Cu(NEIBMPH₃)₂].⁶¹

Table 5.3.2 Assignment of the stretching vibrations of the phosphonic acid groups in the ir spectra (cm⁻¹) of some metal complexes with NEIBMPH₄.^a

Compound	$\nu_{\text{sym}} \text{P-(OH)}$	$\nu_{\text{sym}} \text{PO}_2^{2-}$	$\nu_{\text{asy}} \text{PO}_2^{2-}$	$\nu_{\text{asy}} \text{P=O}$
NEIBMPH ₄	939 ^b , 974 ^c	1025 ^b	1124, 1175 ^b	1214 ^b
[Mn(NEIBMPH ₃) ₂]	932	1073 ^b	1143	1201, 1219
[Cu(NEIBMPH ₃) ₂]	928	1044, 1068, 1088 ^d	1152	1202 ^b
[Cd(NEIBMPH ₃) ₂]	934	1080	1131, 1160	1197, 1217
[Co(NEIBMPH ₃) ₂]	933	1074	1132, 1156	1200, 1218

^a This work. ^b The band was broad and not fully resolved. ^c Could be due to -P(OH)₂ absorption. ^d The band is split into a triplet.

In all the metal complexes examined by ir spectroscopy, it was noted that there generally was an increase in the value of $\nu_{\text{asy}} \text{PO}_2^{2-}$, as well as a

decrease in the value of ν_{sym} P-OH.

The calculated effective magnetic moment was determined (Section 2.5.9) for the copper complex $[\text{Cu}(\text{NEIBMPH}_3)_2]$ at 297.4 K ($\mu_{\text{eff}} = 2.13$). This value was found to be consistent with values obtained for other copper (II) complexes of aminophosphonic acids (normal μ_{eff} range = 1.73-2.20 BM) and also suggests there is no metal-metal interactions.⁵⁴ This value supports that a mononuclear complex formed, *i.e.* μ_{eff} would have a lower value if a dinuclear metal complex formed, due to metal-metal interactions.⁵⁹

UV-visible spectra were obtained for two of the metal complexes, *i.e.* $[\text{Cu}(\text{NEIBMPH}_3)_2]$ and $[\text{Co}(\text{NEIBMPH}_3)_2]$ (Section 2.5.8). An intense absorption band for the copper (II) complex was observed in the region 273 nm, this probably arises from charge transfer.⁵⁴ Absorption bands in the visible region of the spectrum at 513 nm and 495 nm were observed for the cobalt(II) complex, with another small band at *ca.* 278 nm. These bands observed in the visible region probably corresponds to d-d transitions, with the band at 278 nm being ascribed to charge transfer.

^1H , ^{13}C and ^{31}P nmr spectra were only obtained for $[\text{Cd}(\text{NEIBMPH}_3)_2]$ in deuterated sodium hydroxide (NaOD) (Section 2.2.8). Comparison between the ^1H nmr spectra obtained for the free-ligand with that of the cadmium complex, differences between the chemical shift of the signals and coupling constants are observed (Section 2.2.7). Many of the complexes prepared by other workers, seem to be insoluble in water and common organic solvents and hence this precludes characterisation by nmr spectroscopy.⁵³⁻⁶⁰ However, Govindaraju *et al.*⁶¹ prepared a chromium (III) complex of nitrilotris(methylenephosphonic acid) which was water soluble, hence nmr spectra were obtained. To date, this was the only example found in which nmr spectra were determined for a metal complex with an aminomethylenephosphonic acid.

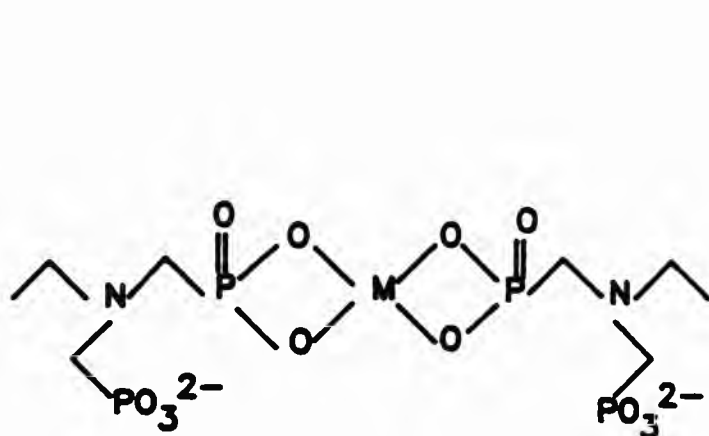
The difference in the chemical shift of the resonance signals in the ^1H and ^{13}C nmr spectra between the free-ligand with that of the cadmium complex, can be influenced by the metal ion as noted by Govindaraju *et al.*⁶¹ However, the differences observed in the spectra obtained for $[\text{Cd}(\text{NEIBMPH}_3)_2]$ can be ascribed to the different solvent used or that the nmr spectra are pH dependent. For the 'free ligand', deuterated water (D_2O) was used, whereas for the cadmium(II) complex, deuterated sodium hydroxide was used.

Differences in the coupling constants obtained for $[\text{Cd}(\text{NEIBMPH}_2)_2]$ i.e. $^3J(\text{CH}_2\text{-P}) = 6.1$ Hz compared to that obtained for the free ligand [$^3J(\text{CH}_2\text{-P}) = 4.4$ Hz] may be ascribed to the electron-withdrawing effect of the metal ion.

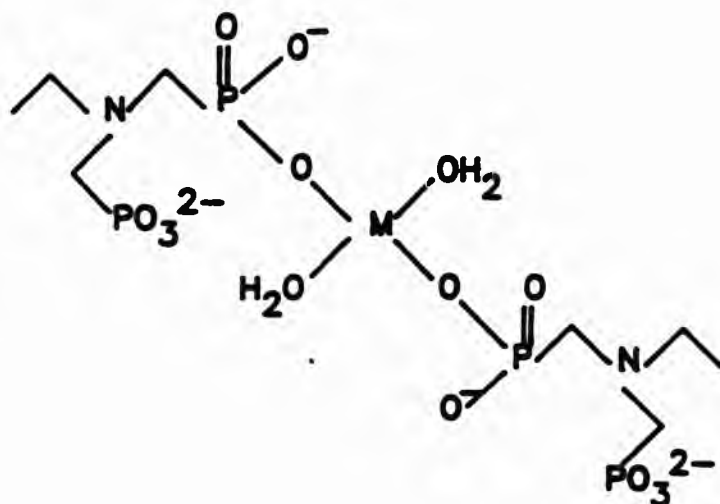
It is evident from the ^{31}P nmr spectra that for $[\text{Cd}(\text{NEIBMPH}_2)_2]$ as well as that for the free ligand, only one phosphorus environment is observed suggesting there is rapid exchange of protons on all the species present in solution (Section 4.3).

In the broad band decoupled ^{31}P nmr spectrum of the cadmium complex, there is evidence of carbon-phosphorus coupling [$^1J(\text{CH}_2\text{-P}) = 142.9$ Hz] which is slightly larger than that for the free ligand $^1J(\text{CH}_2\text{-P}) = 139.3$ Hz.

A possible structure for the cadmium complex can be inferred from the solid state structures of other metal complexes with aminomethylenephosphonic acids, e.g. see below.



X



XI

5.4 References

1. E. N. Rizkalla, *Rev. Inorg. Chem.*, 1983, 5, 223. G. Scharzenbach, H. Ackermann and P. Ruchstuhl, *Helv. Chim. Acta.*, 1949, 32, 1175. K. B. Yatsimirdkii, M. D. Konstantinnovskaya and E. I. Sinyavskaya, *Zh. Neorg. Khim.*, 1989, 34, 2217. CA. 112, 12629f. I. Ya. Polyakova, A. Ya. Fridman and N. M. Dyatlova, *Koord. Khim.*, 1987, 13, 147. E. Matczak-Jon and W. Wojciechowski, *Inorg. Chim. Acta.*, 1990, 173, 85. E. P. Nabirkina, T. I. Ignat'eva, O. A. Raevskii and Yu. P. Belov, *Izv. Akad. Nauk. SSSR, Ser. Khim.*, 1989, 2482; CA 112, 166247s. V. P. Vasil'ev, A. V. Katrotseva and M. P. Perez, *Zh. Neorg. Khim.*, 1991, 36, 2306; CA 115, 241157e. T. Kiss, M. J. Bojczuk, H. Kozlowski, P. Kafarski and K. Antczak, *J. Chem. Soc. Dalton Trans.*, 1991, 2275. M. I. Kabachnik, *Sov. Sci. Rev. B. Chem.*, 1990, 15.
2. K. Sawada, T. Araki and T. Suzuki, *Inorg. Chem.*, 1989, 28, 2687.
3. T. G. Appleton, J. R. Hall and I. J. McMahon, *Inorg. Chem.*, 1986, 25, 720, 726.
4. J. Oakes and E. G. Smith, *J. Chem. Soc. Dalton Trans.*, 1983, 601.
5. R. D. Gillard, P. D. Newman and J. D. Collins, *Polyhedron*, 1989, 8, 2077.
6. E. N. Rizkalla and G. R. Choppin, *Inorg. Chem.*, 1983, 22, 1478.
7. T. A. Babushkina, L. B. Lazukova, V. F. Zolin and L. G. Koreneva, *Koord. Khim.*, 1985, 11, 610.
8. C. F. G. C. Geraldes, A. D. Sherry and G. E. Kiefer, *J. Mag. Res.*, 1992, 97, 290.
9. V. E. Larchenko, K. I. Popov, A. I. Grigor'ev and N. M. Dyatlova, *Koord. Khim.*, 1984, 10, 1187. V. E. Larchenko, K. I. Popov, A. I. Grigor'ev, L. V. Nikitina and N. M. Dyatlova, *Koord. Khim.*, 1984, 10, 492.
10. P. Gans, A. Sabatini and A. Vacca, *J. Chem. Soc., Dalton Trans.*, 1985, 1195.
11. M. Wozniak and G. Nowogrocki, *Talanta*, 1979, 26, 1135.
12. R. P. Carter, M. M. Crutchfield and R. R. Irani, *Inorg. Chem.*, 1967, 6, 939.
13. I. J. Scowen, Ph.D Thesis, University of North London, 1993.
14. K. Sawada, T. Kanda, Y. Naganum and T. Suzkui, *J. Chem. Soc., Dalton Trans.*, 1993, 2557.
15. F. I. Bel'skii, I. B. Goryunova, P. V. Petrovskii, T. Ya. Medved' and M. I. Kabachnik, *Bull. Acad. Sci. USSR*, 1982, 31, 93.
16. C. F. Baes, R. J. Mesmer, *The Hydrolysis of Cations*, Wiley, New York,

1976. (a) pp 229-237; (b) pp 241-247 and (c) pp 129-138.
17. R. W. Matthews and C. J. L. Silwood, unpublished results.
 18. R. J. Motekaitis, FORTRAN 77 program SPE, 1987: A. E. Martell and R. J. Motekaitis, *The Determination of Stability Constants*, 1988, VCH Publishers, New York. C. Crees, TURBO-C program SPECIES, unpublished, 1990. C. J. L. Silwood, GW-BASIC program HPLOT, unpublished, 1990.
 19. H. Irving and R. J. P. Williams, *J. Chem. Soc.*, 1952, 3192.
 20. N. N. Greenwood and A. Earnshaw, *Chemistry of the Elements*, 1986, Pergamon Press, Oxford.
 21. K. F. Purcell and J. C. Kotz, *Inorganic Chemistry*, 1985, W. B. Saunders, Philadelphia.
 22. K. S. Rajan, I. Murase and A. E. Martell, *J. Am. Chem. Soc.*, 1969, 91, 4408.
 23. R. J. Motekaitis, I. Murase and A. E. Martell, *J. Inorg. Nucl. Chem.*, 1971, 33, 3353.
 24. R. J. Motekaitis and A. E. Martell, *J. Coord. Chem.*, 1985, 14, 139.
 25. M. I. Kabachnik, T. Ya. Medved, N. M. Dyatlova, M. N. Rusina and M. V. Rudomino, *Izv. Akad. Nauk SSSR*, 1967, 7, 1501.
 26. N. M. Dyatlova, M. I. Kabachnik, T. Ya. Medved, M. V. Rudomino and Yu. F. Belugin, *Dok. Akad. Nauk SSSR*, 1965, 161, 607.
 27. N. Choi, I. Khan, R. W. Matthews, M. McPartlin and B. P. Murphy, *Polyhedron*, 1994, 13, 847.
 28. L. M. Shkol'nikova, A. L. Poznyak, V. K. Bel'skii, M. V. Rudomino and N. M. Dyatlova, *Koord. Khim.*, 1986, 12, 981.
 29. P. Fenot, J. Darriet, C. Garrigou-Largange and A. Cassaigne, *J. Mol. Struct.*, 1978, 43, 49.
 30. T. Glowiak, W. Sawka-Dobrowolska and B. Jezowska-Trzebiatowska, *J. Cryst. Mol. Struct.*, 1980, 10, 1.
 31. T. Glowiak, W. Sawka-Dobrowolska and B. Jezowska-Trzebiatowska, *Inorg. Chim. Acta.*, 1980, 45, L105.
 32. Y. Ortiz-Avila, P. R. Rudolf and A. Clearfield, *J. Coord. Chem.*, 1989, 20, 109.
 33. M. I. Kabachnik, M. Yu. Antipin, B. K. Shcherbakov, A. P. Baranov, Yu. T. Struchkov, T. Ya. Medved and Yu. M. Polikarpov, *Koord. Khim.*, 1988, 14, 536.
 34. M. Yu. Antipin, *Dokl. Akad. Nauk SSSR*, 1986, 130, 40.
 35. F. A. Cotton, G. Wilkinson and P. L. Gaus, *Basic Inorganic Chemistry*, 1987, Second Edition, John Wiley & Sons, New York.

36. R. B. Lauffer, *Chem. Rev.*, 1987, 87, 901.
37. J. E. Bollinger and M. Roundhill, *Inorg. Chem.*, 1993, 32, 2821.
38. E.g. M. Kodama, T. Koike, A. B. Mahatma and E. Kimura, *Inorg. Chem.*, 1991, 30, 1270. D. D. Dischino, E. J. Delaney, J. E. Emswiler, G. T. Gougham, J. S. Prasad, S. K. Srivaskava and M. T. Tweedle, *Inorg. Chem.*, 1991, 30, 1265.
39. K. Sawada, M. Kuribayashi, T. Suzuki and H. Miyamoto, *J. Sol. Chem.*, 1991, 20, 829.
40. I. Lazar, R. Ramaswamy, E. Brucher, C. F. G. C. Geraldés and A. D. Sherry, *Inorg. Chim. Acta.*, 1992, 195, 89.
41. P. L. Brown, J. Ellis and R. N. Sylva, *J. Chem. Soc. Dalton Trans.*, 1983, 31.
42. C. V. Banks and R. E. Yerrick, *Anal. Chim. Acta.*, 1959, 20, 301.
43. M. I. Kabachnik, T. Ya. Medved', N. M. Dyatlova, O. G. Arkhipova and M. V. Rudomino, *Russ. Chem. Revs.*, 1968, 37, 503.
44. E. N. Rizkalla, *Rev. Inorg. Chem.*, 1983, 5, 223. G. Andergg, *Talanta*, 1993, 40, 243.
45. R. D. Hancock and A. E. Martell, *Chem. Rev.*, 1989, 89, 1875.
46. R. L. Smith and A. E. Martell, *Critical Stability Constants: Volume 1 Amino Acids*, 1974, Plenum Press, New York.
47. M. Cotrait, *Acta. Cryst.*, 1972, B28, 781.
48. L. M. Shkol'nikova, G. V. Polyanchuk, N. M. Dyatlova, M. A. Porai-Koshits and V. G. Yashunskii, *Zh. Strukt. Khim.*, 1983, 24, 92.
49. I. K. Adzhamli, H. Gries, D. Johnson and M. Blau, *J. Med. Chem.*, 1989, 32, 139; CA. 110, 36204y.
50. R. Padros, L. G. Stadtherr, H. Donato Jr. and R. B. Matrin, *J. Inorg. Nucl. Chem.*, 1974, 36, 689. J. E. Bollinger and D. Roundhill, *Inorg. Chem.*, 1993, 32, 2821.
51. M. T. M. Zaki and E. N. Rizkalla, *Talanta*, 1980, 27, 709.
52. R. J. Motekaitis, I. Murase and A. E. Martell, *Inorg. Chem.*, 1976, 15, 2303.
53. N. Palta, B. V. Rao, S. N. Dubey and D. M. Puri, *Ind. J. Chem.*, 1984, 23A, 397; B. V. Rao and D. M. Puri, *Ind. J. Chem.*, 1987, 26A, 1048.
54. I. Lukes, Z. Kvaca and I. Dominak, *Collect. Czech. Chem. Commun.*, 1988, 53, 987.
55. N. D. Mitrofanova, B. Kh. Kushikbaeva, S. A. Ii'ichev and L. I. Martynenko, *Zh. Neorg. Khim.*, 1987, 32, 1153.
56. N. D. Mitrofanova, B. Kh. Kushikbaeva, L. I. Martynenko and S. A.

- Ii'ichev, *Zh. Neorg. Khim.*, 1989, 34, 128.
57. R. Kh. Samakaev, N. M. Dyatlova, M. Z. Gurevich, N. F. Shugal and G. F. Yaroshenka, *Zh. Obsh. Khim.*, 1984, 54, 1720, 1726.
58. B. V. Rao and D. M. Puri, *Polyhedron*, 1989, 8, 453.
59. N. Palta, B. V. Rao, S. N. Dubey and D. M. Puri, *Polyhedron*, 1984, 3, 527.
60. I. Lukes, D. Rejskova, R. Odvarko and P. Vojtisek, *Polyhedron*, 1986, 5, 2063.
61. K. Govindaraju, T. Ramasami and D. Ramaswamy, *Inorg. Chim. Acta.*, 1987, 133, 71.

*Chapter 6 Alkylaminomethylenephosphonic acids: Some studies
relevant to their stabilising action on hydrogen peroxide*

Therefore, the pH-dependence of the ^{31}P nmr chemical shift for DEAMPH_2 which had been treated with *aqueous* hydrogen peroxide was monitored during titrations against base (Section 2.4).

In another approach, the N-oxide derivative of NEIBMPH_4 was prepared and characterised by nmr spectroscopy and C, H, N micro analysis. The protonation scheme for the N-oxide, and its complexation behaviour with Cu(II) , were examined by potentiometry and nmr spectroscopy (where possible).

The examination of the possible interaction between an α -aminomethylene-phosphonic acid, DEAMPH_2 , and sodium stannate was investigated by determining the pH-dependence of $(\delta)^{31}\text{P}$ during titrations of DEAMPH_2 in the presence of sodium stannate (Section 2.4.7).

6.1.1 The pH-dependence of the ^{31}P nmr chemical shift for DEAMPH_2 after treatment with *aqueous* hydrogen peroxide

All the nmr/pH titrations were carried out as in Section 2.4. The ^{31}P broad band proton decoupled nmr spectra were obtained at 40.52 MHz on a WP80 FT spectrometer, using 85% phosphoric acid (H_3PO_4) as an external reference by sample substitution. The lock signal for the spectrometer in this case was 10 % v/v D_2O (Section 2.4.6). As only 10 % D_2O was employed, the pH was not corrected.⁸

The ligand DEAMPH_2 was treated with *aqueous* solutions of hydrogen peroxide and the pH of each solution was adjusted with either *aqueous* nitric acid or *aqueous* ammonia (see Section 2.4.6). The resulting solutions were left for a period of one week and thereafter the hydrogen peroxide was decomposed over platinum wire at 60 °C. The pH was re-determined and recorded.

All the ^{31}P nmr spectra obtained showed only one signal for the phosphorus environment over the pH range 0.5-11.49, indicating that rapid exchange of protons between all the species occurs in solution at each point. Under conditions of fast proton exchange among the various species, L^i , the observed average chemical shift of the nucleus N ($\delta_{\text{obs}}^{\text{N}}$) is given by:

$$\delta_{\text{obs}}^{\text{N}} = \sum_1^i \delta_i^{\text{N}} \chi_i \quad \text{Equation 6.1.1}$$

where δ_i^{N} is the intrinsic chemical shift of the *i*th species, and χ_i is the

mole fraction of the i th species.³ The ^{31}P chemical shift vs pH profile obtained for the treated ligand, DEAMP₂ (Figure 6.1.1, denoted as "□") was significantly different to that obtained for the untreated ligand (Figure 6.1.1, denoted as "Δ").

As the titration proceeds there is an upfield shift of the phosphorus signal from ca. 9 ppm to ca. 8 ppm (between pH 0.5 and 2.2). This is indicative of a phosphonate oxygen-bound proton being neutralized, as seen in the case of the untreated ligand DEAMP₂ (Section 4.3). As the pH is increased from 2.2 to 10, another upfield shift in the phosphorus signal is observed of ca. 3.5 ppm. This suggests that the nitrogen is not deprotonated and, indeed, may not be protonated after treatment with hydrogen peroxide.

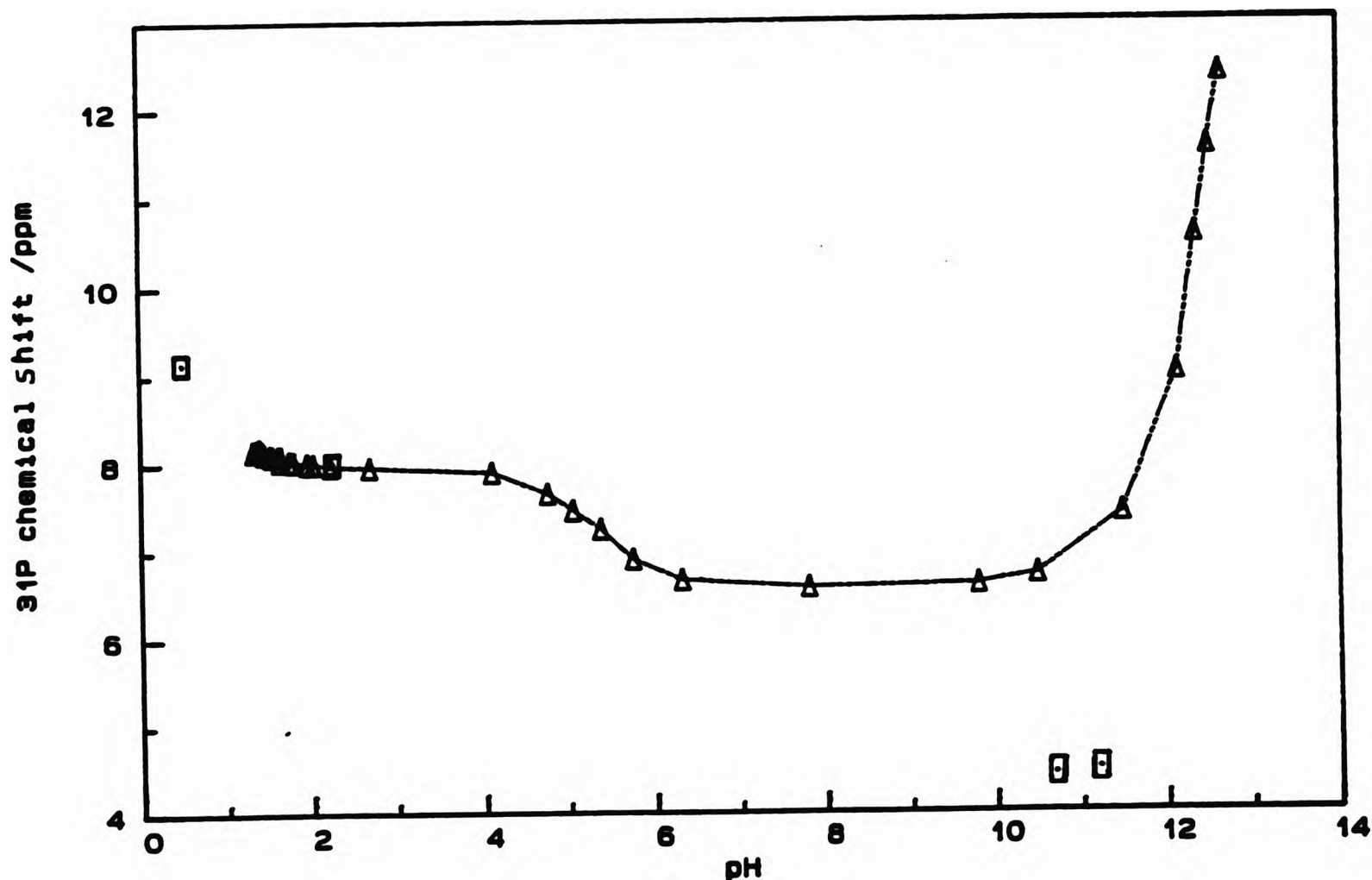
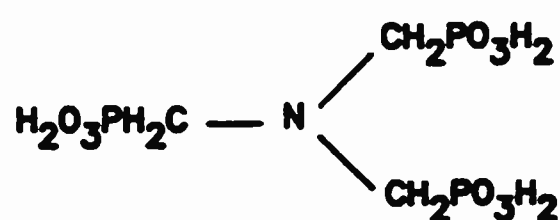


Figure 6.1.1 The pH-dependence of $\delta^{31}\text{P}$ for DEAMP₂ on its own (denoted as "Δ") and after treatment with aqueous hydrogen peroxide (denoted as "□").

The pH dependence of $\delta^{31}\text{P}$ for DEAMPH_2 after treatment with *aqueous* solutions of hydrogen peroxide (pH adjusted) was also carried out by another worker at the University of North London.[†] A similar plot of $\delta^{31}\text{P}$ vs pH was obtained suggesting that hydrogen peroxide reacted with the nitrogen of DEAMPH_2 to form of the N-oxide derivative in basic solutions.[†]

The overall profile obtained for DEAMPH_2 after treatment with hydrogen peroxide is similar to the dependence of ^{31}P chemical shift on the number of equivalents of deuterated sodium hydroxide which Carter *et al.* determined for titrations of the N-oxide derivative of NTMPH_5 .⁴ The difference between the two profiles for the N-oxide derivative of NTMPH_5 and the parent acid is similar to DEAMPH_2 and its N-oxide derivative.



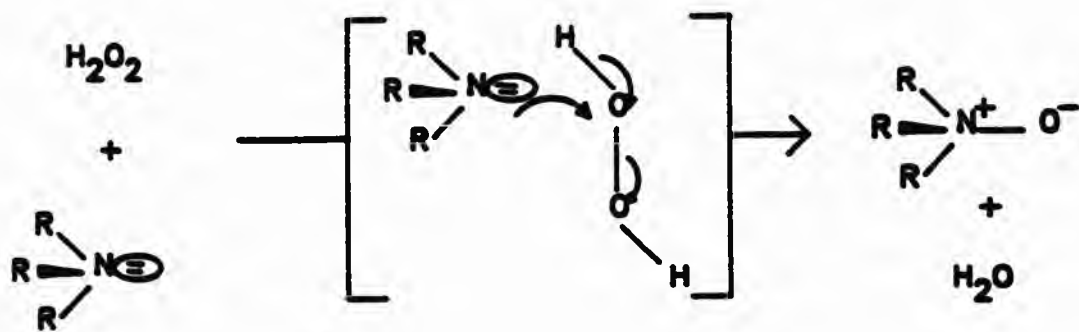
NTMPH_5

6.1.2 Synthesis and characterisation of the N-oxide derivative of NEIBMPH_4
 The N-oxide derivative of NEIBMPH_4 was prepared as described in Section 2.2.5, by a method adapted from a procedure reported by Carter *et al.*⁴ The ligand, NEIBMPH_4 , was heated under reflux for 24 h with hydrogen peroxide at 60 °C. The resulting solution was decomposed for a period of one week by passing dry air through the mixture. On addition of ethanol to the oily residue, a white precipitate was obtained.

The product was characterised by C, H, and N elemental analysis and nmr spectroscopy (^1H , ^{31}P and ^{13}C , Section 2.2.5).

The mechanism by which the alkylaminomethylenephosphonic acid is oxidised to its N-oxide derivative by hydrogen peroxide has not been described in the literature to date. However, the mechanism may be similar to that for oxidation of a tertiary amine by hydrogen peroxide.¹⁰

[†] I. J. Scowen, Ph.D Thesis, University of North London, 1993.



Comparison between the ^1H nmr spectra obtained for the N-oxide derivative [Figure 6.1.2(a)] and that for NEIBMPH₄ [Figure 6.1.2(b)], revealed some major differences.

The methyl protons of the ethyl group (CH_2CH_3) coupled through three bonds to the adjacent protons (CH_2) in the same group, are observed in ^1H nmr spectra for both the N-oxide (1.17 ppm) and for NEIBMPH₄ (1.37 ppm).

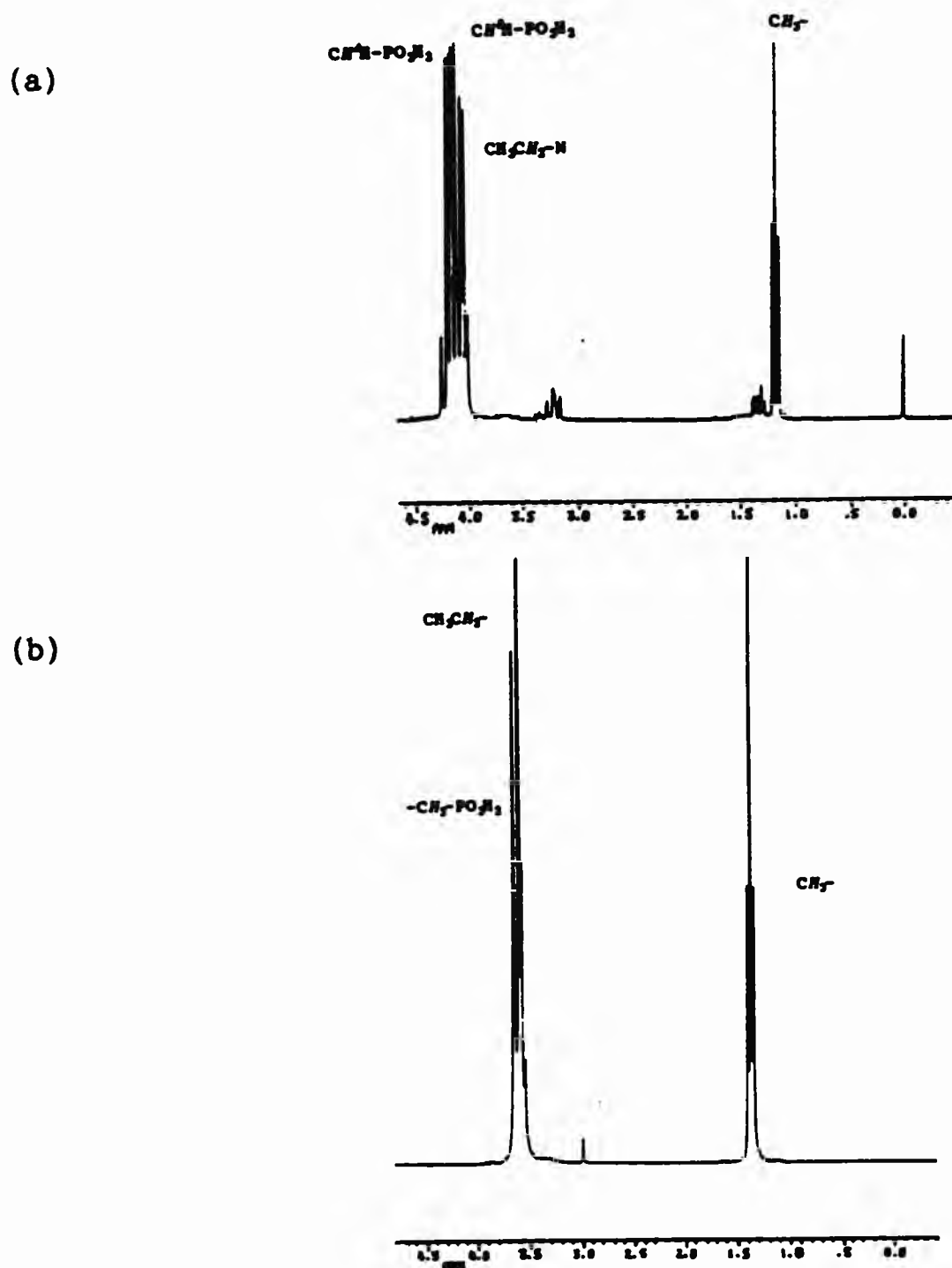


Figure 6.1.2 ^1H nmr spectra for aqueous (D_2O) solutions of (a) the N-oxide derivative of NEIBMPH₄ and (b) NEIBMPH₄.

The expected splitting pattern for the methylenephosphonate protons ($\text{CH}_2\text{-PO}_3\text{H}_2$) is a doublet, arising from the protons coupling through two bonds to the adjacent phosphorus atom [$^2\text{J}(\text{HP})$]. The CH_2 protons in the ethyl group are also expected to couple through three bonds to the adjacent methyl protons resulting in a quartet. In the ^1H nmr spectrum obtained for NEIBMPH_2 , the signals arising from the methylenephosphonate protons ($\text{CH}_2\text{-PO}_3\text{H}_2$) and the protons in the ethyl group (CH_2CH_3) are overlapped (ca. 3.4-3.7 ppm).

However, the signals arising from $\text{CH}_2\text{-PO}_3\text{H}_2$ and CH_2CH_3 in the ^1H nmr spectrum for the N-oxide [Figure 6.1.2(b)] are clearly defined and are slightly shifted downfield by ca. 0.7 ppm compared to the positions of the signals in the 'free-ligand'. The region between 4.0-4.3 ppm when expanded clearly shows two quartet-like multiplets with another quartet slightly at higher field (Figure 6.1.3). The latter quartet (4.04 ppm) can be assigned to the CH_2CH_3 protons, which are coupled through three bonds to the adjacent methyl protons. The remaining two multiplets in this region are assigned to the methylenephosphonate protons. The methylenephosphonate protons in the N-oxide derivative are anisochronous ($\text{CH}^1\text{H}^2\text{PO}_3\text{H}_2$). This arises from the *prochiral* environment of the nitrogen atom and results in the protons H^1 and H^2 being coupled to each other and further coupled through two bonds to the phosphorus atom giving an ABX spin system. The two AB subspectra are shown in Figure 6.1.3.

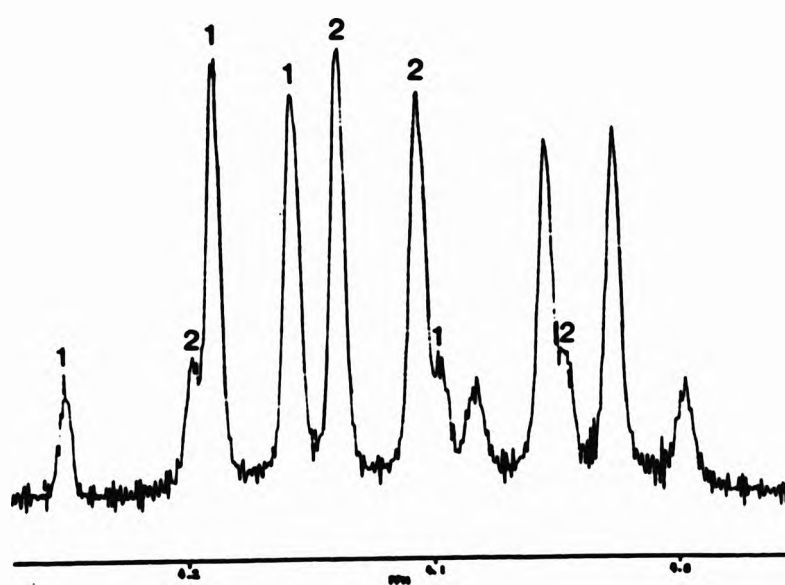


Figure 6.1.3 The two AB subspectra observed in the ^1H nmr spectrum for the N-oxide derivative of NEIBMPH_2 . The quartet arising from the CH_2CH_3 protons is not labelled.

The X part of the ABX spin system, theoretically six signals, is observed in the ^{31}P nmr spectrum as a triplet centred at 5.14 ppm. The ^{31}P chemical shift is significantly upfield (5.14 ppm) of the phosphorus signal in the ^{31}P nmr spectrum for NEIBMPH₄ (9.14 ppm).

Analysis of the AB subspectra¹¹ yields two different sets of parameters (Table 6.1.1), both of which satisfy this part of the spectrum. However, the parameter set appropriate for this spin system (set 1) can be chosen on the basis of the X spectrum (proton coupled, ^{31}P nmr spectrum). Parameter set 1 predicts that only four of the six lines in the X spectrum have significant intensity and that the inner two lines of the symmetrical pattern are overlapped, yielding a triplet pattern. Parameter set 2 predicts a symmetrical pattern of five signals each with sufficient intensity.

Table 6.1.1 Analysis of the AB subspectra to give two sets of parameters.^a

	ν_A	ν_B	J_{AX}	J_{BX}	J_{AB}
Set 1	1046.15 (4.18)	1028.09 (4.11)	12.87	12.67	14.90
Set 2	1037.47 (4.15)	1037.37 (4.15)	30.21	-4.67	14.90

^a Values are in Hz, except for the values in parentheses which are in ppm.

Major differences were also observed between the ^{13}C nmr spectra obtained for NEIBMPH₄ and its N-oxide derivative. Oxidation of the nitrogen of NEIBMPH₄ by hydrogen peroxide to form the N-oxide results in a downfield shift for all ^{13}C nmr signals by ca. 8-13 ppm. This suggests that all the carbons are being deshielded due to the highly electronegative oxygen atom of the N-oxide group withdrawing electron density away from the methylene carbons.

Based on this and other observations,⁴ it is clear that treatment of NEIBMPH₄ with hydrogen peroxide forms the N-oxide derivative.

6.1.3 Protonation equilibria for the N-oxide derivative of NEIBMPH₄

The N-oxide derivative of NEIBMPH₄ has five possible protonation sites, the four phosphonate oxygen atoms and the amine oxygen atom.



Three potentiometric titrations of the ligand at three different concentration of the N-oxide (Figure 6.1.4) were carried out over the pH range as before (Section 2.3) in the absence of any metal ions. The shape of the potentiometric titration curves obtained for the N-oxide, are somewhat different to those obtained for NEIBMPH₄ (Section 4.3). Approximately three equivalents of base are consumed by the N-oxide system by the end-point at pH ca. 8 on the titration curve. For each data file the fully deprotonated ligand was defined as $L = [CH_3CH_2N(O)(CH_2PO_3)_2]^{4-}$. Using the SUPERQUAD¹² program, refinements of the datafiles for a model which included the species LH_3^+ , LH_2^{2+} , LH_1^+ and LH_0 were successful (Table 6.1.2). Using arguments previously applied to the determination of the protonation scheme of NEIBMPH₄ (Section 4.4), the fully protonated species LH_3^+ probably exists only in very acidic conditions. The titration curves gave no indication that the N-oxide was unstable over the pH range studied.

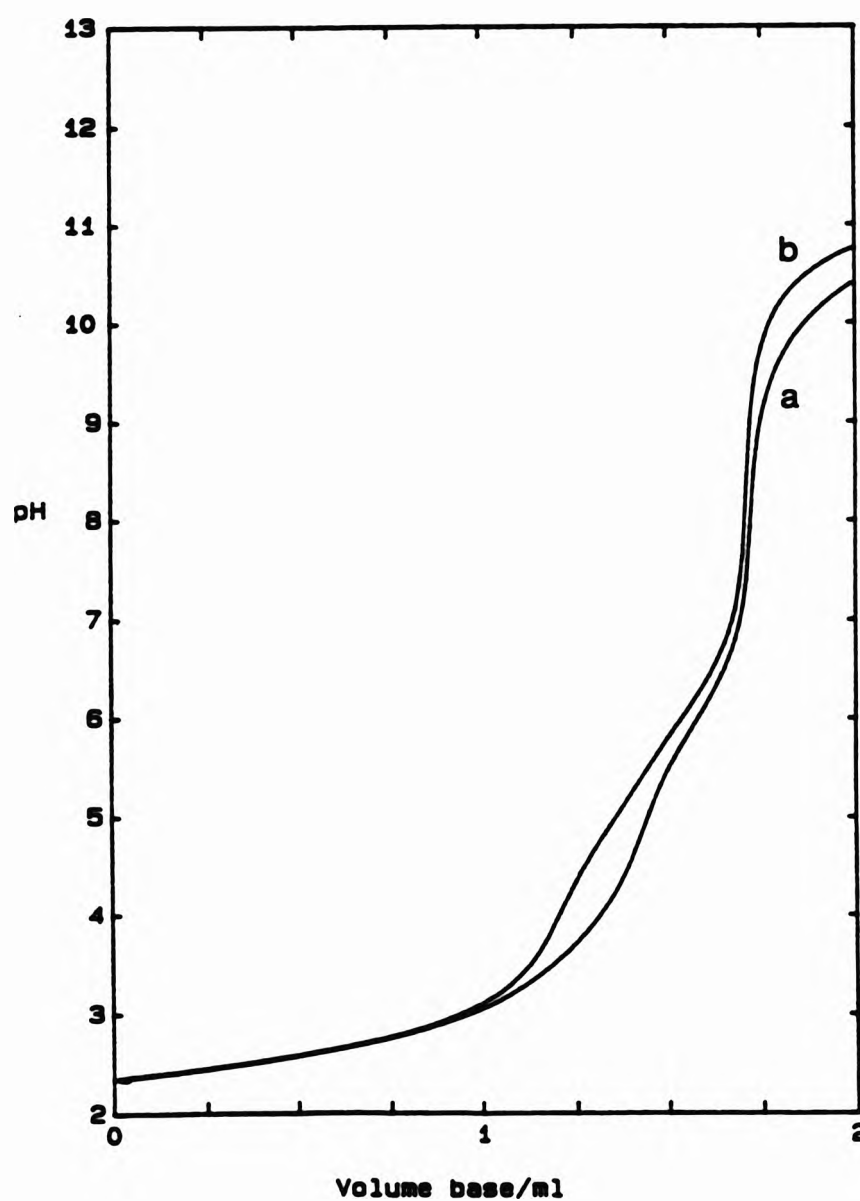


Figure 6.1.4 Titration curves (pH vs volume of base added) for (a) [N-oxide] ca. 0.001 mol dm⁻³ and (b) [NEIBMPH₄] ca. 0.001 mol dm⁻³.

Table 6.1.2 Protonation constants for N-oxide, where L = [EtN(O)(CH₂PO₃)₂]⁴⁻.^a

Datafile	M087 ^b	M088 ^c	M090 ^d	Mean ^e
log β ₀₁₁	10.12(0.010)	9.99(0.020)	10.02(0.014)	10.04 ±0.08
log β ₀₁₂	16.28(0.016)	16.13(0.033)	16.11(0.022)	16.17 ±0.11
log K ₀₁₂	6.16	6.14	6.09	6.13 ±0.04
log β ₀₁₃	20.89(0.022)	20.71(0.051)	20.66(0.030)	20.75 ±0.14
log K ₀₁₃	4.61	4.58	4.55	4.58 ±0.03
log β ₀₁₄	23.26(0.009) ^f		22.88(0.010) ^g	23.07 ±0.19
log K ₀₁₄	2.37		2.22	2.30 ±0.08

^a I = 0.1 mol dm⁻³ KNO₃, 25.0 ±0.1 °C. Figures in parentheses are standard deviations obtained from SUPERQUAD. Convention: β_{MLH} for M_nL_mH_n. ^b Fit parameters obtained from SUPERQUAD, χ² = 2.57, σ = 0.0915; pH 2.81-11.12; 130 data points. ^c Fit parameters obtained from SUPERQUAD, χ² = 5.60, σ = 0.0798; pH 2.97-11.09; 111 data points. ^d Fit parameters obtained from SUPERQUAD, χ² = 3.32, σ = 0.0902; pH 5.08-9.71; 31 data points. ^e Unweighted mean of values from each refinement; error limits are derived from the ranges obtained for each log β_{MLH} (and log K_{MLH}). ^f Fit parameters obtained from SUPERQUAD, χ² = 4.36, σ = 0.0711; pH 2.71-3.32; 44 data points. ^g Fit parameters obtained from SUPERQUAD, χ² = 3.78, σ = 0.0812; pH 2.64-3.42; 54 data points.

To date, relatively few studies have been concerned with the determination of protonation constants for N-oxide derivatives of α-aminomethylenephosphonic acids. Carter *et al.* prepared the N-oxide derivative of nitrilotris(methylene phosphonic acid), NTMPH₆ and determined its protonation and complexation behaviour by potentiometry and nmr spectroscopy where appropriate.⁴ Carter *et al.*⁴ noted the occurrence of one weakly acidic proton of the N-oxide derivative and interpreted this as the proton bound to the amine oxygen. Carter also suggested that the large difference between the values log K₀₁₁ and log K₀₁₂ (Table 6.1.3) for the N-oxide derivative of NTMPH₆ (ca. 5.1 log units) could be ascribed to protonation of two different functions in the molecule, *i.e.* the amine oxygen and the phosphonate oxygen.⁴

Carter confirmed the protonation scheme of the N-oxide derivative of NTMPH₆ by carrying out ³¹P vs pH nmr titrations of both the N-oxide and NTMPH₆.⁴ Differences were observed in the resulting plots of (δ)³¹P vs equivalents of base at high pH.⁴ As with other alkylaminomethylenephosphonic acids, the δ³¹P

Table 6.1.3 Protonation constants of the α -aminomethylenephosphonic acids, NTMPH₆ and NEIBMPH₄, and their N-oxide derivatives.

ligand	log K ₀₁₁	log K ₀₁₂	log K ₀₁₃	log K ₀₁₄	log K ₀₁₅	log K ₀₁₆
NTMPH ₆ ^a	12.34	6.66	5.46	4.30	< 2	< 2
N-oxide ^a	12.05	6.95	5.26	3.28	< 2	< 2
NEIBMPH ₄ ^b	12.00	6.28	4.89	1.94		
N-oxide ^b	10.04	6.13	4.58	2.54		

^a Ref. 4. I = 0.1 mol dm⁻³ KNO₃, 25.0 °C. ^b This work, I = 0.1 mol dm⁻³ KNO₃, 25.0 ± 0.1 °C.

vs equivalents of base profile for NTMPH₆ and the N-oxide showed a gradual upfield shift in the phosphorus signal as the titration progressed in acidic medium; this was ascribed to the deprotonation of the phosphonate oxygen atoms (Section 4.3). At high pH, the profile of $\delta^{31}\text{P}$ vs equivalents of base for the N-oxide derivative showed a slight downfield shift in the phosphorus signal, whereas the unconverted ligand showed a very large downfield shift at high pH. Carter suggested that this much smaller downfield shift for the N-oxide was consistent with the amine oxygen atom being deprotonated and that the deprotonation site, being an extra atom away from the phosphorus atom, has a much smaller influence on the phosphorus chemical shift than the tertiary nitrogen atom in NTMPH₆.⁴

Therefore, in order to clarify the protonation scheme of the N-oxide derivative of NEIBMPH₄, ³¹P nmr vs pH titrations for both the N-oxide and NEIBMPH₄ were determined.

The resulting profiles of $\delta^{31}\text{P}$ vs pH (Figure 6.1.5) for the N-oxide and NEIBMPH₄ are significantly different. The steady upfield shift in the phosphorus signal is ascribed to the deprotonation of phosphonate oxygens and the large downfield shift in the phosphorus signal thereafter, is ascribed to deprotonation of the nitrogen-bound proton (Section 4.4). However, for the N-oxide derivative there is only a slight downfield shift (ca. 0.5 ppm) in the phosphorus signal observed at high pH [Figure 6.1.5(a)]. By analogy with

Carters work on NTMPH_2 ,¹ this slight downfield shift may be due to deprotonation on the amine oxygen.

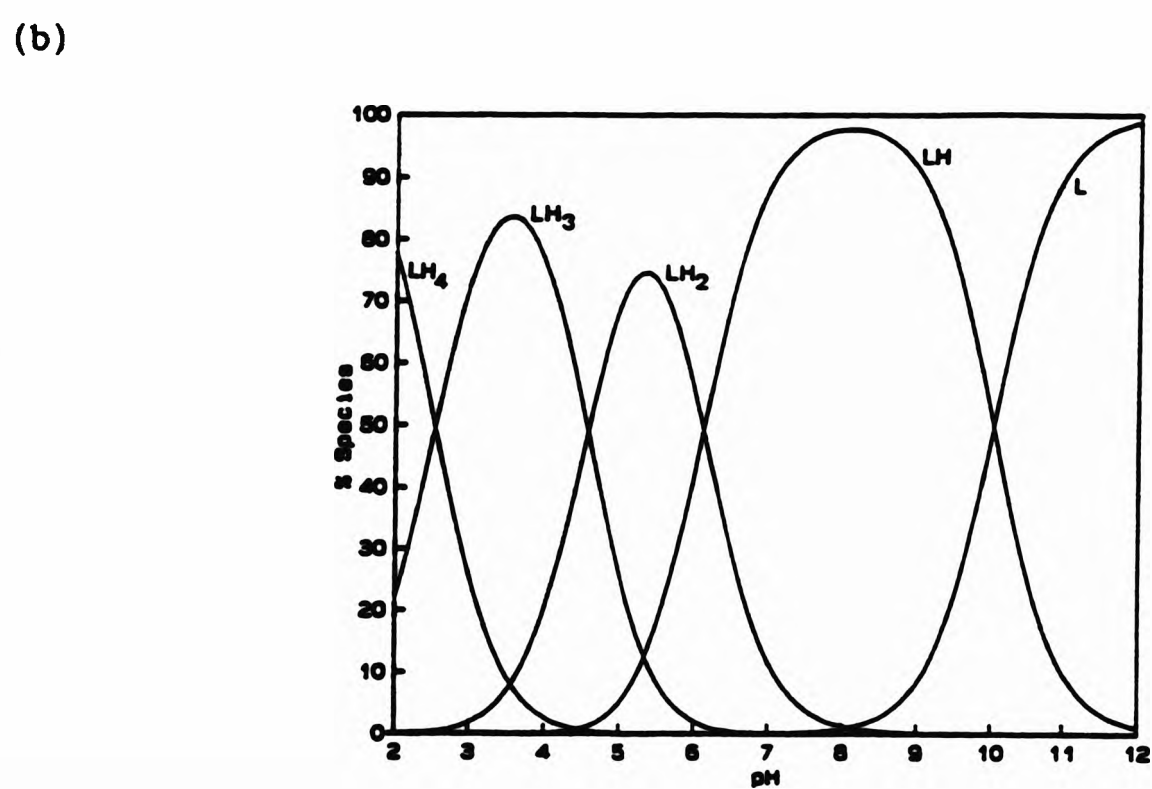
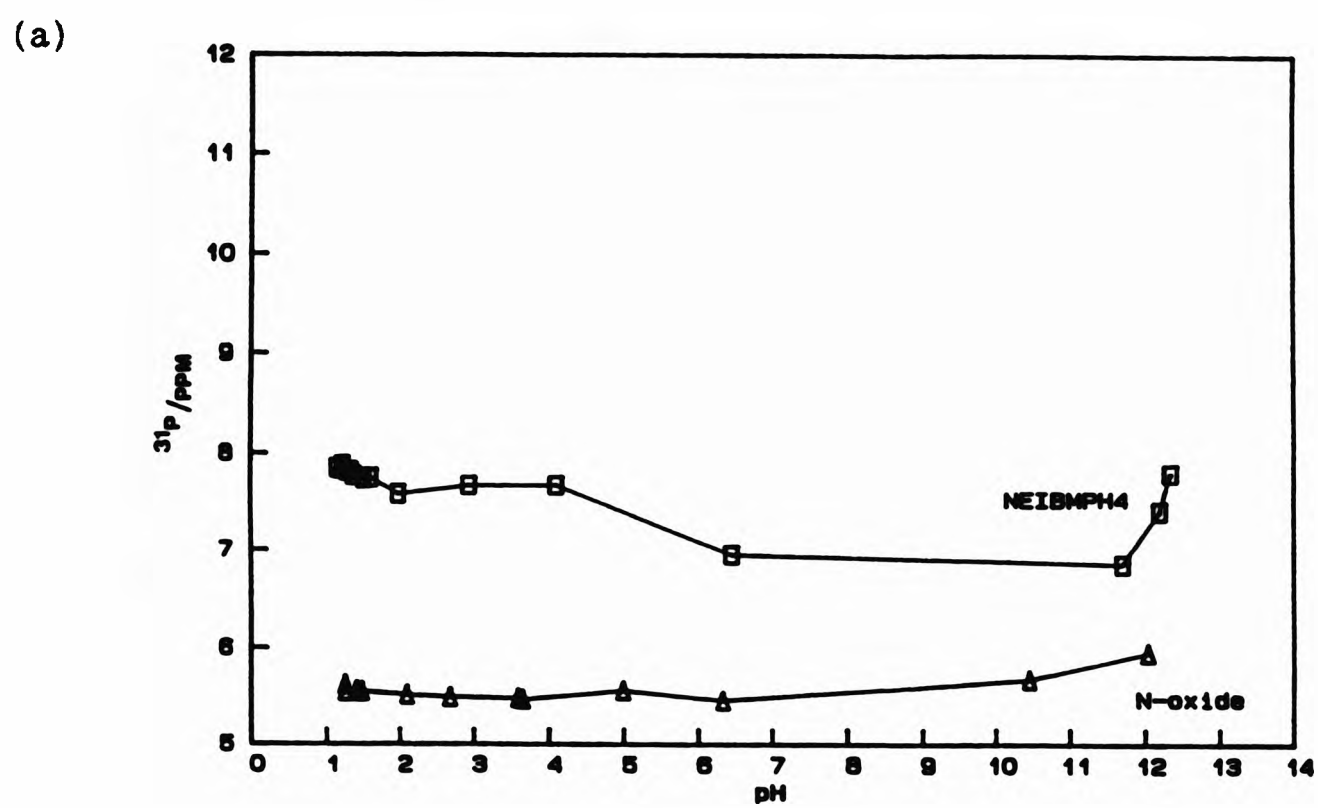
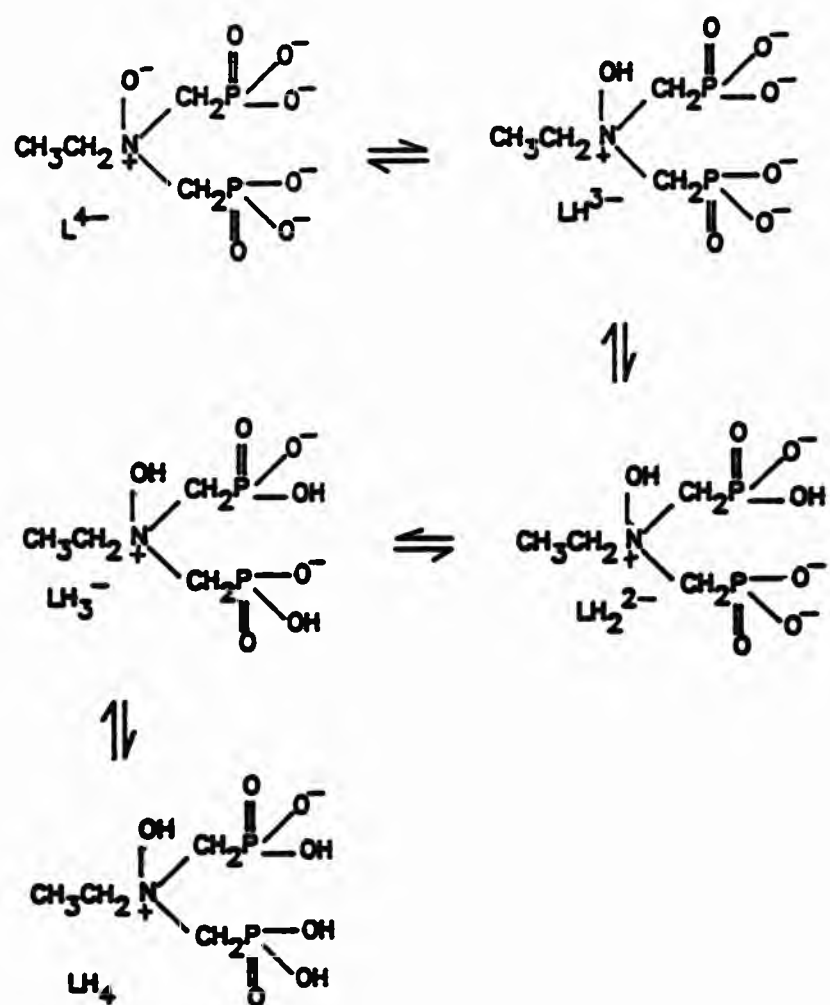


Figure 6.1.5 (a) The pH-dependence of $\delta^{31}\text{P}$ vs pH for NEIBMPH_4 and the N-oxide and (b) species distribution curves¹³ for the N-oxide.

The following protonation scheme has been assigned to the protonation constants determined for the N-oxide derivative of NEIBMPH₄.



6.1.3(a) Preliminary examination of the stability of Cu(II) complexes of the N-oxide derivative

Limited potentiometric studies for the N-oxide derivative of NEIBMPH₄ with Cu(II) were carried out (Section 2.3.6). Potentiometric titrations for the N-oxide with Cu(II) were obtained at metal:ligand ratios of ca. 1:1 and 1:2. Significant deviation of the 'metal-ligand' curve from the 'ligand-only' curve occurs at a ca. pH 3 (Figure 6.1.6) indicating the formation of metal complexes.

The previously determined protonation constants for the N-oxide were held as constant in the SUPERQUAD¹² input files. Subsequent refinements of the data files for a model which included the species [ML]²⁻, [MLH]⁻ and [MLH₂] were successful. The metal stability constants are summarised in Table 6.1.4.

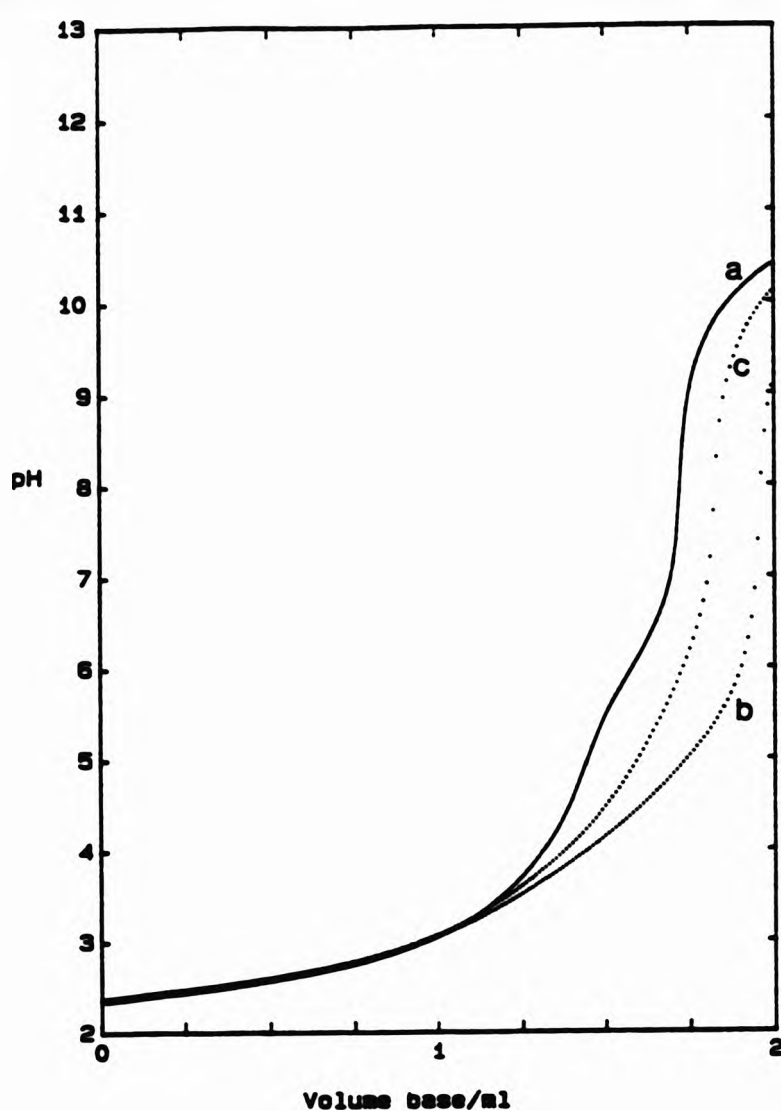


Figure 6.1.6 Titration curves (pH vs volume of base added) for acidified solutions of N-oxide; (a) [N-oxide] ca. $0.001 \text{ mol dm}^{-3}$; (b) $\text{Cu}(\text{NO}_3)_2$ with N-oxide, [M]:[L] ca. 1:1 and (c) $\text{Cu}(\text{NO}_3)_2$ with N-oxide, [M]:[L] ca. 1:2.

Table 6.1.4 Metal stability constants for the N-oxide derivative with Cu(II).^a

Datafile	$\log \beta_{110}$	$\log \beta_{111}$	$\log K_{111}$	$\log \beta_{112}$	$\log K_{112}$
M091 ^b	11.14(0.010)	16.36(0.006)	5.22	20.35(0.010)	3.99
M092 ^c	11.13(0.009)	16.39(0.004)	5.26	20.01(0.009)	3.62
Mean ^d	11.14 ± 0.01	16.38 ± 0.02	5.24 ± 0.02	20.18 ± 0.17	3.81 ± 0.18

^a $I = 0.1 \text{ mol dm}^{-3} \text{ KNO}_3$, $25.0 \pm 0.1 \text{ }^\circ\text{C}$. Figures in parentheses are standard deviations obtained from SUPERQUAD. Convention: β_{MLH} for $M_nL_mH_p$. ^b Fit parameters obtained from SUPERQUAD, $\chi^2 = 3.74$, $\sigma = 0.0280$; pH = 3.50–5.89, 46 data points. ^c Fit parameters obtained from SUPERQUAD, $\chi^2 = 4.53$, $\sigma = 0.0431$; pH = 3.51–6.92, 60 data points. ^d Unweighted mean of values from each refinement; error limits are derived from the ranges obtained from each $\log \beta_{MLH}$ (and $\log K_{MLH}$).

The species distribution curves¹³ for the N-oxide derivative of NEIBMPH₄ in the presence of Cu(II) is shown in Figure 6.1.7.

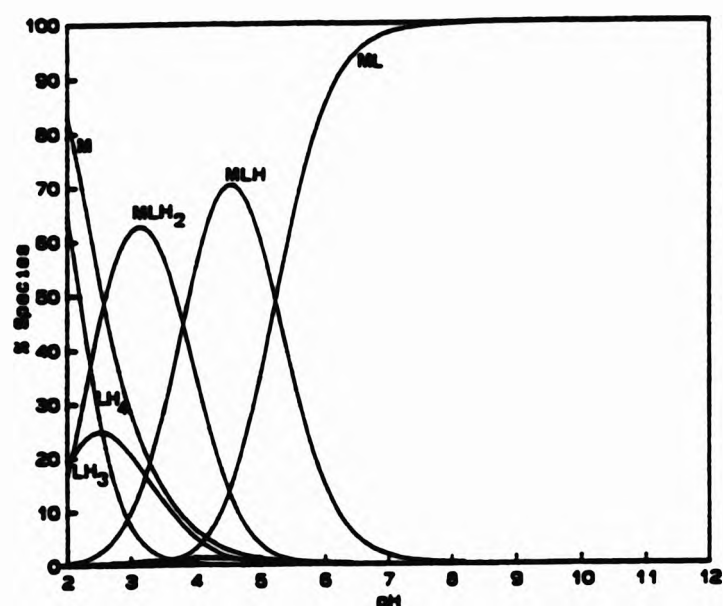
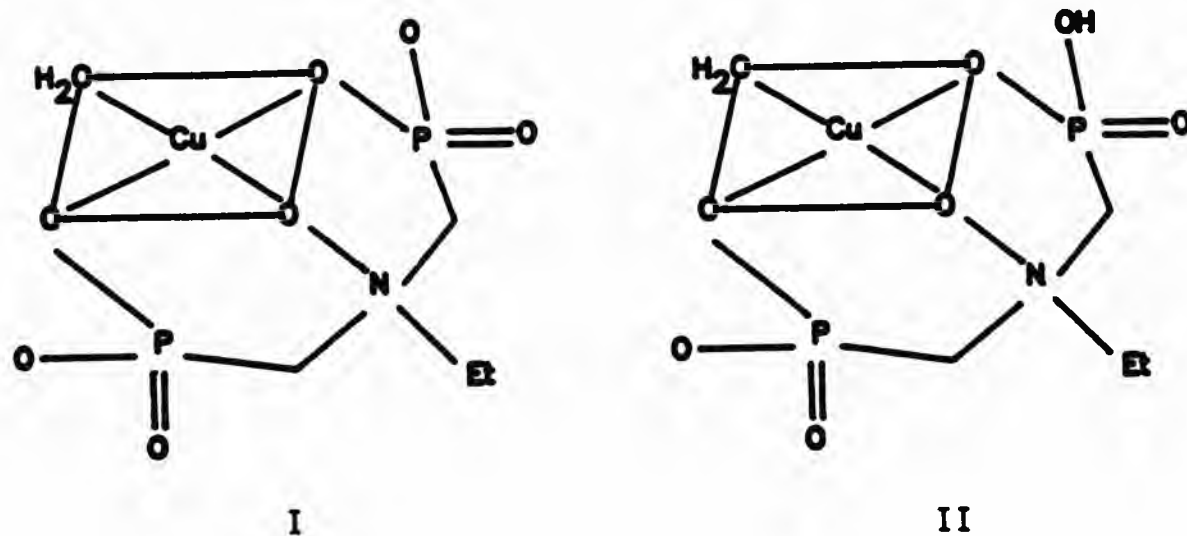


Figure 6.1.7 Species distribution curves¹³ for N-oxide derivative with Cu(II) at [M]:[L] ca. 1:1.

As already mentioned in Section 5.1.4, the basicity of uncoordinated oxygens (O^-) on the N-oxide is expected to decrease on coordination of the ligand to a the metal ion *via* another site on the ligand. The process of protonating the complex $[CuL]^{2-}$ ($[CuL]^{2-} + H^+ \rightleftharpoons [CuLH]^-$) to give the monoprotonated species has a value of $\log K_{111} = 5.24$. This value is less than that for the process of protonation a phosphonate oxygen of the 'free-ligand' ($\log K_{012} = 6.13$); consequently, this indicates that protonation of $[CuL]^{2-}$ occurs at a phosphonate oxygen rather than on the amine oxygen atom. This can be taken as evidence that the amine oxygen atom is coordinated to the Cu(II) ion, as proposed in structure I $[CuL]^{2-}$ and structure II $[CuLH]^-$.



It seems reasonable to assume that formation of two six-membered chelate rings by involving the amine oxygen in coordination to Cu(II) contributes to the stability of these complexes.

Stability constants for metal complexes of some N-oxide derivatives obtained by Carter *et al.*⁴ suggest that the ligands ability to coordinate metal ions [e.g. Ca(II) and Mg(II)] is reduced slightly on conversion to the N-oxide. The difference in the values of $\log K_{110}$ for Cu(II) with the N-oxide (11.14) and NEIBMPH₄ (13.28) is ca. 3 log units.

In summary, in *aqueous* solutions of hydrogen peroxide, α -aminomethylene phosphonic acids are converted to the N-oxide derivatives. The metal stability constants of the N-oxide derivative of NEIBMPH₄ with Cu(II) indicate that the ligand can still complex metal ions, but the stability of the resulting complexes are somewhat less than the analogous complexes with the parent acid.

6.1.4 Preliminary investigations of the possible interaction between DEAMPH₂ and sodium stannate

The combination of alkylaminomethylenephosphonic acids and sodium stannate produces improved stability of hydrogen peroxide which is not achieved by either the aminophosphonic acid or sodium stannate alone.^{14,15} The mechanism of stability enhancement is not known.

Sodium stannate has the composition Na₂SnO₃·3H₂O. However, the water cannot be removed by prolonged desiccation and can only be removed at 140 °C *in vacuo*, during which the nature of the substance is altered.¹⁶ Williams suggested that in the solid state, the three water molecules form part of an ion, [Sn(OH)₆]²⁻, a deduction which is supported by Wyckoff's X-ray evidence that the lattice of potassium stannate is similar to that of potassium hexachloroplatinate(II) with six anionic ligand groups octahedrally arranged around the central metal atom.¹⁷

6.1.4(a) The pH-dependence of the ³¹P nmr chemical shift of DEAMPH₂ in the presence of sodium stannate

The interest in sodium stannate/phosphonate interactions originated from a project to "clone" a hydrogen peroxide formulation which is used as a cleaner for contact lens. The interaction between CDTMPH₃ and sodium stannate was

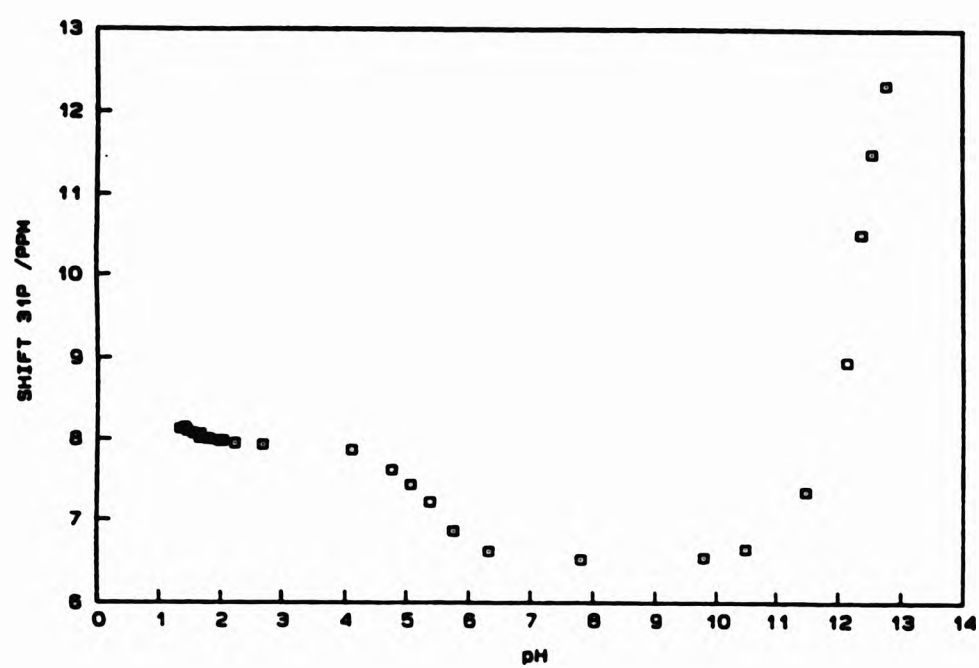
implied, in a decrease in the concentration of the free phosphonic acid, as determined by ion chromatography.¹⁵ It was suggested that the phosphonic acid was bound to stannate in some way and hence could not be detected. The sodium stannate was also added to solutions of N-oxide derivatives of aminomethylene-phosphonic acids and the concentration of the N-oxide was also found to decrease. However, the exact nature of this interaction has not been fully characterised. It was suggested that a tin-phosphonate complex is formed which may bind to the free metal ions reducing the instability of hydrogen peroxide (Chapter 3).¹⁵

Investigation of the possible interaction of an alkylaminomethylene-phosphonic acid with sodium stannate was carried out by using nmr/pH titrations. A solution of the ligand DEAMPH₂ and sodium stannate in a 2:1 molar ratio, was prepared (Section 2.4.7). All ³¹P nmr spectra showed one signal for the phosphorus environment over the pH range 1.65-13.00. This again indicated rapid proton exchange. The resulting profile of $\delta^{31}\text{P}$ vs pH for DEAMPH₂ with sodium stannate was similar to that for DEAMPH₂ alone [Figure 6.1.8(a) and (b)].

As the titration proceeds [Figure 6.1.8(b) there is an upfield shift of the phosphorus signal of ca. 1.5 ppm. As determined before (Section 4.3) this is ascribed to the phosphonate bound proton being neutralised. As more base is added (ca. pH 11) there is a rapid downfield shift of the phosphorus signal of ca. 5.5 ppm, similar to that observed for the untreated ligand DEAMPH₂.

This suggests that the phosphorus atom is being deshielded as in the free phosphonic acid alone (Section 4.3), implying that the nitrogen is being deprotonated (as before). Since the pH-dependence of ³¹P for DEAMPH₂ in the presence of sodium stannate is not significantly different to that for the untreated ligand, the basic structure of DEAMPH₂ appears to be retained and this experiment provides no further evidence for interaction.

(a)



(b)

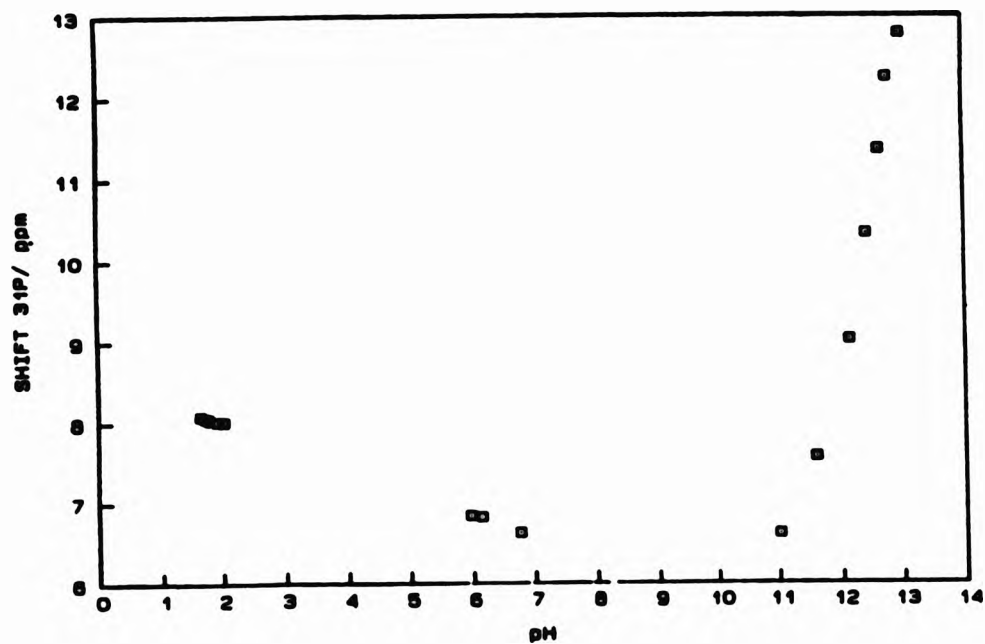


Figure 6.1.8 The pH-dependence of $\delta^{31}\text{P}$ for (a) DEAMPH_2 alone and (b) DEAMPH_2 in the presence of sodium stannate.

6.2 References

1. M. Hollmann, R. Opitz and K. Haage, Ger.(East) 144073, CA 94, 210645f, 1980. K. J. Radimer, Eur. Pat. Appl. EP. 97305, CA 100, 123537w, 1984. G. W. Morris, N. D. Feasey, P. A. Ferguson, D. Van Hemelrijk and M. Charlot, PCT Int. Appl. WO 900134, CA 113, 6601v.
2. R. D. Gillard and P. D. Newman, *Polyhedron*, 1989, 48, 2077.
3. D. F. Evans and M. W. Upton, *J. Chem. Soc., Dalton Trans.*, 1985, 2525.
4. E.g. R. P. Carter, M. M. Crutchfield and R. R. Irani, *Inorg. Chem.*, 1967, 6, 943.
5. S. Croft, B. C. Gilbert, J. R. L. Smith, J. K. Stell and W. R. Sanderson, *J. Chem. Soc., Perkin Trans. 2*, 1992, 153. J. K. Stell, Ph.D Thesis, University of York, 1991.
6. E.g. J. L. Sudmeier and C. N. Reilley, *Polyhedron*, 1964, 36, 1699. J. F. Desreux, E. Merciny and M. F. Loncin, *Inorg. Chem.*, 1981, 20, 987. C. F. G. C. Geraldès, M. C. Alpoim, M. P. M. Marques, A. D. Sherry and M. Singh, *Inorg. Chem.*, 1985, 24, 3876. S. Cortes, E. Bruncher, C. F. G. C. Geraldès and A. D. Sherry, *Inorg. Chem.*, 1990, 29, 5. C. F. G. C. Geraldès, A. D. Sherry, M. P. M. Marques, M. C. Alpoim and S. Cortes, *J. Chem. Soc., Perkin Trans. 2*, 1991, 137.
7. T. G. Appleton, J. R. Hall, A. D. Harris H. A. Kimlin and I. J. McMahon, *Aust. J. Chem.*, 1984, 37, 1833.
8. K. Mikkelsen and S. O. Nielsen, *J. Phys. Chem.*, 1960, 64, 632. P. K. Glasoe and F. A. Long, *J. Phys. Chem.*, 1960, 64, 188.
9. C. F. G. C. Geraldès, A. D. Sherry and W. P. Cacheris, *Inorg. Chem.*, 1989, 28, 3336.
10. S. N. Lewis in, *Oxidation: Volume 1*, Ed. R. L. Augustine, 1969, Marcel Dekker, New York.
11. R. A. Hoffman, S. Forsen and B. Gestblom, *Analysis of NMR Spectra, in NMR Basic Principles and Progress*, 1971, 5, Springer-Verlag.
12. P. Gans, A. Sabatini and A. Vacca, *J. Chem. Soc., Dalton Trans.*, 1985, 1195.
13. R. J. Motekaitis, FORTRAN 77 program SPE, 1987. C. Crees, TURBO-C program SPECIES, 1990. C. J. L. Silwood, GW-BASIC program HPLOT, 1990.
14. S. Lynch and G. W. Morris, personal communication.
15. S. Lynch and N. Chalkley, *Internal report*, Interlox Research & Development, 1990.
16. R. L. Williams and R. J. Pace, *J. Chem. Soc.*, 1957, 4143.

17. R. W. G. Wyckoff, *Amer. J. Sci.*, 1928, 15, 297.

*Chapter 7 Determination of the solid state structures
of N, N-diethylaminomethylenephosphonic acid
and (±)-transcyclohexane-1,2-diamine-
tetrakis(methylenephosphonic acid) by single
crystal X-ray diffraction*

7.1 Introduction

The coordination behaviour of alkylaminomethylenephosphonic acids has been widely studied since 1960, by a number of workers (Chapter 5) e.g. Banks,¹ Kabachnik,² Westerback,³ Motekiatis⁴ and Sawada⁵ to name but a few. Further insight into the nature of the species of metal complexes with α -aminomethylenephosphonic acids is hampered by the lack of information about the ways in which these acids coordinate to metal ions. There are relatively few crystal structures of the metal complexes⁶⁻¹⁰ because suitable crystals for X-ray analysis are particularly difficult to obtain,^{10,11} compared to the free acids, e.g. refs. 12-14. In this work, attempted syntheses of metal complexes of CDTMPH₃ were unsuccessful, probably because they were difficult to isolate. Solid metal complexes of NEIBMPH₄ were isolated and characterised, but it was not possible to obtain them in crystalline form (Chapter 5).

In contrast, the solid state structures of the 'free acids' have proved more readily accessible (e.g. refs. 12-22), but success in obtaining crystals of any given aminomethylenephosphonic acid appears to be largely fortuitous. In particular, isolating solid products from reactions to synthesise *N, N*-di-alkylaminomethylenephosphonic acids has been reported as particularly difficult.²³

N, N-Diethylaminomethylenephosphonic acid, DEAMPH₂,²⁴ was reacted with *n*-butylstannonic acid in order to prepare a complex, but the colourless crystals isolated from the reaction mixture were found to be the 'free ligand', DEAMPH₂, and not the desired complex (again, indicating the difficulty in preparing solid metal complexes of α -aminomethylenephosphonic acids). The crystals were suitable for X-ray crystal structural analysis (Table 7.1.1).

Crystals of (\pm)-*trans*-cyclohexane-1,2-diamine *tetrakis*(methylenephosphonic acid), CDTMPH₃, were originally isolated by another worker,²⁵ and were used for X-ray crystal structural analysis (Table 7.1.1). Subsequently, however, during the course of this work, beautiful, colourless rectangular crystals of CDTMPH₃ were also isolated after allowing a reaction mixture to stand for nine months (Section 2.2.4).

The crystals of *N, N*-diethylaminomethylenephosphonic acid and (\pm)-*trans*-cyclohexane-1,2-diamine *tetrakis*(methylenephosphonic acid) used for X-ray structural

analysis were fully characterised by C, H, N elemental analysis and nmr spectroscopy (Section 2.2). The nmr spectra obtained for the crystals were consistent with those obtained for the bulk samples, as described in Section 2.2.

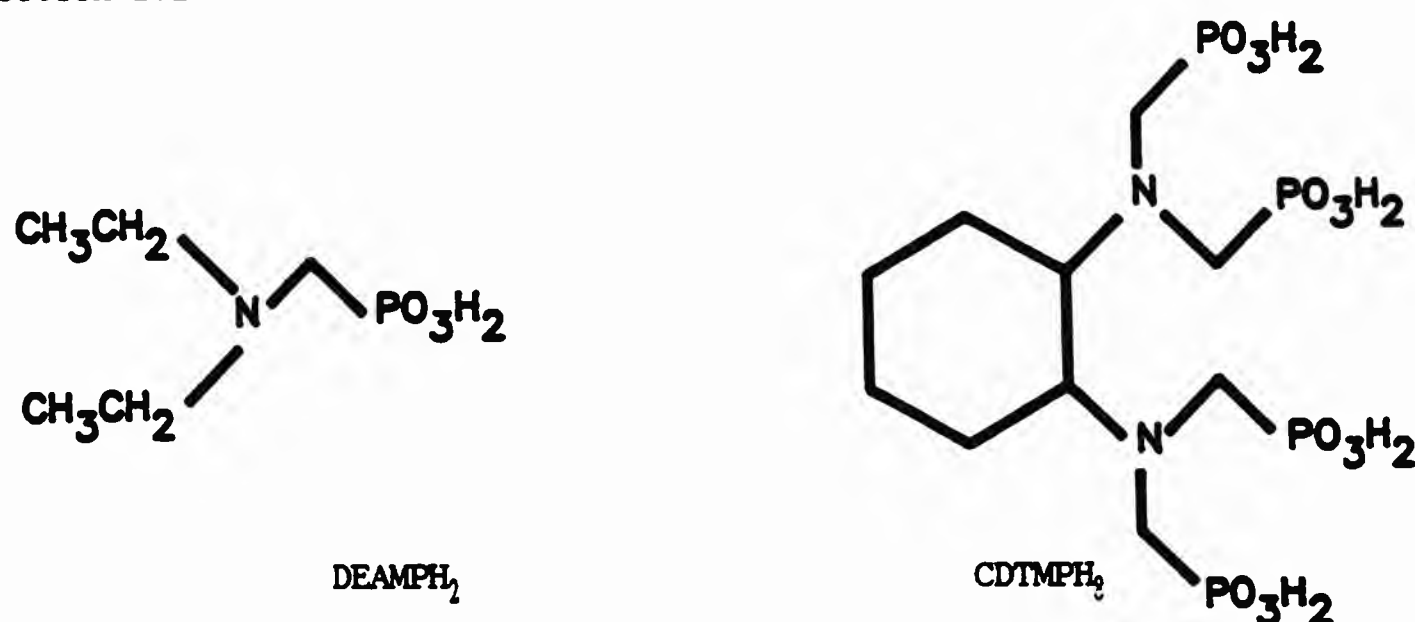


Table 7.1.1 Crystal data obtained for *N,N*-diethylaminomethylenephosphonic acid and (\pm)-*trans*-cyclohexane-1,2-diamine tetrakis(methylene-phosphonic acid).

	DEAMPH ₂	CDTMPH ₃ · H ₂ O
Molecular formula	C ₅ H ₁₄ NO ₃ P	C ₁₀ H ₂₃ N ₂ O ₁₃ P ₄
Relative molecular weight	167.145	508.233
Lattice type	monoclinic	monoclinic
Space group	P2 ₁ /n	P2 ₁ /c
<i>a</i> / Å	7.708(2)	10.660(3)
<i>b</i> / Å	11.398(3)	10.512(3)
<i>c</i> / Å	9.435(2)	18.778(3)
β / °	105.3(2)	105.474(2)
<i>U</i> / Å ³	779.54	2027.95
<i>Z</i>	4	4
<i>F</i> (000)	360	1064
<i>D</i> _c / g cm ⁻³	1.389	1.665
μ (Mo-K α) / cm ⁻¹	2.9	4.3
λ	0.71069	0.71069
Final R(<i>R</i> _v)	0.0498(0.0489)	0.0420(0.0420)
Number of reflections	856	2552
Dimensions /mm	0.20 × 0.20 × 0.15	0.25 × 0.30 × 0.20

X-Ray data²⁶ were collected on a Philips PW1100 four-circle diffractometer as described in Section 2.6. The structure solution and refinement of DEAMPH₂ and CDTMPH₃ are described in Sections 2.6.2 and 2.6.3, respectively.

7.2 Description of the solid state structure of *N, N*-diethylaminomethylene-phosphonic acid, DEAMPH₂

The tables of fractional atomic coordinates, anisotropic thermal parameters, bond lengths, bond angles, inter- and intra-molecular distances are given in Appendix 1 (Tables 1-7).

The structure of the DEAMPH₂ molecule in the solid state is shown in Figure 7.2.1.²⁷ Overall, the molecule has virtual C_s symmetry (mirror symmetry) along the nitrogen-carbon-phosphorus bonds, if the proton on the phosphonate oxygen atom is neglected.

DEAMPH₂ was found to be zwitterionic^{10,12-14,17,20} (Figure 7.2.1), with the nitrogen atom and one phosphonate oxygen atom each protonated. The positively charged nitrogen atom has a distorted tetrahedral coordination sphere (Table 7.2.1).

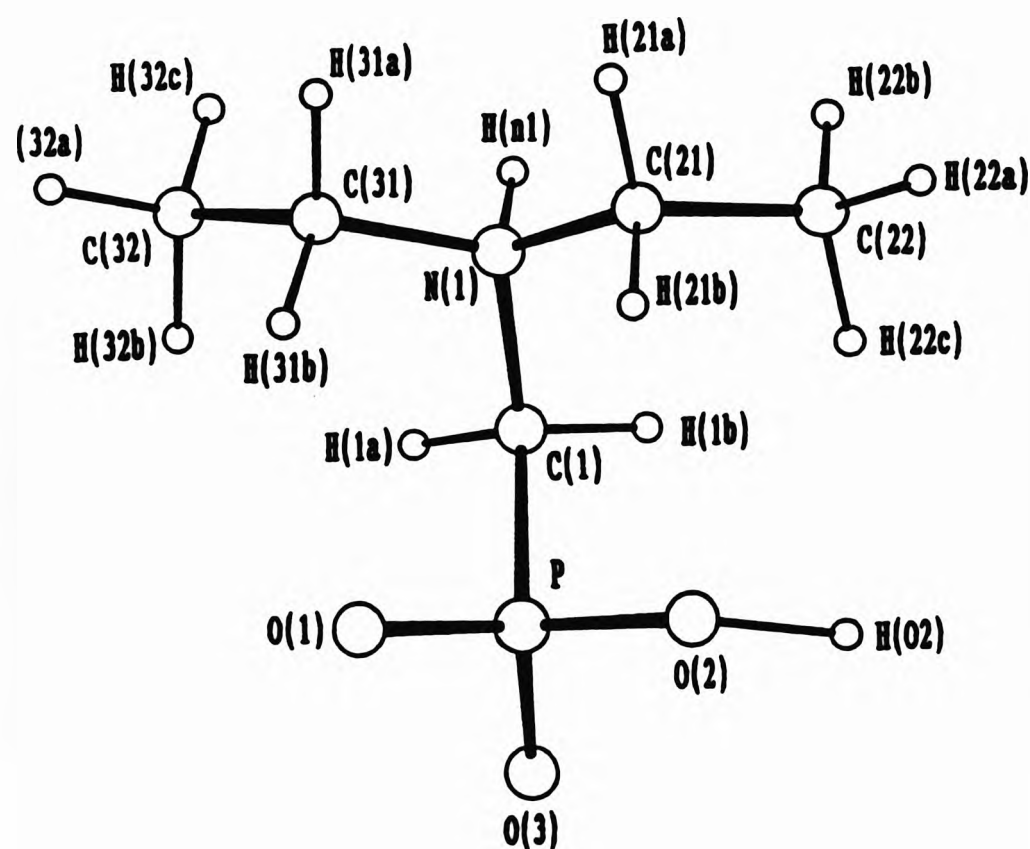


Figure 7.2.1 Molecular structure of DEAMPH₂, including hydrogen atoms.

Table 7.2.1 Bond angles (°) around the nitrogen atom in the DEAMPH₂ molecule.^a

C(31)-N(1)-C(1)	114.0(3)	H(n1)-N(1)-C(1)	101(3)
C(21)-N(1)-C(1)	113.7(3)	H(n1)-N(1)-C(31)	107(3)
C(31)-N(1)-C(21)	110.2(3)	H(n1)-N(1)-C(21)	110(3)

^a Values in parentheses are estimated standard deviations.

The C-N-C bond angles are all slightly greater than the idealised tetrahedral angle of 109.45°, whereas the bond angles involving the proton on the nitrogen atom H(n1); *i.e.* H(n1)-N(1)-C, are in a lower range, 101-110°. Comparison of the C-N-C bond angles with those for other α -aminomethylenephosphonic acids indicates that a pattern is observed (Table 7.2.2).^{17,20,21} Where there are two or more methylenephosphonate groups, the greatest C-N-C angle is between the substituent methylenephosphonate carbons. For example, this C-N-C angle between C-N-C in *N*-ethyliminobis(methylenephosphonic acid) is 113.1(3)°,¹⁷ whereas the angles C-N-C between the methylenephosphonate groups and the ethyl group are equal at 112.1(3)°.¹⁷

Table 7.2.2 Bond angles (°) at nitrogen for some related α -aminomethylene-phosphonic acids.^a

	NEIBMPH ₄ ^b	NTMPH ₆ ^c	EDTMPH ₈ ^d
Angles between CH ₂ PO ₃ H ₂ groups	113.1(3)	113.0(2)	111.4(3)
		112.4(2)	111.7(3)
		112.3(2)	
Angles between CH ₂ PO ₃ H ₂ and alkyl groups	112.1(3)		109.6(3)
	112.1(3)		109.9(3)
			108.2(3)
			110.9(3)

^a Values in parentheses are estimated standard deviations. ^b Ref, 17. *N*-ethyliminobis(methylenephosphonic acid). ^c Ref, 20. Nitriлотris(methylenephosphonic acid). ^d Ref, 21. Ethylenediaminetetrakis(methylenephosphonic acid).

In DEAMPH₂, there is only one substituent methylenephosphonate group, but it

is interesting that the angles at nitrogen involving the methylenephosphonate carbon are much larger [C(21)-N(1)-C(1) = 113.7(3)°, C(31)-N(1)-C(1) = 114.0(3)°] than the angle between the two ethyl groups [C(31)-N(1)-C(21) = 110.2(3)°]. In DEAMPH₂ there is significant repulsion between the phosphonate group and the two ethyl groups resulting in the ethyl groups at nitrogen being 'pushed' away from the monoprotonated phosphonate group. Whereas, in the solid state structure of NEIBMPH₄,¹⁷ the angles around the nitrogen atom involving the methylene carbons are similar, suggesting that repulsion between the phosphonate groups and the ethyl groups is not as great as for DEAMPH₂.

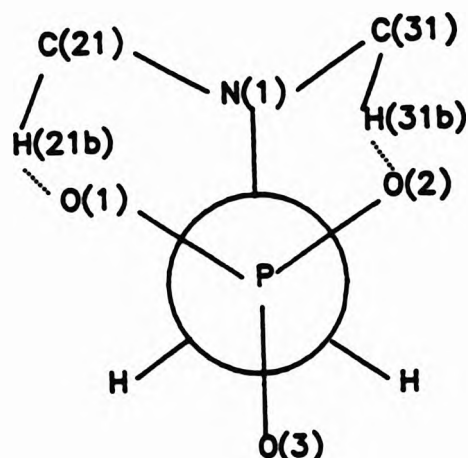
In DEAMPH₂, the bond angle subtended by the nitrogen atom and the phosphorus atom at the carbon atom is extremely large, N(1)-C(1)-P(1) = 120.2(3)°, compared to the range of values (110.9-117.9°) found for other related α -aminomethylenephosphonic acids (Table 7.2.3). This very large angle indicates considerable distortion in the environment of the methylene carbon, and it appears that this may be due to the staggered conformation of the phosphonate group with respect to the protonated nitrogen. However, the eclipsed conformation of both methylene carbons at the nitrogen atom, *i.e.* C(21) and

Table 7.2.3 N-C-P bond angles (°) for some related α -aminomethylenephosphonic acids.^a

Ligand	N-C-P	No. of substituent phosphonate groups
DEAMPH ₂ ^b	120.2(3)	1
DMAMBPH ₄ ^c	115.6(1), 112.0(1)	2
NEIBMPH ₄ ^d	117.9(3), 114.0(2)	2
EDTMPH ₈ ^e	115.2(3), 116.9(3)	4
	116.7(3), 115.7(3)	
NTMPH ₆ ^f	112.6(2), 113.5(2), 117.9(2)	3
AMPH ₂ ^g	110.9(1)	1

^a Values in parentheses are estimated standard deviations. ^b This work. *N,N*-Diethylaminomethylenephosphonic acid. ^c Ref, 14. *N,N*-Dimethylaminobis(methylenephosphonic acid). ^d Ref, 17. *N*-ethyliminobis(methylenephosphonic acid). ^e Ref, 21. Ethylenediaminetetrakis(methylenephosphonic acid). ^f Ref, 20. Nitrilotris(methylenephosphonic acid). ^g Ref, 19. Aminomethylenephosphonic acid.

C(31) with the phosphonate oxygens O(1) and O(2) provides evidence of some interaction between the protons on the methylene carbons and the phosphonate



oxygen atoms, *i.e.* $H(21b)\dots O(1) = 2.39 \text{ \AA}$ and $H(31b)\dots O(2) = 2.48 \text{ \AA}$ resulting in the large N-C-P angle observed.²⁷

The carbon to carbon bond lengths in the ethyl groups of DEAMP₂ are themselves similar, $C(21)-C(22) = 1.515(7) \text{ \AA}$ and $C(31)-C(32) = 1.488(7) \text{ \AA}$ although the difference is of low significance, and both distances are smaller than the carbon to carbon single bond length 1.54 \AA found by Makaranets in the solid state structure of *N*-ethyliminobis(methylenephosphonic acid).¹⁷ In DEAMP₂, the three C-N bond lengths are also slightly different, but it is of low significance.

7.2.1 Classification of phosphorus to oxygen bond lengths

The protonated phosphonate oxygen has a bond length [$P-O(2) = 1.543(3) \text{ \AA}$] which is significantly longer than the other two phosphorus to oxygen bond lengths in the molecule, $P-O(1) = 1.487(3) \text{ \AA}$ and $P-O(3) = 1.520(3) \text{ \AA}$.

The $P-O(1)$ bond length [$1.487(3) \text{ \AA}$] falls at the upper end of the range, $1.456-1.489 \text{ \AA}$, for $P=O$ in fully protonated phosphonate groups ($-PO_3H_2$) of 1-aminoalkanephosphonic acids.²¹ However, the phosphorus to oxygen bond, $P-O(3)$ [$1.520(3) \text{ \AA}$] probably reflects some degree of double bond character since it is close to the upper end of the range ($1.49-1.51 \text{ \AA}$) for bond lengths between phosphorus and non-protonated oxygens in monoprotonated groups (PO_3H^-) of 1-aminoalkanephosphonic acids.²¹ There is, therefore, some evidence for regarding $P-O(1)$ and $P-O(3)$ as involving partial double bond character. The difference in these bonds lengths may be related to the nature of the intermolecular hydrogen bonding interactions involving the oxygen atoms.²²

The bond length from phosphorus to the protonated oxygen atom [$P-O(2) =$

1.543(3) Å] is similar to other bond lengths for P-O(H) groups (1.51-1.57) in related aminophosphonic acids.^{10,12-14} The two types of phosphorus to oxygen bond found in the solid structure of DEAMPH₂ are summarised in Table 7.2.4.

The angles around the phosphorus atom are slightly distorted away from that expected for a idealised tetrahedral, 111.6(2)°, 111.7(2)° and 114.3(2)°. The largest angle is found between the two unprotonated oxygen atoms, [O(3)-P-O(1) = 114.3(2)° and is consistent with mutual repulsion between the bonds to the two oxygen atoms due to their partial double bond character. An even larger O-P-O bond angle was found by Makaranets in the solid structure of NEIBMPH₄, O(1)-P(1)-O(3) = 116.0(2)° between the two P-O bonds with partial double bond character.¹⁷

Table 7.2.4 Classification of the phosphorus-oxygen bonds in DEAMPH₂.^a

Phosphorus-oxygen bond length / Å	Assignment
P-O(2) = 1.543(3)	P-O(H)
P-O(1) = 1.487(3)	P=O
P-O(3) = 1.520(3)	P=O

^a Values in parentheses are estimated standard deviations.

7.2.2 Hydrogen bonding interactions

There is a strong hydrogen bond between the protonated nitrogen atom and a phosphonate oxygen, H(n1)...O(1)' = 1.67 Å of a molecule related by the 2₁ screw axis. Figure 7.2.2(a) shows the infinite spiral chain along the b axis, which results from this interaction.

A second strong intermolecular hydrogen bond was also found between the protonated phosphonate oxygen atom O(2) and a phosphonate oxygen atom of a molecule related by an inversion centre [O(2)...O(3)' = 2.53 Å], hence forming a bridged dimer, Figure 7.2.2(b). These hydrogen bonded pairs link each helical chain to a parallel chain on either side, so that a two-dimensional hydrogen-bonded 'sheet' [Figure 7.2.2(c)] is present in the solid state crystal.

Significantly, no intramolecular hydrogen bonding was found in the structure

of DEAMPH₂. A similar situation was observed for the related acid, NEIBMPH₄.¹⁷

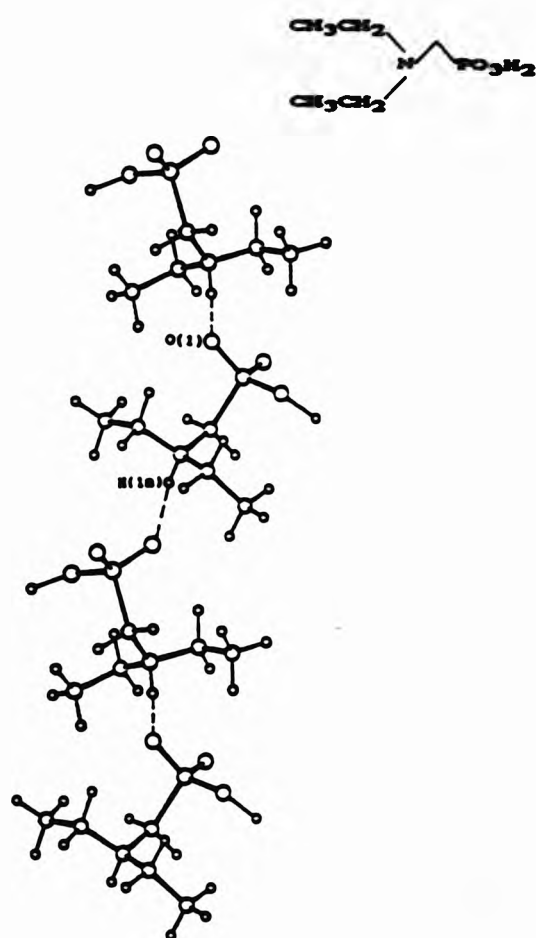


Figure 7.2.2 (a) Intermolecular hydrogen bonding present in DEAMPH₂: molecules of DEAMPH₂, related by a 2₁ screw axis forming long spiral chains held together by hydrogen bonding between the protonated nitrogen atom and the phosphonate oxygen atom.

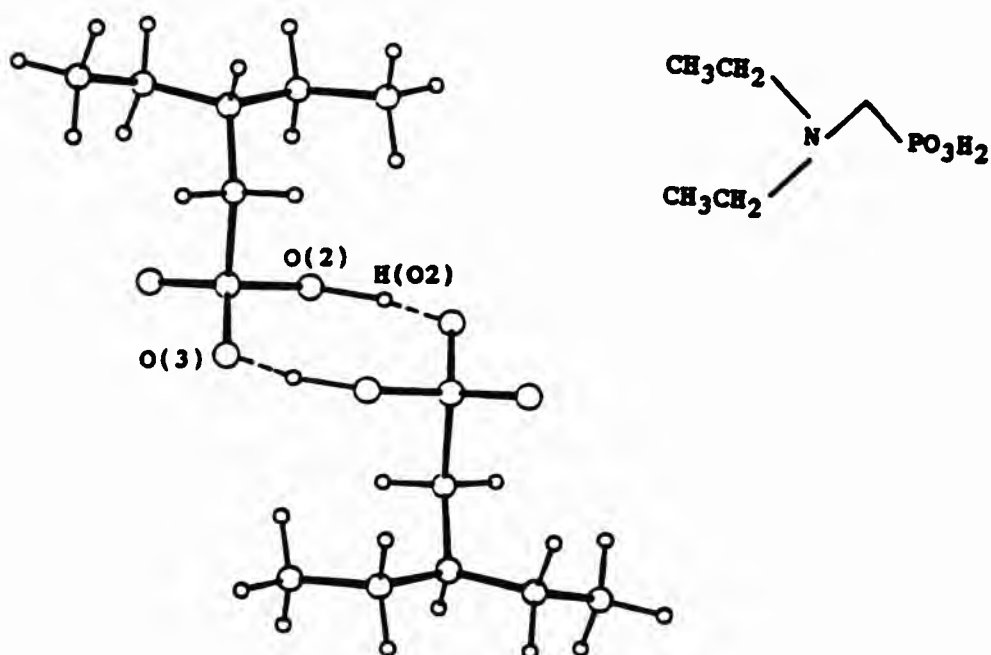


Figure 7.2.2 (b) Intermolecular hydrogen bonding present in DEAMPH₂: Molecules of DEAMPH₂ forming a bridged dimer between the protonated phosphonate oxygen O(2) and a phosphonate oxygen atom O(3)' of an adjacent molecule across an inversion centre.

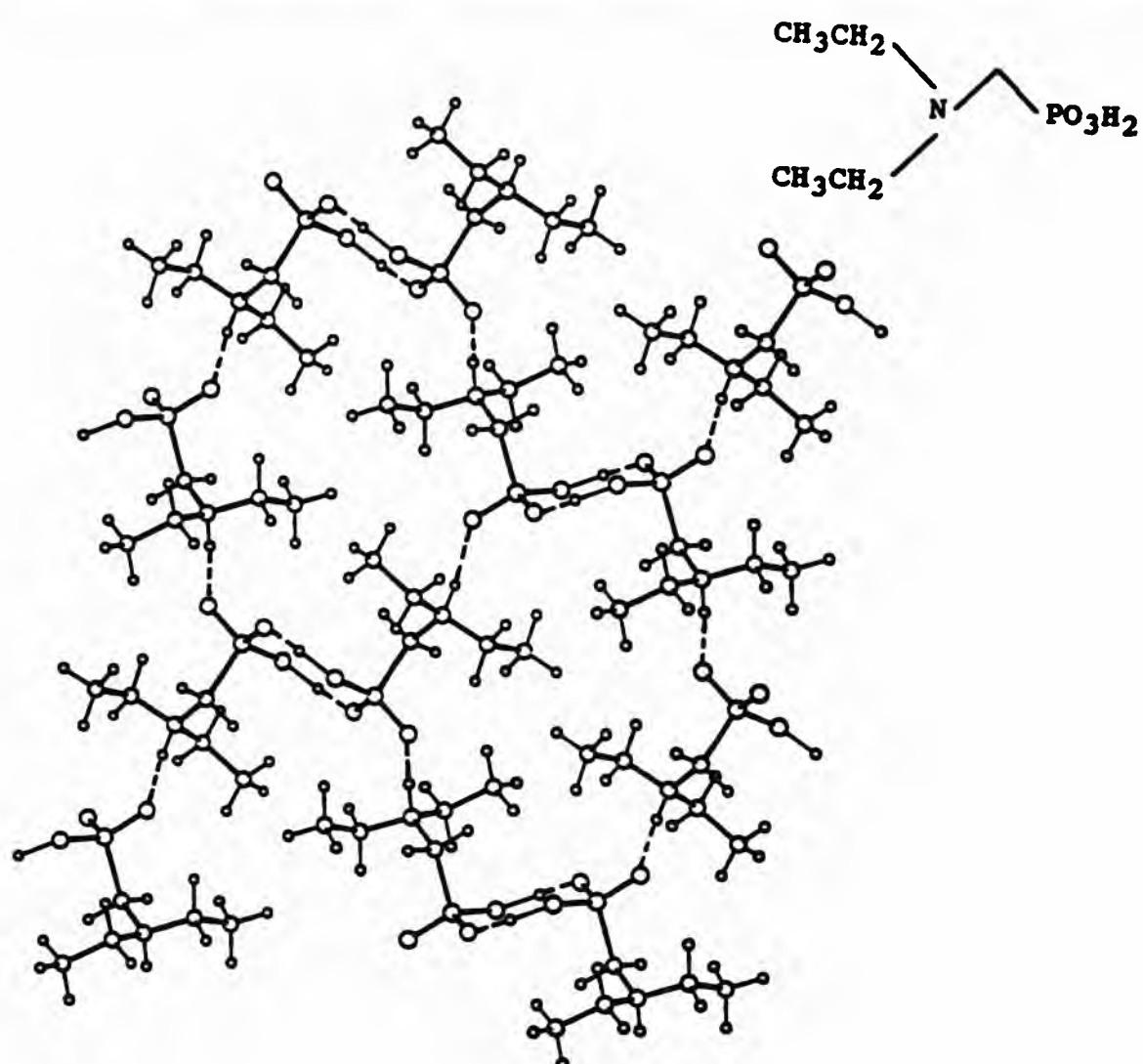


Figure 7.2.2 (c) Two-dimensional hydrogen-bonded sheet of molecules of DEAMPH₂ in the solid state.

7.3 Description of the solid state structure of (±)-*trans*-cyclohexane-1,2-diaminetetrakis(methylenephosphonic acid), CDTMPH₄·H₂O

Tables of fractional atomic coordinates, anisotropic thermal parameters, bond lengths, bond angles, inter- and intra-molecular distances are given in Appendix 2 (Tables 1-7).

The solid state structure of the molecule of CDTMPH₄ is shown in Figure 7.3.1.²⁷ The (±)-*trans* form of CDTMPH₄ can have two possible configurations at the chiral carbons [C(1) and C(2)] involving the substituent aminomethylenephosphonic groups, *i.e.* *aa* or *ee*[†] and hence there are four possible stereoisomers, *i.e.* RS, SR, RR and SS. However, in the solid state structure of CDTMPH₄, the substituent aminomethylenephosphonic acid groups are in the more favourable *ee* conformation, as expected,²⁸ and hence only two stereoisomers are possible, *i.e.* RR and SS. Therefore, in the solid state

[†] *a* = axial, *e* = equatorial.

structure of CDTMPH_3 , the isomers present will be an equal amount of both RR and SS.

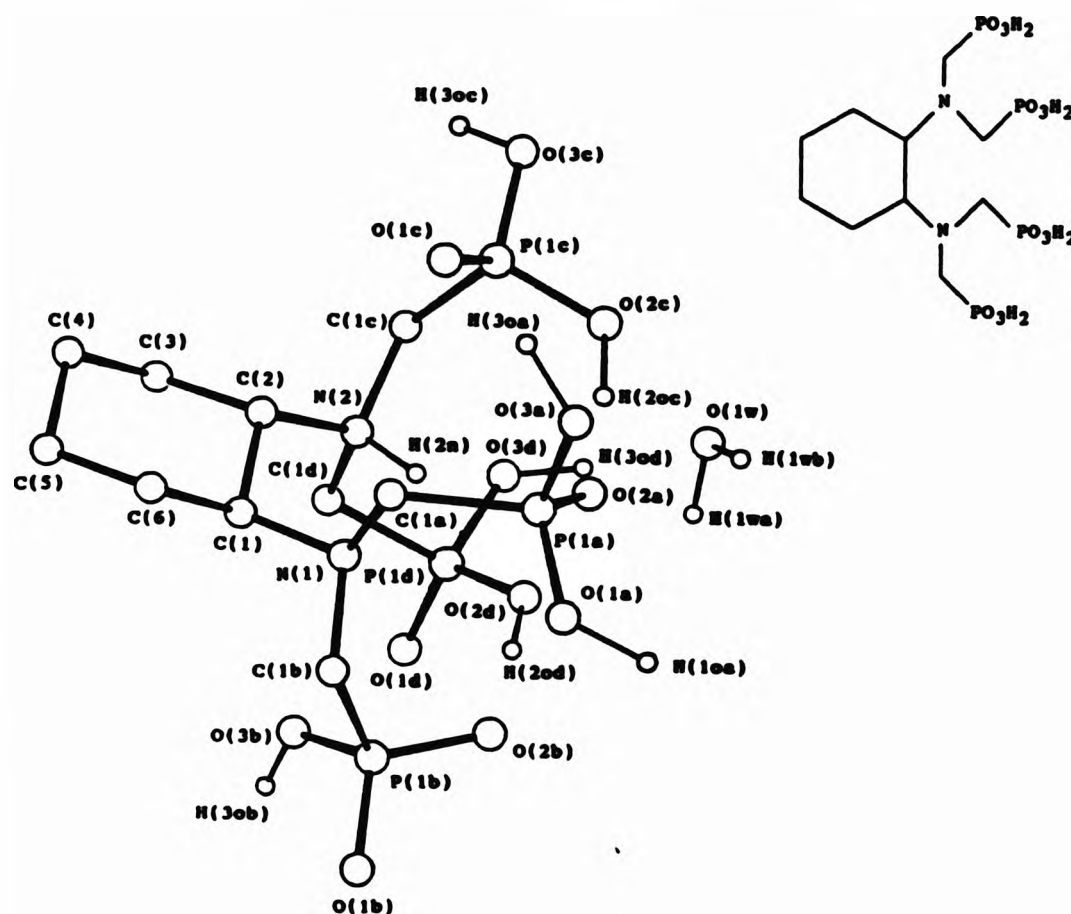


Figure 7.3.1 Molecular structure of $\text{CDTMPH}_3 \cdot \text{H}_2\text{O}$. The hydrogen atoms on the cyclohexyl ring, and the methylenephosphonate groups ($\text{CH}_2\text{-P}$) have been omitted for clarity.

The conformation of the cyclohexyl ring in CDTMPH_3 is a distorted chair. The molecule of CDTMPH_3 was found to be singly zwitterionic; *i.e.* only one nitrogen atom was found to be protonated. In contrast to the solid state structure of CDTMPH_3 , the structure of ethylenediamine *tetrakis*(methylenephosphonic acid) was found to have both nitrogen atoms protonated.²¹ The solid state structure of the carboxylic analogue of CDTMPH_3 , *i.e.* *trans*-cyclohexane-1,2-diaminetetraacetic acid, (CDTAH_4) also shows that only one nitrogen atom is protonated.²⁹ This difference in the protonation state of the nitrogen atoms in polyaminophosphonic and carboxylic acids, may be ascribed to the effects of flexibility in the ethylene backbone chain.²⁹

The bond angles around the nitrogen atom which is not protonated, are all greater than the idealised tetrahedral angle; $\text{C}(1)\text{-N}(1)\text{-C}(1a) = 114.5(3)^\circ$, $\text{C}(1)\text{-N}(1)\text{-C}(1b) = 110.9(3)^\circ$ and $\text{C}(1b)\text{-N}(1)\text{-C}(1a) = 112.0(3)^\circ$. The corresponding angles around the protonated nitrogen atom also show deviation

from the idealised tetrahedral angle; C(1d)-N(2)-C(1c) = 110.7(3)°, C(2)-N(2)-C(1c) = 110.8(3)° and C(2)-N(2)-C(1d) = 113.1(3)°. In contrast, the angles involving the proton on the nitrogen atom are all in a range lower than expected 106-109°, *i.e.* H(2n)-N(2)-C(1c) = 108.8(3)°, H(2n)-N(2)-C(1d) = 107.1(3)° and H(2n)-N(2)-C(2) = 106.1(3)°.

The bond lengths around the nitrogen atoms also show significant differences; the unprotonated nitrogen atom [N(1)], has shorter nitrogen to carbon bond lengths, *i.e.* N(1)-C(1a) = 1.472(5), N(1)-C(1) = 1.482(5) and N(1)-C(1b) = 1.486(5), than the protonated nitrogen atom [N(2)], *i.e.* N(2)-C(1d) = 1.500(4), N(2)-C(1c) = 1.512(5) and N(2)-C(2) = 1.525(5). This reflects the reduced bond strength expected for HN⁺-C compared to N-C.

Bond lengths of carbon to nitrogen atoms of related aminomethylenephosphonic acids (Table 7.3.1) compare well with the values obtained for CDTMPH₈ in this work, *e.g.* in the solid state structure of 1,4,7-triazacyclononanetris(methylenephosphonic acid) a mean C-N bond length of 1.46 Å was found for the nitrogen atom which was unprotonated.²²

Table 7.3.1 Mean bond lengths (Å) around nitrogen atoms in same related aminomethylenephosphonic acids.

Ligand	Protonated nitrogen atom	unprotonated nitrogen atom
DEAMPH ₂ ^a	1.496	
CDTMPH ₈ ^a	1.512	1.480
NEIBMPH ₄ ^b	1.509	
CIBMPH ₄ ^c	1.515	
NTMPH ₅ ^d	1.504	
AMPH ₂ ^e	1.485	
TACNTMPH ₆ ^f	1.510	1.462
EDTMPH ₈ ^g	1.512	

^a This work. ^b Ref, 17. *N*-Ethyliminobis(methylenephosphonic acid). ^c Ref, 18. Cyclohexaneiminobis(methylenephosphonic acid). ^d Ref, 20. Nitrilotris(methylenephosphonic acid). ^e Ref, 19. Aminomethylenephosphonic acid. ^f Ref, 22. 1,4,7-triazacyclononanetris(methylenephosphonic acid) ^g Ref, 21. Ethylenediamine tetrakis(methylenephosphonic acid).

Differences in the carbon to nitrogen bond lengths in two aminocarboxylic acids which contain both protonated and unprotonated nitrogen atoms were also observed. In the structure of *trans*-cyclohexane-1,2-diaminetetraacetic acid (CDTAH₄), the mean C-N bond length involving the protonated nitrogen atom is also longer, *i.e.* 1.514 Å, than the mean bond length involving the unprotonated nitrogen atom, *i.e.* 1.463 Å.²⁹ A similar situation also exists in the structure of diethylenetriaminepentaacetic acid, DETPAH₅.³⁰

In CDTMPH₃, the phosphorus carbon bond lengths (CH₂-P) themselves show some degree of variation. For example, one phosphorus to carbon length is slightly shorter than the other three, *i.e.* P(1b)-C(1b) = 1.788(4) Å, *cf.* P(1a)-C(1a) = 1.806(4) Å, P(1c)-C(1c) = 1.809(4) Å and P(1d)-C(1d) = 1.811(4) Å. This slightly shorter phosphorus to carbon bond length [1.788(4) Å] is associated with the aminomethylenephosphonate group containing the unprotonated nitrogen atom and the monoprotated phosphonate group (PO₃H⁻). This behaviour was also observed by Clegg *et al.* in the structure of 1,4,7-triazacyclononanetris(methylenephosphonic acid), in which the shortest C-P bond was 1.820 Å and was found in the aminomethylenephosphonate group containing the monoprotated phosphonate group and the unprotonated nitrogen atom.²²

In CDTMPH₃, the angles subtended by the protonated nitrogen atom and the phosphorus atom at the carbon atom (N-C-P) [N(2)-C(1c)-P(1c) = 115.6(3)° and N(2)-C(1d)-P(1d) = 113.3(3)°] are larger than the corresponding angles involving the unprotonated nitrogen atom [N(1)-C(1b)-P(1b) = 112.9(3)° and N(1)-C(1a)-P(1a) = 111.9(3)°].

In the structure of *N*-ethyliminobis(methylenephosphonic acid), NEIBMPH₄, the largest N-C-P angle 117.9(3) ° was found in the aminomethylenephosphonate group which contained the protonated nitrogen and the monoprotated phosphonate group (PO₃H⁻).¹⁷ In the structure of ethylenediaminetetrakis(methylenephosphonic acid) the two large N-C-P angles of 116.7(3) ° and 116.9(3) ° were found in the aminomethylenephosphonate groups which involved the protonated nitrogen atoms, and contained the monoprotated phosphonate group (PO₃H⁻) and the other was found in a fully protonated methylenephosphonate group (PO₃H₂).²¹ Clegg found, in the structure of 1,4,7-triazacyclononanetris(methylenephosphonic acid), that the largest N-C-P angle involved the unprotonated nitrogen atom, N(2)-C(21)-P(2) = 118.1(1)° and also contained a monoprotated phosphonate group.²²

Based on these observations there seems to be no correlation of the size of the N-C-P angle with either the state of protonation of the nitrogen atoms or the phosphonate groups. In CDTPH₃, as with DEAMPH₂ (N-C-P = 120°), the large N-C-P angles may be due to the interaction of hydrogen atoms with phosphonate oxygens, *i.e.* there is a close interaction between the proton attached to the chiral carbon atom [C(2)] and a phosphonate oxygen atom, H(2)...O(1c) = 2.30 Å.

7.3.1 Classification of phosphorus-oxygen bond lengths

In CDTPH₃, seven out of the eight phosphonate oxygens were found to be protonated, *i.e.* three out of the four phosphonate groups are fully protonated (PO₃H₂). In the monoprotonated phosphonate group, two phosphorus to oxygen bond lengths are identical, *i.e.* P(1b)-O(1b) = 1.509(3) Å and P(1b)-O(2b) = 1.508(3) Å. These bond lengths between phosphorus and non-protonated phosphonate oxygens fall in the range for monoprotonated phosphonate groups (PO₃H⁻) in 1-aminoalkanephosphonic acids as found by Polyanchuk (1.49-1.51 Å).²¹ This indicates that both P(1b)-O(1b) and P(1b)-O(2b) have the negative charge spread over the two oxygen atoms, producing bonds intermediate between single and double.

The three remaining unprotonated oxygens in the fully protonated phosphonate groups (PO₃H₂), *i.e.* O(2a), O(1c) and O(1d) also have varying bond lengths; P(1a)-O(2a) = 1.496(3) Å, P(1c)-O(1c) = 1.484(3) Å and P(1d)-O(1d) = 1.474(3) Å. The bond length P(1d)-O(1d) (1.474 Å) has considerably double bond character. The other two phosphorus-oxygen lengths, P(1a)-O(2a) = 1.496(3) Å and P(1c)-O(1c) = 1.484(3) Å, fall at the upper end of the range for P=O in 1-aminoalkanephosphonic acids as summarised by Polyanchuk 1.456-1.489 Å.²¹

An attempt has been made to classify the P-O bond lengths in CDTPH₃ from the data available from the solid state structures of other related α -aminomethylenephosphonic acids. This data establishes a characteristic range of values for the various phosphorus to oxygen bond lengths, *i.e.* P-O(H), P=O and P=O. Analysis of the data in Table 7.3.2 indicates the ranges for the various type of phosphorus to oxygen bond lengths, *i.e.* 1.46-1.48 Å for P=O; 1.51-1.56 Å for P-O(H) and 1.48-1.52 for P=O. These ranges overlap and the distinction between the values obtained for P=O, P=O and P-O(H) are not well defined. These ranges differ slightly to those determined by Polyanchuk, who

Table 7.3.2 The phosphorus-oxygen bond lengths (Å) of some α -aminomethylene-phosphonic acids.

Acid	P-O(H)	P=O	P=O	Ref.
AMPH ₂ ^a	1.567(3)		1.512(2) 1.493(2)	19
NEIBMPH ₂ ^b	1.557(4) 1.541(3) 1.517(3)		1.491(3) 1.512(3) 1.504(3)	17
NTMPH ₃ ^c	1.537(3) 1.519(3) 1.538(3) 1.543(3) 1.534(3)	1.456(3)	1.499(3) 1.503(3) 1.489(3)	20
EDTMPH ₃ ^d	1.547(3) 1.529(3) 1.542(3) 1.527(3) 1.557(3) 1.553(3)	1.476(3) 1.468(3)	1.486(3) 1.500(3) 1.507(3) 1.505(3)	21
CIBMPH ₄ ^e	1.544(2) 1.542(2) 1.549(2)	1.479(2)	1.498(2) 1.514(2)	18
DEAMPH ₂ ^f	1.540(3)		1.524(3) 1.489(3)	This work
CDTMPH ₃ ^g	1.510(4) 1.548(3) 1.544(3) 1.516(3) 1.505(3) 1.547(3) 1.536(3)	1.474(3)	1.509(3) 1.508(3) 1.496(3) 1.484(3)	This work

^a Aminomethylenephosphonic acid. ^b *N*-Ethyliminobis(methylenephosphonic acid).
^c Nitrilotris(methylenephosphonic acid). ^d Ethylenediamine tetrakis(methylene-phosphonic acid). ^e Cyclohexaneiminobis(methylenephosphonic acid). ^f *N,N*-Diethylaminomethylenephosphonic acid. ^g (\pm)-*trans*-Cyclohexanediamine tetrakis(methylenephosphonic acid).

defined two different geometries of the phosphonate group: that is monoprotinated (PO_3H^-) and fully protonated (PO_3H_2).²¹ Polyanchuk's ranges are: 1.47-1.48 Å for P=O; 1.55-1.57 Å for P-O(H) (in monoprotinated phosphonate group); 1.53-1.55 Å for P-O(H) (in fully protonated phosphonate group) and 1.49-1.51 Å for P=O.²¹

The phosphorus to oxygen bond length in the structure of DEAMPH_2 , P(1)-O(2) = 1.540 Å, was found to be significantly longer than some of the corresponding phosphorus to oxygen bond lengths involving protonated oxygen atoms in CDTMPH_3 , (Table 7.3.2) e.g. in CDTMPH_3 P(1a)-O(1a) = 1.510(4) Å and P(1d)-O(2d) = 1.505(3) Å. These differences between phosphorus to oxygen bonds may be related to the nature of intermolecular and intramolecular hydrogen bonds in which the oxygen atom is involved as discussed in Section 7.3.2.

The four types of phosphorus to oxygen bond found in the solid state structure of CDTMPH_3 are summarised in Table 7.3.2.

7.3.2 Intramolecular hydrogen bonding interactions

In CDTMPH_3 a number of intramolecular hydrogen bonds were found, which is in contrast to the structure of DEAMPH_2 , in which no intramolecular hydrogen bonds were observed. There are two strong intramolecular hydrogen bonds between phosphonate oxygen atoms, i.e. O(2c)...O(2a) = 2.57 Å and O(2d)...O(2b) = 2.48 Å. A further strong hydrogen bond between a protonated phosphonate oxygen atom and the oxygen atom of the water molecule [H(3od)...O(1w) = 1.55 Å] was also found, as shown in Figure 7.3.2.

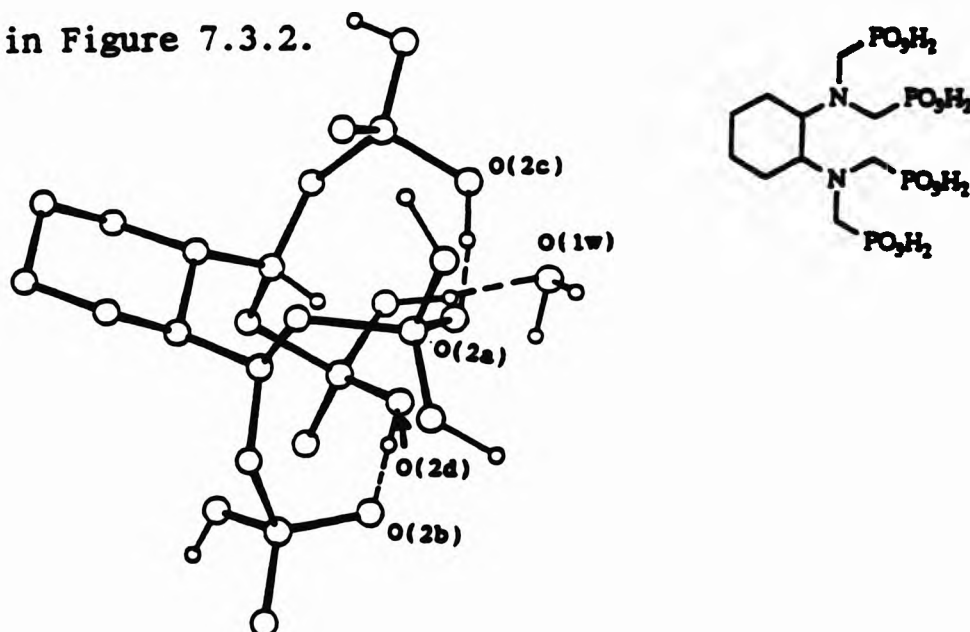


Figure 7.3.2 Intramolecular hydrogen bonding in $\text{CDTMPH}_3 \cdot \text{H}_2\text{O}$: between (a) the phosphonate oxygen atoms, O(2c)-O(2a), O(2d)-O(2b) and (b) water molecule and a protonated phosphonate oxygen atom, O(1w)-H(3od).

In CDTMPH₃, the N(2)...N(1) distance of 2.78 Å is slightly smaller than that observed by Shkol'nikova in the structure of the carboxylate analog of CDTMPH₃, CDTAH₄, N(1)...N(2) = 2.825(3) Å.²⁹ Shkol'nikova suggested that, in the solid state structure of CDTAH₄, the value of the nitrogen to nitrogen distance of 2.825(3) Å placed it in the range (2.9–3.0 Å) for a intramolecular hydrogen bond.²⁹ A similar distance was observed in the structure of diethylenetriamine-pentaacetic acid, N(2)...N(1) = 2.826 Å, which Shkol'nikova also suggested to be an intramolecular hydrogen bond (Table 7.3.3).³⁰ In CDTMPH₃, the distance

Table 7.3.3 (N)-H⁺...N distances (Å) in some related acids.

Distance	TACNTMPH ₆ ^a	CDTAH ₄ ^b	DETPH ₆ ^c	CDTMPH ₃ ^d
N-H	0.83, 0.86	0.99	0.95	1.05
H...N	2.39, 2.39	2.25	2.23	2.21
N...N	2.77, 2.81	2.83	2.83	2.78

^a Ref, 22. 1,4,7-triazacyclononanetriyltris(methylenephosphonic acid). ^b Ref, 29. *trans*-Cyclohexane-1,2-diaminetetraacetic acid. ^c Ref, 30. Diethylenetriaminepentaacetic acid. ^d This work. (±)-*trans*-cyclohexane-1,2-diaminetetrakis(methylenephosphonic acid).

between the proton on the nitrogen atom and the other unprotonated nitrogen atom, H(N2)...N(1) = 2.21 Å, is slightly less than that observed for diethylenetriaminepentaacetic acid, H(N1)...N(2) = 2.25(4) Å (Table 7.3.3). However, although the two nitrogen atoms in the structure of CDTMPH₃ are reasonably close (2.78 Å), there is no intramolecular hydrogen-bonding between the protonated and the unprotonated nitrogen atoms;²⁷ all the hydrogen atoms have been determined in the structure, leaving no doubt about their positions.

The strong intramolecular hydrogen bonding interactions between the methylenephosphonate groups (Figure 7.3.2) in the molecule of CDTMPH₃ hold the four substituent methylenephosphonic acid groups in fixed positions with respect to each other and hence produces a relatively *rigid* structure. As observed in the nmr spectra of CDTMPH₃ (Section 4.2.2) the *rigidity* of the molecule of CDTMPH₃ seems to be retained in solution. This feature of the structure can then be used to plausibly assign the protonation scheme of CDTMPH₃ (Section 4.5) and may also affect the stability of any metal complexes form (Section 5.2).

7.3.3 Intermolecular hydrogen bonding interactions

There are a number of strong hydrogen bonding interactions between phosphonate oxygen atoms and the molecule of water in CDTMPH_3 (Table 7.3.4).

The way in which a strong intermolecular hydrogen bond between a protonated phosphonate oxygen atom and a phosphonate oxygen atom of a molecule related by an inversion centre, $\text{H}(3\text{oa})\dots\text{O}(1\text{c})' = 1.36 \text{ \AA}$ forms a bridged dimer is shown in Figure 7.3.3 (a).

Table 7.3.4 Intermolecular hydrogen bonding interactions for $\text{CDTMPH}_3 \cdot \text{H}_2\text{O} / \text{ \AA}$.

$\text{H}(3\text{oa})\dots\text{O}(1\text{c})^{\text{d}} = 1.36$	$\text{H}(1\text{oa})\dots\text{O}(1\text{d})^{\text{b}} = 1.25$
$\text{H}(1\text{wb})\dots\text{O}(1\text{b})^{\text{b}} = 1.74$	$\text{H}(3\text{ob})\dots\text{O}(2\text{a})^{\text{c}} = 1.58$
$\text{H}(3\text{oc})\dots\text{O}(1\text{b})^{\text{d}} = 1.47$	

^a $-1-x, -y, -1-z.$ ^b $-x, -0.5+y, -1.5-z.$ ^c $-x, 0.5+y, -0.5-z.$ ^d $-1+x, y, z.$

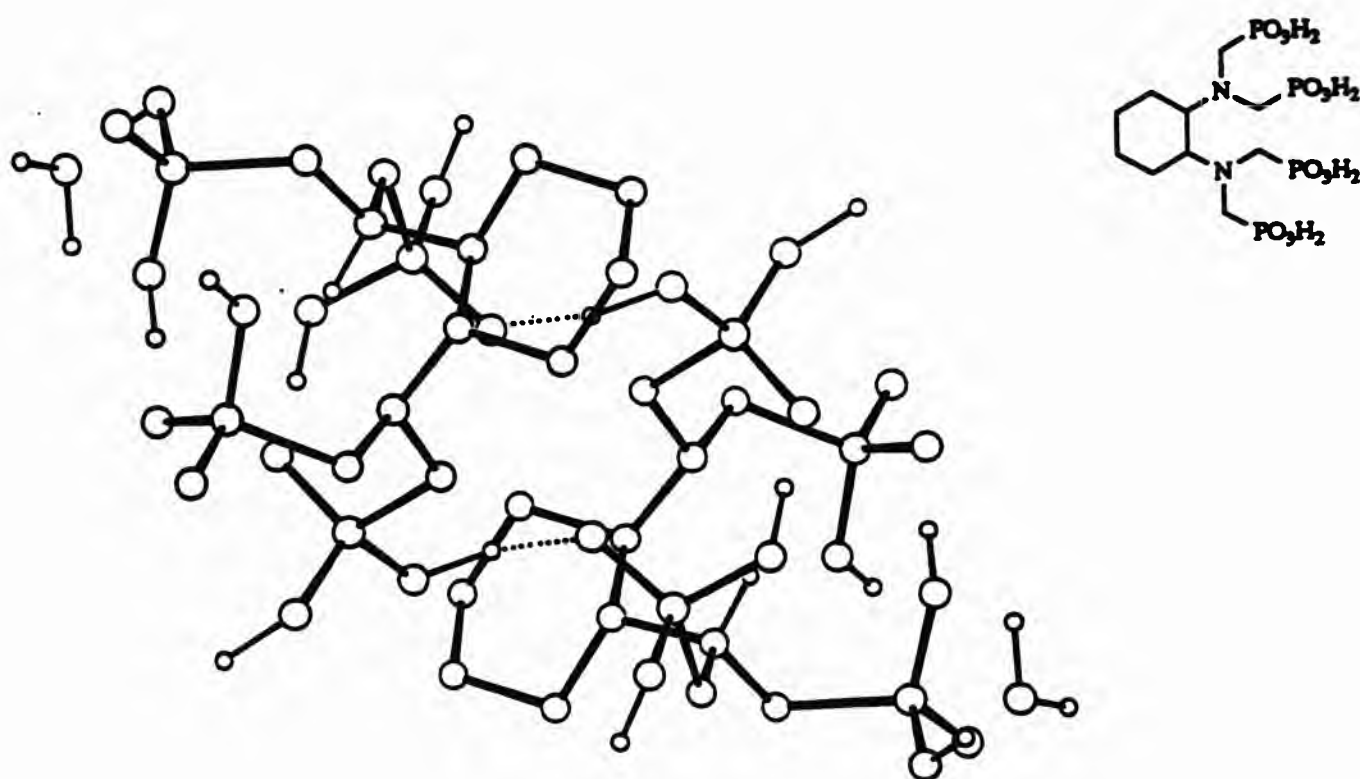


Figure 7.3.3 (a) Intermolecular hydrogen bonding in CDTMPH_3 : molecules of CDTMPH_3 forming a bridged dimer through hydrogen bonding between the protonated phosphonate oxygen atom $\text{O}(3\text{a})$ and a phosphonate oxygen atom $\text{O}(1\text{c})'$ of an adjacent molecule across an inversion centre.

A further four strong intermolecular hydrogen bonds were found between three protonated phosphonate oxygen atoms and phosphonate oxygen atoms of molecules related by the 2_1 screw axes (Table 7.3.4). One intermolecular hydrogen bond involves the proton on the water molecule H(1wb) and an unprotonated phosphonate oxygen atom of a molecule related by the 2_1 screw axes. These hydrogen bonding interactions of molecules related by the 2_1 screw axes are shown in Figure 7.3.3 (b).

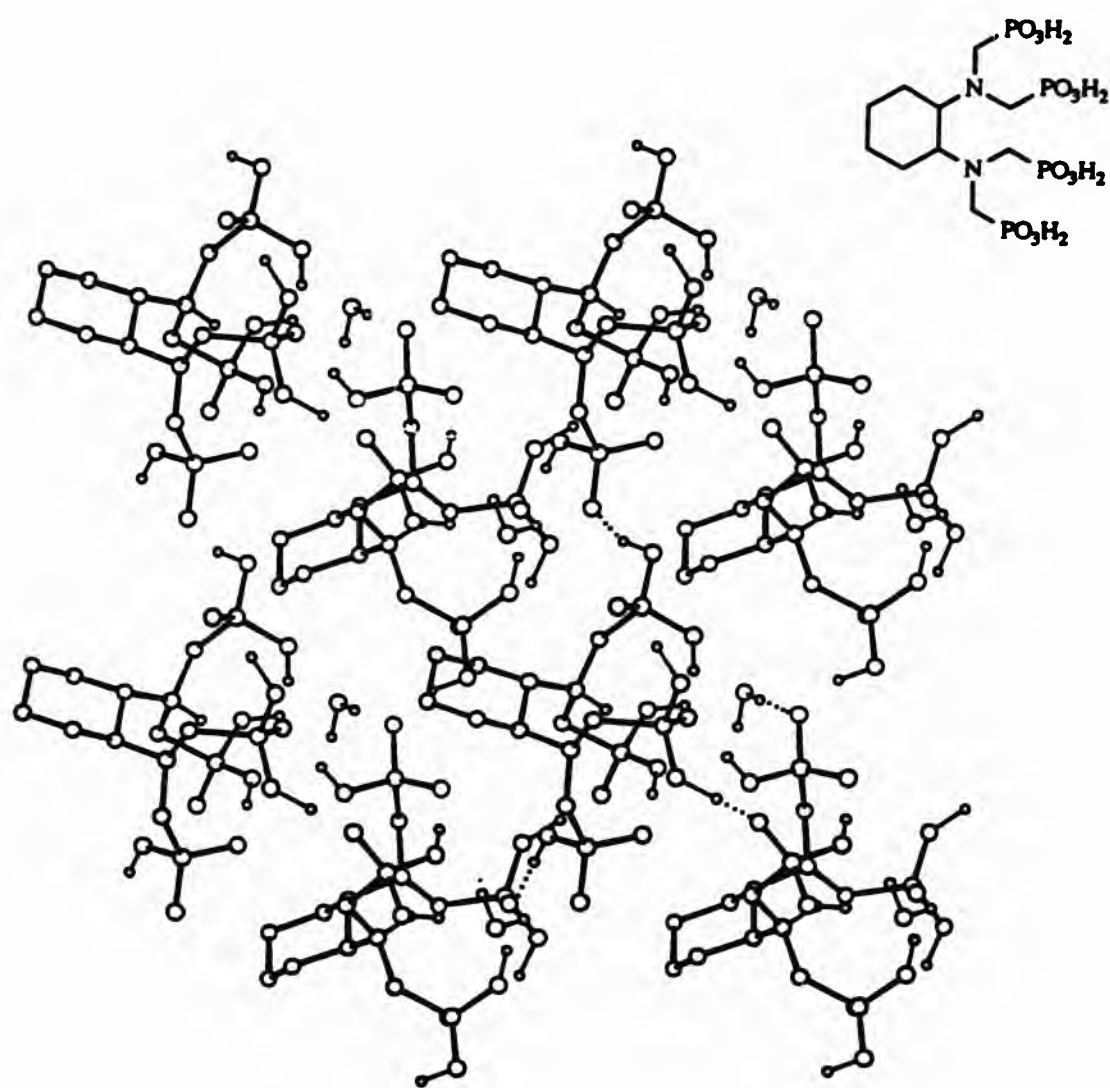


Figure 7.3.3 (b) Intermolecular hydrogen bonding in CDTMPH_3 : molecules of CDTMPH_3 forming long spiral chains held together by hydrogen bonding interactions.

These hydrogen bonding interactions link each helical chain to a parallel chain on either side, so that a two-dimensional hydrogen bonded 'sheet' is present. Hydrogen bonding interactions also link the helical chains in the hydrogen bonded 'sheet' to other 'sheets' above and below it, so that a three-dimensional network of hydrogen bonding is present in the solid state.²⁷

7.3.4 Conformation of the cyclohexyl ring in $CDTMPH_9 \cdot H_2O$

Evaluation of the conformation of saturated rings can be made from a mathematical combination of the torsion angles. This analysis is based upon consideration of the approximate symmetry possessed by most rings. The conformation of a ring is conveniently characterised by the torsion angles.³¹ There are two types of symmetry that need to be considered in order to define conformation, the mirror planes perpendicular to the dominant ring and the twofold axes lying in the ring. The location of symmetry in a ring depends upon the number of atoms comprising that ring. In rings containing an even number of atoms, symmetry elements may pass through two ring atoms located directly across the ring from each other or bisect two opposite ring bonds (Figure 7.3.4).³¹

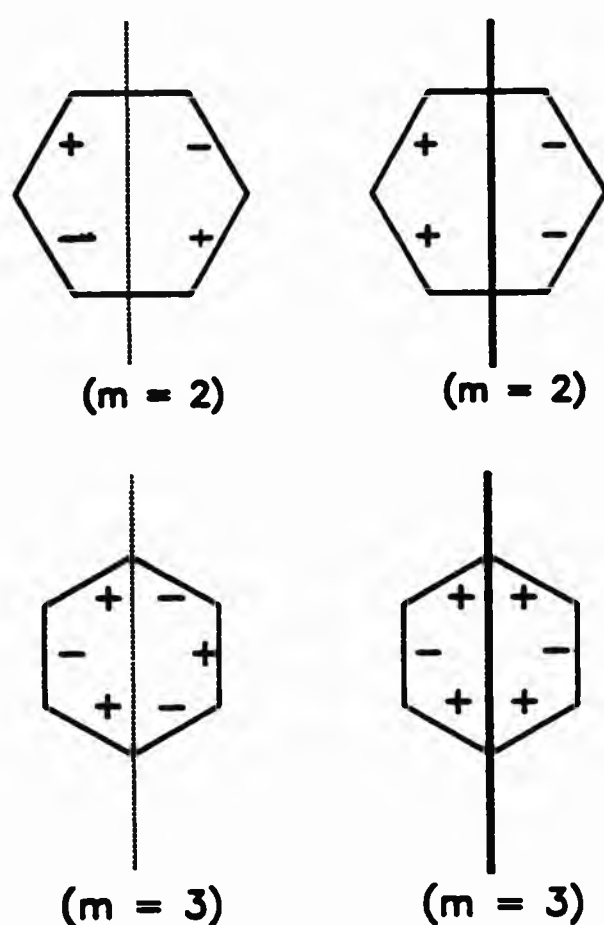


Figure 7.3.4 The signs of the torsion angles in six-membered rings describe the symmetrical positions of atoms related by the symmetry operation. Torsion angles of atoms sequence related by mirrors (....), have opposite signs, whereas torsion angles of atomic sequences related by rotations (—) have the same signs.³¹

Six-membered, saturated rings possess twelve potential symmetry elements that must be considered in order to determine the ring's conformation (Figure 7.3.5).

The asymmetry parameters defined by Duax *et al.*,³¹ precisely define the conformation of any ring relative to ideal conformations (chair, boat, *etc.*) and relative to any other ring of similar compositions. The asymmetry parameters of non-ideal systems measure the degree of departure from ideal symmetry (*i.e.* asymmetry) at any of the possible symmetry locations. Related torsion angles are compared in a way that will result in a value of zero if the symmetry in question is present.

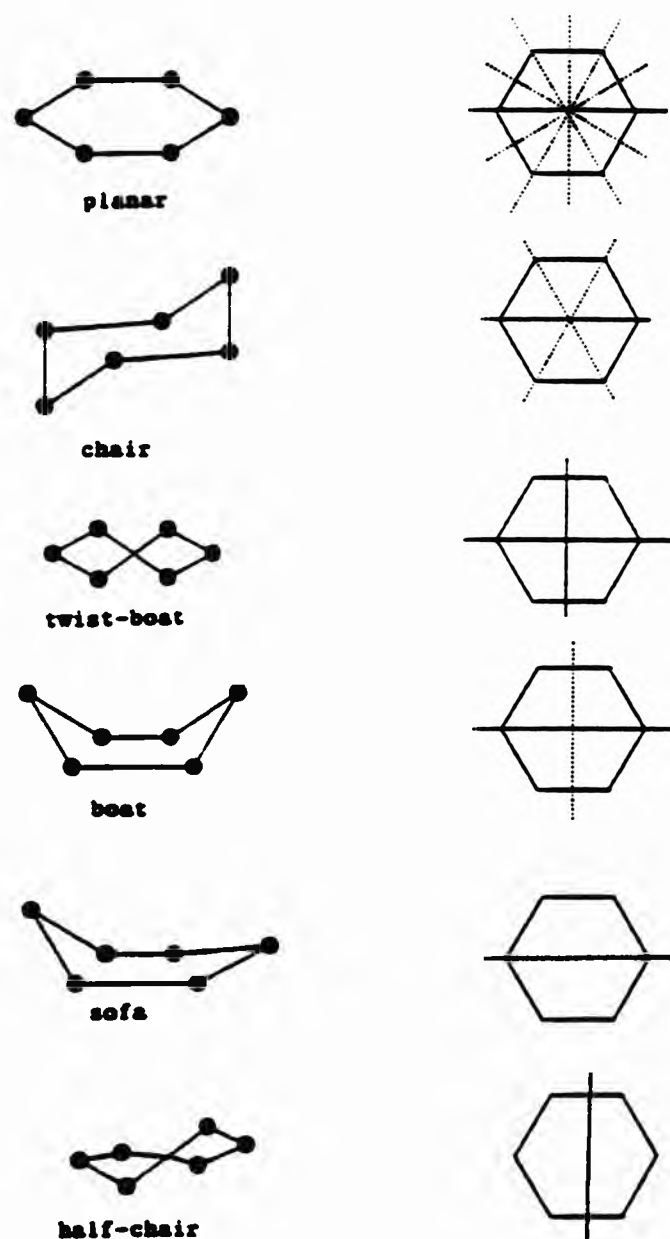


Figure 7.3.5 The most commonly observed conformations of saturated six-membered rings. The mirror (....) and twofold (—) rotational symmetries are also shown.³¹

Mirror-related torsion angles are inversely related (same magnitude, opposite signs) and are compared by addition. The root-mean-square calculation of these individual values then yields a measure of the ring deviation from ideal symmetry at the symmetry location in question:

$$\Delta C_s = \sqrt{\frac{\left(\sum_{i=1}^m (\theta_i + \theta'_i)^2\right)}{m}} \quad \text{Equation 7.3.1}$$

where m is the number of individual comparisons and θ_i and θ'_i are the symmetry-related torsion angles. Equation 7.3.1 is used to calculate mirror-plane asymmetry parameters (ΔC_s), the units of which are degrees. The asymmetry parameters of six-membered rings are useful in detecting the nature of distortions brought about by ring junction and substituents strains. In a perfectly symmetric saturated ring in the chair conformation, six asymmetry parameters would have a magnitude of zero.¹¹

Calculation of the asymmetry parameters for CDTMPH₂ (Figure 7.3.6) using Equation 7.3.1, confirmed the deviation of the cyclohexyl ring from the ideal chair conformation (Table 7.3.5). At carbon 2 [$\Delta C_s(2)$], there is excellent mirror symmetry [$\Delta C_s(2) = 0.7$]. The remaining carbons in the cyclohexyl ring show deviation from the symmetry expected for the chair conformation.

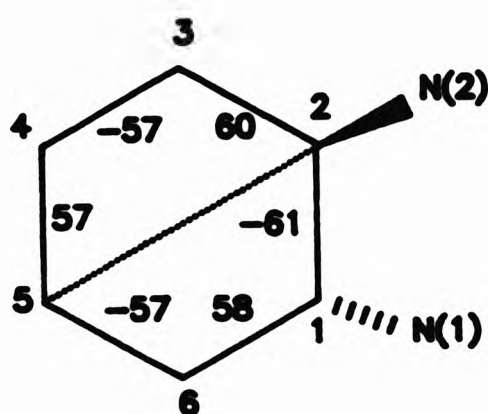


Figure 7.3.6 The nomenclature used for defining the location of asymmetry parameters in the cyclohexyl ring of CDTMPH₂.H₂O. The torsion angles and symmetry axes (----) are also shown.¹¹

Table 7.3.5 Calculated asymmetry parameters ($^{\circ}$) for the cyclohexyl ring in $\text{CDTMPH}_3 \cdot \text{H}_2\text{O}$.

$\Delta C_3(1) = 2.40$	$\Delta C_3(4) = 2.40$
$\Delta C_3(2) = 0.67$	$\Delta C_3(5) = 0.67$
$\Delta C_3(3) = 3.05$	$\Delta C_3(6) = 3.05$

The strain in the cyclohexyl ring can also be seen from the values obtained for the torsion angles (Table 7.3.6). Comparing the mirror symmetries obtained for $\text{CDTMPH}_3 \cdot \text{H}_2\text{O}$ with those observed in the commonly observed conformations (Figure 7.3.5), it can be seen that the conformation of the cyclohexyl ring in CDTMPH_3 deviates from the ideal chair towards the "sofa" conformation, which only has one mirror symmetry. It is clearly seen from the torsion angles the two angles with values of 60° are at the apex of the cyclohexyl ring that points above the plane of the ring. The remaining angles (57°) form the flattened plane of the ring (Figure 7.3.7).

Table 7.3.6 Values of the torsion angles (τ) in the cyclohexyl ring of $\text{CDTMPH}_3 \cdot \text{H}_2\text{O}$.

Angle	$\tau/^{\circ}$	Angle	$\tau/^{\circ}$
C6-C1-C2-C3	-60.92	C2-C3-C4-C5	-57.62
C2-C1-C6-C5	58.61	C3-C4-C5-C6	56.73
C1-C2-C3-C4	60.47	C4-C5-C6-C1	-57.12

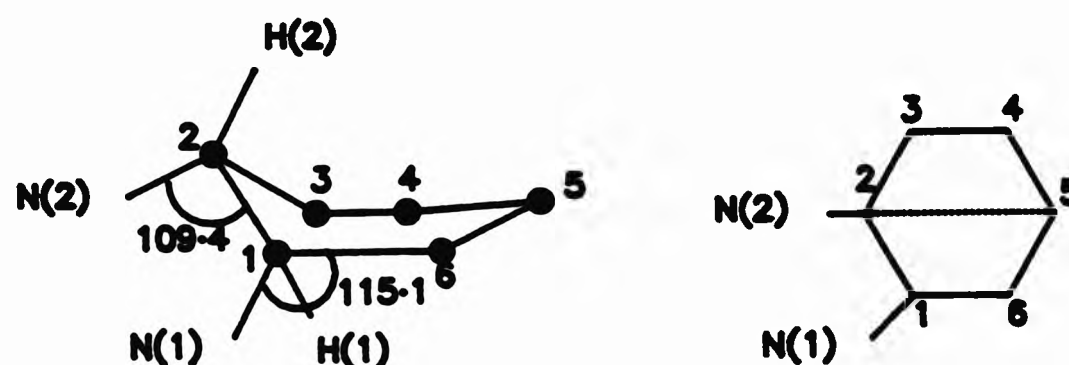


Figure 7.3.7 Schematic diagram of the "sofa" conformation of the cyclohexyl ring in $\text{CDTMPH}_3 \cdot \text{H}_2\text{O}$.

The mirror symmetry of the cyclohexyl ring is through the carbons numbered C(2) and C(5).

Again distortion is observed at the angles relating to the nitrogens attached to the methylene carbons of the cyclohexyl ring, *i.e.* N-C-C angles. The carbon, C(2), which lies along the mirror symmetry and is attached to the nitrogen N(2), has an almost perfect tetrahedral angle [N(2)-C(2)-C(1) = 109.4°]. However, at the other carbon (C1) attached to the nitrogen (N1), the angle is greater than the 109.4° [N(1)-C(1)-C(3) = 110.7°].

Table 7.3.7 Angles (°) involving the chiral carbon atoms C(1) and C(2).

C(2)-C(1)-N(1) = 110.7	C(3)-C(2)-C(1) = 110.9
C(6)-C(1)-C(2) = 108.3	C(3)-C(2)-N(2) = 113.2
C(6)-C(1)-N(1) = 115.1	C(1)-C(2)-N(2) = 109.4

7.3.5 The configuration of the substituent groups

In the solid state structure of the straight chain analog, EDTMPH₃, the aminomethylenephosphonate groups are almost at right angles to each other (86°) along the N-C-C-N backbone and they are also in a *gauche* (skew) conformation to each other [Figure 7.3.8 (b)].²¹ This may maximise the charge separation between the ligating groups as suggested by Hancock *et al.*³²

Differences in the torsion angles between the substituent groups (N-C-C-N) were observed for both CDTMPH₃·H₂O and its carboxylate analog, CDTAH₄·H₂O.²⁶ The torsion angle (N-C-C-N) for CDTAH₄·H₂O, is slightly greater than the idealised *gauche* conformation of 60° (63.50°).²⁹ However, in the case of CDTMPH₃·H₂O, the N-C-C-N torsion angle is much less than the idealised angle of 60° (46.52°), which was not expected. The bulky aminomethylenephosphonate groups seem to lie closer together, probably held together by the strong intramolecular hydrogen bonding between the phosphonate oxygens (Section 7.3.2).

This apparent flexibility of the substituent groups in EDTMPH₃ (*i.e.* the large torsion angle) may explain the greater thermodynamic stability of the metal complexes formed compared with those formed with CDTMPH₃ (Section 5.2). Therefore, the N-C-C-N torsion angles of the ligating groups may greatly affect the stability of any metal complexes with CDTMPH₃ formed in *aqueous*

solution (Section 5.2).

If the N-C-C-N angle is too large (*i.e.* greater than 90°) and there is maximum charge separation between the substituents as in EDTAH_4 , then energy is required to reorganised the ligating groups to the correct orientation for complexation. If the N-C-C-N angle is too small, as in CDTMPH_3 (46°) then energy must again be expended to reorganised the substituents and break any strong hydrogen bonds present.

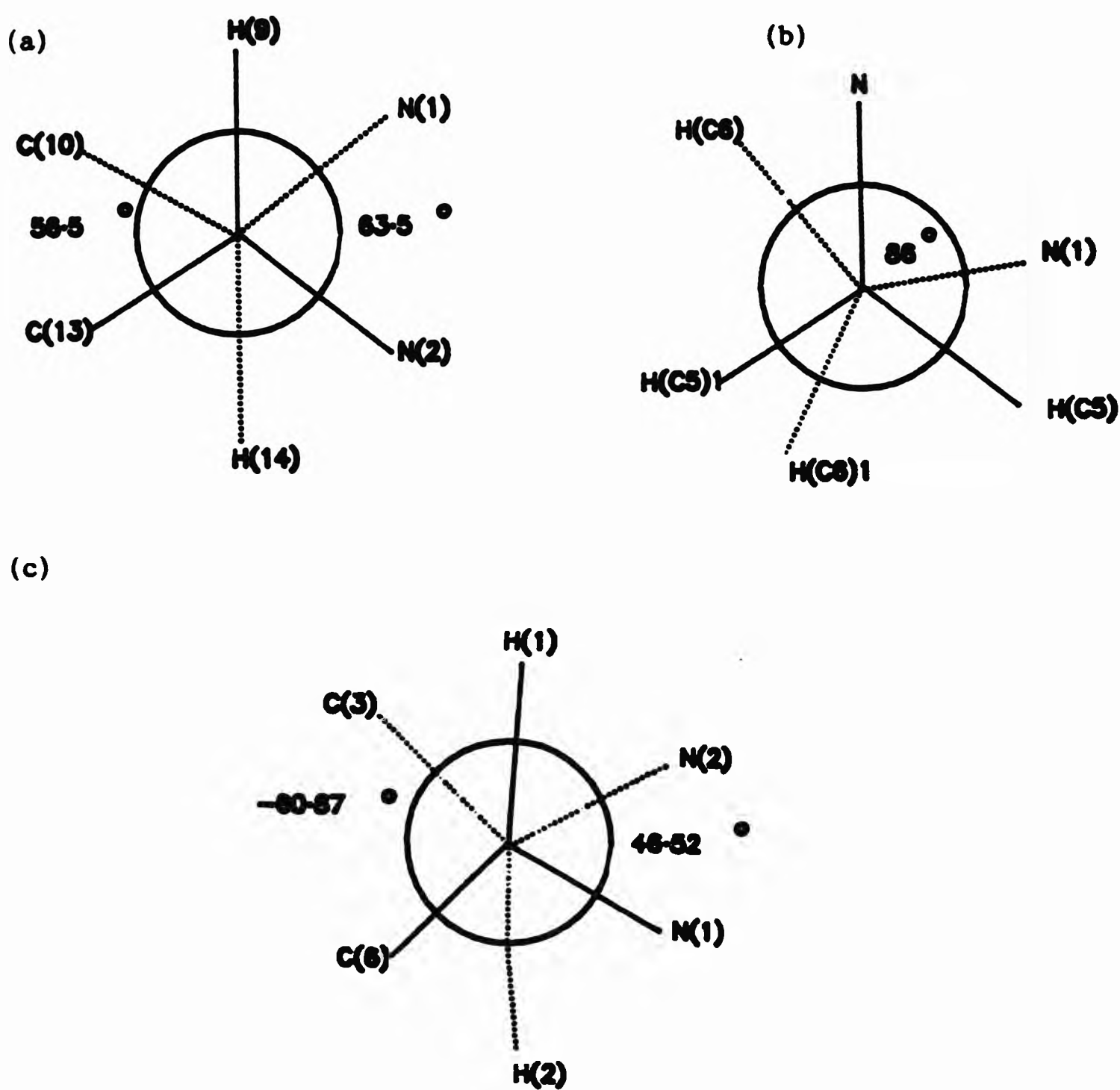


Figure 7.3.8 Newman projections for (a) $\text{CDTAH}_4 \cdot \text{H}_2\text{O}$, along bonds C(9)-C(14); (b) $\text{EDTMPH}_3 \cdot \text{H}_2\text{O}$, along bonds C(5)-C(6); (c) $\text{CDTMPH}_3 \cdot \text{H}_2\text{O}$, along bonds C(1)-C(2).

7.4 References

1. C. V. Banks and R. E. Yerick, *Anal. Chim. Acta.*, 1959, 20, 301.
2. M. I. Kabachnik, T. Ya. Medved', N. M. Dyatlova, O. G. Arkhipova and M. V. Rudomino, *Russ. Chem. Revs.*, 1968, 37, 503.
3. S. Westerback, I. Murase and A. E. Martell, *Inorg. Nucl. Chem. Lett.*, 1971, 7, 1103.
4. R. J. Motekaitis, I. Murase and A. E. Martell, *Inorg. Chem.*, 1976, 15, 2303.
5. K. Sawada, T. Araki and T. Suzuki, *Inorg. Chem.*, 1987, 26, 1199.
6. P. Fenot, J. Darriet, C. Garrigou-Lagrange and A. Cassaigne, *J. Mol. Struct.*, 1978, 43, 49.
7. Y. Ortiz-Avila, P. R. Rudolf and A. Clearfield, *J. Coord. Chem.*, 1989, 20, 109.
8. M. I. Kabachnik, M. Yu. Antipin, B. K. Shcherbakov, A. P. Baranov, Yu. T. Struchkov, T. Ya. Medved' and Yu. M. Polikarpov, *Koord. Khim.*, 1988, 14, 536.
9. L. M. Shkol'nikova, A. L. Poznyak, V. K. Bel'skii, M. V. Rudomino and N. M. Dyatlova, *Koord. Khim.*, 1986, 12, 981.
10. N. Choi, I. Khan, R. W. Matthews, M. McPartlin and B. P. Murphy, *Polyhedron*, 1994, 13, 847.
11. I. Lukes, Z. Kvaca and I. Dominak, *Collect. Czech. Chem. Commun.*, 1988, 53, 987.
12. Y. Okaya, *Acta. Cryst.*, 1966, 20, 712.
13. L. M. Shkol'nikova, G. V. Polyanchuk, V. E. Zavodnik, M. V. Rudomino, S. A. Pisareva, N. M. Dyatlova, B. V. Zhadanov and I. A. Polyakova, *Zh. Strukt. Khim.*, 1987, 28, 124.
14. S. Kulpe, I. Seidel and K. Szulzewsky, *Crys. Res. Technol.*, 1984, 19, 669.
15. Z. Galdecki and W. M. Wolf, *Acta. Cryst.*, 1990, C46, 271.
16. I. Lazar, D. C. Hrnčir, W.-D. Kim, G. E. Kiefer and A. D. Sherry, *Inorg. Chem.*, 1992, 31, 4422.
17. B. I. Makaranets, T. N. Polynova, V. K. Bel'skii, S. A. Ii'ichev and M. A. Porai-Koshits, *Zh. Strukt. Khim.*, 1985, 26, 131.
18. L. M. Shkol'nikova, G. V. Polyanchuk, N. M. Dyatlova, I. B. Geryunova and M. I. Kabachnik, *Izv. Akad. Nauk SSSR, Ser. Khim.*, 1985, 5, 1035.
19. M. Darriet, J. Darriet, A. Cassaigne and E. Neuzil, *Acta. Cryst.*, 1975, B31, 469.

20. J. J. Daly and P. J. Wheatley, *J. Chem. Soc. (A)*, 1967, 212.
21. G. V. Polyanchuk, L. M. Shkol'nikova, M. V. Rudomino, N. M. Dyatlova and S. S. Makarevich, *Zh. Strukt. Khim.*, 1985, 26, 109.
22. W. Clegg, P. B. Iveson and J. C. Lockhart, *J. Chem. Soc., Dalton Trans.*, 1992, 3291.
23. K. Moedritzer and R. R. Irani, *J. Org. Chem.*, 1966, 31, 1603.
24. I. J. Scowen, Ph. D. Thesis, University of North London, 1993.
25. I. D. C. Hales, B.Sc. Project, University of North London, 1992.
26. M. K. Cooper, P. J. Guerny and M. McPartlin, *J. Chem. Soc., Dalton Trans.*, 1982, 757.
27. N. Y. Choi, unpublished results. M. McPartlin, personal communication.
28. E. L. Eliel, N. L. Allinger, S. J. Angyal and G. A. Morrison, *Conformational Analysis*, Interscience Publishers, New York, 1967.
29. L. M. Shkol'nikova, G. V. Polyanchuk, N. M. Dyatlova, M. A. Porai-Koshits and V. G. Yashunskii, *Zh. Strukt. Khim.*, 1983, 24, 92.
30. L. M. Shkol'nikova, G. V. Polyanchuk, N. M. Dyatlova and I. A. Polyakova, *Zh. Strukt. Khim.*, 1984, 25, 103.
31. W. L. Duax, C. M. Weeks and R. C. Roher, *Topics in Stereochemistry*, 1976, 9, 271.
32. R. D. Hancock and A. E. Martell, *Chem. Rev.*, 1989, 89, 1875.

Appendix 1

Table 1 Fractional atomic coordinates and thermal parameters (\AA^2) for DEAMPH₂.

Atom	x	y	z	Uiso or Ueq
P	0.11879(15)	0.96233(9)	0.33597(13)	0.0346(6)
O(1)	0.1597(4)	0.8856(3)	0.2215(3)	0.045(2)
O(2)	-0.0847(4)	0.9866(3)	0.3050(3)	0.045(2)
O(3)	0.1984(4)	0.9203(3)	0.4925(3)	0.048(2)
C(1)	0.2283(5)	1.1041(3)	0.3375(4)	0.033(2)
N(1)	0.1994(4)	1.1734(3)	0.1995(4)	0.033(2)
C(21)	0.0068(6)	1.2024(5)	0.1301(5)	0.045(3)
C(31)	0.2837(6)	1.1203(4)	0.0875(5)	0.048(3)
C(32)	0.4834(7)	1.1201(5)	0.1401(7)	0.070(4)
C(22)	-0.0724(6)	1.2744(5)	0.2331(6)	0.062(3)

Table 2 Fractional atomic coordinates for the hydrogen atoms for DEAMPH₂.

Atom	x	y	z	
H(1a)	0.371(1)	1.089(1)	0.377(1)	0.08
H(1b)	0.184(1)	1.159(1)	0.415(1)	0.08
H(21a)	-0.003(1)	1.252(1)	0.031(1)	0.08
H(21b)	-0.069(1)	1.122(1)	0.103(1)	0.08
H(31a)	0.244(1)	1.171(1)	-0.013(1)	0.08
H(31b)	0.237(1)	1.031(1)	0.066(1)	0.08
H(32a)	0.539(1)	1.082(1)	0.057(1)	0.08
H(32b)	0.525(1)	1.069(1)	0.240(1)	0.08
H(32c)	0.532(1)	1.209(1)	0.161(1)	0.08
H(22a)	-0.212(1)	1.294(1)	0.180(1)	0.08
H(22b)	0.002(1)	1.355(1)	0.260(1)	0.08
H(22c)	-0.064(1)	1.225(1)	0.332(1)	0.08
H(n1)	0.267(7)	1.244(5)	0.236(6)	0.08
H(o2)	-0.151(6)	1.038(5)	0.392(6)	0.08

Table 3 Anisotropic thermal parameters (\AA^2) for DEAMPH₂.

Atom	U11	U22	U33	U23	U13
P	0.037(1)	0.032(1)	0.035(1)	0.001(1)	0.010(1)
O(1)	0.057(2)	0.036(2)	0.041(2)	-0.004(1)	0.018(1)
O(2)	0.033(2)	0.052(2)	0.049(2)	-0.001(2)	0.014(1)
O(3)	0.058(2)	0.048(2)	0.038(2)	0.014(1)	0.015(1)
C(1)	0.036(2)	0.037(2)	0.025(2)	0.002(2)	0.001(2)
N(1)	0.035(2)	0.037(2)	0.028(2)	-0.003(2)	0.004(1)
C(21)	0.028(2)	0.061(3)	0.046(3)	0.015(2)	-0.004(2)
C(31)	0.056(3)	0.047(3)	0.042(3)	-0.009(2)	0.020(2)
C(32)	0.058(3)	0.070(4)	0.082(4)	-0.004(3)	0.035(3)
C(22)	0.046(3)	0.058(3)	0.081(4)	0.013(3)	0.022(3)

Table 4 Bond lengths (Å) for DEAMPH₇.

P	-O(1)	1.487(3)	P	-O(2)	1.543(3)
P	-O(3)	1.520(3)	P	-C(1)	1.821(4)
C(1)	-N(1)	1.489(5)	N(1)	-C(21)	1.493(5)
N(1)	-C(31)	1.506(5)	C(21)	-C(22)	1.517(7)
C(31)	-C(32)	1.488(7)			
O(2)	-H(o2)	1.23(6)	C(1)	-H(1a)	1.080(1)
C(1)	-H(1b)	1.080(1)	N(1)	-H(n1)	0.97(6)
C(21)	-H(21a)	1.080(1)	C(21)	-H(21b)	1.080(1)
C(31)	-H(31a)	1.080(1)	C(31)	-H(31b)	1.080(1)
C(32)	-H(32a)	1.080(1)	C(32)	-H(32b)	1.080(1)
C(32)	-H(32c)	1.080(1)	C(22)	-H(22a)	1.080(1)
C(22)	-H(22b)	1.080(1)	C(22)	-H(22c)	1.080(1)

Table 5 Bond angles (°) for DEAMPH₂.

O(2) -P -O(1)	111.6(2)	O(3) -P -O(1)	114.3(2)
O(3) -P -O(2)	111.7(2)	C(1) -P -O(1)	109.9(2)
C(1) -P -O(2)	106.8(2)	C(1) -P -O(3)	101.8(2)
N(1) -C(1) -P	120.1(3)	C(21) -N(1) -C(1)	113.7(3)
C(31) -N(1) -C(1)	114.0(3)	C(31) -N(1) -C(21)	110.2(3)
C(22) -C(21) -N(1)	111.1(4)	C(32) -C(31) -N(1)	111.5(4)
H(o2) -O(2) -P	123(2)	H(1a) -C(1) -P	106.8(1)
H(1b) -C(1) -P	106.7(1)	H(1b) -C(1) -H(1a)	109.5(1)
N(1) -C(1) -H(1a)	106.9(2)	N(1) -C(1) -H(1b)	106.6(2)
H(n1) -N(1) -C(1)	101(3)	H(n1) -N(1) -C(21)	110(3)
H(n1) -N(1) -C(31)	107(3)	H(21a) -C(21) -N(1)	109.0(2)
H(21b) -C(21) -N(1)	109.1(2)	H(21b) -C(21) -H(21a)	109.5(1)
C(22) -C(21) -H(21a)	109.0(3)	C(22) -C(21) -H(21b)	109.0(3)
H(31a) -C(31) -N(1)	108.9(2)	H(31b) -C(31) -N(1)	109.1(2)
H(31b) -C(31) -H(31a)	109.5(1)	C(32) -C(31) -H(31a)	108.9(3)
C(32) -C(31) -H(31b)	109.0(3)	H(32a) -C(32) -C(31)	109.3(3)
H(32b) -C(32) -C(31)	109.5(3)	H(32b) -C(32) -H(32a)	109.5(1)
H(32c) -C(32) -C(31)	109.6(3)	H(32c) -C(32) -H(32a)	109.5(1)
H(32c) -C(32) -H(32b)	109.5(1)	H(22a) -C(22) -C(21)	109.5(2)
H(22b) -C(22) -C(21)	109.5(3)	H(22b) -C(22) -H(22a)	109.5(1)
H(22c) -C(22) -C(21)	109.5(3)	H(22c) -C(22) -H(22a)	109.5(1)
H(22c) -C(22) -H(22b)	109.5(1)		

Table 6 Intermolecular distances (Å) for DEAMPH₂.

Atom1	Atom2	Dist	S	A	B	C
P	...P	4.08	-1	0.0	2.0	1.0
O(2)	...P	3.52	-1	0.0	2.0	1.0
O(3)	...P	3.53	-1	0.0	2.0	1.0
H(o2)	...P	2.51	-1	0.0	2.0	1.0
N(1)	...P	3.63	-2	1.0	1.0	1.0
H(32c)	...P	3.11	-2	1.0	1.0	1.0
H(n1)	...P	2.78	-2	1.0	1.0	1.0
C(21)	...O(1)	3.38	-1	0.0	2.0	0.0
H(21a)	...O(1)	2.84	-1	0.0	2.0	0.0
H(21b)	...O(1)	2.96	-1	0.0	2.0	0.0
C(1)	...O(1)	3.41	-2	1.0	1.0	1.0
N(1)	...O(1)	2.67	-2	1.0	1.0	1.0
C(21)	...O(1)	3.32	-2	1.0	1.0	1.0
H(32c)	...O(1)	2.88	-2	1.0	1.0	1.0
C(22)	...O(1)	3.35	-2	1.0	1.0	1.0
H(22b)	...O(1)	2.59	-2	1.0	1.0	1.0
H(n1)	...O(1)	1.72	-2	1.0	1.0	1.0
O(3)	...O(2)	2.54	-1	0.0	2.0	1.0
H(o2)	...O(2)	2.97	-1	0.0	2.0	1.0
H(22a)	...O(2)	2.72	-2	0.0	1.0	1.0
H(32b)	...O(3)	2.85	-1	1.0	2.0	1.0
H(22c)	...O(3)	2.73	-1	0.0	2.0	1.0
H(o2)	...O(3)	1.33	-1	0.0	2.0	1.0
H(31a)	...O(3)	2.88	-2	1.0	1.0	1.0
H(21a)	...C(1)	2.89	2	-1.0	2.0	-1.0
H(22a)	...C(32)	3.02	1	-1.0	0.0	0.0
H(32a)	...C(32)	2.93	-1	1.0	2.0	0.0
C(22)	...H(32c)	3.04	1	-1.0	0.0	0.0

Symmetry Transformations:

The second atom is related to the first atom, at (x,y,z), by the symmetry operation S with (A,B,C) added to the (x',y',z') of S.

Where S = 1 x, y, z
 2 0.5+x, 0.5-y, 0.5+z

Table 7 Intramolecular distances (Å) for DEAMPH₂.

H(1a) ...P	2.37	H(1b) ...P	2.37
N(1) ...P	2.87	C(21) ...P	3.33
H(21b)...P	2.92	C(31) ...P	3.45
H(31b)...P	3.03	H(22c)...P	3.31
H(o2)...P	2.44	O(2) ...O(1)	2.51
O(3) ...O(1)	2.53	C(1) ...O(1)	2.71
H(1a) ...O(1)	2.99	N(1) ...O(1)	3.31
C(31) ...O(1)	3.21	H(31b)...O(1)	2.39
O(3) ...O(2)	2.54	C(1) ...O(2)	2.70
H(1b) ...O(2)	2.84	C(21) ...O(2)	3.14
H(21b)...O(2)	2.48	C(22) ...O(2)	3.36
H(22c)...O(2)	2.73	C(1) ...O(3)	2.60
H(1a) ...O(3)	2.72	H(1b) ...O(3)	2.81
H(o2) ...O(3)	2.94	C(21) ...C(1)	2.50
H(21b)...C(1)	2.74	C(31) ...C(1)	2.51
H(31b)...C(1)	2.71	C(32) ...C(1)	3.05
H(32b)...C(1)	2.71	C(22) ...C(1)	2.98
H(22c)...C(1)	2.63	H(n1)...C(1)	1.92
N(1) ...H(1a)	2.08	C(31) ...H(1a)	2.66
C(32) ...H(1a)	2.63	N(1) ...H(1b)	2.07
C(21) ...H(1b)	2.72	C(22) ...H(1b)	2.61
H(21a)...N(1)	2.11	H(21b)...N(1)	2.11
H(31a)...N(1)	2.12	H(31b)...N(1)	2.12
C(32) ...N(1)	2.47	H(32b)...N(1)	2.71
H(32c)...N(1)	2.71	C(22) ...N(1)	2.48
H(22b)...N(1)	2.72	H(22c)...N(1)	2.72
C(31) ...C(21)	2.46	H(31a)...C(21)	2.57
H(31b)...C(21)	2.81	H(22a)...C(21)	2.14
H(22b)...C(21)	2.14	H(22c)...C(21)	2.14
H(n1) ...C(21)	2.04	C(31) ...H(21a)	2.61
C(22) ...H(21a)	2.13	C(31) ...H(21b)	2.76
C(22) ...H(21b)	2.13	H(32a)...C(31)	2.11
H(32b)...C(31)	2.11	H(32c)...C(31)	2.11
H(n1) ...C(31)	2.02	C(32) ...H(31a)	2.10
C(32) ...H(31b)	2.10	H(n1) ...C(32)	2.53
H(n1) ...C(22)	2.63		

Appendix 2

Table 1 Fractional atomic coordinates and thermal parameters (Å) for CDTMPH₈·H₂O.

Atom	x	y	z	Uiso or Ueq
P(1a)	-0.20043(11)	-0.09241(11)	-0.43235(6)	0.0265(6)
O(1a)	-0.0665(3)	-0.1286(3)	-0.4383(2)	0.044(2)
O(2a)	-0.2238(3)	-0.1275(3)	-0.3598(2)	0.032(2)
O(3a)	-0.3028(3)	-0.1534(3)	-0.4978(2)	0.039(2)
P(1b)	0.09507(10)	0.13967(10)	-0.28649(6)	0.0222(5)
O(1b)	0.2341(2)	0.1501(3)	-0.2906(2)	0.031(2)
O(2b)	0.0650(3)	0.0130(3)	-0.2571(2)	0.029(2)
O(3b)	0.0597(2)	0.2487(3)	-0.2410(1)	0.029(1)
P(1c)	-0.51139(10)	0.00206(11)	-0.34561(6)	0.0229(5)
O(1c)	-0.5076(3)	0.0362(3)	-0.4217(1)	0.029(2)
O(2c)	-0.4358(3)	-0.1219(3)	-0.3189(2)	0.040(2)
O(3c)	-0.6455(3)	-0.0178(3)	-0.3342(2)	0.033(2)
P(1d)	-0.15159(10)	0.10883(10)	-0.15018(6)	0.0235(5)
O(1d)	-0.0507(3)	0.1720(3)	-0.0917(2)	0.041(2)
O(2d)	-0.1071(3)	0.0020(3)	-0.1909(2)	0.041(2)
O(3d)	-0.2624(3)	0.0572(3)	-0.1192(2)	0.033(2)
N(1)	-0.1471(3)	0.1505(3)	-0.3833(2)	0.022(2)
N(2)	-0.3070(3)	0.1742(3)	-0.2887(2)	0.019(2)
C(1a)	-0.2187(4)	0.0768(4)	-0.4481(2)	0.026(2)
C(1b)	-0.0060(4)	0.1591(4)	-0.3786(2)	0.028(2)
C(1c)	-0.4361(3)	0.1253(4)	-0.2810(2)	0.027(2)
C(1d)	-0.2277(4)	0.2289(4)	-0.2170(2)	0.023(2)
C(1)	-0.2021(4)	0.2781(4)	-0.3768(2)	0.021(2)
C(2)	-0.3271(3)	0.2673(4)	-0.3531(2)	0.020(2)
C(3)	-0.3736(4)	0.3977(4)	-0.3359(2)	0.026(2)
C(4)	-0.3993(4)	0.4797(4)	-0.4053(2)	0.035(3)
C(5)	-0.2785(4)	0.4909(4)	-0.4327(2)	0.036(3)
C(6)	-0.2295(4)	0.3601(4)	-0.4471(2)	0.032(2)
O(1w)	-0.3006(3)	-0.1803(3)	-0.1127(2)	0.049(2)

Table 2 Fractional atomic coordinates (Å) for the hydrogen atoms for
CDTMPH₈·H₂O.

Atom	x	y	z	
H(1a1)	-0.321(1)	0.101(1)	-0.461(1)	0.08
H(1a2)	-0.182(1)	0.102(1)	-0.495(1)	0.08
H(1b1)	0.018(1)	0.086(1)	-0.413(1)	0.08
H(1b2)	0.013(1)	0.251(1)	-0.399(1)	0.08
H(1c1)	-0.421(1)	0.088(1)	-0.226(1)	0.08
H(1c2)	-0.503(1)	0.205(1)	-0.289(1)	0.08
H(1d1)	-0.152(1)	0.288(1)	-0.228(1)	0.08
H(1d2)	-0.290(1)	0.286(1)	-0.193(1)	0.08
H(1)	-0.127(1)	0.326(1)	-0.336(1)	0.08
H(2)	-0.404(1)	0.229(1)	-0.398(1)	0.08
H(3a)	-0.462(1)	0.388(1)	-0.319(1)	0.08
H(3b)	-0.300(1)	0.442(1)	-0.292(1)	0.08
H(4a)	-0.428(1)	0.574(1)	-0.393(1)	0.08
H(4b)	-0.476(1)	0.437(1)	-0.448(1)	0.08
H(5a)	-0.301(1)	0.545(1)	-0.483(1)	0.08
H(5b)	-0.203(1)	0.539(1)	-0.391(1)	0.08
H(6a)	-0.302(1)	0.314(1)	-0.491(1)	0.08
H(6b)	-0.141(1)	0.370(1)	-0.464(1)	0.08
H(2n)	-0.254	0.098	-0.302	0.08
H(1wa)	-0.215	-0.156	-0.079	0.08
H(1wb)	-0.278	-0.234	-0.154	0.08
H(1oa)	-0.010	-0.226	-0.423	0.08
H(3oa)	-0.398	-0.101	-0.529	0.08
H(3ob)	0.124	0.294	-0.202	0.08
H(2oc)	-0.345	-0.132	-0.340	0.08
H(3oc)	-0.678	0.064	-0.316	0.08
H(2od)	-0.040	0.004	-0.221	0.08
H(3od)	-0.272	-0.036	-0.116	0.08

Table 3 Anisotropic thermal parameters (Å) for $\text{CDTMPH}_8 \cdot \text{H}_2\text{O}$.

Atom	U11	U22	U33	U23	U13
	U12				
P(1a)	0.028(1)	0.027(1)	0.024(1)	0.000(1)	0.006(1)
	0.007(1)				
O(1a)	0.041(2)	0.042(2)	0.049(2)	0.005(2)	0.021(1)
	0.019(2)				
O(2a)	0.025(1)	0.040(2)	0.031(2)	0.008(1)	0.003(1)
	0.005(1)				
O(3a)	0.053(2)	0.029(2)	0.037(2)	-0.010(1)	-0.008(1)
	0.009(1)				
P(1b)	0.018(1)	0.023(1)	0.025(1)	-0.001(1)	0.006(1)
	0.002(1)				
O(1b)	0.020(1)	0.031(2)	0.042(2)	0.003(1)	0.010(1)
	-0.001(1)				
O(2b)	0.028(1)	0.024(2)	0.036(2)	0.005(1)	0.011(1)
	0.002(1)				
O(3b)	0.022(1)	0.030(2)	0.034(2)	-0.011(1)	0.006(1)
	0.001(1)				
P(1c)	0.022(1)	0.023(1)	0.023(1)	0.001(1)	0.007(1)
	0.000(1)				
O(1c)	0.026(1)	0.035(2)	0.025(1)	-0.002(1)	0.007(1)
	-0.003(1)				
O(2c)	0.038(2)	0.035(2)	0.047(2)	0.009(2)	0.018(1)
	0.013(1)				
O(3c)	0.025(1)	0.028(2)	0.046(2)	-0.006(1)	0.016(1)
	-0.007(1)				
P(1d)	0.027(1)	0.023(1)	0.021(1)	0.001(1)	0.005(1)
	-0.004(1)				
O(1d)	0.051(2)	0.042(2)	0.031(2)	0.009(1)	-0.011(1)
	-0.018(2)				
O(2d)	0.046(2)	0.026(2)	0.051(2)	0.003(2)	0.028(2)
	0.006(1)				
O(3d)	0.041(2)	0.028(2)	0.032(2)	0.001(1)	0.018(1)
	-0.006(1)				
N(1)	0.019(2)	0.026(2)	0.020(2)	-0.002(1)	0.007(1)
	0.003(1)				

[Table 3 continued]

N(2)	0.018(1)	0.024(2)	0.015(2)	0.000(1)	0.005(1)
	-0.001(1)				
C(1a)	0.028(2)	0.033(2)	0.015(2)	-0.003(2)	0.004(2)
	0.006(2)				
C(1b)	0.022(2)	0.037(2)	0.026(2)	0.000(2)	0.008(2)
	0.005(2)				
C(1c)	0.021(2)	0.038(3)	0.022(2)	0.002(2)	0.008(2)
	-0.005(2)				
C(1d)	0.025(2)	0.025(2)	0.018(2)	-0.001(2)	0.001(2)
	-0.002(2)				
C(1)	0.022(2)	0.022(2)	0.020(2)	0.003(2)	0.009(2)
	0.002(2)				
C(2)	0.018(2)	0.026(2)	0.017(2)	0.000(2)	0.003(1)
	0.002(2)				
C(3)	0.031(2)	0.023(2)	0.024(2)	0.001(2)	0.005(2)
	0.005(2)				
C(4)	0.038(3)	0.031(3)	0.037(3)	0.009(2)	0.006(2)
	0.008(2)				
C(5)	0.049(3)	0.026(2)	0.033(2)	0.013(2)	0.010(2)
	0.005(2)				
C(6)	0.039(2)	0.031(2)	0.026(2)	0.008(2)	0.012(2)
	0.000(2)				
O(1w)	0.059(2)	0.030(2)	0.059(2)	-0.003(2)	0.030(2)
	-0.004(2)				

Table 4 Bond lengths (Å) for CDTMPH₃·H₂O.

P(1a) -O(1a)	1.510(4)	P(1a) -O(2a)	1.496(3)
P(1a) -O(3a)	1.548(3)	P(1a) -C(1a)	1.806(4)
P(1b) -O(1b)	1.509(3)	P(1b) -O(2b)	1.508(3)
P(1b) -O(3b)	1.536(3)	P(1b) -C(1b)	1.788(4)
P(1c) -O(1c)	1.484(3)	P(1c) -O(2c)	1.544(3)
P(1c) -O(3c)	1.516(3)	P(1c) -C(1c)	1.809(4)
P(1d) -O(1d)	1.474(3)	P(1d) -O(2d)	1.505(3)
P(1d) -O(3d)	1.547(4)	P(1d) -C(1d)	1.811(4)
N(1) -C(1a)	1.472(5)	N(1) -C(1b)	1.486(5)
N(1) -C(1)	1.482(5)	N(2) -C(1c)	1.512(5)
N(2) -C(1d)	1.500(4)	N(2) -C(2)	1.525(5)
C(1) -C(2)	1.517(6)	C(1) -C(6)	1.537(6)
C(2) -C(3)	1.522(6)	C(3) -C(4)	1.526(6)
C(4) -C(5)	1.513(7)	C(5) -C(6)	1.521(7)
O(1a) -H(1oa)	1.181(3)	O(2a) -H(2oc)	1.433(3)
O(3a) -H(3oa)	1.162(3)	O(1b) -H(3oc)	1.466(3)
O(2b) -H(2od)	1.454(3)	O(3b) -H(3ob)	0.982(3)
O(2c) -H(2oc)	1.149(3)	O(3c) -H(3oc)	1.023(3)
O(2d) -H(2od)	1.030(4)	O(3d) -H(3od)	0.990(3)
N(2) -H(2n)	1.046(3)	C(1a) -H(1a1)	1.080(6)
C(1a) -H(1a2)	1.080(6)	C(1b) -H(1b1)	1.080(6)
C(1b) -H(1b2)	1.080(6)	C(1c) -H(1c1)	1.080(6)
C(1c) -H(1c2)	1.080(6)	C(1d) -H(1d1)	1.080(6)
C(1d) -H(1d2)	1.080(6)	C(1) -H(1)	1.080(5)
C(2) -H(2)	1.080(5)	C(3) -H(3a)	1.080(7)
C(3) -H(3b)	1.080(5)	C(4) -H(4a)	1.080(7)
C(4) -H(4b)	1.080(6)	C(5) -H(5a)	1.080(6)
C(5) -H(5b)	1.080(6)	C(6) -H(6a)	1.080(6)
C(6) -H(6b)	1.080(7)	O(1w) -H(1wa)	0.995(3)
O(1w) -H(1wb)	1.043(4)		

Table 5 Bond angles (°) for CDTMPH₃·H₂O.

O(2a) -P(1a) -O(1a)	113.3(2)	O(3a) -P(1a) -O(1a)	108.5(2)
O(3a) -P(1a) -O(2a)	111.6(2)	C(1a) -P(1a) -O(1a)	107.4(2)
C(1a) -P(1a) -O(2a)	110.8(2)	C(1a) -P(1a) -O(3a)	104.8(2)
O(2b) -P(1b) -O(1b)	113.0(2)	O(3b) -P(1b) -O(1b)	111.4(2)
O(3b) -P(1b) -O(2b)	110.4(2)	C(1b) -P(1b) -O(1b)	106.8(2)
C(1b) -P(1b) -O(2b)	108.8(2)	C(1b) -P(1b) -O(3b)	106.2(2)
O(2c) -P(1c) -O(1c)	111.8(2)	O(3c) -P(1c) -O(1c)	116.0(2)
O(3c) -P(1c) -O(2c)	105.5(2)	C(1c) -P(1c) -O(1c)	110.5(2)
C(1c) -P(1c) -O(2c)	106.6(2)	C(1c) -P(1c) -O(3c)	105.7(2)
O(2d) -P(1d) -O(1d)	116.7(2)	O(3d) -P(1d) -O(1d)	110.9(2)
O(3d) -P(1d) -O(2d)	107.7(2)	C(1d) -P(1d) -O(1d)	107.7(2)
C(1d) -P(1d) -O(2d)	108.2(2)	C(1d) -P(1d) -O(3d)	105.0(2)
C(1b) -N(1) -C(1a)	112.0(3)	C(1) -N(1) -C(1a)	114.5(3)
C(1) -N(1) -C(1b)	110.9(3)	C(1d) -N(2) -C(1c)	110.7(3)
C(2) -N(2) -C(1c)	110.8(3)	C(2) -N(2) -C(1d)	113.1(3)
N(1) -C(1a) -P(1a)	111.9(3)	N(1) -C(1b) -P(1b)	112.9(3)
N(2) -C(1c) -P(1c)	115.6(3)	N(2) -C(1d) -P(1d)	113.3(3)
C(2) -C(1) -N(1)	110.7(3)	C(6) -C(1) -N(1)	115.1(3)
C(6) -C(1) -C(2)	108.3(3)	C(1) -C(2) -N(2)	109.4(3)
C(3) -C(2) -N(2)	113.2(3)	C(3) -C(2) -C(1)	110.9(3)
C(4) -C(3) -C(2)	108.7(4)	C(5) -C(4) -C(3)	111.1(4)
C(6) -C(5) -C(4)	110.7(4)	C(5) -C(6) -C(1)	110.5(4)
H(1oa)-O(1a) -P(1a)	129.0(3)	H(2oc)-O(2a) -P(1a)	128.3(2)
H(3oa)-O(3a) -P(1a)	122.6(2)	H(3oc)-O(1b) -P(1b)	133.7(2)
H(2od)-O(2b) -P(1b)	119.6(2)	H(3ob)-O(3b) -P(1b)	123.4(2)
H(2oc)-O(2c) -P(1c)	112.4(2)	H(3oc)-O(3c) -P(1c)	110.6(2)
H(2od)-O(2d) -P(1d)	129.1(3)	H(3od)-O(3d) -P(1d)	118.4(3)
H(2n) -N(2) -C(1c)	108.8(3)	H(2n) -N(2) -C(1d)	107.1(3)
H(2n) -N(2) -C(2)	106.1(3)	H(1a1)-C(1a) -P(1a)	108.9(4)
H(1a1)-C(1a) -N(1)	109.0(4)	H(1a2)-C(1a) -P(1a)	108.9(4)
H(1a2)-C(1a) -N(1)	108.7(4)	H(1a2)-C(1a) -H(1a1)	109.5(4)
H(1b1)-C(1b) -P(1b)	108.6(3)	H(1b1)-C(1b) -N(1)	108.7(4)
H(1b2)-C(1b) -P(1b)	108.6(3)	H(1b2)-C(1b) -N(1)	108.5(4)
H(1b2)-C(1b) -H(1b1)	109.5(5)	H(1c1)-C(1c) -P(1c)	108.0(4)
H(1c1)-C(1c) -N(2)	107.9(3)	H(1c2)-C(1c) -P(1c)	107.9(3)
H(1c2)-C(1c) -N(2)	107.9(4)	H(1c2)-C(1c) -H(1c1)	109.5(5)
H(1d1)-C(1d) -P(1d)	108.5(3)	H(1d1)-C(1d) -N(2)	108.4(4)

[Table 5 continued]

H(1d2)-C(1d) -P(1d)	108.6(3)	H(1d2)-C(1d) -N(2)	108.6(3)
H(1d2)-C(1d) -H(1d1)	109.5(5)	H(1) -C(1) -N(1)	104.3(3)
C(2) -C(1) -H(1)	111.9(4)	C(6) -C(1) -H(1)	106.4(4)
H(2) -C(2) -N(2)	107.2(4)	H(2) -C(2) -C(1)	110.1(4)
C(3) -C(2) -H(2)	106.0(4)	H(3a) -C(3) -C(2)	109.8(4)
H(3b) -C(3) -C(2)	109.5(4)	H(3b) -C(3) -H(3a)	109.5(5)
C(4) -C(3) -H(3a)	109.6(4)	C(4) -C(3) -H(3b)	109.8(4)
H(4a) -C(4) -C(3)	109.0(5)	H(4b) -C(4) -C(3)	109.2(5)
H(4b) -C(4) -H(4a)	109.5(5)	C(5) -C(4) -H(4a)	109.0(5)
C(5) -C(4) -H(4b)	109.1(5)	H(5a) -C(5) -C(4)	109.2(5)
H(5b) -C(5) -C(4)	109.2(5)	H(5b) -C(5) -H(5a)	109.5(5)
C(6) -C(5) -H(5a)	109.3(5)	C(6) -C(5) -H(5b)	109.0(4)
H(6a) -C(6) -C(1)	109.3(4)	H(6a) -C(6) -C(5)	109.1(4)
H(6b) -C(6) -C(1)	109.2(4)	H(6b) -C(6) -C(5)	109.2(5)
H(6b) -C(6) -H(6a)	109.5(5)	H(1wb)-O(1w) -H(1wa)	105.7(3)
O(2c) -H(2oc)-O(2a)	170.4(2)	O(3c) -H(3oc)-O(1b)	158.8(2)
O(2d) -H(2od)-O(2b)	173.2(2)		

Table 6 Intermolecular distances (Å) for CDTMPH₈.H₂O.

Atom1	Atom2	Dist	S	A	B	C
O(1c) ...P(1a)		3.60	-1	-1.0	0.0	-1.0
O(3b) ...P(1a)		3.61	-2	0.0	1.0	0.0
O(1d) ...P(1a)		3.59	-2	0.0	1.0	0.0
H(3ob)...P(1a)		2.71	-2	0.0	1.0	0.0
P(1d) ...O(1a)		3.70	-2	0.0	1.0	0.0
O(1d) ...O(1a)		2.43	-2	0.0	1.0	0.0
H(3ob)...O(1a)		2.97	-2	0.0	1.0	0.0
P(1b) ...O(2a)		3.66	-2	0.0	1.0	0.0
O(3b) ...O(2a)		2.56	-2	0.0	1.0	0.0
H(3ob)...O(2a)		1.58	-2	0.0	1.0	0.0
P(1c) ...O(3a)		3.46	-1	-1.0	0.0	-1.0
O(1c) ...O(3a)		2.50	-1	-1.0	0.0	-1.0
O(1w) ...O(3a)		2.78	2	0.0	-1.0	0.0
H(1wa)...O(3a)		2.82	2	0.0	-1.0	0.0
O(3c) ...P(1b)		3.54	1	-1.0	0.0	0.0
H(3oc)...P(1b)		2.73	1	-1.0	0.0	0.0
H(3b) ...P(1b)		3.09	-2	0.0	1.0	0.0
H(1wb)...P(1b)		2.82	-2	0.0	0.0	0.0
P(1c) ...O(1b)		3.51	1	-1.0	0.0	0.0
O(3c) ...O(1b)		2.45	1	-1.0	0.0	0.0
H(1c2)...O(1b)		2.86	1	-1.0	0.0	0.0
H(3b) ...O(1b)		2.67	-2	0.0	1.0	0.0
O(1w) ...O(1b)		2.77	-2	0.0	0.0	0.0
H(1wb)...O(1b)		1.74	-2	0.0	0.0	0.0
O(3b) ...O(2b)		3.08	-2	0.0	1.0	0.0
H(1d1)...O(2b)		2.58	-2	0.0	1.0	0.0
H(1) ...O(2b)		2.59	-2	0.0	1.0	0.0
H(3b) ...O(2b)		2.54	-2	0.0	1.0	0.0
H(5b) ...O(2b)		2.80	-2	0.0	1.0	0.0
O(2d) ...O(3b)		3.05	-2	0.0	0.0	0.0
H(2od)...O(3b)		2.76	-2	0.0	0.0	0.0
H(3oa)...P(1c)		2.52	-1	-1.0	0.0	-1.0
H(1d2)...P(1c)		3.31	-2	-1.0	1.0	0.0
O(1c) ...O(1c)		3.08	-1	-1.0	0.0	-1.0
H(1a1)...O(1c)		2.86	-1	-1.0	0.0	-1.0
H(3oa)...O(1c)		1.36	-1	-1.0	0.0	-1.0

[Table 6 continued]

H(1c2)...O(2c)	2.92	-2	-1.0	1.0	0.0
C(1d) ...O(3c)	3.25	-2	-1.0	1.0	0.0
H(1d2)...O(3c)	2.27	-2	-1.0	1.0	0.0
C(3) ...O(3c)	3.27	-2	-1.0	1.0	0.0
H(3a) ...O(3c)	2.96	-2	-1.0	1.0	0.0
H(3b) ...O(3c)	2.62	-2	-1.0	1.0	0.0
H(1oa)...P(1d)	2.57	-2	0.0	0.0	0.0
H(6b) ...O(1d)	2.85	2	0.0	0.0	-1.0
H(1oa)...O(1d)	1.25	-2	0.0	0.0	0.0
H(3ob)...O(2d)	2.95	-2	0.0	1.0	0.0
H(5a) ...O(3d)	2.90	2	0.0	0.0	-1.0
C(6) ...O(3d)	3.28	2	0.0	0.0	-1.0
H(6a) ...O(3d)	2.90	2	0.0	0.0	-1.0
H(6b) ...O(3d)	2.96	2	0.0	0.0	-1.0
O(1w) ...H(1c2)	2.69	-2	-1.0	0.0	0.0
O(1w) ...H(3a)	2.61	-2	-1.0	0.0	0.0
H(4b) ...C(4)	2.86	-1	-1.0	1.0	-1.0
C(5) ...H(4b)	3.05	-1	-1.0	1.0	-1.0
O(1w) ...H(5a)	2.82	2	0.0	0.0	0.0
H(3oc)...O(1w)	2.98	-2	-1.0	1.0	0.0

Symmetry Transformations:

The second atom is related to the first atom, at (x,y,z), by the symmetry operation S with (A,B,C) added to the (x',y',z') of S.

Where S =	1	x,	y,	z
	2	x,	0.5-y,	0.5+z

Table 7 Intramolecular distances (Å) for CDTMPH₃·H₂O.

O(1c) ...P(1a)	3.60	O(2c) ...P(1a)	3.71
N(1) ...P(1a)	2.72	H(1a1)...P(1a)	2.38
H(1a2)...P(1a)	2.38	C(1b) ...P(1a)	3.35
H(1b1)...P(1a)	2.94	H(2n) ...P(1a)	3.33
H(1oa)...P(1a)	2.43	H(3oa)...P(1a)	2.38
H(2oc)...P(1a)	2.64	O(2a) ...O(1a)	2.51
O(3a) ...O(1a)	2.48	N(1) ...O(1a)	3.30
C(1a) ...O(1a)	2.68	H(1a2)...O(1a)	2.79
C(1b) ...O(1a)	3.23	H(1b1)...O(1a)	2.43
O(3a) ...O(2a)	2.52	P(1c) ...O(2a)	3.43
O(2c) ...O(2a)	2.57	N(1) ...O(2a)	3.10
C(1a) ...O(2a)	2.72	H(2n) ...O(2a)	2.66
C(1a) ...O(3a)	2.66	H(1a1)...O(3a)	2.78
H(1a2)...O(3a)	2.97	O(2d) ...P(1b)	3.47
N(1) ...P(1b)	2.73	H(1b1)...P(1b)	2.37
H(1b2)...P(1b)	2.37	C(1) ...P(1b)	3.49
H(1) ...P(1b)	3.02	H(3ob)...P(1b)	2.23
H(2od)...P(1b)	2.56	O(2b) ...O(1b)	2.52
O(3b) ...O(1b)	2.52	C(1b) ...O(1b)	2.65
H(1b1)...O(1b)	2.87	H(1b2)...O(1b)	2.87
H(3ob)...O(1b)	2.74	O(3b) ...O(2b)	2.50
P(1d) ...O(2b)	3.59	O(2d) ...O(2b)	2.48
N(1) ...O(2b)	3.16	C(1b) ...O(2b)	2.68
H(1b1)...O(2b)	2.94	P(1d) ...O(3b)	3.49
N(1) ...O(3b)	3.15	C(1b) ...O(3b)	2.66
H(1b2)...O(3b)	2.87	C(1d) ...O(3b)	3.22
H(1d1)...O(3b)	2.37	C(1) ...O(3b)	3.25
H(1) ...O(3b)	2.43	H(2od)...O(3b)	2.85
N(2) ...P(1c)	2.82	H(1c1)...P(1c)	2.38
H(1c2)...P(1c)	2.38	C(2) ...P(1c)	3.43
H(2) ...P(1c)	2.93	H(2n) ...P(1c)	2.83
H(2oc)...P(1c)	2.25	H(3oc)...P(1c)	2.11
O(2c) ...O(1c)	2.51	O(3c) ...O(1c)	2.55
N(2) ...O(1c)	3.17	C(1a) ...O(1c)	3.28
H(1a1)...O(1c)	2.39	C(1c) ...O(1c)	2.71
C(2) ...O(1c)	3.15	H(2) ...O(1c)	2.30
H(3oa)...O(1c)	2.96	H(2oc)...O(1c)	2.66

[Table 7 continued]

O(3c) ...O(2c)	2.44	C(1c) ...O(2c)	2.69
H(1c1)...O(2c)	2.79	H(2n) ...O(2c)	2.98
C(1c) ...O(3c)	2.66	H(1c1)...O(3c)	2.92
H(1c2)...O(3c)	2.80	N(2) ...P(1d)	2.77
C(1c) ...P(1d)	3.36	H(1c1)...P(1d)	2.85
H(1d1)...P(1d)	2.38	H(1d2)...P(1d)	2.39
O(1w) ...P(1d)	3.59	H(2n) ...P(1d)	2.77
H(1wa)...P(1d)	3.24	H(2od)...P(1d)	2.30
H(3od)...P(1d)	2.20	O(2d) ...O(1d)	2.54
O(3d) ...O(1d)	2.49	C(1d) ...O(1d)	2.66
H(1d1)...O(1d)	2.78	O(3d) ...O(2d)	2.46
N(2) ...O(2d)	3.02	C(1d) ...O(2d)	2.69
H(2n) ...O(2d)	2.46	H(3od)...O(2d)	2.56
N(2) ...O(3d)	3.33	C(1c) ...O(3d)	3.19
H(1c1)...O(3d)	2.27	C(1d) ...O(3d)	2.67
H(1d2)...O(3d)	2.76	O(1w) ...O(3d)	2.54
H(1wa)...O(3d)	2.37	N(2) ...N(1)	2.78
H(1a1)...N(1)	2.09	H(1a2)...N(1)	2.09
H(1b1)...N(1)	2.10	H(1b2)...N(1)	2.10
H(1) ...N(1)	2.04	C(2) ...N(1)	2.47
H(2) ...N(1)	2.80	C(6) ...N(1)	2.55
H(6a) ...N(1)	2.82	H(6b) ...N(1)	2.78
H(2n) ...N(1)	2.21	H(1c1)...N(2)	2.11
H(1c2)...N(2)	2.11	H(1d1)...N(2)	2.11
H(1d2)...N(2)	2.11	C(1) ...N(2)	2.48
H(1) ...N(2)	2.82	H(2) ...N(2)	2.11
C(3) ...N(2)	2.54	H(3a) ...N(2)	2.76
H(3b) ...N(2)	2.81	C(1b) ...C(1a)	2.45
H(1b1)...C(1a)	2.43	H(1b2)...C(1a)	3.02
C(1) ...C(1a)	2.48	C(2) ...C(1a)	3.10
H(2) ...C(1a)	2.89	C(6) ...C(1a)	2.98
H(6a) ...C(1a)	2.70	H(2n) ...C(1a)	2.88
H(3oa)...C(1a)	2.81	C(1) ...H(1a1)	2.55
C(2) ...H(1a1)	2.68	C(6) ...H(1a1)	2.88
C(1b) ...H(1a2)	2.54	C(1) ...H(1a2)	2.94
C(6) ...H(1a2)	2.95	C(1) ...C(1b)	2.44
H(1) ...C(1b)	2.44	C(6) ...C(1b)	3.19

[Table 7 continued]

H(6b) ...C(1b)	2.89	C(1) ...H(1b2)	2.45
C(6) ...H(1b2)	2.75	C(1d) ...C(1c)	2.48
H(1d2)...C(1c)	2.57	C(2) ...C(1c)	2.50
H(2) ...C(1c)	2.55	C(3) ...C(1c)	3.17
H(3a) ...C(1c)	2.85	H(2n) ...C(1c)	2.10
H(3oc)...C(1c)	2.57	C(1d) ...H(1c1)	2.51
C(1d) ...H(1c2)	2.89	C(2) ...H(1c2)	2.57
C(3) ...H(1c2)	2.73	C(1) ...C(1d)	3.13
H(1) ...C(1d)	2.91	C(2) ...C(1d)	2.53
C(3) ...C(1d)	2.95	H(3b) ...C(1d)	2.64
H(2n) ...C(1d)	2.07	C(1) ...H(1d1)	2.70
C(2) ...H(1d1)	2.59	C(3) ...H(1d1)	2.90
C(2) ...H(1d2)	2.92	C(3) ...H(1d2)	2.84
H(2) ...C(1)	2.14	C(3) ...C(1)	2.50
H(3b) ...C(1)	2.73	C(4) ...C(1)	2.93
C(5) ...C(1)	2.51	H(5b) ...C(1)	2.76
H(6a) ...C(1)	2.15	H(6b) ...C(1)	2.15
H(2n) ...C(1)	2.51	C(2) ...H(1)	2.17
C(3) ...H(1)	2.74	C(5) ...H(1)	2.71
C(6) ...H(1)	2.11	H(3a) ...C(2)	2.14
H(3b) ...C(2)	2.14	C(4) ...C(2)	2.48
H(4b) ...C(2)	2.72	C(5) ...C(2)	2.91
C(6) ...C(2)	2.47	H(6a) ...C(2)	2.71
H(2n) ...C(2)	2.08	C(3) ...H(2)	2.10
C(4) ...H(2)	2.64	C(6) ...H(2)	2.67
H(4a) ...C(3)	2.14	H(4b) ...C(3)	2.14
C(5) ...C(3)	2.51	H(5b) ...C(3)	2.76
C(6) ...C(3)	2.93	C(4) ...H(3a)	2.14
C(4) ...H(3b)	2.15	C(5) ...H(3b)	2.76
H(5a) ...C(4)	2.13	H(5b) ...C(4)	2.13
C(6) ...C(4)	2.50	H(6a) ...C(4)	2.75
C(5) ...H(4a)	2.13	C(5) ...H(4b)	2.13
C(6) ...H(4b)	2.75	H(6a) ...C(5)	2.13
H(6b) ...C(5)	2.14	C(6) ...H(5a)	2.14
C(6) ...H(5b)	2.13	H(3od)...O(1w)	1.55

Appendix 3

Published in the *Journal of Inorganic Biochemistry*, 1993, vol.51, 439.

STRUCTURAL AND STABILITY STUDIES OF SOME AMINOMETHYLENEPHOSPHONIC ACIDS AND THEIR METAL COMPLEXES

T. Candy,^b N. Choi,^a G. Hägele,^c I. Khan,^a H-W. Kropp,^c R.W. Matthews,^a M. McPartlin,^a M. Constantinou^a,

^aSchool of Applied Chemistry, The University of North London, Holloway Road, London N7 8DB, U.K. ^bInterox Research & Development, Moorfield Road, Widnes, Cheshire WA8 0FE, U.K. ^cHeinrich Heine University, Universitätsstraße 1, D-4000 Düsseldorf, Germany.

Potential biological applications of aminophosphonic acids (e.g. as medical therapeutic and diagnostic reagents[1], and as biocidal agents[2]) have come under close scrutiny. In particular, some aminomethylene-phosphonic acids involving cyclic moieties have been identified as bone resorption inhibitors and antiinflammatory agents[3].

Two polyaminophosphonic acids of this type, L^1H_8 and L^2H_4 , have been synthesised and their solid state structures and solution chemistries determined to provide a basis for investigating biological activity. Both compounds are zwitterionic. Protonation schemes have been elucidated using a combination of pK_a measurements, obtained from an automated potentiometric



titration apparatus, and ^{31}P nmr vs pH data, obtained using a stopped-flow apparatus. Stoichiometric stability constants ($\log \beta$'s) have been determined for complexes of L^1H_8 with a range of metal ions including Gd(III). In contrast to the relatively strong complexes formed by L^1H_8 , L^2H_4 showed significant binding only with Cu(II). However, protonated complexes of L^2H_4 with Cd(II) and Pb(II) were isolated in the solid state and their crystal structures determined. $Cd(L^2H_4) \cdot 4H_2O$ is a simple linear polymer with Cd octahedrally coordinated to two phosphonate oxygens and four water molecules. In contrast, the structure of $[Pb_4(L^2H_4)_2(ClO_4)_4] \cdot 5.5H_2O$ consists of a complex 3-D network of phosphonate groups bridging the lead atoms in several different modes.

1. I.K. Adzamli, H. Gries, D. Johnson, and M. Blau, *J. Med. Chem.*, 32, 139 (1989).
2. D. Cameron, H.R. Hudson, I. Lagerlund, and M. Pianka, *Eur. Pat.* 153 284.
3. I. Yasuo, T. Makoto, S. Shuichi, and A. Tetsushi, *Eur. Pat. Appl.* EP 325,482 (1989).

THE BRITISH LIBRARY

BRITISH THESIS SERVICE

TITLE SYNTHESSES, STRUCTURE AND STABILITY OF
SOME ALKYLPHOSPHONIC ACIDS AND THEIR
METAL COMPLEXES.

AUTHOR Maria
CONSTANTINO

DEGREE Ph.D

**AWARDING
BODY** University of North London

DATE 1994

**THESIS
NUMBER** DX184780

THIS THESIS HAS BEEN MICROFILMED EXACTLY AS RECEIVED

The quality of this reproduction is dependent upon the quality of the original thesis submitted for microfilming. Every effort has been made to ensure the highest quality of reproduction. Some pages may have indistinct print, especially if the original papers were poorly produced or if awarding body sent an inferior copy. If pages are missing, please contact the awarding body which granted the degree.

Previously copyrighted materials (journals articles, published texts etc.) are not filmed.

This copy of the thesis has been supplied on condition that anyone who consults it is understood to recognise that its copyright rests with its author and that no information derived from it may be published without the author's prior written consent.

Reproduction of this thesis, other than as permitted under the United Kingdom Copyright Designs and Patents Act 1988, or under specific agreement with the copyright holder, is prohibited.

C12.

DX

184780